Related titles

Surface modification of biomaterials
(ISBN 978-1-84569-640-5)

Coatings for biomedical applications
(ISBN 978-1-84569-568-2)

Metals for biomedical devices
(ISBN 978-1-84569-434-0)

Woodhead Publishing Series in Biomaterials: Number 94

Surface Coating and Modification of Metallic Biomaterials

Edited by

Cuie Wen



AMSTERDAM • BOSTON • CAMBRIDGE • HEIDELBERG
LONDON • NEW YORK • OXFORD • PARIS • SAN DIEGO
SAN FRANCISCO • SINGAPORE • SYDNEY • TOKYO
Woodhead Publishing is an imprint of Elsevier



Woodhead Publishing is an imprint of Elsevier
80 High Street, Sawston, Cambridge, CB22 3HJ, UK
225 Wyman Street, Waltham, MA 02451, USA
Langford Lane, Kidlington, OX5 1GB, UK

Copyright © 2015 Elsevier Ltd. All rights reserved.

No part of this publication may be reproduced, stored in a retrieval system or transmitted in any form or by any means electronic, mechanical, photocopying, recording or otherwise without the prior written permission of the publisher.

Permissions may be sought directly from Elsevier's Science & Technology Rights Department in Oxford, UK: phone (+44) (0) 1865 843830; fax (+44) (0) 1865 853333; email: permissions@elsevier.com. Alternatively you can submit your request online by visiting the Elsevier website at http://elsevier.com/locate/permissions, and selecting Obtaining permission to use Elsevier material.

Notice
No responsibility is assumed by the publisher for any injury and/or damage to persons or property as a matter of products liability, negligence or otherwise, or from any use or operation of any methods, products, instructions or ideas contained in the material herein. Because of rapid advances in the medical sciences, in particular, independent verification of diagnoses and drug dosages should be made.

British Library Cataloguing in Publication Data
A catalogue record for this book is available from the British Library

Library of Congress Control Number: 2015932575

ISBN 978-1-78242-303-4 (print)
ISBN 978-1-78242-316-4 (online)

For information on all Woodhead Publishing publications visit our website at http://store.elsevier.com/

Typeset by TNQ Books and Journals
www.tnq.co.in
Printed and bound in the United Kingdom



List of contributors

A. Atrens The University of Queensland, Brisbane, QLD, Australia

C.C. Berndt Swinburne University of Technology, Hawthorn, VIC, Australia; Stony Brook University, Stony Brook, NY, USA

C. Blawert Helmholtz-Zentrum Geesthacht, Centre for Materials and Coastal Research, Institute of Materials Research, Geesthacht, Germany

A.R. Boccaccini Imperial College London, London, UK; University of Erlangen-Nuremberg, Erlangen, Germany

S. Cabanas-Polo University of Erlangen-Nuremberg, Erlangen, Germany

F. Cao The University of Queensland, Brisbane, QLD, Australia

S. Chung Northeastern University, Boston, MA, USA

L. Cordero-Arias University of Erlangen-Nuremberg, Erlangen, Germany

M.S. Dargusch The University of Queensland, Brisbane, QLD, Australia

J.A. Gan Swinburne University of Technology, Hawthorn, VIC, Australia; La Trobe University, Melbourne, VIC, Australia

Y. Guven Istanbul University, Istanbul, Turkey

T. Hanawa Tokyo Medical and Dental University, Chiyoda-ku, Tokyo, Japan

B.D. Hatton University of Toronto, Toronto, ON, Canada

T. Kokubo Chubu University, Kasugai, Japan

J. Li Shanghai Institute of Ceramics, Chinese Academy of Sciences, Shanghai, China

X. Lin VU University and University of Amsterdam, Amsterdam, The Netherlands; University of Nanjing, Nanjing, China

X. Liu Shanghai Institute of Ceramics, Chinese Academy of Sciences, Shanghai, China

Y. Liu VU University and University of Amsterdam, Amsterdam, The Netherlands

G. Mani University of South Dakota, Sioux Falls, SD, USA

A. Nouri Institute of Biomaterials and Biomedical Engineering, University of Toronto, Toronto, ON, Canada

Y. Oshida Indiana University School of Dentistry, Indianapolis, IN, USA; University of California San Francisco School of Dentistry, Orinda, CA, USA

R.M. Pilliar University of Toronto, Toronto, ON, Canada

F. Pishbin Imperial College London, London, UK

N. Scharnagl Helmholtz-Zentrum Geesthacht, Centre for Materials and Coastal Research, Institute of Materials Research, Geesthacht, Germany

Z. Shi The University of Queensland, Brisbane, QLD, Australia

N.C. Verissimo State University of Campinas, Campinas, State of São Paulo, Brazil

D. Wang VU University and University of Amsterdam, Amsterdam, The Netherlands

T.J. Webster Northeastern University, Boston, MA, USA; Center of Excellence for Advanced Materials Research, King Abdulaziz University, Jeddah, Saudi Arabia

C. Wen School of Aerospace, Mechanical and Manufacturing Engineering, RMIT University, Bundoora, VIC, Australia

G. Wu VU University and University of Amsterdam, Amsterdam, The Netherlands

S. Yamaguchi Chubu University, Kasugai, Japan

Woodhead Publishing Series in Biomaterials

1 **Sterilisation of tissues using ionising radiations**
Edited by J. F. Kennedy, G. O. Phillips and P. A. Williams
2 **Surfaces and interfaces for biomaterials**
Edited by P. Vadgama
3 **Molecular interfacial phenomena of polymers and biopolymers**
Edited by C. Chen
4 **Biomaterials, artificial organs and tissue engineering**
Edited by L. Hench and J. Jones
5 **Medical modelling**
R. Bibb
6 **Artificial cells, cell engineering and therapy**
Edited by S. Prakash
7 **Biomedical polymers**
Edited by M. Jenkins
8 **Tissue engineering using ceramics and polymers**
Edited by A. R. Boccaccini and J. Gough
9 **Bioceramics and their clinical applications**
Edited by T. Kokubo
10 **Dental biomaterials**
Edited by R. V. Curtis and T. F. Watson
11 **Joint replacement technology**
Edited by P. A. Revell
12 **Natural-based polymers for biomedical applications**
Edited by R. L. Reiss et al
13 **Degradation rate of bioresorbable materials**
Edited by F. J. Buchanan
14 **Orthopaedic bone cements**
Edited by S. Deb
15 **Shape memory alloys for biomedical applications**
Edited by T. Yoneyama and S. Miyazaki
16 **Cellular response to biomaterials**
Edited by L. Di Silvio
17 **Biomaterials for treating skin loss**
Edited by D. P. Orgill and C. Blanco
18 **Biomaterials and tissue engineering in urology**
Edited by J. Denstedt and A. Atala

19 **Materials science for dentistry**
B. W. Darvell
20 **Bone repair biomaterials**
Edited by J. A. Planell, S. M. Best, D. Lacroix and A. Merolli
21 **Biomedical composites**
Edited by L. Ambrosio
22 **Drug–device combination products**
Edited by A. Lewis
23 **Biomaterials and regenerative medicine in ophthalmology**
Edited by T. V. Chirila
24 **Regenerative medicine and biomaterials for the repair of connective tissues**
Edited by C. Archer and J. Ralphs
25 **Metals for biomedical devices**
Edited by M. Ninomi
26 **Biointegration of medical implant materials: Science and design**
Edited by C. P. Sharma
27 **Biomaterials and devices for the circulatory system**
Edited by T. Gourlay and R. Black
28 **Surface modification of biomaterials: Methods analysis and applications**
Edited by R. Williams
29 **Biomaterials for artificial organs**
Edited by M. Lysaght and T. Webster
30 **Injectable biomaterials: Science and applications**
Edited by B. Vernon
31 **Biomedical hydrogels: Biochemistry, manufacture and medical applications**
Edited by S. Rimmer
32 **Preprosthetic and maxillofacial surgery: Biomaterials, bone grafting and tissue engineering**
Edited by J. Ferri and E. Hunziker
33 **Bioactive materials in medicine: Design and applications**
Edited by X. Zhao, J. M. Courtney and H. Qian
34 **Advanced wound repair therapies**
Edited by D. Farrar
35 **Electrospinning for tissue regeneration**
Edited by L. Bosworth and S. Downes
36 **Bioactive glasses: Materials, properties and applications**
Edited by H. O. Ylänen
37 **Coatings for biomedical applications**
Edited by M. Driver
38 **Progenitor and stem cell technologies and therapies**
Edited by A. Atala
39 **Biomaterials for spinal surgery**
Edited by L. Ambrosio and E. Tanner
40 **Minimized cardiopulmonary bypass techniques and technologies**
Edited by T. Gourlay and S. Gunaydin
41 **Wear of orthopaedic implants and artificial joints**
Edited by S. Affatato
42 **Biomaterials in plastic surgery: Breast implants**
Edited by W. Peters, H. Brandon, K. L. Jerina, C. Wolf and V. L. Young

43 **MEMS for biomedical applications**
Edited by S. Bhansali and A. Vasudev
44 **Durability and reliability of medical polymers**
Edited by M. Jenkins and A. Stamboulis
45 **Biosensors for medical applications**
Edited by S. Higson
46 **Sterilisation of biomaterials and medical devices**
Edited by S. Lerouge and A. Simmons
47 **The hip resurfacing handbook: A practical guide to the use and management of modern hip resurfacings**
Edited by K. De Smet, P. Campbell and C. Van Der Straeten
48 **Developments in tissue engineered and regenerative medicine products**
J. Basu and J. W. Ludlow
49 **Nanomedicine: Technologies and applications**
Edited by T. J. Webster
50 **Biocompatibility and performance of medical devices**
Edited by J-P. Boutrand
51 **Medical robotics: Minimally invasive surgery**
Edited by P. Gomes
52 **Implantable sensor systems for medical applications**
Edited by A. Inmann and D. Hodgins
53 **Non-metallic biomaterials for tooth repair and replacement**
Edited by P. Vallittu
54 **Joining and assembly of medical materials and devices**
Edited by Y. (Norman) Zhou and M. D. Breyen
55 **Diamond-based materials for biomedical applications**
Edited by R. Narayan
56 **Nanomaterials in tissue engineering: Fabrication and applications**
Edited by A. K. Gaharwar, S. Sant, M. J. Hancock and S. A. Hacking
57 **Biomimetic biomaterials: Structure and applications**
Edited by A. J. Ruys
58 **Standardisation in cell and tissue engineering: Methods and protocols**
Edited by V. Salih
59 **Inhaler devices: Fundamentals, design and drug delivery**
Edited by P. Prokopovich
60 **Bio-tribocorrosion in biomaterials and medical implants**
Edited by Y. Yan
61 **Microfluidic devices for biomedical applications**
Edited by X-J. James Li and Y. Zhou
62 **Decontamination in hospitals and healthcare**
Edited by J. T. Walker
63 **Biomedical imaging: Applications and advances**
Edited by P. Morris
64 **Characterization of biomaterials**
Edited by M. Jaffe, W. Hammond, P. Tolias and T. Arinzeh
65 **Biomaterials and medical tribology**
Edited by J. Paolo Davim
66 **Biomaterials for cancer therapeutics: Diagnosis, prevention and therapy**
Edited by K. Park

67 **New functional biomaterials for medicine and healthcare**
E. P. Ivanova, K. Bazaka and R. J. Crawford
68 **Porous silicon for biomedical applications**
Edited by H. A. Santos
69 **A practical approach to spinal trauma**
Edited by H. N. Bajaj and S. Katoch
70 **Rapid prototyping of biomaterials: Principles and applications**
Edited by R. Narayan
71 **Cardiac regeneration and repair Volume 1: Pathology and therapies**
Edited by R-K. Li and R. D. Weisel
72 **Cardiac regeneration and repair Volume 2: Biomaterials and tissue engineering**
Edited by R-K. Li and R. D. Weisel
73 **Semiconducting silicon nanowires for biomedical applications**
Edited by J. L. Coffer
74 **Silk biomaterials for tissue engineering and regenerative medicine**
Edited by S. Kundu
75 **Biomaterials for bone regeneration: Novel techniques and applications**
Edited by P. Dubruel and S. Van Vlierberghe
76 **Biomedical foams for tissue engineering applications**
Edited by P. Netti
77 **Precious metals for biomedical applications**
Edited by N. Baltzer and T. Copponnex
78 **Bone substitute biomaterials**
Edited by K. Mallick
79 **Regulatory affairs for biomaterials and medical devices**
Edited by S. F. Amato and R. Ezzell
80 **Joint replacement technology Second edition**
Edited by P. A. Revell
81 **Computational modelling of biomechanics and biotribology in the musculoskeletal system: Biomaterials and tissues**
Edited by Z. Jin
82 **Biophotonics for medical applications**
Edited by I. Meglinski
83 **Modelling degradation of bioresorbable polymeric medical devices**
Edited by J. Pan
84 **Perspectives in total hip arthroplasty: Advances in biomaterials and their tribological interactions**
S. Affatato
85 **Tissue engineering using ceramics and polymers Second edition**
Edited by A. R. Boccaccini and P. X. Ma
86 **Biomaterials and medical-device associated infections**
Edited by L. Barnes and I. R. Cooper
87 **Surgical techniques in total knee arthroplasty (TKA) and alternative procedures**
Edited by S. Affatato
88 **Lanthanide oxide nanoparticles for molecular imaging and therapeutics**
G. H. Lee
89 **Surface modification of magnesium and its alloys for biomedical applications Volume 1: Biological interactions, mechanical properties and testing**
Edited by T. S. N. Sankara Narayanan, I. S. Park and M. H. Lee

90 **Surface modification of magnesium and its alloys for biomedical applications Volume 2: Modification and coating techniques**
Edited by T. S. N. Sankara Narayanan, I. S. Park and M. H. Lee

91 **Medical modelling: the application of advanced design and rapid prototyping techniques in medicine Second Edition**
Edited by R. Bibb, D. Eggbeer and A. Paterson

92 **Switchable and responsive surfaces for biomedical applications**
Edited by Z. Zhang

93 **Biomedical textiles for orthopaedic and surgical applications: fundamentals, applications and tissue engineering**
Edited by T. Blair

94 **Surface coating and modification of metallic biomaterials**
Edited by C. Wen

95 **Hydroxyapatite (HAP) for biomedical applications**
Edited by M. Mucalo

96 **Implantable neuroprostheses for restoring function**
Edited by K. Kilgore

97 **Shape memory polymers for biomedical applications**
Edited by L. Yahia

98 **Regenerative engineering of musculoskeletal tissues and interfaces**
Edited by S. P. Nukavarapu, J. W. Freeman and C. T. Laurencin

99 **Advances in cardiac imaging: techniques and applications**
Edited by K. Nieman, O. Gaemperli, P. Lancellotti and S. Plein

Introduction to surface coating and modification for metallic biomaterials

1

A. Nouri[1], C. Wen[2]
[1]Institute of Biomaterials and Biomedical Engineering, University of Toronto, Toronto, ON, Canada; [2]School of Aerospace, Mechanical and Manufacturing Engineering, RMIT University, Bundoora, VIC, Australia

1.1 Introduction

The demand for safe and effective materials is greatly increasing in biomedical engineering due to the annual increase of the world's population, the growing number of older people, and the high functional demands of younger people. The fundamental requirement of a biomaterial is that the material and the surrounding physiological environment should coexist without having any undesirable effect on one another. Because the surface is the interface where the biomaterials meet and interact with the biological environment (i.e., bone, soft tissue, blood), the surface properties are the major factors that ultimately determine the rejection or acceptance of a biomaterial in the body. The biological events that regulate host responses to materials such as protein adsorption and cell adhesion occur at the biomaterial−tissue interface and are modulated by the physicochemical properties of the material (Anderson, 2001).

Although the bulk properties of the biomaterial are critical determinants of the biological performance of the material, it is rare that a biomaterial with suitable bulk properties also possesses appropriate surface characteristics for clinical applications, and very few surfaces are truly biocompatible. In these cases, a biocompatible modified layer with suitable wear and corrosion resistance would mitigate the above problems. In addition, despite the fact that the mechanical properties of biomaterials are dictated by the bulk properties, tissue−biomaterial interactions are governed by surface properties. These interactions have been hypothesized to occur within a narrow zone of less than 1 nm (Ong and Lucas, 1998).

Because the top layer of surface atoms are those that are in immediate contact with the other phases (i.e., gas, liquid, or solid), this top layer of surface atoms could be regarded as the surface. On the other hand, the structure and chemistry of that top layer of atoms or molecules are significantly determined by the atoms or molecules immediately below. This implies that the surface could be the top 2−10 atomic or molecular layers (say, 0.5−3 nm) (Vickerman, 2009). Atoms at the surface of metallic materials are considered partly reactive to the environment because atomic configuration terminates at the surface. Due to high surface energy, a single molecular layer readily forms on the solid surface where gas molecules are adsorbed at 1 Pa

Surface Coating and Modification of Metallic Biomaterials. http://dx.doi.org/10.1016/B978-1-78242-303-4.00001-6
Copyright © 2015 Elsevier Ltd. All rights reserved.

in 10^{-4} s. For example, in the presence of oxygen atoms, oxygen and metal atoms chemically bond together to form an oxide layer. This means that the surface composition of a metal is different from its bulk composition in the order of nanometers (Hanawa, 2004).

Surface treatment of biomaterials offers the ability to improve material and biological responses through changes in a material's surface chemistry, topography, energy, and charge, while still maintaining the bulk properties of the implant. Surface modifications can broadly be classified into three categories: (1) addition of materials of desirable functions to the surface; (2) conversion of the existing surface into more desirable compositions and/or topographies; and (3) removal of material from the existing surface to create specific topographies (Duan and Wang, 2006).

Surface modification of biomaterials can yield a more profitable return in a much shorter time compared to the painstaking and laborious processes of inventing novel materials. With surface modification, chemical and mechanical durability and tissue compatibility of a surface layer would be improved. From an economical point of view, surface modification is considered an inexpensive process because only the surface layer needs to be modified. In other words, with surface modification, the key physical properties of a biomaterial can be retained while only the outermost surface is modified to tailor to the biointeractions. The chief purpose of surface modification is to improve corrosion resistance, wear resistance, antibacterial property, bioadhesion (bone ingrowth), and biocompatibility, while other important requirements such as adequate mechanical strength and processability are governed by the bulk material properties. Surface modifications should provide distinct properties of interaction with biomolecules or cells of the biological environment. These would promote, for example, the adaptation or in growth of cells onto the surface of fixation elements of artificial joints, or prevention of cellular interaction with the surface to inhibit endothelial cell proliferation to provide cardiovascular devices with a suitable blood compatible surface (Thull, 2010).

There is no universal technique for the surface modification that can be applied to all biomaterials, and variations exist depending on the application and the type of materials. For instance, in bone implant materials, rapid bone conductivity is required; materials of cardiac stents have to be structured to avoid cell proliferation provoking restenosis; in cardiovascular devices, blood compatibility or antithrombogenecity is required; in dental implants, soft-tissue compatibility is required to prevent bacteria invasion from the crevice, which is between the dental implant and gingival epithelium (Hanawa, 2004).

The choice of a suitable method is dependent on many factors, including the substrate material, component design and geometry, cost, and the end applications in which two aspects of the surface engineering process, coating thickness and process temperature, are often highlighted.

1.1.1 Reasons for surface modification

The environment inside the body is mechanically, chemically, and electrically active, and the interface between an implanted biomaterial and the biological environment

(such as hard and soft tissue, blood, body liquid, or saliva) is the location of a variety of dynamic biochemical processes and reactions. The biological response from living tissues to the biomaterials is reliant on the surface properties such as chemical composition, cleanliness, topography, surface energy, corrosion resistance, and the tendency to denaturalize neighboring proteins.

Unfavorable conditions, e.g., premature loading that leads to micromotion, will disrupt the newly forming tissue and lead to the formation of a fibrous capsule (Puleo and Nanci, 1999). The interface of such fibrous capsule is mechanically weak and is susceptible to micromotion, which results in premature loosening. The surface properties can be selectively modified to enhance biological and/or tribological performance of the implants for a variety of orthopedic and dental applications. To this end, the development of novel surfaces has been the principle driving force behind many studies to promote bone formation and firm implant−bone attachment by reducing the implant micromotion and minimizing fibrous tissue formation around the implant. The fast fixation of an implant to hard tissue (or the early implant−bone integration) allows early physiologic loading and thus prevents the bone from disuse atrophy (Duan and Wang, 2006). It also reduces the hospitalization time and cost and improves the quality of life for patients.

When considering the surface modification for a blood-contacting material or device, scientists and engineers should develop materials that suppress the adsorption of blood components (such as proteins, lipids, or calcium) onto the surface of the material and the adhesion of blood cells or components of blood cells onto the surface of the material (Dee et al., 2002).

1.1.2 Pros and cons of metallic biomaterials

Metals are inorganic materials characterized by nondirectional metallic bonds with highly mobile electrons. In addition to their ability to conduct electricity, metals are strong, and most of them have the ability to form into complex shapes using relatively straightforward techniques. The desired mechanical properties of metals can be achieved through thermal and mechanical processes during or after final shaping. In addition, a degree of corrosion and wear resistance can be attained by proper treatment of parts made from selected metal compositions (Pilliar, 1991).

Metals have been used in medical implants for many centuries. Gold has been selected for use in dental material as early as 500 BC, and noble metals have been used in structural dentistry in fillings, crowns, bridges, and dentures since the fifteenth century (Williams, 1990). Today, metals account for a substantial percentage of clinically used materials and, for many applications, still represent the benchmark for success. This is due to a combination of acceptable biocompatibility and appropriate mechanical properties, especially for use as bone substitute materials, such as the high strength and toughness of the α- and β-Ti alloys (Williams, 2001), the low friction coefficient and the high wear resistance of the Co−Cr alloys (Marti, 2000), the superelasticity and shape memory effect of the Nitinol (Hanawa, 2012), etc.

In orthopedics, metals are used for bone and joint replacement in the form of fracture fixation plates, metallic wires, and screws. While the most prominent use of metallic biomaterials is for orthopedic applications, metallic biomaterials have also been widely used for dental implants, orthodontic archwires and unloaded and purely functional devices, such as electrodes in neural implants, prosthetic heart valves, protective cases in pacemakers, artificial hearts, stents, circulatory devices, and catheter guide wires. Surgical instruments, dental instruments, needles, staples, and implantable drug pump housings are also made from metallic materials (Davis, 2003). Due to the importance of metals in orthopedics and dentistry, the main focus of this chapter is on the application and characteristics of metallic biomaterials for hard-tissue replacements.

Most implanted metallic biomaterials have a tendency to lose electrons in solution. As a result, they show a high potential to corrode and leak corrosion products or abrasive particles into the biological environments, which usually causes inflammation and osteolysis. Additionally, their low surface hardness, high friction coefficient, and poor wear resistance are also limiting factors in their biomedical application. It is reported that wear and corrosion are the main reasons for degradation of surgical implants such as hip and knee joint implants, which normally occurs after 10−15 years of use (Spector, 1992). Another problem associated with metallic implants is that they are typically artificial materials and have biological inertness. Bioinert materials are incapable of inducing positive connective osteogenesis or new bone ingrowth; thus only low fixation strength can be achieved between the implant and the host bone (Wang and Zreiqat, 2010). Metallic surfaces are not suitable for endothelial cell coverage and they generally induce the adhesion of platelets that stimulate the proliferation of smooth muscle cells and lead to restenosis (Derkaoui et al., 2012). To address these limitations, new alloy designs and tremendous surface modification techniques have been researched and even commercialized (Hanawa, 2012). Table 1.1 summarizes the essential requirements for metallic biomaterials.

1.2 Surface characteristics of metallic biomaterials

One fundamental principle of cellular biology consists of "what a cell touches has a major role in determining what a cell does" (Getzenberg et al., 1990). Since the first cell−surface interactions occur at the interface, the control of the physicochemical and biochemical properties of a metallic biomaterial is one of the most important criteria in the design of biomedical devices. Depending on a specific application, a suitable surface modification method may result in an increase or reduction of protein adsorption, alteration of surface thrombogenicity, control of cell adhesion, growth and differentiation, modulation of fibrous encapsulation, etc. Surface characteristics of metallic biomaterials are highly influenced by production treatments such as grit blasting, chemical treatments, acid and alkaline attacks, electrochemical and biochemical treatments, etc. (Bagno and Di Bello, 2004).

Table 1.1 Essential requirements of metals for biomedical applications

Property	Application	Effect
Elongation to fracture	Spinal fixation; maxillofacial plate	Improvement of durability
Elastic modulus	Bone fixation; spinal fixation	Prevention of bone resorption and loosening of the implant by stress shielding
Superelasticity; shape memory effect	Multipurpose	Improvement of mechanical compatibility
Fatigue strength	Artificial hip joint; prosthetic heart valve	Improvement of durability and life span
Corrosion resistance	All implant devices excluding intrauterine device (IUD)	Improvement of durability and host tissue response
Wear resistance	Artificial hip joint; knee prostheses	Prevention of generation of wear debris; improvement of durability
Biodegradability	Stent; artificial bone; bone fixation	Elimination of materials after healing; no need for retrieval surgery
Bone formation; bone bonding	Stem and cup of artificial hip joint; dental implant	Fixation of devices in bone
Prevention of bone formation	Bone screw; bone nail	Prevention of assimilation
Adhesion of soft tissue	Dental implant; trans skin device; external fixation; protective cases in pacemakers	Fixation in soft tissue; prevention of inflectional disease
Inhibition of platelet adhesion	Blood-contacting devices	Antithrombotic properties
Inhibition of biofilm formation	All implant devices; treatment tools and apparatus	Prevention of infectious disease
Low magnetic susceptibility	All implant devices; treatment tools and apparatus	No artifact in magnetic resonance imaging

Adapted from Hanawa (2012).

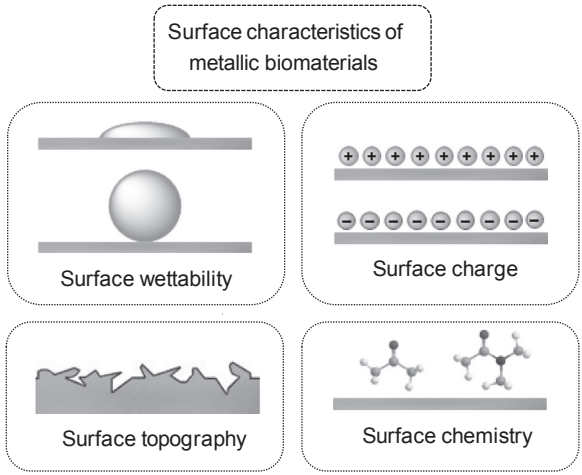


Figure 1.1 The variety of surface characteristics that influence the biological response to an implanted material.

In hard-tissue engineering, it is believed that surface chemistry, topography, and mesoporosity of biomaterials account for the promotion of cell adhesion (Vitale-Brovarone et al., 2007) and hydroxyapatite nucleation (Kokubo et al., 2003; Tanahashi and Matsuda, 1997), whereas biomaterials' macrostructure is involved in scaffold vascularization process and bone growth (Ni et al., 2006). However, it must be noted that cellular response and bone formation are affected by a series of surface properties, not a single property alone. The role of a specific surface characteristic has to be investigated in the context of the other characteristics; otherwise misleading conclusions may be drawn. Figure 1.1 summarizes the key surface characteristics that affect tissue–biomaterials interactions.

1.2.1 Surface chemistry

Surface chemical composition is an important surface characteristic in the design of biomaterials because it determines which functional groups are available for interaction with the biomolecules. Depending on the type of species available and its exposure, the biomolecules may have different affinities for various surfaces (Schmidt et al., 2009). Modification of surface chemistry is the most direct way to influence protein adsorption and cell behavior. There is a more direct effect caused by the presence of well-known specific functional groups, peptide motifs, or proteins that are known to react with certain cell structures and consequently trigger specific behaviors. By tailoring the functional groups available at the material surface, the surface wettability, surface electrical charges, and free energy will also be altered. It is postulated that the material's surface chemistry could stimulate inflammation, the secretion of cytokines/fibrogenic factors, and development of a fibrous capsule. Differences in surface chemistry were shown to modulate

fibronectin expression in vitro (Chou et al., 1996). For instance, the blood compatibility of the surface of a vascular substitute (i.e., protein adsorption, platelet adhesion, thrombogenicity, and patency) can be controlled by the chemical properties of the surface (García, 2008).

The most straightforward approach to modify the surface chemistry of an implant is the application of coatings. The surface chemistry can also be regulated by the deposition of another material with a suitable adhesion onto the implant. Such coatings can be realized with organic or mineral layers. In titanium surfaces, the biological effects of surface chemistry are related mainly to the architecture of the titanium oxide (titania, TiO_2) layer (Sul et al., 2002c). The addition of ions such as calcium (Sul et al. 2002a), sulfur (Sul et al., 2002b), phosphorus (Sul et al., 2002b), or magnesium (Sul et al., 2009) to the native titanium oxide layer through electrochemical oxidation methods has been used extensively to modify the surface chemistry of the metallic implants. Because osseointegration is related directly to the dynamic thickening of the TiO_2 layer, implants with thick TiO_2 layers, such as anodized implants, exhibit a strong bone response in that they increase the bone mineral matrix precipitation on the implant surface (Dohan Ehrenfest et al., 2010).

1.2.2 Topography and surface roughness

The topography of the implant surface is a key factor affecting cellular morphology, self-orientation, proliferation, and differentiation and has a significant influence on cell−cell signaling of implant−adherent cell (Flemming et al., 1999). Topographical modification of biomaterial surfaces is aimed at creating three-dimensional features in the form of micropores and nanopores, gratings, columns, microgroove, dots, pits, and random surface roughness. The surface topography is typically characterized by a succession of peaks and valleys, which can be quantified using either two-dimensional profiles or three-dimensional parameters. All implant materials intended for bioactive applications must contain complex topographical features. This aspect is inspired by biological processes that occur naturally in bone remodeling. The resorption surface of old bone by osteoclasts provides a highly topographically complex surface into which the new bone matrix will be deposited and subsequently becomes interdigitated and interlocked (Davies, 2007).

Similarly, rough, textured, and porous surfaces could stimulate cell attachment and formation of ECM (Boyan et al., 1996). Substrates with more topographical features will expose more surface area for possible interaction with proteins. For example, surfaces with grooves or pores have greater surface area compared with smooth surfaces. Other surface features, such as machine marks introduced during processing, provide additional sites for protein interaction (Dee et al., 2002). Presence of surface roughness provides initial stabilization until bone can grow and attach to the implant surface to provide further improvement in implant bonding (Narayanan et al., 2008). On the contrary, very smooth materials (i.e., endothelium-mimicking surfaces) are typically used in blood-contact applications (Dee et al., 2002). Surface topography is such an important characteristic that one cannot expect bone bonding to occur to artificial

biomaterials (even in the case of calcium phosphate biomaterials) without any surface topographical features (Mendes et al., 2007). Nevertheless, nonbonding materials can be rendered bone bonding by modifying their surface topography (Davies, 2007). The role of a specific surface characteristic has to be investigated in the context of the other characteristics. For instance, Le Guéhennec et al. (2008) observed lower cell viability on a smooth titanium substrate than on plastics, although both substrates have similar hydrophilicity and roughness. This lower cell viability is ascribed to a different surface composition. The role of surface topography versus surface chemistry in controlling biological responses is still under debate. While chemical hypotheses have generally been adopted in the open literature to explain bone bonding, there are experimental evidences demonstrating that bonding is achieved by micro-mechanical interdigitation of the highly conserved extracellular interfacial matrix, known as cement line, with the highly topographically complex surface at the submicron level (Davies, 2007; Mendes et al., 2007, 2009)

Depending on the scale of irregularities of the material surface, surface roughness can be categorized into three main groups—macroroughness (100 μm−milimeters), microroughness (100 nm−100 μm), and nanoroughness (<100 nm)—each with its specific influence on cell response (Chang and Wang, 2011). The macroroughness scale is directly related to implant geometry, with threaded screw and macroporous surface treatments giving surface roughness of more than 10 μm. The microtopographic maximizes the interlocking between mineralized bone and the surface of the implant (Wennerberg et al., 1998). Surface profiles in the nanometer range play an important role in the adsorption of proteins, adhesion of osteoblastic cells, and thus the rate of osseointegration (Brett et al., 2004). To meet the requirements for an enhanced bone implant contact formation, various methods have been developed to create micro- and nano-featured surfaces. Some of these methods include blasting, acid-etching, anodization, and plasma-spraying (Bauer et al., 2013; Le Guéhennec et al., 2007).

The response of cells to microtopographic or nanotopographic features depends mainly on the type and size of the cell. For larger cells, such as osteoblasts and neurons, macroscopic descriptions of the surface roughness could be reasonable (Donoso et al., 2007). It has also been demonstrated that metal surfaces with low microscale to nanophase topography enhance adhesion of osteoblasts (Liu et al., 2010). Ward and Webster (2007) investigated the enhanced functions of osteoblasts on nanophase metals and indicated that more calcium and phosphorus deposition is observed on the surface of nanophase metals. Because more particle boundaries are present on the surface of nanophase compared to conventional metals, this may be an explanation for the measured increase in osteoblast adhesion. For smaller cells, such as human vein endothelial cells, surface roughness at nanometer scale ($\leq$100 nm) could enhance cell adhesion and growth (Chung et al., 2003). However, because proteins are entities smaller than cells, microscale topographic structures are too large and cannot be sensed by proteins. Thus, proteins can be stimulated by using smaller features, in this case, nanotopographic features are closer to the dimension scale of proteins and adjust better to their size (Planell et al., 2010).

Cells commonly show different shapes when cultured on substrates with different roughness and topographic features (Brunette, 1988). When cells are cultured on an anisotropic topography such as a groove, cells orientate themselves along the axis of the groove to find a more suitable place for their further development. This phenomenon is called "contact guidance" and has been only observed in vitro (Anselme et al., 2010). When the surface is polished in only one direction, the edges can give a clear orientation to the cells like moving guides (Eisenbarth et al., 1996). When the surface consists of an organized array of pillars, the cells are able to identify this organization and orient themselves in the orthogonal direction (Su et al., 2006). It was shown that osteoblast cells also react by changing their morphology to suit the environment that they grow in. Osteoblasts maintain a rounded shape without extensions when they are on a flat titanium surface, whereas the titanium nanotube array causes the cells to become elongated, showing an increased number of extensions and filopodia (Subramanian et al., 2012). However, despite the effect of surface anisotropic or isotropic features on cell shape and orientation, there is no considerable difference in bone bonding and osseointegration between these two features. Göransson and Wennerberg (2005), who considered isotropic and anisotropic implant titanium surfaces with similar roughness levels, reported that titanium implants prepared with isotropic and anisotropic surfaces of similar roughness integrate similarly to bone during the three months after implantation. Nevertheless, it is difficult to define the topographic features for implant surfaces prepared by classical processes, such as plasma spraying or sandblasting, that display rather isotropic surfaces (Anselme et al., 2010). Human mesenchymal stem cells (hMSCs) were shown to differentiate better on surfaces presenting slight disorder of 120-nm-diameter nanopits (displaced square placements) compared to a hexagonal, square, or even random placement (Anselme et al., 2010). Last but not least, cells may also sense the viscoelastic properties of substrata. Soft, flexible substrata may inhibit attachment and spreading, while stiff, solid surfaces may promote it (Pelham and Wang, 1997).

Indeed, altering the surface topography will concomitantly lead to the modification of the surface chemistry (Meyer et al., 2005). One possibility to overcome this difficulty is to process model materials, i.e., materials with homogenous composition (not alloyed), and use a process that does not apply too strong an amount of energy. The approaches based, for example, on nano- and micro-patterning are effectively very useful for understanding the mechanisms of cell response to topography, but they produce surface morphology and surface chemistry very different from what is observed on a real implant surface (Ponche et al., 2010). Another possibility to discriminate the relative influence of topography and chemistry is to cover the surface with a thin layer of another material to control the surface chemistry, but without changing the surface topography (at least at the micrometer scale) (Anselme and Bigerelle, 2006b).

The surface topography can be altered by creating porous structures throughout the bulk or only on the surface (e.g., porous coatings) of the metallic biomaterials. As a result, the porous implant material can be strongly bonded to bone by infiltrating the bone into the interconnected pores. The bone ingrowth into porous

surface can cause strong interlocking between the porous implant and the surrounding bone tissue, providing greater mechanical stability at this critical interface. The porous biomaterials also possess a low modulus of elasticity, which minimize or eliminate the stress shielding effect, preventing loosening of the implants (Geetha et al., 2009). The detailed studies made by several authors lead us to conclude that the size of the pores should be in the range of 200−500 μm for better osseointegration (Nouri et al., 2010).

1.2.3 Surface charge

Considering the role of electrostatic interactions in many biological events, the presence of surface charge at the solid−solution interface is one of the major metallic properties that modulate both protein adsorption and cell adhesion (Hamamoto et al., 1995; Krukowski et al., 1990). Positively charged surfaces promote cell adhesion, while negatively charged surfaces reduce it (Bongrand et al., 1982).

It is notable that the cell adhesion on negatively charged surfaces becomes low or negligible at low ionic strength, when the range of electrostatic force is long. On the other hand, cell adhesion is strong at high ionic strength when electrostatic repulsion becomes negligible and van der Waals attraction dominates (Trommler et al., 1985). In another study investigating the adsorption of albumin onto metal oxides, it was reported that on positively charged metal oxides, i.e., TiO_2, ZrO_2, and Al_2O_3, the adsorption was dependent on the surface charge density (Fukuzaki et al., 1996). The adsorption of albumin onto metal oxides showed an increasing trend from TiO_2 to ZrO_2 and finally to Al_2O_3. In general, proteins adsorb to positively charged surfaces and stimulate osteoblast attachment and spreading (Anselme, 2000). The OH^- groups on rough and higher surface energy titanium surfaces dissociate to give positive charges, favoring cell attachment and proliferation (Feng et al., 2003; Zeng et al., 2005). The adsorption was also demonstrated to have a high affinity character, with the negatively charged groups of the protein, mostly carboxyl groups, oriented toward the surfaces. Fragalà and Satriano also showed that the protein adsorption is dependent on both the surface and protein charges due to the mutual electrostatic interactions between them (Fragalà and Satriano, 2010).

It should be noted that Ag and Au are highly electropositive with respect to hydrogen in the electrochemical series. Ti is difficult to assess in terms of its position in the electrochemical series owing to its ability to be readily passivated. But other metals shown to adsorb similar low levels of albumin, for example Ni, are lower in the electrochemical series than Ag or Au. The relatively high levels of protein adsorption to Ag and Au could be related to their ability of binding readily to proteins in vivo and in vitro (Williams and Williams, 1989).

1.2.4 Surface energy and wettability

The surface of a material is a termination of an extended, three-dimensional structure and thus generally represents an increase in energy, i.e., the surface energy. On the

atomic scale, this energy is present as unterminated chemical bonds. Because the bonding energy of the surface molecule is less than the bonding energy associated with a bulk phase molecule, the chemical bonds will "dangle" into the space outside the solid material and will result in the surface atoms having higher energy than the atoms in the bulk. As a result, surface atoms will attempt to reduce free energy by rearranging and/or bonding to any available reactive molecules, such as air or water at a metal surface, to reach a more favorable energy state (Dee et al., 2002; Kasemo and Lausmaa, 1994; Paital and Dahotre, 2009). Therefore, the surface of a material usually has a different chemical composition than its bulk. Well-known examples are the presence of oxide layers on almost all metals and hydroxylated ceramic surfaces. If a surface is exposed to a new environment such as the tissue, it is likely to react again to further lower the energy of the system (Kasemo and Lausmaa, 1994).

The term surface energy is also closely linked with wettability. Whereas surface energy describes interactions with a range of materials, surface wettability (i.e., hydrophilicity and hydrophobicity) describes these interactions with liquid only. The wettability is the extent to which a solid surface is wetted by a liquid, usually expressed as wetting angle (Tyrkiel and Deardney, 1995). Since liquids (e.g., water) have a huge capacity for bonding, a material of high surface energy can enter into more interactions with liquids and consequently will be more hydrophilic. Hydrophilic surfaces such as glass, therefore, have high surface energies, whereas hydrophobic surfaces such as polytetrafluoroethylene or polystyrene have low surface energies. Indeed, the hydrophilicity or hydrophobicity of a material surface is a result of its surface energy, which in turn is associated with the distribution of electrical charges. Concurrently, the distribution of electrical charges is a consequence of the surface chemistry and crystallinity, and all these properties are affected by the surface topography (Planell et al., 2010).

Contact angle measurements are probably the most frequently used technique to measure the average wettability of a surface. A zero degree (0°) wetting angle corresponds to complete wetting, while angles higher than 70° or 80° correspond to poor wetting (Tyrkiel and Deardney, 1995). For titanium implant surfaces, contact angle measurements give values ranging from 0° (hydrophilic) to 140° (hydrophobic) (Le Guéhennec et al., 2007).

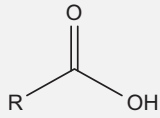
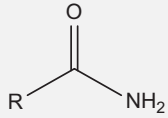
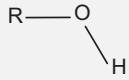
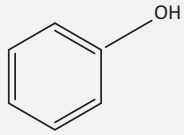
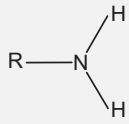
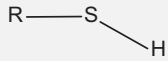
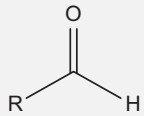
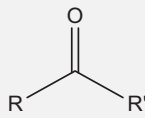
The wettability of a material's surface is vitally important for the adsorption of proteins and the cell adhesion. When an implant material is placed inside a human body, the wetting of the implant material is among the first and foremost plethora of events that take place by the physiological fluids. This further controls the adsorption of proteins, followed by attachment of cells to the implant surface. Hence, surface wettability is considered an important criterion that can dictate the biocompatibility of the implant material (Paital and Dahotre, 2009). The three most important factors that affect the wettability of a surface are its chemical composition, microstructural topography, and surface charge (Meiron et al., 2004). Many studies mentioned that different cell behaviors, related to different surface wettability, may be mediated by protein absorption, because surface wettability modified the type and the quantity of adsorbed cell adhesion molecules. Low energy (hydrophobic) surfaces tend to adsorb more proteins, while high energy (hydrophilic) surfaces tend to resist protein adsorption

(Dietschweiler, 2008; Latour, 2005; Silva-Bermudez and Rodil, 2013; Xu and Siedlecki, 2007). Apart from various hydrophilic biomaterials that have been shown to reduce platelet adhesion and thrombus formation (Dee et al., 2002), as compared to more hydrophobic biomaterials, it has also been reported that very highly hydrophobic surfaces suppress protein and platelet adsorption and thus ensure good blood compatibility (Lin et al., 1992; Sun et al., 2005).

The reason for high affinity of protein adsorption on hydrophobic surfaces is not well investigated, but is believed to be related to lower water heat of adsorption on hydrophobic surfaces and increased unfolding of adsorbed proteins, due to interactions between internal hydrophobic protein domains and the hydrophobic surface (Tengvall, 2003). These interactions lead to greater denaturation and increased internal protein entropy. In general, protein molecules change their conformations to a larger extent on hydrophobic surfaces than on hydrophilic surfaces. Proteins are generally structured with their hydrophobic residues buried within the core of the protein and their hydrophilic residues (charged and polar) lining the protein's solvent accessible surface. If the surface is hydrophobic, the protein will tend to adsorb by the various hydrophobic patches of residues present on the protein's amphiphilic surface, with the protein then tending to unfold and spread its hydrophobic core over the surface. This is due to the thermodynamic driving force acting to reduce the net hydrophobic surface area of the system exposed to the solvent. On the other hand, hydrophilic surfaces tend to interact with the charged and polar functional groups of the protein's surface, thus influencing adsorbed protein orientation, but with a lower tendency to cause the protein to unfold and spread over the surface (Dietschweiler, 2008; Latour, 2005).

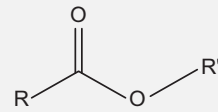
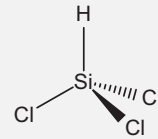
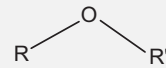
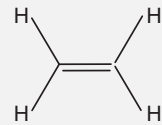
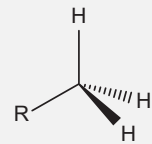
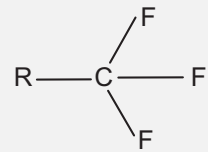
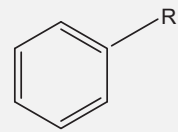
On the contrary, numerous studies have shown that a hydrophilic surface experiences a significant increase in cell attachment, spreading, proliferation, and differentiation (Altankov and Groth, 1994; Anselme, 2000; Chang and Wang, 2011; Eriksson et al., 2004; Protivínský et al., 2007). For example, in an investigation on the relationship between surface characteristics of titanium and initial interactions of titanium−osteoblasts, Feng et al. (2003), reported greater numbers of adhered osteoblasts and higher cell activity on the surfaces with higher surface energy (hydrophilic) and surfaces with more hydroxyl groups. It has also been confirmed in another study that the differentiation of osteoblasts is higher on hydrophilic substrates (OH^- and NH_2^- terminated self-assembled monolayers (SAMs)) than on hydrophobic substrates ($COOH^-$ and CH_3^- terminated SAMs) (Keselowsky et al., 2005). By using SAMs of alkanethiols on gold with different terminal functional groups (COOH, OH, and CH_3), Barbosa et al. (2006) observed thicker fibrous capsules formed around the implanted surfaces coated with CH_3^- terminated SAMs compared to $COOH^-$ and OH^- terminated SAMs. Some in vitro studies have compared osteoblastic cell adhesion and proliferation on different biomaterials with almost the same finish treatment. These studies revealed better results on the more hydrophilic materials with a higher protein adsorption (Hunter et al., 1995). Taking these studies into account, it can be concluded that osteoblast cells generally adhere to and proliferate better on moderate to highly hydrophilic substrates, and this probably explains the higher adsorption of proteins observed, such as fibronectin (Anselme et al., 2010). Table 1.2 summarizes different

Table 1.2 List of polar (hydrophilic) and nonpolar (hydrophobic) functional groups and their chemical structures

Name	Polarity	Chemical structure
Carboxylic acids	Strongly polar	
Amides	Strongly polar	
Hydroxyl (e.g., alcohol)	Strongly polar	
Phenols	Strongly polar	
Amines	Strongly polar	
Thiols	Polar	
Aldehydes	Polar	
Ketones	Polar	

Continued

Table 1.2 Continued

Name	Polarity	Chemical structure
Esters	Polar	
Trichlorosilanes	Polar	
Ethers	Polar	
Alkenes (e.g., ethylene)	Slightly polar	
Methyl	Nonpolar	
Trifluoromethyl	Nonpolar	
Aryl (e.g., phenyl)	Nonpolar	

The letter R represents an alkyl group.

polar and nonpolar functional groups used in the construction of hydrophobic and hydrophilic surfaces.

Osteoblast adhesion was reported to decrease when the contact angle of surface increased from 0° to 106°. Fibroblasts were found to have maximum adhesion when contact angles were between 60° and 80° (Tamada and Ikada, 1993; Wei et al., 2009). Nebe et al. (2007) compared the influence of roughness and surface energy of polymeric and metal surfaces on fibroblast adhesion and concluded that surface energy was more important than surface roughness in determining cell adhesion and proliferation. This finding suggests that the influence of roughness on cell adhesion strength may be secondary to the surface energy for high surface energy materials (i.e., metals).

At the nanoscale, the surface energy can be increased by a more textured surface topography. One of the methods to obtain a high surface energy in metallic biomaterials is the refinement of coarse grains into the nanometer scale. The resulting nanograined materials are materials in which the atoms are clustered to such a degree that each grain consists of only few atoms with the grain size in the nanometer scale when compared to the conventional materials that have grain sizes in the micron scale. It is worth noting that despite the fact that nanograined materials have lesser number of atoms in each grain, the number of atoms on the surface is very high, and hence it possesses a large surface energy (Geetha et al., 2009).

1.3 Types of metals used

The main considerations in selecting metals and alloys for biomedical applications are biocompatibility, appropriate mechanical properties, corrosion/wear resistance, and reasonable cost (Dee et al., 2002). Although pure metals are sometimes used, improved material properties such as strength and corrosion resistance can be provided by metal alloys. Metals generally find applications in the fabrication of implant devices such as hip joint prostheses, knee joint prostheses, dental implants, cardiovascular devices, surgical instruments, etc.

Major metals used in biomedical applications today include: stainless steels (primarily type 316L), cobalt-based alloys (primarily cast Co−Cr−Mo, wrought Co−Ni−Cr−Mo, and wrought Co−Cr−W−Ni), commercially pure titanium (cp Ti) and its alloys (largely the $\alpha + \beta$ alloys, Ti−6Al−4V and Ti−Al−Nb, and several newer β-Ti alloys), NiTi alloys, Au-based materials, and dental amalgam (Ag−Sn alloys).

1.3.1 Stainless steels

Stainless steel is the most frequently used biomaterial for internal fixation devices due to a favorable combination of mechanical properties, corrosion resistance, and cost effectiveness when compared to other metallic implant materials (Frosch and Stürmer, 2006). Stainless steels were the first metals to be used in orthopedics in 1926. However, it was not until 1943 that ASTM 304 was recommended as a standard

implant alloy material (Hallab et al., 2004). The "vanadium steel" was the first metal alloy developed specifically for human use as bone fracture plates (Sherman plates) and screws (Park and Kim, 2000). The first stainless steel used for implant fabrication was the 18−8 (type 302 in modern classification), which is stronger and more resistant to corrosion than the vanadium steel (Park and Kim, 2000). The introduction of 18−8 SMo stainless steel, which contains a small percentage of molybdenum, was a great improvement in the corrosion resistance of steels in chloride solution (salt water). This alloy became known as type 316 stainless steel. In the 1950s, a better corrosion resistance was achieved by reduction of the carbon content of 316 stainless steel from 0.08 to a maximum amount of 0.03 wt.%, and thus this alloy became known as type 316L stainless steel. However, due to potential corrosion of 316L stainless steel inside the body under certain circumstances (for example, in a highly stressed and oxygen-depleted region), surface modification methods, such as anodization, passivation, and glow-discharge nitrogen-implantation, are widely used to improve corrosion resistance, wear resistance, and fatigue strength of 316L stainless steel (Bordji et al., 1996).

The biocompatibility of stainless steel has been proven by successful human implantation for decades. Some strict metallurgical requirements have been laid down to ensure sufficient corrosion resistance, nonmagnetic response, and satisfactory mechanical properties in stainless steel implants (Disegi and Eschbach, 2000). In orthopedic surgery, stainless steel is mainly used when stiffness is the major requirement. The ductility of stainless steel is higher than that of cp Ti (with hexagonal crystal structure). This makes contouring of stainless steel plates easier, compared to titanium plates (Ganesh et al., 2005).

The main concern regarding the application of stainless steel bone plates for the internal fixation of fractured bones is the high stiffness of these plates, which results in excessive stress shielding of the bone (Frosch and Stürmer, 2006). The low tendency of stainless steel implants to return to their original shape after being deformed (low elasticity) can cause delayed callus formation and bone healing (Ganesh et al., 2005). It has also been reported that the high nickel content (10−14%) of stainless steel implants can cause allergic tissue reactions and dermatitis (Kanerva and Förström, 2001), which encouraged the development of new Ni−free austenitic stainless steels with excellent mechanical and technological properties (Disegi and Eschbach, 2000). Moreover, despite the appropriate mechanical properties of 316L, it lacks bioactivity, which prohibits bone bonding and, therefore, limits the lifetime of the implant (Adawy and Abdel-Fattah, 2013).

1.3.2 Cobalt−chromium alloys

Cobalt−chromium (Co−Cr) alloys are one of the commonly used metals in biomedicine and have superior wear resistance with respect to stainless steel and titanium (Jagielski et al., 2006; Marti, 2000). This class of alloys has been extensively used in dentistry and maxillofacial surgery as (1) partial dentures, (2) dental implants, and (3) maxillofacial implants. This class of alloys also has applications in orthopedics surgery such as (1) fracture fixation plates and screws, and (2) hip and knee prostheses

(Mani et al., 2009). Despite a lower biocompatibility than cp Ti, Co−Cr-based alloys have advantages in joint arthroplasty, with a lower rate of aseptic loosening. It has also been shown that Ti6Al4V has a lower mechanical resistance and a higher production of wear debris compared to Co-based femoral components in knee arthroplasty (Peterson et al., 1988).

There are fundamentally two types of Co−Cr alloys: (1) the castable Co−Cr−Mo alloy and (2) the Co−Ni−Cr−Mo alloy, which is usually wrought by (hot) forging. The castable Co−Cr−Mo alloy has been used for many decades in dentistry and, relatively recently, in making artificial joints. The wrought Co−Ni−Cr−Mo alloy is used for making the stems of prostheses for heavily loaded joints, such as the knee and hip (Park and Kim, 2000). The ASTM lists four types of Co−Cr alloys that are recommended for surgical implant applications: (1) cast Co−Cr−Mo alloy (F75), (2) wrought Co−Cr−W−Ni alloy (F90), (3) wrought Co−Ni−Cr−Mo alloy (F562), and (4) wrought Co−Ni−Cr−Mo−W−Fe alloy (F563). Currently, only F75 and F562 alloys are used extensively in implant fabrications. The superior fatigue and ultimate tensile strength of the wrought Co−Ni−Cr−Mo alloy make it suitable for the applications that require long service life without fracture or stress fatigue, such as the stems of the hip joint prostheses (Park and Kim, 2000). The molybdenum is added to produce finer grains, which results in higher strengths after casting or forging. The chromium addition enhances corrosion resistance and solid solution strengthening of the alloy.

For the stainless steel or Co−Cr alloys, in which the corrosion resistance is mainly provided by the Cr_2O_3 surface layer, the presence of chromium represents a source of concern because the release of Cr ions can be triggered by chemical dissolution, which is enhanced in protein-containing media (Kocijan et al., 2012; Lundin et al., 2012) or wear processes. In general, Cr (III) ions are not toxic; nevertheless, a high concentration of Cr (VI) ions in the human body bears a carcinogenic risk (Silva-Bermudez and Rodil, 2013). In vitro studies have indicated that particulate Co is toxic to human osteoblast-like cell lines and inhibits synthesis of type-I collagen, osteocalcin, and alkaline phosphatase in the culture medium. However, particulate Cr and Co−Cr alloy are well tolerated by cell lines with no significant toxicity (Granchi et al., 1996; Park and Kim, 2000).

1.3.3 Titanium and its alloys

Titanium and its alloys are among the most biocompatible metallic materials. They possess outstanding mechanical properties, excellent corrosion resistance, and low density (4.5 g/cm^3), which provide them with very high strength-to-weight ratio. Moreover, their Young's modulus is about one-half that of stainless steel and Co−Cr alloys. In view of these properties, Ti and its alloys are promising candidates for orthopedic and dental applications.

Titanium is an allotropic material, which exists as a hexagonal close-packed structure (hcp, α-Ti) up to 882 °C and body-centered cubic structure (bcc, β-Ti) above that temperature. Since its introduction for bone plates and screws in 1965, commercially pure titanium (cp Ti) has found an increasing application as an implant material in

medicine. Cp Ti is, in fact, a Ti alloy with up to 0.5% oxygen. It possesses high corrosion resistance, an outstanding biocompatibility, and does not cause allergic reactions (Pohler, 2000). One reason for these advantages may be a protective oxide layer that spontaneously forms on the surface of implants in the presence of oxygen. The excellent chemical inertness, corrosion resistance, repassivation ability, and even biocompatibility of titanium and most other titanium alloys are thought to result from the chemical stability and structure of the titanium oxide film that is typically only a few nanometers thick. The amorphous or nanocrystalline oxide film is typically 3−7 nm thick and mainly composed of the stable oxide TiO_2 (Liu et al., 2004). Slight color shifts can occur spontaneously forms on after multiple sterilization; however, they do not have any adverse effects (Pohler, 2000). Cp Ti has various degrees of purity (graded from 1 to 4). This purity is characterized by oxygen, carbon, and iron content. Most dental implants are made from grade 4 cp Ti, because it is stronger than other grades (Le Guéhennec et al., 2007). Increasing amounts of trace elements elevate tensile strength, but reduce ductility of cp Ti (Frosch and Stürmer, 2006).

The mechanical properties of Ti alloys can be tailored over a wide range through compositional variations and thermomechanical processing techniques. The addition of alloying elements to Ti enables it to have a broad range of types, including α-type, α + β-type, and β-type alloys, according to the quantities and types of their alloying elements (Park and Kim, 2000). The α-type alloy has a single-phase microstructure that possesses good weldability. As a single-phase alloy, the α-type alloys cannot be heat-treated for precipitation hardening. The controlled addition of β-stabilizers lowers the transformation temperature. The precipitates of β-phase will appear by heat treatment in the solid solution temperature and subsequent quenching, followed by aging at a relatively lower temperature.

Ti−6Al−4V ELI (extra low interstitial), a typical α + β-type alloy, is the most commonly used Ti alloy in orthopedic applications due to a good combination of mechanical properties and corrosion resistance (Hanawa, 2012; Williams, 2001). However, the release of potentially toxic ions from aluminum (Al) and vanadium (V) during in vivo corrosion of the implant remains a matter of concern. Over the last two decades, researchers working on Ti alloys have discovered new Ti alloys for orthopedic and dental applications. The goal has been focused on fabricating Ti based alloys that have: (1) little or no toxic elements in their composition; (2) a low elastic modulus close to that of cortical bone; (3) a high strength and long fatigue life; and (4) a large room-temperature plasticity so that it can be readily formed. Some of the Ti alloys developed over the last decades for biomedical applications are Ti−Al−Nb and Ti−Al−Nb−Ta (Sasaki et al., l996; Semlitsch et al., 1992), Ti−Nb−Ta−Zr (Niinomi et al., 2004), Ti−Zr−Nb (Yu et al., 2001), Ti−Sn−Nb (Nouri et al., 2008, 2011), and Ti−Ni−Ta (Lekston and Goryczka, 2007).

The wear resistance of Ti and its alloy is relatively low. Ion implantation of Ti (like other metallic materials) can harden the surface and reduce the friction coefficient, ultimately improving the wear resistance (Cui and Luo, 1999). The ductility of titanium is low compared to that of stainless steel, because of its crystal structure. This makes contouring of titanium plates difficult, compared to stainless steel plates (Ganesh et al., 2005). Similarly, Ti and its alloy are not suitable for bone fixation

wires and sternal wires that require ligatures, because of insufficient ductility for wrapping and twisting the wire (Frosch and Stürmer, 2006; Hanawa, 2012). Ti has poor shear strength, making it less desirable for bone screws, plates, and similar applications. It also tends to gall or seize when in sliding contact with itself or another metal (Park and Kim, 2000). In cardiovascular applications, the advantages of Ti lie in its strength, inertness, and nonmagnetic property (Liu et al., 2004). Nevertheless, artificial hearts made entirely of Ti have not been very successful clinically, mainly due to problems with blood-clotting occurring on the device surface (Rintoul et al., 1993). Stainless steels, NiTi, and Co−Cr alloys, as well as Ta, are, in fact, more often used in cardiovascular applications (Hanawa, 2009).

1.3.4 Shape memory and superelastic alloys

Nickel−titanium (NiTi) is the unique class of materials known as shape memory alloys. This alloy is a stoichiometric compound of Ti and Ni and exhibits distinctive mechanical properties, such as shape memory effect, superelasticity, and high damping properties. NiTi shape memory alloy with 55 wt.% of Ni and 45 wt.% of Ti is often called Nitinol (Liu et al., 2004). The equiatomic intermetallic compound NiTi exhibits the shape memory effect that allows for the spontaneous recovery of shape after being subjected to macroscopic deformation higher than its elastic limit. Shape recovery occurs after the deformed material snaps back to its previous shape following heating of the material (Park and Kim, 2000). Another unusual property of this class of materials is the superelasticity. In contrast to other metals such as stainless steel, the stress in these alloys does not increase with increased strain after the initial elastic stress region, and on release of the stress or strain, the metal springs back to its original shape. The superelasticity of Nitinol is used in orthodontic archwires because it allows the archwires to exert a constant force or moment on a large range of deactivation. The low stiffness of NiTi is also preferred over the conventional stainless steel wires that are too stiff and harsh for the tooth. In addition, the shape memory effect can also be used.

Owing to its unique properties NiTi alloy finds wide applications in industry and medicine. Their medical applications include orthodontic archwires for dental, endodontic reamers and files, intravascular stents, catheter guide wire, bone fracture fixtures, staples for healing small bone fractures, etc. (Duerig et al., 1990; Hanawa, 2012). Stents of NiTi alloys must be carefully designed to avoid fractures during service. In particular, during expansion, unexpectedly high local deformation may generate fractures. The fatigue and fracture mechanisms of the superelastic NiTi alloy have only been partly elucidated (Gall et al., 2008; Robertson and Ritchie, 2008). Due to some reported allergic reactions to Ni, the use of NiTi alloy with about 50 mol% Ni in medicine is limited by safety. Therefore, there is a great demand for Ni-free shape memory and superelastic alloys to solve such problems. Ti−Nb−Sn (Takahashi et al., 2002), Ti−Nb−Al (Hosoda et al., 2003), Ti−Mo−Sn/Ag (Maeshima and Nishida, 2004), and Ti−Nb−Zr (Kim et al., 2005b) alloy systems exhibit shape-memory effect and superelasticity, while the recovery strain and superelastic deformation stress of these alloys are still lower than those of the NiTi alloy.

1.3.5 Dental metals

The early failure of Maggiolo's design to implant gold tooth roots into fresh extraction sockets in 1809 encouraged researchers to further investigate and use various metals to replace missing teeth (Alla et al., 2011). In the late 1800s, various researchers unsuccessfully attempted to use different metals, including platinum posts coated with lead, gold, or iridium tubes, silver capsules, etc. (Anusavice, 2006). However, it was not until the late 1930s when Venable created a new alloy composition, Vitallium (Co−Cr−Mo alloy), that became the first long-term successful implant material (Anusavice, 2006).

Dental metals are mostly used as dental amalgams for direct fillings in teeth. Dental amalgam is an alloy made of liquid mercury and other solid metal particulate alloys consisting of silver, tin, copper, etc. The solid alloy is mixed with (liquid) mercury in a mechanical vibrating mixer, and the resulting material is packed into the prepared cavity (Park and Kim, 2000). Noble metals such as gold and platinum have their application in fabricating crowns and bridges. Gold and gold alloys are useful metals in dentistry as a result of their durability, stability, and corrosion resistance (Nielsen, 1986). The noble metal alloy compositions are primarily gold (Au)- or platinum (Pd)-based, with alloying additions of nonnoble (base) metals such as Ag, Cu, Pt, Zn, and some other trace elements (Pilliar, 2009). Softer alloys containing more than 83% gold are used for inlays, which are not subjected to much stress. Harder alloys containing less gold are chosen for crowns and cusps, which are more heavily stressed. Copper, alloyed with gold, significantly increases its strength. Platinum also improves the strength, but no more than about 4% can be added or the melting point of the alloy will be elevated excessively. Silver compensates for the color of copper. A small amount of zinc may be added to lower the melting point and to scavenge oxides formed during melting (Park and Kim, 2000). Base metal alloys have been used in partial denture frameworks. While cp Ti and Ti−6Al−4V have been mostly used for fabricating dental implants, wrought stainless steel, Co−Cr−Ni (Elgiloy), β-Ti, and Nitinol alloys are used for making orthodontic wires in which high yield strength and preferably low elastic modulus provide high "working range" characteristics. The requirement of low elastic modulus favors the selection of β-Ti and NiTi alloys for orthodontic wires, although all four alloys are currently used (Pilliar, 2009).

As in the orthopedic applications, the major advantage of metals for the dental applications is their acceptable biocompatibility, sufficient strength, toughness, and wear and corrosion resistance. Dental implant materials with requirements very similar to materials used for orthopedic applications are usually made from commercially pure titanium or titanium alloys (Pilliar, 2009).

1.3.6 Other metals

Magnesium (Mg): Metallic biomaterials are stiff and are permanent by nature. For instance, in load-bearing orthopedic applications, their high modulus of elasticity (as compared to bone) leads to the implant retaining a large fraction of the mechanical

load applied to the bone. This phenomenon is commonly known as "stress shielding," which results in bone resorption, implant loosening, and, consequently, the need for future revision surgery. Metallic biomaterials also interfere with radiologic imaging of the underlying skeleton. In view of these problems, bioabsorbable implants play a promising role because they will degrade over time and gradually allow the bone and soft tissue to carry an increasing load (Maurus and Kaeding, 2004). Currently, there are two candidates for bioabsorbable metallic materials: magnesium alloy (Heublein et al., 2003; Li and Zheng, 2013; Wu et al., 2013) and pure iron (Peuster et al., 2001).

Mg alloys are essential to human metabolism (Saris et al., 2000) and have outstanding advantages, including biocompatibility and the possibility to eliminate the need of a second operation for implant removal, thereby minimizing trauma to the patients and decreasing medical costs (Yang et al., 2010). The tensile strength, yield strength, modulus of elasticity ($E = 41-45$ GPa), and density of Mg alloy present structural properties very similar to human bone tissue ($E = 3-20$ GPa) exhibit better mechanical properties than other metals (Wu et al., 2013; Yang et al., 2010). Nevertheless, due to the extreme activity of Mg, control of the corrosion rate for safe use in the human body is a key factor in the use of Mg for medical devices. To this end, surface modification and alloying are necessary to control the corrosion rate of Mg implant materials.

Platinum group metals (PGM) are found as a compound that includes six pure metals with high melting points, comprising platinum (Pt), palladium (Pd), rhodium (Rh), iridium (Ir), ruthenium (Ru), and osmium (Os). These metals have the ability to stay stable at high temperatures and are extremely resistant to corrosion. Due to their high corrosion resistance and low threshold potentials for electrical conductivity, they are mainly used as alloys for electrodes such as pacemaker tips, implantable defibrillators, catheters, stents, and neuromodulation devices (Cowley and Woodward, 2011; Park and Kim, 2000). Electrodes used for neuromodulation stimulation (including "brain pacemakers" used, for example, to treat Parkinson's disease and cochlear implants to restore hearing) should be made of materials that are corrosion resistant under extreme voltage potential and charge transfer conditions. The PGM metals and alloys such as Pt and Pt−Ir satisfy these conditions and are the principle materials used for making electrodes for electrical stimulation and sensing purposes. The Pt−Ir alloys (10−30 wt.% Ir) also offer the advantage of higher mechanical properties (scratch resistance) compared with unalloyed Pt because of solid solution strengthening (Pilliar, 2009).

Silver: Silver salts, silver complexes, and the metal itself have played an important part in the development of medicine. Metallic silver is used in a number of surgical applications, both for structural devices (e.g., cranial support plates, suture wire, aneurysm clips, and tracheostomy tubes) and for prostheses (e.g., silicon−silver penile implants). Silver can prevent the growth of microorganisms responsible for disease (Grashoff and King, 1990). The antimicrobial properties of silver are used in the form of silver salts and complexes that break down to release silver ions (Ag^+) (Davis, 2003). Silver is also one of the metals that displays high levels of protein adsorption, as opposed to titanium and tantalum with lower affinities for proteins (Williams and Williams, 1989).

Tantalum has been studied for biomedical applications and has shown suitable biocompatibility and osteoconductivity (Matsuno et al., 2001). However, its high modulus of elasticity and high density (16.68 g/cm^3) has restricted the biomedical use of tantalum to few applications, such as wire sutures for plastic surgeons and neurosurgeons and a radioisotope for bladder tumors. Furthermore, the extremely high melting temperature of tantalum (3020 °C) and its high affinity for oxygen make it difficult to process tantalum structures via conventional processing methods. Despite these drawbacks, tantalum implants have been used successfully in general surgery and neurosurgery as monofilament and braided suture wires for skin closure, tendon, and nerve repair; as foils and sheets for nerve anastomoses; as clips for the ligation of vessels; as staples for abdominal surgery; and as pliable sheets and plates for cranioplasty and reconstructive surgery (Davis, 2003). The fabrication of porous structures made of tantalum not only decreases the apparent density of tantalum, but also reduces its high modulus of elasticity in a proper range similar to that of human bone (3−20 GPa), which leads to the reduction of stress shielding (Yang et al., 2013).

Zirconium alloys: Zirconium (Zr) belongs to group four in the periodic table of elements, with titanium, hafnium (Hf), and rutherfordium (Rf). Zirconium has chemical properties similar to its known family member titanium, including its high affinity for oxygen. Zirconium is very resistant to corrosive attacks in most mineral and organic acids, strong alkalis, and saline solutions. Zirconium has largely found its application in biomaterials as an alloying additive in titanium alloys. As a pure element or as an alloy, Zr is known as an excellent bioactive metallic biomaterial because it can form a bone-like apatite layer on its surfaces in the living body (Chen et al., 2008; Sista et al., 2013). A zirconium alloy knee implant with a hard ceramic (zirconia) surface has also been developed (Davis, 2003).

1.4 Biological interactions on the surface of metallic biomaterials

A criterion for the suitability of a biomaterial in a physiological environment is the physicochemical reactivity of the surface. Once the biomaterial is implanted in vivo, it comes in direct contact with body fluid. Body fluid is a corrosive aqueous medium containing different types of ions and molecules, such as proteins, polysaccharides, and enzymes, as well as different types of cells (Planell et al., 2010). On implantation, the initial dynamic events that take place on the biomaterial surface will strongly affect the lifespan of the implant. As mentioned earlier, the surface properties of the metallic biomaterials have significant influence over the initial events occurring at the biomaterial's surface.

The tissue−biomaterial interaction events occurring at different time and dimension scales are shown in Figure 1.2. When a biomaterial is implanted into the body, the first molecules to reach its surface are water molecules. The water interaction and binding on surfaces are influenced by the surface characteristics, subsequently influencing the proteins and other molecules that arrive later (Kasemo, 2002). The formation of water

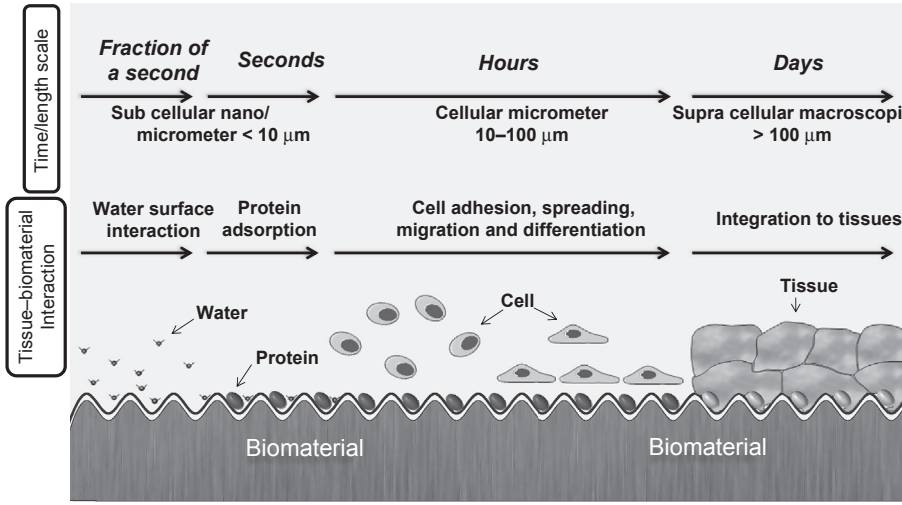


Figure 1.2 Tissue−biomaterial interactions: illustration of events occurring at the interface between biological systems and biomaterial surface at varying time and length scale.

coating layer on the surface of the material occurs within a period of nanoseconds. Depending on the anatomical location of the implanted biomaterial, the implants are surrounded by different types of tissues. In the case of artificial joints, bone fixation devices, and dental implants, the surface of the material attaches to both hard and soft tissues. Orthodontic wires, crowns, and bridges are used in oral cavities where their environments vary drastically. Stents, clips, and artificial hearts for circulatory diseases are exposed to blood and soft tissue (Hiromoto, 2008).

The biological reactions are characterized by two components, the response of the host to the implant and the implant behavior in the host. The host response to implants involves a series of cell and substrate reactions and is influenced by a wide range of factors, including anatomical location, shape and size of implant, surgical procedure, modality and direction of loading, biological fluids, age and gender, and in particular, surface characteristics. The host response to implants is essentially an inflammatory response that continues as long as there is a foreign body present to which to respond. An inflammatory reaction involves the migration of neutrophils and monocytes/macrophages to the injury site by chemotaxis of different cytokines to phagocytose cellular debris and all the material perceived as foreign. Neutrophils disappear after finishing their task, and macrophages predominate after the initial period. A macrophagic response is typical of a chronic inflammatory reaction and is common for most implants (Planell et al., 2010). The sustained presence of macrophages leads to formation of multinucleated giant cells or foreign body giant cells to overcome the frustrated process of phagocytosis process experienced by single cells (Dee et al., 2002). At this stage, macrophages give place to fibroblasts as the main cell line. Concurrently, fibroblasts begin secreting a collagen I and III-based extracellular matrix (ECM) that will encapsulate the material. The thickness of this ECM, known as a fibrous capsule,

will vary depending on the movement of the implanted device and serve to isolate the material from host tissue (Planell et al., 2010). For a long time, this encapsulation by fibrous connective tissue, which was found even around clinically successful orthopedic and dental skeletal implants, was considered the only possible interface between living bone tissue and a foreign material (Plenk, 1998). In the case of implantable devices, these adverse responses, including the fibrous encapsulation, bacterial adhesion, and inflammation, can be traced back to the initial biointerfacial interactions.

1.4.1 Protein adsorption on the surface of metallic biomaterials

The interaction of the biomaterial surface with macromolecules found in the physiological medium such as proteins is the second stage of the implant reaction and occurs after hydration. This usually takes seconds up to hours after implantation (Figure 1.2). In the aqueous medium containing both proteins and cells, the smaller protein molecules (of which the number/concentration is usually higher than that of the cells) cover the implant surface before the cells arrive. Hence, as a rule, the cells adhere onto an adsorbed proteinaceous layer (Norde, 2006). These proteins first come from blood and tissue fluids at the wound site and later from cellular activity in the periprosthetic region (Puleo and Nanci, 1999). With sufficient passing of time, molecules with greater affinity for the surface arrive, but with a slower rate (because of lower concentration and/or larger size) of approach. The surface, however, may already be covered by a monolayer of protein. In this case, the only way for new molecules to bind to the surface is if previously adsorbed molecules detach (Dee et al., 2002). As bonds between the adsorbed molecule and the surface are periodically broken, new protein molecules can occupy the binding sites. The first molecule is detached from the surface when all of its contacts with the substrate become occupied by the new molecule. Exchange proceeds until the surface is populated by proteins with strong interaction with the substrate. This hierarchical series of collision, adsorption, and exchange processes has been termed “the Vroman effect” (Dee et al., 2002; Planell et al., 2010). This process is schematically illustrated in Figure 1.3.

Finally, cellular contact and interaction with the adsorbed proteins on the surface of the implant is the third stage, which usually takes from minutes up to days. The adsorbed proteins act as a translator between the surface properties of the material and the cell receptors, determining the fate of the implant in the biological environment (Carré and Lacarriere, 2010; Parhi et al., 2010). This third stage is highly influenced by complex interactions among the ECM proteins, cell membrane proteins, and cytoskeleton proteins, surface chemistry and topography, the micro and macrostructure of the material (porosity, pore size and geometry, interconnectivity), and the potential degradation products of the material (Planell et al., 2010). The behavior of proteins at surfaces plays a vital role in determining the nature of the tissue−implant interface. Adsorbed proteins affect blood coagulation and complement activation and bacterial and cell adhesion.

There are several proteins in the human blood plasma. Albumin is a very well characterized globular transport protein and is widely used in protein adsorption studies due to its high abundance in plasma; it constitutes about 50% of the plasma

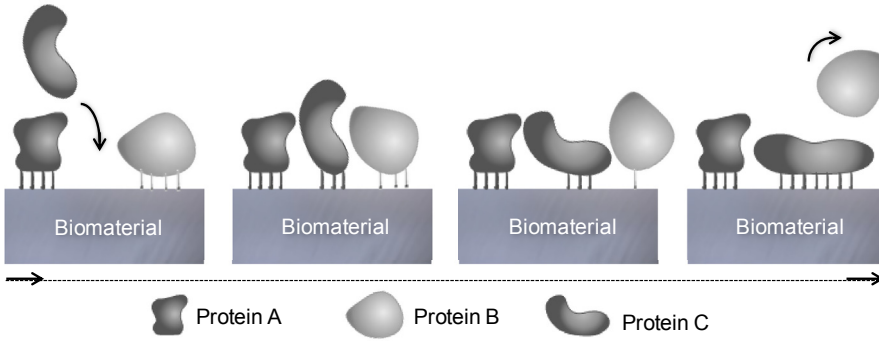


Figure 1.3 Schematic illustration of the Vroman effect. The various conformations of proteins that are adsorbed onto the biomaterial surface are denoted here as proteins A, B, and C. In the course of time, protein B is displaced from the surface and replaced by protein C through an exchange reaction. The latter protein C has higher affinity with surface sites, thus forms more stable bonds with the available biniding sites on the surface.

proteins and consequently is present for almost all kinds of implants (Carré and Lacarriere, 2010; Wilson et al., 2005). Whereas the adsorption of albumin is expected to inhibit cell adhesion, vitronectin or fibronectin are the ECM proteins responsible for cell adhesion (Geetha et al., 2009). The adhesive properties of such proteins lie in their arginine−glycine−aspartic acid (RGD) sequence, which is specific to the fixation of cell membrane receptors like integrins (fibronectin, osteopontin, bone sialoprotein, thrombospondin, type I collagen, and vitronectin) (Meyer and Wiesmann, 2006). Human osteoblasts were shown in in vitro studies to strongly adhere to RGD-containing proteins such as fibronectin (as compared with type I and type IV collagen) and vitronectin, but weakly to laminin and type V collagen. These RGD sequence-containing ECM proteins (vitronectin and fibronectin) can act as binding elements between artificial surfaces and skeletal cells, exerting strong effects on cell adhesion, matrix maturation, and mineralization (Rezania and Healy, 2000). Fibronectin is a key component of ECM proteins and promotes attachment of cells to the biomaterial surface through its central binding domain RGD sequence. For instance, fibronectin can rapidly bind to exposed titanium oxide surfaces in vitro. The presence of even low levels of this protein enhances cell binding (Narayanan et al., 2008). Recent developments in biocompatible surface coating technologies for adherent cells concentrate on fixing the ECM proteins like fibronectin and vitronectin or amino acid sequences of these proteins on the surface (Ohl and Schroder, 1999).

Fibrinogen is an ECM protein highly involved in the blood coagulation cascade and consequently in the blood compatibility processes, which in vitro has also been related to the promotion of cell adhesion. Adsorption of fibrinogen is expected to lead to fibrin formation enhancing the activation of the coagulation cascade and platelet adhesion (Sperling et al., 2009). Other common proteins are those related to the immune system such as the lysozyme and some globulins, for instance the

immunoglobulins. These proteins control the immune response toward a foreign material, directing the acceptance of the implant by the body or triggering immunological responses of rejection. Structural proteins such as collagen are also very relevant for the interaction between connective tissues and foreign surfaces (Wilson et al., 2005). Another group of essential proteins that are involved in a cell's capacity to adhere, spread, divide, and migrate are the myosins (Baker and Titus, 1998). They are actin-based motor proteins that translocate along actin fibers and allow their contraction.

The protein−surface interactions are dependent on several properties, including (Dee et al., 2002):

1. *Size*: Larger protein molecules are expected to have more sites of contact with the surface than a smaller one, which thus usually exhibit greater surface activity.
2. *Charge*: The charge and the distribution of charge on the protein surface can greatly influence the protein adsorption. Because proteins represent copolymers of different amino acids, most proteins carry acidic and basic groups and hydrophilic and hydrophobic moieties. Therefore they are both amphoteric and amphiphilic (Groth et al., 2010). Depending on the isoelectrical point of proteins, they may possess a positive or negative net charge at physiological conditions (Andrade and Hlady, 1986). Molecules near the isoelectric point are generally being adsorbed more readily to the surfaces. Charged amino acids are generally located on the outside of proteins and are potentially available to interact with surfaces.
3. *Unfolding rate*: Molecules that rapidly unfold can expose more sites (points) for protein−surface contact.
4. *Structure stability*: Molecules with less intramolecular crosslinking are considered to be less stable molecules. These molecules can unfold to a greater extent and form more contact points with the surfaces. Additionally, unfolding of proteins can expose hydrophobic regions (hydrophobic residues are generally located on the interior of the molecule) and allow interaction with the surface.

1.4.2 Cell adhesion and cell−surface interaction

After the interaction of the biomaterial surface with macromolecules (i.e., proteins), cell adhesion is the next stage occurring between the biomaterial and biological environment where the cells make contact with the adsorbed layer of ECM proteins on the surface of implant (see Figure 1.2). Apart from contact, cell adhesion also involves spreading of cells over the surface, followed by the subsequent differentiation and growth of cells. Once the proteins are adsorbed onto the implant surface, they act as the interface between the surface and the cells. As a result, cells interact indirectly with the biomaterial surface through the adsorbed layer of ECM proteins (not to the native surface). Binding is mediated by the cell cytoplasm, in particular, through cell structures known as lamellipodia or pseudopodia depending on the cell type (Anselme, 2000). These lamellipodia possess smaller extensions that are also formed by actin filaments. These are very thin and long structures that sense the ECM and material surface. Fillopodia are actuators of the adhesion, spreading, and motility processes. Integrins located within these long and thin cytoplasm extensions interact with the substrate surface, creating focal contacts that are points at which several integrin receptors meet to form stronger adhesion points. Depending on the surface conditions,

the fillopodia will receive more or fewer signals, allowing the cell to attach or separate from the surface, to move in one direction or another, to adopt a very spread out or rounded morphology, etc. (Beningo et al., 2001; Margel et al., 1993).

In addition to their major role as anchoring molecules, integrins are also involved in important cellular processes such as tissue organization, cell migration during embryogenesis, cellular differentiation, and immune and inflammatory responses (Albelda and Buck, 1990; Ruoslahti and Pierschbacher, 1987). The type of cells closest to the surface and their activities will change with time. For example, depending on the type of initial interaction, the final results may be fibrous capsule formation or tissue integration (Park and Kim, 2000). Murphy-Ulrich (2001) distinguished three adhesion stages: the weak adhesion involving attachment of cells because of the integrin-ligand bindings; the intermediate adhesion when cell spreading occurs; and the strong adhesion when the formation of focal adhesions and stress fibers is achieved.

On the interactions between osteoblasts and biomaterials for orthopedic implants, Wilson et al. (2005) concluded that cells respond most favorably to charged and hydrophilic surfaces, as a consequence of the large adsorption of cell adhesion-promoting proteins (fibronectin, vinculin, etc.) on these surfaces and the small degree of denaturation (better bioactivity) of the adsorbed proteins.

The kinetic aspects of cell adhesion were described by Bigerelle and Anselme using eukaryotic cells on surfaces (Bigerelle and Anselme, 2005). Findings demonstrated that cell adhesion is influenced by different phenomena and it was concluded that (1) in the early stages, the cell interaction is more related to the surface properties because the protein configuration on the surface is driven by the surface properties, and (2) the long-term cell adhesion is more related to the kinetics of the ECM formation and remodeling. Qualitatively, cell adhesion is evaluated by observing the cells adhering to the surface under a microscope. However, to develop new biomaterials with superior biocompatibility, it is absolutely necessary to quantitatively evaluate a material's affinity for cells. Because cells do not directly adhere to solid surfaces, but through cell adhesion proteins such as fibronectin and vitonectin, the adhesion force to a material is determined by the adsorption of proteins to the materials surface and the activity of the cell itself (Hanawa, 2004).

ECM is a complex structural entity surrounding and supporting cells and is commonly referred to as the noncellular component of tissues. The ECM is composed of three major classes of biomolecules: (1) structural fibrillar proteins (e.g., collagen and elastin); (2) an amorphous interfibrillar matrix composed mainly of proteoglycans; and (3) specialized proteins (e.g., fibrillin, fibronectin, and laminin). ECM proteins are generally specialized for a particular function (Lee and Laurencin, 2008). The composition of the ECM proteins can have profound effects directly on cellular behavior because many of these protein molecules are highly tissue and cell specific. These proteins provide attachment to cellular receptors, mainly integrins, and they cluster to form focal adhesions. The ECM proteins deliver signals important for survival, growth, and differentiation (Groth et al., 2010). Focal adhesions are closed junctions in which the distance between the substrate surface and the cell membrane is between 10 and 15 nm. All these biochemical and mechanical interactions allow signal transduction to the nucleus that either induces cell death through apoptosis

if the adhesion is not possible or cell growth and cell differentiation if cell adhesion and spreading can be achieved (Anselme et al., 2010). It has been found that the strength of adhesion controls the degree of cell spreading and hence the shape of cells on a substratum (Huang and Ingber, 1999). After adhesion and migration, cells divide and proliferate across the surface. They further differentiate and synthesize the molecules that they normally synthesize in their tissue of origin. For instance, osteoblasts will synthesize collagen and other proteins that are normally found in bone tissue (Meyer et al., 2005).

1.5 Overview of coating and modification

The main reason for coating and modification of metallic biomaterials is to modify biological response of the host tissue in the peri-implant region. Existing treatments of metallic implants involve alterations to the atoms, compounds, molecules, or textures on the material surface that can be divided into surface chemistry modification treatments or topographical treatments. It is worth noting that a commercial solution often uses a combination of the two to maximize cellular response. As a matter of fact, impacting topography of a metallic surface by physical methods inevitably leads to significant modification of the chemistry of surfaces.

The following sections give an overview of the principles and techniques used for the surface modification and coating of the metallic biomaterials. Although coating is generally classified as surface modification, it is plausible to separate coating methods from other physicochemical surface modification of metallic biomaterials. However, it is beyond the scope of this chapter to discuss all the surface modification and coating techniques in existence; thus, this section only attempts to discuss the most frequently used surface modification and coating techniques. Some of the most typical methods used for surface modification and coating of metallic biomaterials are schematically illustrated in Figure 1.4.

1.5.1 Surface modification of metallic biomaterials

Surface modification processes of metallic materials generally fall into two classes of physicochemical and biochemical treatments (Puleo and Nanci, 1999). The first class is mainly composed of treatments impacting morphology, like grit blasting, electro-erosion, plasma treatments, or smoothing; the chemical category includes acidic or alkaline treatments and electrochemical deposition. The biochemical treatments are related to conjugation of biological molecules to mimic biointerfaces (Ponche et al., 2010). However, many of these treatments are interconnected, and hence, it is almost impossible to control one aspect without affecting other characteristics of the material in use. For example, if these treatments are mainly devoted to the control of topography, a change in the surface chemistry cannot be avoided, and the wettability and contact angle measurements are strongly affected (Rupp et al., 2006).

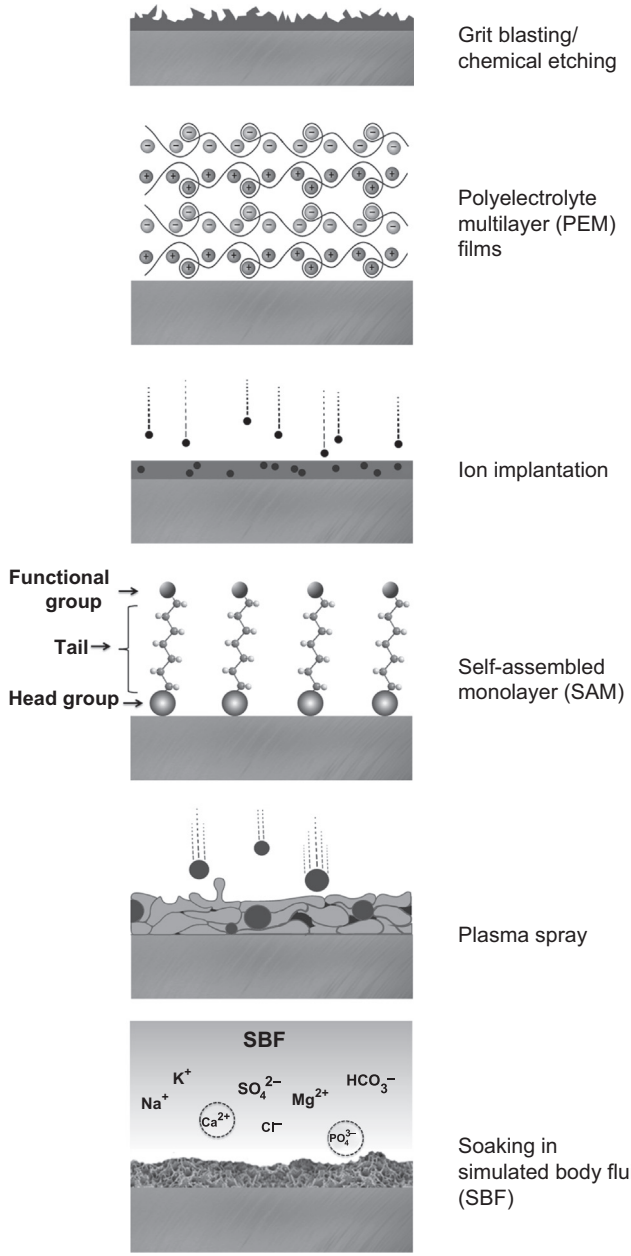


Figure 1.4 Schematic illustration of some of the typical methods used for surface modification and coating of metallic biomaterials.

1.5.1.1 Physicochemical surface modification

A variety of physicochemical surface modification strategies have emerged to (1) regulate cellular events and induce specific biological responses at a metallic surface; (2) improve the amount and stability of biomolecules; and (3) finally, obtain a desired tissue response (Kohn, 1998). Physicochemical surface modification techniques include surface coating (which will be discussed separately in the section that follows), machining, polishing, grit blasting, acid etching, alkali etching, anodization, vapor deposition, and surface self-assembly methods. Physical interactions related to these techniques are electrostatic interaction, van der Waals force, hydrogen bonding, hydrophobic interaction, etc. Physical techniques are simple methods that often do not require large and expensive equipment (Groth et al., 2007). In most of these techniques, the material's surface topography can be tailored by adding a new material that covers the implants (e.g., plasma treatment) or by removing material from the surface as in the case of grit-blasting, chemical etching, or electrochemical methods.

Among the numerous physicochemical surface treatments, the most frequently used techniques are as follows:

(i) *Grit blasting*: Grit blasting is a physical technique that leads to the formation of a porous layer on the implant surface through the collision with microscopic particles. For grit blasting, aluminum oxide (Al_2O_3), titanium dioxide (TiO_2), or calcium carbonate ($CaCO_3$) particles are projected by a fluid carrier (compressed air or liquid) onto the surface. Such erosion processes have an effect down to the micrometer scale, depending on the size of particles used for blasting, and give surfaces an average roughness index of less than 1 μm.

(ii) *Chemical etching:* Chemical etching acts on the dissolution of native oxide layer of metals. It can be carried out in acidic or alkaline conditions. Strong acids like HCl, HNO_3, H_2SO_4, H_3PO_4, and even HF are usually used for the chemical etching of titanium and its alloys. The combination of strong acids is also an effective way of creating a thin grid of nanopits on a titanium surface (diameter 20−100 nm) (Variola et al., 2011). As a consequence, acidic etching modifies the oxide surface by introducing Ti−OH acidic hydroxyl groups (doubly coordinated by titanium atoms). Alkaline treatment with NaOH increases the density and stabilizes the basic hydroxyl groups (singly coordinated to titanium atoms) at the surface of the metallic oxide owing to the high pH value (Ponche et al., 2010). Acid-etching processes are also known to dissolve alumina particles embedded in the layer after a grit-blasting process.

Apart from a chemical or electrochemical process, an etched surface can also be achieved, depending on the material, by exposing the surface to a reactive plasma in a chamber wherein a reactive plasma produces a reaction product with the surface, thereby etching the surface (Thull, 2010). Nevertheless, the major shortcoming of the sand/grit-blasting and chemical etching is that they are a random process, thus it is hard to control the uniformity and distribution of nanostructures on the implant surfaces (Subramanian et al., 2012).

(iii) *Electrochemical methods:* Electrochemical methods consist of immersing the implant in a solution of electrolytes (acids, ions, or oxidants) and connecting it to a pole of an electrical circuit. The electrochemical methods can be split into three

experimental techniques including anodization, electropolishing, and electroerosion. *Anodization* (also referred to as anodic oxidation) is a powerful technique that can produce surfaces with improved oxide layer or increased oxide thickness of up to micron size, compared to 3−4 nm of the native oxide layer. The anodization treatment renders the material to form topographically complex surfaces at the submicron level, creates porous coatings, and/or leads to enhanced corrosion protection and decreased ion release (due to increased oxide thickness). It has been shown that the nanosized texture produced by anodization technique provides an efficient means to enhance attachment and proliferation of osteoblast cells (Bayram et al., 2014; Sista et al., 2013). Voltage and direct current (galvanic current) are used to thicken the oxide layer throughout the implant surface. The titanium substrates serves as the anode in the process, while an inert platinum sheet provides the cathode (Bressan et al., 2013). The structural and chemical properties of anodic oxides on titanium can be varied significantly by controlling the process variables, such as anode potential, electrolyte composition, temperature, and current. Different diluted acids (H_2SO_4, H_3PO_4, acetic acid, and others) are commonly used electrolytes for anodic oxidation of titanium (Lausmaa, 2001).

Electropolishing is a widely used industrial method for surface finishing of metal components. The process essentially acts as a controlled electrochemical dissolution of the amorphous native oxide to give a polycrystalline metallic surface. On this basis, the new oxide layer is devoid of defects, dense, and exhibits a reduced roughness. For titanium, depending on the exact process parameters, the rate of material removal (dimensional change) will be in the range of 1−10 μm per minute (Lausmaa, 2001). For the *electro-erosion* process, the vicinity of a Cu−Zn wire from the surface initiates a plasma zone, which locally melts the surface of the titanium implants and grows a TiO_2 layer. Bigerelle et al. (2002) reported that the main influential characteristics of the electro-eroded surfaces may be their isotropic and smooth aspects of the relief as a result of surface fusion during the process. Contaminations with copper and zinc can also occur (Anselme and Bigerelle, 2006a). The temperature of fusion of materials during the electro-erosion process would remove all surface inclusions and uniformly cover a thickened oxidized layer on the surface.

(iv) *Ion beam-based processes:* Ion-beam-based processes, such as ion implantation, ion-beam-assisted deposition (IBAD), and plasma treatment, which is based on ionized particle bombardment, can provide beneficial surface layers with desirable properties (Cui and Luo, 1999). When ion impacts material surface, attaching, sputtering, and implantation may occur proportional to the ion's energy. In metallic biomaterials, these physical changes can often result in the formation of highly disordered and sometimes amorphous structures (Chu et al., 2002). The advantages of ion-beam-based processes are the possibility of accurate dose and depth control, low-temperature processing, versatility of ion species, nonequilibrium process, and reliability. In addition, the treatment can be selectively applied only to specific areas of the surface. Nevertheless, shallow penetration depth and its relatively high cost are the main drawbacks of this technique (Jagielski et al., 2006; Rautray et al., 2011).

The surface modification techniques using ion-beam technology fall into two categories, including thin film formation and surface-modified layer formation

(Hanawa, 1999). The thin film formation is aimed at improving specific surface properties of an implant and can have a different chemistry from the substrate. For example, ion implantation of calcium and phosphorus on titanium implants (e.g., apatite film) leads to formation of a thin film with different surface polarities and electrokinetic potentials compared to pure medical grade titanium (Krischok et al., 2007). Likewise in bone conductivity, other surface properties such as corrosion resistance and wear resistance can also be improved by the formation of thin films of TiO_2 and TiN, respectively. The thin film formation technique is also an effective method to fabricate functionally graded materials. Although the film composition can be easily modulated by the film formation technique, the film adhesion to the substrate is weak. The second category of ion-beam technology is the surface-modified layer, which can be produced by ion implantation and ion mixing. The advantage of the surface-modified layer is the graded composition and an obscure interface between the surface layer and substrate, making surface delamination less of a problem (Liu et al., 2004).

(v) *Laser surface modification*: Lasers can be used to modify the metallic surfaces and tailor the surface properties without unduly affecting the underlying properties of a material. In fact, the laser energy can be focused precisely on the surface only where it is needed. The electromagnetic radiation of a laser beam is absorbed within the first atomic layers for opaque materials, such as metals. There are no associated hot gas jets, eddy currents, or even radiation spillage outside the optically defined beam area (Hao and Lawrence, 2005). Laser surface modification of metallic biomaterials can lead to transformation hardening, surface melting, and/or surface alloying. Common advantages of laser surface modification, in particular for biomedical applications, include, but are not limited to: chemical cleanliness, controlled thermal penetration and profile, remote noncontact processing, and relative ease to automate (Bandyopadhyay et al., 2011; Hao and Lawrence, 2005). Lasers have also been applied to coat titanium with tricalcium phosphate (TCP) ceramics to improve bone cell−biomaterials interactions. Using optimized laser parameters, a coating thickness of 200−700 μm has been obtained (Roy et al., 2008). It was found that the thickness of the coating is enhanced by increasing laser power and/or powder feed rate. However, coating thickness decreased with increasing laser scan speed.

1.5.1.2 Biochemical surface modification

Recent advances in cell and molecular biology have led biologists, chemists, and material scientists to design and develop biomaterials equipped with molecular cues mimicking certain aspects of structure or function of natural ECM. Therefore, biochemical surface modification involves changing the biochemical properties of biomaterials by immobilizing biomolecules (i.e., peptides, proteins, enzymes, or growth factors) representing such molecular cues on the surface of biomaterials. The rationale for these hybrid materials integrating synthetic and biological components is to convey biofunctionality and elicit desired biological responses. Adsorption, entrapment, and covalent attachment are the three major mechanisms by which biomolecules are immobilized on the surface of a biomaterial (García, 2008; Paital and Dahotre, 2009). While binding proteins to polymers is relatively widespread,

covalent binding of proteins to metallic surfaces has long been problematic and elusive (Wise et al., 2009).

Bone formation on the surface of metallic biomaterials is accelerated when biomolecules concerning bone formation are immobilized on the material surface. Several immobilization methods and biomolecules have been exploited in the literature to enhance the bone formation on the surface of biomaterials. The amount of proteins bound to metallic biomaterials can be modulated by the choice of the surface treatment, immobilization chemistry, and material itself. For instance, in case of titanium and its alloys, the modified layer does not make direct contact with the substrate due to the presence of native oxide (i.e., TiO_2) on titanium substrates. Because TiO_2 is a relatively inert surface, only a few organic reagents, such as organosilanes, organophosphates, and photosensitive chemicals are able to form strong chemical bonds (Liu et al., 2004; Yang et al., 2006).

The surface of metals is first converted into reactive groups, and then biomolecules are conjugated to the surface by reacting with the reactive groups. The most commonly used method is through covering of a surface by self-assembly with organofunctional alkoxysilane molecules. This process is usually referred to as silanization. For example, the surfaces are converted into amino groups (e.g., by 3-aminopropyltriethoxysilane) and further into aldehyde groups (e.g., by glutaraldehyde) (Nanci et al., 1998) or maleimide groups (e.g., by succinimidyl ester maleimide) (Xiao et al., 1998). The monolayer coatings of biomaterials by means of silane and thiols with different end groups offer a wide variety of surface chemical properties. These coatings can be used to control the hydrophilicity of the surface and introduce specific chemical functional groups (e.g., methyl, hydroxyl, or carboxyl groups) at the surface (Palmquist et al., 2010). Peptides/proteins then can be conjugated to the surface through the amino-terminal group (i.e., formation of Schiff's base) or through cysteine (i.e., addition of HS−) (Xiao et al., 1998). Various peptides containing the ubiquitous Arg-Gly-Asp (RGD) sequence have been immobilized and received significant interest because RGD is the essential sequence mediating cell adhesion in many ECM proteins (e.g. vitronectin, fibronectin) (Dee et al., 2002; Duan and Wang, 2006; Ruoslahti and Pierschbacher, 1987). To improve hard-tissue response, Puleo et al. (2002) immobilized bone morphogenetic protein-4 (BMP-4) on Ti−6Al−4V alloy through lysozyme.

It has been accepted that collagen positively affects cellular adhesion, proliferation, and differentiation of many cell types in culture (Kleinman et al., 1981). The cellular response induced by collagen is mainly mediated through the amino acid sequence Arg−Gly−Asp (RGD), which is recognized by the integrin receptors located at the cell membrane (Ruoslahti and Pierschbacher, 1987). For this reason, collagen has successfully been used to modify biomaterial surfaces, which has been shown, for example, on surfaces of stainless steel (Müller et al., 2005) and titanium (Morra et al., 2003).

In some applications such as blood-contacting devices, it is necessary to reduce surface protein adsorption. The simplest approach to reduce protein adsorption is to passivate the surface with a layer of an inert protein such as albumin. Cells do not have adhesion receptors for albumin, and for this reason albumin has been

used to passivate surfaces against cell adhesion. The anticoagulant and antithrombotic are immobilized on the biomaterial surface either for controlled release or for a longer-term presence. In the case of polymeric materials, an anticoagulant may be incorporated into the chemical structure of a polymer, becoming an integral part of the biomaterial (Dee et al., 2002). Heparin is a common biomolecule that has been immobilized on biomaterials surface with excellent anticoagulant and antithrombotic properties (Li et al., 2011). The covalent immobilization of tropoelastin on the plasma- coated stainless steel surface was subsequently found to have improved biocompatibility by promoting endothelial cell attachment and proliferation relative to uncoated stainless steel controls (Yin et al., 2009). Various antithrombotic molecules (covalent, ionic, and physical adsorption) with specific chemical groups (e.g., −COOH, $-NH_2$, and −OH) were immobilized onto the surface of clinical vascular devices and held great promise in terms of blood biocompatibility (Li et al., 2011).

1.5.2 Coating of metallic biomaterials

In orthopedic and dental applications, some ceramics, such as Bioglass, sintered hydroxyapatite, and glass-ceramic A-W, spontaneously form a bone-like apatite layer on their surface in the living body and bond to bone through the apatite layer. These materials are called bioactive ceramics and are clinically important for use as bone-repairing materials (Kokubo et al., 2004). The formed apatite is very similar to bone mineral in its composition and structure. Thus, osteoblasts preferentially proliferate and differentiate to produce apatite and collagen on this apatite layer. However, compared with human cortical bone, ceramics have lower fracture toughness and higher elastic modulus. Metals (especially cp Ti and β-Ti alloys), on the other hand, possess higher toughness and closer elastic modulus to those of human cortical bone, but are bioinert materials in elemental form, which generally results in the encapsulation of the metal implant by a thin layer of fibrous tissue after the implantation into the living bone. When a metal implant is coated with hydroxyapatite, bone cells adhere onto the surface of the apatite coating without any intervening layers. The hydroxyapatite matrix of the bone cells later becomes integral with the hydroxyapatite coating, and there is excellent adhesion of the coated implant to the bone (Batchelor and Chandrasekaran, 2004).

Surface coatings of metallic biomaterials have been developed as a means of sheathing a metal in a coating that is more acceptable to the human body. The chemistry or biochemistry of coating layer remains only superficially associated with the bulk material, even if partial impregnation might be unavoidable. To further proceed on the nature and mechanisms of coating of metallic biomaterials, it is important to first define the surface and the bulk. Ideally, the surface modification should be confined to the outermost molecular layer ($\sim$10−15 Å), but in practice, thicker layers (10−100 nm) are used to ensure uniformity, durability, and functionality (García, 2008). In many titanium implants, the pristine thickness of the TiO_2 layer varies from 10 to 100 nm (Jarmar et al., 2008). However, the definition of coating and bulk material might become difficult in some cases, and wide

discrepancies are reported in the literature in terms of coating thickness. Whereas coatings thicker than 100 nm have been considered bulk material (Dohan Ehrenfest et al., 2010), calcium phosphate deposition of ~50 μm thick is considered to be a thin coating (Søballe, 1993).

The coating process must be consistent with the substrate to be coated, and an attempt should be made to keep the substrate intact during the coating process. For instance, in the case of Ti and its alloys, subjecting the substrate to high temperatures may adversely affect the characteristic and properties of the material. Furthermore, the coating process must not introduce impurities on the surface, which may affect the interface properties (Thull, 2010). Subsequently, failure in substrate-coating adhesion is usually unacceptable for any application because it results in the release of debris or ions into the human body, in addition to the evident failure of the biocompatibility or biofunctionality properties conferred to the biomaterial by the coating (Silva-Bermudez and Rodil, 2013).

1.5.2.1 Calcium phosphate coatings

The most important objective of surface modification of metallic biomaterials for hard-tissue engineering is the improvement of bone conductivity, through formation of a bioactive layer. Given that ~70 wt.% of the bone material is a mineral similar to nonstoichiometric hydroxyapatite (HA; $Ca_{10}(OH)_2(PO_4)_6$) (Brown and Chow, 1976), coating metallic implants with a layer of HA (or rather the generic term of calcium phosphate (CaP)) appears to be a plausible choice. The rationale is that because of their chemical similarities, bone may not recognize HA as foreign and therefore may heal faster and integrate with CaP-coated implants more firmly (Duan and Wang, 2006). Hydroxyapatites are resorbable materials in the living organism. Slowly resorbed hydroxyapatite is a building material for growing bone tissue (Batory et al., 2012). The most common CaP phases are HA, brushite [DCPD; $CaHPO_4.2H_2O$], and tricalcium phosphate (TCP; $Ca_3(PO_4)_2$) (Narayanan et al., 2008). The combination of the high mechanical strength of metals with the osteoconductive properties of CaP make HA coatings on titanium implants widely used in orthopedic surgery.

Several techniques have been undertaken to coat the metallic biomaterials with a thin layer of bone-like CaP. The most frequently used methods are plasma spraying (Chu et al., 2002; Ong et al., 2006); laser methods (Bao et al., 2006; Clèries et al., 2000a); sol−gel (Piveteau et al., 1999; Wen et al., 2007); biomimetic coating using simulated body fluids (Chen et al., 2007; Nouri et al., 2007); IBAD (Pham et al., 2000; Sioshansi and Tobin, 1996); laser methods (Bandyopadhyay et al., 2011; Lusquiños et al., 2005); radio frequency sputtering (Ong et al., 1992; Yang et al., 2005); electrochemical cathodic deposition (Kumar et al., 1999; Kuo and Yen, 2002); electrophoretic deposition (Hamagami et al., 2004; Wei et al., 2005); glow-discharge plasma (Aronsson et al., 1997); and physical vapor deposition (Paschoal et al., 2003).

The detailed review of all these techniques is beyond the scope of this chapter, and only some of the most popular methods are briefly discussed as follows.

Plasma-spraying method: Plasma spraying is one of the most widely used techniques to coat HA on Ti and its alloys substrate (Cook et al., 1992; Heimann, 1996; Liu et al., 2002). Plasma-spraying processes involve complex thermal changes between the plasma zone, powder particles, and the substrate. Particles injected into the 10,000 °C plasma jet undergo an extremely high heating rate within a few seconds. Although particles experience melting or even boiling, some large particles may not be completely molten because of their short duration in the plasma zone. The droplets are propelled and finally impact the substrate surface, forming splats (Narayanan et al., 2008). When in contact with the surface, the melted particles condense and form a film of several tenths of microns with an average roughness of several micrometers. Roughness associated with HA provides good bone-screw fixation.

Nevertheless, this well-accepted coating method exhibits some major drawbacks. A very rough surface will have more particulate concentration around the implant. Other problems include failure within the coating, discontinued dissolution of the coating after implantation, variation in bond strength at the coating−metal interface, variations in coating density as a result of the process, poor adhesion between the coatings and substrates, microcracks on the coating surface, and tendency to delaminate. Plasma-sprayed HA coatings of 20−50 μm thickness can be applied to microrough surfaces. However, the mechanical resistance of the interface between the coating and titanium is considered to be a weak point and will be fractured under a relatively low stress, because of low joint strength and low toughness of the sprayed layer itself (Dohan Ehrenfest et al., 2010; Hanawa, 1999). The process is, therefore, limited to thermally stable phases such as HA, and it makes it almost impossible to immobilize bone morphogenetic proteins on the surface so as to stimulate bone healing. Furthermore, the plasma-spraying method can only be applied to areas that are in direct line-of-sight; that is, only the parts of the substrate that are directly in the line of the spray are coated. Therefore, it is difficult to uniformly coat implants of complex shapes and the internal surfaces of porous structures or scaffolds widely used in orthopedic and dental implants (Duan and Wang, 2006; Habibovic et al., 2002). Despite the mentioned drawbacks, plasma-sprayed HA coatings in general exhibit suitable adhesion strength and are quickly deposited on the surface. Therefore, this method is widely accepted for clinical applications.

Treatment in simulated body fluid: The development of simulated body fluid (SBF) is based on the concept that the essential prerequisite to evaluate the bone-binding abilities of a biomaterial is the formation of apatite layer on its surface when implanted into the living body (Kokubo et al., 1990; Kokubo and Takadama, 2006). The apatite layer can form on the ceramics, metals, and polymers when they are soaked in SBF with ion concentrations nearly equal to those of human blood plasma. On the formation of apatite nuclei on a material, they can grow spontaneously by consuming the CaP ions from the surrounding SBF. A bioactive coating method using this apatite-forming ability is often carried out under physiological conditions of temperature (37 °C) and pH (7.4) and thus is called a "biomimetic method." The apatite formed is often called "bone-like apatite."

Human body fluid is supersaturated with apatite under normal conditions. Functional groups on the surface of the synthetic material can serve as effective apatite

nucleation sites, and apatite nuclei will readily form on its surface and continue to grow by consuming calcium and phosphate ions from the surrounding body fluid (Kokubo et al., 2004). Thus, two essential prerequisites required for the formation of apatite layer on materials using SBF are: (1) the existence of surface functional groups that induce the nucleation of apatite (e.g., Si−OH, Ti−OH, Nb−OH, Ta−OH, COOH, and PO_4H_2 groups); and (2) increase in the supersaturation concerning apatite around the surface of the materials (Kokubo et al., 1990, 1996). Treatment of Ti-based alloys with an aqueous solution of NaOH at 60 °C for 24 h, followed by heat treatment at 500−800 °C, is the most well-known technique to form functional group of Ti−OH on the surface of Ti alloys. This alkaline and heat treatment technique results in a thin titanate layer, which can then form a dense bone-like apatite layer when soaked in physiological solution and, ultimately, enhance the strength of the bone/implant interface. Coatings are typically 10−15 μm in thickness (Liu and Hunziker, 2009). Coating thickness can be modified by changing the volume of the coating solution, concentration of CaP in the solution, and, most importantly, the duration of the coating process (soaking time).

The biomimetic treatment in SBF has an advantage over conventional coating techniques because (1) it forms nanosized apatite crystals with high bioactivity and good resorption characteristics; (2) it is a low-temperature process applicable to any heat-sensitive substrate including polymer substrates; (3) it can uniformly coat porous implants or implants of complex geometries; (4) as a low-temperature coating method, it allows the incorporation of thermally unstable biologically active compounds such as growth factors, e.g., BMP, adhesion molecules, and antibiotics, that may be used to improve the clinical performance of the metallic biomaterials; and finally, (5) it is a simple and cost-effective method (Habibovic et al., 2004). However, SBF is a metastable solution, so it must be prepared only before being used. Although it can be stored refrigerated, the solution can only be kept for a limited period of no more than one month (Vallet-Regi et al., 2013).

Sol−gel: Sol−gel is another popular method of HA coatings on titanium alloy substrate (Liu et al., 2001; Peltola et al., 1998; Piveteau et al., 1999; Wen et al., 2007). In this method, CaP coatings are prepared by dipping the titanium in calcium (usually nitrate salt) and phosphorus gels for an appropriate time. The biological performance of HA coatings obtained by sol−gel coating is generally better than sputtering and plasma-spraying techniques. This is because the formation of rough and porous coatings through this method favors the circulation of physiological fluids and facilitates transport of nutrients and tissue ingrowth when it is used for biomedical application (Liu et al., 2001). Presence of hydroxyl groups in the sol−gel method promotes the calcium and phosphate precipitation and hence improves the interactions with osteoblasts (Narayanan et al., 2008; Ramires et al., 2001).

The sol−gel method offers several advantages, such as better control of the chemical composition of the coating, the possibility of preparing homogeneous films, control of the film microstructure, and a reduction in the densification temperature of the ceramic layer. In addition, the sol−gel method requires less equipment than most available techniques and is potentially less expensive (Piveteau, 2001). Nevertheless,

the CaP coatings obtained through this method are porous, less dense, and fail to adhere properly to the substrate. The poor adhesion is a detrimental factor that limits their use. To improve the adhesion and density of the coatings, the coatings are sintered at high temperatures; and depending on the applied temperature, different CaP phases can be obtained (Metikoš-Huković et al., 2003).

As reviewed by Narayanan (Narayanan et al., 2008), the CaP coatings are characterized by the following features:

Stability of the coatings: Stability of a modified surface is a crucial requirement for adequate biological performance. Mechanical stability (i.e., resistance to cracking, delamination, and debonding) and chemical stability, especially in aggressive and chemically active environments such as physiological fluids, are two criteria that together account for surface stability (García, 2008). Highly crystalline CaP coatings generally have low dissolution rate in physiological fluids and can provide long-term stability of the implant. However, coatings with a low dissolution rate also have a low reprecipitation rate, which may not be an ideal situation. On the other hand, amorphous CaP coatings (e.g., those coatings produced by IBAD and laser methods) possess both high dissolution rates and reprecipitation rates, that make them a desirable choice. However, there is concern regarding the coating stability, because the mechanical stability of the implant surface at the early stage of implantation should be assured so as to provide primary mechanical strength. Seemingly, a coating with controllable dissolution/reprecipitation and sufficient stability is plausible to tackle with the excessive dissolution of CaP coatings for long-term stability, while retaining a certain degree of bioactivity for enhanced tissue attachment (Narayanan et al., 2008). Biomimetic and electrochemical calcium phosphate coatings deposited from solutions at ambient temperatures present compositional and structural features closely mimicking those of bone.

Coating thickness: Thin surface modifications are preferred for most applications because thicker coatings often negatively influence the mechanical and functional properties of the material. If the coatings have high thicknesses, the outer layers tend to detach from the substrate, resulting in poor adhesion to the substrate. The higher coating thickness (>100 μm) associated with the plasma-spraying technique is not desirable because it can cause failure due to fatigue under tensile loading conditions. Furthermore, the residual stresses within the coatings are increased with increasing thickness, and its energy release may initiate cracking at the substrate/coating interface (Jansen and León, 2009). However, the coating stability would also be affected if the thicknesses are low and have poor crystallinity. The thickness of a CaP coating is always, theoretically, a compromise between the dissolution and mechanical properties of the coating. Although cells and tissues interact with only the top layers of the coating and a 10-nm coating would be sufficient for cell activity, 10-μm thick coatings are suggested to be good for apposition. Plasma-spraying produces coatings with thicknesses ranging from 30−200 μm. Electrochemical methods can also produce wide thicknesses depending on the current density. On the other hand, the coating thickness of wet techniques like sol−gel or soaking in SBF is usually low. Use of high-temperature techniques like RF sputtering, IBAD, or laser methods produce significantly thinner coatings.

Coating adhesion to the substrate: Bond strength of the CaP coating on the titanium implant material is crucial because it has to withstand crevice and bone growth stress. Adhesion strengths of the coatings can be measured by tensile and scratch tests, among others. The coating on the implant surface should also have higher or at least comparable bond strength with natural human bone ($\geq$18 MPa). For a dense coating under tensile loading, failure occurs at the interface of the coating and substrate, and the cohesive strength is higher than the bond strength. For a porous coating, the cohesive strength is low and the fracture occurs inside the coating (Han et al., 2001). On a surface-modified Ti samples featuring discrete crystalline deposition (DCD) of CaP nanocrystals, Mendes et al. reported that the resistance to detachment resulted in fracture of the bone tissue as opposed to failure at the interface (Mendes et al., 2007). The amorphous coatings have a more brittle nature and less adhesion compared to the crystalline ones (Clèries et al., 2000b).

The adhesion of a deposited film to a surface can be enhanced by different strategies such as removing contaminant layers, changing the surface chemistry, generating a microscopically rough surface, increasing the nucleation density by forming nucleation site defects, introducing thermal energy directly into the surface region (thereby promoting reaction and diffusion), and so on (Thull and Grant, 2001). Another strategy is to introduce negative functional groups onto the surface of metal substrate. Acid-etched titanium discs and rods were treated by CO_2 plasma and then incubated in a modified SBF (*m*-SBF) to prepare an HA layer. It was found that after the treatment with CO_2 plasma, the hydrophilicity of the titanium sample was improved, and hydroxyl groups on the titanium surface were increased. The hydroxyapatite formability on the surface of sandblasted-acid etched titanium was enhanced by CO_2 plasma pretreatment, due to the increased negative charge of the titanium surface (Hu et al., 2011).

1.5.2.2 Calcium phosphate glass-ceramic coatings

Another important class in the bioactive coating family is glass ceramics, such as Bioglass® and Cerabone® A-W (Hench and Anderson, 1993). Glass ceramics contain both a glass phase and a tough ceramic microstructure that reinforces the material. Glass ceramics exhibit a wide range of compositions, but are generally composed of SiO_2, CaO, and P_2O_5, although small amounts of MgO, Na_2O, or CaF_2 can also be present (Hertz and Bruce, 2007). Three kinds of methods are usually used to apply the glasses as coatings: (1) enameling or glazing using glass frits; (2) flame spray coating; and (3) rapid-immersion coating, in which the heated metal is rapidly inserted into the molten glass (Hench, 1991). The glassy structure of these materials can be partially dissolved by body fluids, releasing Ca^{2+} and P^{5+} ions and forming large amounts of bioactive Si−OH groups. The Si−OH groups on the coating surface are beneficial for the nucleation and growth of apatite in the body fluids, which is supersaturated with respect to CaP (Hench and Anderson, 1993). Plasma spraying and sol−gel coating techniques are used more frequently for producing bioglass coatings (Wang and Zreiqat, 2010).

1.5.2.3 Composite coatings

Biomaterials can be made as composites for advanced applications if a single material is incapable of fulfilling the various requirements of the given application. Composite coatings are an emerging area of surface modification of metallic biomaterials in which a functional surface layer with the required physical, mechanical, or biological properties covers a bulk biomaterial. For instance, titanium/porous titanium composites have advantageous mechanical properties, Ti/ceramic composite show special biological properties with improved osseointegration features, and the special physical properties of Ti/ceramic composites make them suitable for heart pacemaker leads (Breme et al., 2000). In the course of developing metallic biomaterials, various combinations such as ceramic/ceramic and ceramic/polymer have been proposed recently.

The incorporation/immobilization of biomolecules into calcium phosphate has received a considerable interest in the coating of metallic biomaterials. The presence of appropriate biomolecules at the surface may provide signals to selected types of cells and promote their adhesion or function (Duan and Wang, 2006). To increase the Ti ability to bond with bone, a mixture of titanium dioxide (TiO_2) and CaP was fabricated and deposited as a coating (Piveteau et al., 1999). Therefore, CaP/TiO_2 coatings can be expected to combine the advantages of TiO_2 with those of CaP. Inspired from the structure of natural bone, biopolymers such as collagen, gelatin, silk fibroin, chitosan, and poly(lactide-co-glycolide) have been used to make composite with bioactive inorganic materials such as calcium phosphate (Carlo Reis et al., 2011). Hahn et al. (2011) prepared a dense and well-adherent HA−chitosan composite coating on an AZ31 Mg alloy. The resultant composites are mechanically superior to individual component due to the ductile properties of the biopolymer, which increase the fracture toughness of the inorganic component (Wang and Zreiqat, 2010). Besides biocompatibility and osseoconduction, the composite coatings may also enhance the corrosion resistance. In an attempt to rectify the disadvantages of a single CaP or polymer coating, a composite coating composed of dicalcium phosphate dehydrate (DCPD) and polycaprolactone (PCL) was prepared on the Mg−Zn alloy (Wang et al., 2012). Compared to the DCPD-coated alloy, the DCPD−PCL-coated alloy showed higher corrosion resistance, as manifested by the elevated corrosion potential, reduced corrosion current, and less hydrogen released.

1.5.2.4 Oxide coatings

Typically used metallic biomaterials, such as surgical stainless steels, cobalt−chromium-based alloys, titanium, and titanium-based alloys, have a strong tendency to spontaneously form a very fine and stable oxide layer (a so-called passive film) on its surface in the reaction with atmospheric oxygen or most aqueous environments (Bauer et al., 2013). The native oxide layers are only few nanometers thick and act as a highly protective surface barrier between the bulk metal and the aggressive biological environment, conferring biocompatibility to the metallic surfaces (Silva-Bermudez and Rodil, 2013; Virtanen et al., 2008). It has been widely recognized that most of the properties related to the biocompatibility (inertness) of the metallic biomaterials

are due to the properties of their native oxides. For example, titanium oxides increase calcium ion interactions, which are important for protein and subsequent osteoblast adhesion (Ellingsen, 1991).

The protective quality of an oxide layer is kinetically determined by the ion transfer through the layer and the stability of the oxide layer against dissolution (Schultze and Lohrengel, 2000). A variety of factors, such as oxide composition, thickness, microstructure, homogeneity, and defect concentration, influence the ionic transport through the oxide layer and the stability of the layer in different environments. These factors are interrelated and can affect one another. For instance, the thickness of the oxide film not only affects the homogeneity and porosity of the film, but also alters the roughness, the surface energy, and the wettability (Silva-Bermudez and Rodil, 2013). Following long-term exposure to biological fluids, the thin oxide layer (5−6 nm) failed to protect the Ti from corrosion, whereas a thicker and homogeneous Ti oxide coating (100 nm), significantly enhanced the long-term biocorrosion resistance of Ti, showing a similar cellular response (Ochsenbein et al., 2008). Sharma and Paul (1992) reported that increasing the thickness of the oxide layer on Ta substrates, increased the surface hydrophilicity and therefore enhanced fibrinogen adsorption on Ta oxide-coated surfaces, as compared to the bare Ta surfaces with a native oxide layer. Other properties, such as the oxide crystallinity, have clearly been associated with protein adsorption (Kurrat et al., 1994), showing that the changes in other surface properties due to the different crystalline structures were the influencing factor for protein adsorption.

It must be noted that the composition of the oxide layer can lead to a variety of cellular responses. For instance, vanadium, even in its oxidized state, V_2O_5, has been shown to cause an adverse cellular response due to the release of toxic V ions (Eisenbarth et al., 2004; Okazaki et al., 1996). Aluminum has a poorer biocompatibility than Nb or Ta (Scotchford et al., 2003) and in high concentrations may act as a neurotoxic substance (Mjoberg et al., 1997; Nag et al., 2005; Okazaki et al., 1996). This knowledge has been realized in the design and development of metallic alloys for orthopedic implants, in which elements such as V and Al have been substituted by additions of Sn, Nb, or Zr (Nouri, 2008; Nouri et al., 2007).

Consequently, the design of metal oxide-based biocompatible coatings has emerged from the need to obtain metallic biomaterials with suitable biocorrosion resistance and cellular response. TiO_2 (titania) is the most frequently studied metal oxide-based coatings. TiO_2 is a hard, adherent, and protective layer being used as a coating on other materials to create biocompatible interfaces and to promote chemical bonding between bone tissue and implant materials (Hertz and Bruce, 2007). The corrosion resistance is also known to increase with increasing thickness of the TiO_2 coating. Several coating methods have been used to deposit TiO_2 on the surface of metallic biomaterials, including dip-coating, microsphere precipitation, or plasma-spraying. TiO_2 exists in three different crystallographic forms: rutile and anatase with tetragonal structure, and brookite with orthorhombic structure. Surface oxides on titanium can vary in thickness from a few nanometers up to several micrometers, depending on the method of preparation and the temperatures

involved. TiO_2 coatings between the HA and titanium have been used to improve the bonding strength of the HA layer and the Ti substrate. Wen et al. reported that the existing cracks on TiO_2-coated surface could be filled in and completely covered by the subsequent HA coating (Wen et al., 2007).

1.5.2.5 Other coatings

Carbon layer coatings: Thin carbon layers in the form of nanocrystalline diamond or diamond-like carbon (DLC) make metallic surface generally more biocompatible and more resistant to fibrous encapsulation (biofilm). Diamond has the outstanding reputation of being chemically inert and uniquely biocompatible and has found a number of applications in medicine (Freitas, 2003). In orthopedic surgery, the use of a diamond coating on metallic biomaterials reduces generation of macrophages and improves the wearability of devices (Santavirta et al., 1999). In addition to very high wear-resistance and excellent biocompatibility, chemical inertness and corrosion resistance of DLC also make it a perfect coating material to protect the surfaces of surgical instruments against the aggressive biological environment and to solve the tribological problems (i.e., friction, lubrication, and wear characteristics) (Jakubowski et al., 2004; Kim et al., 2005).

Because of the high hardness and low friction coefficients of DLC, sputtering and IBAD are the two most frequently used techniques to prepare DLC coatings on metallic biomaterials (Goto et al., 2011). Kobayashi et al. (2007) prepared a DLC coating on NiTi archwires to test in vitro whether nickel release could be reduced. This investigation concluded that there was a reduction in the concentration of nickel ions in physiological saline, which makes DLC noncytotoxic in a corrosive environment. Another possible alternative to solve tribological problems is to protect the alloy surface by means of biocompatible titanium carbo-nitride (Ti−C−N) coatings. The Ti−C−N coatings improve the general response of the biomaterial (Sáenz De Viteri et al., 2012). It was also reported that the preparation of titanium nitride (Ti−N) or Ti−C−N layers on the titanium alloy (Ti−6Al−4V) modulate the thrombogenicity of the surface (Walkowiak, 2007).

Layer-by-layer method: The layer-by-layer (LbL) method consists of alternately depositing polyelectrolytes that self-assemble and self-organize on the surface of the material, leading to the formation of polyelectrolyte multilayer (PEM) films (Crouzier et al., 2011). This technique is based on the consecutive adsorption of polyanions and polycations via electrostatic interactions. The electrostatic attraction between positively and negatively charged molecules appears to be a suitable choice as a driving force for multilayer build-up. The procedure is simple and applicable to a variety of substrates. Different types of films containing charged species have been successfully prepared, including biological molecules (polypeptides, polysaccharides, DNA, proteins, and viruses) and various kinds of nanoparticles (clay platelets, carbon nanotubes, etc.) (Decher and Schlenoff, 2003). The LbL assembled heparin/fibronectin biofunctional films were prepared on titanium surface to enhance the blood anticoagulation and accelerate the formation of endothelial tissue simultaneously (Li et al., 2011). The LbL assembled chitosan/heparin coating on a coronary

stainless steel stent significantly promoted the formation of endothelial tissue and proved to be safer than bare metal stents due to its superior anticoagulative effect (Meng et al., 2009). To improve the surface biocompatibility of titanium oxide layers, a LbL self-assembly technique, based on the polyelectrolyte-mediated electrostatic adsorption of chitosan and gelatin, was used, leading to the formation of multilayers on the titanium thin layers. Cells adhered to this modified surface have a more flattened morphology and better cell−cell/cell−substrate interactions than that of a control (Cai et al., 2005).

Hydrogels containing heparin and dopamine prepared by enzyme reaction have been used as an alternative coating method for enhancing blood compatibility of metallic biomaterials (Joung et al., 2012). The hydrogel on a surface not only provides a smooth and slippery surface, but also averts the formation of fibrous tissue and interaction with blood components (Joung et al., 2012). Coating the surfaces with heparin is also an effective approach to improve the blood compatibility of artificial materials (Riesenfeld et al., 1995).

1.6 Conclusions and future trends

Among the various biomedical materials, metals represent the benchmark for success due to a combination of acceptable biocompatibility and superb mechanical properties. These properties make metals promising biomaterials for functional and load-bearing applications such as cardiovascular devices and orthopedic implants. The most commonly used metals in biomedical applications are stainless steel, cobalt−chromium alloys, commercially pure titanium, and titanium alloys. Because the surface is the interface where the biomaterials meet and interact with the biological environment (i.e., bone, soft tissue, and blood), the foremost challenge in improving the function and the lifespan of implants is the proper surface treatment prior to implantation. Surface modifications of biomaterials represent promising routes to engineer biofunctionality at the material−tissue interface to modulate biological responses without altering material bulk properties. It was reviewed that a biomaterial's surface chemistry, topography, charge, and wettability are the most crucial aspects in the design of biomedical devices.

Understanding the mechanisms of protein adsorption and cell adhesion at the material−tissue interface will provide robust means for researchers to select proper biomaterials and surface modification techniques. The specific surface treatments have to be adopted based on the materials substrate, the specific biological environment consisting of the kind of adjacent tissue, and the given application, so as to enhance biomaterial performance in vivo. This chapter is aimed at reviewing some of the current surface modification techniques for metallic biomaterials, including physicochemical, biochemical, and coating techniques. Most modifications can alter the surface chemistry and topography of the metallic biomaterials, in particular for better osseointegration or blood compatibility.

It is anticipated that technical breakthroughs in synthetic chemistry, biofunctionalization, micro- and nano-engineering, and surface characterization will lead to

the fabrication of more advanced and bioactive surfaces. In particular, surfaces that are highly topographically complex at the submicron level are thought to interact with some proteins more effectively and, thus, are expected to provide unparalleled control over cellular activities and healing responses. A surface modification process that is too complex will be difficult and expensive to commercialize. It is more appropriate to minimize the number of steps or design each step to be relatively insensitive to small changes in the experimental conditions.

Acknowledgements

This research is financially supported by the Australian Government under the Australia−India Strategic Research Fund through AISRF project ST060048.

References

Adawy, A., & Abdel-Fattah, W. I. (2013). An efficient biomimetic coating methodology for a prosthetic alloy. *Materials Science and Engineering C, 33*, 1813−1818.

Albelda, S. M., & Buck, C. A. (1990). Integrins and other cell adhesion molecules. *FASEB Journal, 4*, 2868−2880.

Alla, R. K., Ginjupalli, K., Upadhya, N., Shammas, M., Ravi, R. K., & Sekhar, R. (2011). Surface roughness of implants: a review. *Trends in Biomaterials and Artificial Organs, 25*, 112−118.

Altankov, G., & Groth, T. (1994). Reorganization of substratum-bound fibronectin on hydrophilic and hydrophobic materials is related to biocompatibility. *Journal of Materials Science: Materials in Medicine, 5*, 732−737.

Anderson, J. M. (2001). Biological responses to materials. *Annual Review of Materials Research, 31*, 81−110.

Andrade, J. D., & Hlady, V. (1986). Protein adsorption and materials biocompatibility: a tutorial review and suggested hypotheses. *Advances in Polymer Science, 79*, 1−63.

Anselme, K. (2000). Osteoblast adhesion on biomaterials. *Biomaterials, 21*, 667−681.

Anselme, K., & Bigerelle, M. (2006a). Effect of a gold−palladium coating on the long-term adhesion of human osteoblasts on biocompatible metallic materials. *Surface and Coatings Technology, 200*, 6325−6330.

Anselme, K., & Bigerelle, M. (2006b). Statistical demonstration of the relative effect of surface chemistry and roughness on human osteoblast short-term adhesion. *Journal of Materials Science: Materials in Medicine, 17*, 471−479.

Anselme, K., Ponche, A., & Bigerelle, M. (2010). Relative influence of surface topography and surface chemistry on cell response to bone implant materials. Part 2: biological aspects. *Proceedings of the Institution of Mechanical Engineers H, 224*, 1487−1507.

Anusavice, K. J. (2006). *Phillips' science of dental materials*. Elsevier.

Aronsson, B. O., Lausmaa, J., & Kasemo, B. (1997). Glow discharge plasma treatment for surface cleaning and modification of metallic biomaterials. *Journal of Biomedical Materials Research, 35*, 49−73.

Bagno, A., & Di Bello, C. (2004). Surface treatments and roughness properties of Ti-based biomaterials. *Journal of Materials Science: Materials in Medicine, 15*, 935−949.

Baker, J. P., & Titus, M. A. (1998). Myosins: matching functions with motors. *Current Opinion in Cell Biology, 10*, 80−86.

Bandyopadhyay, A., Krishna Balla, V., Roy, M., & Bose, S. (2011). Laser surface modification of metallic biomaterials. *JOM, 63*, 94−99.

Bao, Q., Chen, C., Wang, D., Lei, T., & Liu, J. (2006). Pulsed laser deposition of hydroxyapatite thin films under Ar atmosphere. *Materials Science and Engineering A, 429*, 25−29.

Barbosa, J. N., Madureira, P., Barbosa, M. A., Aguas, A. P. (2006). The influence of functional groups of self-assembled monolayers on fibrous capsule formation and cell recruitment. 76, 737−743.

Batchelor, A. W., & Chandrasekaran, M. (2004). *Service characteristics of biomedical materials and implants* (Vol. 3). London: Imperial College Press.

Batory, D., Gawronski, J., Kaczorowski, W., & Niedzielska, A. (2012). C−HAp composite layers deposited onto AISI 316L austenitic steel. *Surface & Coatings Technology, 206*, 2110−2114.

Bauer, S., Schmuki, P., Von Der Mark, K., & Park, J. (2013). Engineering biocompatible implant surfaces part I: materials and surfaces. *Progress in Materials Science, 58*, 261−326.

Bayram, C., Demirbilek, M., Yalçın, E., Bozkurt, M., Doğan, M., & Denkbaş, E. B. (2014). Osteoblast response on co-modified titanium surfaces via anodization and electrospinning. *Applied Surface Science, 288*, 143−148.

Beningo, K. A., Dembo, M., Kaverina, I., Small, J. V., & Wang, Y. L. (2001). Nascent focal adhesions are responsible for the generation of strong propulsive forces in migrating fibroblasts. *Journal of Cell Biology, 153*, 881−888.

Bigerelle, M., & Anselme, K. (2005). A kinetic approach to osteoblast adhesion on biomaterial surface. *Journal of Biomedical and Materials Research A, 75*, 530−540.

Bigerelle, M., Anselme, K., Noël, B., Ruderman, I., Hardouin, P., & Iost, A. (2002). Improvement in the morphology of Ti-based surfaces: a new process to increase in vitro human osteoblast response. *Biomaterials, 23*, 1563−1577.

Bongrand, P., Capo, C., & Depieds, R. (1982). Physics of cell adhesion. *Progress in Surface Science, 12*, 217−285.

Bordji, K., Jouzeau, J. Y., Mainard, D., Payan, E., Delagoutte, J. P., & Netter, P. (1996). Evaluation of the effect of three surface treatments on the biocompatibility of 316L stainless steel using human differentiated cells. *Biomaterials, 17*, 491−500.

Boyan, B. D., Hummert, T. W., Dean, D. D., & Schwartz, Z. (1996). Role of material surfaces in regulating bone and cartilage cell response. *Biomaterials, 17*, 137−146.

Breme, J., Biehl, V., & Hoffmann, A. (2000). Tailor-made composites based on titanium for medical devices. *Advanced Engineering Materials, 2*, 270−275.

Bressan, E., Sbricoli, L., Guazzo, R., Tocco, I., Roman, M., Vindigni, V., et al. (2013). Nanostructured surfaces of dental implants. *International Journal of Molecular Sciences, 14*, 1918−1931.

Brett, P. M., Harle, J., Salih, V., Mihoc, R., Olsen, I., Jones, F. H., et al. (2004). Roughness response genes in osteoblasts. *Bone, 35*, 124−133.

Brown, W. E., & Chow, L. C. (1976). Chemical properties of bone mineral. *Annual Review of Materials Science, 6*, 213−236.

Brunette, D. M. (1988). The effects of implant surface topography on the behavior of cells. *International Journal of Oral & Maxillofacial Implants, 3*, 231−246.

Cai, K., Rechtenbach, A., Hao, J., Bossert, J., & Jandt, K. D. (2005). Polysaccharide-protein surface modification of titanium via a layer-by-layer technique: characterization and cell behaviour aspects. *Biomaterials, 26*, 5960−5971.

Carlo Reis, E. C., Borges, A. P., Araújo, M. V., Mendes, V. C., Guan, L., & Davies, J. E. (2011). Periodontal regeneration using a bilayered PLGA/calcium phosphate construct. *Biomaterials, 32*, 9244−9253.

Carré, A., & Lacarriere, V. (2010). How substrate properties control cell adhesion. A physical−chemical approach. *Journal of Adhesion Science and Technology, 24*, 815−830.

Chang, H. I., & Wang, Y. (2011). Cell responses to surface and architecture of tissue engineering scaffolds. In D. Eberli (Ed.), *Regenerative medicine and tissue engineering—cells and biomaterials* (pp. 569−588). InTech.

Chen, X. B., Nouri, A., Hodgson, P. D., & Wen, C. E. (2007). Surface modification of TiZr alloy for biomedical application. *Advanced Materials Research, 15−17*, 89−94.

Chen, X. B., Nouri, A., Li, Y., Lin, J., Hodgson, P. D., & Wen, C. (2008). Effect of surface roughness of Ti, Zr, and TiZr on apatite precipitation from simulated body fluid. *Biotechnology and Bioengineering, 101*, 378−387.

Chou, L., Firth, J. D., Nathanson, D., Uitto, V. J., & Brunette, D. M. (1996). Effects of titanium on transcriptional and post-transcriptional regulation of fibronectin in human fibroblasts. *Journal of Biomedical and Materials Research A, 31*, 209−217.

Chu, P. K., Chen, J. Y., Wang, L. P., & Huang, N. (2002). Plasma-surface modification of biomaterials. *Materials Science and Engineering R, 36*, 143−206.

Chung, T. W., Liu, D. Z., Wang, S. Y., & Wang, S. S. (2003). Enhancement of the growth of human endothelial cells by surface roughness at nanometer scale. *Biomaterials, 24*, 4655−4661.

Clèries, L., Fernandez-Pradas, J. M., & Morenza, J. L. (2000a). Bone growth on and resorption of calcium phosphate coatings obtained by pulsed laser deposition. *Journal of Biomedical and Materials Research A, 49*, 43−52.

Clèries, L., Martínez, E., Fernández-Pradas, J. M., Sardin, G., Esteve, J., & Morenza, J. L. (2000b). Mechanical properties of calcium phosphate coatings deposited by laser ablation. *Biomaterials, 21*, 967−971.

Cook, S. D., Thomas, K. A., Dalton, J. E., Volkman, T. K., Whitecloud, T. S. R., & Kay, J. F. (1992). Hydroxylapatite coating of porous implants improves bone ingrowth and interface attachment strength. *Journal of Biomedical Materials Research, 26*, 989−1001.

Cowley, A., & Woodward, B. (2011). A healthy future: platinum in medical applications. *Platinum Metals Review, 55*, 98−107.

Crouzier, T., Boudou, T., Ren, K., & Picart, C. (2011). Coating of material surfaces with layer-by-layer assembled polyelectrolyte films. In S. Zhang (Ed.), *Biological and biomedical coatings handbook: processing and characterization* (pp. 333−376). Boca Raton, FL: CRC Press.

Cui, F. Z., & Luo, Z. S. (1999). Biomaterials modification by ion-beam processing. *Surface and Coatings Technology, 112*, 278−285.

Davies, J. E. (2007). Bone bonding at natural and biomaterial surfaces. *Biomaterials, 28*, 5058−5067.

Davis, J. R. (2003). *Handbook of materials for medical devices*. ASM International.

Decher, G., & Schlenoff, J. B. (2003). *Multilayer thin films: sequential assembly of nanocomposite materials*. Weinheim, Germany: Wiley-VCH.

Dee, K. C., Puleo, D. A., & Bizios, R. (2002). *An introduction to tissue-biomaterial interactions*. Hoboken, NJ: Wiley & Sons Inc.

Derkaoui, S. M., Labbé, A., Chevallier, P., Holvoet, S., Roques, C., Avramoglou, T., et al. (2012). A new dextran-graft-polybutylmethacrylate copolymer coated on 316L metallic stents enhances endothelial cell coverage. *Acta Biomaterialia, 8*, 3509−3515.

Dietschweiler, C. 2008. Protein adsorption at solid surfaces. Term paper. Zürich: Swiss Federal Institute of Technology.

Disegi, J. A., & Eschbach, L. (2000). Stainless steel in bone surgery. *Injury, 31*(Suppl. 4), 2−6.

Dohan Ehrenfest, D. M., Coelho, P. G., Kang, B. S., Sul, Y. T., & Albrektsson, T. (2010). Classification of osseointegrated implant surfaces: materials, chemistry and topography. *Trends in Biotechnology, 28*, 198−206.

Donoso, M. G., Méndez-Vilas, A., Bruque, J. M., & González-Martin, M. L. (2007). On the relationship between common amplitude surface roughness parameters and surface area: implications for the study of cell−material interactions. *International Biodeterioration & Biodegradation, 59*, 245−251.

Duan, K., & Wang, R. (2006). Surface modifications of bone implants through wet chemistry. *Journal of Materials Chemistry, 16*, 2309−2321.

Duerig, T. W., Melton, K. N., Stockel, D., & Wayman, C. M. (1990). *Engineering aspects of shape memory alloys*. London: Butterworth-Heinemann.

Eisenbarth, E., Meyle, J., Nachtigall, W., & Breme, J. (1996). Influence of the surface structure of titanium materials on the adhesion of fibroblasts. *Biomaterials, 17*, 1399−1403.

Eisenbarth, E., Velten, D., Müller, M., Thull, R., & Breme, J. (2004). Biocompatibility of beta-stabilizing elements of titanium alloys. *Biomaterials, 25*, 5705−5713.

Ellingsen, J. E. (1991). A study on the mechanism of protein adsorption to TiO_2. *Biomaterials, 12*, 593−596.

Eriksson, C., Nygren, H., & Ohlson, K. (2004). Implantation of hydrophilic and hydrophobic titanium discs in rat tibia: cellular reactions on the surfaces during the first 3 weeks in bone. *Biomaterials, 25*, 4759−4766.

Feng, B., Weng, J., Yang, B. C., Qu, S. X., & Zhang, X. D. (2003). Characterization of surface oxide films on titanium and adhesion of osteoblast. *Biomaterials, 24*, 4663−4670.

Flemming, R. G., Murphy, C. J., Abrams, G. A., Goodman, S. L., & Nealey, P. F. (1999). Effects of synthetic micro- and nano-structured surfaces on cell behavior. *Biomaterials, 20*, 573−588.

Fragalà, M. E., & Satriano, C. (2010). Selective protein adsorption on ZnO thin films for bio-functional nano-platforms. *Journal of Nanoscience and Nanotechnology, 10*, 5889−5893.

Freitas, R. A. (2003). Biocompatibility. In *Nanomedicine* (volume IIA). Georgetown, TX: Landes Bioscience.

Frosch, K. H., & Stürmer, K. M. (2006). Metallic biomaterials in skeletal repair. *European Journal of Trauma, 32*, 149−159.

Fukuzaki, S., Urano, H., & Nagata, K. (1996). Adsorption of bovine serum albumin onto metal oxide surfaces. *Journal of Fermentation and Bioengineering, 81*, 163−167.

Gall, K., Tyber, J., Wilkesanders, G., Robertson, S. W., Ritchie, R. O., & Maier, H. J. (2008). Effect of microstructure on the fatigue of hot rolled and cold drawn NiTi shape memory alloys. *Materials Science and Engineering A, 486*, 389−403.

Ganesh, V. K., Ramakrishna, K., & Ghista, D. N. (2005). Biomechanics of bone-fracture fixation by stiffness-graded plates in comparison with stainless-steel plates. *Biomedical Engineering Online, 4*, 46.

García, A. J. (2008). Surface modification of biomaterials. In A. Atala, R. Lanza, J. A. Thomson & R. M. Nerem (Eds.), *Principles of regenerative medicine* (pp. 656−665). Burlington: Academic Press, Elsevier.

Geetha, M., Singh, A. K., Asokamani, R., & Gogia, A. K. (2009). Ti based biomaterials, the ultimate choice for orthopaedic implants—a review. *Progress in Materials Science, 54*, 397−425.

Getzenberg, R. H., Pienta, K. J., & Coffey, D. S. (1990). The tissue matrix: cell dynamics and hormone action. *Endocrine Reviews, 11*, 399−417.

Göransson, A., & Wennerberg, A. (2005). Bone formation at titanium implants prepared with iso- and anisotropic surfaces of similar roughness: an in vivo study. *Clinical Implant Dentistry and Related Research, 7*, 17−23.

Goto, T., Narushima, T., & Ueda, K. (2011). Bioceramic coating on titanium by physical and chemical vapor deposition. In S. Zhang (Ed.), *Biological and biomedical coatings handbook: processing and characterization* (pp. 229−332). Boca Raton, FL: CRC Press.

Granchi, D., Ciapetti, G., Savarino, L., Cavedagna, D., Donati, M. E., & Pizzoferrato, A. (1996). Assessment of metal extract toxicity on human lymphocytes cultured in vitro. *Journal of Biomedical and Materials Research A, 31*, 183−191.

Grashoff, G. J., & King, R. O. (1990). Silver in medical applications. In D. Williams (Ed.), *Concise encyclopedia of medical & dental materials* (pp. 321−326). Pergamon Press and The MIT Press.

Groth, T., Liu, Z. M., Niepel, M., Peschel, D., Kirchhof, K., Altankov, G., et al. (2007). Chemical and physical modifications of biomaterial surfaces to control adhesion of cells. In V. P. Shastri, G. Altankov, & A. Lendlein (Eds.), *Advances in regenerative medicine: role of nanotechnology, and engineering principles* (pp. 253−284). Dordrecht, The Netherlands: Springer.

Groth, T., Liu, Z. M., Niepel, M., Peschel, D., Kirchhof, K., Altankov, G., et al. (2010). Chemical and physical modifications of biomaterial surfaces to control adhesion of cells. In V. P. Shastri, G. Altankov, & A. Lendlein (Eds.), *Advances in regenerative medicine: role of nanotechnology, and engineering principles* (pp. 253−284). Springer.

Habibovic, P., Barrére, F., & De Groot, K. (2004). New biomimetic coating technology and incorporation of bioactive agents and properties. In R. L. Reis & S. Weiner (Eds.), *Learning from nature how to design new implantable biomaterials* (pp. 105−121). Dordrecht: Kluwer Academic.

Habibovic, P., Barrére, F., Van Blitterswijk, C. A., De Groot, K., & Layrolle, P. (2002). Biomimetic hydroxyapatite coating on metal implants. *Journal of the American Ceramic Society, 85*, 517−522.

Hahn, B., Park, D., Choi, J., Ryu, J., Yoon, W., Choi, J., et al. (2011). Aerosol deposition of hydroxyapatite−chitosan composite coatings on biodegradable magnesium alloy. *Surface & Coatings Technology, 205*, 3112−3118.

Hallab, N. J., Jacobs, J. J., & Katz, J. L. (2004). Application of materials in medicine, biology, and artificial organs: orthopedic applications. In B. D. Ratner, A. S. Hoffman, F. Schoen, & J. E. Lemons (Eds.), *Biomaterials science: an introduction to materials in medicine* (2nd ed., pp. 526−555). Elsevier Academic Press.

Hamagami, J. I., Ato, Y., & Kanamura, K. (2004). Fabrication of highly ordered macroporous apatite coating onto titanium by electrophoretic deposition method. *Solid State Ionics, 172*, 331−334.

Hamamoto, N., Hamamoto, Y., Nakajima, T., & Ozawa, H. (1995). Histological, histocytochemical and ultrastructural study on the effects of surface charge on bone formation in the rabbit mandible. *Archives of Oral Biology, 40*, 97−106.

Hanawa, T. (1999). In vivo metallic biomaterials and surface modification. *Materials Science and Engineering A, 267*, 260−266.

Hanawa, T. (2004). Surface modification of metallic biomaterials. In S. H. Teoh (Ed.), *Engineering materials for biomedical applications* (pp. 4−(1−36)). Singapore: World Scientific Publishing.

Hanawa, T. (2009). Materials for metallic stents. *Journal of Artificial Organs, 12*, 73−79.

Hanawa, T. (2012). Research and development of metals for medical devices based on clinical needs. *Science and Technology of Advanced Materials, 13*, 1−15.

Han, Y., Fu, T., Lu, J., & Xu, K. (2001). Characterization and stability of hydroxyapatite coatings prepared by an electrodeposition and alkaline-treatment process. *Journal of Biomedical Materials Research, 54*, 96−101.

Hao, L., & Lawrence, J. (2005). *Laser surface treatment of bio-implant materials*. West Sussex, England: John Wiley & Sons.

Heimann, R. B. (1996). *Plasma-spray coating*. Weinheim: VCH.

Hench, L. L. (1991). Bioceramics: from concept to clinic. *Journal of American Ceramic Society, 74*, 1487−1510.

Hench, L. L., & Anderson, Ö. (1993). Bioactive glass coatings. In L. L. Hench, & L. Wilson (Eds.), *An introduction to bioceramics* (pp. 239−260). Singapore: World Scientific.

Hertz, A., & Bruce, I. J. (2007). Inorganic materials for bone repair or replacement applications. *Nanomedicine, 2*, 899−918.

Heublein, B., Rohde, R., Kaese, V., Niemeyer, M., Hartung, W., & Haverich, A. (2003). Biocorrosion of magnesium alloys: a new principle in cardiovascular implant technology? *Heart, 89*, 651−656.

Hiromoto, S. (2008). Corrosion of metallic biomaterials in cell culture environments. *The Electrochemical Society Interface, 17*, 41−44.

Hosoda, H., Fukui, Y., Inamura, T., Wakashima, K., Miyazaki, S., & Inoue, K. (2003). Mechanical properties of Ti-base shape memory alloys. *Materials Science Forum, 426-432*, 3121−3126.

Huang, S., & Ingber, D. E. (1999). The structural and mechanical complexity of cell growth control. *Nature Cell Biology, 1*, E131−E138.

Hunter, A., Archer, C. W., Walker, P. S., & Blunn, G. W. (1995). Attachment and proliferation of osteoblasts and fibroblasts on biomaterials for orthopaedic use. *Biomaterials, 16*, 287−295.

Hu, X., Shen, H., Shuai, K., Zhang, E., Bai, Y., Cheng, Y., et al. (2011). Surface bioactivity modification of titanium by CO2 plasma treatment and induction of hydroxyapatite: in vitro and in vivo studies. *Applied Surface Science, 257*, 1813−1823.

Jagielski, J., Piatkowska, A., Aubert, P., Thomé, L., Turos, A., & Abdul Kader, A. (2006). Ion implantation for surface modification of biomaterials. *Surface & Coatings Technology, 200*, 6355−6361.

Jakubowski, W., Bartosz, G., Niedzielski, P., Szymanski, W., & Walkowiak, B. (2004). Nanocrystalline diamond surface is resistant to bacterial colonization. *Diamond and Related Materials, 13*, 1761−1763.

Jansen, J. A., & León, B. (2009). Introduction. In B. León & J. A. Jansen (Eds.), *Thin calcium phosphate coatings for medical implants* (pp. 1−8). New York: Springer.

Jarmar, T., Palmquist, A., Brånemark, R., Hermansson, L., Engqvist, H., & Thomsen, P. (2008). Characterization of the surface properties of commercially available dental implants using scanning electron microscopy, focused ion beam, and high-resolution transmission electron microscopy. *Clinical Implant Dentistry and Related Research, 10*, 11−22.

Joung, Y. K., You, S. S., Park, K. M., Go, D. H., & Park, K. D. (2012). In situ forming, metal-adhesive heparin hydrogel surfaces for blood-compatible coating. *Colloids and Surfaces B: Biointerfaces, 99*, 102−107.

Kanerva, L., & Förström, L. (2001). Allergic nickel and chromate hand dermatitis induced by orthopaedic metal implant. *Contact Dermatitis, 44*, 103−104.

Kasemo, B. (2002). Biological surface science. *Surface Science, 500*, 656−677.

Kasemo, B., & Lausmaa, J. (1994). Surface properties and processes of the biomaterial-tissue interface. *Materials Science and Engineering C, 1*, 115−119.

Keselowsky, B. G., Collard, D. M., & García, A. J. (2005). Integrin binding specificity regulates biomaterial surface chemistry effects on cell differentiation. *Proceedings of the National Academy of Sciences U S A, 102*, 5953−5957.

Kim, H. G., Ahn, S. H., Kim, J. G., Park, S. J., & Lee, K. R. (2005a). Electrochemical behavior of diamond-like carbon films for biomedical applications. *Thin Solid Films, 475*, 291−297.

Kim, J. I., Kim, H. Y., Inamura, T., Hosoda, H., & Miyazaki, S. (2005b). Shape memory characteristics of Ti−22Nb−(2−8)Zr(at.%) biomedical alloys. *Materials Science and Engineering A, 403*, 334−339.

Kleinman, H. K., Klebe, R. J., & Martin, G. R. (1981). Role of collagenous matrices in the adhesion and growth of cells. *Journal of Cell Biology, 88*, 473−485.

Kobayashi, S., Ohgoe, Y., Ozeki, K., Hirakuri, K., & Aoki, H. (2007). Dissolution effect and cytotoxicity of diamond-like carbon coatings on orthodontic archwires. *Journal of Materials Science: Materials in Medicine, 18*, 2263−2268.

Kocijan, A., Conradi, M., & Schön, P. M. (2012). Austenitic and duplex stainless steels in simulated physiological solution characterized by electrochemical and X-ray photoelectron spectroscopy studies. *Journal of Biomedical and Materials Research B, 100*, 799−807.

Kohn, D. H. (1998). Metals in medical applications. *Current Opinion in Solid State and Materials Science, 3*, 309−316.

Kokubo, T., Kim, H. M., & Kawashita, M. (2003). Novel bioactive materials with different mechanical properties. *Biomaterials, 24*, 2161−2175.

Kokubo, T., Kim, H. M., Kawashita, M., & Nakamura, T. (2004). Bioactive metals: preparation and properties. *Journal of Materials Science: Materials in Medicine, 15*, 99−107.

Kokubo, T., Kushitani, H., Sakka, S., Kitsugi, T., & Yamamuro, T. (1990). Solutions able to reproduce in vivo surface-structure changes in bioactive glass-ceramics A-W3. *Journal of Biomedical Materials Research, 24*, 721−734.

Kokubo, T., Miyaji, F., & Kim, H. M. (1996). Spontaneous formation of bonelike apatite layer on chemically treated titanium metals. *Journal of American Ceramic Society, 4*, 1127−1129.

Kokubo, T., & Takadama, H. (2006). How useful is SBF in predicting in vivo bone bioactivity. *Biomaterials, 27*, 2907−2915.

Krischok, S., Blank, C., Engel, M., Gutt, R., Ecke, G., Schawohl, J., et al. (2007). Influence of ion implantation on titanium surfaces for medical applications. *Surface Science, 601*, 3856−3860.

Krukowski, M., Shively, R. A., Osdoby, P., & Eppley, B. L. (1990). Stimulation of craniofacial and intramedullary bone formation by negatively charged beads. *Journal of Oral and Maxillofacial Surgery, 48*, 468−475.

Kumar, M., Dasarathy, H., & Riley, C. (1999). Electrodeposition of brushite coatings and its transformation to hydroxyapatite in simulated body fluid. *Journal of Biomedical and Materials Research A, 45*, 302−310.

Kuo, M. C., & Yen, S. K. (2002). The process of electrochemical deposited hydroxyapatite coatings on biomedical titanium at room temperature. *Materials Science and Engineering C, 20*, 153−160.

Kurrat, R., Ramsden, J. J., & Prenosil, E. (1994). Kinetic model for serum albumin adsorption : experimental verification. *Journal of the Chemical Society, Faraday Transactions, 90*, 587−590.

Latour, R. A. (2005). Biomaterials: protein-surface interactions. In G. L. Bowlin & G. Wnek (Eds.), *Encyclopedia of biomaterials and biomedical engineering* (pp. 1−15). Taylor & Francis.

Lausmaa, J. (2001). Mechanical, thermal, chemical and electrochemical surface tretament of titanium. In D. M. Brunette, P. Tengvall, M. Textor, & P. Thomsen (Eds.), *Titanium in medicine* (pp. 231−266). Heidelberg: Springer-Verlag.

Le Guéhennec, L., Lopez-Heredia, M. A., Enkel, B., Weiss, P., Amouriq, Y., & Layrolle, P. (2008). Osteoblastic cell behaviour on different titanium implant surfaces. *Acta Biomaterialia, 4*, 535−543.

Le Guéhennec, L., Soueidan, A., Layrolle, P., & Amouriq, Y. (2007). Surface treatments of titanium dental implants for rapid osseointegration. *Dental Materials, 23*, 844−854.

Lee, D. A., & Laurencin, C. T. (2008). Surface modification of biomaterials at the nanoscale: biomimetic scaffolds for tissue engineering applications. In C. T. Laurencin, & L. S. Nair (Eds.), *Nanotechnology and tissue engineering: the scaffold* (pp. 163−196). Boca Raton: CRC Press.

Lekston, Z., & Goryczka, T. (2007). Phase transformation in Ti−Ni−Ta shape memory alloy. *Solid State Phenomena, 130*, 147−150.

Lin, Y. S., Hlady, V., & Janatova, J. (1992). Adsorption of complement proteins on surfaces with a hydrophobicity gradient. *Biomaterials, 13*, 497−504.

Liu, X., Chu, P. K., & Ding, C. (2004). Surface modification of titanium, titanium alloys, and related materials for biomedical applications. *Materials Science and Engineering R, 47*, 49−121.

Liu, X., Chu, P. K., & Ding, C. (2010). Surface nano-functionalization of biomaterials. *Materials Science and Engineering R, 70*, 275−302.

Liu, Y., & Hunziker, E. B. (2009). Biomimetic coatings and their biological functionalization. In B. Leon, & J. A. Jansen (Eds.), *Thin calcium phosphate coatings for medical implants* (pp. 301−314). New York: Springer.

Liu, X., Tao, S., & Ding, C. (2002). Bioactivity of plasma sprayed dicalcium silicate coatings. *Biomaterials, 23*, 963−968.

Liu, D. M., Troczynski, T., & Tseng, W. J. (2001). Water-based sol-gel synthesis of hydroxyapatite: process development. *Biomaterials, 22*, 1721−1730.

Li, G., Yang, P., & Huang, N. (2011). Layer-by-layer construction of the heparin/fibronectin coatings on titanium surface:stability and functionality. *Physics Procedia, 18*, 112−121.

Li, N., & Zheng, Y. (2013). Novel magnesium alloys developed for biomedical application: a review. *Journal of Materials Science and Technology, 29*, 489−502.

Lundin, M., Hedberg, Y., Jiang, T., Herting, G., Wang, X., Thormann, E., et al. (2012). Adsorption and protein-induced metal release from chromium metal and stainless steel. *Journal of Colloid and Interface Science, 366*, 155−164.

Lusquiños, F., Pou, J., Boutinguiza, M., Quintero, F., Soto, R., León, B., et al. (2005). Main characteristics of calcium phosphate coatings obtained by laser cladding. *Applied Surface Science, 247*, 486−492.

Maeshima, T., & Nishida, M. (2004). Shape memory properties of biomedical Ti−Mo−Ag and Ti−Mo−Sn alloys. *Materials Transactions, 45*, 1096.

Mani, G., Feldman, M. D., Oh, S., & Agrawal, C. M. (2009). Surface modification of cobalt−chromium−tungsten−nickel alloy using octadecyltrichlorosilanes. *Applied Surface Science, 255*, 5961−5970.

Margel, S., Vogler, E. A., Firment, L., Watt, T., Haynie, S., & Sogah, D. Y. (1993). Peptide, protein, and cellular interactions with self-assembled monolayer model surfaces. *Journal of Biomedical and Materials Research A, 27*, 1463−1476.

Marti, A. (2000). Cobalt-base alloys used in bone surgery. *Injury, 31*(Suppl. 4), 18−21.

Matsuno, H., Yokoyama, A., Watari, F., Uo, M., & Kawasaki, T. (2001). Biocompatibility and osteogenesis of refractory metal implants, titanium, hafnium, niobium, tantalum and rhenium. *Biomaterials, 22*, 1253−1262.

Maurus, P. B., & Kaeding, C. C. (2004). Bioabsorbable implant material review. *Operative Techniques in Sports Medicine, 12*, 158−160.

Meiron, T. S., Marmur, A., & Saguy, I. S. (2004). Contact angle measurement on rough surfaces. *Journal of Colloid and Interface Science, 274*, 637−644.

Mendes, V. C., Moineddin, R., & Davies, J. E. (2007). The effect of discrete calcium phosphate nanocrystals on bone-bonding to titanium surfaces. *Biomaterials, 28*, 4748−4755.

Mendes, V. C., Moineddin, R., & Davies, J. E. (2009). Discrete calcium phosphate nanocrystalline deposition enhances osteoconduction on titanium-based implant surfaces. *Journal of Biomedical Materials Research A, 90*, 577−585.

Meng, S., Liu, Z., Shen, L., Guo, Z., Chou, L. L., Zhong, W., et al. (2009). The effect of a layer-by-layer chitosan-heparin coating on the endothelialization and coagulation properties of a coronary stent system. *Biomaterials, 30*, 2276−2283.

Metikoš-Huković, M., Tkalčec, E., Kwokal, A., & Piljac, J. (2003). An in vitro study of Ti and Ti-alloys coated with sol−gel derived hydroxyapatite coatings. *Surface and Coatings Technology, 165*, 40−50.

Meyer, U., Büchter, A., Wiesmann, H. P., Joos, U., & Jones, D. B. (2005). Basic reactions of osteoblasts on structured material surfaces. *European Cells and Materials, 26*, 39−49.

Meyer, U., & Wiesmann, H. P. (2006). *Bone and cartilage engineering*. Berlin: Springer-Verlag.

Mjoberg, B., Hellquist, E., Mallmin, H., & Lindh, U. (1997). Aluminum, Alzheimer's disease and bone fragility. *Acta Orthopaedica Scandinavica, 68*, 511−514.

Morra, M., Cassinelli, C., Cascardo, G., Cahalan, P., Cahalan, L., Fini, M., et al. (2003). Surface engineering of titanium by collagen immobilization. Surface characterization and in vitro and in vivo studies. *Biomaterials, 24*, 4639−4654.

Müller, R., Abke, J., Schnell, E., Macionczyk, F., Gbureck, U., Mehrl, R., et al. (2005). Surface engineering of stainless steel materials by covalent collagen immobilization to improve implant biocompatibility. *Biomaterials, 26*, 6962−6972.

Murphy-Ullrich, J. E. (2001). The de-adhesive activity of matricellular proteins: is intermediate cell adhesion an adaptive state? *Journal of Clinical Investigation, 107*, 785−790.

Nag, S., Banerjee, R., & Fraser, H. L. (2005). Microstructural evolution and strengthening mechanisms in Ti−Nb−Zr−Ta, Ti−Mo−Zr−Fe and Ti−15Mo biocompatible alloys. *Materials Science and Engineering C, 25*, 357−362.

Nanci, A., Wuest, J. D., Peru, L., Brunet, P., Sharma, V., Zalzal, S., et al. (1998). Chemical modification of titanium surfaces for covalent attachment of biological molecules. *Journal of Biomedical and Materials Research A, 40*, 324−335.

Narayanan, R., Seshadri, S. K., Kwon, T. Y., & Kim, K. H. (2008). Calcium phosphate-based coatings on titanium and its alloys. *Journal of Biomedical Materials Research B, 85*, 279−299.

Nebe, J. G., Luethen, F., Lange, R., & Beck, U. (2007). Interface interactions of osteoblasts with structured titanium and the correlation between physicochemical characteristics and cell biological parameters. *Macromolecular Bioscience, 7*, 567−578.

Ni, S., Chang, J., Chou, L. (2006). A novel bioactive porous $CaSiO_3$ scaffold for bone tissue engineering. 76, 196−205.

Nielsen, J. P. (1986). Dental noble-metal casting alloys: composition and properties. In M. B. Bever (Ed.), *Encyclopedia of materials science and engineering* (pp. 1093−1095). Oxford: Pergamon Press.

Niinomi, M., Hattori, T., & Niwa, S. (2004). Material characteristics and biocompatibility of low ridgidity titanium alloys for biomedical applications. In M. J. Yaszemski, D. J. Trantolo, K. U. Lewandrowski, V. Hasirci, D. E. Altobelli, & D. L. Wise (Eds.), *Biomaterials in orthopedics* (pp. 41−62). New York: Marcel Dekker, Inc.

Norde, W. (2006). Surface modifications to influence adhesion of biological cells and adsorption of globular proteins. In J. P. Blitz & V. M. Gun'ko (Eds.), *Surface chemistry in biomedical and environmental science* (pp. 159−176). Dordrecht, The Netherlands: Springer.

Nouri, A. (2008). Novel metal structures through powder metallurgy for biomedical applications. PhD, Deakin University.

Nouri, A., Chen, X. B., Hodgson, P. D., & Wen, C. E. (2007). Preparation of bioactive porous Ti−Sn−Nb alloy for biomedical applications. In *Proceeding of 5th international conference on porous metals and metallic foams (MetFoam 2007)* (Montreal, Canada).

Nouri, A., Chen, X. B., Li, Y. C., Yamada, Y., Hodgson, P. D., & Wen, C. E. (2008). Synthesis of Ti−Sn−Nb alloy by powder metallurgy. *Materials Science and Engineering A, 485*, 562−570.

Nouri, A., Hodgson, P. D., & Wen, C. E. (2010). Biomimetic porous titanium scaffolds for orthopedic and dental applications. In A. Mukherjee (Ed.), *Biomimetics learning from nature* (pp. 415−450). InTech.

Nouri, A., Hodgson, P. D., & Wen, C. E. (2011). Effect of ball-milling time on the structural characteristics of biomedical porous Ti−Sn−Nb alloy. *Materials Science and Engineering C, 31*, 921−928.

Ochsenbein, A., Chai, F., Winter, S., Traisnel, M., Breme, J., & Hildebrand, H. F. (2008). Osteoblast responses to different oxide coatings produced by the sol-gel process on titanium substrates. *Acta Biomaterialia, 4*, 1506−1517.

Ohl, A., & Schroder, K. (1999). Plasma-induced chemical micropatterning for cell culturing applications: a brief review. *Surface and Coatings Technology, 116−119*, 820−830.

Okazaki, Y., Ito, Y., Kyo, K., & Tateishi, T. (1996). Corrosion resistance and corosion fatigue strength of new titanium alloys for medical implants without V and Al. *Materials Science and Engineering A, 213*, 138−147.

Ong, J. L., Appleford, M., Oh, S., Yang, Y., Chen, W. H., Bumgardner, J. D., et al. (2006). The characterization and development of bioactive hydroxyapatite coatings. *JOM, 58*, 67−69.

Ong, J. L., & Lucas, L. C. (1998). Auger electron spectroscopy and its use for the characterization of titanium and hydroxyapatite surfaces. *Biomaterials, 19*, 455−464.

Ong, J. L., Lucas, L. C., Lacefield, W. R., & Rigney, E. D. (1992). Structure, solubility and bond strength of thin calcium phosphate coatings produced by beam sputter deposition. *Biomaterials, 13*, 249−254.

Paital, S. R., & Dahotre, N. B. (2009). Calcium phosphate coatings for bio-implant applications: materials, performance factors, and methodologies. *Materials Science and Engineering R, 66*, 1−70.

Palmquist, A., Omar, O. M., Esposito, M., Lausmaa, J., & Thomsen, P. (2010). Titanium oral implants: surface characteristics, interface biology and clinical outcome. *Journal of the Royal Society Interface, 7*, S515−S527.

Parhi, P., Golas, A., & Vogler, E. A. (2010). Role of proteins and water in the initial attachment of mammalian cells to biomedical surfaces: a review. *Journal of Adhesion Science and Technology, 24*, 853−888.

Park, J. B., & Kim, Y. K. (2000). Metallic biomaterials. In J. D. Bronzino (Ed.), *The biomedical engineering handbook* (2nd ed.). FL, USA: Boca Raton: CRC Press.

Paschoal, A. L., Vanâncio, E. C., Canale, L. C., Da Silva, O. L., Huerta-Vilca, D., & Motheo Ade, J. (2003). Metallic biomaterials TiN-coated: corrosion analysis and biocompatibility. *Artificial Organs, 27*, 461−464.

Pelham, R. J., & Wang, Y. L. (1997). Cell locomotion and focal adhesions are regulated by substrate flexibility. *Proceedings of the National Academy of Sciences U. S. A, 94*, 13661−13665.

Peltola, T., Pätsi, M., Rahiala, H., Kangasniemi, I., & Yli-Urpo, A. (1998). Calcium phosphate induction by sol-gel-derived titania coatings on titanium substrates in vitro. *Journal of Biomedical Materials Research Part A, 41*, 504−510.

Peterson, C. D., Hillberry, B. M., & Heck, D. A. (1988). Component wear of total knee prostheses using Ti−6Al−4V, titanium nitride coated Ti−6Al−4V, and cobalt-chromium-molybdenum femoral components. *Journal of Biomedical and Materials Research A, 22*, 887−903.

Peuster, M., Wohlsein, P., Brugmann, M., Ehlerding, M., Seidler, K., Fink, C., et al. (2001). A novel approach to temporary stenting: degradable cardiovascular stents produced from corrodible metal—results 6−18 months after implantation into New Zealand white rabbits. *Heart, 86*, 563−569.

Pham, M. T., Matz, W., Reuther, H., Richter, E., Steiner, G., Oswald, S. (2000). Ion beam sensitizing of titanium surfaces to hydroxyapatite formation. 128−129, 313−319.

Pilliar, R. M. (1991). Modern metal processing for improved load-bearing surgical implants. *Biomaterials, 12*, 95−100.

Pilliar, R. M. (2009). Metallic biomaterials. In R. Narayan (Ed.), *Biomedical materials* (pp. 41−81). Springer.

Piveteau, L. D. (2001). Sol-Gel coatings on titanium. In D. M. Brunette, P. Tengvall, M. Textor, & P. Thomsen (Eds.), *Titanium in medicine* (pp. 267−282). Heidelberg: Springer-Verlag.

Piveteau, L. D., Girona, M. I., Schlapbach, L., Barboux, P., Boilot, J. P., & Gasser, B. (1999). Thin films of calcium phosphate and titanium dioxide by a sol-gel route: a new method for coating medical implants. *Journal of Materials Science: Materials in Medicine, 10*, 161−167.

Planell, J. A., Navarro, M., Altankov, G., Aparicio, C., Engel, E., Gil, J., et al. (2010). Materials surface effects on biological interactions. In V. P. Shastri, G. Altankov, & A. Lendlein (Eds.), *Advances in regenerative medicine: role of nanotechnology, and engineering principles* (pp. 233−252). Springer.

Plenk, H. (1998). Prosthesis−bone interface. *Journal of Biomedical Materials Research, 43*, 350−355.

Pohler, O. E. M. (2000). Unalloyed titanium for implants in bone surgery. *Injury, 31*(Suppl. 4), D7−D13.

Ponche, A., Bigerelle, M., & Anselme, K. (2010). Relative influence of surface topography and surface chemistry on cell response to bone implant materials. Part 1: physico-chemical effects. *Proceedings of the Institution of Mechanical Engineers H, 224*, 1471−1486.

Protivínský, J., Appleford, M., Strnad, J., Helebrant, A., & Ong, J. L. (2007). Effect of chemically modified titanium surfaces on protein adsorption and osteoblast precursor cell behavior. *International Journal of Oral & Maxillofacial Implants, 22*, 542−550.

Puleo, D. A., Kissling, R. A., & Sheu, M. S. (2002). A technique to immobilize bioactive proteins, including bone morphogenetic protein-4 (BMP-4), on titanium alloy. *Biomaterials, 23*, 2079−2087.

Puleo, D. A., & Nanci, A. (1999). Understanding and controlling the bone-implant interface. *Biomaterials, 20*, 2311−2321.

Ramires, P. A., Romito, A., Cosentino, F., & Milella, E. (2001). The influence of titania/hydroxyapatite composite coatings on in vitro osteoblasts behavior. *Biomaterials, 22*, 1467−1474.

Rautray, T. R., Narayanan, R., & Kim, K. H. (2011). Ion implantation of titanium based biomaterials. *Progress in Materials Science, 56*, 1137−1177.

Rezania, A., & Healy, K. E. (2000). The effect of peptide surface density on mineralization of a matrix deposited by osteogenic cells. *Journal of Biomedical and Materials Research A, 52*, 595−600.

Riesenfeld, J., Olsson, P., Sanchez, J., & Mollnes, T. E. (1995). Surface modification with functionally active heparin. *Medical Device Technology, 6*, 24−31.

Rintoul, T. C., Butler, K. C., Thomas, D. C., Carriker, J. W., Maher, T. R., Kiraly, R. J., et al. (1993). Continuing development of the Cleveland Clinic-Nimbus total artificial heart. *ASAIO, 39*, 168−171.

Robertson, S. W., & Ritchie, R. O. (2008). A fracture-mechanics-based approach to fracture control in biomedical devices manufactured from superelastic Nitinol tube. *Journal of Biomedical and Materials Research B, 84*, 26−33.

Roy, M., Vamsi Krishna, B., Bandyopadhyay, A., & Bose, S. (2008). Laser processing of bioactive tricalcium phosphate coating on titanium for load-bearing implants. *Acta Biomaterialia, 4*, 324−333.

Ruoslahti, E., & Pierschbacher, M. D. (1987). New perspectives in cell adhesion: RGD and integrins. *Science, 238*, 491−497.

Rupp, F., Scheideler, L., Olshanska, N., De Wild, M., Wieland, M., & Geis-Gerstorfer, J. (2006). Enhancing surface free energy and hydrophilicity through chemical modification of microstructured titanium implant surfaces. *Journal of Biomedical and Materials Research A, 76*, 323−334.

Sáenz De Viteri, V., Barandika, M. G., De Gopegui, U. R., Bayón, R., Zubizarreta, C., Fernández, X., et al. (2012). Characterization of Ti-C-N coatings deposited on Ti6Al4V for biomedical applications. *Journal of Inorganic Biochemistry, 117*, 359−366.

Santavirta, S., Takagi, M., Gomez-Barrena, E., Nevalainen, J., Lassus, J., Salo, J., et al. (1999). Studies of host response to orthopedic implants and biomaterials. *Journal of Long-Term Effects of Medical Implants, 9*, 67−76.

Saris, N.E., Mervaala, E., Karppanen, H., Khawaja, J.A., Lewenstam, A. (2000). Magnesium. an update on physiological, clinical and analytical aspects. 294, 1−26.

Sasaki, Y., Doi, K., & Matsushita, T. (1996). New titanium alloys for artificial hip joints. *Kinzoku, 66*, 812−817.

Schmidt, D. R., Waldeck, H., & Kao, W. J. (2009). Protein adsorption to biomaterials. In D. A. Puleo, & R. Bizios (Eds.), *Biological interactions on materials surfaces* (pp. 1−18). Springer.

Schultze, J. W., & Lohrengel, M. M. (2000). Stability, reactivity and breakdown of passive films. Problems of recent and future research. *Electrochimica Acta, 45*, 2499−2513.

Scotchford, C. A., Ball, M., Winkelmann, M., Vörös, J., Csucs, C., Brunette, D. M., et al. (2003). Chemically patterned, metal-oxide-based surfaces produced by photolithographic techniques for studying protein- and cell-interactions. II: protein adsorption and early cell interactions. *Biomaterials, 24*, 1147−1158.

Semlitsch, M. F., Weber, H., Streicher, R. M., & Schon, R. (1992). Joint replacement components made of hot-forged and surface treated Ti6Al6Nb alloy. *Biomaterials, 13*, 781−788.

Sharma, C. P., & Paul, W. (1992). Protein interaction with tantalum: changes with oxide layer and hydroxyapatite at the interface. *Journal of Biomedical Materials Research A, 26*, 1179−1184.

Silva-Bermudez, P., & Rodil, S. E. (2013). An overview of protein adsorption on metal oxide coatings for biomedical implants. *Surface & Coatings Technology, 233*, 147−158.

Sioshansi, P., & Tobin, E. J. (1996). Surface treatment of biomaterials by ion beam process. *Surface and Coatings Technology, 83*, 175−182.

Sista, S., Nouri, A., Li, Y., Wen, C., Hodgson, P. D., & Pande, G. (2013). Cell biological responses of osteoblasts on anodized nanotubular surface of a titanium-zirconium alloy. *Journal of Biomedical and Materials Research A, 101*, 3416−3430.

Søballe, K. (1993). Hydroxyapatite ceramic coating for bone implant fixation. Mechanical and histological studies in dogs. *Acta Orthopaedica Scandinavica Supplement, 255*, 1−58.

Spector, M. (1992). Biomaterial failure. *Orthopedic Clinics of North America, 23*, 211−217.

Sperling, C., Fischer, M., Maitz, M. F., & Werner, C. (2009). Blood coagulation on biomaterials requires the combination of distinct activation processes. *Biomaterials, 30*, 4447−4456.

Subramanian, K., Tran, D., & Nguyen, K. T. (2012). Cellular responses to nanoscale surface modifications of titanium implants for dentistry and bone tissue engineering applications. In K. Subramani, & W. Ahmed (Eds.), *Emerging nanotechnologies in dentistry*. Oxford: Elsevier.

Su, W. T., Chu, I. M., Yang, J. Y., & Lin, C. D. (2006). The geometric pattern of a pillared substrate influences the cell-process distribution and shapes of fibroblasts. *Micron, 37*, 699−706.

Sul, Y. T., Johansson, C. B., & Albrektsson, T. (2002a). Oxidized titanium screws coated with calcium ions and their performance in rabbit bone. *International Journal of Oral & Maxillofacial Implants, 17*, 625−634.

Sul, Y. T., Johansson, C. B., Kang, Y., Jeon, D. G., & Albrektsson, T. (2002b). Bone reactions to oxidized titanium implants with electrochemical anion sulphuric acid and phosphoric acid incorporation. *Clinical Implant Dentistry and Related Research, 4*, 78−87.

Sul, Y. T., Johansson, C. B., Röser, K., & Albrektsson, T. (2002c). Qualitative and quantitative observations of bone tissue reactions to anodised implants. *Biomaterials, 23*, 1809−1817.

Sul, Y. T., Kang, B. S., Johansson, C. B., Um, H. S., Park, C. J., & Albrektsson, T. (2009). The roles of surface chemistry and topography in the strength and rate of osseointegration of titanium implants in bone. *Journal of Biomedical and Materials Research A, 89*, 942−950.

Sun, T., Tan, H., Han, D., Fu, Q., & Jiang, L. (2005). No platelet can adhere—largely improved blood compatibility on nanostructured superhydrophobic surfaces. *Small, 1*, 959−963.

Takahashi, E., Sakurai, T., Watanabe, S., Masahashi, N., & Hanada, S. (2002). Effect of heat treatment and Sn content on superelasticity in biocompatible TiNbSn alloys. *Materials Transactions, 43*, 2978−2983.

Tamada, Y., & Ikada, Y. (1993). Effect of preadsorbed proteins on cell adhesion to polymer surfaces. *Journal of Colloid and Interface Science, 155*, 334−339.

Tanahashi, M., & Matsuda, T. (1997). Surface functional group dependence on apatite formation on self-assembled monolayers in a simulated body fluid. *Journal of Biomedical and Materials Research A, 34*, 305−315.

Tengvall, P. (2003). How surfaces interact with the biological environment. In J. E. Ellingsen & S. P. Lyngstadaas (Eds.), *Bio-implant interface, improving biomaterials and tissue reactions* (pp. 285−303). Boca Raton: CRC Press.

Thull, R. (2010). Surface treatment. In M. Niinomi (Ed.), *Metals for biomedical devices* (pp. 251−259). Boca Raton: Woodhead Publishing.

Thull, R., & Grant, D. (2001). Physical and chemical vapor deposition and plasma-assisted techniques for coating titanium. In D. M. Brunette, P. Tengvall, M. Textor, & P. Thomsen (Eds.), *Titanium in medicine* (pp. 283−341). Heidelberg: Springer-Verlag.

Trommler, A., Gingell, D., & Wolf, H. (1985). Red blood cells experience electrostatic repulsion but make molecular adhesions with glass. *Biophysical Journal, 48*, 835−841.

Tyrkiel, E., & Deardney, P. (1995). *A guide to surface engineering terminology*. London: The Insititute of Materials.

Vallet-Regi, M., García, M. M., & Colilla, M. (2013). *Biomedical applications of mesoporous ceramics*. Boca Raton, FL: CRC Press.

Variola, F., Brunski, J., Orsini, G., Tambasco De Oliveira, P., Wazen, R., & Nanci, A. (2011). Nanoscale surface modifications of medically relevant metals: state-of-the art and perspectives. *Nanoscale, 3*, 335−353.

Vickerman, J. C. (2009). Introduction. In J. C. Vickerman & I. S. Gilmore (Eds.), *Surface analysis: the principal techniques* (pp. 1−8). Singapore: John Wiley & Sons.

Virtanen, S., Milosev, I., Gomez-Barrena, E., Trebse, R., Salo, J., & Konttinen, Y. T. (2008). Special modes of corrosion under physiological and simulated physiological conditions. *Acta Biomaterialia, 4*, 468−476.

Vitale-Brovarone, C., Verné, E., Robiglio, L., Appendino, P., Bassi, F., Martinasso, G., et al. (2007). Development of glass-ceramic scaffolds for bone tissue engineering: characterisation, proliferation of human osteoblasts and nodule formation. *Acta Biomaterialia, 3*, 199−208.

Walkowiak, B. (2007). Surface-modified metallic biomaterials in contact with blood and endothelial cells. *Macromolecular Symposia, 253*, 122−127.

Wang, H., Zhao, C., Chen, Y., Li, J., & Zhang, X. (2012). Electrochemical property and in vitro degradation of DCPD−PCL composite coating on the biodegradable Mg−Zn alloy. *Materials Letters, 68*, 435−438.

Wang, G., & Zreiqat, H. (2010). Functional coatings or films for hard-tissue applications. *Materials, 3*, 3994−4050.

Ward, B. C., & Webster, T. J. (2007). Increased functions of osteoblasts on nanophase metals. *Materials Science and Engineering C, 27*, 575−578.

Wei, J., Igarashi, T., Okumori, N., Igarashi, T., Maetani, T., Liu, B., et al. (2009). Influence of surface wettability on competitive protein adsorption and initial attachment of osteoblasts. *Biomedical Materials, 4*, 045002.

Wei, M., Ruys, A. J., Swain, M. V., Milthorpe, B. K., & Sorrell, C. C. (2005). Hydroxyapatite-coated metals: Interfacial reactions during sintering. *Journal of Materials Science: Materials in Medicine, 16*, 101−106.

Wennerberg, A., Hallgren, C., Johansson, C., & Danelli, S. (1998). A histomorphometric evaluation of screw-shaped implants each prepared with two surface roughnesses. *Clinical Oral Implants Research, 9*, 11−19.

Wen, C. E., Xu, W., Hu, W. Y., & Hodgson, P. D. (2007). Hydroxyapatite/titania sol-gel coatings on titanium-zirconium alloy for biomedical applications. *Acta Biomaterialia, 3*, 403−410.

Williams, D. F. (1990). *Concise encyclopedia of medical and dental materials*. Oxford: Pergamon Press.

Williams, D. F. (2001). Titanium for medical applications. In D. M. Brunette, P. Tengvall, M. Textor, & P. Thomsen (Eds.), *Titanium in medicine* (pp. 11−24). Heidelberg: Springer-Verlag.

Williams, R. L., & Williams, D. F. (1989). The spatial resolution of protein adsorption on surfaces of heterogeneous metallic biomaterials. *Journal of Biomedical Materials Research, 23*, 339−350.

Wilson, C. J., Clegg, R. E., Leavesley, D. I., & Pearcy, M. J. (2005). Mediation of biomaterial-cell interactions by adsorbed proteins: a review. *Tissue Engineering, 11*, 1−18.

Wise, S. G., Mithieux, S. M., & Weiss, A. S. (2009). Engineered tropoelastin and elastin-based biomaterials. In D. S. Eisenberg & A. Mcpherson (Eds.), *Advances in protein chemistry and structural biology* (vol. 78, pp. 1−24). Oxford, UK: Elsevier.

Wu, G., Ibrahim, J. M., & Chu, P. K. (2013). Surface design of biodegradable magnesium alloys-a review. *Surface and Coatings Technology, 233*, 2−12.

Xiao, S., Textor, M., & Spencer, N. (1998). Covalent attachment of cell-adhesive, (Arg−Gly−Asp)-containing peptides to titanium surfaces. *Langmuir, 14*, 5507−5516.

Xu, L. C., & Siedlecki, C. A. (2007). Effects of surface wettability and contact time on protein adhesion to biomaterial surfaces. *Biomaterials, 28*, 3273−3283.

Yang, J., Cui, F. Z., Lee, I. S., & Wang, X. (2010). Plasma surface modification of magnesium alloy for biomedical application. *Surface and Coatings Technology, 205*, S182−S187.

Yang, Y., Kim, K. H., & Ong, J. L. (2005). A review on calcium phosphate coatings produced using a sputtering process—an alternative to plasma spraying. *Biomaterials, 26*, 327−337.

Yang, H., Li, J., Zhou, Z., & Ruan, J. (2013). Structural preparation and biocompatibility evaluation of highly porous tantalum scaffolds. *MaterialsLetters, 100*, 152−155.

Yang, Y., Oh, N., Liu, Y., Chen, W., Oh, S., Appleford, M., et al. (2006). Enhancing osseointegration using surface-modified titanium implants. *JOM, 58*, 71−76.

Yin, Y., Wise, S. G., Nosworthy, N. J., Waterhouse, A., Bax, D. V., Youssef, H., et al. (2009). Covalent immobilisation of tropoelastin on a plasma deposited interface for enhancement of endothelialisation on metal surfaces. *Biomaterials, 30*, 1675−1681.

Yu, S. Y., Scully, J. R., & Vitus, C. M. (2001). Influence of niobium and zirconium alloying additions on the anodic dissolution behavior of activated titanium in HCl solutions. *Journal of the Electrochemical Society, B148*, 68−78.

Zeng, Q., Chen, Z. Q., Li, Q. L., Li, G., & Darvell, B. W. (2005). Surface modification of titanium implant and in vitro biocompatibility evaluation. *Key Engineering Materials, 288-289*, 315−318.

Surface properties and characterization of metallic biomaterials

2

G. Mani
University of South Dakota, Sioux Falls, SD, USA

2.1 Introduction

The surface properties of biomaterials play a crucial role in determining the success of medical implants and devices. Although a biomaterial has excellent bulk properties for a specific application, if the surface properties are not suitable, the implant will fail. For example, a metallic biomaterial developed for an orthopedic application may have excellent load-bearing mechanical properties, but if the material surface does not support osseointegration, it cannot be used for this application unless the surface is modified. In another example, a metallic biomaterial developed for a coronary stent application may have excellent mechanical properties for implantation using balloon catheters, but if the material surface is not anti-thromogenic, the material cannot be used for this application. Generally, when a biomaterial is implanted inside the body, the proteins will first adsorb onto the material surface within few seconds (Dee et al., 2002). Once a monolayer of proteins is adsorbed in few minutes, then the cells will arrive and interact with the proteins that are already adsorbed onto the biomaterial surface. Hence, the cell−biomaterial interaction is mediated only through the proteins adsorbed on the biomaterial surface (Dee et al., 2002). The type, amount, and orientation of proteins adsorbed on biomaterials are determined by the surface properties of the biomaterials and by the properties of the proteins (Dee et al., 2002). The proteins adsorbed on a material surface will strongly influence the adhesion, proliferation, and differentiation of cells. Hence, the nature of protein adsorption on a biomaterial surface plays a major role in determining the implant−tissue interface. Also, the proteins adsorbed can alter the surface properties and degradation properties of the biomaterial (Dee et al., 2002). In this chapter, the surface properties of metallic biomaterials and the different instrumentation that are commonly used to characterize the surface of biomaterials are discussed.

2.2 Surface properties and characterization techniques

The surface properties that play a major role in determining the success of biomaterials are surface chemistry, surface wettability, surface texture, and surface charges. Most of the commonly used metallic biomaterials, such as titanium, titanium alloy

Surface Coating and Modification of Metallic Biomaterials. http://dx.doi.org/10.1016/B978-1-78242-303-4.00002-8
Copyright © 2015 Elsevier Ltd. All rights reserved.

(Ti-6Al-4V), 316L stainless steel, cobalt−chromium alloys, and nitinol, have a stable surface oxide layer that provides excellent corrosion-resistant properties. The surface chemistry of these metals is primarily determined by the chemical composition of a surface oxide layer, which is primarily the metal oxides corresponding to the metal. From wettability perspective, the surfaces of metals can be hydrophilic, hydrophobic, or in between. Regarding surface texture, there are numerous textures that are available on metals in macroscale, microscale, and nanoscale. The surface charges of metals can be positive, negative, or neutral. A variety of instruments are currently available to characterize the different surface properties of metals. Fourier transform infrared spectroscopy (FTIR), X-ray photoelectron spectroscopy (XPS), and time-of-flight secondary ion mass spectrometry (Tof-SIMS) are the instruments commonly used to characterize the surface chemistry. Contact angle goniometry is used to characterize the surface wettability. Scanning electron microscopy (SEM), atomic force microscopy (AFM), and profilometry techniques are commonly used to characterize the surface texture. The zeta potential analysis technique is used to characterize the surface charges. In this chapter, the surface properties of biomaterials and the different instruments that are used to characterize them are covered.

2.3 Surface chemistry

Most metallic biomaterials that are commonly used are metal oxide systems. These systems have an oxide layer on the surface. Hence, the surface chemistry of these systems directly depends on the chemical composition of the surface oxide layer. The oxide layer is mainly composed of metal oxides corresponding to that metal. For example, titanium has a titanium oxide (TiO_2) layer on its surface. 316L stainless steel contains mainly chromium oxide (Cr_2O_3) and some iron oxide (Fe_2O_3) in its oxide layer. Similarly, cobalt−chromium alloys have chromium oxide (Cr_2O_3) and cobalt oxide (CoO) in their oxide layer. The native oxide layer of most metal oxide systems contains some hydroxyl (−OH) group functionalities (Mani et al., 2010). The density of −OH groups on metal oxides varies greatly because it depends on the conditions in which the metal was processed and cleaned. Hydrocarbon ($-CH_3$, $-CH_2$, and −CH functionalities) contamination on the surface oxide layer is also very common with the metal oxide systems (Mani et al., 2008, 2010). Hence, the metallic biomaterials are typically cleaned using a variety of organic solvents to remove hydrocarbons and other contaminations from the surface oxide layer. The metallic biomaterials are commonly surface modified for a variety of biomedical applications. The surface modification typically involves either altering the original surface or depositing a coating on the existing surface (Ratner et al., 2004). In both the cases, all the surface properties including surface chemistry will then depend on the nature of modified surfaces and not on the original surfaces. For example, titanium can be surface modified using titanium nitride to improve its wear resistance. In this case, the surface chemistry will depend on the titanium nitride and not on the original titanium oxide surface. The surface modification can provide a variety of reactive functional groups, such as carboxylic acid (−COOH), amine ($-NH_2$), and hydroxyl (−OH) on metal

oxide surfaces. Because the surface chemistry of metals has an important role in determining protein adsorption and the following cellular behavior, the surfaces need to be characterized thoroughly for the surface chemistry. FTIR, XPS, and Tof-SIMS are some of the instruments commonly used to characterize the surface chemistry of metallic biomaterials.

2.3.1 Fourier transform infrared spectroscopy

FTIR is a standard analytical instrument that is used to characterize the surface chemistry of biomaterials. It provides information regarding the vibrations of atomic and molecular species. Atoms in molecules undergo vibrations such as stretching (change in bond length) and bending (change in bond angle) (Robinson et al., 2005). When the infrared radiation is allowed to interact with the vibrating molecule on a sample, a portion of the radiation with frequencies equal to the frequencies of vibrations is absorbed by the molecule (Robinson et al., 2005; Sibilia et al., 1988). The analysis of the remaining portion of the radiation transmitted through the sample provides information regarding the structure of the molecule (Robinson et al., 2005; Sibilia et al., 1988). Conventionally, the infrared spectroscopy consists of an infrared radiation source, a monochromator, and a detector (Leng, 2008; Robinson et al., 2005). The infrared radiation produced from the source has a wide range of wavelengths. The radiation passes through the sample and the monochromator, where the radiation is dispersed into its constituent wavelengths, and the wavelengths are processed one at a time. The detector then measures the intensities of different wavelengths. The main limitation of conventional infrared spectroscopy is the longer scanning time (Robinson et al., 2005). However, in the modern day FTIR, interferometers are used instead of monochromators (Cox, 1992; Roberts, 1992; Robinson et al., 2005; Sibilia et al., 1988). With the use of interferometers, all wavelengths of the radiation are processed simultaneously. Hence, the data are obtained at a faster rate. A Fourier transformation is applied to convert the obtained interferogram (a plot of signal intensity versus time) into the final infrared spectrum (a plot of wavenumber versus absorbance intensity or % transmittance) (Leng, 2008; Robinson et al., 2005; Zhang et al., 2008). The FTIR is well known for its high sensitivity and providing spectra with low signal-to-noise ratio. Also, in most cases, it can be used as a nondestructive technique. Different types of sampling modes can be used in FTIR to characterize a wide variety of samples. The commonly used different sampling modes are: (1) attenuated total reflection (ATR); (2) specular reflectance; and (3) diffuse reflectance infrared Fourier transform infrared spectroscopy (DRIFTS) (Figure 2.1).

2.3.2 Attenuated total reflection

The ATR mode is commonly used to characterize the surface chemistry of metallic, polymeric, and ceramic biomaterials (Ratner et al., 2004). In ATR, the sample to be characterized is tightly pressed on a crystal with high refractive index (Figure 2.1(a)). The infrared beam is allowed to pass through the crystal and internally reflected several times. This process creates evanescent waves that pass into the sample at a depth

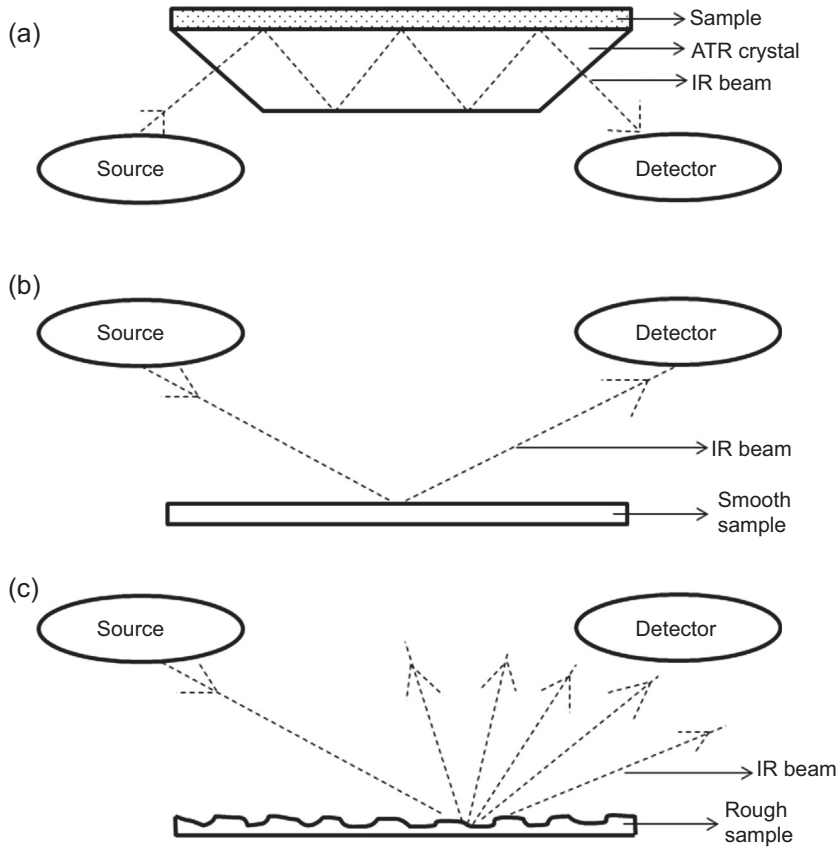


Figure 2.1 Schematic of (a) attenuated total reflection, (b) specular reflectance, (c) diffuse reflectance infrared Fourier transform infrared spectroscopy.

of 1−5 μm (Ratner et al., 2004; Robinson et al., 2005). In the infrared regions, where the sample absorbed energy, the evanescent waves will be attenuated. The attenuated energy of evanescent waves is passed back to the IR beam coming out at the opposite end of the crystal and enters the detector. Because the ATR has large penetration depth, it is not considered as an entirely surface-sensitive technique. However, it provides ample information regarding the molecular structure of organic coatings, polymer coatings, and proteins and other biomolecules deposited on metallic biomaterials (Ratner et al., 2004).

2.3.3 Specular reflectance

The specular reflectance mode is used to characterize thin films on smooth and highly reflective surfaces (Figure 2.1(b)). In this mode, when an IR beam is allowed to pass through the thin film-coated polished surface, the two events, absorption and reflection, occur (Robinson et al., 2005). The absorption event occurs when the IR beam

passes through the film, while the reflection event occurs when the beam is reflected from the polished surface underlying thin films. The analysis of the IR beam reflected back provides information regarding the IR energy absorbed by the thin film. In specular reflectance, the angle of reflection of an IR beam is equivalent to its angle of incidence. Typically, an angle of 30°−45° from the normal is used in this mode to study thin films with information obtained from a depth of 0.5−100 μm (Robinson et al., 2005). The advanced version of specular reflectance is called infrared reflection absorption spectroscopy (IRRAS), in which the angle of incidence of an infrared beam is 80° or greater. This highly surface-sensitive technique is also known as grazing angle analysis. This technique is used to characterize the molecular coatings, which have a thickness typically less than 10 nm, on metal surfaces (Ratner et al., 2004). A polarizer can be used in IRRAS to determine the orientation of molecules on the metal surfaces.

2.3.4 Diffuse reflectance infrared Fourier transform spectroscopy

The DRIFTS mode is used to characterize the surface chemistry of high-surface-area materials, such as powders, particles, and rough surfaces (Figure 2.1(c)). When the IR beam is allowed to pass through a sample of particles, the beam can either reflect back from a particle surface or it can transmit through the particle and reflect back from another particle surface. This transmission−reflection event occurs multiple times inside the sample. After that, the IR beam coming out of the sample is collected and focused onto the detector using an ellipsoid or a paraboloid mirror. During the IR beam−particles interaction, a part of the IR energy is absorbed by the particles, and this information is used to generate an IR spectrum. The size of the particles used for this characterization should be 5 μm or less. The powder samples can be analyzed as they are. If a sample absorbs too much energy, it should be diluted in nonabsorbent matrix such as KBr and KCl. The penetration depth of an infrared radiation in this sampling mode is about 100 μm (Robinson et al., 2005).

2.3.5 X-ray photoelectron spectroscopy

XPS is a surface-sensitive technique that is used to determine quantitative elemental composition and molecular composition of a material surface. This technique is also known as electron spectroscopy for chemical analysis (Ratner, 2004; Wachtman, 1993). XPS works on the principle of photoelectric effect (Brundle, 1992; Ratner, 2004; Wachtman, 1993). In XPS, a beam of X-rays is allowed to irradiate a sample to eject electrons from the inner shells of atoms present on the surface. The electrons that are ejected are called photoelectrons. The kinetic energy of the photoelectrons is measured, and the binding energy of the electrons is then calculated using the following equation (Brundle, 1992; Kibel, 1992; Ratner, 2004; Wachtman, 1993):

$$\mathrm{BE} = h\nu - \mathrm{KE} \tag{2.1}$$

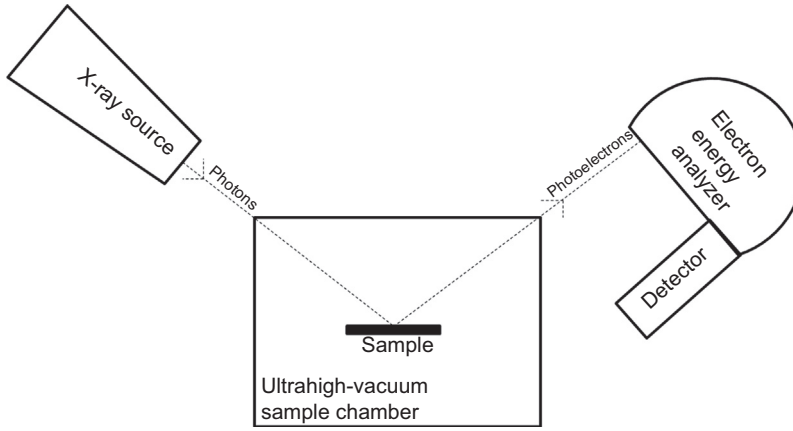


Figure 2.2 Schematic of an X-ray photoelectron spectrometer.

In the above Eqn (2.1), BE is the binding energy of the photoelectrons, $h\nu$ is the energy of the photons with h as Planck's constant (6.626×10^{-34} Js) and ν as the frequency of the radiation, and KE is the kinetic energy of the photoelectrons.

The primary components of an XPS system include: (1) an X-ray source; (2) an ultrahigh-vacuum sample chamber; (3) an electron energy analyzer; and (4) a computer (Figure 2.2). The two X-ray sources that are commonly used in XPS are Mg K_α radiation with an $h\nu$ of 1253.6 eV and Al K_α radiation with an $h\nu$ of 1486.6 eV (Kibel, 1992; Leng, 2008). The samples to be analyzed are placed in an ultrahigh-vacuum chamber to avoid any contamination and to maximize the number of photoelectrons reaching the energy analyzer. The energy analyzer calculates the kinetic energy of the photoelectrons. The emitted photoelectrons will have kinetic energies in the range of 0−1250 eV or 0−1480 eV, depending on the type of X-ray source used in the system. Once the kinetic energies are determined, the computer then calculates the binding energies of the photoelectrons. Because the binding energies of electrons present in the different orbitals (1s, 2s, 2p, etc.) of atoms are already known from the literature, the type of elements present on the material surface is determined.

XPS detects all elements except hydrogen and helium (Brundle, 1992; Ratner, 2004). The chemical bonding of elements can also be determined by XPS. It provides information regarding the top 1−10 nm of the material surface. The detection limit varies from 0.1 to 1.0 atom% (Wachtman, 1993; Zhang et al., 2008). Depending on the system design, the area of analysis varies from 10 to 200 μm (Zhang et al., 2008). Depth profiling is a technique that is used in XPS for determining the elemental information in the subsurface of a material (Kibel, 1992; Leng, 2008; Zhang et al., 2008). In depth profiling, the sample surface is slowly etched over a period, and the new surfaces obtained are characterized at regular intervals to determine the elements present in the subsurface for up to a depth of 1 μm. In this way, XPS provides quantitative information regarding the elements present at different depths of the sample surface.

2.3.6 Secondary ion mass spectrometer

SIMS is one of the most surface-sensitive techniques that is currently available to determine the atomic and molecular compositions of a material surface at a depth of 1−2 nm. It can detect all elements, including hydrogen, on the material surface. The elements with a concentration less than 1 ppm can also be measured using SIMS.

The primary components of a SIMS system include: (1) a primary ion gun; (2) an ultrahigh-vacuum sample chamber; (3) an energy analyzer; (4) a mass analyzer; (5) a detector; and (6) a computer (Figure 2.3). In most cases, the primary ions used for bombarding the samples are from noble gas such as Argon (Ar) (Leng, 2008; Macdonald and King, 1992). The ions from other gases, such as cesium, oxygen, and gallium, have also been used (Leng, 2008; Macdonald and King, 1992). SIMS works on the principle of sputtering (Vickerman and Swift, 1997). An ultrahigh-vacuum chamber is needed to prevent the contamination of samples during the analysis and to maximize the number of secondary ions reaching the detector. A beam of primary ions is allowed to collide with the material surface to generate secondary

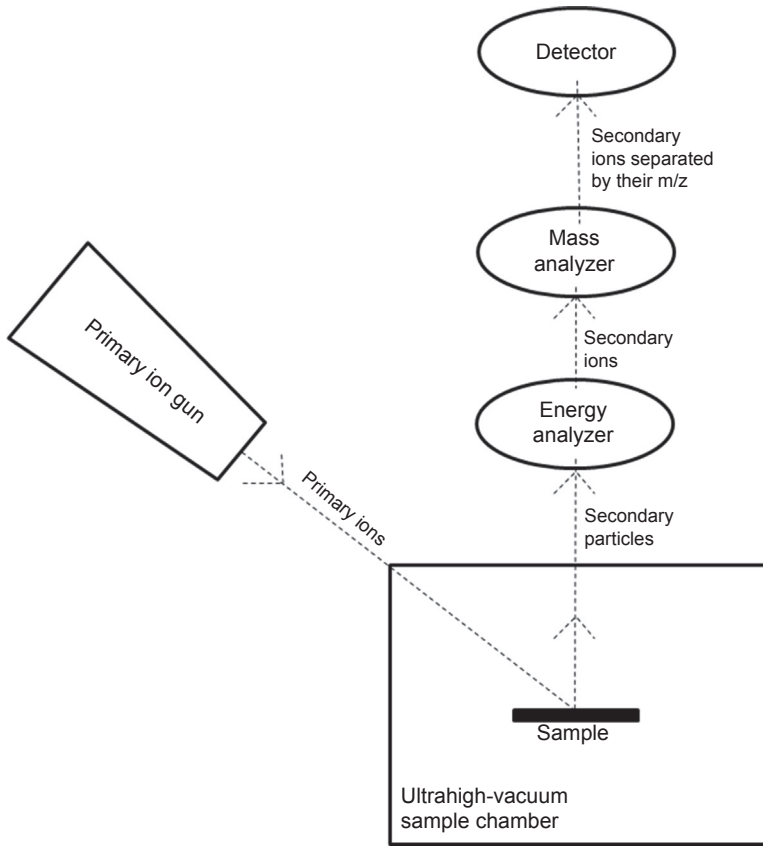


Figure 2.3 Schematic of a secondary ion mass spectrometer.

particles; it consists of mostly neutral species and few (~1%) positive and negative ion species (secondary ions) (Leng, 2008; Macdonald and King, 1992; Vickerman and Swift, 1997). The energy analyzer separates the secondary ions from the secondary particles and passes them onto the mass analyzer, which separates the secondary ions based on their mass-to-charge ratio (*m*/*z*) (Macdonald and King, 1992). The detector then counts the number of ions according to their *m*/*z*. The three different types of mass analyzers used in SIMS are: (1) sector; (2) quadrupole; and (3) time-of-flight (Tof). The Tof is the most sensitive and commonly used mass analyzer in SIMS (Leng, 2008). The Tof works on the principle of measuring the time taken by the secondary ions to reach the detector.

SIMS can be operated in two different modes, static SIMS and dynamic SIMS (Leng, 2008; Ratner, 2004; Vickerman and Swift, 1997). In static SIMS, the dose of primary ions used to colloid the sample surface is low ($<10^{13}$ ions/cm^2). Only 10% of the atoms or molecules on the sample surface are sputtered in this mode. Hence, the sample surface is minimally damaged in this mode of analysis. However, dynamic SIMS is a destructive technique (Vickerman and Swift, 1997). In this mode, a high dose of primary ions is used to etch the sample surface for a period, and the chemical composition is obtained at regular intervals at different depths. This method, which is similar to XPS depth profiling, provides elemental and chemical information of the material surface at different depths.

Although SIMS is a highly surface-sensitive technique, there are two limitations. First, unlike XPS, SIMS is not a quantitative technique because the intensity of secondary ions is not directly proportional to the elemental concentrations on the sample surface (Leng, 2008). Second, unlike XPS spectra, the spectra of SIMS are complex for interpretation (Agrawal et al., 2014). Hence, extensive training and experience are necessary for interpreting SIMS spectra.

2.4 Surface wettability

When a drop of liquid is placed on a solid sample, the extent to which the liquid drop spreads on the sample surface defines the wettability. This is determined by measuring the angle made by a liquid at the boundary at which liquid, solid, and gas phases intersect (Agrawal et al., 2014). The angle that is measured is called contact angle. A contact angle value of 0° represents a surface that is completely wettable, whereas a contact angle value of 180° represents a surface that is completely nonwettable. Typically, the surfaces that show water contact angles less than 30° are called hydrophilic, while the surfaces that show water contact angles greater than 90° are called hydrophobic. The surfaces that show water contact angles in between those of hydrophilic and hydrophobic surfaces are called moderately wettable.

For hydrophilic surfaces, the force between the molecules of water (cohesive force) will be lower than the force between water molecules and molecules at the solid surface (adhesive force). Hence, the water spreads on the surfaces. For hydrophobic surfaces, the cohesive force will be greater than the adhesive force. Hence, the water beads up on the surfaces. A balance between the surface tensions of solid−gas,

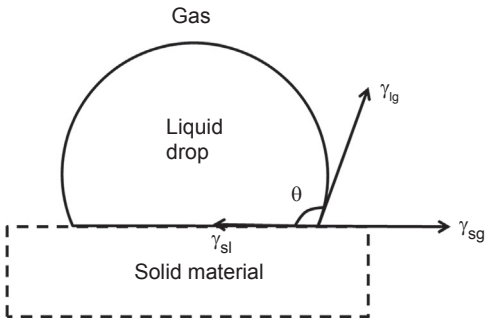


Figure 2.4 Schematic illustrating the balance between the surface tensions of solid−gas, liquid−gas, and solid−liquid interfaces.

liquid−gas, and solid−liquid interfaces primarily determines how much the liquid will be spread on a solid surface (Figure 2.4). The relationship between the interfacial tensions and contact angle is provided by Young's equation (Ratner, 2004; Zhang et al., 2008):

$$\gamma_{sg} = \gamma_{sl} + \gamma_{lg} \cos \theta \tag{2.2}$$

in which γ_{sg} is the interfacial tension between the solid and the gas; γ_{sl} is the interfacial tension between the solid and the liquid; γ_{lg} is the interfacial tension between the liquid and the gas; and θ is the contact angle measured.

In the above Eqn (2.2), the two unknown parameters are γ_{sg} and γ_{sl}. These parameters can be determined either by Zisman method or by solving simultaneous equations (Ratner et al., 2004). The Zisman method involves measuring contact angles (θ) on a solid surface using multiple liquids with known surface tension values (γ_{lg}). A plot will then be made with γ_{lg} versus θ. The value of γ_{sg} will be determined by extrapolating the plot to the contact angle value of 0°. The determined γ_{sg} value is also known as critical surface tension value (γ_c) of the material. The method of determining γ_{sg} by solving simultaneous equations involves the use of two different liquids with known values of γ_{lg}. The contact angle values on a solid surface will be determined using the two liquids. Then, the contact angle and γ_{lg} values of the two liquids will be substituted in Eqn (2.2) to obtain two equations with two unknown variables (γ_{sg} and γ_{sl}). These two simultaneous equations will be solved to determine the value for γ_{sg}.

Surface wettability plays a crucial role in determining the cell behavior on biomaterials (Arima and Iwata, 2007; Lee et al., 1998; Mani et al., 2009; Wachem et al., 1985, 1987). Several studies in the literature have shown that moderately wettable surfaces favor the adhesion and growth of cells (Arima and Iwata, 2007; Lee et al., 1998; Mani et al., 2009; Wachem et al., 1985, 1987). This could be due to the preferential adsorption of cell-adhesive proteins such as fibronectin and vitronectin on moderately wettable surfaces when compared to more hydrophilic or hydrophobic surfaces. In general, hydrophilic surfaces resist protein adsorption, while hydrophobic surfaces favor protein adsorption (Ratner et al., 2004). When a material surface resists the

adsorption of proteins, the cell growth is expected to be poor on the surface because the cell−material interaction mainly occurs through adsorbed proteins. Hydrophobic surfaces tend to strongly adsorb the non-cell-adhesive proteins such as albumin due to their higher concentration, smaller size, and quicker arrival to the biomaterial surface. Hence, the albumin layer on the biomaterial surface will be hard to replace by cell-adhesive proteins such as fibronectin due to its lower concentration, larger size, and late arrival to the biomaterial surface. The structure of most proteins in its original conformation contains hydrophilic functional groups on the outside of its coiled structure, while the hydrophobic functional groups are hidden inside the structure. When the proteins adsorb onto hydrophobic surfaces, the structure could unfold (denature) due to hydrophobic−hydrophobic interactions occurring between the hydrophobic functional groups of protein and hydrophobic material surface. The altered conformation of adsorbed proteins could also result in poor cell growth on the biomaterial surfaces. Thus, surface wettability is one of the important parameters that influence the biocompatibility of biomaterials. The instrument that is commonly used to measure surface wettability of a solid material is the contact angle goniometer.

2.4.1 Contact angle goniometry

The currently available contact angle goniometers consist of: (1) a flat platform to hold the sample; (2) a syringe to place a drop of liquid on the sample surface; (3) a source to shed light on the liquid drop; (4) a charge-coupled camera to capture an image of the liquid drop placed on the sample surface; and (5) a computer to process the image to determine the contact angle.

Contact angles are typically measured by two different methods (Agrawal et al., 2014). The first method involves simply measuring the contact angle of a liquid drop placed on a material surface. In the second method, a liquid drop is first placed on a material surface, and the contact angle is measured. After that, additional liquid drops are gradually added to the original liquid drop to maximize its volume, but without increasing the solid and liquid interfacial area. The contact angles are measured regularly after the addition of every liquid drop. The contact angles measured will reach a plateau after reaching a maximum value, and the angle at the plateau is called the advancing contact angle. The liquid drops are then gradually removed to minimize the volume of the expanded liquid drop without decreasing the solid and liquid interfacial area. The contact angles measured will reach a plateau after reaching a minimum value, and the angle at the plateau is called the receding contact angle. The difference between advancing and receding contact angles is called contact angle hysteresis. The hysteresis provides information regarding whether a material surface is homogeneous or heterogeneous (Agrawal et al., 2014). A low hysteresis value indicates a homogeneous material surface, while a high hysteresis value indicates a heterogeneous material surface (Agrawal et al., 2014).

The advantages of contact angle goniometry are its inexpensive instrumentation and the simplicity of the technique (Ratner et al., 2004). The limitations include variations in the assignment of tangent and base lines of the liquid drop by different operators.

Although the use of software systems significantly minimizes this discrepancy, still it is a concern for reflective or nonconventional samples. The liquids used to measure contact angles can sometimes change the original structure of the material surface by swelling, dissolving, or re-orienting (Ratner et al., 2004). Also, the liquids used can get contaminated during the procedure, especially when receding contact angles are measured.

2.5 Surface texture

Textured surfaces are commonly used in orthopedic, dental, and cardiovascular implants and devices. Surface textures assist in the growth of different types of cells on various medical implants and devices (Flemming et al., 1999). The favorable response could be due to some of the textured surfaces mimicking the extracellular matrix. Also, the textured surfaces can serve as reservoirs for delivering therapeutic drugs, proteins, or other biomolecules (Lancaster et al., 2012). In the biomedical literature, the term surface texture generally encompasses the surface morphological (two-dimensional) and surface topographical (three-dimensional (3D)) features of a biomaterial surface. The surface textures can be either engineered or created randomly (Hamilton et al., 2008). The engineered surface textures include grooves, ridges, steps, pits, holes, tunnels, and tubes (Hamilton et al., 2008). These textures can be created using various techniques, including lithography, casting, printing, and stamping. The randomly created nonstructured rough surfaces are prepared by sandblasting and etching (Hamilton et al., 2008). Several different types of cells, including chondrocytes, endothelial cells, epithelial cells, fibroblasts, leucocytes, macrophages, neurons, osteoblasts, and osteoclasts, have been shown to react to surface textures (Curtis and Wilkinson, 1997, 1998). The changes in gene expression and cytoskeletal and morphological changes have been observed for the cells interacting with various surface textures (Curtis and Wilkinson, 1997, 1998). The specific response of cells depends on the type and dimensions of surface texture that these are interacting with. The instrumentations that are commonly used for characterizing surface textures of biomaterials are SEM, AFM, and profilometry techniques.

2.5.1 Scanning electron microscopy

SEM is one of the commonly used microscopy techniques to image the texture of a material surface. It provides 3D-like images of surface morphology at nanometer resolutions (Brandon and Kaplan, 1999; Leng, 2008; Ratner, 2004; Zhang et al., 2008). The main advantages of SEM are its easy usage and maintenance. SEM consists of: (1) an electron gun; (2) electromagnetic lenses and apertures; (3) scanning coils; (4) a specimen holding chamber; (5) a detector; and (6) a computer (Figure 2.5).

In SEM, a high-energy (30-keV) electron beam is generated by heating a tungsten filament. The electron beam is initially focused onto the specimen surface by the electromagnetic lenses and apertures and then rastered across the surface of the specimen using scanning coils. The electrons collided on the specimen surface undergo both

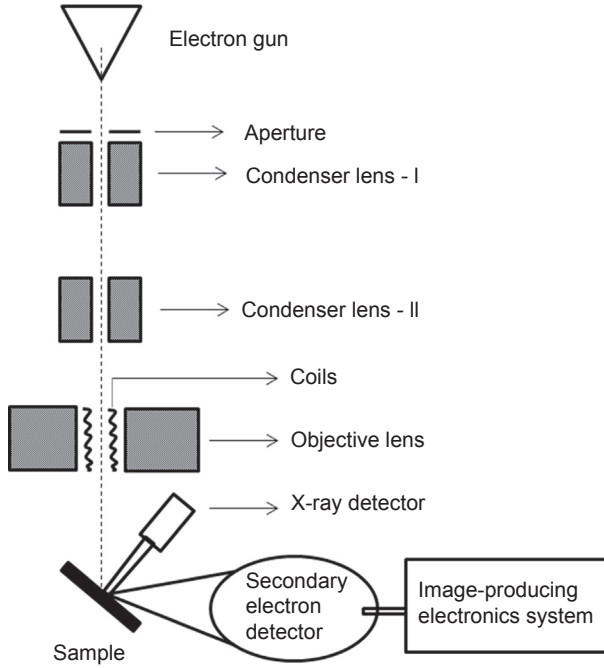


Figure 2.5 Schematic of a scanning electron microscope.

elastic and inelastic scattering to produce secondary electrons, backscattered electrons, X-rays, auger electrons, and cathodoluminescence radiation. During elastic scattering, no energy is transferred from the electrons to the colliding atoms, and the electrons are simply bounced off from the specimen surface as backscattered electrons. However, during inelastic scattering, all or at least part of the energy is transferred from the electrons to the colliding atoms, and the excess energy obtained is released by the atoms as secondary electrons or X-rays. The secondary electrons are then collected in the detector and processed further to obtain images of the material surface. The secondary electrons, backscattered electrons, and X-rays detected are analyzed for obtaining information regarding topography, atomic number, and chemical composition, respectively (Leng, 2008). An X-ray energy dispersive spectrometer is commonly used to analyze the energy and intensity of X-rays generated for determining the elemental composition of the material surface (Leng, 2008; Ratner, 2004). An X-ray energy dispersive spectrometer is not a surface-sensitive technique, because the X-rays are generated from the depth of a micron or more within the specimen.

For SEM characterization, a specimen has to be conductive or semiconductive (Bindell, 1992; Ratner, 2004). Because most metallic biomaterials are conductive, the specimens can be imaged as it is. However, if the metallic biomaterials are surface modified with nonconductive materials such as polymers, biological, or organic materials, then the specimens have to be coated with a thin film of conductive material

(e.g., gold−palladium alloy) to prevent build-up of negatively charged electrons on the specimen surface (Bindell, 1992; Ratner, 2004). In this way, good-quality images of the nonconductive material surfaces can be obtained.

2.5.2 Atomic force microscopy

AFM is used to characterize the 3D topography of a material surface with extremely high resolution in nanometers or angstroms (Leng, 2008). The primary components of an AFM include: (1) a cantilever with a sharp tip (probe) at its end; (2) a piezoelectric scanner that is capable of moving the sample in x, y, and z directions; (3) a source of laser; (4) a position-sensitive detector; and (5) a computer to process the data (Figure 2.6).

In AFM analysis, when the probe is carefully brought close to the sample surface at a distance of few angstroms, the forces such as van der Waals, capillary, or electrostatic that are generated between the probe and sample surface deflect the cantilever (Leggett, 1997; Leng, 2008; Zhang et al., 2008). To maintain a constant force between the probe and sample surface, the piezoelectric scanner moves the sample up and down, so that the probe follows the contour of the material surface. The deflection of the probe is accurately measured by passing the laser beam to reflect from the cantilever and passed onto the detector. The signal received by the detector is ultimately converted into an image.

The force generated between the probe and sample surface is quantitatively calculated by Hooke's law:

$$F = -kx \tag{2.3}$$

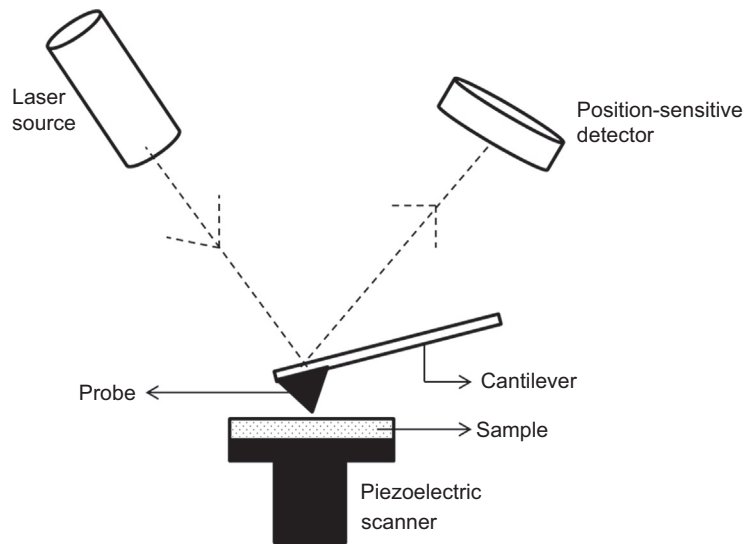


Figure 2.6 Schematic of an atomic force microscope.

In this Eqn (2.3), F is the force generated between the probe and sample surface, k is the spring constant of the cantilever, and x is the cantilever deflection.

The two different types of modes in which the AFM can acquire images are contact mode and tapping mode (Ratner, 2004; Zhang et al., 2008). In contact mode, the probe makes physical contact with the sample surface in such a gentle way that the electron clouds of atoms present on the probe and the sample surface overlap. In this mode, a constant force is maintained between the probe and sample surface by maintaining constant deflection of the cantilever. This mode is commonly used for rigid samples such as metallic biomaterials. However, if the metallic biomaterials are surface modified with soft materials such as polymers, proteins, or other biological materials, then the contact mode AFM imaging is not preferred because the force exerted in a small focused area can easily damage the soft coating. In tapping mode, the probe taps on the specimen surface and is oscillated at or closer to its fundamental frequency. In this case, the amplitude of the oscillation, which is affected by the force of interaction between the probe and specimen surface, is kept constant for obtaining the images. The tapping mode is very commonly used for imaging polymeric, biological, and other soft specimens. This mode can be used for characterizing hard materials as well.

The AFM images of a material surface can be obtained at atomic resolutions (Leng, 2008). Also, no surface treatments or vacuum conditions are necessary for AFM imaging. This characterization can be carried out at room temperature or even in an aqueous environment using a fluid cell accessory. The limitations of AFM include its limited XY scan area ($\sim 100 \times 100\ \mu m$) and vertical scan range ($\sim 10\ \mu m$) (Agrawal et al., 2014).

2.5.3 Profilometry techniques

The two different types of profilometers that are commonly used for characterizing biomaterials are a contact profilometer and a noncontact profilometer (Ratner et al., 2004). A contact profilometer is used for measuring the roughness of the material surface. In this profilometer, a diamond stylus is brought down to the sample surface and is moved laterally across the specimen for a specified distance at a specified constant force. The small variations on the sample surface are detected by measuring the displacement of stylus in the vertical direction as a function of position. The height position of the stylus produces an analog signal that is then converted into a digital signal and displayed. The advantages of a contact profilometer are its simplicity and inexpensive instrumentation. It can be used for measuring the roughness of metallic and other biomaterials. However, for soft specimens, because there is a physical contact between the stylus and specimen surface, a distortion of the surface profile can occur (Ratner et al., 2004). In the noncontact profilometer, the stylus is replaced by a beam of light or laser (Ratner et al., 2004). Hence, there is no physical contact with the specimen surface. The light or laser beam is focused on the sample surface and moved laterally to get the light or laser beam reflected back from the specimen surface. The reflected light or laser is then converted into an electrical signal to obtain images of the surface. The advantage of a noncontact profilometer is its vertical resolution, which is in nanometers. However, the lateral resolution is poor. The other limitation is that the

specimen surface has to provide at least some reflectivity for characterization using a noncontact profilometer (Ratner et al., 2004).

2.6 Surface charges

Surface charge is one of the four important surface properties that determine the biomaterial−tissue interactions. However, it is difficult to evaluate the effect of surface charge alone because it often depends on the wettability or chemistry of the material surface. For example, charged surfaces are typically hydrophilic. In another example, the carboxylic acid (−COOH) functional groups exist as negatively charged carboxylate ions ($-COO^-$) under physiological conditions. The amine ($-NH_2$) functional groups exist as positively charged ammonium ion ($-NH_3+$) under physiological conditions. These examples clearly show how the surface charge is closely related to surface wettability or chemistry and the difficulties in evaluating the sole effect of surface charge. In general, cell growth is better on charged surfaces when compared to neutral surfaces. The instrument that is commonly used to measure surface charges is zeta potential.

2.6.1 Zeta potential analysis

The surface charge of a material is determined by zeta potential analysis (Hunter, 1981). For solid materials, the analysis is carried out at the interface between the solid and the liquid using a streaming potential technique (Smoluchowski, 1921). Solid objects in solution carry a surface charge. Hence, the ions are distributed near the solid surface. When a liquid is allowed to flow over the solid surface, the distribution of ions on the solid surface is disrupted to create a potential difference, which is called streaming potential. In this characterization technique, a fluid is allowed to flow over the solid surface at different pressures, and the streaming potential is measured. The measured streaming potential is then converted into zeta potential. This technique can be used to determine the surface charges of metallic, polymeric, and other biomaterials.

2.7 Summary

The surface properties, such as surface chemistry, surface wettability, surface texture, and surface charges, are crucial for determining the success of biomedical implants and devices. A variety of instruments are used to study the different surface properties of biomaterials. A single characterization technique alone cannot provide information regarding all the surface properties of a biomaterial. FTIR provides molecular structure and chemical bonding information, while the XPS and ToF-SIMS provides elemental composition and chemical bonding information of material surfaces. A contact angle goniometer provides wettability information of a biomaterial. SEM provides surface morphological information, while AFM provides surface topographical information

of a biomaterial surface. Zeta potential analysis provides information regarding the surface charges of a biomaterial. It is essential to use multiple instruments for thoroughly characterizing all the different surface properties of biomaterials.

References

Agrawal, C. M., Ong, J. L., Appleford, M. R., & Mani, G. (2014). *Introduction to biomaterials basic theory with engineering applications*. New York: Cambridge University Press.

Arima, Y., & Iwata, H. (2007). Effect of wettability and surface functional groups on protein adsorption and cell adhesion using well-defined mixed self-assembled monolayers. *Biomaterials, 28*, 3074−3082.

Bindell, J. B. (1992). Scanning electron microscopy. In C. R. Brundle, C. A. Evans, & S. Wilson (Eds.), *Encyclopedia of materials characterization*. Stoneham: Butterworth-Heinemann.

Brandon, D., & Kaplan, W. D. (1999). *Microstructural characterization of materials*. West Sussex: John Wiley & Sons.

Brundle, C. R. (1992). X-ray photoelectron spectroscopy. In C. R. Brundle, C. A. Evans, & S. Wilson (Eds.), *Encyclopedia of materials characterization*. Stoneham: Butterworth-Heinemann.

Cox, J. N. (1992). Fourier transform infrared spectroscopy. In C. R. Brundle, C. A. Evans, & S. Wilson (Eds.), *Encyclopedia of materials characterization*. Stoneham: Butterworth-Heinemann.

Curtis, A., & Wilkinson, C. (1997). Topographical control of cells. *Biomaterials, 18*, 1573−1583.

Curtis, A., & Wilkinson, C. (1998). Reactions of cells to topography. *Journal of Biomaterials Science, Polymer Edition, 9*, 1313−1329.

Dee, K., Puleo, D., & Bizios, R. (2002). *An introduction to tissue−biomaterials interactions*. New Jersey: John Wiley & Sons, Inc.

Flemming, R. G., Murphy, C. J., Abrams, G. A., Goodman, S. L., & Nealey, P. F. (1999). Effects of synthetic micro- and nano-structured surfaces on cell behavior. *Biomaterials, 20*, 573−588.

Hamilton, D. W., Ghrebi, S., Kim, H., Chehroudi, B., & Brunette, D. M. (2008). Surface topography and cell behavior. In G. E. Wnek & G. L. Bowlin (Eds.), *Encyclopedia of biomaterials and biomedical engineering* (2nd ed.). New York: Informa Health Care USA, Inc.

Hunter, R. J. (1981). *Zeta potential in colloids science*. New York: Academic Press.

Kibel, M. H. (1992). X-ray photoelectron spectroscopy. In D. J. O'connor, B. A. Sexton, & R. S. C. Smart (Eds.), *Surface analysis methods in materials science*. Berlin Heidelberg: Springer-Verlag.

Lancaster, S., Kakade, S., & Mani, G. (2012). Microrough cobalt−chromium alloy surfaces for paclitaxel delivery: preparation, characterization, and in vitro drug release studies. *Langmuir, 28*, 11511−11526.

Lee, J., Khang, G., Lee, J., & Lee, H. (1998). Interaction of different types of cells on polymer surfaces with wettability gradient. *Journal of Colloid and Interface Science, 205*, 323−330.

Leggett, G. J. (1997). Scanning tunnelling microscopy and atomic force microscopy. In J. C. Vickerman (Ed.), *Surface analysis—the principal techniques*. West Sussex: John Wiley & Sons.

Leng, Y. (2008). *Materials characterization: Introduction to microscopic and spectroscopic methods*. Singapore: John Wiley & Sons (Asia) Pte Ltd.

Macdonald, R. J., & King, B. V. (1992). SIMS—secondary ion mass spectrometry. In D. J. O'connor, B. A. Sexton, & R. S. C. Smart (Eds.), *Surface analysis methods in materials science*. Berlin Heidelberg: Springer-Verlag.

Mani, G., Chandrasekar, B., Feldman, M. D., Patel, D., & Agrawal, C. M. (2009). Interaction of endothelial cells with self-assembled monolayers for potential use in drug-eluting coronary stents. *Journal of Biomedical Materials Research Part B: Applied Biomaterials, 90B*, 789−801.

Mani, G., Johnson, D., Marton, D., Dougherty, V. L., Feldman, M. D., Patel, D., et al. (2008). Stability of self-assembled monolayers on titanium and gold. *Langmuir, 24*, 6774−6784.

Mani, G., Macias, C. E., Feldman, M. D., Marton, D., Oh, S., & Agrawal, C. M. (2010). Delivery of paclitaxel from cobalt−chromium alloy surfaces without polymeric carriers. *Biomaterials, 31*, 5372−5384.

Ratner, B. D. (2004). Surface properties and surface characterization of materials. In B. D. Ratner, A. S. Hoffman, F. J. Schoen, & J. E. Lemons (Eds.), *Biomaterials science: An introduction to materials in medicine* (2nd ed.). London: Elsevier Academic Press.

Ratner, B. D., Hoffman, A. S., Schoen, F. J., & Lemons, J. E. (2004). *Biomaterials science: An introduction to materials in medicine*. London: Elsevier Academic Press.

Roberts, N. K. (1992). Fourier transform infrared spectroscopy of surfaces. In D. J. O'connor, B. A. Sexton, & R. S. C. Smart (Eds.), *Surface analysis methods in materials science*. Berlin Heidelberg: Springer-Verlag.

Robinson, J. W., Frame, E. M. S., & Frame, G. M. (2005). *Undergraduate instrumental analysis*. New York: Marcel Dekker.

Sibilia, J. P., Hammond, W. B., & Szobota, J. S. (1988). Molecular spectroscopy. In Sibilia, J.P. (Ed.), *A guide to materials characterization and chemical analysis*. Weinheim: Wiley-VCH Verlag GmbH & Co. KGaA.

Smoluchowski, M. (1921). *Handbook of electricity and magnetism*. Leipzig: Barth.

Vickerman, J. C., & Swift, A. J. (1997). Secondary ion mass spectrometry—the surface mass spectrometry. In J. C. Vickerman (Ed.), *Surface analysis—the principal techniques*. West Sussex: John Wiley & Sons.

Wachem, P. V., Beugeling, T., Feijen, J., Bantjes, A., Detmers, J., & Aken, W. V. (1985). Interaction of cultured human endothelial cells with polymeric surfaces of different wettabilities. *Biomaterials, 6*, 403−408.

Wachem, P. V., Hogt, A., Beugeling, T., Feijen, J., Bantjes, A., Detmers, J., et al. (1987). Adhesion of cultured human endothelial cells onto methacrylate polymers with varying surface wettability and charge. *Biomaterials, 8*, 323−328.

Wachtman, J. B. (1993). *Characterization of materials*. Manning, Butterworth-Heinemann.

Zhang, S., Li, L., & Kumar, A. (2008). *Materials characterization techniques*. Boca Raton: CRC Press.

Corrosion of Mg for biomedical applications

3

A. Atrens, F. Cao, Z. Shi, M.S. Dargusch
The University of Queensland, Brisbane, QLD, Australia

3.1 Introduction

This review of Mg corrosion for biomedical applications is based on our recent review by Atrens et al. (2013). There is considerable interest in the use of Mg alloys for biodegradable medical implants (Atrens et al., 2011; Ding et al., 2014; Taltavull et al., 2014; Zainal Abidin et al., 2011, 2013, 2015), particularly for applications where some mechanical strength is needed, such as for example as bone fixation plates. The concept is that the Mg implant provides mechanical support while the body heals, and thereafter the Mg implant corrodes away completely, obviating the second surgery that is necessary to remove a nonbiodegradable implant made from e.g. stainless steel. The understanding of Mg corrosion in medical applications can build upon the extensive research on Mg corrosion (Atrens et al., 2009, chap. 3; Song and Atrens, 1999, 2003) for transport applications.

3.2 Stainless magnesium

3.2.1 Tolerance limits and the corrosion of pure Mg

Corrosion of pure Mg involves a partially protective film, consisting of MgO in contact with the metallic Mg, with a surface layer of $Mg(OH)_2$ (Liu et al., 2009b). The MgO layer is probably very thin and provides the protection, whereas the surface $Mg(OH)_2$ is bulky and probably fairly porous (Baril et al., 2007).

High-purity (HP) Mg has the lowest corrosion rate for any form of Mg. No element has been found that produces a solid solution Mg alloy with a corrosion rate lower than that of HP Mg. Corrosion rates are large if the concentration of any of the impurity elements (Fe, Ni, Cu and Co) is greater than its tolerance limit, see Figure 3.1. Fe is of most significant concern because it can be readily picked up by molten Mg contained in steel vessels and can be picked up on the surface of Mg alloys during mechanical forming operations with Fe tools. Thus, Song and Xu (2010) showed that the corrosion rate of AZ31B could be reduced by a factor of 50 by a simple cleaning operation to remove the Fe impurity particles embedded in the surface. Figure 3.1 shows that the corrosion rate is large for Mg alloys above the tolerance limit (Liu et al., 2009a).

Surface Coating and Modification of Metallic Biomaterials. http://dx.doi.org/10.1016/B978-1-78242-303-4.00003-X
Copyright © 2015 Elsevier Ltd. All rights reserved.

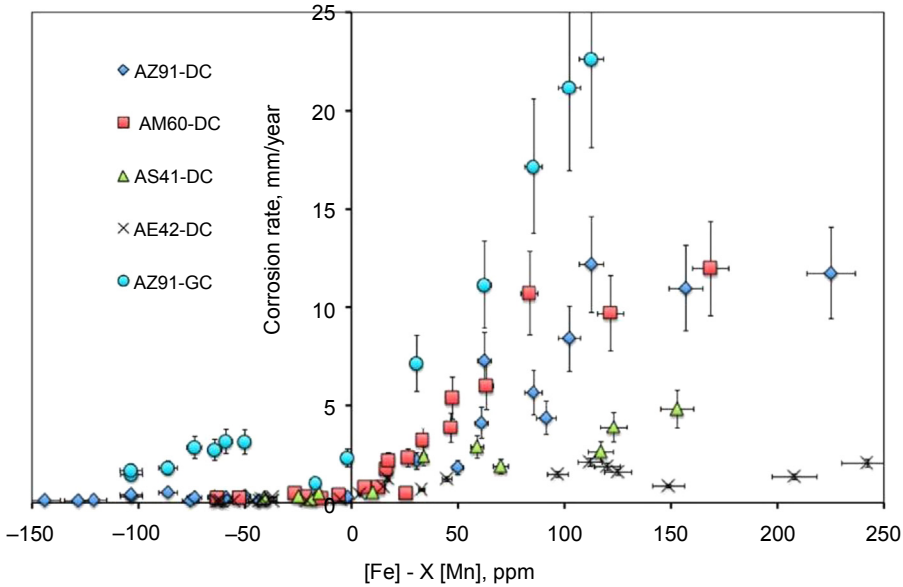


Figure 3.1 Literature values of the corrosion rate for Mg alloys die-cast (DC) AZ91, AM60, AS41 and AE42 and gravity-cast (GC) AZ91 re-plotted as a function of the Fe content above the tolerance limit from Liu et al. (2009a).

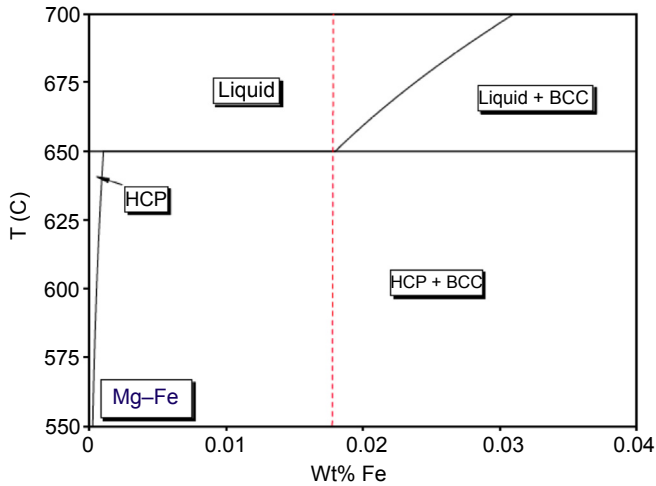


Figure 3.2 Mg−Fe phase diagram after (Liu et al., 2009a) used to explain the tolerance limit for Fe.

Liu et al. (2009a) explained the tolerance limit of Fe using the Mg−Fe phase diagram which is presented in Figure 3.2. The tolerance limit for Fe in cast pure Mg corresponds to the eutectic concentration of 0.018% Fe (180 wt ppm). Cooling an alloy from the melt with a greater Fe concentration causes the solid to contain the Fe-rich

body-centred cubic (BCC) phase. This phase is an extremely efficient cathode which allows the cathodic reaction of hydrogen evolution to proceed at a fast rate. The corresponding anodic reaction must also proceed at the same rate; as a consequence, the overall corrosion rate is high. In contrast, solidification of an Mg alloy with a lower Fe content typically results in the formation of only the HCP alpha-Mg phase with the Fe in metastable solid solution. The solidification of such an Mg alloy proceeds quickly through the two-phase (liquid + solid) phase field, too quickly to permit formation of the Fe-rich BCC phase. As a consequence, an Mg casting normally has a low corrosion rate if the Fe content is below the tolerance limit for Fe.

Figure 3.2 indicates however that such a single-phase Mg casting is in a metastable condition, and that the Fe-rich phase is expected to precipitate if the casting is heat-treated, which is confirmed by the data in Figure 3.3 (Liu, et al., 2009a).

Figure 3.3 shows that the hydrogen evolution rate increased linearly with immersion time for HP Mg (open circles). One molecule of hydrogen is evolved for each atom of Mg dissolved, so that the measurement of evolved hydrogen is a convenient way in which to monitor Mg corrosion (Song and Atrens, 2003). Figure 3.3 shows that the corrosion rate of the HP Mg was increased significantly after heat treatment at 550 °C (open triangles and squares) because of the precipitation of particles of the Fe-rich phase as predicted by Figure 3.2.

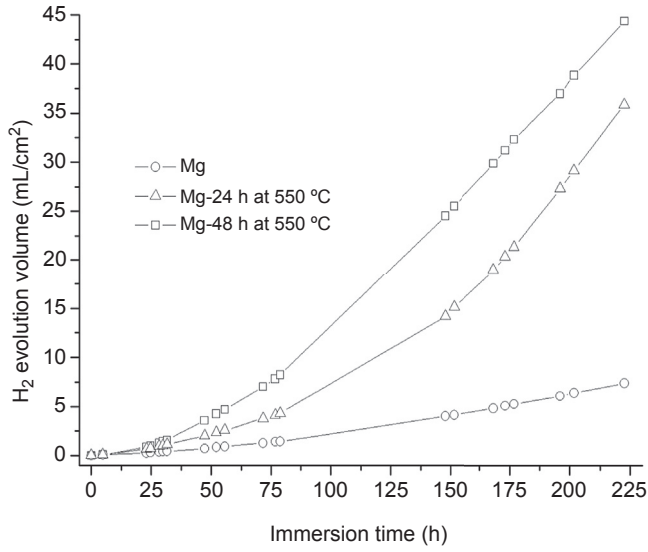


Figure 3.3 Hydrogen evolution data for high-purity (HP) Mg, and for HP Mg after heat treatment at 550 °C (Liu et al., 2009a). The Mg−Fe phase diagram indicates that high-purity Mg containing an Fe content less than the eutectic concentration contains on normal solidification only alpha-Mg, all the Fe is in metastable solid solution, and the corrosion rate is low, shown by the slow increase in hydrogen evolution, see open circles. However, heat treatment causes the Fe-rich BCC phase to precipitate, and causes the corrosion rate to increase, shown by the higher rate of hydrogen evolution (open triangles and open squares).

Figure 3.2 may also apply to Mg alloys, indicating that Mg alloys may have high corrosion rates after heat treatment or after such hot working operations as extrusion.

Figure 3.2 also implies that the Fe-rich BCC could form during normal cooling, even if the Fe content is well below 180 ppm, and that the corrosion rates are high if that happens. Figure 3.4 illustrates the corrosion rates of such a case for specimens 19 and 28 from the Helmholtz Zentrum Geesthacht (HZG) ingot containing 32 ppm Fe compared with those for specimens 26 and 27 from University of Queensland (UQ) HP Mg containing 20 ppm (Qiao et al., 2012). The important point is the higher corrosion rates of specimens 19 and 28 resulting from micro-galvanic acceleration of the corrosion rate by Fe-rich particles that formed during solidification, for the HZG Mg. Figure 3.5(a) provides a typical appearance of the corrosion of HZG Mg. Some grains showed deep-layered corrosion, whereas adjacent grains showed filiform corrosion. The differences are partly explicable in terms of the crystallographic dependence of corrosion with close-packed planes showing significantly lower corrosion rates (Liu et al., 2008; Song, 2012; Song et al., 2010; Song and Xu, 2012). In any case, the substantial corrosion rates of the HZG correlated with the significant corrosion damage on the specimen surfaces after the immersion tests. In

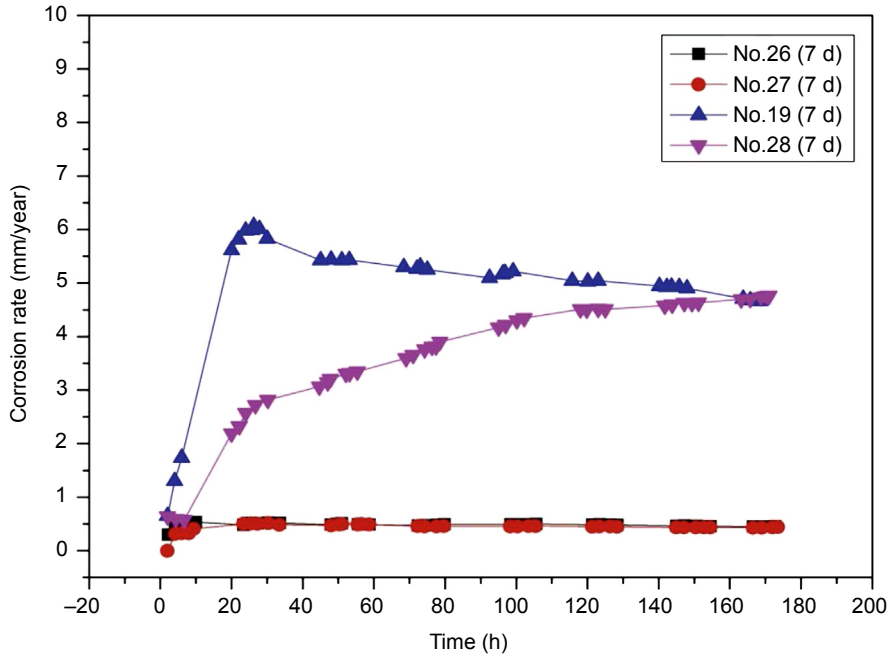


Figure 3.4 Corrosion rate from the hydrogen evolution data, P_H, for the plug-in specimens immersed for 7 days at the open circuit potential in 3.5% NaCl saturated with $Mg(OH)_2$ (Qiao et al., 2012). Specimens 19 and 28 are from the HZG Mg ingot (Qiao et al., 2012). Specimens 26 and 27 are from UQ HP Mg.

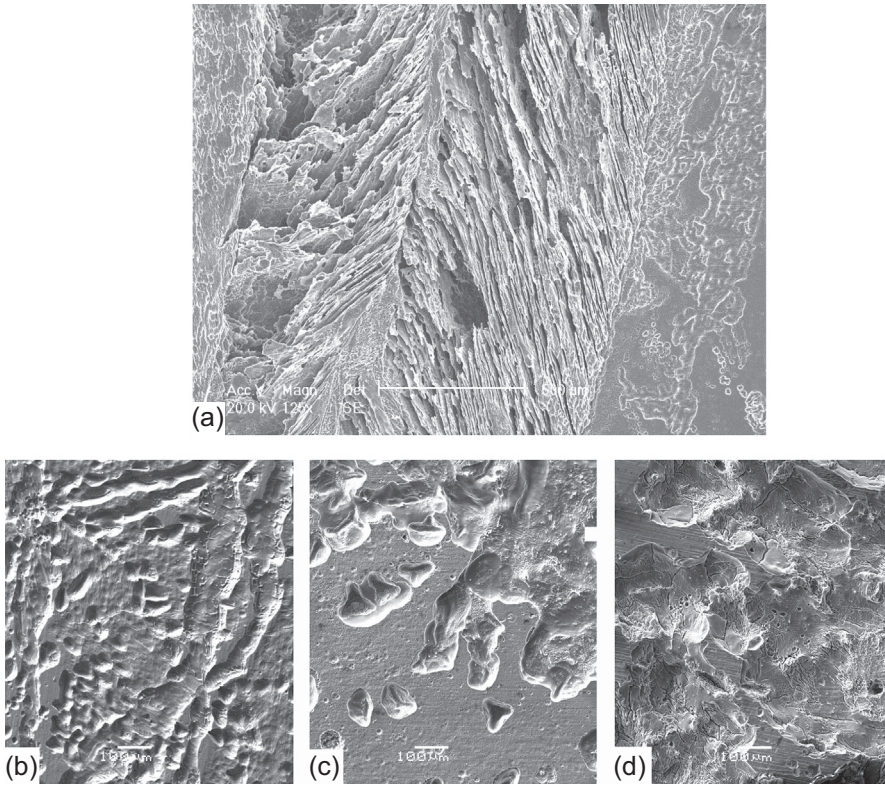


Figure 3.5 (a) Typical corrosion morphology was different in the adjoining grains for corrosion of the HZG Mg. Some grains exhibited superficial corrosion with some filiform corrosion. The adjacent grains exhibited deep-layered corrosion. HZG Mg ingot after immersion for 7 days (Qiao et al., 2012). (b–d) Scanning electron microscope images (Shi and Atrens, 2011) for surfaces after removal of corrosion products for (b) high-purity (HP) Mg specimens hung with fishing line in 3.5% NaCl solution saturated with $Mg(OH)_2$ for 5 days, and (c) and (d) for HP Mg plug-in specimens immersed in the same solution for (c) 7 days and (d) 31 days. Corrosion for short time immersion took the form of shallow pit which gradually linked up and some filiform corrosion. Corrosion after 31 days had in addition significant crack-like features and crevice-like features at the bottom of the corrosion cavities.

contrast, the corrosion morphology of HP Mg showed shallow pits that gradually linked up and some filiform corrosion as illustrated in Figure 3.5(b) and (c). Figure 3.5(d) shows that at longer immersion times there developed some crack-like features at the bottom of the corrosion cavities. Nevertheless, even after 32 days' immersion, there were parts of the original surface that had suffered no corrosion attack. This indicates that corrosion takes time to develop for HP Mg.

The reason for the precipitation of Fe-rich phase particles in the HZG Mg, and not in the UQ HP Mg, is not understood. Useful insights into the metallurgy of Mg solidification were provided by the recent article by Liu and Song (2013).

Particles in the microstructure may also degrade the corrosion performance (Cao et al., 2013b; Shi et al., 2013).

Recently, Cao et al. (2013a) concluded that the intrinsic corrosion rate was 0.25 ± 0.07 mm/year for ultra-high-purity (UP) Mg in 3.5% NaCl solution saturated with $Mg(OH)_2$.

3.2.2 Requirement for UP Mg alloys

Figure 3.6 provides a recent compilation (Cao et al., 2013b; Shi et al., 2013) of corrosion data for Mg alloys, showing that the corrosion rates of typical Mg alloys are greater than that of HP Mg. The Mg alloys typically two or more phases, each of which causes microgalvanic acceleration of the corrosion rate of the alpha-Mg matrix phase. Figure 3.7 illustrates one exception, that occurs when (1) there is a high density of second-phase particles so that the second-phase particles form a continuous network and (2) the corrosion rate of the second phase is significantly lower than that of the

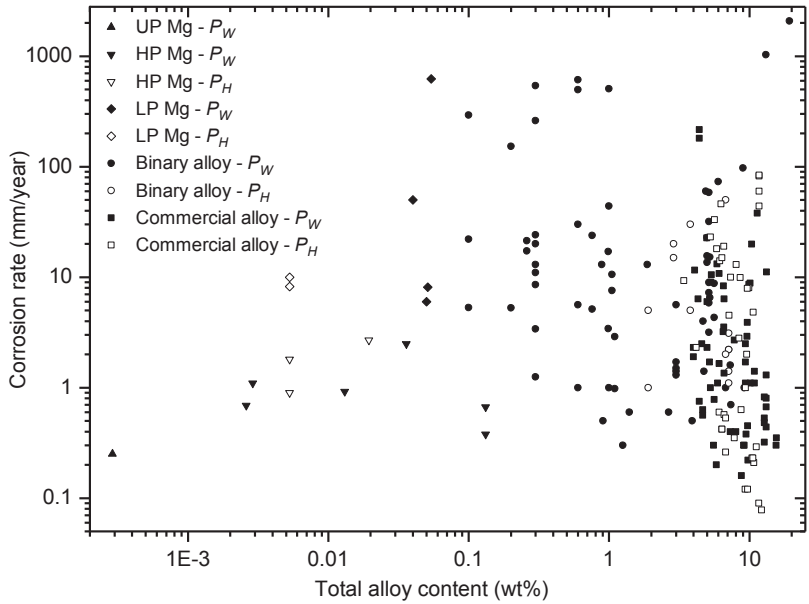


Figure 3.6 Corrosion of Mg alloys (Cao et al., 2013b; Shi et al., 2013). No alloying element has been identified that consistently gives corrosion rates lower than that of high-purity (HP) Mg in a technically relevant solution like 3.5% NaCl solution saturated with $Mg(OH)_2$. Ultra-high-purity (UP) Mg had an intrinsic corrosion rate of 0.25 ± 0.07 mm/year in 3.5% NaCl solution saturated with $Mg(OH)_2$, only slightly lower than the intrinsic corrosion rate HP Mg, 0.38 ± 0.24 mm/year in the same solution (Cao et al., 2013a), although individual specimens do give somewhat higher corrosion rates. The vast bulk of Mg alloys give corrosion rates higher than that of HP Mg. The corrosion rate measured by hydrogen evolution for low corrosion rates underestimates the real corrosion rate because the amount of hydrogen dissolved in the Mg specimen causes a significant error in the corrosion rate at low corrosion rates.

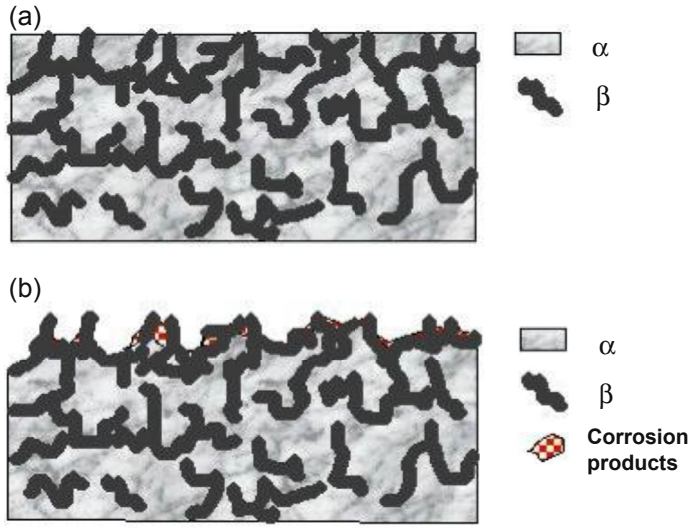


Figure 3.7 (a) A cross-section of an Mg alloy containing a continuous second phase (beta) in an alpha matrix is exposed to the solution at only the top surface (Song and Atrens, 1999, 2003). Figure 3.7(a) shows initial state. Exposed to the solution are both the alpha-matrix and the beta phase. The second phase is assumed to have a corrosion rate significantly lower than that of the matrix, alpha-phase. Initially the corrosion is essentially characteristic of that the alpha-phase, until the alpha-phase has corroded away. Figure 3.7(b) illustrates steady state. The corrosion is dominated by that of the second phase. However, second phases in Mg alloys are intermetallics and are typically brittle. Thus, this strategy in unlikely to produce a high performance Mg alloy with a low corrosion rate.

alpha-Mg. Another exception is that Mg-0.4As was reported to have a low corrosion rate in 0.1 M NaCl attributed to arsenic poisoning the cathodic reaction of hydrogen evolution (Birbilis et al., 2013).

In contrast to the substantial corrosion rates for two-phase Mg alloys, an Mg alloy with a corrosion rate substantially lower than that of HP Mg might be theoretically be produced if an alloying element could be found so that the surface film on the alloy was based on the alloying element rather than on Mg. This was suggested by Song and Atrens (2003) based on the analogy of stainless steels which are Fe−Cr alloys on which forms a protective passive film for a Cr content higher than 10.5%, and similarly on Ni and Co alloys higher than a critical Cr concentration (Bruesch et al., 1984, 1985; Burstein and Daymond, 2009; Heine and Kirchheim, 1999; Jin and Atrens, 1987; Kirchheim et al., 1989; Lim and Atrens, 1992a, 1992b; Olefjord and Elfstron, 1982; Schneider et al., 1990).

This strategy could be explored to for Mg alloys, if homogeneous solid-solution Mg−X alloys could be produced in UP form with impurity contents, particularly Fe, less than ∼2 ppm. To date, this strategy could not be explored because heat treatment of Mg alloys of existing purity causes the precipitation of the Fe-rich BCC phase, and consequent high corrosion rates. In contrast, UP Mg−X alloys could be heat

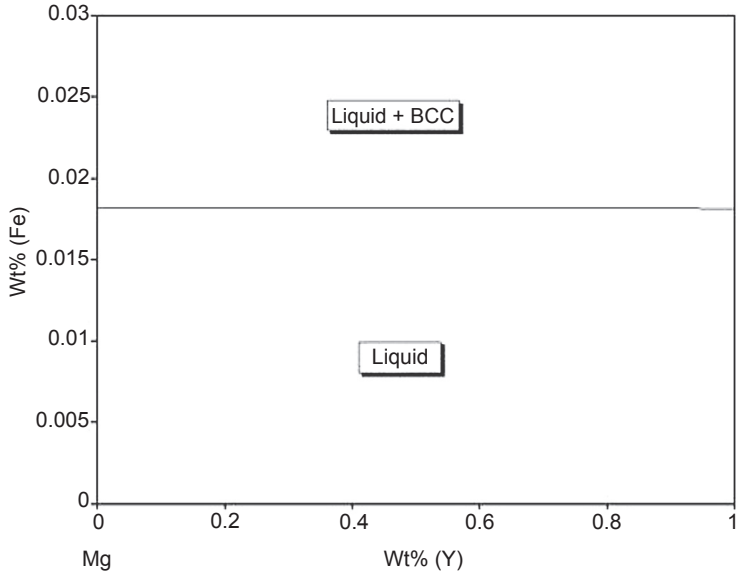


Figure 3.8 Isothermal section through the Mg−Fe−Y phase diagram at 651 °C, just above the eutectic temperature, indicating that Y has no influence on the Fe solubility in molten Mg (Prasad et al., 2012). Similarly there was no influence from a large number of elements including Sn, Ca, Sr, Ce, Gd, Nd and Z (Prasad et al., 2012).

treated to solutionize the alloying elements into the solid solution, and then the corrosion behaviour of these alloys could be studied. This has not been possible to date.

3.2.3 Melt purification

UP Mg−X alloys can be produced by melt purification with Zr as shown by our recent theoretical and experimental research (Prasad et al., 2012). Many elements, including Y, Sn, Ca, Sr, Ce, Gd, Nd and Zn, have little influence on the Mg−Fe phase diagram shown in Figure 3.2. This is illustrated in Figure 3.8 which indicates no influence of yttrium on Fe solubility. Zr, in contrast, significantly reduces Fe solubility as shown in Figure 3.9. Thus, sufficient Zr in the melt at equilibrium at 660 °C (0.2%) can reduce the Fe content to 2 ppm.

3.3 Biocorrosion

3.3.1 Key issues

The potential of Mg as a biodegradable implant material requires control of their degradation rates (Song and Song, 2007), and there is a lot of work on alloying and surface treatment (Song, 2007a,b; Wang et al., 2007). The other key issue is to be able to relate in vitro corrosion rates to behaviour in vivo (Staiger et al., 2011;

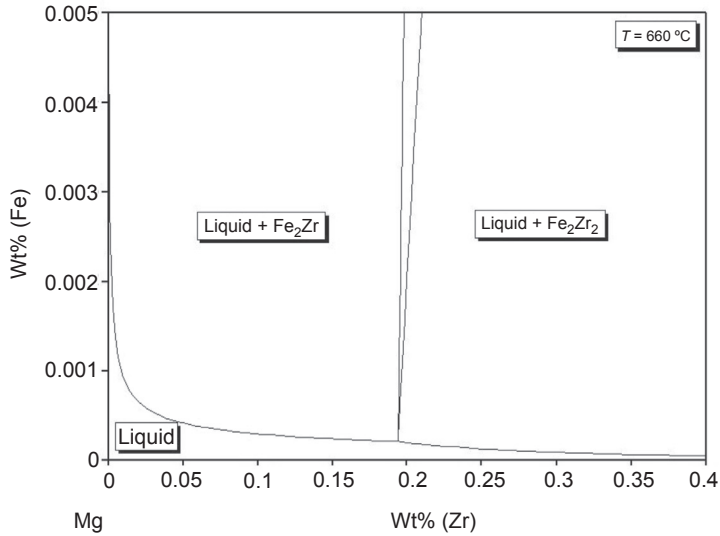


Figure 3.9 Methodology (Prasad et al., 2012) by which a Mg−X alloy can be produced with the required Fe impurity concentration of 2 ppm. The melt is equilibrated at 700 °C, sufficient Zr (or master alloy containing Zr) is added to achieve a Zr concentration of 0.2%, the melt is cooled to 660 °C and the $FeZr_2$ is allowed to settle from the top part of the melt.

Zainal Abidin et al., 2011, 2013). Zainal Abidin et al. (2011, 2013) suggested that this requires sufficient understanding of Mg corrosion to be able to identify the main determining factors for Mg biocorrosion.

3.3.2 *In vitro/in vivo comparison*

Zainal Abidin et al. (2011) found that literature in vitro corrosion rates related well to behaviour in vivo, when the literature data were selected on the basis of the known factors that influence the corrosion rate of Mg: chloride ion concentration, pH, buffer system and temperature.

Subsequently, Zainal Abidin et al. (2013) showed that there was a good correlation between in vitro tests in Nor's solution and in vivo behaviour for HP Mg and WE21 which had moderate corrosion rates, see Table 3.1. Nor's solution was a

Table 3.1 Corrosion rates in vitro (immersed in Nor's solution at 37 ± 2 °C) and in vivo (Zainal Abidin et al., 2013)

	Corrosion rate, P_W, mm/year		
Alloy	**Nor's solution**	**In vivo 30 days**	**In vivo 60 days**
HP Mg	0.9 ± 0.3	1.0 ± 0.3	0.7 ± 0.3
WZ21	1.0 ± 1.0	1.8 ± 0.4	1.0 ± 0.2

modification of Hank's solution, in that the pH was maintained constant at the appropriate value by bubbling CO_2 through the solution at the appropriate partial pressure. This made use of the same buffer system that maintains blood at the physiological pH value.

Similarly, Walker et al. (2012) found good agreement between in vitro and in vivo behaviour for pure Mg, and the Mg alloys AZ31, Mg0.8Ca, Mg1Zn, Mg1Mn and Mg1.3Ca3Zn.

3.4 Corrosion rate measurement

3.4.1 Measurement techniques

The study of Mg corrosion benefits from the fact that there are a number of independent techniques by which to measure the corrosion rate. The instantaneous corrosion rate can be measured using (1) evolved hydrogen, P_H, (2) the Tafel extrapolation of polarization curves, P_i, and (3) electrochemical impedance spectroscopy (EIS), $P_{i,EIS}$ (see e.g. Cao et al., 2013a,b; Shi et al., 2013). The average corrosion rate over the whole immersion period can be evaluated from the total amount of evolved hydrogen, P_{AH}, and from weight loss, P_W. It is best practise to measure the corrosion rate by a number of independent methods to check for consistency.

However, Song and Atrens (2003) pointed out that the Tafel extrapolation has often not provided corrosion rates consistent with those measured by weight loss or hydrogen evolution, see also Shi et al. (2010), Shi et al. (2012a,b). An example is provided in Figure 3.10 which is an adaptation from Qiao et al. (2012) from the published data of Gandel et al. (2014), King et al. (2014), Sudholtz et al. (2011). One issue is that polarization curves are often measured soon after specimen immersion in solution, whereas the corrosion rate can increase with immersion time, as is known to occur for Mg−Y alloys (Liu et al., 2010) or may decrease with immersion time (King et al., 2014).

3.4.2 Plug-in specimen

Plug-in specimens were developed by Shi and Atrens (2011) and Shi et al. (2012c), see Figures 3.11 and 3.12, and allow reproducible and simultaneous measurement of P_H, P_i and $P_{i,EIS}$. Furthermore, P_{AH} has typically been in good agreement with P_W in our measurements (Cao et al., 2013a,b; Qiao et al., 2012; Shi et al., 2013; Song and Atrens, 2003; Zhao et al., 2008a,b), with the following two exceptions: (1) at low corrosion rates, see Figure 3.13, and (2) in Nor's solution (Zainal Abidin et al., 2011, 2013), see Figure 3.14. In these cases, P_{AH} is less than P_W attributed to dissolution of some hydrogen in the Mg specimen.

In contrast, P_i and $P_{i,EIS}$ are always less than P_W and P_H (Cao et al., 2013a,b; Shi et al., 2013).

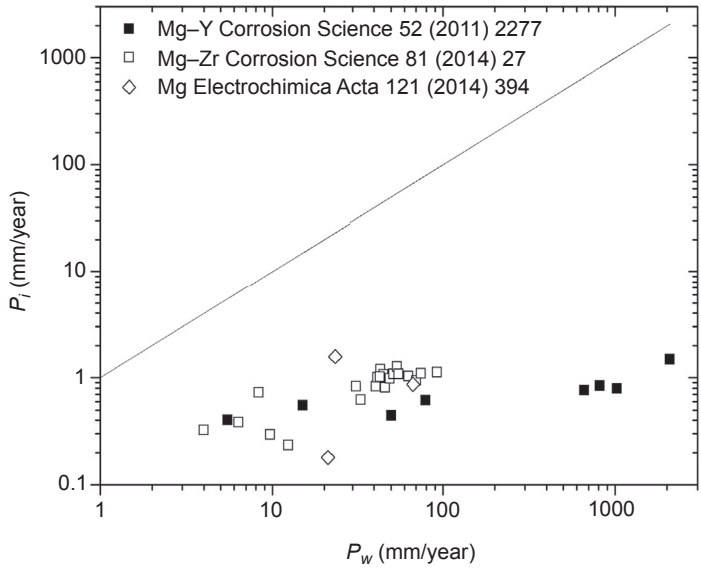


Figure 3.10 P_i (evaluated from the *iR*-compensated polarization curves) versus P_W (open diamonds) from the work of King et al. (2014). These data are compared with a cross-plot of P_i and P_W values evaluated from Gandel et al. (2014) as open squares and from Sudholz et al. (2011) squares. The data relate to various Mg alloys corroding in various chloride solutions. The line drawn as a guide to the eye corresponds to the condition of equality.

3.4.3 Crevice corrosion

Shi and Atrens (2011) found that crevice corrosion could significantly increase the measured corrosion rate when using a typical mounted specimen such as that illustrated in Figure 3.15. Thus it is good practise to examine each specimen after each corrosion test for crevice corrosion. Shi and Atrens (2011) developed the fishing-line specimen as illustrated in Figure 3.16 to have no crevice. The typical corrosion morphology, see Figure 3.17, was similar to that illustrated previously in Figure 3.5(b) and (c).

3.4.4 Measurement time

For research that aims to understand long-term service corrosion in, for example the body, care is needed with short-term tests. For example, Kirkland et al. (2012) recommended that P_i be measured soon after specimen immersion in the solution. This must be assessed in the context of the fact that the Mg corrosion rate typically changes with immersion time. In many solutions, the initial corrosion rate is small, and then the corrosion rate increases with immersion time (Song, 2007b; Song and Song, 2007; Staiger et al., 2011; Wang et al., 2007). A typical example is shown by specimens 19 and 28 in Figure 3.4 (Qiao et al., 2012). The quality of the recommendation of Kirkland et al. (2012) can be assessed by considering the data of

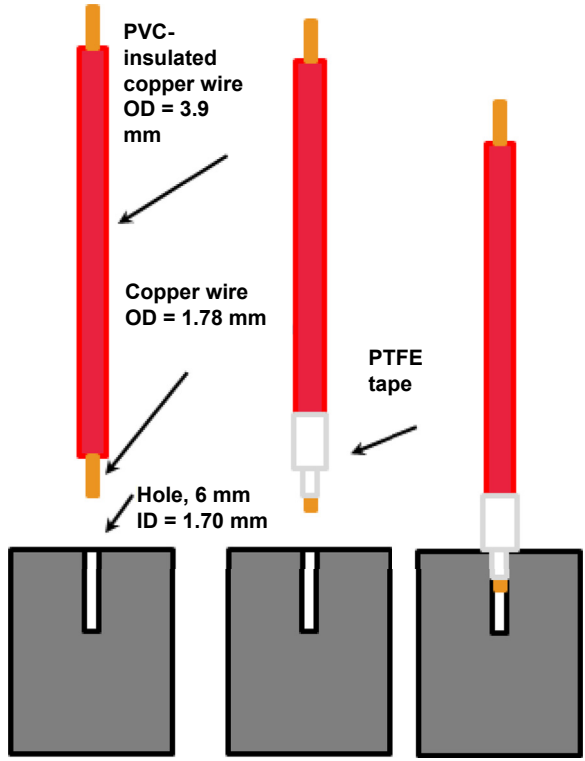


Figure 3.11 The plug-in specimen (Shi and Atrens, 2011; Shi et al., 2012c). An oversized bared copper conductor is forced into an undersized hole in the side of a rectangular Mg specimen providing a robust mechanical joint with good conductivity. The careful assembly of the plug-in specimen and the Teflon tape ensures that there is no crevice corrosion.

Figure 3.4. The same initial corrosion rate is shown by specimens 19, 28, 26 and 27. However, the steady-state corrosion rate for specimens 19 and 28 is about an order of magnitude higher than that for specimens 26 and 27. The initial measurements cannot predict this difference in the steady-state corrosion rate.

3.4.5 Measurement issues

Each of the techniques for the measurement of Mg corrosion needs care. Key issues are discussed by Atrens et al. (2013).

3.4.6 Solutions

Zainal Abidin et al. (2011, 2013) developed Nor's solution and showed that this solution was a good starting model for Mg biodegradation for medical applications. Nor's solution corresponds to Hank's solution through which CO_2 is bubbled at a partial pressure of 0.9 atm. The interaction of the CO_2 and the bicarbonate concentration

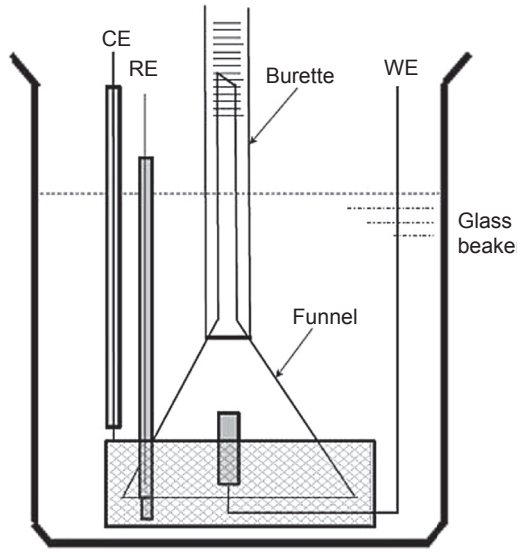


Figure 3.12 A typical experimental setup with the plug-in specimen in a standard three-electrode cell (Shi and Atrens, 2011; Shi et al., 2012c). The instantaneous corrosion rate can be evaluated from (1) the evolved hydrogen, P_H, (2) the Tafel extrapolation of polarization curves, P_i, and (3) electrochemical impedance spectroscopy, $P_{i,EIS}$, and the average corrosion rate over the whole immersion test can be evaluated from the weight loss, P_W, and the total amount of evolved hydrogen, P_{AH}.

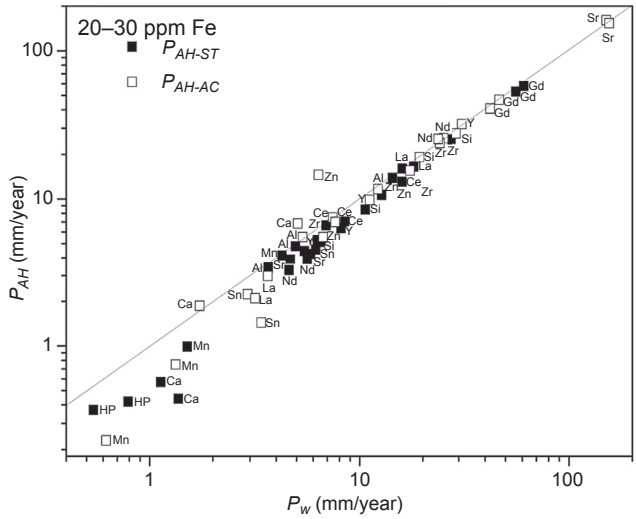


Figure 3.13 Good agreement at high corrosion rates between P_{AH} and P_W. At low corrosion rate P_{AH} was less than P_W attributed to the dissolution of some hydrogen in the Mg specimen. Data from Cao et al. (2013b), Shi et al. (2013).

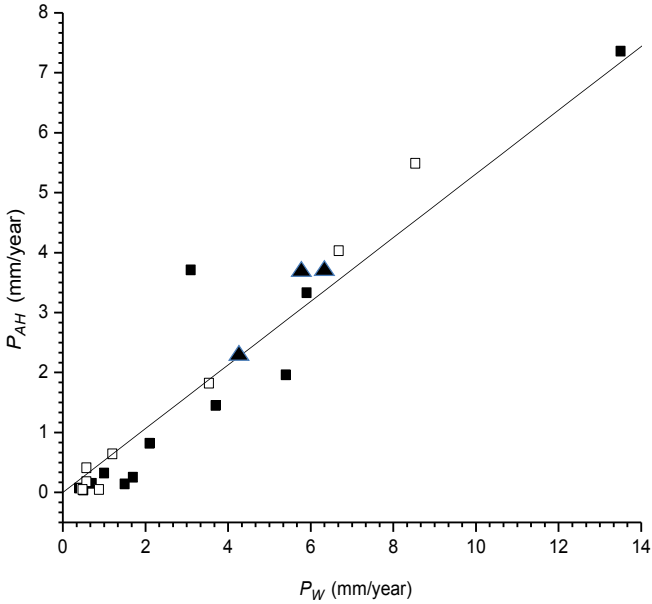


Figure 3.14 There was a good correlation between P_{AH} and P_W in Nor's solution, but P_{AH} was significantly lower than P_W, attributed to some hydrogen dissolving in the Mg specimen (Zainal Abidin et al., 2011, 2013). In addition, the triangles represent data from Kirkland et al. (2012).

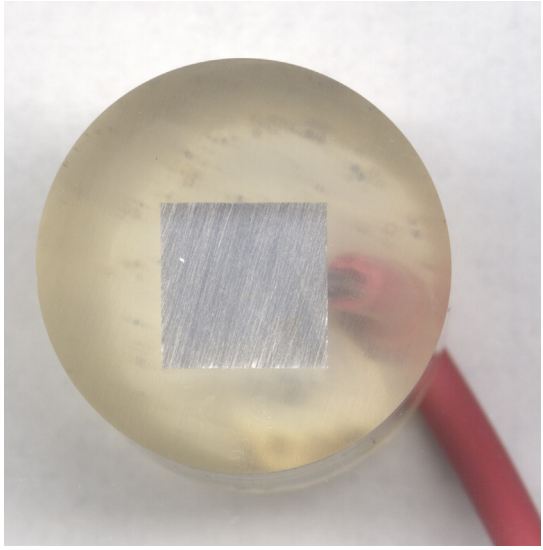


Figure 3.15 A typical mounted specimen widely used in Mg corrosion research, particularly for electrochemical measurements. This specimen type is quick and easy to prepare. The surface exposed to the solution can be prepared to any desired finish. Shi and Atrens [49] found that there could be significant crevice corrosion between the specimen and the mount. Such crevice corrosion could be an issue whenever the specimen is mounted to produce a crevice.



Figure 3.16 A typical fishing-line specimen designed to have the least possible minimal crevice (Shi and Atrens, 2011). The specimen is supported in a cradle of fishing line and suspended in the solution without touching any surface. The corrosion rate can be evaluated from the evolved and the weight loss.

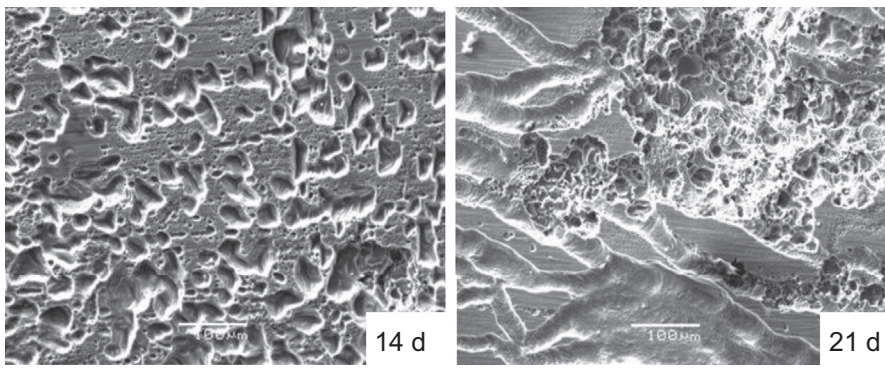


Figure 3.17 Typical corrosion morphology for high-purity (HP) Mg fishing-line specimens after immersion in 3.5% NaCl solution saturated with $Mg(OH)_2$, for the stated duration and after removal of the corrosion products (Shi and Atrens, 2011).

maintains the pH at 7.4. This is the same buffer as in blood. Moreover, Nor's solution contains a chloride concentration similar to that in blood, and consequently the corrosiveness is expected to be similar, because the chloride ions are the most aggressive of the inorganic ions in blood. The chemistry was considered in detail by Zainal Abidin et al. (2011).

Research to understand the corrosion in service and to understand the corrosion mechanism often uses concentrated chloride solutions. Mg corrosion in such solutions causes a pH increase typically in a few hours towards a pH value ~10.4. This is because of the low solubility of $Mg(OH)_2$ as explained by Atrens et al. (2013). Consequently, there are advantages in the use of chloride solutions saturated with $Mg(OH)_2$ because these solutions are typical of the local pH at a corrosion Mg surface and moreover do not change with immersion time. We have often used such solutions (Cao et al., 2013a,b; Shi et al., 2013; Shi and Atrens, 2011).

3.4.7 Apparent valence of Mg

Let it be assumed that (1) an electrochemical measurement of the Mg corrosion rate, P_i, provides a valid measurement of the Mg corrosion that is under electrochemical control, and (2) the total corrosion rate is measured from the corresponding measurement of the corrosion rate evaluated from hydrogen evolution, P_H, or weight loss, P_W. Then, the apparent valence of Mg corrosion can be evaluated from

$$V_{iH} = \frac{2P_i}{P_H} \tag{3.1}$$

Shi and Atrens (2011) measured

$$V_{iH} = \frac{2P_i}{P_H} = 1.45 \tag{3.2}$$

from simultaneous measurements of P_i and P_H such as those in Figure 3.18. Figure 3.5(b) and (c) indicates that the corrosion morphology consisted of relatively open corrosion cavities (which tended to link up) and some filiform corrosion.

This is consistent with a corrosion mechanism that is only partly under electrochemical control. The mechanism assumes that the overall anodic partial reaction

$$Mg \rightarrow Mg^{++} + 2e \tag{3.3}$$

occurs through a short-lived extremely reactive intermediate the uni-positive Mg^+ that can react with water in the following reaction:

$$Mg^+ + H_2O + OH^- \rightarrow Mg(OH)_2 + \tfrac{1}{2} H_2 \tag{3.4}$$

Figure 3.19 presents data for the simultaneous measurements of P_i and P_H that include the data in Figure 3.18. For immersion times greater than about 16 days, there was no change in the corrosion rate as measured by the electrochemical technique (full circles), whereas there was a significant increase in the actual corrosion rate as evaluated from hydrogen evolution (open circles). This indicated

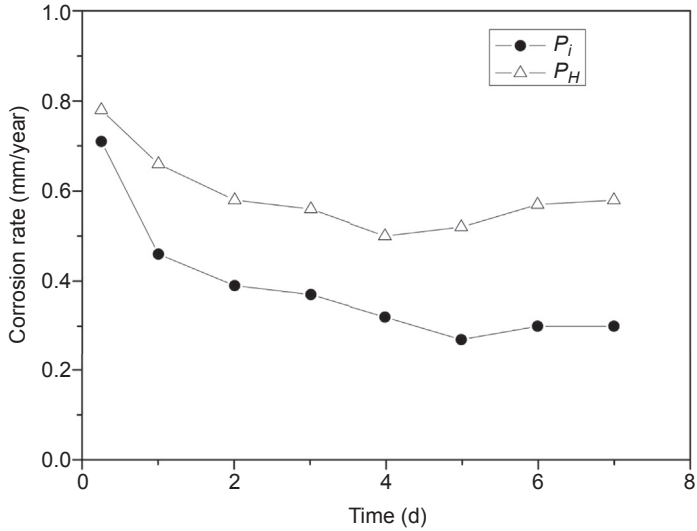


Figure 3.18 Comparison of P_i and P_H for an HP Mg plug-in specimen immersed for 7 days in 3.5% NaCl saturated with $Mg(OH)_2$ (Shi and Atrens, 2011).

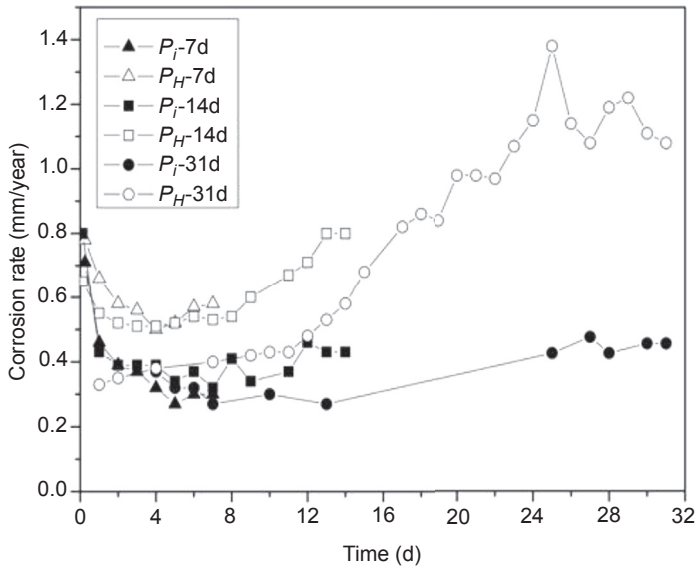


Figure 3.19 Instantaneous corrosion rate for HP Mg determined from hydrogen evolution, P_H, open symbols, and the corresponding corrosion rate determined from the corrosion current density from the polarization curve, P_i, full symbols, plotted versus immersion time, for immersion at the open-circuit potential in 3.5% NaCl solution saturated with $Mg(OH)_2$ at 25 °C (Shi and Atrens, 2011). The triangles represent data from specimen PMg1-4, squares represent data from specimen PMg1-5 and circles represent data from specimen PMg1-3.

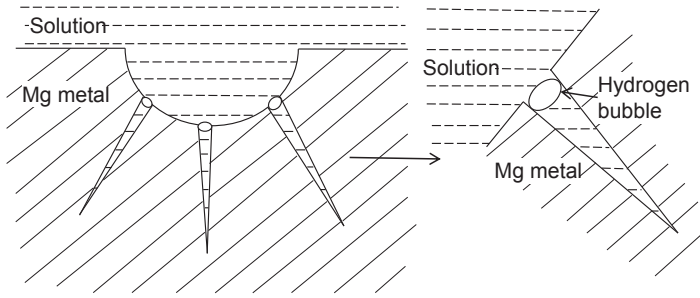


Figure 3.20 A schematic idealization of the corrosion morphology corresponding to Figure 3.5(d). Corrosion can proceed within the crack-like or crevice-like features at the bottom of the corrosion cavities. If the evolved hydrogen collects as a bubble at the mouth of the crack-like or crevice-like feature, then the hydrogen bubble can isolate the corrosion within the feature from the outside environment, and in particular the corrosion inside the features can proceed without being measured or influenced by the electrochemical measurement system. Corrosion can proceed inside with local anodes being balanced by local cathodes, and with no influence of the external polarization on the corrosion within the crack-like or crevice-like features.

that the actual corrosion was isolated from the electrochemical measurement system. Figure 3.5(d) presents the relevant corrosion morphology, and Figure 3.20 provides a mechanism by which the evolving hydrogen bubbles can cause the isolation of the corrosion from the electrochemical measurement system.

A perceived deficiency of the uni-positive Mg^{+} corrosion mechanism has been the lack of observations of Mg^{+}. However, Mg^{+} is common in stars as MgH (Bernath et al., 1985). Furthermore, gas-phase studies have shown (Harms et al., 1994; Missizu et al., 1992) that Mg^{+} reacts spontaneously within microseconds with even a few water molecules. This is consistent with the proposed role of the Mg^{+} ion as an extremely reactive intermediate between Mg and Mg^{2+}.

3.5 Magnesium corrosion mechanism

Atrens et al. (2013) recently carried out a critical evaluation of the possible mechanisms for Mg corrosion. They concluded that the most probable mechanism remains that based on the uni-positive Mg^{+} ion, as developed by Song and coworkers (Song et al., 1997; Song and Atrens, 2003; Song, 2006, 2011, 2013): that (1) Mg has a partially protective film and the film-free area increases with anodic polarization potential in a catalytic activation process and (2) corrosion occurs at breaks in the partial protective film involving the uni-positive Mg ion. There may be some self-corrosion, such as dissolution within deep crevice-like features on a severely damaged surface.

However, self-corrosion is clearly more important for cases where the apparent valence is less than 1.0.

Acknowledgements

This work was supported by the Australian Research Council Centre of Excellence Design of Light Alloys and the Defence Materials Technology Centre. Thanks to the China Scholarship Council to provide a scholarship under the State Scholarship Fund to Fuyong Cao.

References

Atrens, A., Liu, M., & Zainal Abidin, N. I. (2011). Corrosion mechanism applicable to biodegradable magnesium implants. *Materials Science and Engineering B, 176*, 1609−1636.

Atrens, A., Liu, M., Zainal Abidin, N. I., & Song, G. (2009). Corrosion of magnesium (Mg) alloys and metallurgical influence. In G. L. Song (Ed.), *Corrosion of magnesium alloys* (pp. 117−165). Woodhead Cambridge, 2011.

Atrens, A., Song, G. L., Cao, F., Shi, F., & Bowen, P. K. (2013). Advances in Mg corrosion and research suggestions. *Journal of Magnesium and Alloys, 1*, 177−200.

Baril, G., Galicia, G., Deslouis, C., Pebere, N., Tribollet, B., & Vivier, V. (2007). An impedance investigation of the mechanism of pure magnesium corrosion in sodium sulphate solutions. *Journal of the Electrochemical Society, 154*, C108−C113.

Bernath, P. F., Black, J. H., & Brault, J. W. (1985). The spectrum of MgH. *The Astrophysical Journal, 298*, 375−381.

Birbilis, N., Williams, G., Gusieva, K., Samaniego, A., Gibson, M. A., & McMurray, H. N. (2013). Poisoning the corrosion of magnesium. *Electrochemistry Communications, 34*, 295−298.

Bruesch, P., Atrens, A., Muller, K., & Neff, H. (1984). Korrosion von rostfreien Stählen in Chloridlösungen. Eine XPS-Untersuchung der Passivfilme. *Fresenius Jounal Analytical Chemie, 319*, 812−821.

Bruesch, P., Muller, K., Atrens, A., & Neff, H. (1985). Corrosion of stainless steels in chloride solution: an XPS investigation of passive films. *Applied Physics A, 38*, 1−18.

Burstein, G. T., & Daymond, B. T. (2009). The remarkable passivity of austenitic stainless steel in sulphuric acid solution and the effect of repetitive temperature cycling. *Corrosion Science, 51*, 2249−2252.

Cao, F., Shi, Z., Hofstetter, J., Uggowitzer, P. J., Song, G., Liu, M., et al. (2013a). Corrosion of ultra-high-purity Mg in 3.5% NaCl solution saturated with $Mg(OH)_2$. *Corrosion Science, 75*, 78−99.

Cao, F., Shi, Z., Song, G. L., Liu, M., & Atrens, A. (2013b). Corrosion behaviour in salt spray and in 3.5% NaCl solution saturated with $Mg(OH)_2$ of as-cast and solution heat-treated binary Mg−X alloys: X = Mn, Sn, Ca, Zn, Al, Zr, Si, Sr. *Corrosion Science, 76*, 60−97.

Ding, D., Wen, C., Hodgson, P., & Li, Y. (2014). Effect of alloying elements on the corrosion behavior and biocompatibility of biodegradable magnesium alloys: a review. *Journal of Chemistry B, 2*, 1912−1933.

Gandel, D. S., Easton, M. A., Gibson, M. A., Abbot, T. A., & Birbilis, N. (2014). The influence of zirconium additions on the corrosion of magnesium. *Corrosion Science, 81*, 27−35.

Harms, A. C., Khanna, S. N., Chen, B., & Castleman, A. W., Jr. (1994). Dehydrogenation reactions in $Mg^+(H_2O)_n$ clusters. *Journal of Chemical Physics, 100*, 3540−3544.

Heine, B., & Kirchheim, R. (1999). Dissolution rates of iron and chromium and Fe−Cr-alloys in the passive state. *Corrosion Science, 31*, 533−538.

Jin, J., & Atrens, A. (1987). ESCA-studies of the structure and composition of the passive film formed on stainless steels by various immersion times in 0.1 M NaCl solution. *Applied Physics A, 42*, 149−165.

King, A. D., Birbilis, N., & Scully, J. R. (2014). Accurate electrochemical measurement of magnesium corrosion rates; a combined impedance, mass-loss and hydrogen collection study. *Electrochimica Acta, 121*, 394−406.

Kirchheim, R., Heine, B., Fischmeister, H., Hofmann, S., Knote, H., & Stolz, U. (1989). The passivity of iron−chromium alloys. *Corrosion Science, 29*, 899−917.

Kirkland, N. T., Birbilis, N., & Staiger, M. P. (2012). Assessing the corrosion of biodegradable magnesium implants: a critical review of current methodologies and their limitations. *Acta Biomaterialia, 8*, 925−936.

Lim, A. S., & Atrens, A. (1992a). ESCA studies of Cr−Co alloys. *Applied Physics A, 54*, 270−278.

Lim, A. S., & Atrens, A. (1992b). ESCA studies of Ni−Cr alloys. *Applied Physics A, 54*, 343−349.

Liu, M., Qiu, D., Zhao, M., Song, G., & Atrens, A. (2008). The effect of crystallographic orientation on the active corrosion of pure magnesium. *Scripta Materialia, 58*, 421−424.

Liu, M., Schmutz, P., Uggowitzer, P. J., Song, G., & Atrens, A. (2010). The influence of yttrium (Y) on the corrosion of Mg−Y binary alloys. *Corrosion Science, 52*, 3687−3701.

Liu, M., & Song, G. L. (2013). Impurity control and corrosion resistance of magnesium−aluminium alloy. *Corrosion Science*. http://dx.doi.org/10.1016/j.corsci.2013.07.037.

Liu, M., Uggowitzer, P. J., Nagasekhar, A. V., Schmutz, P., Easton, M., Song, G., & Atrens, A. (2009a). Calculated phase diagrams and the corrosion of die-cast Mg−Al alloys. *Corrosion Science, 51*, 602−619.

Liu, M., Zanna, S., Ardelean, H., Frateur, I., Schmutz, P., Song, G., Atrens, A., & Marcus, P. (2009b). A first quantitative XPS study of the surface films formed, by exposure to water, on Mg and on the Mg−Al intermetallics: Al_3Mg_2 and $Mg_{17}Al_{12}$. *Corrosion Science, 51*, 1115−1127.

Missizu, F., Sanekata, M., Tsukamoto, K., & Fuke, F. (1992). Photodissociation of size-selected $Mg^+(H_2O)_n$ ions for $n = 1$ and 2. *Journal of Physics and Chemistry, 96*, 8259−8264.

Olefjord, I., & Elfstrom, B. O. (1982). The composition of the surface during passivation of stainless steels. *Corrosion, 38*, 47−52.

Prasad, A., Uggowitzer, P. J., Shi, Z., & Atrens, A. (2012). Production of high purity magnesium alloys by melt purification with Zr. *Advanced Engineering Materials, 14*, 477−490.

Qiao, Z., Shi, Z., Hort, N., Zainal Abidin, N. I., & Atrens, A. (2012). Corrosion behaviour of a nominally high purity Mg ingot produced by permanent mould direct chill casting. *Corrosion Science, 61*, 185−207.

Schneider, A., Kuron, D., Hofmann, S., & Kirchheim, R. (1990). AES analysis of pits and passive films formed on Fe−Cr Fe−Mo and Fe−Cr−Mo alloys. *Corrosion Science, 31*, 191−196.

Shi, Z., & Atrens, A. (2011). An innovative specimen configuration for the study of Mg corrosion. *Corrosion Science, 53*, 226−246.

Shi, Z., Cao, F., Song, G. L., Liu, M., & Atrens, A. (2013). Corrosion behaviour in salt spray and in 3.5% NaCl solution saturated with $Mg(OH)_2$ of as-cast and solution heat-treated binary Mg−RE alloys: RE = Ce, La, Nd, Y, Gd. *Corrosion Science, 76*, 98−118.

Shi, Z., Jia, J. X., & Atrens, A. (2012a). Galvanostatic anodic polarisation curves and galvanic corrosion of high purity Mg in 3.5% NaCl saturated with $Mg(OH)_2$. *Corrosion Science, 60*, 296−308.

Shi, Z., Jia, J. X., & Atrens, A. (2012b). Galvanostatic anodic polarisation curves and galvanic corrosion of AZ31B in 0.01 M Na_2SO_4 saturated with $Mg(OH)_2$. *Advanced Engineering Materials, 14*, 324−334.

Shi, Z., Liu, M., & Atrens, A. (2010). Measurement of the corrosion rate of magnesium alloys using Tafel extrapolation. *Corrosion Science, 52*, 579−588.

Shi, Z., Prasad, A., & Atrens, A. (2012c). Plug-in specimens for the measurement of the corrosion rate of Mg alloys. *JOM, 64*(6), 657−663,.

Song, G. L. (2006). *Corrosion and protection of magnesium alloys*. Beijing: Chemical Industry Press (宋光铃编著《镁合金腐蚀与防护》化学工业出榜社).

Song, G. (2007a). Control of biodegradation of biocompatible magnesium alloys. *Corrosion Science, 49*, 1696−1701.

Song, G. (2007b). Control of degradation of biocompatible magnesium in a pseudo-physiological environment by a ceramic like anodized coating. *Advanced Materials Research, 29−30*, 95−98.

Song, G. L. (2011). Chapter 1 electrochemistry of Mg and its alloys. In G. L. Song (Ed.), *Corrosion of magnesium alloys*. UK: Woodhead Publishing Limited.

Song, G. L. (2012). Effect of texture on the corrosion behavior of AZ31 Mg alloy. *JOM, 64*(6), 671−679.

Song, G. L. (2013). Chapter 1 corrosion behavior and prevention strategies for magnesium (Mg) alloys. In G. L. Song (Ed.), *Corrosion prevention of magnesium alloys*. UK: Woodhead Publishing Limited.

Song, G., & Atrens, A. (1999). Corrosion mechanisms of magnesium alloys. *Advanced Engineering Materials, 1*, 11−33.

Song, G., & Atrens, A. (2003). Understanding magnesium corrosion mechanism: a framework for improved alloy performance. *Advanced Engineering Materials, 5*, 837−858.

Song, G. L., Atrens, A., StJohn, D., Wu, X., & Nairn, J. (1997). The anodic dissolution of magnesium in chloride and sulphate solutions. *Corrosion Science, 39*, 1981−2004.

Song, G. L., Mishra, R., & Xu, Z. (2010). Crystallographic orientation and electrochemical activity of AZ31 Mg alloy. *Electrochemistry Communications, 12*, 1009−1012.

Song, G., & Song, S. (2007). A possible biodegradable magnesium implant material. *Advanced Engineering Materials, 9*, 298−302.

Song, G. L., & Xu, Z. (2010). The surface, microstructure and corrosion of magnesium alloy AZ31 sheet. *Electrochimica Acta, 55*, 4148−4161.

Song, G. L., & Xu, A. (2012). Crystal orientation and electrochemical corrosion of polycrystalline Mg. *Corrosion Science, 63*, 100−112.

Staiger, M. P., Feyerabend, F., Willumeit, R., Sfeir, G. S., Zheng, Y. F., Virtanen, S., et al. (2011). Summary of the panel discussions at the 2nd symposium on biodegradable metals, Maratea, Italy, 2010. *Materials Science and Engineering B, 176*, 1596−1599.

Sudholz, A. D., Gusieva, K., Chen, X. B., Muddle, B. C., Gibson, M. A., & Birbilis, N. (2011). *Corrosion Science, 53*, 2277.

Taltavull, C., Shi, Z., Torres, B., Rams, J., & Atrens, A. (2014). Influence of the chloride ion concentration on the corrosion of high-purity Mg, ZE41 and AZ91 in buffered Hank's solution. *Journal of Materials Science: Materials in Medicine, 25*, 329−345.

Walker, J., Shadanbaz, S., Kirkland, N. T., Stace, E., Woodfield, T., Staiger, M. P., et al. (2012). Magnesium alloys: predicting in vivo corrosion with in vitro immersion testing. *Journal of Biomedical Materials Research B, 100*, 1134−1141.

Wang, H., Estrin, Y., Fu, H. M., Song, G., & Zúberová, Z. (2007). The effect of pre-processing and grain structure on the bio-corrosion and fatigue resistance of magnesium alloy AZ31. *Advanced Engineering Materials, 9*, 967−972.

Zainal Abidin, N. I., Atrens, A. D., Martin, D., & Atrens, A. (2011). The corrosion of high purity Mg, Mg2Zn0.2Mn, ZE41 and AZ91 in Hank's solution at 37 °C. *Corrosion Science, 53*, 3542−3556.

Zainal Abidin, N. I., Da Forno, A., Bestetti, M., Martin, D., Beer, A., & Atrens, A. (2015). Evaluation of coatings for Mg alloys for biomedical applications. *Advanced Engineering Materials, 17*(1), 58−67.

Zainal Abidin, N. I., Rolfe, B., Owen, H., Malisano, J., Martin, D., Hofstetter, J., et al. (2013). The in vivo and in vitro corrosion of high-purity magnesium and magnesium alloys WZ21 AND AZ91. *Corrosion Science, 75*, 354−366.

Zhao, M. C., Liu, M., Song, G., & Atrens, A. (2008a). Influence of the β-phase morphology on the corrosion of the Mg alloy AZ91. *Corrosion Science, 50*, 1939−1953.

Zhao, M. C., Liu, M., Song, G. L., & Atrens, A. (2008b). Influence of homogenization annealing of AZ91 on mechanical properties and corrosion behavior. *Advanced Engineering Materials, 10*, 93−103.

Plasma surface modification of metallic biomaterials

4

J.A. Gan[1,2], C.C. Berndt[1,3]
[1]Swinburne University of Technology, Hawthorn, VIC, Australia; [2]La Trobe University, Melbourne, VIC, Australia; [3]Stony Brook University, Stony Brook, NY, USA

4.1 Introduction

Plasma is considered the fourth state of matter; it is defined as a gas in the partially ionized state (Friedrich, 2012). It consists of positive ions, free electrons and high-energy atoms and molecules in low, atmospheric or highpressure conditions. Plasma is generated by ionizing atoms or molecules of plasma gas to form positive ions and free electrons. Ionization to form plasma is mostly accomplished by electrical power, but can also be in the form of shock wave excitation or chemical plasmas (Harry, 2010). It is not the focus of this chapter to discuss the aspects of plasma physics, but rather on the plasma processes that are well suited for surface modification of metallic materials. Therefore, only important physical properties of a plasma that are related to the chemistry or surface properties of biomaterials are discussed.

The first part of this chapter provides details on the types of plasma sources and their working environment and the different aspects of plasma surface modification. The specifics of plasma-modification techniques that can be used to alter metallic surfaces, such as plasma implantation and plasma deposition, are discussed in relation to their effects. The second part of this chapter describes the surface property changes that result from plasma modification and the potential biomaterial applications that will benefit from these surface properties. The current challenges in plasma surface modification of biomaterials are considered with the future direction of research and developments in this area.

4.2 An overview of plasma surface modification

Plasma sources can be classified according to their degree of equilibrium and operating pressure. The degree of equilibrium refers to the thermal equilibrium of the plasma, which is defined by the relative temperature of electrons, ions and neutral species within the plasma. A thermal plasma, also known as a hot or high-temperature plasma, is a plasma that is in thermal equilibrium, at which the relative temperature of the ions, T_i, to the temperature of electrons, T_e, is small and can be almost defined by a single temperature. On the other hand, a non-thermal or cold plasma is not in thermal equilibrium, at which the plasma temperature is defined by the temperature of the ions, which

Surface Coating and Modification of Metallic Biomaterials. http://dx.doi.org/10.1016/B978-1-78242-303-4.00004-1
Copyright © 2015 Elsevier Ltd. All rights reserved.

is much lower than the temperature of the electrons ($T_e \gg T_{ion} \approx T_{gas}$). Temperature ranges and examples of thermal and non-thermal plasmas are summarized in Table 4.1.

The differences in thermal energy of plasma systems are attributed to the collision rate and kinetic energy distribution among the electrons, ions, atoms and molecules. Therefore, thermodynamic equilibrium of a plasma system relies substantially on the system's pressure. Generally, a non-thermal plasma is often associated with low pressure, while thermal plasmas operate at high pressure, although recent research revolves around non-thermal plasmas at atmospheric pressure. The mass difference between electrons and other species results in inefficient energy transfer by elastic collisions due to a mismatch in kinetic energy (Friedrich, 2012). The kinetic energy from electrons can only be transferred to atoms and molecules by inelastic collisions, while the kinetic energy can be transferred efficiently among heavy particles such as ions, atoms and molecules.

At low pressure, the density of gaseous atoms and molecules is low, thus the collision rate is also low. In this circumstance, the electrons achieve thermodynamic equilibrium among themselves much faster than achieving equilibrium with ions and neutral species (Friedrich, 2012). Thus, the electrons remain highly energized, while the heavy particles are cooled near to the ambient temperature. Consequently, the ion temperature is much lower than the electron temperature in a non-thermal plasma. At high pressure, the collision rate is much higher, and the kinetic energy transfer from electrons to the heavy particles becomes more efficient. Therefore, all the species within the plasma achieve thermal equilibrium and maintain a similar temperature.

Plasma surface modification is typically accomplished using a low-temperature thermal plasma, Table 4.1(i), or non-thermal plasma, Table 4.1(iii). The use of various plasma technologies to modify surfaces of biomaterials has been proven to be effective in improving their bioactivity, biocompatibility and lifetime (Chu, 2006; Lombardi et al., 2009; Wu et al., 2007). However, it should be noted that there are distinct differences in the plasma surface modification of hard and soft tissues. Hard tissues refer to mineralized tissues or tissues with a rigid intercellular substance, such as bones, while soft tissues are tissues other than bones and joints that connect, support or

Table 4.1 Temperature ranges and examples of thermal and non-thermal plasma

Thermal (hot) plasma		(iii) Non-thermal (cold) plasma
(i) Low temperature	(ii) High temperature	
$T_e \approx T_i \approx T < 2 \times 10^4$ K	$T_e \approx T_i \approx T > 10^7$ K	$T_i \approx T \approx 300$ K $T_i \ll T_e \leq 10^5$ K
e.g. plasma arc at atmospheric pressure (~100 kPa)	e.g. fusion plasma	e.g. glow discharge at low pressure (~100 Pa)

Note: T_e, electron temperature; T_i, ion temperature; T, plasma system temperature.

surround other body structures, e.g. fibrous tissues. This chapter only concerns plasma modification of hard tissues, specifically metallic materials.

There are specific sets of requirements that need to be fulfilled for a material to qualify as a biomaterial. For instance, an artificial joint requires mechanical strength to endure high stress and load bearing, while maintaining good wettability, resistant to corrosion and wear, and biocompatible. A single material rarely possesses all these requirements. Mechanical strength is governed by the bulk properties of the material, whereas wettability, corrosion and wear resistance, and biocompatibility depend on the surface properties. Therefore, surface modification is often required for biomaterials to improve their functionality and lifespan.

The versatility of plasma surface-modification techniques has made it an effective and economical tool to impart functional properties required for osseointegration of metallic materials, such as stainless steel, titanium, titanium alloy and cobalt chromium molybdenum alloy, that are often used as biomaterials due to their high strength and fracture resistance (Pilliar, 2009). Plasma technology is used to modify the surface of metallic biomaterials by (1) chemically or physically altering the surface at the atomic or molecular scale, and/or (2) coating a surface with a material of different composition (Chu et al., 2002).

4.3 Plasma surface-modification techniques

Generally, modification techniques can be classified into three categories, depending on the characteristics of the surface transformation: (1) removal of materials, such as plasma etching and sputtering; (2) change of materials, such as plasma ion implantation; and (3) addition of materials, such as plasma polymerization and plasma spray. Plasma surface-modification techniques associated with each of these categories are depicted in Figure 4.1. Each of these techniques alters the surface properties of biomaterials to a different extent through surface cleaning, surface functionalization and/or deposition of materials that impart desirable surface properties.

4.3.1 Plasma sterilization, sputtering and etching

Naturally, all biomaterials to be used in clinical applications must be free of surface contamination. Surface contaminants can arise from a variety of sources, including residues from surface preparation methods such as grit blasting, processing fluids or sterilization and adsorption of organic molecules from the surrounding environment. Organic contaminants, such as microorganisms, can be removed *via* sterilization, while inorganic contaminants are removed by more vigorous techniques such as sputtering and etching.

Medical devices and biomaterials are conventionally sterilized using techniques such as steam autoclaving, dry heating, gamma and UV light radiation, and ethylene oxide and hydrogen peroxide gas treatment. In addition to having less residue and being more environmental friendly (Feldman and Hui, 1997; Kyi et al., 1995), plasma sterilization presents a cost-effective alternative to conventional sterilization

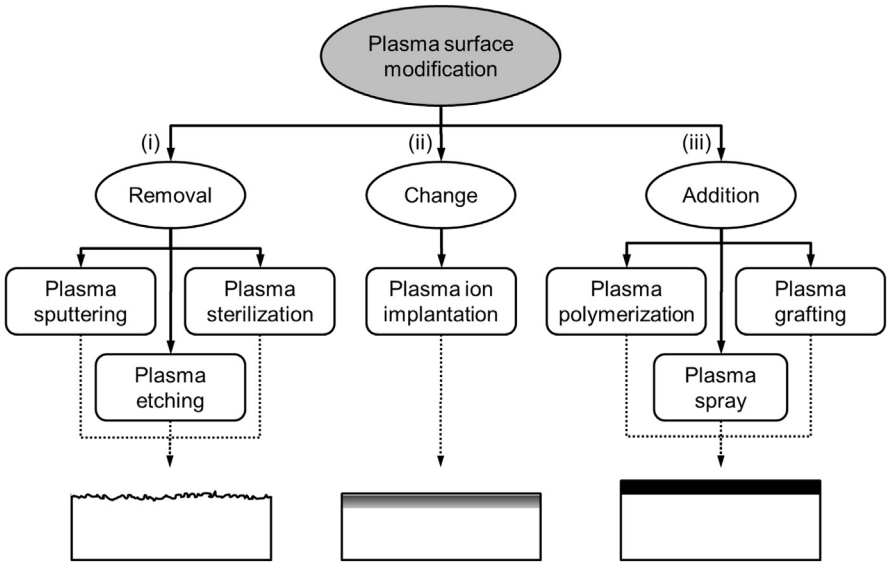


Figure 4.1 Classification of plasma surface-modification techniques.

techniques with regard to the operation costs, processing time and damage afflicted to the treated parts and instrument (Adler et al., 1998).

Despite its potential, the literature on plasma sterilization of biomaterials is focused on polymeric films and scaffolds such as ultrahigh-molecular-weight polyethylene and polylactide (Goldman and Pruitt, 1998; Holy et al., 2001). Studies on plasma sterilization of metallic biomaterials are limited to commercially pure titanium, titanium alloys and nickel−titanium. Laboratory-scale plasma sterilization has been performed using (1) an argon (Aronsson et al., 1997; Shibata and Miyazaki, 2002) or (2) an oxygen plasma (Cvelbar et al., 2006; Park et al., 2012b), while commercial plasma sterilization units used hydrogen peroxide (Sterrad® 100St, Advanced Sterilization Products, Johnson and Johnson, Irvine, CA) or peracetic acid plasma (Plazlyte®, AbTox Inc., Mundelein, IL).

Plasma sterilization operates based on the synergistic effects of ultraviolet (UV) radiation and etching by plasma radicals (Lerouge et al., 2001). The efficiency of sterilization depends not only on the interactions between the plasma radicals with the surfaces, but also on the heating effect from the radical interaction (Cvelbar et al., 2006). Therefore, the substrate material influences the optimization of parameters used in plasma sterilization. The role of plasma parameters on sterilization is depicted in Figure 4.2. Plasma sterilization was reported to improve biocompatibility of the materials (Shibata and Miyazaki, 2002; Thierry et al., 2000).

In plasma sputtering, materials are removed from the surface through bombardment by ions of an inert gas, which is typically argon. The ions are generated by a glow discharge that is initiated and maintained by means of an applied electric potential

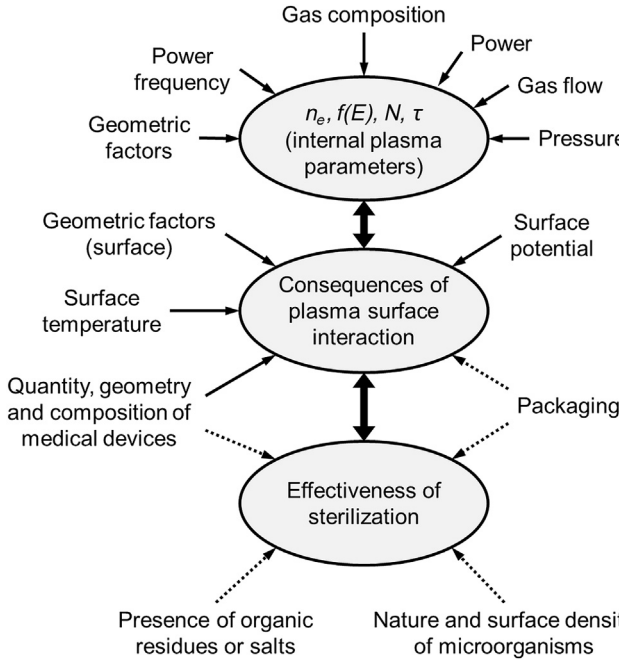


Figure 4.2 Parameters influencing the efficiency of plasma sterilization. Dotted arrows represent factors specific to sterilization. n_e, electron density; $f(E)$, energy distribution function; N, volume concentration of active species; τ, residence time in treatment chamber. Reproduced from Lerouge et al. (2001) with permission from Springer Science and Business Media.

between an anode and a cathode within a low-pressure environment. The ions accelerate toward the target by the applied electric field, where the target, which is also the cathode, is supplied with a negative voltage. Some of the atoms at the target surface will acquire sufficient energy by momentum transfer through elastic and inelastic collisions and be ejected from the target. Note that the sputtering process discussed here is in the context of surface cleaning and material removal, as opposed to material deposition that encompasses both atom removal from a target (cathode) and deposition of the atoms onto a substrate (anode). Surface modification by sputter deposition is discussed in chapter 8.

The first layer of atoms is completely removed with the appropriate sputtering parameters and time, followed by gradual etching of the underlying layers to achieve surface cleaning. Sputtering is often used as a pretreatment to remove contaminants, such as oxides, for subsequent implantation and deposition processes. Surface cleaning of metallic biomaterials by plasma sputtering removes surface contaminants and produces a highly uniform and reproducible composition. Argon plasma was effective in removing impurities such as aluminium, silicon, sulphur, chlorine and calcium from a commercially pure titanium surface, while a combination of oxygen and argon plasmas is required to remove fluorine contaminants (Aronsson et al., 1997).

The sputtering rates are determined by the voltage and pressure of the system. Decreasing the voltage or increasing the system's pressure leads to a low average energy of the impinging ions, thus a low sputtering rate is achieved (Aronsson et al., 1997). A low-energy system and/or short treatment time result in mild and incomplete cleaning. Under these less-optimum conditions, only contaminants at the sharp edges of the surface are removed because the electric field gradient produces higher current intensities and ion fluxes at these locations, thus a higher removal rate. Argon plasma sputtering is also effective in assisting desorption of hydrogen from the titanium surface, which arose from a surface roughening process (Aronsson et al., 2001). However, the gas flow rate of argon needs to be optimized to prevent readsorption onto the clean surface to form hydrides and carbides (Aronsson et al., 1997, 2001).

Plasma etching is a chemical process for removal of targeted materials, as opposed to the physical process of sputtering. In plasma etching, the reactive particle from the plasma adsorbs onto the surface to be etched and forms a chemical bond with the atom at the surface. The product molecule is subsequently desorbed from the surface (Oehrlein, 1990). Plasma etching is mainly used to pattern microelectromechanical systems devices (Hu et al., 2012; Parker et al., 2005), but it has also been applied to biomaterials to improve the surface topography and biofunctionality.

Reactive ion etching (RIE), which is a plasma-based etching technique, is used to etch metallic biomaterials, such as titanium, niobium and tantalum, to improve osteoblast cell attachment by altering the surface topography and surface energy (Pypen et al., 1997). These materials are usually etched using a chlorine-based or fluorine-based plasma that can form volatile metallic halide etching products. Similar to plasma sputtering, the etching rates of RIE are influenced by the voltage and pressure of the systems (Xiao et al., 2010). In addition, the structure and anisotropy of the etched surfaces are influenced by the total gas flow and gas composition (Löffler et al., 2012). Chlorinated RIE has been adopted to produce nanogrooved titanium surfaces by pattern transfer using a mask produced by nanoimprint lithography (Domanski et al., 2012). These nanogrooved surfaces have minimal contamination, good uniformity and are suitable for in vivo implant applications.

4.3.2 Plasma immersion ion implantation

Plasma ion implantation introduces elements into surfaces through implantation of high-energy ions. The ions are accelerated to typically between 20 and 200 keV and directed toward the sample surface. This process operates in a high-vacuum environment and has a relatively shallow treatment depth since the ions are only able to penetrate solid materials up to the depth of several nanometres (Cui and Luo, 1999). The earlier version of this process used an ion beam and is a more selective surface-modification technique because it is a line-of-sight process.

Development of plasma immersion ion implantation (PIII), which is a non-line-of-sight process, has improved the versatility of the ion implantation process. A variation of PIII process is the plasma immersion ion implantation and deposition (PIII&D) process, which incorporates thermal diffusion and deposition into PIII to achieve a greater

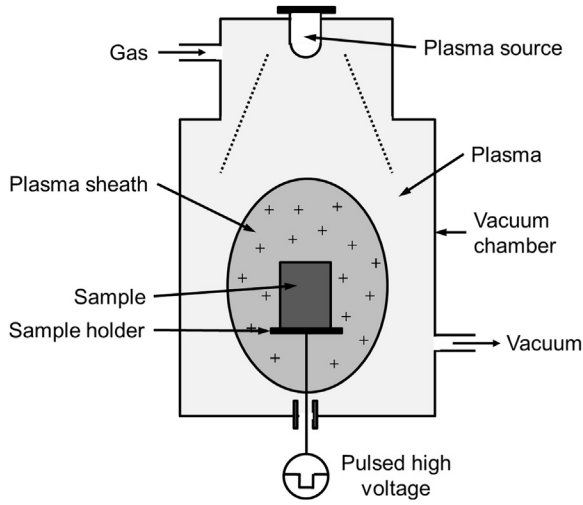


Figure 4.3 Schematic of a plasma immersion ion implantation system.

depth of surface modification. Generally, PIII refers to surface modification by ion implantation without deposition, such as nitrogen implantation to form a nitride, while PIII&D refers to ion implantation that involves the formation of films.

In PIII, the sample is supplied with a high pulsed negative potential and surrounded by a high-density plasma. Ions that are generated in the plasma are accelerated toward the plasma sheath formed around the samples and implanted into the sample surface. A schematic of a PIII system is shown in Figure 4.3. The gaseous plasma in PIII can be generated by direct current, radio frequency glow discharge or electron cyclotron resonance, while a metallic plasma is generated separately or simultaneously using vacuum arc plasma sources (Chu et al., 2002). More than one element can be introduced into the plasma system at any one time.

The properties of the ion-implanted surface depend on the ion species, ion energy, ion dose, plasma density and bias voltage. A high plasma density, short pulse width and high frequency are recommended for good dose uniformity, i.e. good conformity of the plasma sheath shape to that of the sample (Chu et al., 2002). The depth of ion implantation increases with the increase of bias voltage (Liu et al., 2005).

The effects of ion energy level on the microstructure of films produced by ion implantation are shown in Figure 4.4. Low-energy ions result in a columnar structure

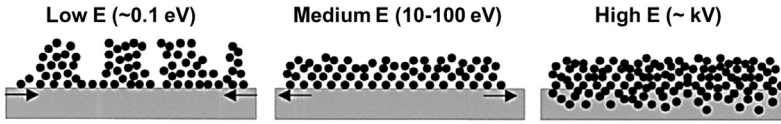


Figure 4.4 Schematics of film microstructure deposited using different ion energy levels. The arrows for the low- and medium-energy processes indicate the direction of strain and the resulting forces on the substrate.
Reproduced from Bilek et al. (2002) with permission from Elsevier.

separated by pores that leads to tensile stress, while energetic ions result in a dense structure with stress that is compressive in nature (Bilek et al., 2002). A high-impact energy allows for significant atomic rearrangement and relaxation of local stress and strain, thus forming a mixing layer at the film−substrate interface that improves adhesion.

Most metallic biomaterials have been documented to be treated by PIII or PIII&D to improve surface properties such as mechanical strength, wear resistance, corrosion resistance and biocompatibility. Examples of such studies are summarized in Table 4.2. Deposition of diamond-like carbon films (DLC) on metallic substrates by PIII&D has also attracted attention in the biomedical field due to their chemical inertness and mechanical properties (Liu et al., 2012; Uzumaki et al., 2008). The DLC films were doped with ions such as nitrogen, calcium and phosphorus to increase their biocompatibility (Chu, 2006; Kwok et al., 2006).

4.3.3 Plasma polymerization

Plasma polymerization involves the formation of a high-molecular-weight polymer from its monomers through activation by an energetic plasma species. The plasma source is used to induce the formation of radicals at solid surfaces and/or gaseous monomers, which are then recombined randomly to form a polymer. The cycle may repeat or propagate through the formation of radicals on the already-deposited polymer. Plasma polymerization can be used to form thin films on many types of surfaces, including metals and polymers. Plasma polymerized films are ultrathin (10 to a few hundred nanometres), smooth, pinhole-free and homogeneous and have good adhesion.

The products of plasma polymerization are often different from that of conventional polymerization due to its unique reaction mechanism, in which the monomers are cross-linked, fragmented or rearranged to form an irregularly structured polymer rather than a polymer with repetitive units (Friedrich, 2011). The irregular structure enhances the films' mechanical properties and resistance toward aging, oxidation and shrinking. The regularity of the polymer can be improved by using pulsed plasma polymerization (Friedrich et al., 2003). The combination of continuous and pulsed plasma polymerization maintains the advantages of both modes, in which the polymer has high density and high stability in an aqueous environment (Li et al., 2009).

Plasma polymerization is an effective surface-modification technique for biomaterials because it promotes osseointegration through the formation of hydrophilic functional groups, such as amine ($-NH_2$) and carboxyl (−COOH). The retention of functional groups in plasma polymerization is higher compared to the retention of the whole monomer structure; hence high concentrations of a single type of functional group can be achieved to promote adhesion or as anchor sites for grafting (Friedrich, 2011).

Table 4.3 summarizes the functional groups and monomers typically used in plasma polymerization of metallic biomaterials. The retention of functional groups increases in the order: allylamine ($-NH_2$), acrylic acid (−COOH), and allylalcohol (−OH),

Table 4.2 Summary of plasma immersion ion implantation of various metallic biomaterials

Substrate	Implanted ion(s)	Phases	Reference(s)
Cobalt chromium molybdenum	Nitrogen	CrN, Cr_2N, $(Co,Cr,Mo)_{2+x}N$	Öztürk et al. (2006), Park et al. (2012a)
Magnesium alloy	Aluminium, zirconium, titanium	Al_2O_3, ZrO_2, TiO_2, MgO, $Mg(OH)_2$	Liu et al. (2007c)
	Oxygen	MgO	Wan et al. (2007)
Nickel−titanium	Carbon	TiC	Poon et al. (2005b), Yeung et al. (2008)
	Nitrogen	TiN, TiO_xN_y	Liu et al. (2007b), Yeung et al. (2007)
	Oxygen	$Ti_{11}Ni_{14}$, TiO_2, TiO	Tan et al. (2003), Yeung et al. (2005), Poon et al. (2005b)
Stainless steel	Nitrogen	Fe_2N, Fe_3N, Fe_4N, CrN, Cr_2N	Liu et al. (2007a), Mello et al. (2009a)
CP-Titanium (commercially pure titanium)	Calcium	$Ca(OH)_2$, $CaCO_3$	Liu et al. (2004b, 2005)
	Nitrogen	TiN	Tang et al. (1998), Pareta et al. (2009)
	Oxygen	TiO_2	Mändl et al. (2001), Thorwarth et al. (2001)
	Phosphorus, sodium	TiO_2[a], TiP[a], P_4O_{10}[a], α-P_3Ti_5[a], Na_2TiO_3	Liu et al. (2004a, b), Maitz et al. (2005)
Ti-6Al-4V	Carbon	TiC	Zhao et al. (2013)
	Nitrogen	TiN, Ti_2N, TiO_2	Ueda et al. (2003), Mello et al. (2009b)
	Nitrogen and oxygen	TiO, Ti_2O, TiO_2, TiN, Ti_2N	Leng et al. (2001), Xiong et al. (2007)

[a]The phases were not indicated in the original references. These phases were noted from the literature of phosphorus ion beam implantation (Baunack et al., 1998; Wieser et al., 1999) rather than plasma immersion ion implantation.

for which the retention of the respective functional groups ranges from 55 to 75% to 90% (Friedrich et al., 2003). Despite having the highest retention, hydroxyl is the least popular functional group used to modify biomaterials due to poor corrosion properties and cytocompatibility compared to amine and carboxyl functionalized surfaces (Jung et al., 2012; Ko et al., 2013).

Table 4.3 Summary of functional groups and monomers used for plasma polymerization of metallic substrates for biomaterial applications

Functional group	Monomer	Substrate[a]	Reference(s)
Amine ($-NH_2$)	Allylamine	CP-Titanium	Finke et al. (2007), Jung et al. (2012), Ko et al. (2012a), Schröder et al. (2010b)
		Magnesium	Ko et al. (2013)
		Stainless steel	Gallino et al. (2010), Yang et al. (2010, 2011a)
		Ti-6Al-4V	Finke et al. (2011)
	Heptylamine	CP-Titanium	Li et al. (2009), Zhao et al. (2011)
Carboxyl ($-COOH$)	Acrylic acid	CP-Titanium	Jung et al. (2012), Ko et al. (2012a), Schroder et al. (2010a)
		Magnesium	Ko et al. (2013)
		Stainless steel	Yang et al. (2011a)
Hydroxyl ($-OH$)	Allyl alcohol	CP-Titanium	Jung et al. (2012), Ko et al. (2012a)
		Magnesium	Ko et al. (2013)

[a]CP-Titanium refers to commercially pure titanium.

The osseointegration of carboxyl plasma-polymerized surfaces is further improved through a cation-exchange approach, in which the hydrogen in $-COOH$ is replaced by the cation (M^{x+}) to form $-COOM$. Ion-exchanged titanium surfaces using calcium, magnesium, and sodium ions showed improved cell spreading and proliferation (Ko et al., 2012b; Lee et al., 2012). A thin (10–100 nm) plasma-polymerized layer has also been used to protect living cells from direct contact with a copper-implanted titanium surface while still maintaining the antimicrobial property of copper to prevent post-operative inflammation (Schröder et al., 2010b).

4.3.4 Plasma grafting

Graft polymerization can be achieved through many means: chemical, radiation, photochemical, plasma, and enzyme treatments (Bhattacharya and Misra, 2004). Plasma grafting has similar radical formation and recombination mechanisms as plasma polymerization. However, instead of forming polymer chains on the

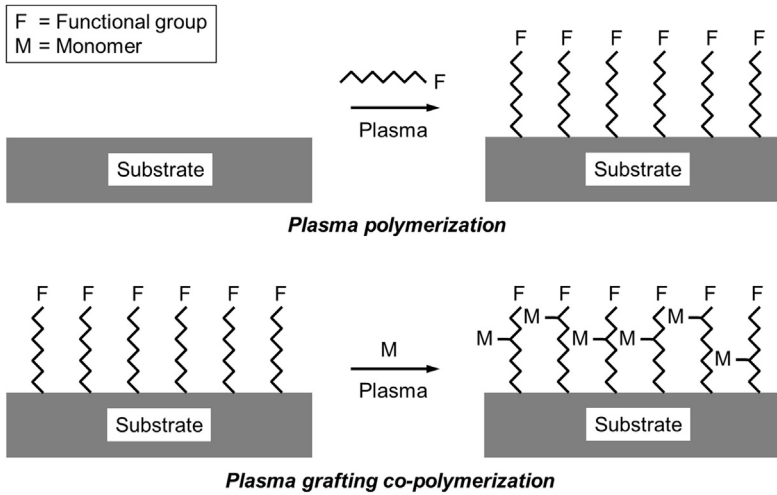


Figure 4.5 Schematic showing the difference between plasma polymerization and plasma-induced grafting. *Note: The site and sequence of monomer attachment in the schematic is not representative of the actual reaction.*

substrate, plasma grafting involves the addition of one or more monomer(s) covalently bonded to an already-deposited polymer layer to form a branched co-polymer. Plasma grafting is initiated by the impact of high-energy electrons from the plasma source, which is usually a glow discharge, and causes cleaving of chemical bonds in the polymer to form radicals. Grafting is propagated by these radical sites on the polymer when combined with monomers, and is terminated when the radical sites combine with monomer radicals. Therefore, plasma grafting of metallic surfaces is often preceded by polymerization or other polymer coating techniques. The difference between plasma polymerization and plasma-induced grafting is shown schematically in Figure 4.5.

Plasma grafting of biomaterials is typically performed to improve the biocompatibility, osseointegration, wettability, and lubricity of the implants. This approach has been used to treat surfaces of metallic biomaterials such as titanium, titanium alloy, and stainless steel (Huang et al., 2011; Ye et al., 2009; Zhang et al., 2001), although cobalt−chromium−molybdenum alloy is also known to be treated by chemical grafting (Kyomoto et al., 2007). Grafting of metallic surfaces is preceded by functionalization of the surfaces by functional groups such as amine, silane or siloxane to provide grafting sites. Such pretreatment is usually accomplished by plasma polymerization, sputter deposition or dip coating.

The functionalized surfaces are then activated by a plasma to provide radical sites for grafting. The grafting process is sometimes followed by UV treatment (Ye et al., 2009; Zhang et al., 2001). Depending on the intended surface function(s), different materials are grafted onto the treated surface. Proteins such as collagen and albumin were grafted to enhance biocompatibility and osseointegration of the implants

(Chang et al., 2008; Huang et al., 2011). Amine was grafted onto a siloxane-functionalized surface to enhance surface lubricity to minimize trauma and tissue abrasion during insertion and removal of medical devices to and from the body (Chen et al., 2009a).

4.3.5 Plasma spraying

Plasma spray belongs to the family of thermal spray processes. Classification of thermal spray processes according to their source of energy is shown in Figure 4.6. Thermal spray is a generic term that is used to refer to a group of coating processes in which a stream of finely divided metallic or nonmetallic particles is applied onto a substrate to form flattened lamellae that stack progressively to form a coating (Davis, 2005; Pawlowski, 2008). Unlike all previously discussed plasma surface-modification techniques that use non-thermal plasma sources, plasma spray uses a thermal plasma source. The heat from a thermal plasma is required to melt the feedstock material, which is accelerated and deposited through formation of a bond that is based on mechanical interlocking.

The energy sources used to generate a thermal plasma are usually direct current (DC), electric arcs or other high-frequency sources. The plasma generator generally consists of a copper anode and a cathode that is usually made of thoriated tungsten because of its high melting point and good thermionic emission properties. A schematic of plasma spray torch is shown in Figure 4.7. The plasma is generated by supplying a high-voltage discharge to ionize the plasma-forming gases to form positive ions and free electrons. The movement of free electrons through the ionized gas maintains the plasma state. Heat and light energy is released when the electrons and ions recombine.

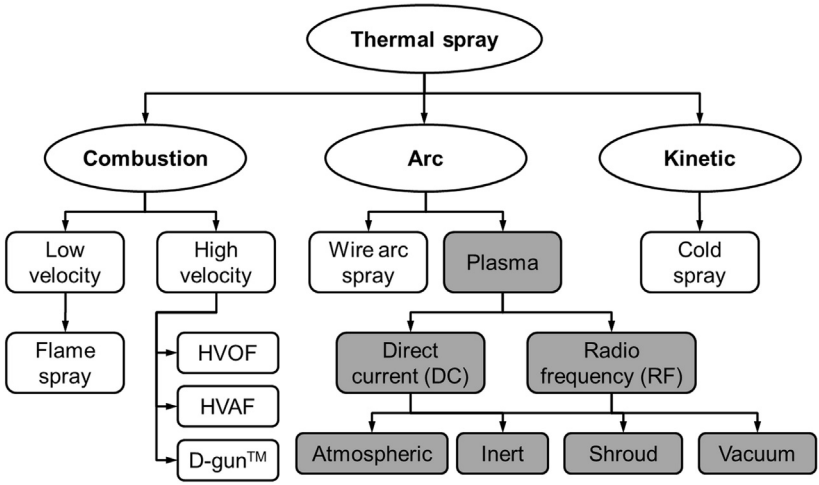


Figure 4.6 Plasma spray process within the thermal spray processes classification. HVOF, high velocity oxygen-fuel; HVAF, high velocity air-fuel; D-gun™, detonation gun.

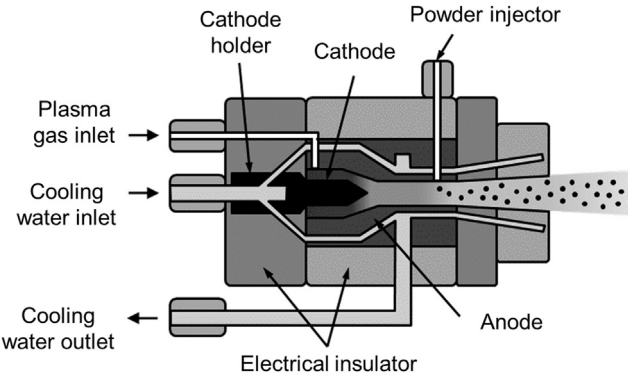


Figure 4.7 Schematic of a plasma spray torch.

The plasma-forming gas directly influences the degree of melting of the feedstock and is usually an inert monoatomic or diatomic gas. Monoatomic gases, such as argon and helium, have lower gas enthalpy, but the generated gas jet could reach high velocity. On the other hand, diatomic gases, such as hydrogen and nitrogen, generate greater enthalpy due to dissociation of their molecular structure and have higher thermal conductivity. Combinations of monoatomic and diatomic gases are used to generate thermal plasmas with high enthalpy and velocity.

The high temperature of the plasma spray process, in which the jet temperature ranges between 8000 and 15,000 °C, allows for the deposition of a wide range of materials including metals, ceramics, polymers, and composites. The feedstock materials used for plasma spray processes are typically in the form of powder, although recent development has favoured the deposition of nanostructured coatings using feedstock in solution or suspension form. The plasma spray process has the advantage of greater treatment depth compared to other plasma-modification techniques, in which the deposit's thickness can range from 50 μm to several millimetres. Also, the plasma spray process is flexible in relation to its working environment. Depending on the material needs, they can be deposited under atmospheric, inert or vacuum conditions. Despite being a line-of-sight process, the plasma spray process can treat substrates with complex geometries, e.g. orthopaedic knees and hips.

Plasma spray has been used to modify surface properties of metallic implants to impart mechanical and biological compatibility. Metallic biomaterials such as titanium and its alloys, cobalt−chromium alloys, and stainless steel have mechanical strength that are well suited for the load-bearing requirement of biomedical implants, but lack the bioactivity for bone bonding and growth. The ability of plasma spray to deposit dense and porous coatings is imperative in providing a favourable surface for bone-implant fixation and bone ingrowth while still maintaining good corrosion resistance. One way of achieving this effect is by depositing coatings with graded porosity (Yang et al., 2000): (1) a dense inner layer to prevent metal ions release; (2) an intermediate layer with a mixture of micro and macropores for calcium phosphate precipitation; and (3) an outer layer with macropores for bone ingrowth.

The most well-known plasma spray application on biomaterials is the deposition of hydroxyapatite (HA), $Ca_{10}(PO_4)_6(OH)_2$, because the structure and composition of HA are similar to the bone mineral that constitutes 60−70 wt% of natural bone (Sun et al., 2001). This chemical similarity promotes the formation of a strong bone−implant bond (De Groot et al., 1987; Geesink et al., 1988; Oonishi et al., 1989), thus improving the fixation and postoperative recovery time. Other calcium phosphate materials such as tricalcium phosphate (Kitsugi et al., 1996) and fluorapatite (Fathi et al., 2009) have also been used to produce similar effects as HA. The low mechanical performance of HA (Akao et al., 1981; Jarcho, 1981; Jarcho et al., 1976) has led to the incorporation of reinforcement materials such as alumina, titania, and zirconia into HA coatings.

Materials other than HA, such as calcium silicate, titanium, titania, and zirconia, have also been deposited directly onto metallic implants to improve the corrosion resistance of the implants. Plasma-sprayed coatings can inhibit the release of metal ions such as aluminium and vanadium caused by dissolution and corrosion of the metallic implants, which may cause long-term health problems (Geurtsen, 2002; Laing et al., 1967). The materials and postspray treatments used in plasma-spray modifications of various metallic substrates for biomedical applications are summarized in Table 4.4.

Plasma-sprayed implants have been widely used in orthopaedics and dentistry, such as hip and knee implants, screws and pins in bone plates, and dental endosteal implants. A review on the clinical performance of plasma-sprayed HA is available in (Sun et al., 2001). However, there have been concerns about the long-term performance of HA due to the dissolution and weakening of HA coatings in the physiological environment.

The presence of (1) amorphous calcium phosphate, (2) thermal decomposition products such as tricalcium phosphate, tetracalcium phosphate, and calcium oxide, and (3) dehydroxylation products such as oxyhydroxyapatite and oxyapatite promotes coating resorption and degradation due to their enhanced solubility in body fluids (Legeros, 1993; Radin and Ducheyne, 1992). The purity and crystallinity of HA coatings can be improved through the control of feedstock quality, selection of appropriate process parameters, and post-deposition heat treatment (Sun et al., 2001).

Although plasma-sprayed implants have shown high mid- to long-term survival (Lombardi et al., 2009), there have been cases of prostheses loosening that require revision surgery after several years postimplantation (Lai et al., 2002; Røkkum et al., 1999). The implant may become loose within the skeletal structure and not be stabilized and fixed in the three-dimensional space. The prime mechanisms for such loosening include: (1) aseptic loosening (Røkkum et al., 1999; Sundfeldt et al., 2006); (2) low coating−implant adhesion relative to the bone-coating bond (Müller and Patsalis, 1997); and (3) insufficient load transfer due to bone-implant elastic moduli mismatch (Dujovne et al., 1993). Various bond coat materials have been introduced to improve implant fixation and stabilization; Table 4.5.

In addition to improving the coating−implant adhesion, bond coats also (Heimann, 2007; Kurzweg et al., 1998): (1) prevent direct contact between HA and the metallic

Table 4.4 Summary of plasma sprayed coatings and post-spray treatments for various metallic biomaterials

Substrate	Coating[a]	Plasma spray system[b]	Post-spray treatment(s)	Reference(s)
Co–Cr–Mo	HA	APS	None	Ducheyne and Healy (1988), Dalton and Cook (1995)
	$Ca_3(PO_4)_2$	APS	None	Chae et al. (1992)
	Titanium	VPS	None	Reclaru et al. (2005)
CP–Titanium	Al_2O_3, Al_2O_3–TiO_2	APS	None	Yilmaz (2009)
	HA	APS	None	García-Sanz et al. (1997), Gross et al. (1998)
			Heat treatment, spark plasma sintering	Yu et al. (2003), Lu et al. (2006)
			Water vapour treatment	Cao et al. (1996), Chen et al. (1997)
	HA/Al_2O_3	APS	None	Mittal et al. (2013)
	HA/YSZ	APS	None	Aydin et al. (2006)
	Titanium	APS	None	Yang and Ong (2003), Simon et al. (2005)
			Ion implanted with NH_2^+	Yang et al. (2002)
	Titanium	VPS	[c]CEMEX® acrylic bone cement top layer	Reclaru et al. (2003)
	YSZ	APS	None	Yang and Ong (2003)
Magnesium alloy	TiO_2	APS	Sealing with Na_2SiO_3	Zeng et al. (2008)
Nickel–titanium	Titanium	APS	Sealing with organic polymers (silicone, epoxy, cyanoacryl or polyamide) or physical vapour deposition of titanium	Okuyama et al. (2004)

Continued

Table 4.4 Continued

Substrate	Coating[a]	Plasma spray system[b]	Post-spray treatment(s)	Reference(s)
Stainless steel	Bioglass	APS	Silver ion-exchange	Miola et al. (2009)
	$Ca_5(PO_4)_3F$/ Niobium	APS	None	Fathi et al. (2009)
	HA	APS	None	Sun et al. (2002), Heleno et al. (2009)
			Heat treatment	Gross and Berndt (1994)
	HA/TiO_2	APS	None	Ye et al. (2007)
	TiO_2	SPPS	Alkaline (NaOH) treatment	Chen et al. (2008)
Ti-6Al-4V	Bioglass	APS	None	Kitsugi et al. (1996)
			Silver ion-exchange	Miola et al. (2009)
	Ca_2SiO_4	APS	None	Liu et al. (2002)
	$Ca_3(PO_4)_2$	APS	None	Kitsugi et al. (1996)
	$CaSiO_3-TiO_2$	APS	None	Liu and Ding (2002)
	$CaTiSiO_5$	APS	None	Wu et al. (2009)
	HA	APS	None	Yang et al. (1995), Sergo et al. (1997)
			Alkaline (NaOH) and heat treatment	Lee et al. (2004a)
			Heat treatment	Kweh et al. (2002), Dong et al. (2003)
			Polymer (polyhydroxybutyrate, polyhydroxyvalerate or polymethylmethacrylate) top coat	Chebbi and Stokes (2012)

	HA	VPS	None	Heimann and Vu (1997), Tsui et al. (1998a), Gledhill et al. (1999)
			Heat treatment	Tsui et al. (1998b)
	HA/bioglass	APS	None	Ding et al. (2000)
	HA/$CaSiO_3$	APS	None	Kitsugi et al. (1996)
	HA/silicon	APS	None	Gomes et al. (2010)
	HA/titanium	APS	None	Zheng et al. (2000)
	HA/TiO_2	SPSS	None	Varadaraajan et al. (2009)
	HA/TiO_2 (graded)	CAPS	Heat treatment	Cannillo et al. (2008)
	HA/YSZ	APS	None	Chang et al. (1997), Fu et al. (2000), Lee et al. (2004b)
	Titanium	VPS	Chemical treatment with NaOH and Ag	Chen et al. (2009b, 2010)

[a]HA and YSZ are abbreviations for hydroxyapatite, $Ca_{10}(PO_4)_6(OH)_2$, and yttria-stabilized zirconia, Y_2O_3-ZrO_2, respectively.
[b]APS, CAPS, SPSS, and VPS are abbreviations for atmospheric plasma spray, controlled atmosphere plasma spray, solution precursor plasma spray, and vacuum plasma spray, respectively. VPS can also be termed as LPPS (low pressure plasma spray).
[c]CEMEX® is a trade name for acrylic bone cement manufactured by Tecres S.P.A. Corporation (Verona, Italy).

Table 4.5 Summary of bond coat materials used in plasma spray modifications of metallic implants

Substrate	Bond coat	Top coat[a]	Thickness (μm)		Reference(s)
			Bond coat	Top coat	
CP-Titanium	Al_2O_3/TiO_2	HA	25–50	100–170	Oktar et al. (2006)
	HA/Ti	HA	100	100	Rakngarm and Mutoh, (2009)
	HA/TiO_2	HA	…	…	Lu et al. (2004)
	Ni–Al	Al_2O_3, Al_2O_3–TiO_2	185–193	447–608	Yilmaz (2009)
	Titanium	HA	50–100	100	Yang and Ong (2003), Rakngarm and Mutoh (2009)
	TiO_2	YSZ-HA	…	…	Aydin et al. (2006)
	ZrO_2	Ha	…	…	Yang and Ong (2003)
Ti-6Al-4V	Calcium silicate, Ca_2SiO_4	HA	10–50	30–130	Lamy et al. (1996), Kurzweg et al. (1998)
	Titanium	HA	5–100	40–400	Tsui et al. (1998b), Gledhill et al. (1999)
	TiO_2, TiO_2–ZrO_2	HA	10–15	150–180	Kurzweg et al. (1998), Heimann (1999)
	Y_2O_3–ZrO_2	HA	15	135	Chou and Chang (2001), Chou and Chang (2003)

[a]HA and YSZ are abbreviations for hydroxyapatite, $Ca_{10}(PO_4)_6(OH)_2$, and yttria-stabilized zirconia, Y_2O_3–ZrO_2, respectively.

substrate that catalyses thermal decomposition of HA; (2) reduce metal ion release; (3) reduce the thermal gradient at the substrate-coating interface; (4) reduce coating-substrate thermal expansion coefficient mismatch; and (5) cushion coating damage initiated by cyclic micromotions of the implant immediately after operations. An extensive review of bond coats in plasma-sprayed biomedical implants is available in (Heimann, 2007).

4.4 Surface properties from plasma modification

There are three primary aspects that must be considered for clinical applications of metallic biomaterials: (1) biocompatibility; (2) physical and mechanical properties; and (3) manufacturing practicality (Hoeppner and Chandrasekaran, 1994). The ideal biomaterial for hard tissue replacements should exhibit a biocompatible chemical composition to avoid adverse tissue reactions, excellent resistance to degradation in the human body environment, acceptable mechanical strength to sustain cyclic loading, low modulus to minimize bone resorption, and high wear resistance to minimize debris generation (Long and Rack, 1998). All these requirements are rarely exhibited by a single material, but may be largely achieved by engineering the surface properties. The material properties that can be imparted on biomaterials through surface modifications are summarized in Figure 4.8.

4.4.1 Surface morphology

It has been established that the surface morphology of biomaterials directly influences protein adsorption; cell attachment and proliferation; contact guidance; and differentiation (Anselme and Bigerelle, 2011; Deligianni et al., 2001; Ismail et al., 2007; Kieswetter et al., 1996). Plasma surface modification creates topographical features, such as grooves, pits, pores, and roughness, which mimic the natural extracellular matrix. The surface features can be: (1) well-defined; e.g. submicron patterning achieved through plasma etching, Figure 4.9(a); or (2) disordered; e.g. the roughness of plasma-sprayed surfaces, Figure 4.9(e). The cell response toward surface topography depends on the cell types since cell adhesion is promoted by different proteins that adsorb preferentially on surfaces (Curtis and Wilkinson, 1997; Masters and Anseth, 2004). Figure 4.9 compares the surface morphology of titanium or titanium-based alloys treated by different plasma processes.

Plasma sterilization and sputtering do not generally alter the topography of the treated surfaces significantly since these techniques were used mainly to remove surface contaminants on medical devices and surgery tools, which are often within the nanometre-range thickness (Aronsson et al., 1997). However, non-optimized treatment parameters may result in non-uniform material removal, thus a change in surface morphology. This is often the case when a low-energy system and/or short treatment time is used to treat a rough surface. Under these circumstances, only the contaminants at the sharp edges of the surface are removed because the removal rate is higher with

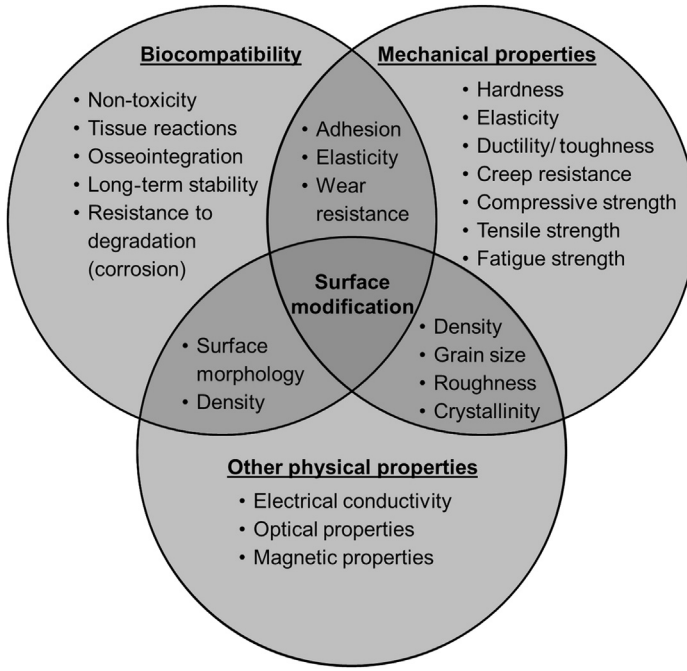


Figure 4.8 Primary requirements of metallic biomaterials achieved through surface modification. The intersection of the three primary requirements represents the topical area where surface modification has the greatest potential.

the higher current intensities and ion fluxes at these locations (Aronsson et al., 1997). Plasma sterilization increases the surface roughness (Park et al., 2012b), while plasma sputtering decreases surface roughness (Aronsson et al., 1997; Lin et al., 2005). Table 4.6 compares the arithmetic average roughness of various plasma-modified surfaces.

Plasma etching for surface cleaning purposes may exhibit similar outcomes as sterilized and sputtered surfaces. However, the use of plasma etching for surface patterning result in well-defined surface features, such as grooves and pillars, that were transferred using an etch mask (Domanski et al., 2012; Löffler et al., 2012); Figure 4.9(a). These nanopatterns resemble the highly organized nanometric-scale topography of the extracellular matrix of certain hard tissues; e.g. type I collagen, which is the basic building block of bones, has a groove-like fibrillar structure with 68-nm gaps (Weiner and Wagner, 1998). The cell response, which is measured by the cell adhesion, orientation and growth rate, relies on the cell type and the nanopattern topography and dimensions (Curtis and Wilkinson, 1997); e.g. osteoblasts are responsive to nanogrooves down to 75 nm in width and 33 nm in depth (Lamers et al., 2010). The surface roughness of plasma-etched surfaces generally increased after the etching process, although the extent of increment depended on the initial roughness and the etching parameters.

Despite the fact that the surface morphology of materials modified with PIII, plasma polymerization and plasma grafting exhibited discernible surface features,

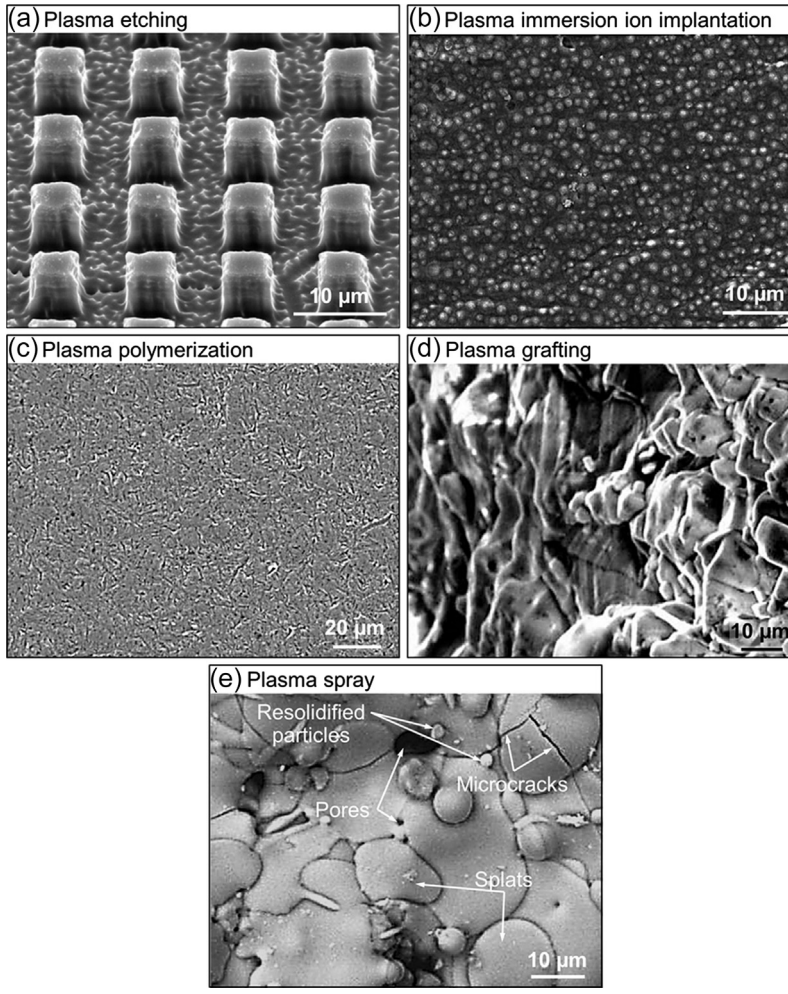


Figure 4.9 Surface morphology of titanium or titanium-based alloys modified by: (a) reactive ion etching to form patterned titanium pillars, reproduced from Löffler et al. (2012) with permission from Elsevier; (b) plasma immersion ion implantation with calcium, reproduced from Liu et al. (2005) with permission from Elsevier; (c) plasma polymerization with allylamine, reproduced from Wu et al. (2007) with permission from the Japan Institute of Metals and Materials; (d) plasma grafted with type I collagen, reproduced from Chang et al. (2008) with permission from the Japanese Society for Dental Materials and Devices; and (e) plasma sprayed with HA reproduced from Yu et al. (2003) with permission from Elsevier. The microstructural features in (e) have been highlighted for clarity.

Figure 4.9(b)–(d), the significance of these processes lies on the surface chemistry changes rather than physical ones. However, the increased surface roughness after the respective plasma-modification processes was shown to have beneficial effects on cell adhesion and proliferation (Liu et al., 2007b; Pareta et al., 2009; Seo et al., 2010).

Table 4.6 Comparison of the arithmetic roughness average values, R_a, for surfaces treated with various plasma surface modification processes

Plasma process	Initial average roughness, ${}_iR_a$ (nm) [μin]	Final average roughness, ${}_fR_a$ (nm) [μin]	References
Plasma sterilization	5 [0.20]	10−11 [0.39−0.43]	Thierry et al. (2000)
Plasma sputtering	17.20 [0.68]	2.02 [0.08]	Lin et al. (2005)
Plasma etching	7 ± 3 [0.28 ± 0.12]	38−116 [1.50−4.57]	Domanski et al. (2012)
Plasma immersion ion implantation	1.78 [0.07]	5.8−12.1 [0.23−0.48]	Öztürk et al. (2006)
Plasma polymerization	6.361 [0.25]	21.750 [0.86]	Seo et al. (2010)
Plasma grafting	350 [13.78]	310 [12.21]	Sawano et al. (2010)
Plasma spray	1100 ± 100 [43.31 ± 3.94]	5700−8200 [224.41−322.84]	Tsui et al. (1998a)

Note that this table is provided for the comparison of the general trend of surface roughness changes after the respective plasma-modification process. The range of surface roughness values depends on the initial R_a values and various processing parameters of the respective processes.

On the contrary, a smoother surface has better resistance toward corrosion because the surface area available for the initiation of pitting corrosion is smaller within such biomaterials (Tan et al., 2003; Wan et al., 2007). The surface morphology of PIII surfaces varies substantially with the implantation voltage, ion types, and incident ion dose (Liu et al., 2007b; Tan et al., 2003), while that of plasma-polymerized and grafted surfaces depend largely on the film thickness, monomer type, and power (Ko et al., 2012a; Myung et al., 2013).

Plasma-sprayed surfaces are relatively rough compared to those modified by other plasma-modification techniques. Such rough surfaces are attributed to the need for substrate surface asperities for good bonding of plasma-sprayed materials, which is achieved through mechanical interlocking. The surface of metallic substrates is typically roughened by grit blasting, and the average surface roughness usually ranges between 2 and 6 μm; depending on the blasting parameters and material needs. The surface roughness generally increases after plasma spray deposition because the substrate surface irregularities are transmitted to the next layer of coating surface during deposition and enhanced by new protuberances such as porosity and unmelted particles during coating growth (Cirolini et al., 1991). Distinctive morphological features are observable on the coating surface, including flattened particles known as splats, unmelted particles, resolidified particles, and microcracks; Figure 4.9(e). The

variability of each of these surface features depends on the degree of particle melting, particle impact velocity, spray distance, and substrate temperature.

The variability of the plasma-modified surface morphology strongly influences the cell response toward the biomaterial (Borsari et al., 2005a; Lamers et al., 2010), through alteration of surface energy and wettability. Surface roughness has been established to have a direct influence over surface wettability (Cassie and Baxter, 1944; Wenzel, 1936) and, therefore, the surface energy. However, the cell sensitivity and response toward surface morphology depends on the cell phenotype; e.g. fibroblasts adhere well on smooth surfaces, while osteoblasts adhere better on rough surfaces (Anselme and Bigerelle, 2011). Surface topography and roughness also have significant roles on the mechanical, wear, and corrosion behaviour of biomaterials.

4.4.2 Surface chemistry

Surface chemistry dictates the free energy and functionality of interfaces, and therefore directly influences cell adhesion and proliferation of biomaterials. However, it is often difficult to distinguish the relative effects of surface chemistry and surface topography because independent variation of these two surface characteristics is technically difficult (Anselme et al., 2000; Hallab et al., 2001). Short-term cell adhesion and proliferation on Ti-6Al-4V were found to depend more on surface chemistry, while surface roughness is more influential on long-term cell adhesion (Anselme and Bigerelle, 2006a, 2006b). Although the variability of surface topography is often associated with a change in the surface chemistry, this section will focus on plasma-modification approaches that impart more direct surface chemistry modifications rather than surface chemistry alterations associated with topography changes.

Introduction of high-energy ions through PIII results in the formation of new phases on the implanted surfaces, Table 4.2, which directly transforms the surface properties. The commonly implanted ions include carbon, nitrogen, and oxygen, which result in the formation of carbides, nitrides, and oxides, respectively. These phases impart mechanical strength, wear resistance, and corrosion resistance on metallic biomaterials. For instance, carbon-PIII improves the corrosion resistance of NiTi alloys, which significantly reduces the leaching of metal ions and improves the cytocompatibility (Poon et al., 2005b). On the other hand, implantation with bioactive ions such as calcium and sodium substantially accelerates calcium phosphate formation on metallic substrates in vivo (Hanawa et al., 1997; Maitz et al., 2005). Similar improvement of osteoconduction is achieved through plasma spraying of bioactive ceramic coatings, such as HA and bioglass, on metallic biomaterials (Sun et al., 2001; Verné et al., 1998).

Plasma polymerization and plasma grafting are used to modify metallic biomaterials by introducing functional groups such as amine, carboxyl, hydroxyl, and collagen onto the interfaces. The chemical reactivity of such functional groups aids the immobilization of biologically active protein molecules on bioinert metallic surfaces (Puleo et al., 2002). In addition, protonation or deprotonation of the amine or carboxyl groups in aqueous solutions at physiological pH values produces positively and negatively charged surfaces, respectively, that exhibit high affinity for opposite-charged cells due to electrostatic interaction (Lee et al., 1994). The coatings with tunable surface

density of hydrophilic functional groups also help enhance the wettability of biomaterial surfaces for cell adhesion and spreading over a larger area (Bacakova et al., 2011), as well as provide high-lubricity surfaces for improved wear resistance (Kyomoto et al., 2007).

Finke et al. (2007) found that the cell response of a high-density amine functionalized titanium surface is similar to that of a collagen-bonded surface. Yang et al. (2010) discovered that heparin grafting on allylamine plasma-polymerized surface exhibits excellent anticoagulant properties and promotes endothelial cell adhesion and proliferation. The cell proliferation on plasma-polymerized metallic surfaces can be further improved by ion exchange of bioactive ions, such as magnesium, onto the polymeric thin film containing functional groups (Ko et al., 2012b). On the other hand, grafting of metallic surfaces with lysozyme or poly(ethylene glycol) deteriorates protein adsorption and bacterial adhesion through steric repulsion by the long and dense polymeric chains, thus preventing biofilm growth, and could potentially be used as antifouling agents on metallic biomaterials (Caro et al., 2009; Zhang et al., 2001).

4.4.3 Biocompatibility and bioactivity

The biocompatibility of a material is dictated by its in vivo biological responses, such as non-toxicity, tissue response, and long-term stability. The ideal characteristics would depend on the specific applications of the biomaterials. For instance, protein adsorption is desirable for cell proliferation and osseointegration in joint replacements, while such adhesion in biomaterial components in direct contact with blood, e.g. artificial heart valves, would cause medical complications. Therefore, the biocompatibility of plasma-modified surfaces will be discussed with consideration to these differences. Note that it is not the intention of this section to provide a comprehensive review on the biological responses of plasma-modified surfaces, but to indicate how such responses are altered with plasma modifications. Generally, all plasma-cleaned and sterilized surfaces exhibit increased surface energy and good wettability, which encourages cell attachment, proliferation, and differentiation (Aronsson et al., 1997; Park et al., 2012b; Pypen et al., 1997). Again, such biological responses depend largely on the surface morphology and surface chemistry of the biomaterials.

4.4.3.1 Plasma immersion ion-implanted surfaces

Plasma immersion ion implantation (PIII) induces the formation of rough surfaces and significant surface chemistry alterations, which resulted in improved osteoblast and fibroblast cell adhesion, proliferation, and new bone formation (Mändl et al., 2001; Pareta et al., 2009; Poon et al., 2005b). Zhao et al. (2013) indicated that surface chemistry is more important for in vitro cytocompatibility, while surface roughness is more important for new bone formation in vivo. Combination of water and hydrogen-PIII improves cell adhesion and spreading through the formation of -OH functional groups that catalyse apatite nucleation through calcium titanate formation and subsequent phosphate adsorption (Xie et al., 2005). On the other hand, calcium-PIII enhances bioactivity and bone conduction through the formation of calcium hydroxide and

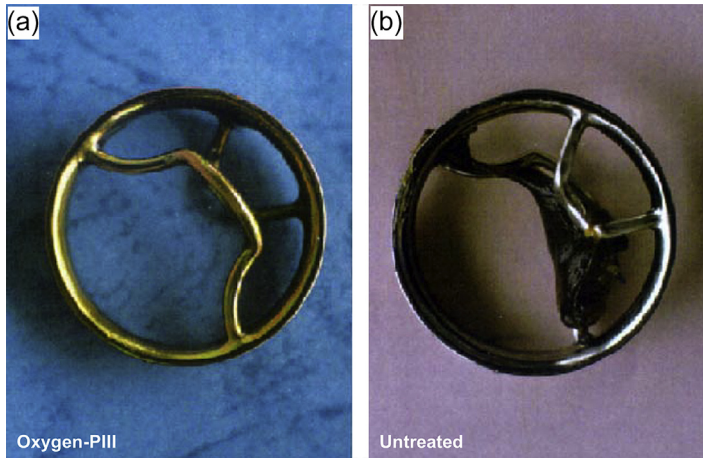


Figure 4.10 Comparison of surface conditions of mechanical heart valve cages after 30 days of in vivo test: (a) modified with oxygen plasma immersion ion implantation remains thrombus-free, and (b) untreated surface encapsulated by thrombus.
Reproduced from Huang et al. (2004) with permission from Elsevier.

calcium carbonate, which dissolve gradually in simulated body fluid to form HA on the surface (Chu, 2007b; Hanawa et al., 1997).

Calcium- and phosphorus-PIII enhance hemocompatibility by promoting the absorption and unfolding of proteins (Kwok et al., 2006). The degree of protein conformational changes directly influences the behaviour of platelets; e.g. albumin and fibrinogen are platelet inhibiting and activating proteins, respectively. The calcium- and phosphorus-PIII surfaces exhibited less platelet adhesion and activation compared to the low-temperature isotropic pyrolytic carbon (LTIC) (Kwok et al., 2006), which has the best hemocompatibility among clinically applied materials for artificial heart valves. Formation of *n*-type semiconductor Ti−O films through oxygen-PIII also decreased platelet adhesion and clotting by preventing protein denaturation through electron transfer (Huang et al., 2004; Mändl et al., 2001). The platelet adhesion decreased by a factor of four, while the clotting time is doubled compared to LTIC (Wang et al., 2000). Figure 4.10 shows thrombus formation on the surface of an untreated mechanical heart valve cage after 30 days of in vivo test, while the PIII-modified surface remains unaffected.

4.4.3.2 Plasma-polymerized and plasma-grafted surfaces

Plasma polymerization of metallic surfaces with amine groups was reported to be more favourable for immobilization of proteins because the positively charged surface tends to promote osteoblastic response during initial contact with the negatively charged hyaluronan matrix (Finke et al., 2007, 2011; Jung et al., 2012). On the other hand, Ko et al. (2012a) reported plasma polymerization of carboxyl groups exhibit better cell proliferation due to entrapment of calcium ions by the $-COO^-$ function to form a columnar

calcium framework for apatite nuclei formation. Both amine and carboxyl groups facilitated cell osteogenic differentiation, although the mechanisms of the functional groups influence on differentiation were unclear (Schröder et al., 2010a; Seo et al., 2010).

Immobilization of lysozyme and heparin on plasma-polymerized surfaces resulted in improved biomolecule retention at the cell−biomaterial interface (Puleo et al., 2002) and reduction of platelet adhesion (Yang et al., 2010), respectively. Immobilization of heparin, which is a negatively charged anticoagulant, on the stainless steel surface plasma polymerized with allylamine improved the adhesion and proliferation of endothelial cells (Yang et al., 2010). Formation of a homogeneous endothelium layer on the surface helped inhibit thrombus formation (Yang et al., 2010). The platelet adhesion and activation of plasma-polymerized and heparin-immobilized surfaces were decreased from 64.2 to 10.1% and from 42.1 to 12.8%, respectively (Yang et al., 2010).

Plasma grafting of proteins such as collagen I and albumin onto plasma-polymerized metallic surfaces leads to better attachment and activation of human osteoblast-like cells (Chang et al., 2008; Huang et al., 2011; Lin et al., 2005). Extracellular fibres, which are the primary mineralization sites, were evidenced on collagen- and albumin-grafted surfaces, indicating enhanced mineralization during osteoblastic differentiation (Chang et al., 2008; Huang et al., 2011). On the contrary, protein adsorption is inhibited by poly(ethylene glycol)methacrylate (PEGMA) grafting, which is effective against bovine serum albumin and γ-globulin adsorption, thus improving the resistance to thrombosis and failure (Zhang et al., 2001). The irreversible protein adsorption onto a metallic surface is prevented through steric repulsion by the bulky side groups of PEGMA, in which the grafted surface is completely free of adsorbed protein at a PEGMA concentration of 0.05 mol/L (Zhang et al., 2001). Plasma grafting of biocompatible phospholipid poly(2-methacryloxyloxyethyl phosphorylcholine) was also proven to be effective against thrombosis (Ye et al., 2009) and periprosthetic osteolysis (Moro et al., 2004).

4.4.3.3 Plasma-sprayed surfaces

Plasma-sprayed HA coatings on metallic implants have been proven to accelerate fixation and improve bone ingrowth and bonding (Cook et al., 1992; Geesink et al., 1988). Such coatings have shown high long-term survivorship in clinical studies (Lombardi et al., 2006; Vallecillo Capilla et al., 2007). The clinical performance of plasma-sprayed HA coatings has been reviewed by Sun et al. (2001). Partial dissolution of HA coatings in the physiological medium causes localized supersaturation of Ca^{2+} and PO_4^{3-} ions, which increases the ionic activity product of apatite followed by precipitation on the coating surface (Kweh et al., 2002). Decomposition products of plasma-sprayed HA such as amorphous HA and β-tricalcium phosphate significantly increase the rate of dissolution and apatite precipitation due to their higher solubility (Yu et al., 2003; Zheng et al., 2000). Osseointegration proceeds through the formation of a layer of carbonated calcium phosphate that incorporates collagenous matrix, followed by bone remodelling, bidirectional growth, and formation of a bonding layer between the host bone and HA coating (Sun et al., 2001).

Other plasma-sprayed coatings, such as TiO_2, ZrO_2-reinforced HA, and $CaSiO_3$−TiO_2, have also shown to improve bioactivity of metallic implants (Chen et al., 2008; Liu and Ding, 2002; Yugeswaran et al., 2012), while silver-doped and TiN coatings were demonstrated to be effective against bacterial adhesion (Miola et al., 2009; Scaranoet al., 2003). The roughness and porosity of plasma-sprayed coatings provide a high specific area for contact with the physiological medium, thus improving the physicochemical interactions at the bone−implant interface that promotes bone ingrowth (Sun et al., 2001; Tsui et al., 1998a). However, the influence of surface roughness on cell response diminishes when the roughness values become greater than the cell dimensions (20−80 μm) (Borsari et al., 2005b).

4.4.4 Mechanical properties

Mechanical properties play a crucial role in the stability and long-term performance of biomaterials. Implant materials should have sufficient strength to endure high stress and load bearing, while exhibiting an elastic modulus that is close to that of the original hard tissue. Inadequate strength or mechanical property mismatch result in fractures or implant loosening that will lead to implant failure. Orthopaedic implants must have high fatigue strength to withstand cyclic loading. Despite the importance of mechanical properties, this aspect of plasma-modified metallic biomaterials has not been well documented. Reports of mechanical data have centralized on PIII and plasma-sprayed surfaces, while the mechanical properties of other plasma-modified surfaces are rarely mentioned.

Hardness is often used as a measure of mechanical strength of biomaterials, while elastic modulus determines the extent of load transfer and fatigue behaviour during cyclic loading. Figure 4.11 maps the published hardness-elastic modulus values of various plasma-modified materials in comparison with bone and untreated metallic biomaterials. This form of data presentation follows that of Ashby (2011) and that has been formalized for thermal spray materials by Ang et al. (2013). The elastic modulus of metallic biomaterials are significantly higher than that of bone, which ranges between 0.1 and 30 GPa, depending on the type of bone (Zysset et al., 1999), mineral volume fractions (Evans et al., 1990), and measurement direction (Katz, 1980). The mismatch in elastic modulus leads to stress shielding and bone resorption due to insufficient load transfer (Long and Rack, 1998; Sun et al., 2001). Plasma modifications improved the hardness of the material, while effectively decreasing the elastic modulus to a value closer to that of the bone. Elastic moduli as low as 0.5−5.3 GPa were obtained for plasma-spray coatings of HA on Ti-6Al-4V (Tsui et al., 1998a). Surfaces modified with PIII exhibit a higher hardness and elastic modulus than plasma-sprayed surfaces due to a higher density and formation of carbides, nitrides, and oxides.

Good bond strength between the modified layer and the metallic implant ensure its long-term stability and prevent osteolysis, which is a bone/implant degeneration process that is triggered by wear debris. There has been little mention of the bond strength of PIII surfaces in the literature, *viz* a shear strength of 2.9 MPa for oxygen−PIII titanium alloy (Mändl et al., 2003). Bond strengths of greater than

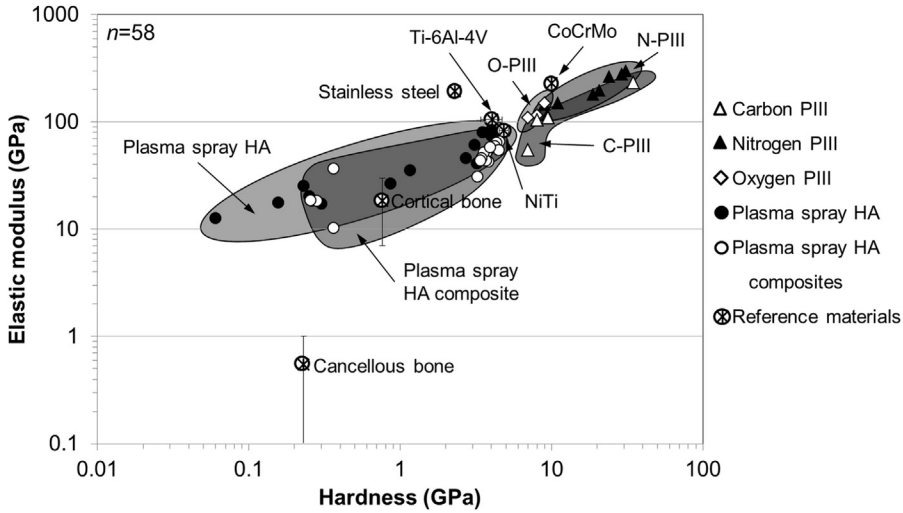


Figure 4.11 Hardness-elastic modulus map of various plasma-modified metallic biomaterials. PIII, plasma immersion ion implantation; HA, hydroxyapatite.

25 MPa have been reported for plasma-sprayed HA coatings (Heimann and Vu, 1997; Yang and Ong, 2003), which are well above the minimum value of 15 MPa established by the ISO 13,779-2 standard (2008). Yang et al. (1997) reported an increased shear strength of HA coatings after 24 weeks of implantation, while Heimann and Vu (1997) reported decreased coating tensile strength after a 7-day in vitro test. Such differences indicated the importance of bonding between the implant and host bone for implant fixation. In fact, thin ($\sim$50 μm) coatings provide better implant fixation due to its stronger coating-substrate bond strength (Yang et al., 1997). The implant fixation reliability is evidenced by the difference of failure sites, in which a 50-μm coating failed at the coating-bone interface rather than at the coating-substrate interface observed in a 200-μm coating. The bond strength was increased by greater than 25% with the use of a bond coat (Chou and Chang, 2002; Yang and Yang, 2013), see Table 4.5, while reinforced HA coatings exhibited an increased bond strength by up to 78% (Fu et al., 2000; Zheng et al., 2000).

The residual stress of plasma-sprayed HA coatings was reported to range between 21 and 100 MPa (Gledhill et al., 1999; Sergo et al., 1997; Tsui et al., 1998a). The nature of the residual stresses, which are tensile and compressive when deposited in air and vacuum, respectively, determines the coating dissolution behaviour in physiological solution and the extent of crack formation (Sergo et al., 1997). The interfacial fracture toughness of plasma-sprayed HA coatings on Ti-6Al-4V have been evaluated using three mode I tests: (1) the short bar chevron notch test (Filiaggi et al., 1991); (2) the single-edge notch-bend test (Tsui et al., 1998a); and (3) the indentation test (Fu et al., 2000). The K_{Ic} values were reported to range between 0.28 and 1.41 MPa $m^{1/2}$ for HA coatings deposited with different plasma power, secondary gas and heat treatment, compared to fracture toughness of 0.73−1.45 MPa $m^{1/2}$ for bulk HA (Ramesh et al., 2008; Ślósarczyk and Białoskórski, 1998).

The fatigue life of stainless steel was increased by more than two and 5.5 times through nitrogen-PIII and PIII&D of a TiN film, respectively (Liu et al., 2007a, 2013). Nitrogen implantation improves fatigue behaviour by restricting the fatigue crack initiation through (1) inhibition of dislocation movement at the surface that is induced by compressive stress; and (2) restriction of slip band development on the surface that nucleate cracks (Liu et al., 2007a). The fatigue life of low carbon steel was improved by 43% and 46% by plasma-sprayed HA and TiO_2 coatings, respectively (Cizek et al., 2009). Hydroxyapatite coatings can survive up to 10^7 cycles of 120−150 MPa cyclic loading in tension and compression modes (Laonapakul et al., 2012; Rakngarm and Mutoh, 2009). While the fatigue life of Ti-6Al-4V was not affected by HA coatings of thickness less than 100 μm, it is significantly reduced when the coating thickness exceeded 150 μm (Lynn and DuQuesnay, 2002). Fatigue damage of plasma-sprayed HA occurred through three stages: (1) crack nucleation and propagation in the coating; (2) stable crack propagation to the substrate; and (3) unstable crack propagation until final fracture (Laonapakul et al., 2012).

4.4.5 Tribological behaviour

Metal implants exhibit poor lubrication compared to natural joints (friction coefficient, μ of 0.001−0.03) due to their high rigidity, which leads to high friction and fretting wear. Excessive wear of implant materials is the principal failure mode for the long-term use of hard tissue replacement. The accumulation of wear debris causes adverse cellular response that leads to inflammation, osteolysis and aseptic loosening. Wear debris in contemporary artificial implants originates from the following interfaces (Hoeppner and Chandrasekaran, 1994): (1) metal/polymer joint; (2) metal/cement; (3) implant/coating; (4) coating/substrate; (5) coating/bone; and (6) implant/bone. Therefore, fretting wear can be minimized by: (1) reducing the interfaces between components; (2) adopting materials with low elastic modulus; or (3) surface modifications (Wang and Wang, 2004).

Plasma immersion ion implantation increases the surface energy and hardness of metallic surfaces through the formation of nitrides, carbides or oxides, thereby reducing the friction coefficient and improving the wear resistance (Sioshansi and Tobin, 1996). The decrease of friction coefficient arises from the physical changes, such as crystalline structure changes, that occur in the near surface region of the materials (Cui and Luo, 1999). High hardness is generally required to resist abrasion wear, while the increase of surface energy allows better retention of lubricating fluid film that decreases the friction coefficient and wear. The wear rate of nitrogen-PIII Ti-6Al-4V was reduced by 90% (Mello et al., 2009b), while those of stainless steel and CoCrMo were reduced by more than 50% (Çelik et al., 2008; Mello et al., 2009a). Nitrogen-PIII has also been reported to reduce the friction coefficient and wear volume of NiTi alloys (Cheng and Zheng, 2006; Levintant-Zayonts and Kucharski, 2009).

Plasma-sprayed surfaces demonstrate a relatively higher friction coefficient than PIII surfaces due to their high surface roughness; Table 4.6. For instance, plasma-sprayed HA coatings on Ti-6Al-4V reveal a friction coefficient of 0.6−0.8

(Fu et al., 1999; Yugeswaran et al., 2012), while that of PIII Ti-6Al-4V is 0.1−0.5 (Silva et al., 2007; Mello et al., 2009b). However, the friction coefficient of plasma-sprayed coatings was reduced to between 0.2 and 0.3 when tested in a lubricated system used to simulate the body fluid (Fu et al., 1999). The porous nature of plasma-sprayed coatings allows better retention of lubricant, thus maintaining a low and stable friction coefficient and wear rate. Reinforcement of HA using alumina particles contributed to a decrease of wear loss from 0.4787 to 0.1576 kg/m^2, while the wear rate of HA coatings reinforced with 30 wt% of yttria-stabilized zirconia was reduced by 38% (Yugeswaran et al., 2012). Significant improvement of wear resistance has also been reported in other reinforced HA coatings, such as carbon nanotube-HA coatings on Ti-6Al-4V (Balani et al., 2007) and SiO_2/Ti-HA coatings on stainless steel (Morks et al., 2008). Such improvements are attributed to the increased hardness, decreased porosity and anchoring of HA splats by the reinforcing particles (Balani et al., 2007; Yugeswaran et al., 2012).

Plasma polymerization and grafting were used to create lubricious coatings for medical devices, which enables easy insertion and removal from a patient with minimized tissue abrasion and trauma (Chen et al., 2009a; Kyomoto et al., 2007). The lubricity of stainless steel and NiTi surfaces was increased by 20−37% through plasma polymerization of 1,3,5,7-tetramethylcyclotetrasiloxane and grafting of *N*-trimethylsilylallylamine (Chen et al., 2009a). Plasma grafting of 2-methacryloyloxyethyl phosphorylcholine onto CoCrMo produced a bearing interface that mimics that of natural joints (Kyomoto et al., 2007). The plasma-grafted CoCrMo exhibits a low friction coefficient of 0.01, which is as low as that of the natural cartilage interface (Kyomoto et al., 2009). Such a lubricious surface maintains the long-term stability of the implant and prevents the degeneration of articular cartilage, which will lead to the migration of the artificial femoral head into the pelvis (Kyomoto et al., 2010b).

4.4.6 Corrosion resistance

Despite having good biocompatibility, metallic biomaterials show poor corrosion resistance in physiological fluid. Leaching of metal ions such as nickel and cobalt increases the cytotoxicity of the material, which could lead to allergic reactions, osteolysis and implant failure (Shih et al., 2000). According to a study on osteoblast proliferation and viability, the toxicity of metal ions increases in the order: Na < Cr < Mg < Mo, nontoxic or mildly toxic; Al < Ta < Co, moderately toxic; and Ni < Fe < Cu < Mn < V, toxic (Hallab et al., 2002). Plasma surface modification improves the corrosion resistance of metallic biomaterials by forming a barrier layer on the metal substrates, thus restricting ion diffusion from the subsurface alloy. The electrochemical behaviour of various plasma-modified metallic biomaterials in comparison with the original surfaces is summarized in Table 4.7. Generally, the enhancement of corrosion resistance is indicated by a shift toward a more positive corrosion potential, E_{corr} and/or a decrease in current density, I_{corr} (Sui and Cai, 2006).

The concentration of nickel ions leaching from untreated NiTi was detected to be as high as 30.23 ppm after 5 weeks of immersion in simulated body fluid (Chu, 2007b),

Table 4.7 The corrosion current density, i_{corr} and corrosion potential, E_{corr} of plasma-modified metallic biomaterials tested under different conditions

Test conditions[a]	Substrate	i_{corr} (A/cm^2)	E_{corr} (V)	Modification technique[b]	i_{corr} (A/cm^2)	E_{corr} (V)	References
Bovine serum, 37 °C	CoCrMo alloy	9.00×10^{-8}	−0.319	Nitrogen-PIII	5.10×10^{-7}	0.036	Díaz et al. (2011)
Bovine serum, 37 °C	CoCrMo alloy	9.00×10^{-8}	−0.319	Oxygen-PIII	5.00×10^{-9}	0.100	Díaz et al. (2011)
Artificial bone fluid, 37 °C	CoCrMo alloy	2.40×10^{-8}	−0.377	PS titanium	2.20×10^{-6}	−0.165	Reclaru et al. (2005)
SBF, 37 °C	Magnesium	1.68×10^{-4}	−1.980	Chromium-PIII	1.67×10^{-3}	−1.550	Xu et al. (2011)
SBF, 37 °C	AZ31 magnesium alloy	5.61×10^{-4}	−1.730	CO_2-PIII	2.60×10^{-4}	−1.770	Xu et al. (2013)
DMEM, 37 °C	AZ31 magnesium alloy	2.41×10^{-4}	−1.720	CO_2-PIII	3.66×10^{-6}	−1.620	Xu et al. (2013)
3.5% NaCl solution	AZ31 magnesium alloy	…	−1.430	Tantalum-PIII	…	−1.25	Wang et al. (2007)
Hanks' solution, 37 °C	AM60 magnesium alloy	9.90×10^{-5}	−1.536	PS titanium dioxide	1.67×10^{-3}	−1.394	Zeng et al. (2008)
SBF, 37 °C	Nickel-titanium	…	−0.231	Acetylene-PIII	…	−0.114	Yeung et al. (2005)
SBF, 37 °C	Nickel-titanium	…	−0.231	Carbon-PIII	…	−0.114	Poon et al. (2005a)
SBF, 37 °C	Nickel-titanium	…	−0.231	Carbon-PIIID	…	−0.060	Poon et al. (2005b)

Continued

Table 4.7 Continued

Test conditions[a]	Substrate	i_{corr} (A/cm^2)	E_{corr} (V)	Modification technique[b]	i_{corr} (A/cm^2)	E_{corr} (V)	References
Hanks' solution	Nickel-titanium	…	−0.196	Carbon-PIIID	…	0.013	Sui et al. (2007)
SBF, 37 °C	Nickel-titanium	…	−0.231	Nitrogen-PIII	…	−0.163	Poon et al. (2005a)
Hanks' solution	Nickel-titanium	3.70×10^{-7}	−0.370	Oxygen-PIII	4.90×10^{-8}	−0.230	Tan et al. (2003)
SBF, 37 °C	Nickel-titanium	…	−0.231	Oxygen-PIII	…	−0.027	Yeung et al. (2005)
Ringer's solution, 37 °C	Nickel-titanium	8.70×10^{-8}	−0.288	Tantalum-PIII	1.40×10^{-8}	−0.194	Li et al. (2010)
SBF	316L Stainless steel	…	…	PS hydroxyapatite	3.20×10^{-7}	−0.308	Yugeswaran et al. (2012)
SBF	316L Stainless steel	…	…	PS hydroxyapatite-zirconia	1.70×10^{-8}	−0.245	Yugeswaran et al. (2012)
0.90% NaCl solution	316L Stainless steel	3.00×10^{-7}	−0.190	PS fluorapatite	8.00×10^{-8}	−0.120	Fathi et al. (2009)
0.90% NaCl solution	316L Stainless steel	3.00×10^{-7}	−0.190	PS fluorapatite-niobium	2.50×10^{-8}	−0.180	Fathi et al. (2009)
Simulated blood plasma	CP-titanium	6.40×10^{-8}	…	Oxygen-PIII	1.60×10^{-8}	…	Yang et al. (2011)
Artificial bone fluid, 37 °C	CP-titanium	…	…	PS titanium	7.02×10^{-7}	−0.088	Reclaru et al. (2003)

Fusayama-Meyer artificial saliva, 37 °C	CP-titanium	…	…	PS titanium	1.12×10^{-6}	0.022	Simon et al. (2005)
SBF	CP-titanium	6.93×10^{-7}	−0.136	PS hydroxyapatite	9.13×10^{-9}	−0.128	Mittal et al. (2013)
SBF	CP-titanium	6.93×10^{-7}	−0.136	PS hydroxyapatite-alumina	3.73×10^{-7}	−0.122	Mittal et al. (2013)
Hanks' solution, 37 °C	Ti-6Al-4V	5.00×10^{-8}	−0.456	Siloxane PP	4.00×10^{-9}	−0.197	Zhou et al. (2012)
Hanks' solution	Ti−15Mo−3Nb−3Al−0.2Si	1.20×10^{-8}	−0.326	Carbon-PIII	8.50×10^{-8}	−0.248	Mohan et al. (2012)

[a]DMEM, Dulbecco's Modified Eagle Medium; SBF, simulated body fluid.
[b]PIII, plasma immersion ion implantation; PIIID, plasma immersion ion implantation and deposition; PP, plasma polymerization; PS, plasma spray.

which exceeds the 9 ppm cytotoxicity limit of nickel (Shih et al., 2000). Plasma immersion ion implantation reduced the nickel ion concentration to below 0.012 ppm, at which surfaces treated with carbon-PIII exhibited the best corrosion resistance compared to those treated by nitrogen- and oxygen-PIII (Chu, 2007b; Poon et al., 2005a). The enhanced corrosion resistance was attributed to the decreased electrical conductivity of the surface due to carbon film formation, which reduced the exchange of electrical charges and the extent of electrochemical corrosion (Dorner-Reisel et al., 2004).

Similar improvements of corrosion resistance were revealed for PIII-modified CoCrMo (Lutz et al., 2011), magnesium (Xu et al., 2013) and titanium alloys (Mohan et al., 2012); Table 4.7. Leaching of titanium ions was negligible when compared to that of nickel, cobalt and chromium ions; thus the effectiveness of metallic biomaterials in relation to their corrosion resistance increased in the order: stainless steel, nickel−titanium, PIII−nickel−titanium and titanium alloys (Yeung et al., 2007). The ion dose used in PIII must be optimized to have a positive impact on corrosion resistance because high ion bombardment may roughen or create nanopores on the surfaces, which increases the pitting corrosion susceptibility (Tan et al., 2003).

The concentrations of cobalt and chromium ions detected from titanium plasma-sprayed CoCrMo alloys were as high as 1.7 ppm, with a corrosion current density that was higher than that of untreated CoCrMo alloys (Reclaru et al., 2005). The increase of ion leaching was attributed to the accelerated corrosion process at the titanium−CoCrMo interface due to the release of chromium ions at cavities, which is known to provoke local acidification of electrolyte and contribute to amplified localized corrosion (Reclaru et al., 2005). Such high concentrations of ions leaching from the original surface indicated that the plasma-sprayed titanium layer was permeable, mainly due to the porous nature of plasma-sprayed coatings. This circumstance causes a predicament in designing plasma-sprayed implants, because open porosity is desirable for optimal osseointegration, while such a structure is detrimental toward corrosion resistance.

A plasma-sprayed surface that has good osseointegration and corrosion resistance for such corrosion-prone substrates can be produced by depositing two layers of coatings: (1) a first impermeable dense layer, which is deposited using a fine powder and high plasma energy; and (2) a second layer that is rough and porous, which is deposited using a coarser powder and low plasma energy (Reclaru et al., 2003). Other plasma-sprayed coatings, such as titanium dioxide and HA, have also proven effective in improving corrosion resistance of magnesium alloys and stainless steel; Table 4.7. A plasma-polymerized siloxane film on Ti-6Al-4V also improved corrosion resistance due to its insoluble, dense and highly cross-linked structure (Zhou et al., 2012). There was no other information available on the corrosion behaviour of other plasma-modified metallic biomaterial surfaces.

4.5 Potential biomaterial applications

The enhancement of surface properties of plasma-modified metallic materials has invigorated many promising biomedical applications, including surgical tools and

medical devices for orthopaedic, dental and cardiovascular implants. The versatility of plasma techniques provides a wide range of surface-modification capabilities, which allows for applications that span from atomic level cleaning to the structuring of biomedical implants.

Non-reactive plasmas, such as air and argon, have been used to clean and sterilize surgical tools and medical devices by removing proteinaceous contaminants from the surface (Kumar, 2013). Molecular plasma deposition is used to deposit biomolecules such as amino acids in the form of solution or suspension onto biased substrates to improve the bioactivity of metallic implants (Storey et al., 2007). Bioactive agents have also been covalently bonded onto plasma-deposited films such as heptafluorobutyl methacrylate for anti-thrombogenic endovascular stents (Narayanan et al., 1994). Such plasma-modified bioresorbable medical implants can regenerate soft tissues, membranous tissues or organs such as cardiovascular tissues, skin, ligaments, tendons, periodontal fibres or hernia correction by inducing fibrosis (Ip and Yuen, 2012).

Plasma immersion ion implantation with nitrogen and oxygen decreases platelet and leukocyte adhesion, while decreasing restenosis and increasing apoptosis of medical devices such as stents, valves, pacemakers, screws, plates and joints (Chen, 2013; Zamora et al., 2003). Carbon-, nitrogen- and oxygen-PIII are used to modify shape memory alloys such as NiTi for the correction of serious spinal deformities, e.g. scoliosis (Chu, 2007a). The plasma-modified shape memory alloy has enhanced mechanical properties, hydrophilicity, and corrosion and wear resistance and increased cell adhesion (Yeung et al., 2010). In joint prostheses and bearings, oxygen-PIII is used to form hydroxyl groups on the surface, which is bonded to a biocompatible material with phosphorylcholine groups via a binder such as methacrylic acid, to supress wear and the formation of abrasive debris (Kyomoto et al., 2010a).

Plasma polymerization can be used to create both hydrophilic and antithrombogenic surfaces. Hydrophilic surfaces that promote cell adhesion and growth are created through plasma polymerization of (1) monomers with hydrophilic functional groups, such as amines, thiols, hydroxyls and carboxyls (Sill et al., 2012; Vyavahare and Marigliano, 2005); or (2) hydrophilic polymeric units with double-bond (i.e. C═C, C═N or C═O) monomers, such as ethylene oxide, *N*-trimethylsilyl-allylamine and allyl alcohol (Zamora et al., 2007). These plasma-polymerized surfaces with enhanced biocompatibility and cell proliferation are used as matrices for tissue engineering; bone implants and prosthetics including pins, rivets, screws, rods and joints; cardiovascular devices such as stents, vascular valves and occlusion devices; microchips; or electrodes (Ng et al., 2010). For instance, plasma-polymerized allylamine on 316L stainless steel can be used as coronary stents to scaffold the diseased arteries and prevent reblockage during balloon angioplasty (Gallino et al., 2010).

The plasma-polymerized surfaces can be further modified by attaching (1) small organic moieties such as poly(ethylene glycol), monosaccharide and phospholipid to improve biocompatibility and bioactivity (Claude et al., 2007; Sill et al., 2012) or (2) spacer molecules and anti-coagulants such as heparin to provide resistance to plasma proteins and reduce thrombosis (Marchant, 1995). Plasma polymerization is also used to deposit aliphatic hydrocyclosiloxane or other silicone-based polymers onto surgical needles after plasma etching, which significantly reduce the average

tissue penetration force to below that of a standard siliconized surgical needle (Roby, 2003; Vetrecin, 2012). The tip or entire needle can be further grafted with a lubricant such as aminoalkyl siloxane to enhance the surface lubricity (Roby, 2003).

Plasma-sprayed HA implants have been used extensively in orthopaedics and dentistry since the 1980s, e.g. hip bone and joint replacement, screws and pins in bone plates to fix fractures, and endosteal implants (Sun et al., 2001). This biocompatible coating has been clinically proven to prevent infection and short-term rejection (Sun et al., 2001). HA coatings that are free of amorphous $Ca_3(PO_4)_2$ and impurities such as $Ca(OH)_2$, CaO and $CaCO_3$ are obtained through postdeposition treatments: (1) immersion in an aqueous solution of inorganic salt, saccharide, ethylene glycol or glycerol to dissolve the alkaline components (Nakano and Watanabe, 1987); or (2) a hydrothermal process to convert amorphous $Ca_3(PO_4)_2$ to crystalline HA (Story and Burgess, 1998). The treated surfaces exhibit excellent mechanical properties and affinity to cells without haematolysis. Carbonated plasma-sprayed HA coatings, in which the phosphate and/or hydroxyl ions are partially replaced by HCO_3^- ions, exhibit enhanced biocompatibility, osteoconduction, bioactivity and biodegradability (Rey and Ranz, 2001).

Hydroxyapatite coatings with an intrinsic osteoinductive structure to enhance the rate of bone growth are produced by sintering the plasma-sprayed coatings to form a network of coalesced and interconnected porosity (Ripamonti and Kirkbride, 2001). Incorporation of nanostructured reinforcement materials such as titania (Varadaraajan et al., 2009), zirconia (Kumar et al., 2003) and carbon nanotubes (Balani et al., 2007) significantly improves the strength, toughness, wear resistance and adhesion of HA coatings. These nanostructured plasma-sprayed coatings, which consist of a mixture of fully and partially molten particles, have been patented for implants such as artificial hip joints, knee joints and dentures (Lima et al., 2006). Plasma-sprayed coatings from feedstock of metal-coated HA that is incorporated with bioactive agents such as antibiotics, antitumour drugs, anti-inflammatory drugs, adhesion factors and growth factors enable better integration of the implants into the body by preventing infection and facilitating healing and growth (Ahmed and Markx, 2012).

4.6 Challenges and future trends

Plasma processes are becoming an increasingly favoured technique for surface modification of biomaterials due to their versatility and efficacy. Despite the many promising attributes displayed by plasma-modified biomaterials, full implementation of the technology in the biomedical field is still hindered by the lack of understanding on the mechanisms governing the physicochemical and biological changes of the modified surfaces, as well as the long-term physiological effects of the modified components in the human body. The current challenges and future trends of plasma surface modification of metallic biomaterials are summarized in Figure 4.12.

It has been established that the enhancement of surface properties, including the mechanical, biocompatibility, tribological and corrosion aspects, primarily arose from the alterations of surface morphology and/or surface chemistry. Although there

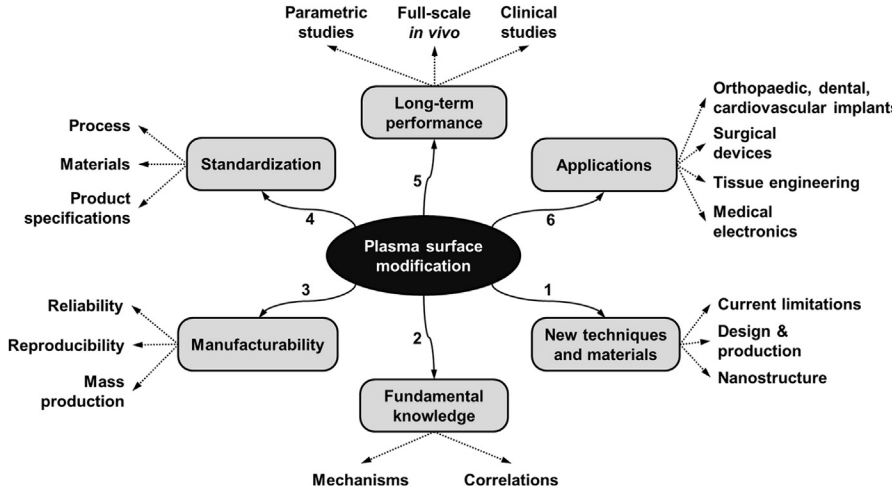


Figure 4.12 Current challenges and future trends of plasma surface modification of metallic biomaterials.

have been substantial studies devoted to surface properties of plasma-modified materials, the exact mechanisms and correlations between the induced morphological and/or chemical changes with the surface properties improvements are yet to be determined. One of the challenges lies in the laborious task of distinguishing the relative effects of morphology and chemistry changes on the surface properties because these changes often occur concurrently during the surface-modification process (Anselme et al., 2000). Thus, it is imperative that such mechanisms and correlations be established to enable precise control of the modification process and surface properties for specific biomedical applications.

Clinical studies present a crucial step toward implementation and marketing of biomaterials. While the clinical performance of plasma-sprayed coatings has been studied extensively in the past decades, data on the clinical performance of other plasma-modified surfaces, especially PIII and plasma-polymerized surfaces, are still limited. The knowledge on the mechanical, tribological, corrosion and biological behaviour of these materials has been restricted to short-term in vivo performances. For instance, the fatigue life of full-scale, load-bearing implants subjected to cyclic stress in a physiological environment is still a controversial subject that has not been fully investigated. The corrosion behaviour of modified metallic biomaterials has mostly been tested *via* the potentio-dynamic polarization method, which only reveals short-term corrosion behaviour. Factors such as the thickness, topography and adhesion of the modified surfaces should be taken into consideration for the evaluation of long-term corrosion behaviour in vivo.

Nanostructured materials have demonstrated many advantages over conventional materials in a variety of industries, including biomedical applications. Many researchers have begun implementing nanostructural considerations to mimic the local tissue environment or increase the surface-to-volume ratio for enhanced performance,

e.g. nanogrooved surfaces and nanocomposite coatings. However, it is critical that the benefits extended by the nanostructured materials be equally assessed with the risks of having artificial nanosized materials integrated in the human body. New plasma-modification techniques and materials are anticipated to emerge to address this need for nanoscaling, as well as to improve the design and manufacturing process of medical devices, e.g. the ability to modify surfaces with a complex geometry.

Plasma modification is still a relatively new surface-modification technique for biomaterials compared to other conventional techniques such as sputter deposition and chemical treatment. Thus, the manufacturing aspects of plasma modification in relation to process control, reliability, and reproducibility are still being scrutinized for the effectiveness of mass production and commercialization. For instance, the current plasma surface-modification services provided by independent businesses are highly variable in terms of process, materials and product specifications. Standardization in these aspects of biomaterial production will be a vital step toward commercialization of high-quality, consistent and reliable medical devices. Plasma surface modification will remain a subject of vigorous study and an effective solution to the clinical development of metallic biomaterials in the foreseeable future.

4.7 Sources of further information

Further information on the plasma technology, including the fundamentals, kinetics, properties and applications, can be found in the books by Boulos et al., (1994), Harry (2010), Gross et al. (1968), and Rossnagel et al. (1990). Information on specific plasma techniques discussed in this chapter can be found in the following references:

- Plasma etching (Manos and Flamm, 1989; Sugawara, 1998).
- Plasma immersion ion implantation (Chu and Tian, 2004; Liu et al., 2008).
- Plasma polymerization (Friedrich, 2011; Inagaki, 1996; Yasuda, 1985).
- Plasma spray (Davis, 2005; Fauchais, 2004; Pawlowski, 2008).

For more information on specific work on plasma surface modification of metallic biomaterials, the readers are referred to the works by the research teams listed below. The WWW links were accessed on 05 December 2013.

- Plasma immersion ion implantation: The City University of Hong Kong, Hong Kong http://www6.cityu.edu.hk/appkchu/plasma/default.htm
- Plasma polymerization: Leibniz-Institute for Plasma Science and Technology, Germany http://www.leibniz-gemeinschaft.de/en/institute-museen/einrichtungen/inp/
- Thermal spray deposition: Swinburne University of Technology, Australia http://www.swinburne.edu.au/engineering/iris/deposition-technologies/
- Thermal spray deposition: Stony Brook University, New York, USA http://www.ctsr-sunysb.org/new/index.shtml

Acknowledgements

The authors would like to acknowledge the financial support by the Australia−India Strategic Research Fund (AISRF, ST 060048).

References

Adler, S., Scherrer, M., & Daschner, F. D. (1998). Costs of low-temperature plasma sterilization compared with other sterilization methods. *Journal of Hospital Infection, 40*(2), 125−134.

Ahmed, R. & Markx, G.H. (2012). *Coating method.* RRG Coatings Limited. US patent 2012/0141775 A1, published June 7, 2012.

Akao, M., Aoki, H., & Kato, K. (1981). Mechanical properties of sintered hydroxyapatite for prosthetic applications. *Journal of Materials Science, 16*(3), 809−812.

Ang, A. S. M., Sanpo, N., Sesso, M. L., Kim, S. Y., & Berndt, C. C. (2013). Thermal spray maps: material genomics of processing technologies. *Journal of Thermal Spray Technology, 22*(7), 1170−1183.

Anselme, K., & Bigerelle, M. (2006a). Effect of a gold-palladium coating on the long-term adhesion of human osteoblasts on biocompatible metallic materials. *Surface and Coatings Technology, 200*(22−23 SPEC. ISS.), 6325−6330.

Anselme, K., & Bigerelle, M. (2006b). Statistical demonstration of the relative effect of surface chemistry and roughness on human osteoblast short-term adhesion. *Journal of Materials Science: Materials in Medicine, 17*(5), 471−479.

Anselme, K., & Bigerelle, M. (2011). Role of materials surface topography on mammalian cell response. *International Materials Reviews, 56*(4), 243−266.

Anselme, K., Linez, P., Bigerelle, M., Le Maguer, D., Le Maguer, A., Hardouin, P., et al. (2000). The relative influence of the topography and chemistry of TiAl6V4 surfaces on osteoblastic cell behaviour. *Biomaterials, 21*(15), 1567−1577.

Aronsson, B. O., Hjörvarsson, B., Frauchiger, L., Taborelli, M., Vallotton, P. H., & Descouts, P. (2001). Hydrogen desorption from sand-blasted and acid-etched titanium surfaces after glow-discharge treatment. *Journal of Biomedical Materials Research, 54*(1), 20−29.

Aronsson, B. O., Lausmaa, J., & Kasemo, B. (1997). Glow discharge plasma treatment for surface cleaning and modification of metallic biomaterials. *Journal of Biomedical Materials Research, 35*(1), 49−73.

Ashby, M. F. (2011). *Chapter 4—Material property charts, materials selection in mechanical design* (4th ed.). Burlington, MA: Butterworth-Heinemann.

Aydin, M. M., Ozyegin, L. S., Oktar, F. N., Erkmen, E. Z., Anzabi, O., & Gross, K. (2006). Plasma sprayed zirconia-hydroxyapatite composite coatings. *Key Engineering Materials, 309−311*, 631−634.

Bacakova, L., Filova, E., Parizek, M., Ruml, T., & Svorcik, V. (2011). Modulation of cell adhesion, proliferation and differentiation on materials designed for body implants. *Biotechnology Advances, 29*(6), 739−767.

Balani, K., Chen, Y., Harimkar, S. P., Dahotre, N. B., & Agarwal, A. (2007). Tribological behavior of plasma-sprayed carbon nanotube-reinforced hydroxyapatite coating in physiological solution. *Acta Biomaterialia, 3*(6), 944−951.

Baunack, S., Oswald, S., & Scharnweber, D. (1998). Depth distribution and bonding states of phosphorus implanted in titanium investigated by AES, XPS and SIMS. *Surface and Interface Analysis, 26*(6), 471−479.

Bhattacharya, A., & Misra, B. N. (2004). Grafting: a versatile means to modify polymers: techniques, factors and applications. *Progress in Polymer Science (Oxford), 29*(8), 767−814.

Bilek, M. M. M., McKenzie, D. R., Tarrant, R. N., Lim, S. H. M., & McCulloch, D. G. (2002). Plasma-based ion implantation utilising a cathodic arc plasma. *Surface and Coatings Technology, 156*(1−3), 136−142.

Borsari, V., Giavaresi, G., Fini, M., Torricelli, P., Salito, A., Chiesa, R., et al. (2005a). Physical characterization of different-roughness titanium surfaces, with and without hydroxyapatite coating, and their effect on human osteoblast-like cells. *Journal of Biomedical Materials Research—Part B Applied Biomaterials, 75*(2), 359−368.

Borsari, V., Giavaresi, G., Fini, M., Torricelli, P., Tschon, M., Chiesa, R., et al. (2005b). Comparative in vitro study on a ultra-high roughness and dense titanium coating. *Biomaterials, 26*(24), 4948−4955.

Boulos, M. I., Fauchais, P., & Pfender, E. (1994). *Thermal plasmas: Fundamentals and applications*. New York, NY: Plenum Press.

Cannillo, V., Lusvarghi, L., & Sola, A. (2008). Production and characterization of plasma-sprayed TiO_2-hydroxyapatite functionally graded coatings. *Journal of the European Ceramic Society, 28*(11), 2161−2169.

Cao, Y., Weng, J., Chen, J., Feng, J., Yang, Z., & Zhang, X. (1996). Water vapour-treated hydroxyapatite coatings after plasma spraying and their characteristics. *Biomaterials, 17*(4), 419−424.

Caro, A., Humblot, V., Méthivier, C., Minier, M., Salmain, M., & Pradier, C. M. (2009). Grafting of lysozyme and/or poly(ethylene glycol) to prevent biofilm growth on stainless steel surfaces. *Journal of Physical Chemistry B, 113*(7), 2101−2109.

Cassie, A. B. D., & Baxter, S. (1944). Wettability of porous surfaces. *Transactions of the Faraday Society, 40*, 546−551.

Çelik, A., Bayrak, Ö., Alsaran, A., Kaymaz, I., & Yetim, A. F. (2008). Effects of plasma nitriding on mechanical and tribological properties of CoCrMo alloy. *Surface and Coatings Technology, 202*(11), 2433−2438.

Chae, J. C., Collier, J. P., Mayor, M. B., Surprenant, V. A., & Dauphinais, L. A. (1992). Enhanced ingrowth of porous-coated CoCr implants plasma-sprayed with tricalcium phosphate. *Journal of Biomedical Materials Research, 26*(1), 93−102.

Chang, E., Chang, W. J., Wang, B. C., & Yang, C. Y. (1997). Plasma spraying of zirconia-reinforced hydroxyapatite composite coatings on titanium part I phase, microstructure and bonding strength. *Journal of Materials Science: Materials in Medicine, 8*(4), 193−200.

Chang, W. J., Ou, K. L., Lee, S. Y., Chen, J. Y., Abiko, Y., Lin, C. T., et al. (2008). Type I collagen grafting on titanium surfaces using low-temperature glow discharge. *Dental Materials Journal, 27*(3), 340−346.

Chebbi, A., & Stokes, J. (2012). Thermal spraying of bioactive polymer coatings for orthopaedic applications. *Journal of Thermal Spray Technology, 21*(3−4), 719−730.

Chen, M. (Meng Chen), (2013). *Plasma modified medical devices and methods*. US patent 2013/0046375, published February 21, 2013.

Cheng, Y., & Zheng, Y. F. (2006). Deposition of TiN coatings on shape memory NiTi alloy by plasma immersion ion implantation and deposition. *Thin Solid Films, 515*(4), 1358−1363.

Chen, M., Hsieh, T. T., Osaki, S., Zamora, P. O., & Tsang, R. (2009a). Improvement of surface lubricity of polymers and metals by a glow-discharge plasma cross-linking process. *Journal of Biomaterials Science, Polymer Edition, 20*(4), 511−527.

Chen, D., Jordan, E. H., Gell, M., & Wei, M. (2008). Apatite formation on alkaline-treated dense TiO_2 coatings deposited using the solution precursor plasma spray process. *Acta Biomaterialia, 4*(3), 553−559.

Chen, J., Tong, W., Cao, Y., Feng, J., & Zhang, X. (1997). Effect of atmosphere on phase transformation in plasma-sprayed hydroxyapatite coatings during heat treatment. *Journal of Biomedical Materials Research, 34*(1), 15−20.

Chen, Y., Zheng, X., Li, B., Xie, Y., & Ding, C. (2010). In vitro bioactivity, cytotoxicity and blood compatibility of anti-bacterial vacuum plasma sprayed titanium coatings. *Materials Science Forum, 658*, 511−514.

Chen, Y., Zheng, X., Xie, Y., Ji, H., & Ding, C. (2009b). Antibacterial properties of vacuum plasma sprayed titanium coatings after chemical treatment. *Surface and Coatings Technology, 204*(5), 685−690.

Chou, B. Y., & Chang, E. (2001). Interface investigation of plasma-sprayed hydroxyapatite coating on titanium alloy with ZrO_2 intermediate layer as bond coat. *Scripta Materialia, 45*(4), 487−493.

Chou, B. Y., & Chang, E. (2002). Plasma-sprayed zirconia bond coat as an intermediate layer for hydroxyapatite coating on titanium alloy substrate. *Journal of Materials Science: Materials in Medicine, 13*(6), 589−595.

Chou, B. Y., & Chang, E. (2003). Influence of deposition temperature on mechanical properties of plasma-sprayed hydroxyapatite coating on titanium alloy with ZrO_2 intermediate layer. *Journal of Thermal Spray Technology, 12*(2), 199−207.

Chu, P. K. (2006). Bioactivity of plasma implanted biomaterials. *Nuclear Instruments and Methods in Physics Research, Section B: Beam Interactions with Materials and Atoms, 242*(1−2), 1−7.

Chu, P. K. (2007a). Enhancement of surface properties of biomaterials using plasma-based technologies. *Surface and Coatings Technology, 201*(19−20), 8076−8082.

Chu, P. K. (2007b). Plasma surface treatment of artificial orthopedic and cardiovascular biomaterials. *Surface and Coatings Technology, 201*(9−11), 5601−5606.

Chu, P. K., Chen, J. Y., Wang, L. P., & Huang, N. (2002). Plasma-surface modification of biomaterials. *Materials Science and Engineering R: Reports, 36*(5−6), 143−206.

Chu, P. K., & Tian, X. B. (2004). Plasma-based surface modification. In G. E. Totten, & H. Liang (Eds.), *Surface modification and mechanisms: Friction, stress, and reaction engineering*. New York, NY: Marcel Dekker.

Cirolini, S., Harding, J. H., & Jacucci, G. (1991). Computer simulation of plasma-sprayed coatings. I. Coating deposition model. *Surface and Coatings Technology, 48*(2), 137−145.

Cizek, J., Khor, K. A., Siegl, J., & Bensch, J. (2009). A study on the influence of plasma deposited HA and TiO_2 coatings on fatigue lives of low-carbon steel specimens with respect to various powder in-flight properties. In B. R. Marple, M. M. Hyland, Y.-C. Lau, C.-J. Li, R. S. Lima, & G. Montavon (Eds.), *Expanding thermal spray performance to new markets and applications, May 4−7, 2009* (pp. 361−365). Las Vegas: NV. ASM International.

Claude, C.D., Hossainy, S.F.A., & Malik, S.M. (2007). *Plasma-generated coatings for medical devices and methods for fabricating thereof.* Advanced Cardiovascular Systems, Inc. US patent 7,201,935 B1, published April 10, 2007.

Cook, S. D., Thomas, K. A., Dalton, J. E., Volkman, T. K., Whitecloud, T. S., III, et al. (1992). Hydroxylapatite coating of porous implants improves bone ingrowth and interface attachment strength. *Journal of Biomedical Materials Research, 26*(8), 989−1001.

Cui, F. Z., & Luo, Z. S. (1999). Biomaterials modification by ion-beam processing. *Surface and Coatings Technology, 112*(1−3), 278−285.

Curtis, A., & Wilkinson, C. (1997). Topographical control of cells. *Biomaterials, 18*(24), 1573−1583.

Cvelbar, U., Vujoševič, D., Vratnica, Z., & Mozetič, M. (2006). The influence of substrate material on bacteria sterilization in an oxygen plasma glow discharge. *Journal of Physics D: Applied Physics, 39*(16), 3487−3493.

Dalton, J. E., & Cook, S. D. (1995). In vivo mechanical and histological characteristics of HA-coated implants vary with coating vendor. *Journal of Biomedical Materials Research, 29*(2), 239−245.

Davis, J. R. (Ed.). (2005). *Handbook of thermal spray technology*. Materials Park, OH: ASM International.

De Groot, K., Geesink, R., Klein, C. P. A. T., & Serekian, P. (1987). Plasma sprayed coatings of hydroxylapatite. *Journal of Biomedical Materials Research, 21*(12), 1375−1381.

Deligianni, D. D., Katsala, N., Ladas, S., Sotiropoulou, D., Amedee, J., & Missirlis, Y. F. (2001). Effect of surface roughness of the titanium alloy Ti-6Al-4V on human bone marrow cell response and on protein adsorption. *Biomaterials, 22*(11), 1241−1251.

Díaz, C., García, J. A., Mändl, S., & Rodríguez, R. J. (2011). Plasma immersion ion implantation for the prevention of metal ion release from CoCrMo alloys. *IEEE Transactions on Plasma Science, 39*(11 PART 2), 3045−3048.

Ding, S. J., Ju, C. P., & Chern Lin, J. H. (2000). Morphology and immersion behavior of plasma-sprayed hydroxyapatite/bioactive glass coatings. *Journal of Materials Science: Materials in Medicine, 11*(3), 183−190.

Domanski, M., Luttge, R., Lamers, E., Walboomers, X. F., Winnubst, L., Jansen, J. A., et al. (2012). Submicron-patterning of bulk titanium by nanoimprint lithography and reactive ion etching. *Nanotechnology, 23*(6).

Dong, Z. L., Khor, K. A., Quek, C. H., White, T. J., & Cheang, P. (2003). TEM and STEM analysis on heat-treated and in vitro plasma-sprayed hydroxyapatite/Ti-6Al-4V composite coatings. *Biomaterials, 24*(1), 97−105.

Dorner-Reisel, A., Schürer, C., Irmer, G., & Müller, E. (2004). Electrochemical corrosion behaviour of uncoated and DLC coated medical grade Co28Cr6Mo. *Surface and Coatings Technology, 177−178*, 830−837.

Ducheyne, P., & Healy, K. E. (1988). The effect of plasma-sprayed calcium phosphate ceramic coatings on the metal ion release from porous titanium and cobalt-chromium alloys. *Journal of Biomedical Materials Research, 22*(12), 1137−1163.

Dujovne, A. R., Bobyn, J. D., Krygier, J. J., Miller, J. E., & Brooks, C. E. (1993). Mechanical compatibility of noncemented hip prostheses with the human femur. *Journal of Arthroplasty, 8*(1), 7−22.

Evans, G. P., Behiri, J. C., Currey, J. D., & Bonfield, W. (1990). Microhardness and Young's modulus in cortical bone exhibiting a wide range of mineral volume fractions, and in a bone analogue. *Journal of Materials Science: Materials in Medicine, 1*(1), 38−43.

Fathi, M. H., Zahrani, E. M., & Zomorodian, A. (2009). Novel fluorapatite/niobium composite coating for metallic human body implants. *Materials Letters, 63*(13−14), 1195−1198.

Fauchais, P. (2004). Understanding plasma spraying. *Journal of Physics D: Applied Physics, 37*(9), R86−R108.

Feldman, L. A., & Hui, H. K. (1997). Compatibility of medical devices and materials with low-temperature hydrogen peroxide gas plasma. *Medical Device and Diagnostic Industry, 19*(12), 57−62.

Filiaggi, M. J., Coombs, N. A., & Pilliar, R. M. (1991). Characterization of the interface in the plasma sprayed HA coating/Ti-6Al-4V implant system. *Journal of Biomedical Materials Research, 25*(10), 1211−1229.

Finke, B., Hempel, F., Testrich, H., Artemenko, A., Rebl, H., Kylián, O., et al. (2011). Plasma processes for cell-adhesive titanium surfaces based on nitrogen-containing coatings. *Surface and Coatings Technology, 205*(Suppl. 2), S520−S524.

Finke, B., Luethen, F., Schroeder, K., Mueller, P. D., Bergemann, C., Frant, M., et al. (2007). The effect of positively charged plasma polymerization on initial osteoblastic focal adhesion on titanium surfaces. *Biomaterials, 28*(30), 4521−4534.

Friedrich, J. (2011). Mechanisms of plasma polymerization—reviewed from a chemical point of view. *Plasma Processes and Polymers, 8*(9), 783−802.

Friedrich, J. (2012). *Plasma, the plasma chemistry of polymer surfaces*. Weinheim, Germany: Wiley-VCH Verlag GmbH & Co. KGaA.

Friedrich, J., Mix, R., Kühn, G., Retzko, I., Schönhals, A., & Unger, W. (2003). Plasma-based introduction of monosort functional groups of different type and density onto polymer surfaces. Part 2: pulsed plasma polymerization. *Composite Interfaces, 10*(2−3), 173−223.

Fu, Y., Batchelor, A. W., & Khor, K. A. (1999). Fretting wear behavior of thermal sprayed hydroxyapatite coating lubricated with bovine albumin. *Wear, 230*(1), 98−102.

Fu, L., Khor, K. A., & Lim, J. P. (2000). Yttria stabilized zirconia reinforced hydroxyapatite coatings. *Surface and Coatings Technology, 127*(1), 66−75.

Gallino, E., Massey, S., Tatoulian, M., & Mantovani, D. (2010). Plasma polymerized allylamine films deposited on 316L stainless steel for cardiovascular stent coatings. *Surface and Coatings Technology, 205*(7), 2461−2468.

García-Sanz, F. J., Mayor, M. B., Arias, J. L., Pou, J., León, B., & Pérez-Amor, M. (1997). Hydroxyapatite coatings: a comparative study between plasma-spray and pulsed laser deposition techniques. *Journal of Materials Science: Materials in Medicine, 8*(12), 861−865.

Geesink, R. G. T., De Groot, K., & Klein, C. P. A. T. (1988). Bonding of bone to apatite-coated implants. *Journal of Bone and Joint Surgery—Series B, 70*(1), 17−22.

Geurtsen, W. (2002). Biocompatibility of dental casting alloys. *Critical Reviews in Oral Biology and Medicine, 13*(1), 71−84.

Gledhill, H. C., Turner, I. G., & Doyle, C. (1999). Direct morphological comparison of vacuum plasma sprayed and detonation gun sprayed hydroxyapatite coatings for orthopaedic applications. *Biomaterials, 20*(4), 315−322.

Goldman, M., & Pruitt, L. (1998). Comparison of the effects of gamma radiation and low temperature hydrogen peroxide gas plasma sterilization on the molecular structure, fatigue resistance, and wear behavior of UHMWPE. *Journal of Biomedical Materials Research, 40*(3), 378−384.

Gomes, P. S., Botelho, C., Lopes, M. A., Santos, J. D., & Fernandes, M. H. (2010). Evaluation of human osteoblastic cell response to plasma-sprayed silicon-substituted hydroxyapatite coatings over titanium substrates. *Journal of Biomedical Materials Research—Part B Applied Biomaterials, 94*(2), 337−346.

Gross, K. A., & Berndt, C. C. (1994). Structural changes of plasma sprayed hydroxyapatite coating during in-vitro testing. In E. Horowitz, & J. E. Parr (Eds.), *Characterization and performance of calcium phosphate coatings for implants*. Philadelphia, PA: ASTM International.

Gross, K. A., Berndt, C. C., & Herman, H. (1998). Amorphous phase formation in plasma-sprayed hydroxyapatite coatings. *Journal of Biomedical Materials Research, 39*(3), 407−414.

Gross, B., Grycz, B., & Miklóssy. (1968). *Plasma technology*. London: Iliffe Books Ltd.

Hallab, N. J., Bundy, K. J., O'Connor, K., Moses, R. L., & Jacobs, J. J. (2001). Evaluation of metallic and polymeric biomaterial surface energy and surface roughness characteristics for directed cell adhesion. *Tissue Engineering, 7*(1), 55−70.

Hallab, N. J., Vermes, C., Messina, C., Roebuck, K. A., Glant, T. T., & Jacobs, J. J. (2002). Concentration- and composition-dependent effects of metal ions on human MG-63 osteoblasts. *Journal of Biomedical Materials Research, 60*(3), 420−433.

Hanawa, T., Kamiura, Y., Yamamoto, S., Kohgo, T., Amemiya, A., Ukai, H., et al. (1997). Early bone formation around calcium-ion-implanted titanium inserted into rat tibia. *Journal of Biomedical Materials Research, 36*(1), 131−136.

Harry, J. E. (2010). *Introduction to plasma technology: Science, engineering and applications*. Weinheim, Germany: Wiley-VCH Verlag GmbH & Co. KGaA.

Heimann, R. B. (1999). Design of novel plasma sprayed hydroxyapatite-bond coat bioceramic systems. *Journal of Thermal Spray Technology, 8*(4), 597−604.

Heimann, R. B. (2007). Novel approaches towards design and biofunctionality of plasma-sprayed osteoconductive calcium phosphate coatings for biomedical implants: the concept of bond coats. In P. J. Pannone (Ed.), *Trends in biomaterials research*. New York, NY: Nova Science Publishers.

Heimann, R. B., & Vu, T. A. (1997). Low-pressure plasma-sprayed (LPPS) bioceramic coatings with improved adhesion strength and resorption resistance. *Journal of Thermal Spray Technology, 6*(2), 145−149.

Heleno, R. A., Wagner, N. S., & Branco, J. R. T. (2009). Performance evaluation of hydroxyapatite coatings thermally sprayed on surgical fixation pins. *Key Engineering Materials, 396−398*, 69−75.

Hoeppner, D. W., & Chandrasekaran, V. (1994). Fretting in orthopaedic implants: a review. *Wear, 173*(1−2), 189−197.

Holy, C. E., Cheng, C., Davies, J. E., & Shoichet, M. S. (2001). Optimizing the sterilization of PLGA scaffolds for use in tissue engineering. *Biomaterials, 22*(1), 25−31.

Huang, H. M., Hsieh, S. C., Teng, N. C., Feng, S. W., Ou, K. L., & Chang, W. J. (2011). Biological surface modification of titanium surfaces using glow discharge plasma. *Medical and Biological Engineering and Computing, 49*(6), 701−706.

Huang, N., Yang, P., Leng, Y. X., Wang, J., Sun, H., Chen, J. Y., et al. (2004). Surface modification of biomaterials by plasma immersion ion implantation. *Surface and Coatings Technology, 186*(1−2), 218−226.

Hu, J., Zhang, Y., Chen, S., He, S., Li, N., & Chen, J. (2012). Inductively coupled plasma etching of bulk molybdenum. In *IEEE 25th International Conference on Micro Electro Mechanical Systems (MEMS), Jan. 29−Feb. 2, 2012, Paris, France* (pp. 267−270).

Inagaki, N. (1996). *Plasma surface modification and plasma polymerization*. Lancaster, PA: Technomic Publishing Company, Inc.

International Organization for Standardization. (2008). *Hydroxyapatite—Part 2: Coatings of hydroxyapatite. Implants for surgery*. Switzerland: ISO 13779-2:2008(E), International Organization for Standardization.

Ip, W.Y., & Yuen, C.K. (2012). *Implant for tissue engineering*. The University of Hong Kong. US patent 8,172,908 B2, published May 8, 2012.

Ismail, F. S. M., Rohanizadeh, R., Atwa, S., Mason, R. S., Ruys, A. J., Martin, P. J., et al. (2007). The influence of surface chemistry and topography on the contact guidance of MG63 osteoblast cells. *Journal of Materials Science: Materials in Medicine, 18*(5), 705−714.

Jarcho, M. (1981). Calcium phosphate ceramics as hard tissue prosthetics. *Clinical Orthopaedics and Related Research, 157*, 259−278.

Jarcho, M., Bolen, C. H., Thomas, M. B., Bobick, J., Kay, J. F., & Doremus, R. H. (1976). Hydroxylapatite synthesis and characterization in dense polycrystalline form. *Journal of Materials Science, 11*(11), 2027−2035.

Jung, S. C., Lee, K., & Kim, B. H. (2012). Biocompatibility of plasma polymerized sandblasted large grit and acid titanium surface. *Thin Solid Films, 521*, 150−154.

Katz, J. L. (1980). Anisotropy of Young's modulus of bone. *Nature, 283*(5742), 106−107.

Kieswetter, K., Schwartz, Z., Hummert, T. W., Cochran, D. L., Simpson, J., Dean, D. D., et al. (1996). Surface roughness modulates the local production of growth factors and cytokines by osteoblast-like MG-63 cells. *Journal of Biomedical Materials Research, 32*(1), 55−63.

Kitsugi, T., Nakamura, T., Oka, M., Senaha, Y., Goto, T., & Shibuya, T. (1996). Bone-bonding behavior of plasma-sprayed coatings of Bioglass^{R}, AW-glass ceramic, and tri-calcium phosphate on titanium alloy. *Journal of Biomedical Materials Research, 30*(2), 261−269.

Ko, Y. M., Lee, K., & Kim, B. H. (2012a). Bone like apatite formation on modified Ti surfaces with COOH, NH_2, and OH functional groups by plasma polymerization. *Thin Solid Films, 521*, 128−131.

Ko, Y. M., Lee, K., & Kim, B. H. (2012b). Effect of Mg ion on formation of bone-like apatite on the plasma modified titanium surface. *Surface and Coatings Technology, 228 (Supplement 1)*, S404−S407.

Ko, Y. M., Lee, K., & Kim, B. H. (2013). Effect of functional groups on biodegradation and pre-osteoblastic cell response on the plasma-polymerized magnesium surface. *Japanese Journal of Applied Physics, 52*(1 PART2).

Kumar, S. (2013). *Cleaning and sterilising method for biomedical surfaces*. University of South Australia. WO patent 2013/037008 A1, published March 21, 2013.

Kumar, R., Cheang, P., & Khor, K. A. (2003). Radio frequency (RF) suspension plasma sprayed ultra-fine hydroxyapatite (HA)/zirconia composite powders. *Biomaterials, 24*(15), 2611−2621.

Kurzweg, H., Heimann, R. B., Troczynski, T., & Wayman, M. L. (1998). Development of plasma-sprayed bioceramic coatings with bond coats based on titania and zirconia. *Biomaterials, 19*(16), 1507−1511.

Kweh, S. W. K., Khor, K. A., & Cheang, P. (2002). An in vitro investigation of plasma sprayed hydroxyapatite (HA) coatings produced with flame-spheroidized feedstock. *Biomaterials, 23*(3), 775−785.

Kwok, S. C. H., Ha, P. C. T., McKenzie, D. R., Bilek, M. M. M., & Chu, P. K. (2006). Biocompatibility of calcium and phosphorus doped diamond-like carbon thin films synthesized by plasma immersion ion implantation and deposition. *Diamond and Related Materials, 15*(4−8), 893−897.

Kyi, M. S., Holton, J., & Ridgway, G. L. (1995). Assessment of the efficacy of a low temperature hydrogen peroxide gas plasma sterilization system. *Journal of Hospital Infection, 31*(4), 275−284.

Kyomoto, M., Ishihara, K., Iwasaki, Y., Moro, T., Nakamura, K., Takatori, Y., et al. (2010a). *Biomaterial, joint prosthesis using the biomaterial and method of producing the same*. Japan Medical Materials corporation, the University of Tokyo and National University Corporation Tokyo Medical and Dental University. US patent 2010/0262237 A1, published October 14, 2010.

Kyomoto, M., Iwasaki, Y., Moro, T., Konno, T., Miyaji, F., Kawaguchi, H., et al. (2007). High lubricious surface of cobalt-chromium-molybdenum alloy prepared by grafting poly(2-methacryloyloxyethyl phosphorylcholine). *Biomaterials, 28*(20), 3121−3130.

Kyomoto, M., Moro, T., Iwasaki, Y., Miyaji, F., Kawaguchi, H., Takatori, Y., et al. (2009). Superlubricious surface mimicking articular cartilage by grafting poly(2-methacryloyloxyethyl phosphorylcholine) on orthopaedic metal bearings. *Journal of Biomedical Materials Research—Part A, 91*(3), 730−741.

Kyomoto, M., Moro, T., Saiga, K. I., Miyaji, F., Kawaguchi, H., Takatori, Y., et al. (2010b). Lubricity and stability of poly(2-methacryloyloxyethyl phosphorylcholine) polymer layer on Co-Cr-Mo surface for hemi-arthroplasty to prevent degeneration of articular cartilage. *Biomaterials, 31*(4), 658−668.

Lai, K. A., Shen, W. J., Chen, C. H., Yang, C. Y., Hu, W. P., & Chang, G. L. (2002). Failure of hydroxyapatite-coated acetabular cups. *Journal of Bone and Joint Surgery—Series B, 84*(5), 641−646.

Laing, P. G., Ferguson, A. B., Jr., & Hodge, E. S. (1967). Tissue reaction in rabbit muscle exposed to metallic implants. *Journal of Biomedical Materials Research, 1*(1), 135−149.

Lamers, E., Walboomers, X. F., Domanski, M., te Riet, J., van Delft, F. C. M. J. M., Luttge, R., et al. (2010). The influence of nanoscale grooved substrates on osteoblast behavior and extracellular matrix deposition. *Biomaterials, 31*(12), 3307−3316.

Lamy, D., Pierre, A. C., & Heimann, R. B. (1996). Hydroxyapatite coatings with a bond coat of biomedical implants by plasma projection. *Journal of Materials Research, 11*(3), 680−686.

Laonapakul, T., Otsuka, Y., Nimkerdphol, A. R., & Mutoh, Y. (2012). Acoustic emission and fatigue damage induced in plasma-sprayed hydroxyapatite coating layers. *Journal of the Mechanical Behavior of Biomedical Materials, 8*, 123−133.

Lee, J. H., Jung, H. W., Kang, I. K., & Lee, H. B. (1994). Cell behaviour on polymer surfaces with different functional groups. *Biomaterials, 15*(9), 705−711.

Lee, B. H., Kim, J. K., Kim, Y. D., Choi, K., & Lee, K. H. (2004a). In vivo behavior and mechanical stability of surface-modified titanium implants by plasma spray coating and chemical treatments. *Journal of Biomedical Materials Research—Part A, 69*(2), 279−285.

Lee, K., Ko, Y. M., & Kim, B. H. (2012). Biocompatibility of cation coated on plasma-polymerized Ti surface. *Japanese Journal of Applied Physics, 51*(8 PART 2).

Lee, T. M., Yang, C. Y., Chang, E., & Tsai, R. S. (2004b). Comparison of plasma-sprayed hydroxyapatite coatings and zirconia-reinforced hydroxyapatite composite coatings: in vivo study. *Journal of Biomedical Materials Research—Part A, 71*(4), 652−660.

Legeros, R. Z. (1993). Biodegradation and bioresorption of calcium phosphate ceramics. *Clinical Materials, 14*(1), 65−88.

Leng, Y. X., Yang, P., Chen, J. Y., Sun, H., Wang, J., Wang, G. J., et al. (2001). Fabrication of Ti-O/Ti-N duplex coatings on biomedical titanuim alloys by metal plasma immersion ion implantation and reactive plasma nitriding/oxidation. *Surface and Coatings Technology, 138*(2−3), 296−300.

Lerouge, S., Wertheimer, M. R., & Yahia, L. H. (2001). Plasma sterilization: a review of parameters, mechanisms, and limitations. *Plasmas and Polymers, 6*(3), 175−188.

Levintant-Zayonts, N., & Kucharski, S. (2009). Surface characterization and wear behavior of ion implanted NiTi shape memory alloy. *Vacuum, 83*(Suppl. 1), S220−S223.

Li, L., Dai, X. J., Xu, H. S., Zhao, J. H., Yang, P., Maurdev, G., et al. (2009). Combined continuous wave and pulsed plasma modes: for more stable interfaces with higher functionality on metal and semiconductor surfaces. *Plasma Processes and Polymers, 6*(10), 615−619.

Li, Y., Zhao, T., Wei, S., Xiang, Y., & Chen, H. (2010). Effect of Ta_2O_5/TiO_2 thin film on mechanical properties, corrosion and cell behavior of the NiTi alloy implanted with tantalum. *Materials Science and Engineering C, 30*(8), 1227−1235.

Lima, R., Marple, B., Li, H., & Khor, K.A. (2006). *Biocompatible thermal spray coating made from a nanostructured feedstock*. National Research Council of Canada and Nanyang Technological University. published as US 2006/0199024 A1, on September 7, 2006, published Application pending.

Lin, C. C., Cheng, H. C., Huang, C. F., Lin, C. T., Lee, S. Y., Chen, C. S., et al. (2005). Enhancement of biocompatibility on bioactive titanium surface by low-temperature plasma treatment. *Japanese Journal of Applied Physics, Part 1: Regular Papers and Short Notes and Review Papers, 44*(12), 8590−8598.

Liu, X., & Ding, C. (2002). Plasma sprayed wollastonite/TiO_2 composite coatings on titanium alloys. *Biomaterials, 23*(20), 4065−4077.

Liu, X., Fu, R. K. Y., & Chu, P. K. (2008). Surface modification of biomaterials using plasma immersion ion implantation and deposition. In P. K. Chu, & X. Y. Liu (Eds.), *Biomaterials fabrication and processing handbook*. Boca Raton, FL: CRC Press/Taylor and Francis.

Liu, H., Jiang, Y., Zhou, R., & Tang, B. (2013). Mechanical property and rolling contact fatigue life of TiN film on bearing steel by plasma immersion ion implantation and deposition. *Reviews on Advanced Materials Science, 33*(2), 131−136.

Liu, X., Poon, R. W. Y., Chu, P. K., & Ding, C. X. (2004a). *Surface modification of titanium by phosphorus plasma immersion ion implantation, 7th World Biomaterials Congress, May 17−21, 2004*. Sydney, Australia. Red Hook, NY: Curran Associates, Inc., 1112.

Liu, X., Poon, R. W. Y., Kwok, S. C. H., Chu, P. K., & Ding, C. (2004b). Plasma surface modification of titanium for hard tissue replacements. *Surface and Coatings Technology, 186*(1−2 SPEC. ISS), 227−233.

Liu, X., Poon, R. W. Y., Kwok, S. C. H., Chu, P. K., & Ding, C. (2005). Structure and properties of Ca-plasma-implanted titanium. *Surface and Coatings Technology, 191*(1), 43−48.

Liu, H., Tang, B., Wang, L., Wang, X., & Jiang, B. (2007a). Fatigue life and mechanical behaviors of bearing steel by nitrogen plasma immersion ion implantation. *Surface and Coatings Technology, 201*(9−11), 5273−5277.

Liu, X., Tao, S., & Ding, C. (2002). Bioactivity of plasma sprayed dicalcium silicate coatings. *Biomaterials, 23*(3), 963−968.

Liu, X. M., Wu, S. L., Chan, Y. L., Chu, P. K., Chung, C. Y., Chu, C. L., et al. (2007b). Surface characteristics, biocompatibility, and mechanical properties of nickel-titanium plasma-implanted with nitrogen at different implantation voltages. *Journal of Biomedical Materials Research—Part A, 82*(2), 469−478.

Liu, C., Xin, Y., Tian, X., & Chu, P. K. (2007c). Corrosion behavior of AZ91 magnesium alloy treated by plasma immersion ion implantation and deposition in artificial physiological fluids. *Thin Solid Films, 516*(2−4), 422−427.

Liu, H., Xu, Q., Wang, C., Zhang, X., & Tang, B. (2012). Investigating the microstructure and mechanical behaviors of DLC films on AISI52100 bearing steel surface fabricated by plasma immersion ion implantation and deposition. *Surface and Coatings Technology, 228 (Supplement 1)*, S159−S163.

Löffler, R., Fleischer, M., & Kern, D. P. (2012). An anisotropic dry etch process with fluorine chemistry to create well-defined titanium surfaces for biomedical studies. *Microelectronic Engineering, 97*, 361−364.

Lombardi, A. V., Berend, K. R., & Mallory, T. H. (2006). Hydroxyapatite-coated titanium porous plasma spray tapered stem: experience at 15 to 18 years. *Clinical Orthopaedics and Related Research, 453*, 81−85.

Lombardi, A. V., Jr., Berend, K. R., Mallory, T. H., Skeels, M. D., & Adams, J. B. (2009). Survivorship of 2000 tapered titanium porous plasma-sprayed femoral components. *Clinical Orthopaedics and Related Research, 467*(1), 146−154.

Long, M., & Rack, H. J. (1998). Titanium alloys in total joint replacement - a materials science perspective. *Biomaterials, 19*(18), 1621−1639.

Lu, Y. P., Li, M. S., Li, S. T., Wang, Z. G., & Zhu, R. F. (2004). Plasma-sprayed hydroxyapatite+ titania composite bond coat for hydroxyapatite coating on titanium substrate. *Biomaterials, 25*(18), 4393−4403.

Lu, Y. P., Xiao, G. Y., Li, S. T., Sun, R. X., & Li, M. S. (2006). Microstructural inhomogeneity in plasma-sprayed hydroxyapatite coatings and effect of post-heat treatment. *Applied Surface Science, 252*(6), 2412−2421.

Lutz, J., Díaz, C., García, J. A., Blawert, C., & Mändl, S. (2011). Corrosion behaviour of medical CoCr alloy after nitrogen plasma immersion ion implantation. *Surface and Coatings Technology, 205*(8−9), 3043−3049.

Lynn, A. K., & DuQuesnay, D. L. (2002). Hydroxyapatite-coated Ti-6Al-4V. Part 1: the effect of coating thickness on mechanical fatigue behaviour. *Biomaterials, 23*(9), 1937−1946.

Maitz, M. F., Poon, R. W. Y., Liu, X. Y., Pham, M. T., & Chu, P. K. (2005). Bioactivity of titanium following sodium plasma immersion ion implantation and deposition. *Biomaterials, 26*(27), 5465−5473.

Mändl, S., Krause, D., Thorwarth, G., Sader, R., Zeilhofer, F., Horch, H. H., et al. (2001). Plasma immersion ion implantation treatment of medical implants. *Surface and Coatings Technology, 142−144*, 1046−1050.

Mändl, S., Sader, R., Thorwarth, G., Krause, D., Zeilhofer, H. F., Horch, H. H., et al. (2003). Biocompatibility of titanium based implants treated with plasma immersion ion implantation. *Nuclear Instruments and Methods in Physics Research, Section B: Beam Interactions with Materials and Atoms, 206*, 517−521.

Manos, D. M., & Flamm, D. L. (1989). *Plasma etching: An introduction*. San Diego, CA: Academic Press, Inc.

Marchant, R.E. (1995). *Anticoagulant plasma polymer-modified substrate*. Case Western Reserve University. US patent 5,455,040, published October 3, 1995.

Masters, K. S., & Anseth, K. S. (2004). Cell-material interactions. In N. A. Peppas, & M. V. Sefton (Eds.), *Molecular and cellular foundations of biomaterials*. San Diego, CA: Elsevier Inc.

Mello, C. B., Ueda, M., Lepienski, C. M., & Reuther, H. (2009a). Tribological changes on SS304 stainless steel induced by nitrogen plasma immersion ion implantation with and without auxiliary heating. *Applied Surface Science, 256*(5), 1461−1465.

Mello, C. B., Ueda, M., Silva, M. M., Reuther, H., Pichon, L., & Lepienski, C. M. (2009b). Tribological effects of plasma immersion ion implantation heating treatments on Ti-6Al-4V alloy. *Wear, 267*(5−8), 867−873.

Miola, M., Ferraris, S., Di Nunzio, S., Robotti, P. F., Bianchi, G., Fucale, G., et al. (2009). Surface silver-doping of biocompatible glasses to induce antibacterial properties. Part II: plasma sprayed glass-coatings. *Journal of Materials Science: Materials in Medicine, 20*(3), 741−749.

Mittal, M., Nath, S. K., & Prakash, S. (2013). Improvement in mechanical properties of plasma sprayed hydroxyapatite coatings by Al_2O_3 reinforcement. *Materials Science and Engineering C, 33*(5), 2838−2845.

Mohan, L., Anandan, C., & Grips, V. K. W. (2012). Corrosion behavior of titanium alloy Beta-21S coated with diamond like carbon in Hank's solution. *Applied Surface Science, 258*(17), 6331−6340.

Morks, M. F., Fahim, N. F., & Kobayashi, A. (2008). Structure, mechanical performance and electrochemical characterization of plasma sprayed SiO_2/Ti-reinforced hydroxyapatite biomedical coatings. *Applied Surface Science, 255*(5, Part 2), 3426−3433.

Moro, T., Takatori, Y., Ishihara, K., Konno, T., Takigawa, Y., Matsushita, T., et al. (2004). Surface grafting of artificial joints with a biocompatible polymer for preventing periprosthetic osteolysis. *Nature Materials, 3*(11), 829−836.

Müller, R. T., & Patsalis, T. (1997). Shear and tensile strength of hydroxyapatite coating under loading conditions. An experimental study in dogs. *Archives of Orthopaedic and Trauma Surgery, 116*(6−7), 334−337.

Myung, S. W., Ko, Y. M., & Kim, B. H. (2013). Effect of plasma surface functionalization on preosteoblast cells spreading and adhesion on a biomimetic hydroxyapatite layer formed on a titanium surface. *Applied Surface Science, 287*, 62−68.

Nakano, K. & Watanabe, K. (1987). *Method for the production of endosseous implants*. Sumitomo Chemical Company. US patent 4,687,675, published August 18, 1987.

Narayanan, P.V., Rowland, S.M. & Stanley, K.D. (1994). *Treatment of metallic surfaces using radiofrequency plasma deposition and chemical attachment of bioactive agents*. Cordis Corporation. US patent 5,336,518, published August 9, 1994.

Ng, M.K.C., Waterhouse, A., Weiss, A.S., & Wise, S.G. (2010). *Chemically and biologically modified medical devices*. US patent 2010/0174351 A1, published July 8, 2010.

Oehrlein, G. S. (1990). Reactive ion etching. In S. M. Rossnagel, J. J. Cuomo, & W. D. Westwood (Eds.), *Handbook of plasma processing technology: Fundamentals, etching, deposition and surface interactions*. New Jersey, NJ: Noyes Publications.

Oktar, F. N., Yetmez, M., Agathopoulos, S., Goerne, T. M. L., Goller, G., Ipeker, I., et al. (2006). Bond-coating in plasma-sprayed calcium-phosphate coatings. *Journal of Materials Science: Materials in Medicine, 17*(11), 1161−1171.

Okuyama, M., Kobayashi, J., Take, S., & Itoi, Y. (2004). Effect of plasma spray and surface sealing treatment of Ni-Ti shape memory alloy applying to biomaterials. *Materials Transactions, 45*(4), 1045−1053.

Oonishi, H., Yamamoto, M., Ishimaru, H., Tsuji, E., Kushitani, S., Aono, M., et al. (1989). The effect of hydroxyapatite coating on bone growth into porous titanium alloy implants. *Journal of Bone and Joint Surgery—Series B, 71*(2), 213−216.

Öztürk, O., Türkan, U., & Eroğlu, A. E. (2006). Metal ion release from nitrogen ion implanted CoCrMo orthopedic implant material. *Surface and Coatings Technology, 200*(20−21), 5687−5697.

Pareta, R. A., Reising, A. B., Miller, T., Storey, D., & Webster, T. J. (2009). Increased endothelial cell adhesion on plasma modified nanostructured polymeric and metallic surfaces for vascular stent applications. *Biotechnology and Bioengineering, 103*(3), 459−471.

Parker, E. R., Thibeault, B. J., Aimi, M. F., Rao, M. P., & MacDonald, N. C. (2005). Inductively coupled plasma etching of bulk titanium for MEMS applications. *Journal of the Electrochemical Society, 152*(10), C675−C683.

Park, W. W., Kim, E. K., Jeon, J. H., Choi, J. Y., Moon, S. W., Lim, S. H., et al. (2012a). Wear of UHMWPE against nitrogen-ion-implanted and NbN-coated Co-Cr-Mo alloy formed by plasma immersion ion implantation and deposition for artificial joints. *Applied Surface Science, 258*(20), 8228−8233.

Park, J. H., Olivares-Navarrete, R., Baier, R. E., Meyer, A. E., Tannenbaum, R., Boyan, B. D., et al. (2012b). Effect of cleaning and sterilization on titanium implant surface properties and cellular response. *Acta Biomaterialia, 8*(5), 1966−1975.

Pawlowski, L. (2008). *The science and engineering of thermal spray coatings*. England, UK: John Wiley & Sons.

Pilliar, R. M. (2009). Metallic biomaterials. In R. Narayan (Ed.), *Biomedical materials*. New York, NY: Springer Science + Business Media, LLC.

Poon, R. W. Y., Ho, J. P. Y., Liu, X., Chung, C. Y., Chu, P. K., Yeung, K. W. K., et al. (2005a). Improvements of anti-corrosion and mechanical properties of NiTi orthopedic materials by acetylene, nitrogen and oxygen plasma immersion ion implantation. *Nuclear Instruments and Methods in Physics Research, Section B: Beam Interactions with Materials and Atoms, 237*(1−2), 411−416.

Poon, R. W. Y., Yeung, K. W. K., Liu, X. Y., Chu, P. K., Chung, C. Y., Lu, W. W., et al. (2005b). Carbon plasma immersion ion implantation of nickel-titanium shape memory alloys. *Biomaterials, 26*(15), 2265−2272.

Puleo, D. A., Kissling, R. A., & Sheu, M. S. (2002). A technique to immobilize bioactive proteins, including bone morphogenetic protein-4 (BMP-4), on titanium alloy. *Biomaterials, 23*(9), 2079−2087.

Pypen, C. M. J. M., Plenk, H., Jr., Ebel, M. F., Svagera, R., & Wernisch, J. (1997). Characterization of microblasted and reactive ion etched surfaces on the commercially pure metals niobium, tantalum and titanium. *Journal of Materials Science: Materials in Medicine, 8*(12), 781−784.

Radin, S. R., & Ducheyne, P. (1992). Plasma spraying induced changes of calcium phosphate ceramic characteristics and the effect on in vitro stability. *Journal of Materials Science: Materials in Medicine, 3*(1), 33−42.

Rakngarm, A., & Mutoh, Y. (2009). Characterization and fatigue damage of plasma sprayed HAp top coat with Ti and HAp/Ti bond coat layers on commercially pure titanium substrate. *Journal of the Mechanical Behavior of Biomedical Materials, 2*(5), 444−453.

Ramesh, S., Tan, C. Y., Bhaduri, S. B., Teng, W. D., & Sopyan, I. (2008). Densification behaviour of nanocrystalline hydroxyapatite bioceramics. *Journal of Materials Processing Technology, 206*(1−3), 221−230.

Reclaru, L., Eschler, P. Y., Lerf, R., & Blatter, A. (2005). Electrochemical corrosion and metal ion release from Co-Cr-Mo prosthesis with titanium plasma spray coating. *Biomaterials, 26*(23), 4747−4756.

Reclaru, L., Lerf, R., Eschler, P. Y., Blatter, A., & Meyer, J. M. (2003). Evaluation of corrosion on plasma sprayed and anodized titanium implants, both with and without bone cement. *Biomaterials, 24*(18), 3027−3038.

Rey, C., & Ranz, X. (2001). *Process for preparation of hydroxyapatite coatings*. Biocoatings S.r.l. US patent 6,280,789 B1, published August 28, 2001.

Ripamonti, U., & Kirkbride, A.N. (2001). *Biomaterial and bone implant for bone repair and replacement*. Implico B.V. US patent 6,302,913 B1, published October 16, 2001.

Roby, M.S. (2003). *Plasma treated surgical needles and methods for their manufacture*. Tyco Healthcare Group LP. US patent 6,558,409 B1, published May 6, 2003.

Røkkum, M., Brandt, M., Bye, K., Hetland, K. R., Waage, S., & Reigstad, A. (1999). Polyethylene wear, osteolysis and acetabular loosening with an HA-coated hip prosthesis. A follow-up of 94 consecutive arthroplasties. *Journal of Bone and Joint Surgery—Series B, 81*(4), 582−589.

Rossnagel, S. M., Cuomo, J. J., & Westwood, W. D. (1990). *Handbook of plasma processing technology—Fundamentals, etching, deposition, and surface interactions*. New Jersey, USA: William Andrew Publishing/Noyes.

Sawano, H., Warisawa, S., & Ishihara, S. (2010). Study on wear reduction mechanism of artificial joints grafted with hydrophilic polymer membranes. *Wear, 268*(1), 233−240.

Scarano, A., Piattelli, M., Vrespa, G., Caputi, S., & Piattelli, A. (2003). Bacterial adhesion on titanium nitride-coated and uncoated implants: an in vivo human study. *The Journal of Oral Implantology, 29*(2), 80−85.

Schröder, K., Finke, B., Ohl, A., Lüthen, F., Bergemann, C., Nebe, B., et al. (2010a). Capability of differently charged plasma polymer coatings for control of tissue interactions with titanium surfaces. *Journal of Adhesion Science and Technology, 24*(7), 1191−1205.

Schröder, K., Finke, B., Polak, M., Lüthen, F., Nebe, J. B., Rychly, J., et al. (2010b). Gas-discharge plasma-assisted functionalization of titanium implant surfaces. *Materials Science Forum, 638−642*, 700−705.

Seo, H. S., Ko, Y. M., Shim, J. W., Lim, Y. K., Kook, J. K., Cho, D. L., et al. (2010b). Characterization of bioactive RGD peptide immobilized onto poly(acrylic acid) thin films by plasma polymerization. *Applied Surface Science, 257*(2), 596−602.

Sergo, V., Sbaizero, O., & Clarke, D. R. (1997). Mechanical and chemical consequences of the residual stresses in plasma sprayed hydroxyapatite coatings. *Biomaterials, 18*(6), 477−482.

Shibata, Y., & Miyazaki, T. (2002). Anode glow discharge plasma treatment enhances calcium phosphate adsorption onto titanium plates. *Journal of Dental Research, 81*(12), 841−844.

Shih, C. C., Lin, S. J., Chen, Y. L., Su, Y. Y., Lai, S. T., Wu, G. J., et al. (2000). The cytotoxicity of corrosion products of nitinol stent wire on cultured smooth muscle cells. *Journal of Biomedical Materials Research, 52*(2), 395−403.

Sill, K.N., Skaff, H., & Breitenkamp, K. (2012). *Plasma modification of metal surfaces*. Intezyne Technologies, Inc. US patent 2012/0046735, published February 23, 2012.

Silva, M. M., Ueda, M., Pichon, L., Reuther, H., & Lepienski, C. M. (2007). Surface modification of Ti6Al4V alloy by PIII at high temperatures: effects of plasma potential. *Nuclear Instruments and Methods in Physics Research, Section B: Beam Interactions with Materials and Atoms, 257*(1−2 SPEC. ISS), 722−726.

Simon, M., Lagneau, C., Moreno, J., Lissac, M., Dalard, F., & Grosgogeat, B. (2005). Corrosion resistance and biocompatibility of a new porous surface for titanium implants. *European Journal of Oral Sciences, 113*(6), 537−545.

Sioshansi, P., & Tobin, E. J. (1996). Surface treatment of biomaterials by ion beam processes. *Surface and Coatings Technology, 83*(1−3), 175−182.

Ślósarczyk, A., & Białoskórski, J. (1998). Hardness and fracture toughness of dense calcium-phosphate-based materials. *Journal of Materials Science: Materials in Medicine, 9*(2), 103−108.

Storey, D.M., McGrath, T.S., & Shimpi, T.M. (2007). *Molecular plasma deposition of colloidal materials*. Ionic Fusion Corporation. US patent 7,250,195 B1, published July 31, 2007.

Story, B., & Burgess, A. (1998). *Prosthetic implants coated with hydroxylapatite and process for treating prosthetic implants plasma-sprayed with hydroxylapatite*. Sulzer Calcitek Inc. US patent 5,730,598, published March 24, 1998.

Sugawara, M. (1998). *Plasma etching: Fundamentals and applications*. New York, NY: Oxford University Press Inc.

Sui, J. H., & Cai, W. (2006). Formation of diamond-like carbon (DLC) film on the NiTi alloys via plasma immersion ion implantation and deposition (PIIID) for improving corrosion resistance. *Applied Surface Science, 253*(4), 2050−2055.

Sui, J. H., Gao, Z. Y., Cai, W., & Zhang, Z. G. (2007). Corrosion behavior of NiTi alloys coated with diamond-like carbon (DLC) fabricated by plasma immersion ion implantation and deposition. *Materials Science and Engineering A, 452−453*, 518−523.

Sun, L., Berndt, C. C., Gross, K. A., & Kucuk, A. (2001). Material fundamentals and clinical performance of plasma-sprayed hydroxyapatite coatings: a review. *Journal of Biomedical Materials Research, 58*(5), 570−592.

Sun, L., Berndt, C. C., Khor, K. A., Cheang, H. N., & Gross, K. A. (2002). Surface characteristics and dissolution behavior of plasma-sprayed hydroxyapatite coating. *Journal of Biomedical Materials Research, 62*(2), 228−236.

Sundfeldt, M., Carlsson, L. V., Johansson, C. B., Thomsen, P., & Gretzer, C. (2006). Aseptic loosening, not only a question of wear: a review of different theories. *Acta Orthopaedica, 77*(2), 177−197.

Tan, L., Dodd, R. A., & Crone, W. C. (2003). Corrosion and wear-corrosion behavior of NiTi modified by plasma source ion implantation. *Biomaterials, 24*(22), 3931−3939.

Tang, B. Y., Chu, P. K., Wang, S. Y., Chow, K. W., & Wang, X. F. (1998). Methane and nitrogen plasma immersion ion implantation of titanium metal. *Surface and Coatings Technology, 103−104*, 248−251.

Thierry, B., Tabrizian, M., Savadogo, O., & Yahia, L. H. (2000). Effects of sterilization processes on NiTi alloy: surface characterization. *Journal of Biomedical Materials Research, 49*(1), 88−98.

Thorwarth, G., Mändl, S., & Rauschenbach, B. (2001). Rutile formation and oxygen diffusion in oxygen PIII-treated titanium. *Surface and Coatings Technology, 136*(1−3), 236−240.

Tsui, Y. C., Doyle, C., & Clyne, T. W. (1998a). Plasma sprayed hydroxyapatite coatings on titanium substrates. Part 1: mechanical properties and residual stress levels. *Biomaterials, 19*(22), 2015−2029.

Tsui, Y. C., Doyle, C., & Clyne, T. W. (1998b). Plasma sprayed hydroxyapatite coatings on titanium substrates. Part 2: optimisation of coating properties. *Biomaterials, 19*(22), 2031−2043.

Ueda, M., Silva, M. M., Otani, C., Reuther, H., Yatsuzuka, M., Lepienski, C. M., et al. (2003). Improvement of tribological properties of Ti6Al4V by nitrogen plasma immersion ion implantation. *Surface and Coatings Technology, 169−170*, 408−410.

Uzumaki, E. T., Lambert, C. S., Belangero, W. D., & Zavaglia, C. A. C. (2008). Biocompatibility of titanium based implants with diamond-like carbon coatings produced by plasma immersion ion implantation and deposition. *Key Engineering Materials, 361−363*(I), 677−680.

Vallecillo Capilla, M., Romero Olid, M. N., Olmedo Gaya, M. V., Reyes Botella, C., & Zorrilla Romera, C. (2007). Cylindrical dental implants with hydroxyapatite- and titanium plasma spray-coated surfaces: 5-year results. *The Journal of Oral Implantology, 33*(2), 59−68.

Varadaraajan, V., Visveswaran, R., & Mohanty, P. S. (2009). Nano titania embedded hydroxyapatite coating by precursor plasma. In B. R. Marple, M. M. Hyland, Y.-C. Lau, C.-J. Li, R. S. Lima, & G. Montavon (Eds.), *Expanding thermal spray performance to new markets and applications, May 4−7, 2009* (pp. 354−360). Las Vegas: NV. ASM International.

Verné, E., Ferraris, M., Ventrella, A., Paracchini, L., Krajewski, A., & Ravaglioli, A. (1998). Sintering and plasma spray deposition of bioactive glass-matrix composites for medical applications. *Journal of the European Ceramic Society, 18*(4), 363−372.

Vetrecin, R. (2012). *Process for in situ plasma polymerization of silicone coatings for surgical needles*. Robert Vetrecin. US patent 2012/0321776 A1, published December 20, 2012.

Vyavahare, N.R. & Marigliano, J.J. (2005). *Vascular biomaterial devices and methods*. Clemson University. US patent 6,837,903 B2, published January 4, 2005.

Wan, G. J., Maitz, M. F., Sun, H., Li, P. P., & Huang, N. (2007). Corrosion properties of oxygen plasma immersion ion implantation treated magnesium. *Surface and Coatings Technology, 201*(19−20), 8267−8272.

Wang, C., & Wang, Y. (2004). Tribology of endoprostheses. In D. G. Poitout (Ed.), *Biomechanics and biomaterials in orthopedics*. Singapore: Springer London.

Wang, X., Zeng, X., Wu, G., Yao, S., & Lai, Y. (2007). Effects of tantalum ion implantation on the corrosion behavior of AZ31 magnesium alloys. *Journal of Alloys and Compounds, 437*(1−2), 87−92.

Wang, X., Zhang, F., Li, C., Zheng, Z., Wang, X., Liu, X., et al. (2000). Improvement of blood compatibility of artificial heart valves via titanium oxide film coated on low temperature isotropic carbon. *Surface and Coatings Technology, 128−129*(1), 36−42.

Weiner, S., & Wagner, H. D. (1998). The material bone: structure-mechanical function relations. *Annual Review of Materials Science, 28*(1), 271−298.

Wenzel, R. N. (1936). Resistance of solid surfaces to wetting by water. *Industrial and Engineering Chemistry, 28*(8), 988−994.

Wieser, E., Tsyganov, I., Matz, W., Reuther, H., Oswald, S., Pham, T., et al. (1999). Modification of titanium by ion implantation of calcium and/or phosphorus. *Surface and Coatings Technology, 111*(1), 103−109.

Wu, E. Y., Ou, K. L., & Pan, Y. N. (2007). Enhancement of biocompatibility on bioactive Ti-Nb-based alloy by high-density plasma modification. *Materials Transactions, 48*(12), 3164−3169.

Wu, C., Ramaswamy, Y., Liu, X., Wang, G., & Zreiqat, H. (2009). Plasma-sprayed $CaTiSiO_5$ ceramic coating on Ti-6Al-4V with excellent bonding strength, stability and cellular bioactivity. *Journal of the Royal Society Interface, 6*(1), 159−168.

Xiao, Y. B., Kim, E. H., Kong, S. M., Park, J. H., Min, B. C., & Chung, C. W. (2010). Inductively coupled plasma reactive ion etching of titanium thin films using a Cl_2/Ar gas. *Vacuum, 85*(3), 434−438.

Xie, Y., Liu, X., Huang, A., Ding, C., & Chu, P. K. (2005). Improvement of surface bioactivity on titanium by water and hydrogen plasma immersion ion implantation. *Biomaterials, 26*(31), 6129−6135.

Xiong, D., Gao, Z., & Jin, Z. (2007). Friction and wear properties of UHMWPE against ion implanted titanium alloy. *Surface and Coatings Technology, 201*(15), 6847−6850.

Xu, R., Wu, G., Yang, X., Hu, T., Lu, Q., & Chu, P. K. (2011). Controllable degradation of biomedical magnesium by chromium and oxygen dual ion implantation. *Materials Letters, 65*(14), 2171−2173.

Xu, R., Yang, X., Zhang, X., Wang, M., Li, P., Zhao, Y., et al. (2013). Effects of carbon dioxide plasma immersion ion implantation on the electrochemical properties of AZ31 magnesium alloy in physiological environment. *Applied Surface Science, 286*, 257−260.

Yang, Y., & Ong, J. L. (2003). Bond strength, compositional, and structural properties of hydroxyapatite coating on Ti, ZrO_2-coated Ti, and TPS-coated Ti substrate. *Journal of Biomedical Materials Research—Part A, 64*(3), 509−516.

Yang, Y., Ong, J. L., & Tian, J. (2002). In vivo evaluation of modified titanium implant surfaces produced using a hybrid plasma spraying processing. *Materials Science and Engineering C, 20*(1−2), 117−124.

Yang, Y. Z., Tian, J. M., Tian, J. T., Chen, Z. Q., Deng, X. J., & Zhang, D. H. (2000). Preparation of graded porous titanium coatings on titanium implant materials by plasma spraying. *Journal of Biomedical Materials Research, 52*(2), 333−337.

Yang, Z., Tu, Q., Wang, J., Lei, X., He, T., Sun, H., et al. (2011a). Bioactive plasma-polymerized bipolar films for enhanced endothelial cell mobility. *Macromolecular Bioscience, 11*(6), 797−805.

Yang, C. Y., Wang, B. C., Chang, E., & Wu, J. D. (1995). The influences of plasma spraying parameters on the characteristics of hydroxyapatite coatings: a quantitative study. *Journal of Materials Science: Materials in Medicine, 6*(5), 249−257.

Yang, C. Y., Wang, B. C., Lee, T. M., Chang, E., & Chang, G. L. (1997). Intramedullary implant of plasma-sprayed hydroxyapatite coating: an interface study. *Journal of Biomedical Materials Research, 36*(1), 39−48.

Yang, Z., Wang, J., Luo, R., Maitz, M. F., Jing, F., Sun, H., et al. (2010). The covalent immobilization of heparin to pulsed-plasma polymeric allylamine films on 316L stainless steel and the resulting effects on hemocompatibility. *Biomaterials, 31*(8), 2072−2083.

Yang, C. H., Wang, Y. T., Tsai, W. F., Ai, C. F., Lin, M. C., & Huang, H. H. (2011b). Effect of oxygen plasma immersion ion implantation treatment on corrosion resistance and cell adhesion of titanium surface. *Clinical Oral Implants Research, 22*(12), 1426−1432.

Yang, Y. C., & Yang, C. Y. (2013). Mechanical and histological evaluation of a plasma sprayed hydroxyapatite coating on a titanium bond coat. *Ceramics International, 39*(6), 6509−6516.

Yasuda, H. (1985). *Plasma polymerization*. Orlando, FL: Academic Press, Inc.

Ye, S. H., Johnson, C. A., Jr., Woolley, J. R., Oh, H. I., Gamble, L. J., Ishihara, K., et al. (2009). Surface modification of a titanium alloy with a phospholipid polymer prepared by a plasma-induced grafting technique to improve surface thromboresistance. *Colloids and Surfaces B: Biointerfaces, 74*(1), 96−102.

Ye, F. X., Ohmori, A., Tsumura, T., Nakata, K., & Li, C. J. (2007). Microstructural analysis and photocatalytic activity of plasma-sprayed titania-hydroxyapatite coatings. *Journal of Thermal Spray Technology, 16*(5−6), 776−782.

Yeung, K. W. K., Chan, Y. L., Lam, K. O., Liu, X. M., Wu, S. L., Liu, X. Y., et al. (2008). New plasma surface-treated memory alloys: towards a new generation of "smart" orthopaedic materials. *Materials Science and Engineering C, 28*(3), 454−459.

Yeung, K.W.K., Poon, R.W.Y., Chu, P.K-H., Cheung, K.M.C., & Lu, W.W. (2010). *Surface treated shape memory materials and methods for making same*. Versitech Limited and the City University of Hong Kong. US patent 7,803,234 B2, published September 28, 2010.

Yeung, K. W. K., Poon, R. W. Y., Chu, P. K., Chung, C. Y., Liu, X. Y., Lu, W. W., et al. (2007). Surface mechanical properties, corrosion resistance, and cytocompatibility of nitrogen plasma-implanted nickel-titanium alloys: a comparative study with commonly used medical grade materials. *Journal of Biomedical Materials Research—Part A, 82*(2), 403−414.

Yeung, K. W. K., Poon, R. W. Y., Liu, X. Y., Ho, J. P. Y., Chung, C. Y., Chu, P. K., et al. (2005). Corrosion resistance, surface mechanical properties, and cytocompatibility of plasma immersion ion implantation-treated nickel-titanium shape memory alloys. *Journal of Biomedical Materials Research—Part A, 75*(2), 256−267.

Yilmaz, S. (2009). An evaluation of plasma-sprayed coatings based on Al_2O_3 and Al_2O_3-13 wt% TiO_2 with bond coat on pure titanium substrate. *Ceramics International, 35*(5), 2017−2022.

Yu, L. G., Khor, K. A., Li, H., & Cheang, P. (2003). Effect of spark plasma sintering on the microstructure and in vitro behavior of plasma sprayed HA coatings. *Biomaterials, 24*(16), 2695−2705.

Yugeswaran, S., Yoganand, C. P., Kobayashi, A., Paraskevopoulos, K. M., & Subramanian, B. (2012). Mechanical properties, electrochemical corrosion and in-vitro bioactivity of yttria stabilized zirconia reinforced hydroxyapatite coatings prepared by gas tunnel type plasma spraying. *Journal of the Mechanical Behavior of Biomedical Materials, 9*, 22−33.

Zamora, P.O., Chen, M., Osaki, S., Hsieh, T-T., & Tsang, R. (2007). *Medical device with plasma cross-linked hydrophilic coating*. BioSurface Engineering Technologies, Inc. US patent 7,217,769 B2, published May 15, 2007.

Zamora, P.O., Osaki, S., & Chen, M. (2003). *Plasma-deposited coatings, devices and methods*. BioSurface Engineering Technologies, Inc. US patent 6,613,432 B2, published September 2, 2003.

Zeng, R., Dietzel, W., Chen, J., Huang, W., & Wang, J. (2008). Corrosion behavior of TiO_2 coating on magnesium alloy AM60 in Hank's solution. *Key Engineering Materials, 373−374*, 609−612.

Zhang, F., Kang, E. T., Neoh, K. G., Wang, P., & Tan, K. L. (2001). Surface modification of stainless steel by grafting of poly(ethylene glycol) for reduction in protein adsorption. *Biomaterials, 22*(12), 1541−1548.

Zhao, J. H., Michalski, W. P., Williams, C., Li, L., Xu, H. S., Lamb, P. R., et al. (2011). Controlling cell growth on titanium by surface functionalization of heptylamine using a novel combined plasma polymerization mode. *Journal of Biomedical Materials Research—Part A, 97A*(2), 127−134.

Zhao, Y., Wong, S. M., Wong, H. M., Wu, S., Hu, T., Yeung, K. W. K., et al. (2013). Effects of carbon and nitrogen plasma immersion ion implantation on in vitro and in vivo biocompatibility of titanium alloy. *ACS Applied Materials and Interfaces, 5*(4), 1510−1516.

Zheng, X., Huang, M., & Ding, C. (2000). Bond strength of plasma-sprayed hydroxyapatite/Ti composite coatings. *Biomaterials, 21*(8), 841−849.

Zhou, L., Lv, G. H., Ji, C., & Yang, S. Z. (2012). Application of plasma polymerized siloxane films for the corrosion protection of titanium alloy. *Thin Solid Films, 520*(7), 2505−2509.

Zysset, P. K., Edward Guo, X., Edward Hoffler, C., Moore, K. E., & Goldstein, S. A. (1999). Elastic modulus and hardness of cortical and trabecular bone lamellae measured by nanoindentation in the human femur. *Journal of Biomechanics, 32*(10), 1005−1012.

Chemical surface modification of metallic biomaterials

5

J. Li, X. Liu
Shanghai Institute of Ceramics, Chinese Academy of Sciences, Shanghai, China

5.1 Introduction

Chemical modification of metallic biomaterials mainly depends on the chemical reactions occurring at the interface between biomaterials and reactive solutions, which is suitable for creating hierarchical topographies from the microscale to the nanoscale on the surfaces with large area and the devices with complex three-dimensional (3D) shape due to the non-line-of-sight nature. The common methods are hydrogen peroxide, acid, alkali, and thermal oxidation treatments. Due to the simplicity and flexibility, they are considered promising techniques for the surface modification of biomaterials, especially metallic biomaterials.

5.2 Chemical surface modification methods

5.2.1 Hydrogen peroxide treatment

Much attention has been paid to the corrosion behavior of titanium over hydrogen peroxide (H_2O_2), because it is important for harmless biomedical Ti-based implants and resistant pulp bleaching equipment (Tengvall et al., 1989b, 1989c). A titanium surface reacts with H_2O_2 to generate titania gels, which have been identified to be $Ti^{4+}(OH^-)_2O_2^{2-}$—$Ti^{4+}(OH^-)_2O_2^-$—$Ti^{4+}(OH)_x$—$TiO_2 \cdot nH_2O$ (Tengvall et al., 1989a) and can enhance the bioactivity of Ti-based implants by inducing the formation of apatite when soaked in simulated body fluid (SBF) (Li et al., 1994a, 2013, 1994b; Peltola et al., 1998). Metallic titanium foils underwent a hydrothermal treatment in the H_2O_2 solution at 80 °C from 6 to 72 h to produce nanostructured titania surfaces (Li et al., 2013). The color of the H_2O_2 solution changed to orange soon after the reaction for 6 h, caused by the dissolution of Ti (IV) ions into the solution (Figure 5.1(a)), and a nanopetal structure was formed on the titanium surface (Figure 5.1(b)). Increasing the reaction time to 24 h, the solution turned light orange (Figure 5.1(c)), and the nanopetal morphology maintained with a little expansion (Figure 5.1(d)). Prolonging the oxidation of titanium foil with H_2O_2 solution for 72 h, a homogeneous grey-white film was produced on the surface of titanium foil, during which white precipitations appeared in the solution (Figure 5.1(e)). The top layer was well-aligned nanorods (Figure 5.1(f)).

Surface Coating and Modification of Metallic Biomaterials. http://dx.doi.org/10.1016/B978-1-78242-303-4.00005-3
Copyright © 2015 Elsevier Ltd. All rights reserved.

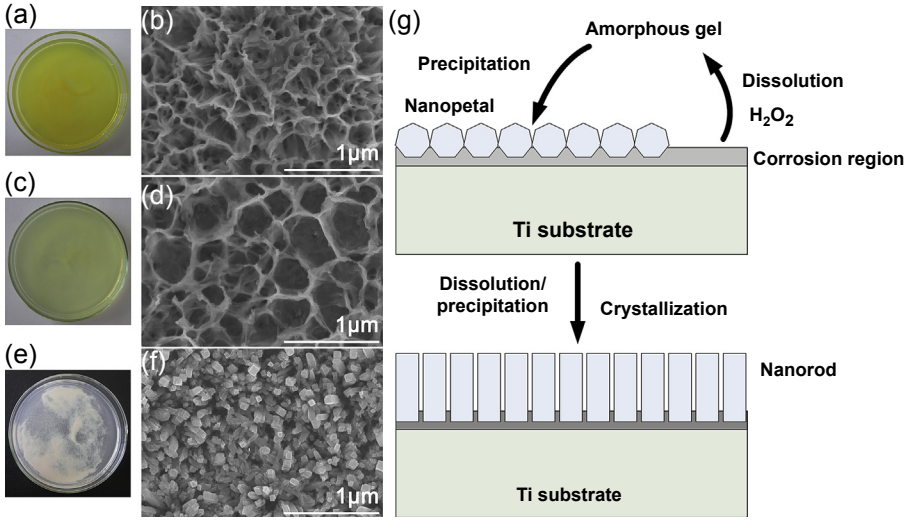


Figure 5.1 Typical photographs of the reaction solution and the corresponding SEM images obtained from the samples immersed in H_2O_2 solution for 6 h (a, b), 24 h (c, d), and 72 h (e, f), showing the structure development of titanium surface. (g) Depicts the schematic illustration of the structure development based on dissolution and precipitation mechanism.
Li et al. (2013). Reprinted with kind permission from Copyright © 2013 The Royal Society of Chemistry.

A dissolution and precipitation mechanism is proposed for the formation of the nanostructured titania films, as illustrated in Figure 5.1(g). These nanostructured titania surfaces were subsequently demonstrated to possess good bioactivity and bacteriostasis effect due to the negative surface potential that can induce apatite formation and inhibit bacterial adhesion. The nanopetal topography can regulate bone marrow mesenchymal stem cell differentiation toward osteoblasts. Furthermore, it is noted that the nanopetals with larger size led to better cell responses (including adhesion, proliferation, and differentiation) (Zhang et al., 2012a). Compared to the pristine surface, the titania nanorod film exhibited a significantly enhanced osteogenic activity (Zhang et al., 2013). Furthermore, it is proposed that the titania gel possessed a double-layer structure, consisting of an outer porous layer and an inner thin (<5 nm) but dense layer (Pan et al., 1996, 1998). The amorphous titania gel can be gradually transformed into the crystalline phase by undergoing heat treatment above 300 °C (Wang et al., 2002). In detail, the amorphous gel mainly crystallized to the anatase phase if the heat treatment was below 600 °C, while the rutile phase predominated above 700 °C, as shown in Figure 5.2(a). Meanwhile, it is observed that the amorphous gel that underwent a heat treatment between 400 and 500 °C had a sole anatase phase and possessed excellent bioactivity (Figure 5.2(b)). A higher treatment temperature will increase the content of the rutile phase in the titania layer and thus decrease the bioactivity.

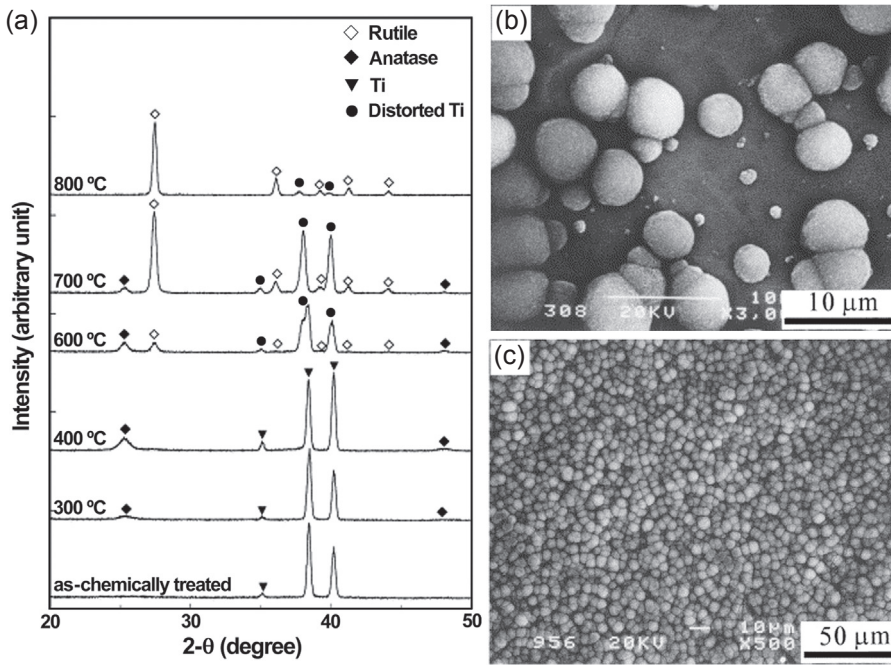


Figure 5.2 (a) XRD patterns of the samples treated with the H_2O_2/HCl solution at 80 °C for 0.5 h and subsequently heat treated at various temperatures for 1 h, indicating the transformation of crystal structure of the gels. (b, c) SEM images of apatite particles deposited on the titanium surfaces after it was soaked in SBF for 2 days (b) and 5 days (c). The titanium surfaces have been treated with the H_2O_2/HCl solution at 80 °C for 0.5 h and subsequently heat treated at 400 °C for 1 h.
Wang et al. (2002). Reprinted with kind permission from Copyright © 2002 Elsevier.

An amorphous titania gel layer can also be generated on the titanium surface through the chemical treatment in H_2O_2/$TaCl_5$ solution, and the amorphous titania can be subsequently transformed into the anatase phase by heat treatment between 300 and 600 °C, showing the bioactivity for apatite formation in SBF. It is interesting that the thicker titania gel layers possess a better bioactivity after soaking in SBF for 1 day when compared to those thinner ones. After soaking for 2 days, the samples' surfaces are nearly entirely covered with apatite (Wang et al., 2000).

After immersing the titanium foil in H_2O_2 solution, the metallic titanium reacts with H_2O_2 molecules to produce Ti−OH groups on the titanium surface, which act as the nucleation sites and play a crucial role in the apatite formation process (Kokubo et al., 2003). After soaking in SBF, Ti−OH groups interact with OH^- ions in SBF to form a negatively charged surface with the functional group Ti−O^- ions as follows (Liu et al., 2005):

$$\mathrm{Ti-OH} + \mathrm{OH^-} \rightarrow \mathrm{Ti-O^-} + \mathrm{H_2O} \tag{5.1}$$

The formation of a negatively charged surface contributes to the apatite nucleation and growth, which is due to the electrostatic attraction with the positively charged calcium ions (Li et al., 1994b). The arrival of calcium ions can increase the local supersaturation around the material surface in SBF. Once reaching the critical nucleation concentration of apatite, apatite will nucleate and grow spontaneously by assembling the remaining calcium, phosphate, and hydrogen carbonate ions around apatite nuclei in SBF and form bone-like apatite (Kokubo et al., 2003). The amount of Ti−OH groups increases with the prolonged reaction time and decreases after the heat treatment (Peltola et al., 1998). The measurement of zeta potential on the material surface is an effective characterization method to predict the bioactivity (Li et al., 2013).

5.2.2 Acid treatment

Acid treatment is often used to produce a clean and uniform surface state by eliminating the oxide layer and contamination. It is reported that nanoscale features are formed on a titanium surface by using titania grit blasting and subsequent HF treatment, which thus improve the osteoconductivity and the bone-specific messenger RNA expression (Guo et al., 2007). When immersing titanium disks in a 0.2 vol.% HF solution and carefully controlling the exposure time and the initial surface topography, the desired surfaces with higher roughness, lower cytotoxicity, and better biocompatibility can be achieved on polished titanium surfaces (Lamolle et al., 2009; Figure 5.3). It is believed that the HF treatment can result in the favorable growth conditions for cells due to the low hydrocarbon content, the existence of fluoride, hydride, and oxide, and the microtopography and nanotopography. When immersing titanium in HF solution, a series of chemical reactions will occur at the

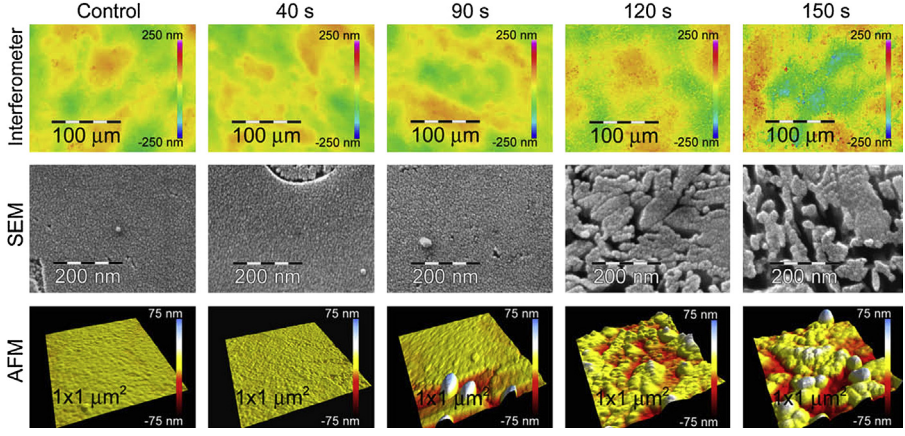


Figure 5.3 Blue light interferometer, SEM and AFM images of the modified titanium disks in 0.2 vol.% HF. Topographical changes at both micro- and nano-level in function of the immersion time with HF were observed, especially after 120 and 150 s.
Lamolle et al. (2009). Reprinted with kind permission from Copyright © 2009 Elsevier.

titanium/solution interface, and the unique F-doped flower-like titania nanostructure will be directly grown on the titanium surface (Wu et al., 2008). By controlling the hydrothermal parameters, the observed results show that the growth of F-doped titania nanoflower involves several steps. First, the metallic titanium reacts with HF under the hydrothermal condition, which produces H_2TiF_6 as follows:

$$Ti + 6HF \rightarrow H_2TiF_6 + 2H_2\uparrow \tag{5.2}$$

As reaction (5.2) continues, more H_2TiF_6 is produced. Subsequently, H_2TiF_6 combines with H_2O, which produces $Ti(OH)_4$:

$$H_2TiF_6 + 4H_2O \rightarrow Ti(OH)_4 + 6HF \tag{5.3}$$

The as-produced $Ti(OH)_4$ slowly decomposes into TiO_2, gradually nucleates, and grows into TiO_2 nanoparticles under the hydrothermal conditions:

$$Ti(OH)_4 \rightarrow TiO_2 + 2H_2O \tag{5.4}$$

It is known that HF is a strong corrosive chemical. The as-produced TiO_2 can also be etched by HF as reaction (5.5):

$$TiO_2 + 6HF \rightarrow H_2TiF_6 + 2H_2O \tag{5.5}$$

At the same time, the as-produced H_2TiF_6 species diffuses to the surface of the titania and new titania is produced and aggregated on the former surface of titania nanoparticles (Macak et al., 2005). The above processes of the dissolution and deposition repeat continuously, which eventually leads to the generation of the F-doped flower-like TiO_2 nanostructure on the titanium surface, as shown in Figure 5.4. In the hydrothermal process, HF not only etches the metallic titanium, which provides a titanium source for the production of titania nanostructure, but also acts as the source of F-dopant.

Hydrochloric acid (HCl) was shown to act as an excellent decontamination agent to a titanium surface because it can readily dissolve titanium salts when compared to $Na_2S_2O_8$ and H_2SO_4 (Takeuchi et al., 2003). A general acid vapor oxidation strategy has been developed to fabricate highly oriented hierarchically nanostructured rutile titania arrays with controllable topographies on metallic titanium (Yang et al., 2009b). By optimizing the initial concentration of HCl, titania array films with different rutile nanostructures (including nanotrees, dendritic nanobundles, and nanorods) can be selectively acquired. The corresponding growth mechanism was investigated by using a time-dependent procedure. On the basis of the observed experimental results, the following growth mechanism of the dendritic rutile titania nanotrees is proposed (Figure 5.5).

In the first step, rutile titania nanorods nucleate and grow vertically along their c-direction on metallic titanium through a direct oxidation in HCl vapor (Figure 5.5(e)). The initial rutile titania nanorods absorb titanium atoms directly

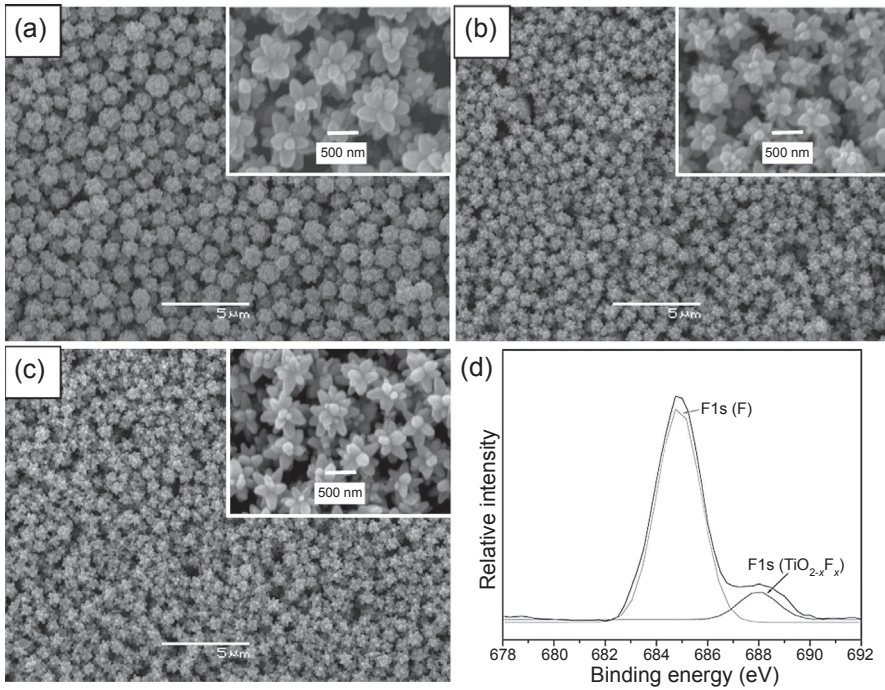


Figure 5.4 SEM images of the samples prepared at 100 °C for 5 h using different concentrations of HF: (a) 1 mM, (b) 5 mM, and (c) 20 mM. (D) F 1 s high-resolution XPS spectrum of the F-doped flower-like TiO_2 nanostructures prepared using the hydrothermal method at 150 °C in 1 mM HF for 5 h. The insets show the corresponding high-magnification images.
Wu et al. (2008b). Reprinted with kind permission from Copyright © 2008 American Chemical Society.

from the substrate and oxygen atoms from the vapor with the help of HCl. It is well-known that metallic titanium can react with hot HCl to produce hydrated Ti^{3+} ions and hydrogen. The further oxidation and instant hydration in hot vapor can produce hydrated titania on the titanium, which can be used for the nucleation of rutile seeds and the growth of rutile nanorods. During the early growth stage, the longitudinal growth along ⟨001⟩ direction predominates, whereas at a later stage, the radial growth along [110] and/or [100] directions becomes more dominant, and the trunk tends to be thicker (Peng and Peng, 2001; Yang et al., 2006). This type of growth behavior may account for the formation of titania nanobundles that consist of the nanowires with orientated attachment of (110) side facets. Meanwhile, the growth of rutile titania nanobundles is highly promoted by using a higher concentration of HCl vapor. Here, the HCl vapor acts as both a catalyst and a chemical corrosive agent, which can promote the formation of rutile phase and introduce defects onto the nanorod surface, respectively. As a result, the rough surfaces are induced as the trunk shell, and the bundled nanowires are produced as the trunk core. In the following step, the (101)

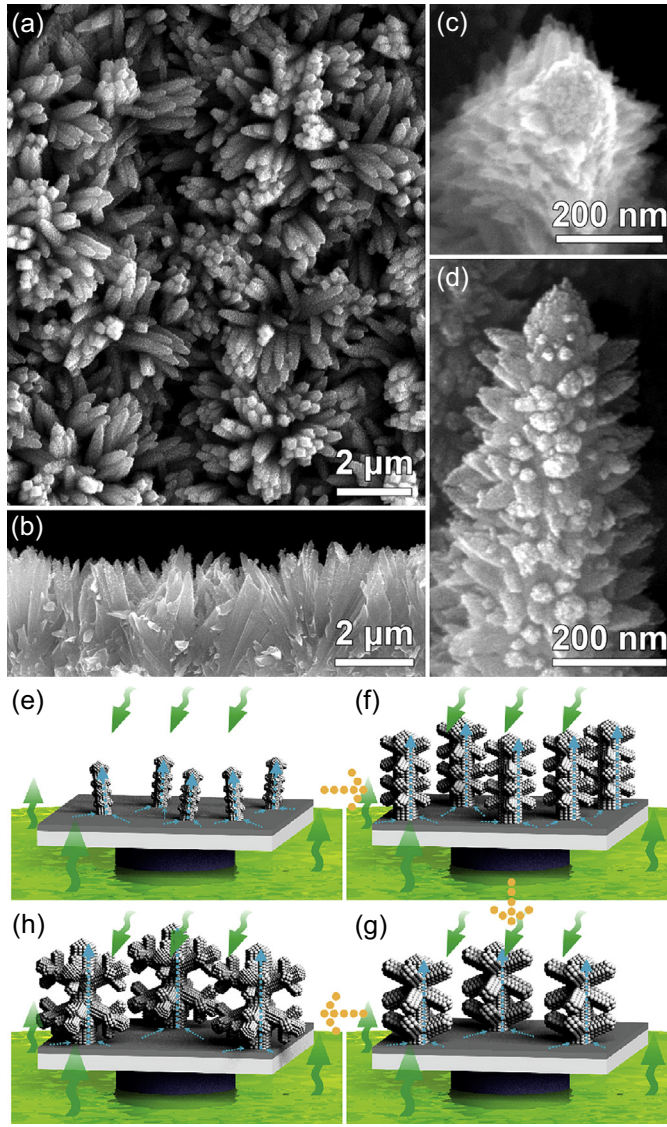


Figure 5.5 (Left panel) SEM images of branched nanotrees grown from and rooted on titanium sputtered substrate: (a, b) top and side view of a nanotree "forest"; and (c, d) a typical individual nanotree. (Right panel) Schematic illustration of the growth process: (e) no densely distributed rod-like trunks grow from the titanium, and the side surfaces are eroded; (f) obvious branches appear, and the trunk tends to be more orientated due to space limitation; (g) both branches and trunks tend to be larger in dimension because of "Ostwald ripening"; (h) ternary growth of the branches.
Yang et al. (2009b). Reprinted with kind permission from Copyright © 2009 American Chemical Society.

twin structures come out from the nucleation and growth of the side branches (Figure 5.5(f)), responding to the surface defects induced by the corrosion of the trunk surfaces with the HCl vapor. Thirdly, with prolonging the aging time, some branches continue to grow while lots of smaller branches begin to disappear, possibly due to "Ostwald ripening" (Figure 5.5(g)). Furthermore, the HCl vapor continually plays an important role in the growth of one-dimensional rutile titania nanostructures and their side branches. Along with the growth of the second branches and the chemical corrosion of HCl vapor on the branches' sides, tertiary branches can be produced on the larger nanobranches that initially grow at the previously eroded sites (Figure 5.5(h)).

A mixed acid is also used to pretreat titanium (Nanci et al., 1998; Schwartz et al., 1996). The mixed acid consisting of 10−30 vol.% of HNO_3 and 1−3 vol.% of HF in deionized water is proposed as a standard solution for acid pretreatment, in which HF molecules can react with metallic titanium to generate the soluble titanium fluorides and hydrogen. In general, acid etching produces a thin oxide layer on the substrate surface (<10 nm).

A combination of acid and H_2O_2 has also received much attention for the surface modification of titanium and its alloys. The mixed acid of pure H_2SO_4 and 30 wt% H_2O_2 with a volume ratio of 1:1 was adopted to manipulate the surface microstructure and nanostructure of the polished Ti−6Al−4V alloy by optimizing the etching parameters (Variola et al., 2008). These optimized surfaces can facilitate the growth of osteoblastic cells, but limit the growth of fibroblastic cells, showing the selectivity on cells. An in vivo study further demonstrated that the titanium implant treated with H_2SO_4/H_2O_2 can significantly enhance the contact osteogenesis when using a dog model, as shown in Figure 5.6 (Tavares et al., 2007). The combination of HCl/H_2O_2 and heat treatments has also attracted numerous interests for the surface modification of titanium and its alloys (He et al., 2009; Shi et al., 2009; Yang et al., 2009a; Zhang et al., 2012b). The integration between Ti−6Al−4V implants and bones was better facilitated by the HCl/H_2O_2 and heat treatments to form a bioactive surface for the protein adsorption, ion enrichment, and cell growth (Shi et al., 2009). The scanning electron microscopy (SEM) morphology of the two samples is shown in Figure 5.7. MC3T3-E1 cells were cultured and examined on these samples after 4, 7, and 14 days. The upregulated gene expressions of ALP, OCN, Col-I, etc. were observed in the test group, showing the significantly enhanced osteoblastic activity than the control group.

5.2.3 Alkali treatment

Alkali and heat treatment strategy was first introduced by Kim et al. (1996) to enhance the bioactivity of titanium and its alloys, which can also induce the deposition of a bioactive bone-like apatite layer on the surfaces of bioactive ceramics, such as Bioglass® (Hench and Andersson, 1993), hydroxyapatite (LeGeros and LeGeros, 1993), and glass−ceramic A/W (Kokubo et al., 1990). As a typical example, the alkali and heat treatment procedures can be described as follows (Kim et al., 1996; Lee et al., 2002). The samples are first immersed in a 5−10 M

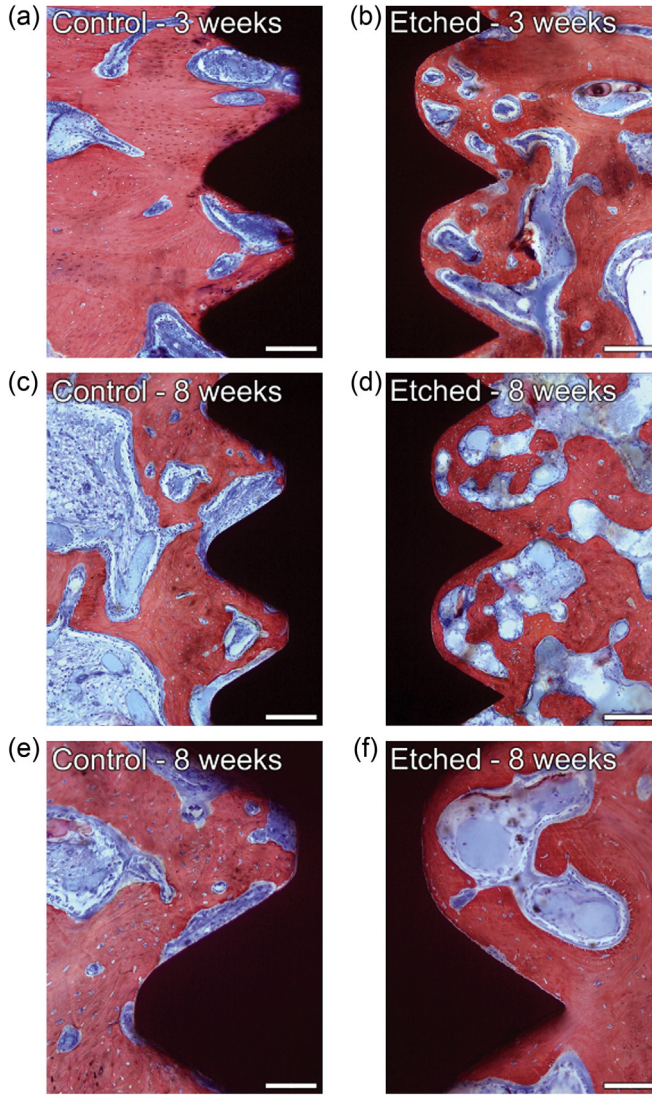


Figure 5.6 Mesiodistal ground sections of control (a, c, e) and etched (b, d, f) titanium implants and the surrounding connective tissues at 3 (a, b) and 8 (c, d, e, f) weeks postimplantation. At 3 and 8 weeks, lamellar bone trabecullae and woven bone were observed adjacent to the control surfaces (a, c, e), whereas a continuous, thin layer of newly formed bone was observed in direct contact with the etched surfaces (b, d, f). Such woven bone formation was connected to trabecullae of parent, lamellar bone. Alizarin red and Stevenel's blue. Scale bars a, b, c, d = 200 μm; e, f = 100 μm.
Tavares et al. (2007). Reprinted with kind permission from Copyright © 2007 Wiley-VCH Verlag GmbH&Co. KGaA.

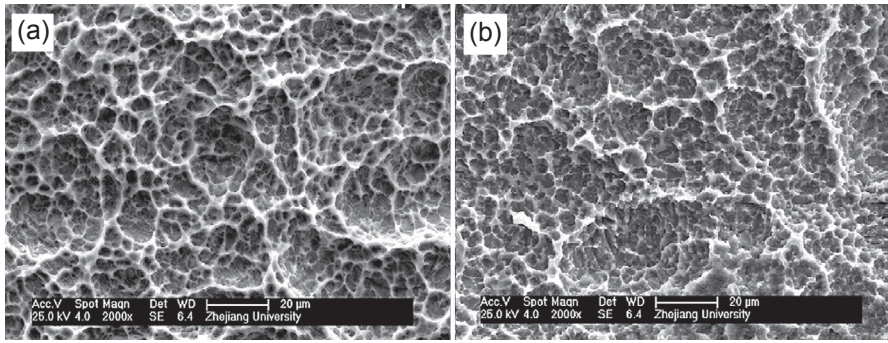


Figure 5.7 SEM images of two different Ti alloy surfaces. (a) Sandblasted, dual acid-etched and HCl/H_2O_2 heat-treated Ti-6Al-4V disc (test group) has an irregular surface with porous network structure; (b) Sandblasted, dual acid-etched treated Ti-6Al-4V disc (control group) has a similar surface; however, the micropits and indentations in this surface seem a little smaller compared with those in the test surface.
Shi et al. (2009). Reprinted with kind permission from Copyright © 2009 Elsevier.

NaOH or KOH solution for 24 h, followed by rinsing with deionized water and ultrasonic cleaning for 5 min. The samples are then dried in an oven at 40 °C for 24 h and finally heated to around 600−800 °C for 1 h. The heat treatment is performed at a pressure of 10^{-4}−10^{-5} Torr due to the strong tendency of metallic titanium to oxidize. After the treatment, a nanoporous film can be produced on the titanium surface (Figure 5.8; Nishiguchi et al., 1999). The thin film XRD (TF-XRD) patterns obtained from the treated titanium surface demonstrate the generation of sodium titanate hydrogel on the titanium surface. A larger amount of sodium titanate and anatase and rutile titania phases crystallize after the heat treatment at 800 °C for 1 h (Figure 5.9; Kim et al., 1996).

Various TiO_2-based nanostructures, including nanoplate, nanowire, nanoflower, nanoneedle, continuous nanowire network films, etc., are hydrothermally formed on a large scale directly on metallic titanium substrate or scaffold in the alkali solutions (Divya Rani et al., 2009; Dong et al., 2007, 2006; Peng and Chen, 2006). The growth mechanism of the novel nanostructures on metallic titanium can be understood by the simultaneous processes of dissolution and reprecipitation reactions (Divya Rani et al., 2009). At a low concentration of aqueous alkali, the two reactions of dissolution and reprecipitation processes can be expressed as follows:

$$\mathrm{Ti} + 4\mathrm{H_2O} \rightarrow \mathrm{Ti(OH)_3^+} + \mathrm{OH^-} + 2\mathrm{H_2} \quad \text{(Dissolution)} \tag{5.6}$$

$$\mathrm{Ti(OH)_3^+} + \mathrm{OH^-} \rightarrow \mathrm{TiO_2} + 2\mathrm{H_2O} \quad \text{(Precipitation)} \tag{5.7}$$

Therefore, at a low concentration of NaOH solution, it is possible that titania can be directly grown on the surface of metallic titanium by hydrothermal reaction without any change in the pH value (as indicated by reactions (5.6) and (5.7)).

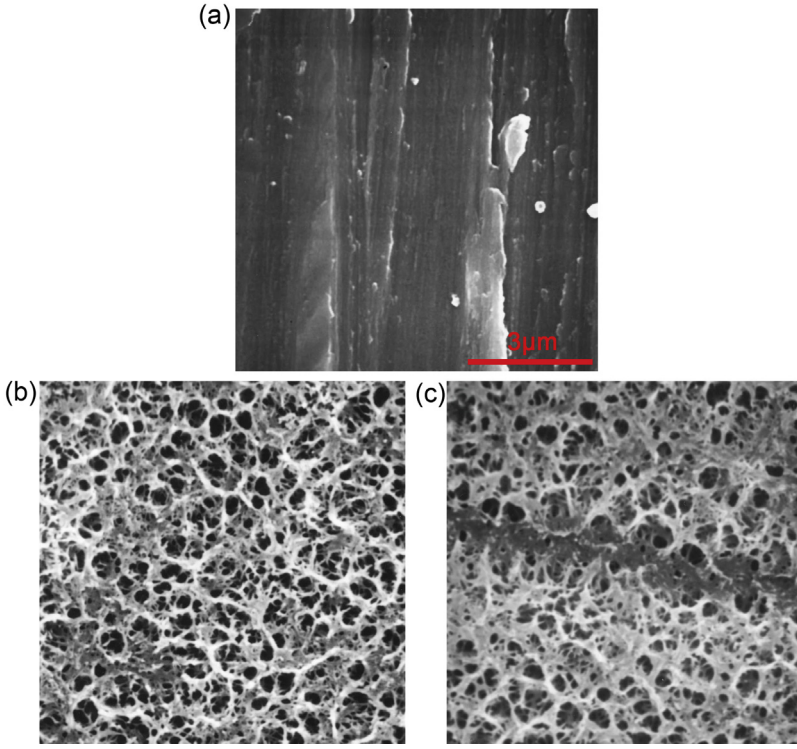


Figure 5.8 SEM images of titanium surfaces. (a) Control titanium with smooth surface. (b) Alkali-treated titanium has a fine trabecular surface. (c) Alkali- and heat-treated titanium. The surface appears to be somewhat densified compared with alkali-treated one. Nishiguchi et al. (1999). Reprinted with kind permission from Copyright © 1999 Elsevier.

However, at a high concentration of aqueous alkali, the general dissolution of titanium species and the reprecipitation of sodium titanate come out. The general dissolution reaction of metallic titanium in aqueous alkali to produce a polytitanate anion can be expressed as:

$$n\mathrm{Ti} + 2n\mathrm{H}^{+} + (2n+m)\mathrm{OH}^{-} \rightarrow [\mathrm{Ti}_n\mathrm{O}_{2n+m}]^{(2m)-} + \left(\frac{4n+m}{2}\right)\mathrm{H}_2 \tag{5.8}$$

The as-produced polytitanate anions in the dissolution step can react with Na^+ cations in NaOH aqueous solution to generate sodium polytitanate (Chi et al., 2007; Wang et al., 2008; Yada et al., 2007). Similarly, the general precipitation reaction of sodium polytitanate can be expressed as:

$$2m\mathrm{Na}^{+} + [\mathrm{Ti}_n\mathrm{O}_{2n+m}]^{(2m)-} \rightarrow \mathrm{Na}_{2m}\mathrm{Ti}_n\mathrm{O}_{2n+m} \tag{5.9}$$

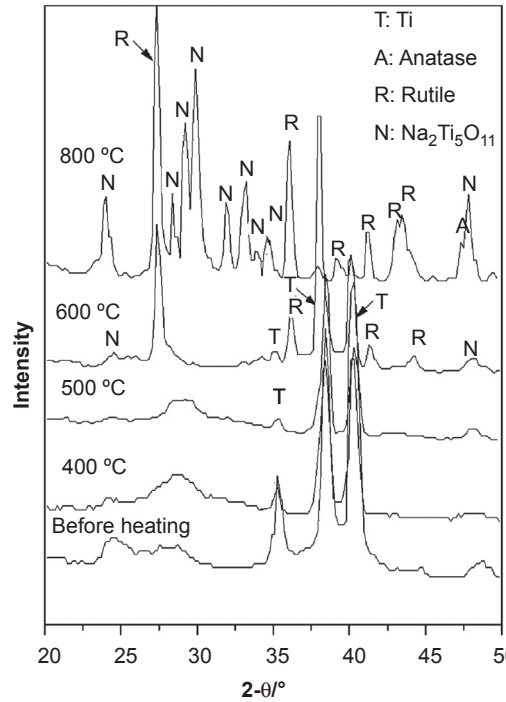


Figure 5.9 TF-XRD patterns of the titanium surface soaked in 10 M NaOH at 60 °C for 24 h then heated at various temperatures for 1 h.
Kim et al. (1996). Reprinted with kind permission from Copyright © 1996 Wiley-VCH Verlag GmbH&Co. KGaA.

The morphology development of the nanostructures formed on the titanium surface by using the hydrothermal method can be well understood in a self-consistent manner based on the kinetics of the dissolution and reprecipitation procedures shown above in the reactions. When the dissolution rate is higher than the precipitation rate, the titanium surface has a tendency to be porous in nature. When the precipitation rate is relatively low, the growth of the nanostructures will be more uniform in all directions. On the contrary, when the precipitation rate is larger than the dissolution rate, the growth will become anisotropic, which can produce some oriented nanostructures.

It has been demonstrated that the chemical treatment of titanium and its alloys in alkali solution is an effective way to obtain bioactivity for the biomedical applications (Kim et al., 1997, 2013; Kokubo et al., 1996; Yamaguchi et al., 2013). A bioactive film that can enrich Ca^{2+} ions and release Mg^{2+} ions was produced on the surface of metallic titanium by alkali and heat treatments, which can induce the deposition of bone-like apatite on the surface within 7 days in SBF, as shown in Figure 5.10 (Yamaguchi et al., 2013).

To figure out the mechanism of the apatite deposition induced by alkali treatment, the zeta potential of the sodium titanate surface was measured by laser electrophoresis at various SBF soaking times (Nakamura et al., 2001). The obtained results showed that the surface of the sodium titanate layer was highly negatively charged once it

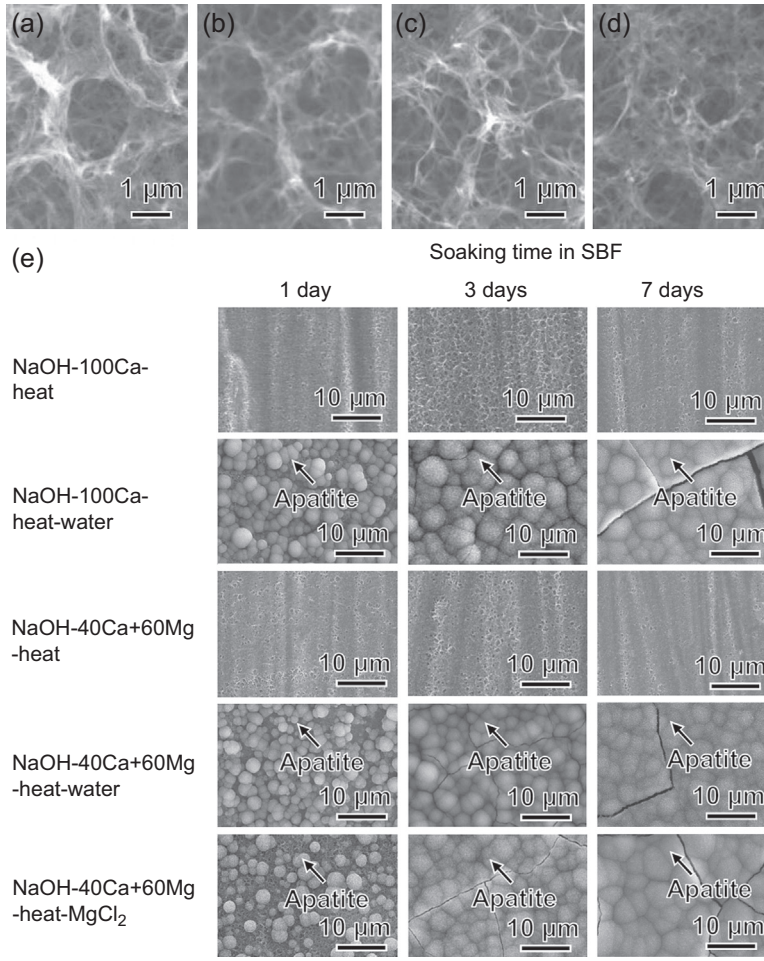


Figure 5.10 FE-SEM photographs of Ti surfaces subjected to (a) 40Ca + 60Mg, (b) subsequent heat, and finally (c) water or (d) $MgCl_2$ treatments following the NaOH treatment. (e) FE-SEM photographs of the Ti surfaces soaked in SBF for different days after heat and subsequent water treatments following NaOH and 100Ca treatments, and after heat and subsequent water or $MgCl_2$ treatments following NaOH and 40Ca + 60 Mg treatments. Yamaguchi et al. (2013). Reprinted with kind permission from Copyright © 2013 The Royal Society of Chemistry.

had been immersed in the SBF, as shown in Figure 5.11. Along with the immersion time increasing, the surface zeta potential would increase up to a maximum positive value. After that, the surface potential would decrease to a negative value again and finally arrive at a constant negative value. On the basis of this observation, the mechanism behind the apatite formation process can be well understood from the viewpoint of the electrostatic interaction between the functional groups on the surface and the

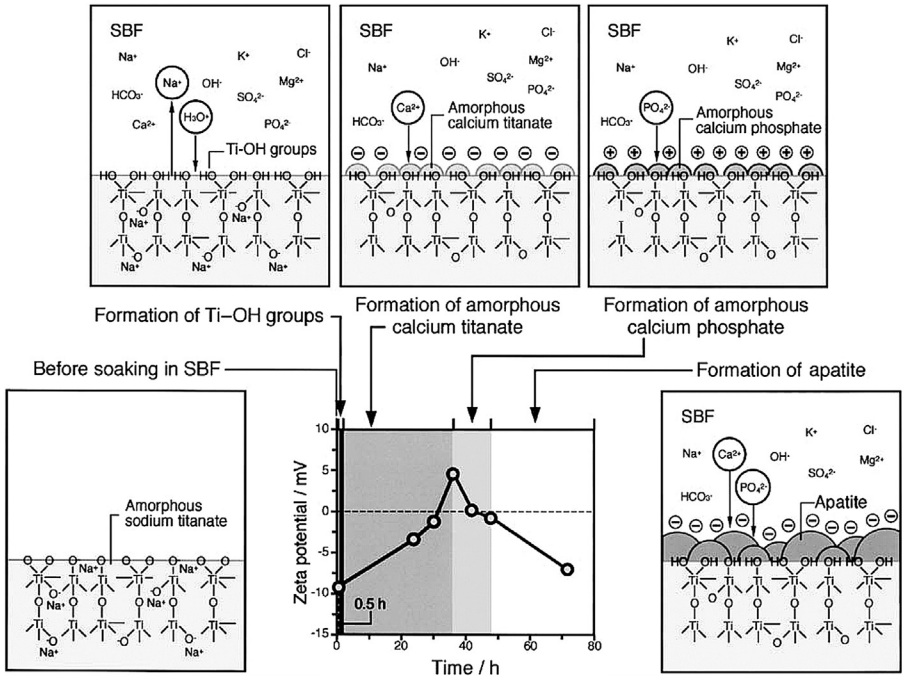


Figure 5.11 Schematic showing the relationship between the changes in surface structure and the potential of amorphous sodium titanate in the apatite formation process on its surface in SBF. Kokubo et al. (2003). Reprinted with kind permission from Copyright © 2003 Elsevier.

ions in the SBF. In detail, when the sodium titanate is immersed in SBF, the Ti−OH groups are produced on the surface, and they are, as indicated in reaction (5.1). As a result, the negatively charged groups can selectively combine with the positively charged Ca^{2+} ions in the SBF to produce calcium titanate, as shown in Figure 5.11 (Kokubo et al., 2003). Along with the accumulation of Ca^{2+} ions on the surface, the surface will gradually obtain an overall positive charge. As a consequence, the positively charged surface combines with the negatively charged phosphate ions to produce the amorphous calcium phosphate. This calcium phosphate can spontaneously transform into the apatite due to the fact that the apatite is the stable phase in the body environment (Tung, 1998). A similar mechanism of electrostatic interaction for apatite deposition is proposed to suit for other functional groups that are effective for apatite nucleation, such as Zr−OH, Ta−OH, Nb−OH, Si−OH, etc., due to the fact that all these functional groups have a zero isoelectric point at the pH value that is much lower than seven. Therefore, these functional groups should be negatively charged in the living body (Kitahara et al., 1997).

It has been reported that large-area nanostructured bioactive titanates can be directly grown on 3D microporous Ti-based metal scaffolds by soaking the scaffolds in a 10-M NaOH aqueous solution at 60 °C (Figure 5.12; Wu et al., 2008a). The nanostructured titanates exhibit the characteristics of one-dimensional nanobelts/nanowires

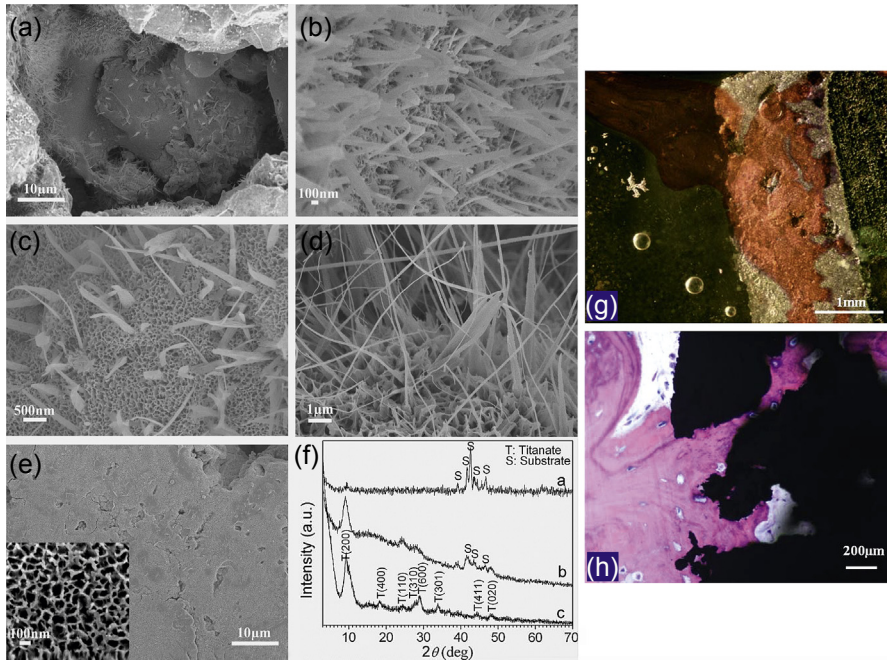


Figure 5.12 (a–f) Morphologies of hydrothermally treated 3D porous NiTi scaffold. (a) Typical surface morphology of exposed internal pore after treatment at 60 °C for 240 h. (b) Morphology of the wall of the exposed pore in (a). (c) Morphology of the bottom of the pore in (a). (d) General growth condition of nanowires/nanobelts on the exposed surface after treatment at 60 °C for 240 h. (e) Hydrothermal reaction at 60 °C for 96 h producing a continuous nanoskeleton. (f) XRD patterns for porous NiTi scaffold: trace a, the untreated; trace b, hydrothermal treatment at 60 °C for 240 h; trace c, hydrothermal treatment at 180 °C for 72 h. The histological analysis of bone tissues on the 3D porous NiTi scaffold. (g) The bone tissue can grow well almost on the entire surface (red color indicating bone tissues). (h) The bone tissues can also grow into the exposed internal pores (black indicating porous NiTi scaffold, and pink indicating bone tissues).
Wu et al. (2008a). Reprinted with kind permission from Copyright © 2008 American Chemical Society.

on a nanoskeleton layer. Interestingly, the as-prepared titanate nanostructure on the exposed surface resembles the lowest level of the hierarchical organization of collagen and hydroxyapatite. In addition, the resultant nanostructure is also similar to the cancellous bone structure at the microscale/macroscale. Furthermore, this chemically modified surface possesses superhydrophilicity and can accelerate apatite deposition and cell attachment and proliferation.

Alkali- and heat-treated titanium surfaces can directly bond to bones, but the only alkali-treated titanium surfaces cannot. To achieve the bone-bonding ability, both the alkali and heat treatments are essential (Nishiguchi et al., 1999). The detaching failure loads of the untreated, alkali-treated, and alkali- and heat-treated titanium groups after

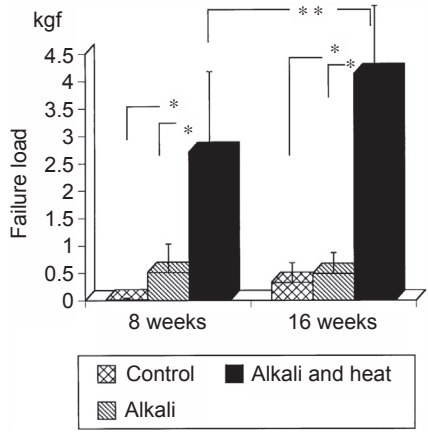


Figure 5.13 Results of detaching test. Failure loads (mean ± standard deviation). Control: control group. Alkali: alkali-treated group. Alkali and heat: alkali- and heat-treated group. (*): $P < 0.001$ (**): $P < 0.05$.
Nishiguchi et al. (1999). Reprinted with kind permission from Copyright © 1999 Elsevier.

the implantation of 8−16 weeks are summarized in Figure 5.13 (Nishiguchi et al., 1999). After 8 weeks, the failure load of the alkali- and heat-treated titanium group was 2.71 ± 1.47 kgf, which is significantly higher than those of the alkali-treated titanium group and the control titanium group with 0.51 ± 0.52 and 0.02 ± 0.03 kgf, respectively. After 16 weeks, the alkali- and heat-treated titanium group had a failure load of 5.13 ± 1.25 kgf, which is significantly higher than that of the same group at 8 weeks and those of the alkali-treated and the control titanium groups at 16 weeks. The failure loads of the alkali-treated and control titanium groups do not increase over the 8-week loads, which are 0.49 ± 0.38 and 0.33 ± 0.36 kgf, respectively. The alkali- and heat-treated titanium is considered to bond to bones through the apatite deposited on the surface (Kim et al., 1996).

Fujibayashi et al. (2001) investigated the effect of sodium elimination on the bone-bonding property of bioactive titanium modified by alkali and heat treatments. Sodium-free bioactive titanium plates were fabricated by soaking in a 5 M NaOH aqueous solution at 60 °C for 24 h, followed by soaking in deionized water at 40 °C for 48 h before heating at 600 °C for 1 h. The in vivo bioactivity was evaluated mechanically and histologically after 4, 8, 16, and 24 weeks. The procedure of sodium elimination showed an enhancement effect on the bone-bonding strength of the bioactive titanium at 4 and 8 weeks postoperatively. Nevertheless, the bone-bonding strength was lower than that of the conventional alkali- and heat-treated titanium at 16 and 24 weeks. Histological examinations after the detaching test indicated the breakage of the modified layer in the sodium-free alkali- and heat-treated titanium group. In conclusion, the sodium elimination can accelerate the in vivo bioactivity of the bioactive titanium and result in a faster bone bonding due to the anatase structure on the surface, but the damage of the surface-graded structure caused by the complete

elimination of sodium will decrease the adhesive strength of the modified layer to the titanium substrate.

Since Kim et al. first introduced the alkali and heat treatments to improve the bioactivity of biomedical titanium and its alloys, many researchers have paid numerous attentions to optimizing this treatment process for better biomedical applications. Lee et al. (Lee et al., 2002) investigated the bioactivity and the surface changes on chemically modified Ti−In−Nb−Ta and Ti−6Al−4V ELI alloys by in vitro tests in SBF. Porous network films of sodium titanate ($Na_2Ti_5O_{11}$ or $Na_2Ti_6O_{13}$) were successfully grown on the surface of titanium alloys by using alkali and heat treatments. The pore size of the inner network structure in the Ti−In−Nb−Ta alloy was lower than that of the Ti−6Al−4V ELI alloy, while the thickness of the sodium titanate film on the Ti−In−Nb−Ta alloy was half that of the Ti−6Al−4V ELI alloy. As a result, the Ti−In−Nb−Ta alloy possesses an enhanced corrosion resistance to alkalis. In addition to Ti and its alloys, direct chemical treatments have also been adopted to modify other metallic biomedical materials. Miyazaki et al. (2000) have confirmed that the apatite formation can be induced on the surface of metallic tantalum in SBF after a short period of immersion by using a pretreatment method in diluted NaOH aqueous solution to produce an amorphous sodium tantalate hydrogel layer on the tantalum surface, which points out the practicability of acquiring the bioactive Ta-based metals for biomedical applications through simple chemical treatments. The mechanism lies behind; that is, the structural changes of tantalum surfaces during the chemical treatment result in the generation of a bioactive tantalate layer that contains alkali ions, which can accelerate the spontaneous nucleation of bone-like apatite layer on the surface of metallic tantalum in SBF (Miyazaki et al., 2002). Uchida et al. (2002) also demonstrated the practicability of acquiring the bioactive metallic zirconium after the alkali treatment with NaOH aqueous solution. The metallic zirconium pretreated in NaOH solution with a concentration of above 5 M can induce a layer of apatite depositing on the surface after soaking in SBF. The nucleation of apatite is induced by the Zr−OH groups within the zirconia hydrogel layer on the metallic zirconium surface produced by the NaOH pretreatment.

Been systematically investigated the corrosion behaviors of grade 2 titanium in alkaline hydrogen peroxide environments by using weight loss corrosion tests, electrochemical impedance spectroscopy, linear polarization resistance measurements, and potentiodynamic polarography (Been, 1998). Nowadays, a mixed solution of NaOH and H_2O_2 is often used to chemically modify the metallic titanium and its alloys. When immersing a titanium substrate in the mixed solution of H_2O_2 and NaOH, the hydroperoxyl ions (OOH^-) resulting from the ionization of H_2O_2 molecules as reaction (5.10) act as active oxidants to oxidize the metallic titanium, followed by the formation of titanium peroxy gel ($Ti(IV)O_2^{2+}$) as reaction (5.11) (Tengvall et al., 1989a):

$$H_2O_2 \rightarrow OOH^- + H^+ \tag{5.10}$$

$$Ti + 2OOH^- \rightarrow Ti(IV)O_2^{2+} + 2OH^- + 2e^- \tag{5.11}$$

In an alkaline environment, both reactions (5.10) and (5.11) can be accelerated, and the titanate ions ($HTiO_3^-$) are produced as reaction (5.12) (Been, 1998; Been and Tromans, 2000):

$$\mathrm{Ti(IV)O_2^{2+} + OOH^- + 2OH^- \rightarrow HTiO_3^- + H_2O + O_2\uparrow} \tag{5.12}$$

When mixing NaOH and H_2O_2 in a Teflon-lined pressure vessel at room temperature, numerous bubbles can be observed in the mixed solution, which indicates the production of O_2 gas from reaction (5.12).

Taking $Na_2Ti_4O_9$ as an example, the as-produced $HTiO_3^-$ ions subsequently combine with Na^+ ions in the solution to form $Na_2Ti_4O_9$ as follows:

$$\mathrm{2Na^+ + 4HTiO_3^- \rightarrow Na_2Ti_4O_9 + H_2O + 2OH^-} \tag{5.13}$$

A delivery platform for bioactive ions, such as Sr^{2+}, Mg^{2+}, Ca^{2+}, Zn^{2+}, etc., is successfully fabricated on the surface of metallic titanium by using a mixed treatment of NaOH and H_2O_2 under a hydrothermal condition, followed by a simple ion exchange process (Li et al., 2014b). The chemically modified surfaces can sustainedly release the bioactive ions at a slow rate during a period. An in vitro SBF test demonstrated that the modified titanium surfaces have good bioactivity along with the controlled release. Furthermore, it is confirmed that the modified surfaces also possess good biocompatibility and osteogenic activity.

5.2.4 Thermal oxidation

Kuznetsov et al. (2012) reported on the direct growth of rutile titania ceramic layers on titanium substrate by a simple calcination in an air atmosphere. Heat treatments of nitinol in air, argon, and partially reduced atmosphere have been much explored for surface oxidation to prevent the Ni ions' release and to promote the bioactivity and biocompatibility in the biological environment (Barison et al., 2004; Firstov et al., 2002; Gu et al., 2005; Michiardi et al., 2006, 2007; Plant et al., 2005; Shabalovskaya et al., 2003).

The biocompatibility of nitinol shape memory alloys has shown promising applications in self-expandable cardiovascular stents, stone extraction baskets, catheter guidewires, and other invasive and minimally invasive biomedical devices. A thin passive layer of titania can be spontaneously grown on the surface of the NiTi intermetallic alloy, which provides its biocompatibility. This oxide layer is considered to stem from the reaction between titanium atoms in the alloy surface and oxygen atoms in the environment, which leads to a depletion of titanium atoms in the subsurface region. And experimental evidence indicates the generation of a Ni-rich layer below the oxide film. Nolan et al. (Nolan and Tofail, 2010) have investigated the initial stages of oxide growth on the (110) surface of NiTi alloy to understand the generation of alloy/oxide interface by using the method of density functional theory simulation. Atomic and molecular oxygen are initially adsorbed on the (110) surface, followed

by the addition of O_2 molecules, up to two monolayers. Oxygen adsorption always leads to a large energy gain. With the help of the atomic oxygen, titanium atoms can be pulled out of the surface layer, which leaves behind a Ni-rich subsurface region. On the other hand, the molecular O_2 adsorbs dissociatively and pulls a titanium atom far out of the surface layer. The addition of more O_2 molecules up to one monolayer is also dissociative and leads to the complete elimination of titanium atoms from the initial surface layer. When further adding O_2 molecules up to two monolayers, the titanium atoms can be pulled farther out of the surface, resulting in the formation of a single thin layer of titania. The electronic structure shows that the NiTi alloy maintains the metallic character, which is consistent with the oxide layer being a passivant.

5.3 Challenges and future trends

Today, a sole surface modification method cannot meet all the clinical requirements, such as inhibiting bacterial infections, enhancing osseointegration, etc. (Goodman et al., 2013; Neoh et al., 2012). To achieve the multifunctional purposes and meet the clinical applications, there is a tendency to combine various modification methods together to functionalize the surface of metallic biomaterials. Many researchers have made positive attempts, as listed in Table 5.1.

Table 5.1 Combined treatment methods for surface modification in previous works

Combined treatments	References
Acid treatment + alkali treatment	Jonášová et al. (2004), Wen et al. (1997), and Wen et al. (1998)
Anodic oxidation + alkali treatment	Xin et al. (2009) and Zhao et al. (2013)
Micro-arc oxidation + alkali treatment	Gao et al. (2014)
Plasma spraying + alkali treatment	Nishiguchi et al. (2001), Lee et al. (2004), and Xue et al. (2005)
H_2O_2 treatment + PIII	Zheng et al. (2012) and Li et al. (2014a)
Alkali treatment + PIII&D	Li et al. (2011)

Note: PIII&D, Plasma immersion ion implantation and deposition.

References

Barison, S., Cattarin, S., Daolio, S., Musiani, M., & Tuissi, A. (2004). Characterisation of surface oxidation of nickel−titanium alloy by ion-beam and electrochemical techniques. *Electrochimica Acta, 50*, 11−18. http://dx.doi.org/10.1016/j.electacta.2004.07.007.

Been, J. (1998). *Titanium corrosion in alkaline hydrogen peroxide environments*. Doctor of Philosophy—PhD. University of British Columbia https://circle.ubc.ca/handle/2429/9456?show=full.

Been, J., & Tromans, D. (2000). Titanium corrosion in alkaline hydrogen peroxide. *Corrosion, 56*, 809—818. http://dx.doi.org/10.5006/1.3280584.

Chi, B., Victorio, E. S., & Jin, T. (2007). Synthesis of TiO_2-based nanotube on Ti substrate by hydrothermal treatment. *Journal of Nanoscience and Nanotechnology, 7*, 668—672. http://dx.doi.org/10.1166/jnn.2007.147.

Divya Rani, V. V., Manzoor, K., Menon, D., Selvamurugan, N., & Nair, S. V. (2009). The design of novel nanostructures on titanium by solution chemistry for an improved osteoblast response. *Nanotechnology, 20*, 195101. http://dx.doi.org/10.1088/0957-4484/20/19/195101.

Dong, W., Zhang, T., Epstein, J., Cooney, L., Wang, H., Li, Y., et al. (2007). Multifunctional nanowire bioscaffolds on titanium. *Chemistry of Materials, 19*, 4454—4459. http://dx.doi.org/10.1021/cm070845a.

Dong, W., Zhang, T., Mcdonald, M., Padilla, C., Epstein, J., & Tian, Z. R. (2006). Biocompatible nanofiber scaffolds on metal for controlled release and cell colonization. *Nanomedicine: Nanotechnology, Biology and Medicine, 2*, 248—252. http://dx.doi.org/10.1016/j.nano.2006.10.005.

Firstov, G. S., Vitchev, R. G., Kumar, H., Blanpain, B., & Van Humbeeck, J. (2002). Surface oxidation of NiTi shape memory alloy. *Biomaterials, 23*, 4863—4871. http://dx.doi.org/10.1016/S0142-9612(02)00244-2.

Fujibayashi, S., Nakamura, T., Nishiguchi, S., Tamura, J., Uchida, M., Kim, H.-M., et al. (2001). Bioactive titanium: effect of sodium removal on the bone-bonding ability of bioactive titanium prepared by alkali and heat treatment. *Journal of Biomedical Materials Research, 56*, 562—570. http://dx.doi.org/10.1002/1097-4636(20010915)56:4<562:AID-JBM1128>3.0.CO;2-M.

Gao, H., Jie, Y. F., Wang, Z. Q., Wan, H., Gong, L., Lu, R. C., et al. (2014). Bioactive tantalum metal prepared by micro-arc oxidation and NaOH treatment. *Journal of Materials Chemistry B, 2*, 1216—1224. http://dx.doi.org/10.1039/C3TB21521K.

Goodman, S. B., Yao, Z., Keeney, M., & Yang, F. (2013). The future of biologic coatings for orthopaedic implants. *Biomaterials, 34*, 3174—3183. http://dx.doi.org/10.1016/j.biomaterials.2013.01.074.

Guo, J., Padilla, R. J., Ambrose, W., De Kok, I. J., & Cooper, L. F. (2007). The effect of hydrofluoric acid treatment of TiO_2 grit blasted titanium implants on adherent osteoblast gene expression in vitro and in vivo. *Biomaterials, 28*, 5418—5425. http://dx.doi.org/10.1016/j.biomaterials.2007.08.032.

Gu, Y. W., Tay, B. Y., Lim, C. S., & Yong, M. S. (2005). Biomimetic deposition of apatite coating on surface-modified NiTi alloy. *Biomaterials, 26*, 6916—6923. http://dx.doi.org/10.1016/j.biomaterials.2005.04.051.

Hench, L. L., & Andersson, Ö. (1993). Bioactive glasses. In *An introduction to bioceramics*.

He, F. M., Yang, G. L., Li, Y. N., Wang, X. X., & Zhao, S. F. (2009). Early bone response to sandblasted, dual acid-etched and H_2O_2/HCl treated titanium implants: an experimental study in the rabbit. *International Journal of Oral and Maxillofacial Surgery, 38*, 677—681. http://dx.doi.org/10.1016/j.ijom.2009.03.716.

Jonšov, L., Muller, F. A., Helebrant, A., Strnad, J., & Greil, P. (2004). Biomimetic apatite formation on chemically treated titanium. *Biomaterials, 25*, 1187—1194. http://dx.doi.org/10.1016/j.biomaterials.2003.08.009.

Kim, C., Kendall, M. R., Miller, M. A., Long, C. L., Larson, P. R., Humphrey, M. B., et al. (2013). Comparison of titanium soaked in 5 M NaOH or 5 M KOH solutions. *Materials Science and Engineering: C, 33*, 327−339. http://dx.doi.org/10.1016/j.msec.2012.08.047.

Kim, H.-M., Miyaji, F., Kokubo, T., & Nakamura, T. (1996). Preparation of bioactive Ti and its alloys via simple chemical surface treatment. *Journal of Biomedical Materials Research, 32*, 409−417. http://dx.doi.org/10.1002/(SICI)1097-4636(199611)32:3<409::AID-JBM14>3.0.CO;2-B.

Kim, H. M., Miyaji, F., Kokubo, T., & Nakamura, T. (1997). Effect of heat treatment on apatite-forming ability of Ti metal induced by alkali treatment. *Journal of Materials Science: Materials in Medicine, 8*, 341−347. http://dx.doi.org/10.1023/A:1018524731409.

Kitahara, K. F., Ozaki, T., & Oshima, H. (1997). *Zeta potential*. Tokyo: Saientisuto-sha.

Kokubo, T., Ito, S., Huang, Z. T., Hayashi, T., Sakka, S., Kitsugi, T., et al. (1990). Ca, P-rich layer formed on high-strength bioactive glass-ceramic A-W. *Journal of Biomedical Materials Research, 24*, 331−343. http://dx.doi.org/10.1002/jbm.820240306.

Kokubo, T., Kim, H.-M., & Kawashita, M. (2003). Novel bioactive materials with different mechanical properties. *Biomaterials, 24*, 2161−2175. http://dx.doi.org/10.1016/S0142-9612(03)00044-9.

Kokubo, T., Miyaji, F., Kim, H.-M., & Nakamura, T. (1996). Spontaneous formation of bonelike apatite layer on chemically treated titanium metals. *Journal of the American Ceramic Society, 79*, 1127−1129. http://dx.doi.org/10.1111/j.1151-2916.1996.tb08561.x.

Kuznetsov, V., Ryabchuk, V., Emeline, A., Mikhaylov, R., Rudakova, A., & Serpone, N. (2012). Thermo- and photo-stimulated effects on the optical properties of rutile titania ceramic layers formed on titanium substrates. *Chemistry of Materials, 25*, 170−177. http://dx.doi.org/10.1021/cm3031736.

Lamolle, S. F., Monjo, M., Rubert, M., Haugen, H. J., Lyngstadaas, S. P., & Ellingsen, J. E. (2009). The effect of hydrofluoric acid treatment of titanium surface on nanostructural and chemical changes and the growth of MC3T3-E1 cells. *Biomaterials, 30*, 736−742. http://dx.doi.org/10.1016/j.biomaterials.2008.10.052.

Lee, B.-H., Do Kim, Y., Shin, J. H., & Hwan Lee, K. (2002). Surface modification by alkali and heat treatments in titanium alloys. *Journal of Biomedical Materials Research, 61*, 466−473. http://dx.doi.org/10.1002/jbm.10190.

Lee, B.-H., Kim, J. K., Kim, Y. D., Choi, K., & Lee, K. H. (2004). In vivo behavior and mechanical stability of surface-modified titanium implants by plasma spray coating and chemical treatments. *Journal of Biomedical Materials Research Part A, 69A*, 279−285. http://dx.doi.org/10.1002/jbm.a.20126.

LeGeros, R. Z., & LeGeros, J. P. (1993). Dense hydroxyapatite. In *An introduction to bioceramics*.

Li, P., Kangasniemi, I., De Groot, K., & Kokubo, T. (1994a). Bonelike hydroxyapatite induction by a gel-derived titania on a titanium substrate. *Journal of the American Ceramic Society, 77*, 1307−1312. http://dx.doi.org/10.1111/j.1151-2916.1994.tb05407.x.

Li, J., Liu, X., Qiao, Y., Zhu, H., & Ding, C. (2014a). Antimicrobial activity and cytocompatibility of Ag plasma-modified hierarchical TiO_2 film on titanium surface. *Colloids and Surfaces B: Biointerfaces, 113*, 134−145. http://dx.doi.org/10.1016/j.colsurfb.2013.08.030.

Li, J., Liu, X., Qiao, Y., Zhu, H., Li, J., Cui, T., et al. (2013). Enhanced bioactivity and bacteriostasis effect of TiO_2 nanofilms with favorable biomimetic architectures on titanium surface. *RSC Advances, 3*, 11214−11225. http://dx.doi.org/10.1039/C3RA23252B.

Li, Z., Meng, F., & Liu, X. (2011). Wettability control by DLC coated nanowire topography. *Nanotechnology, 22*, 135302. http://dx.doi.org/10.1088/0957-4484/22/13/135302.

Li, P., Ohtsuki, C., Kokubo, T., Nakanishi, K., Soga, N., & De Groot, K. (1994b). The role of hydrated silica, titania, and alumina in inducing apatite on implants. *Journal of Biomedical Materials Research, 28*, 7−15. http://dx.doi.org/10.1002/jbm.820280103.

Li, J., Zhang, W., Qiao, Y., Zhu, H., Jiang, X., Liu, X., et al. (2014b). Chemically regulated bioactive ion delivery platform on a titanium surface for sustained controlled release. *Journal of Materials Chemistry B, 2*, 283−294. http://dx.doi.org/10.1039/C3TB21102A.

Liu, X., Zhao, X., Fu, R. K. Y., Ho, J. P. Y., Ding, C., & Chu, P. K. (2005). Plasma-treated nanostructured TiO_2 surface supporting biomimetic growth of apatite. *Biomaterials, 26*, 6143−6150. http://dx.doi.org/10.1016/j.biomaterials.2005.04.035.

Macak, J. M., Tsuchiya, H., & Schmuki, P. (2005). High-aspect-ratio TiO_2 nanotubes by anodization of titanium. *Angewandte Chemie International Edition, 44*, 2100−2102. http://dx.doi.org/10.1002/anie.200462459.

Michiardi, A., Aparicio, C., Planell, J. A., & Gil, F. J. (2006). New oxidation treatment of NiTi shape memory alloys to obtain Ni-free surfaces and to improve biocompatibility. *Journal of Biomedical Materials Research Part B: Applied Biomaterials, 77B*, 249−256. http://dx.doi.org/10.1002/jbm.b.30441.

Michiardi, A., Aparicio, C., Ratner, B. D., Planell, J. A., & Gil, J. (2007). The influence of surface energy on competitive protein adsorption on oxidized NiTi surfaces. *Biomaterials, 28*, 586−594. http://dx.doi.org/10.1016/j.biomaterials.2006.09.040.

Miyazaki, T., Kim, H.-M., Kokubo, T., Ohtsuki, C., Kato, H., & Nakamura, T. (2002). Mechanism of bonelike apatite formation on bioactive tantalum metal in a simulated body fluid. *Biomaterials, 23*, 827−832. http://dx.doi.org/10.1016/S0142-9612(01)00188-0.

Miyazaki, T., Kim, H.-M., Miyaji, F., Kokubo, T., Kato, H., & Nakamura, T. (2000). Bioactive tantalum metal prepared by NaOH treatment. *Journal of Biomedical Materials Research, 50*, 35−42. http://dx.doi.org/10.1002/(SICI)1097-4636(200004)50:1<35::AID-JBM6>3.0.CO;2-8.

Nakamura, T., Kawashita, M., Kokubo, T., Kim, H. M., & Himeno, T. (2001). Zeta-potential variation of bioactive titanium metal during apatite formation on its surface in simulated body fluid. *Key Engineering Materials, 218*, 641−644. http://dx.doi.org/10.4028/www.scientific.net/KEM.218-220.641.

Nanci, A., Wuest, J., Peru, L., Brunet, P., Sharma, V., Zalzal, S., et al. (1998). Chemical modification of titanium surfaces for covalent attachment of biological molecules. *Journal of Biomedical Materials Research, 40*, 324−335. http://dx.doi.org/10.1002/(SICI)1097-4636(199805)40:2<324::AID-JBM18>3.0.CO;2-L.

Neoh, K. G., Hu, X., Zheng, D., & Kang, E. T. (2012). Balancing osteoblast functions and bacterial adhesion on functionalized titanium surfaces. *Biomaterials, 33*, 2813−2822. http://dx.doi.org/10.1016/j.biomaterials.2012.01.018.

Nishiguchi, S., Kato, H., Neo, M., Oka, M., Kim, H.-M., Kokubo, T., et al. (2001). Alkali- and heat-treated porous titanium for orthopedic implants. *Journal of Biomedical Materials Research, 54*, 198−208. http://dx.doi.org/10.1002/1097-4636(200102)54:2<198::AID-JBM6>3.0.CO;2-7.

Nishiguchi, S., Nakamura, T., Kobayashi, M., Kim, H.-M., Miyaji, F., & Kokubo, T. (1999). The effect of heat treatment on bone-bonding ability of alkali-treated titanium. *Biomaterials, 20*, 491−500. http://dx.doi.org/10.1016/S0142-9612(98)90203-4.

Nolan, M., & Tofail, S. A. M. (2010). Density functional theory simulation of titanium migration and reaction with oxygen in the early stages of oxidation of equiatomic NiTi alloy. *Biomaterials, 31*, 3439−3448. http://dx.doi.org/10.1016/j.biomaterials.2010.01.060.

Pan, J., Liao, H., Leygraf, C., Thierry, D., & Li, J. (1998). Variation of oxide films on titanium induced by osteoblast-like cell culture and the influence of an H_2O_2 pretreatment. *Journal of Biomedical Materials Research, 40*, 244−256. http://dx.doi.org/10.1002/(SICI)1097-4636(199805)40:2<244::AID-JBM9>3.0.CO;2-L.

Pan, J., Thierry, D., & Leygraf, C. (1996). Hydrogen peroxide toward enhanced oxide growth on titanium in PBS solution: blue coloration and clinical relevance. *Journal of Biomedical Materials Research, 30*, 393−402. http://dx.doi.org/10.1002/(SICI)1097-4636(199603)30:3<393::AID-JBM14>3.0.CO;2-L.

Peltola, T., Patsi, M., Rahiala, H., Kangasniemi, I., & Yli-Urpo, A. (1998). Calcium phosphate induction by sol-gel-derived titania coatings on titanium substrates in vitro. *Journal of Biomedical Materials Research, 41*, 504−510. http://dx.doi.org/10.1002/(SICI)1097-4636(19980905)41:3<504::AID-JBM22>3.0.CO;2-G.

Peng, X., & Chen, A. (2006). Large-scale synthesis and characterization of TiO_2-based nanostructures on Ti substrates. *Advanced Functional Materials, 16*, 1355−1362. http://dx.doi.org/10.1002/adfm.200500464.

Peng, Z. A., & Peng, X. (2001). Mechanisms of the shape evolution of CdSe nanocrystals. *Journal of the American Chemical Society, 123*, 1389−1395. http://dx.doi.org/10.1021/ja0027766.

Plant, S. D., Grant, D. M., & Leach, L. (2005). Behaviour of human endothelial cells on surface modified NiTi alloy. *Biomaterials, 26*, 5359−5367. http://dx.doi.org/10.1016/j.biomaterials.2005.01.067.

Schwartz, Z., Martin, J., Dean, D., Simpson, J., Cochran, D., & Boyan, B. (1996). Effect of titanium surface roughness on chondrocyte proliferation, matrix production, and differentiation depends on the state of cell maturation. *Journal of Biomedical Materials Research, 30*, 145−155. http://dx.doi.org/10.1002/(SICI)1097-4636(199602)30:2<145::AID-JBM3>3.0.CO;2-R.

Shabalovskaya, S. A., Anderegg, J., Laab, F., Thiel, P. A., & Rondelli, G. (2003). Surface conditions of nitinol wires, tubing, and as-cast alloys. The effect of chemical etching, aging in boiling water, and heat treatment. *Journal of Biomedical Materials Research Part B: Applied Biomaterials, 65B*, 193−203. http://dx.doi.org/10.1002/jbm.b.10001.

Shi, G.-S., Ren, L.-F., Wang, L.-Z., Lin, H.-S., Wang, S.-B., & Tong, Y.-Q. (2009). H_2O_2/HCl and heat-treated Ti-6Al-4V stimulates pre-osteoblast proliferation and differentiation. *Oral Surgery, Oral Medicine, Oral Pathology, Oral Radiology, and Endodontology, 108*, 368−375. http://dx.doi.org/10.1016/j.tripleo.2009.05.033.

Takeuchi, M., Abe, Y., Yoshida, Y., Nakayama, Y., Okazaki, M., & Akagawa, Y. (2003). Acid pretreatment of titanium implants. *Biomaterials, 24*, 1821−1827. http://dx.doi.org/10.1016/S0142-9612(02)00576-8.

Tavares, M. G., Tambasco De Oliveira, P., Nanci, A., Hawthorne, A. C., Rosa, A. L., & Xavier, S. P. (2007). Treatment of a commercial, machined surface titanium implant with H_2SO_4/H_2O_2 enhances contact osteogenesis. *Clinical Oral Implants Research, 18*, 452−458. http://dx.doi.org/10.1111/j.1600-0501.2007.01344.x.

Tengvall, P., Elwing, H., & Lundstrm, I. (1989a). Titanium gel made from metallic titanium and hydrogen peroxide. *Journal of Colloid and Interface Science, 130*, 405−413. http://dx.doi.org/10.1016/0021-9797(89)90117-3.

Tengvall, P., Elwing, H., Sj Qvist, L., Lundstrm, I., & Bjursten, L. M. (1989b). Interaction between hydrogen peroxide and titanium: a possible role in the biocompatibility of titanium. *Biomaterials, 10*, 118−120. http://dx.doi.org/10.1016/0142-9612(89)90043-4.

Tengvall, P., Lundstrm, I., Sj Qvist, L., Elwing, H., & Bjursten, L. M. (1989c). Titanium−hydrogen peroxide interaction: model studies of the influence of the inflammatory response on titanium implants. *Biomaterials, 10*, 166−175. http://dx.doi.org/10.1016/0142-9612(89)90019-7.

Tung, M. S. (1998). *Calcium phosphate in biological and industrial system*. Dordrecht: Kluwer Academic Publishers.

Uchida, M., Kim, H.-M., Miyaji, F., Kokubo, T., & Nakamura, T. (2002). Apatite formation on zirconium metal treated with aqueous NaOH. *Biomaterials, 23*, 313−317. http://dx.doi.org/10.1016/S0142-9612(01)00110-7.

Variola, F., Yi, J.-H., Richert, L., Wuest, J. D., Rosei, F., & Nanci, A. (2008). Tailoring the surface properties of Ti6Al4V by controlled chemical oxidation. *Biomaterials, 29*, 1285−1298. http://dx.doi.org/10.1016/j.biomaterials.2007.11.040.

Wang, Y., Du, G., Liu, H., Liu, D., Qin, S., Wang, N., et al. (2008). Nanostructured sheets of Ti−O nanobelts for gas sensing and antibacterial applications. *Advanced Functional Materials, 18*, 1131−1137. http://dx.doi.org/10.1002/adfm.200701120.

Wang, X.-X., Hayakawa, S., Tsuru, K., & Osaka, A. (2000). Improvement of bioactivity of $H_2O_2/TaCl_5$-treated titanium after subsequent heat treatments. *Journal of Biomedical Materials Research, 52*, 171−176. http://dx.doi.org/10.1002/1097-4636(200010)52:1<171:AID-JBM22>3.0.CO;2-O.

Wang, X.-X., Hayakawa, S., Tsuru, K., & Osaka, A. (2002). Bioactive titania gel layers formed by chemical treatment of Ti substrate with a H_2O_2/HCl solution. *Biomaterials, 23*, 1353−1357. http://dx.doi.org/10.1016/S0142-9612(01)00254-X.

Wen, H. B., Liu, Q., De Wijn, J. R., De Groot, K., & Cui, F. Z. (1998). Preparation of bioactive microporous titanium surface by a new two-step chemical treatment. *Journal of Materials Science: Materials in Medicine, 9*, 121−128. http://dx.doi.org/10.1023/A:1008859417664.

Wen, H. B., Wolke, J. G. C., De Wijn, J. R., Liu, Q., Cui, F. Z., & De Groot, K. (1997). Fast precipitation of calcium phosphate layers on titanium induced by simple chemical treatments. *Biomaterials, 18*, 1471−1478. http://dx.doi.org/10.1016/S0142-9612(97)82297-1.

Wu, S., Liu, X., Hu, T., Chu, P. K., Ho, J., Chan, Y., et al. (2008a). A biomimetic hierarchical scaffold: natural growth of nanotitanates on three-dimensional microporous Ti-based metals. *Nano Letters, 8*, 3803−3808. http://dx.doi.org/10.1021/nl802145n.

Wu, G., Wang, J., Thomas, D. F., & Chen, A. (2008b). Synthesis of F-doped flower-like TiO_2 nanostructures with high photoelectrochemical activity. *Langmuir, 24*, 3503−3509. http://dx.doi.org/10.1021/la703098g.

Xin, Y., Jiang, J., Huo, K., Hu, T., & Chu, P. K. (2009). Bioactive $SrTiO_3$ nanotube arrays: strontium delivery platform on Ti-based osteoporotic bone implants. *ACS Nano, 3*, 3228−3234. http://dx.doi.org/10.1021/nn9007675.

Xue, W., Liu, X., Zheng, X., & Ding, C. (2005). In vivo evaluation of plasma-sprayed titanium coating after alkali modification. *Biomaterials, 26*, 3029−3037. http://dx.doi.org/10.1016/j.biomaterials.2004.09.003.

Yada, M., Inoue, Y., Uota, M., Torikai, T., Watari, T., Noda, I., et al. (2007). Plate, wire, mesh, microsphere, and microtube composed of sodium titanate nanotubes on a titanium metal template. *Langmuir, 23*, 2815−2823. http://dx.doi.org/10.1021/la062654c.

Yamaguchi, S., Matsushita, T., & Kokubo, T. (2013). A bioactive Ti metal with a Ca-enriched surface layer releases Mg ions. *RSC Advances, 3*, 11274−11282. http://dx.doi.org/10.1039/C3RA00054K.

Yang, X.-F., Chen, Y., Yang, F., He, F.-M., & Zhao, S.-F. (2009a). Enhanced initial adhesion of osteoblast-like cells on an anatase-structured titania surface formed by H_2O_2/HCl solution and heat treatment. *Dental Materials, 25*, 473−480. http://dx.doi.org/10.1016/j.dental.2008.09.007.

Yang, X., Konishi, H., Xu, H., & Wu, M. (2006). Comparative sol−hydro(solvo)thermal synthesis of TiO_2 nanocrystals. *European Journal of Inorganic Chemistry, 2006*, 2229−2235. http://dx.doi.org/10.1002/ejic.200500855.

Yang, X., Zhuang, J., Li, X., Chen, D., Ouyang, G., Mao, Z., et al. (2009b). Hierarchically nanostructured rutile arrays: acid vapor oxidation growth and tunable morphologies. *Acs Nano, 3*, 1212−1218. http://dx.doi.org/10.1021/nn900084e.

Zhang, W. J., Li, Z. H., Huang, Q. F., Xu, L., Li, J. H., Jin, Y. Q., et al. (2013). Effects of a hybrid micro/nanorod topography-modified titanium implant on adhesion and osteogenic differentiation in rat bone marrow mesenchymal stem cells. *International Journal of Nanomedicine, 8*, 257−265. http://dx.doi.org/10.2147/IJN.S39357.

Zhang, W. J., Li, Z. H., Liu, Y., Ye, D. X., Li, J. H., Xu, L. Y., et al. (2012a). Biofunctionalization of a titanium surface with a nano-sawtooth structure regulates the behavior of rat bone marrow mesenchymal stem cells. *International Journal of Nanomedicine, 7*, 4459−4472. http://dx.doi.org/10.2147/IJN.S33575.

Zhang, F., Zhang, C. F., Yin, M. N., Ren, L. F., Lin, H. S., & Shi, G. S. (2012b). Effect of heat treatment on H_2O_2/HCl etched pure titanium dental implant: an in vitro study. *Medical Science Monitor, 18*, BR265−BR272. http://dx.doi.org/10.12659/MSM.883204.

Zhao, L., Wang, H., Huo, K., Zhang, X., Wang, W., Zhang, Y., et al. (2013). The osteogenic activity of strontium loaded titania nanotube arrays on titanium substrates. *Biomaterials, 34*, 19−29. http://dx.doi.org/10.1016/j.biomaterials.2012.09.041.

Zheng, Y., Li, J., Liu, X., & Sun, J. (2012). Antimicrobial and osteogenic effect of Ag-implanted titanium with a nanostructured surface. *International Journal of Nanomedicine, 7*, 875. http://dx.doi.org/10.2147/IJN.S28450.

Sol–gel surface modification of biomaterials

6

R.M. Pilliar
University of Toronto, Toronto, ON, Canada

6.1 Introduction

6.1.1 General

The sol–gel process is a wet chemical method for forming inorganic (ceramic) structures as monoliths, fibres, powders, or thin films from colloidal suspension of inorganic or metal organic precursors. The noted advantages of sol–gel processing include precise control of chemistry and structure at the molecular level, porosity at the nano-scale level, and use of lower processing temperatures resulting in unique structures and lower associated costs. Formation of nonequilibrium (amorphous or metastable) structures is possible, and undesired phase transformations and microstructural changes can be avoided because of the low processing temperature treatments. For forming larger monolithic parts (dimensions >1 cm), potential disadvantages include shrinkage during drying and sintering stages resulting in dimensional control and crack formation problems, high raw material costs for some formulations, and relatively low production rates, although batch sample processing can overcome this latter disadvantage. Forming thin films (<1 μm in thickness) as coatings, the focus of this chapter, minimizes some of these concerns.

Formation of thin film coatings by sol–gel methods represents an early commercial application of sol–gel technology. Presently, sol–gel-formed thin films are used extensively in optical and electronic applications. They also offer potential benefits as protective coatings against corrosion or wear, an often-desired feature of implantable devices. For biomaterial applications, the ability to purposely design nano porous structures at implant surfaces represents another potential advantage for control of bioactivity or for delivery of biologics and antibacterial agents.

The field of sol–gel processing is a multidisciplinary one involving physics, inorganic and organic chemistry, and application of these basic sciences to the field of materials engineering and, specifically, biomaterials and biomedical engineering – the focus of this chapter. Several reviews of sol–gel science are available and recommended for readers wishing broader insight (Brinker et al., 1991; Brinker and Scherer, 1990; Hench and West, 1990; Schmidt, 1988).

The process involved in forming sol–gel-derived systems (for bulk parts or thin films and coatings) consists of four often-overlapping stages described as (1) hydrolysis and condensation reactions of inorganic or organic precursors to form particulate or polymeric sols, (2) agglomeration/clustering of sol constituents leading

Surface Coating and Modification of Metallic Biomaterials. http://dx.doi.org/10.1016/B978-1-78242-303-4.00006-5
Copyright © 2015 Elsevier Ltd. All rights reserved.

to eventual formation of gel structures of sufficient stiffness to retain shape and form, (3) drying of the gel, and (4) sintering to form inorganic phases and structures with desired characteristics (i.e., composition, structure, physical, chemical, and mechanical properties and, for biomedical implant applications, bioactivity, and biocompatibility).

6.1.2 The sol–gel process

A sol is a colloidal suspension of fine nano-sized particles in a liquid medium, typically an aqueous or alcohol solution with acid or base catalysts added to promote or control reactions. Typically, particles or polymer networks that form within the sol are 1–5 nm in size, but can be larger. The colloidal sol suspension may consist of dense nonfractal particles forming so-called particulate sols derived from inorganic starting precursor compounds. Such compounds dissociate in solution, releasing ionic species that undergo hydrolysis and condensation reactions (Brinker and Scherer, 1990) to form stable sol particles. Larger particles can form as the sol ages through Ostwald ripening (i.e., dissolution of smaller particles and growth of larger ones). Sols can also be formed from organic precursors (usually metal alkoxides in alcohol or alcohol–water solutions). Hydrolysis of organic precursors is followed by condensation reactions resulting in polymer network formation and so-called polymeric sols. The polymer network structures can be weakly or highly branched with network interaction determining the sol structure. Sols can be formed from combined inorganic and organic precursors that, on reacting in solution, form a desired compound sol precursor. Formation of calcium phosphate precursors by adding a dissociated salt in aqueous medium to an organic-based precursor alcohol/water solution is an important biomaterial-related example. At present, an understanding of the intermediate reaction products that form during the process is limited, but what is known is that, in time, a calcium phosphate sol of desired Ca:P ratio (corresponding to calcium hydroxyapatite, for example) can result.

The next stage in the sol–gel process involves transformation of the sol to a gel. For sols formed from particulate precursors, particle agglomeration occurs with aging of the sol. Agglomerated particles of a certain size can remain separated in suspension as a result of repulsive forces due to surface charge effects overriding the reduction in surface free energy resulting from agglomeration. Particle agglomeration occurs when the attractive van der Waals force between particles is greater than the surface charge–related repulsive force. Increasing agglomerate size and, hence, reactant concentration result in an increased viscosity of the sol. This results in development of solution characteristics suitable for preparing components or coatings. Altering solution pH, which will affect the particle surface charge, will influence agglomeration. As agglomerate growth continues and viscosity increases, a continuous network eventually forms across a part dimension (either a bulk sample held in a mold, a film, or a thin coating). With this, the structure becomes self-supporting and transformation of a sol to a gel defining the gel point results. The time for this to occur is referred to as the gel time. As discussed later, continued gel aging results in aggregate

rearrangement for particulate precursor−derived gels to form more ordered structures. The extent of ordering as well as particulate size will determine the percent porosity of final structures, with greater ordering yielding more close-packed, lower porosity structures. For sols formed from polymeric precursors, continued reaction results in growth of polymer chains by continued condensation reactions and the formation of large macromolecular networks. As with particulate precursor−derived sols, development of a continuous polymer network across a sample cross-section forming a spanning polymer cluster results in a sharp increase in viscosity and elastic resistance at the gel point. Interchain bonding for polymeric precursor−derived gels occurs through covalent bond formation, with the final molecular arrangement dependent on sol aging time and polymer chain conformation (i.e., weakly branched polymers with low steric hindrance resulting in denser structures, whereas highly branched polymers exhibiting greater steric hindrance result in more open structures). The different interatomic bonding forces for particulate-formed gels (van der Waals) compared with those formed by polymeric precursors (covalent) result in different properties for the two systems. Covalently bonded polymeric precursor−derived gels form strong irreversible bonds, whereas particulate precursor−formed gels have weaker reversible bonds that can readily be returned to the sol state through vigorous agitation. Intrinsic characteristics of particle aggregates (size, packing density) and polymer network clusters (size, extent of polymer branching, and cluster interactions) determine the properties and characteristics of the gel and, after further processing, the final inorganic products.

Microstructural changes (aging) for both particulate-formed and polymeric precursor−formed gels continue after the gel point is reached. Aging involves further condensation reactions and polymer network development or particle agglomeration. The result is a continuous increase in elastic modulus and strength of the gel and its shrinkage in concert with liquid phase expulsion, a process referred to as syneresis. During drying, evaporation of liquid phase occurs initially from the sample surface region, whereas retained liquid is drawn inward by capillary and osmotic forces. As the gel stiffens from continued polycondensation and agglomeration, high-residual stresses develop from the differential drying rates at the surface and internal gel regions. These stresses can be large enough to cause cracking. In addition to syneresis, microstructural coarsening of gel structures occurs during aging. The extent of these effects will be dependent on relative rates of condensation/agglomeration and evaporation during the drying stage. For thin sol−gel-derived coatings, drying occurs relatively quickly (seconds to minutes) compared with the much slower drying times associated with bulk samples (days), thereby reducing the probability for cracking because relatively compliant gel structures are maintained during most of the drying process. Drying can be achieved at ambient or elevated temperature, with rapid drying allowing less time for condensation and agglomeration reactions. For polymeric precursor−derived gels, this results in finer network structures with lower porosity and finer pores. In contrast, particulate precursor−formed gels subjected to faster drying will form less ordered structures yielding high-porosity structures. Phase transformations may also occur during the aging process, particularly if elevated temperatures are used during the drying stage. Gelation usually results in formation of

metastable amorphous structures that, with time (accelerated at elevated temperatures), will transform to stable rystalline phases.

Final densification and strength development of dried gel structures are achieved through a sinter anneal. This higher temperature treatment results in sinter neck growth between particles and higher strengths. Sinter neck formation and growth are driven by reduction in surface free energy through a reduced total surface area and the small radius of curvature sinter neck regions. This occurs by mass transport mechanisms at the sinter neck regions with or without significant densification depending on the dominant sintering mechanism. For amorphous gel structures that initially form upon gelation and aging at temperatures below the crystallization temperature of the formed gel reaction products, material transport resulting in sinter neck formation occurs by viscous flow. This involves a relatively low activation energy barrier, thereby allowing sinter neck growth at relatively low temperatures particularly for nano-scale particles and clusters constituting the gel. Even for crystalline samples in which sintering involves volume, grain boundary, and surface diffusion with higher associated activation energies, nano-scale structures allow rapid densification at relatively low sintering temperatures. Sinter neck growth results in increased mechanical and physical properties, the necessary requirement for many ceramic and glass products formed by sol−gel processing. In addition, microstructures and phases may be altered significantly as a result of the sintering treatment. For some applications, including certain coatings used with biomedical implants, attaining a controlled porous structure displaying increased bioactivity is the goal. Selection of precursors and processing to prepare sols and gels are important for appropriate structural and compositional formation of such porous structures. The use of sol−gel coating of implants to form preferred implant surface geometry and/or chemistry represents an important and growing area of use of sol−gel technology.

6.1.2.1 Sol−gel-derived coatings of biomedical implants

Surface modification of implants to promote desired cell response to achieve a preferred implant−tissue interface structure represents a goal of contemporary implant design. Sol−gel-derived coatings, as already noted, offer an attractive means for achieving this goal. For bone-interfacing orthopedic and dental implants in which rapid bone formation and bone juxtaposition to an implant surface yielding secure long-term implant-to-bone fixation is desired, thin sol−gel-formed calcium phosphate coatings have been reported to promote faster rates of osseointegration (Gan et al., 2004b; Nguyen et al., 2004; Tache et al., 2004). Other studies have demonstrated the use of sol−gel-formed titanium oxide films to promote rapid surface formation of hydroxyapatite-like layers in vitro (in synthetic/Strong simulated body fluid [SBF] solution) and of early bone formation in vivo (Areva and Jokinen, 2008; Jokinen et al., 1998; Li and de Groot, 1993; Peltola et al., 1998). Titania sol−gel-formed coatings have also been shown to promote soft tissue-to-implant bonding (Aaritalo et al., 2007; Areva et al., 2004, 2007; Paldan et al., 2008; Rossi et al., 2008).

6.1.3 Formation and characterization of sol−gel-derived coatings

Thin sol−gel-derived coatings over implant substrates can be applied by dip coating or spin coating as well as spray coating. Most reported studies on sol−gel coating of surgical implants have used either dip or spin coating methods which are described as follows.

6.1.3.1 Dip coating

The dip-coating process consists of four stages: substrate immersion into a sol solution, substrate withdrawal, drainage during and after withdrawal, and evaporation and drying during and following sample withdrawal (Figure 6.1). After drying, a heat treatment is often used to complete the dehydration process and to remove any residual organics. This may be part of the sintering heat treatment used to achieve desired coating structure, cohesive strength, and adhesive strength at the coating−substrate interface. For metallic substrates, excessive surface oxidation of the substrate surface that might prevent good coating-to-substrate bonding and substrate microstructural changes resulting in loss of mechanical properties must be avoided.

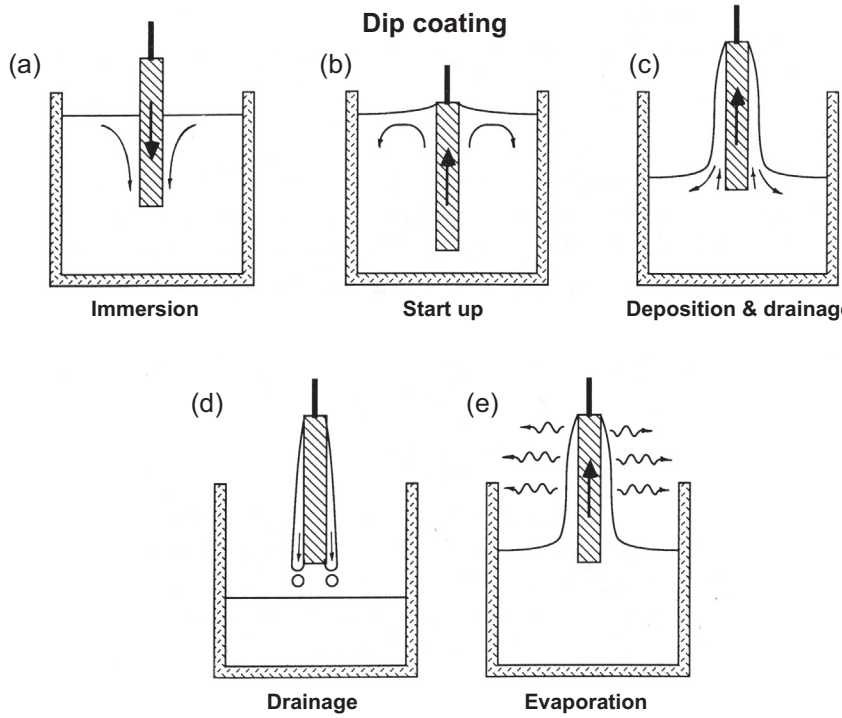


Figure 6.1 Schematic representation of stages of dip-coating process before final sintering anneal.
With permission adapted from Brinker and Scherer (1990), Chapter 13 (Film Formation).

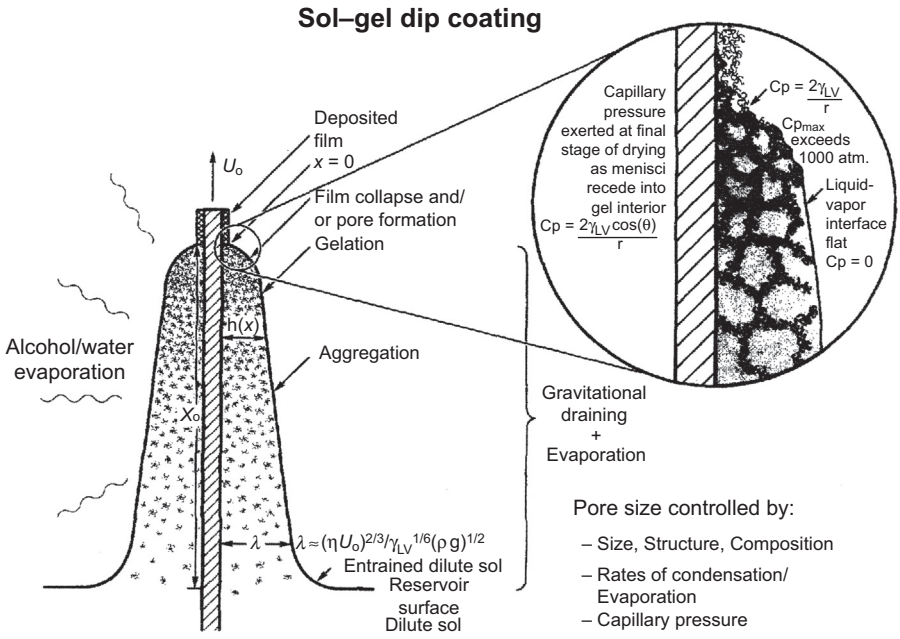


Figure 6.2 Schematic illustration showing steady-state structure development during deposition and drainage stage during dip-coating operation. Insert shows final stages of evaporation and gel collapse and structure before sintering anneal.
With permission Brinker et al. (1991).

Figure 6.2 illustrates the steady-state gel structure that develops during sol–gel coating. In contrast to bulk sol–gel-formed samples, gel formation and drying stages overlap significantly. Because of the relatively limited coating thickness (typically individual layers are less than 0.5-μm thick; multilayering can be used to form thicker overall coatings), evaporation and loss of liquid phase from the gel–liquid complex occur in a matter of seconds or minutes as opposed to the much longer periods (days and weeks) required with bulk samples. This rapid drying limits the time for network development for polymeric precursor–formed coatings, thereby allowing the shorter networks to pack more tightly to form lower porosity coatings. Rapid drying has the opposite effect on particulate precursor–derived coatings with rapid evaporation of liquid and associated reduced gel compliance allowing less time for particle ordering leading to more porous structures. Dip-formed coating thickness is a function of sol viscosity, substrate withdrawal rate, solvent evaporation rate, gel syneresis (a function of liquid–vapor surface energy), and ambient conditions during withdrawal (e.g., pressure, temperature). Prediction of thickness of the gel film, h, has been proposed using the Landau–Levich equation (Eqn (6.1)) (Landau and Levich, 1942);

$$h = 0.94(\eta U)^{2/3}/\gamma_{LV}^{1/6}(\rho g)^{1/2} \tag{6.1}$$

where h is film thickness, η liquid phase viscosity, U withdrawal speed, γ_{LV} liquid–vapor surface tension, ρ sol-specific gravity, and g gravity. The relation holds up well to experimental verification with higher viscosity and withdrawal speed yielding thicker coatings. Subsequent drying, calcining, and sintering processes will result in reduction of coating thickness beyond this predicted gel thickness.

During sample withdrawal from solution, polycondensate clusters and particle aggregates within the coating layer become increasingly concentrated as evaporation occurs (see Figure 6.2). This increased concentration leads to tighter packing of network clusters and particle agglomerates resulting in increased intercluster and interagglomerate bonding and consequent reduced film compliance that, as previously noted, eventually inhibits further restructuring. Characteristics of the gel coating (density, pore size, stiffness) are determined by relative rates of condensation and evaporation, the latter is a function of extrinsic factors including processing temperature, pressure, local airflow, or other ambient atmosphere conditions as well as solvent characteristics (molecular weight, vapor pressure). Thin coatings are especially sensitive to these factors.

6.1.3.2 Spin coating

Figure 6.3 depicts the four stages characterizing the spin-coating process (Bornside et al., 1987). These are (1) deposition of liquid sol, (2) spin-up in which centrifugal forces spread the deposited sol over the substrate surface, (3) spin-off with excess

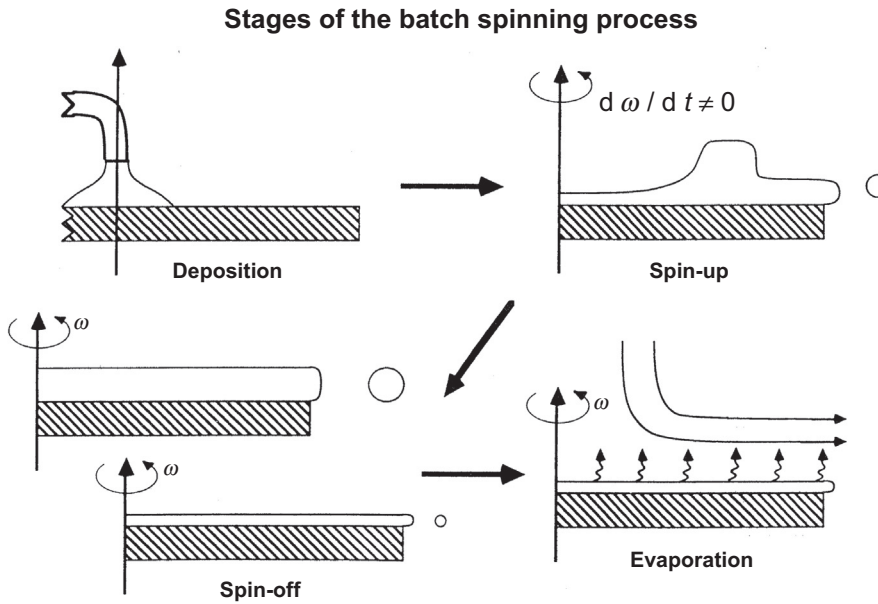


Figure 6.3 Schematic illustration of stages of film development during the spin-coating process. With permission Brinker and Scherer (1990), Chapter 13 (Film Formation).

liquid flowing off the substrate, and (4) evaporation of retained liquid phase. A relation predicting gel thickness layer, $h(t)$, at time t (before excessive evaporation and aging) has been reported (Eqn (6.2)); this suggests the dependence of layer thickness development on liquid viscosity, density (specific gravity), and spin velocity (Emslie et al., 1958; Scriven, 1988);

$$h(t) = h_o/\left(1 + 4\rho\omega^2 h_o^2 t/3\eta\right)^{1/2} \tag{6.2}$$

in which h_o is thickness of the layer at the beginning of the spin-off stage, ρ is the density of the deposit (presumed constant although this is not the case because sol-to-gel transformation and gel aging are occurring during this stage), ω is angular velocity, and η, the sol/gel viscosity (also assumed constant). The final film thickness is determined by gel outflow and evaporation with outflow dominant initially but evaporation being more prominent during gel aging and increasing deposit viscosity. This results in a film thickness in stage 4 that continues to lose solvent by evaporation only. Studies of final film thickness, time to reach this thickness, and parameters determining these quantities have been investigated and compared with analytical predictions based on gel density as a function of time, evaporation rates (a function of time, spin frequency, ambient conditions, and solvent characteristics), and assumptions related to solute and solvent behavior namely Newtonian flow characteristics and a constant evaporation rate during film thinning (Meyerhofer, 1978). Aside from attempted quantitative prediction of film characteristics, the real value of these predictions is the identity of parameters that affect final coating thickness and time to achieve this final thickness.

Evaporation of solvent from deposited films occurs throughout stages 2, 3, and 4 during spin coating. Significant shrinkage of the film occurs during stage 3, with shrinkage occurring principally in the transverse film direction because adherence of the deposited film to the substrate surface (whether by ionic, covalent, or van der Waals bonding) inhibits shrinkage in directions along the substrate-coating interface. The eventual uniform decrease in film thickness during stage 3 over the whole substrate surface (Figure 6.3) is one advantage of spin-coating, with constant final coating thickness resulting over the whole substrate (for planar substrate surfaces). Surface irregularities and geometric discontinuities (for both spin- and dip coating) will result in development of different film thickness at such regions. A major advantage of forming thin coatings over solid substrates by sol−gel methods is the avoidance of cracking on drying of the gel and, consequently, avoidance of cracks within the coating after the calcining/sintering treatment. The buildup of film thickness at substrate irregularities and discontinuities results in thicker coatings in such regions that are more susceptible to cracking during drying. If a design goal is to make completely dense and impervious coatings, as intended for coatings designed to inhibit substrate degradation by corrosion or abrasion for example, crack formation may be unacceptable. The issue may be moot for implants in which coatings are biodegradable and intended for short-term effectiveness only (to promote early bone formation, for example).

6.1.3.3 Coating sintering

Most as-made sol–gel-formed coatings on implants require a degree of mechanical integrity to ensure that preinsertion implant handling and early postimplantation functional loading (either inadvertent or intended) does not result in coating fragmentation and/or delamination. For this reason, coatings, after the drying treatment, are given a sintering anneal to promote strong bonding between clusters and aggregates constituting the gel coating as well as at the coating–substrate interface. The annealing treatment also serves to remove any residual organics that may still be present following drying and that could negatively affect biocompatibility. The extremely fine particles and clusters within the gel result in very rapid rates of sintering at relatively low temperatures. Sinter neck formation and densification can occur by a viscous flow mechanism (with amorphous structures) or volume, grain boundary or surface diffusion mechanisms (with crystalline structures), or a combination of these depending on the specific sintering conditions used. For crystalline structures, initial "green" density, determined by particulate size, packing, and degree of agglomeration for particulate precursor–derived gels and network cluster size and fractal characteristics for polymeric precursor–derived gels determine the density or retained porosity following the sintering treatment. Although studies on the sintering kinetics of coatings are limited, it has been reported that sol–gel-formed coatings appear to densify more rapidly than bulk sol–gel-formed samples of similar composition, precursor type, and processing conditions (Brinker and Mukherjee, 1981). This is believed to be due to the more rapid evaporation associated with coatings resulting in less time for aging and, hence, retention of more compliant gel structures during the drying stage enabling more extensive pore collapse due to capillary forces.

6.1.3.4 Factors affecting coating microstructure

The structure and properties of sol–gel-formed coatings (i.e., density, pore size, surface area, crystallinity, strength, and chemical stability) are determined by both the liquid solution characteristics before coating application during dipping or spinning and the conditions during film formation (i.e., gelation, drying, and sintering). Within the liquid solution before substrate coating by dipping or spinning, the size and conformation of polymer networks or particulate aggregates (i.e., extent of network branching, cluster/agglomerate ordering) and relative rates of evaporation and condensation are important in determining final structure of the deposited gel layer. Evaporation rates can be controlled during the coating operation by appropriate selection of ambient conditions (temperature, pressure) as well as liquid solvent composition and its characteristic equilibrium vapor pressure. Thus, higher molecular weight solvents characterized by higher vapor pressure points will result in slower evaporation rates, potentially yielding more time for condensation, formation of less compliant gels and, hence, higher porosity coatings. To the contrary, slower evaporation rates for particulate precursor–derived gels result in greater ordering leading to denser coatings. Film thickness as determined by withdrawal or spin rate will affect evaporation rate and, consequently, coating porosity. Shear forces that develop during substrate

withdrawal or spin-off stages may also affect gel constituent clustering or agglomeration and, hence, porosity. The relatively rapid deposition and drying times of thin films compared with bulk samples allow less time for aging of gels before and after they reach their gel point (defined for films as the point at which films are able to withstand gravitational or spin-imposed centrifugal forces). Thus, for polymeric precursor–derived films, because less time is available for condensation reactions that otherwise would result in more extensive and more highly crosslinked and stiffer networks, the more compliant films are able to assimilate networks into tighter structures during gel formation and drying thereby reducing the possibility of coating cracking. The resulting tighter structural organization and packing of clusters yields denser coatings. For polymeric sol–derived systems, the extent to which this can occur is dependent on the network characteristics following hydrolysis and condensation of the precursors, which is related to their mass fractal dimension, d_f. Weakly branched networks (i.e., lower d_f) are able to interpenetrate to a greater extent (referred to as being mutually transparent) thereby resulting in higher packing density and lower porosity as the gel is concentrated during evaporation on the substrate surface. For highly branched polymer networks (i.e., $d_f \geq 1.5$), the systems are referred to as being mutually opaque. Network interactions, with further polycondensation and less dense packing of clusters, result in greater retained porosity. The size of precursor clusters also determines the mass fractal dimension and porosity. For particulate precursor–derived gels, agglomerate size, surface charge characteristics (attractive or repulsive van der Waals forces acting between particles during solvent evaporation), and extent of ordering determine the density and porosity characteristics of coatings.

6.1.3.5 Coating characterization

Methods that have been reported for characterizing sol–gel-derived coatings include conventional and thin film X-ray diffraction (to determine crystallinity), X-ray photoelectron spectroscopy, Fourier transform infrared spectroscopy, and Raman spectroscopy (for molecular characterization), scanning electron microscopy (SEM), energy-dispersive X-ray, and atomic force microscopy (for microstructural, compositional, and topographical characterization), differential thermal analysis–thermal gravimetric analysis (to study phase transformation). Transmission electron microscopy (TEM and selected area electron diffraction) using a complex thin-section preparation method to examine the interface zone has also been reported (Gan and Pilliar, 2004). Substrate–coating interface strength measurements have been determined both qualitatively (scratch testing) and quantitatively (interface tensile strength by direct tensile loading of the interface using adhesively bonded platens to transmit forces to the coating–substrate interface). Quantitative pull-off testing is limited by the strength of the adhesives used and their ability to adhesively bond to the sol–gel-formed surface so that reported values represent minimum values at best. Interface shear strength predictions have been made using an indirect method (i.e., shear lag test) (Choudhury and Agrawal, 2011; Filiaggi et al., 1996; Gan et al., 2004a). Results from the shear lag testing suggest very high interface shear strengths for calcium phosphate (Ca-P) and zirconia sol–gel-derived coatings formed on Ti and Ti alloy

substrates (~275–680 MPa). Such high values suggest formation of primary chemical bonds at the interface as a result of either strong bonding related to close interatomic apposition between hydroxylated complexes at the Ti substrate surface and gel layer surface or reaction products that might have formed during the calcining/sintering annealing treatments (Gan and Pilliar, 2004). That study used high-resolution TEM studies and selected area electron diffraction and reported the formation of $CaTiO_3$ at the interface region. Presumably the nano-scale gel structures and associated high thermodynamic reactivity of surface species allow such reactions at the relatively low annealing temperatures used during processing.

6.2 Sol–gel coating applications in biomaterials

6.2.1 Bone-interfacing implants and enhanced osseointegration

Cementless implants became increasingly popular for use in joint replacement procedures beginning in the mid-1980s (initially for femoral hip replacement components, but subsequently for knee and other joint replacement components). Strategies to ensure rapid and secure fixation of these designs represent a major research focus to the present with implant surface modification being a popular design strategy. Successful endosseous dental implants gained credibility in the late 1970s mainly through the pioneering efforts of Swedish investigators (Branemark et al., 1977) (P-I Branemark coined the term "osseointegration" that since then has been commonly used to describe successful cementless implant fixation to bone). With early success of cementless implants in both orthopedics and dentistry has come the increased use of such devices in wider patient indications and with the use of less conservative (i.e., shorter) limited loading periods before a return to near-normal functional loading. For example, commercial dental implants are now offered for early (within days) and immediate (same day) "functional" loading (provided host bone quality is suitable). Although orthopedic practice remains more conservative, there is nevertheless a move to shorter, limited loading periods before allowing patient return to normal or near-normal activities (unfortunately, not always with happy outcomes). Early loading is even encouraged, depending on patient's health and physical condition as a means of maintaining soft-tissue conditioning and faster mechanically stimulated bone formation. A review of published articles from 1990 onwards indicates a large number of reports on surface modification of cementless implants intended for more rapid and reliable osseointegration. Included are studies of sol–gel-coated orthopedic and dental implants. Two general approaches have been reported: (1) formation of calcium phosphate coatings directly on bone-interfacing implant surfaces during implant fabrication, Ti and Ti alloys primarily (Weng, 1999), but also with some studies on CoCrMo and stainless steel implants (Duran et al., 2004; Vijayalakshmi et al., 2008), and (2) sol–gel-formed oxide coatings (primarily TiO_2) that are then treated by soaking in an alkali solution followed by heat treatment to form calcium phosphate surface deposits that promote osseointegration (i.e., a biomimetic approach) (Kim et al., 1996; Kokubo et al., 2000, Chap. 16). Studies with mixed Ti and calcium phosphate sol–gel-formed

deposits have also been reported (Piveteau et al., 1999). All of these investigations have had as their major goal the development of faster osseointegration for load-bearing implants as a result of enhanced osteoconductivity and/or osteoinductivity because of the coating layer.

6.2.1.1 Calcium phosphate (Ca–P) sol–gel-derived coatings

Both particulate (inorganic route–formed) and polymeric (organic route–formed) precursors have been used for the formation of thin sol–gel-derived HAp coatings on different substrates. Based on the review of literature since the early 1990s, polymeric precursor–based gels appear to represent the more commonly used approach. Both precursor types result in thin film coatings of approximately micron or so thickness (often involving multilayer deposition prior to a final sinter anneal to achieve the desired final thickness). The sol–gel-derived coatings appear strongly bonded to the substrate (Choudhury and Agrawal, 2011; Gan et al., 2004a; Weng, 1999). Resulting coatings are often nonstoichiometric HAp (i.e., Ca:P = 1.67, which increases their susceptibility to degradation, a sometimes desirable feature. Some coatings are characterized as calcium-deficient HAp and with carbonate inclusion (mimicking natural bone mineral in that regard). The degree of crystallinity, amount and size of porosity, and microstructure are dependent on the conditions used for coating preparation. The thin sol–gel-formed coatings, as expected, conform closely to the underlying substrate surface features and deposition by dipping or spinning being a non–line-of-site process, three-dimensional features such as sintered porous structures or undercut regions of textured surfaces are able to be totally coated. In vivo (rabbit) studies of sol–gel-derived calcium-deficient HAp coatings have been reported (Gan et al., 2004b; Nguyen et al., 2004; Tache et al., 2004), and the results of those studies indicate that the coatings (both organic and inorganic route–formed) result in more rapid osseointegration with enhanced bone ingrowth rates being demonstrated for the sintered porous-coated Ti-based implants investigated. In those studies, the thin Ca-P coatings were characterized as poorly crystalline, Ca–deficient, carbonated HAp with Ca/P ratios dependent on annealing conditions used during sintering. In studies reported by Gan, Ca/P ratio for inorganic route–formed coatings annealed in air at 500 °C was equal to 1.45, whereas organic route–formed coatings similarly annealed displayed a Ca/P ratio of 2.10 (although both types exhibited diffraction peaks corresponding to HAp crystal structure). However, a recent study using similar sol preparation and gel coating conditions but on a different substrate (calcium polyphosphate) for a different purpose (see Section 6.2.3) reported near-stoichiometric the Ca:P ratios for both organic and inorganic route–formed coatings. In another earlier study (Nguyen et al., 2004) but with the inorganic route–formed coatings sintered in vacuum at 760 °C rather than in air, the Ca/P ratio was equal to 1.70 (very near-stoichiometric HAp). Crystal lattice defects contributing to the observed poorly crystalline structure are expected to result during rapid crystallization on annealing of the initial amorphous Ca–P phase formed by room temperature drying of the gel. Such poorly crystalline carbonated and nonstoichiometric HAp represents a thermodynamically less stable structure compared with highly crystalline HAp and, thus,

is more readily degraded in vivo (compared with stoichiometric HAp). For the intended coating role on porous-surfaced substrates (or presumably other substrates with textured surfaces), namely promotion of faster rates of bone ingrowth into surface features (pores or undercuts), early in vivo degradation but at a rate slow enough to not invoke a chronic inflammatory or toxic response appears to be acceptable and even advantageous—provided that suitable underlying substrate surface topography (i.e., textured, irregular, or porous-surfaced) is available to allow secure bone-to-implant micromechanical attachment for long-term osseointegration). Additionally, the carbonated form of the sol−gel-derived Ca−P coating closely mimics the composition of natural bone mineral and, as such, introduces a buffering agent (released carbonate during degradation) to help maintain a desired pH environment during osteogenesis. The HAp surface modification may also be significant in allowing efficient and rapid absorption of molecular species favoring preosteoblast cell adhesion and differentiation toward rapid osteogenesis. In addition to the Ca^{2+} and PO_4^{3-} local environment resulting from HAp coating degradation, the nano-scale topographical features (texture and porosity) introduced by the sol−gel-derived HAp coatings may also contribute to the observed more rapid osseointegration compared with non-coated "control" substrates.

A brief summary of reported precursor formulations and processing conditions used to form sol−gel-derived HAp coatings is presented next (and Table 6.1). As previously noted, most prior studies used the polymeric precursor approach (organic route) for coating preparation with sols of the desired Ca:P molar ratio (1.67:1) being used to form a gel (although this Ca/P ratio is not necessarily retained in the final coating).

For organic route−formed coatings, a frequently noted P precursor is triethyl phosphite ($P(OC_2H_5)_3$), also designated as ($P(OEt)_3$), a readily hydrolyzable alkoxide that, after a 24-h or so hydrolysis period, forms a suitable P-containing sol. Mixing this sol under vigorous stirring conditions with an appropriate quantity of a calcium nitrate tetrahydrate solution ($Ca(NO_3)_2 \cdot 4H_2O$) dissolved in either water or a water/alcohol solution (to achieve the desired Ca/P molar ratio) results in, after a required aging period (>24 h to allow full hydrolysis of the two precursors and reaction of the P and Ca precursors), formation of an appropriate sol for HAp formation. Dip- or spin coating results in a HAp layer without any other Ca−P phases (Carrado, 2013; Choudhury and Agrawal, 2011; Gan and Pilliar, 2004; Liu et al., 2001, 2002a,b,c,d). Other Ca and P precursor combinations that have been reported include calcium diethoxide ($Ca(OEt)_2$) with $P(OEt)_3$ (Gross et al., 1990), calcium acetate ($Ca(C_2H_3O_2)_2$) and triethyl phosphate ($(C_2H_5)_3PO_4$) (Jillavenkatesa and Condrate, 1998), calcium nitrate and phenyldichlorophosphite ($C_6H_5PCl_2$) (Brendel et al., 1992), calcium nitrate and phosphonoacetic acid ($HOOCCH_2PO(OH)_2$) (Takahashi et al., 1995), calcium nitrate tetrahydrate and diammonium phosphate ($(NH_4)_2HPO_4$) (Esfahani et al., 2012; Mavis et al., 2000), and calcium 2-ethylhexanoate (Ca/EHA) solution mixed with an ethylhexyl-phosphate solution (Metikos-Hukovic et al., 2003).

For HAp coatings formed on Ti or Ti alloy substrates using the inorganic route, P_2O_5 and $Ca(NO_3)_2 \cdot 4H_2O$ starting precursors dissolved in ethanol have been reported. After heating at 90 °C for 24 h, P_2O_5 in ethanol forms oxyalkoxides ($PO(OH)(OR)_2$ and $PO(OH)_2(OR)$) that react with the calcium nitrate solution to form

Table 6.1 Some calcium phosphate coatings for bone bonding—processing and characteristics

Substrate	Precursor (organic/inorganic)	Hydrolysis and aging conditions	Coating method	Drying conditions	Calcining/sintering conditions	Coating characteristics/notes	References
Ti6Al4V - sintered porous coating	Triethyl phosphite (TEP) + calcium nitrate tetrahydrate ($Ca(NO_3)_2 \cdot 4H_2O$) solution	TEP stirred in DDH_2O for 24 h; add Ca nitrate solution; age 4 days @ 40 °C in H_2O, diluted in ethanol (EtOH) + 2 days aging @ RT	Dip coat; withdrawal @ 20 cm/min	In air @ RT	20 min in air @ RT + 500 °C for 10 min	Featureless surface; nanocrystalline carbonated HAp; interface strength (shear lag test) = 280 Mpa; $CaTI_2O_5$ interface reaction product	Gan and Pilliar (2004), Gan et al. (2004a)
Ti6Al4V-sintered porous coating	TEP + $Ca(NO_3)_2 \cdot 4H_2O$ solution	Hydrolyze >4 h with no acid catalyst; few minutes with catalyst; mixture vigorously stirred for 10 min; 24 h aging @ RT	Dip coat	Dried @ 80 °C	Up to 6 h @ 375 °C or 500 °C for 10 min in air; 2 h-aged used for dip coating porous−surfaced dental implants	375 °C sintered coating– > dense, strongly bonded HAp coating	Liu et al. (2002a)

Commercial purity Ti (oxidized @ 500 °C/1 h and furnace cooled)	TEP + $Ca(NO_3)_2 \cdot 4H_2O$ solution	TEP stirred in DDH_2O for 24 h add Ca nitrate solution; age 5 days @ RT in H_2O, diluted with EtOH + 2 days aging @ RT	Dip coat—withdrawal speed = 3 mm/s	Dried @ 100 °C for 1 h	500 °C for 30 min in argon;	Also HAp-ZrO_2 composite coatings (for enhanced fretting wear resistance); interface strength (shear lag test) = 570 Mpa (pure HA) and 678 MPa (composite coating)	Chowdry and Agrawal (2011)
Ti	TEP + calcium diethoxide	Hydrolyzed @ 70 °C for 10 min; aging >24 h	Spin coating @ 2500 rpm for 10 s	Prefired @ 500 °C for 5 min; 7 layers applied	600, 700, 800 °C for 10 min; removal of all organics observed @ 800 °C	Crystallizes @ 550 °C; nanocrystalline (average grain size = 50 nm)	Gross et al. (1990)
Ti, Ti6Al4V, Ti6Al6Nb	Calcium hydroxide suspended in EtOH + ethyl hexanoic acid (EHA) + ethylhexyl-phosphate solution; diluted with EtOH	Stirred for 4 h @ 25 °C	Dip coat @ 25 °C; withdrawal speed ≈ 1 mm/s	Dried in air @ 130 °C for 4 h	Between 400 and 900 °C for 10 min	Well-crystallized HAp andβ-TCP on Ti and A5; poorly crystallized HAp and β-TCP on Ti 6Al6Nb	Metikos-Hukovic et al. (2003)

Continued

Table 6.1 Continued

Substrate	Precursor (organic/inorganic)	Hydrolysis and aging conditions	Coating method	Drying conditions	Calcining/sintering conditions	Coating characteristics/notes	References
Ti6Al4V	P_2O_5 + EtOH solution mixed with $Ca(NO_3)_2 \cdot 4H_2O$ in EtOH	Mixed solution refluxed for 24 h	Dip coat; withdrawal rate = 4 cm/min	Dried @ 150 °C for 15 min	500 °C, 15 min in air; multilayer (10×); some further annealed @ 750 °C in vacuum (10^{-2} Torr), 15 min	500 °C sinter– > HAp; 750 °C– > HAp + β-TCP	Weng (1999)
Ti6Al4V	$Ca(NO_3)_2 \cdot 4H_2O$ dissolved in methyl cellulose and deionized H_2O, NH_4OH added to solution	Solution vigorously stirred @ 60−70 °C for 90 min forming HAp precipitated particles that were blended into a gelatin, glycerol, H_2O solution	Dip coat; withdrawal rate = 15−300 mm/min	Air dried @ 90 °C	840 °C in N_2 for 2−4 h hold time	Highly porous HAp coatings; well-bonded to substrate (interface tensile strength from pull-off test >30 Mpa)	Mavis and Cuneyt Tas (2000)
TiB_2/TiB/Ti	$Ca(NO_3)_2 \cdot 4H_2O$ and diammonium phosphate	Reacted @ 40 °C in aqueous solution, pH > 9	Dip coat; withdrawal rate = 4 cm/min	Dried @ 100 °C	400 °C for 0.5 h in air	HAp formed with a small amount of β-TCP	Esfahani et al. (2012)

RT, room temperature.

the HAp-forming sol that is applied by dip coating. The resulting gel layer is dried at 150 °C for 15 min followed by a 500 °C calcining/sintering heat treatment to form the HAp coating (Weng and Baptista, 1999).

An alcohol-free particulate precursor−derived coating using a solution of calcium nitrate ($Ca(NO_3)_2.4H_2O$) and ammonium dihydrogen phosphate ($NH_4H_2PO_4$) for the Ca and P precursors (with NH_4OH addition for pH control ≈ pH 12) was reported for forming HAp coatings over sintered porous-surfaced Ti6Al4V implants (Chai and Ben-Nissan, 1999; Gan and Pilliar, 2004). This formulation, as described in more detail later, was used in a study comparing microstructure, chemical composition, coating-to-substrate interface shear strength, and in vivo performance of sol−gel-derived HAp coatings formed by organic and inorganic routes (Gan and Pilliar, 2004; Gan et al., 2004a).

The organic and inorganic route for forming sol−gel-derived coatings follows similar processing protocols for aging of precursor solutions before dip- or spin-coating and drying and calcining/sintering after coating. An appropriate solution aging period (usually longer for inorganic precursor solutions) is crucial to ensure complete hydrolysis of the starting precursors and thorough intermixing of Ca and P precursor solutions to form monolithic HAp after drying and calcination/sintering heat treatments. Sol aging periods of up to 7 days at ambient temperatures were used with inorganic route−formed coatings (Gan and Pilliar, 2004); 1−24 h aging periods are more common for organic route−formed films. Intermediate reaction products leading to HAp formation remain poorly defined at present. Higher sol aging temperatures (up to 80 °C) result in significant reduction of required aging times (Liu et al., 2002b). Drying of coatings is achieved at temperatures of 100°−200 °C for times sufficient to ensure complete removal of liquid solvent. Calcining and sintering of the dried gels on Ti and Ti alloy substrates can be achieved at temperatures as low as 400 °C. At such low temperatures, amorphous Ca−P coatings are retained, with crystallization resulting only at temperatures higher than about 500 °C. The use of low annealing temperatures is important in ensuring suitable substrate surfaces and substrate microstructure retention (i.e., avoidance of excessive oxide layer formation and phase transformations and grain coarsening that could lower mechanical properties).

Comparison of particulate precursor− and polymeric precursor−formed coatings with regard to microstructure, chemical composition (Ca/P ratio), and in vivo osseointegration potential has been studied using thin film X-ray diffraction and high-resolution field-emission SEM (FE-SEM), Fourier transform infrared spectroscopy, and diffuse reflectance infrared Fourier transform spectroscopy to compare the two coating types formed by dip coating (Gan and Pilliar, 2004). In vivo osseointegration of implants placed in rabbit femoral condyle sites and implant pull-out strengths and interface zone structures at early postimplantation time (9 days) were also studied (Gan et al., 2004a; Tache et al., 2004). High-resolution FE-SEM studies indicated coarser microstructures for the inorganic route−formed coatings with mesoscopic-sized pores at the outer surface in the 2−50 nm size range and greater volume % porosity (∼40% as qualitatively assessed using FE-SEM imaging; Figure 6.4(a)). Crystals ≈200 nm were observed within the coating (as determined by TEM examination of thin films prepared through the coating thickness). For the organic route−formed coatings, pores and individual grains

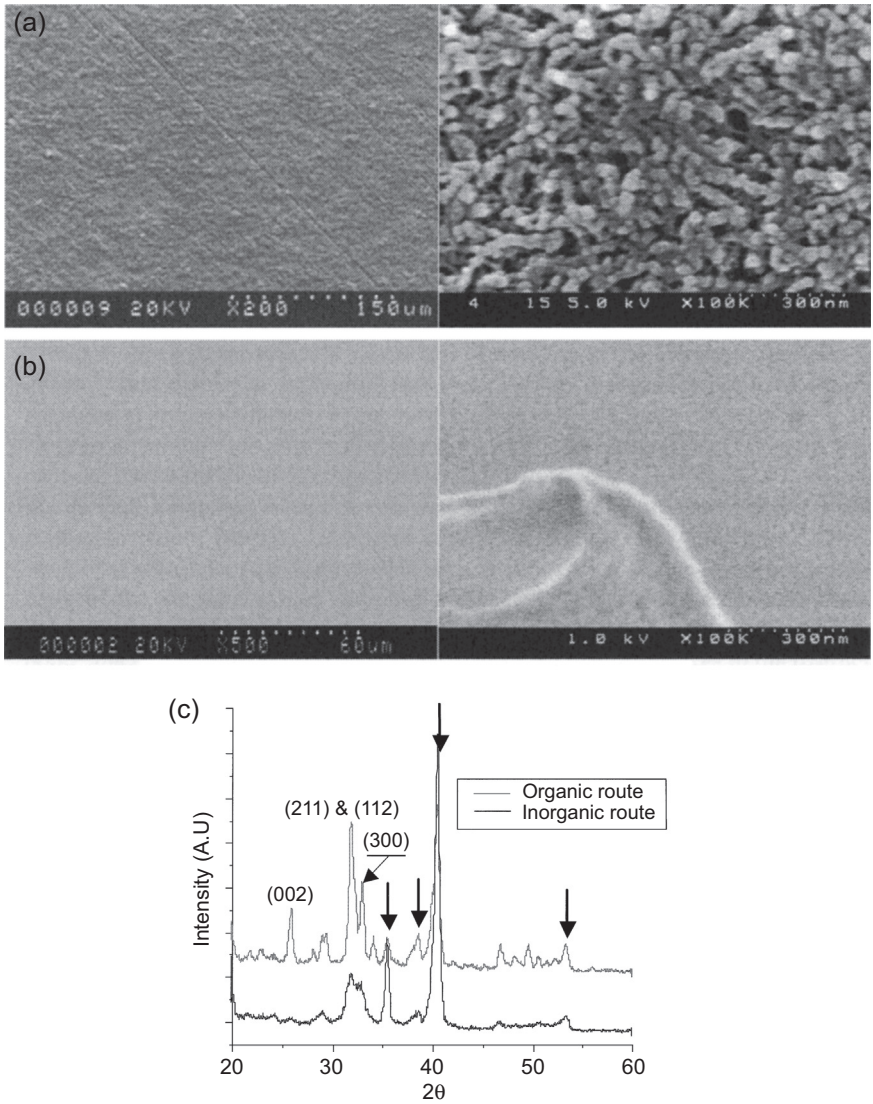


Figure 6.4 Examples of microstructural variation resulting from use of different precursors (inorganic and organic route—formed HAp coatings on Ti6Al4V substrates). Low-resolution SEM (left) and high-resolution FE-SEM (right) of (a) inorganic route sol—gel-formed; (b) organic route sol—gel-formed coating; and (c) XRD spectra confirming the HAp crystal structure of the coatings. The high-resolution image of the inorganic route—formed coating shows a nanocrystalline and nano-porous structure. The organic route—formed coating with an even finer nanocrystalline structure appears featureless. A film defect (lower left corner) is used to focus the image during FE-SEM examination.
With permission Gan and Pilliar (2004).

could not be resolved by high-resolution FE-SEM examination (at 100 K) suggesting nano-scale porosity below the FE-SEM resolution limit (<1 nm − Figure 6.4(b)). Both coating types appeared crystalline (as determined by thin film X-ray diffraction; Figure 6.4(c)) but with broader diffraction peaks compared to well-crystallized HAp "control" samples. This was attributed to the large amount of inherent crystalline defects within the rapidly crystallized sol−gel-formed coatings and, possibly, significant residual strains from strong coating-to-substrate bonding and lattice mismatch at the coating−substrate interface. When examined by optical microscopy, the surface of the organic route−formed coatings appeared smooth and featureless in contrast to the inorganic route−formed coatings that displayed an orange peel−like surface topography, perhaps reflecting a coarser aggregate structure of the particulate precursor sol used to form the coating. Despite these apparent structural differences, the in vivo response showed no significant difference for the two designs in terms of rate of osseointegration as assessed using the pull-out testing of samples implanted in rabbit femoral condyle sites at 9 days postimplantation. Both coating types resulted in significantly faster bone ingrowth compared with uncoated controls that were similarly handled and pull-out tested. In view of the similar in vivo response and that the organic route−formed coatings did not appear to introduce any observable new topographic features to the bone-interfacing implant surfaces, it was concluded that differences in microstructure and surface topography were less significant than surface chemistry in promoting faster osseointegration, at least in this study in which primary fixation was due to bone ingrowth into microscopic (up to 150 μm) interconnected pores. However, the low crystallinity and presumably rapid rate of degradation of both coating types could have resulted in early coating degradation and introduction of new topographical features developing in a short time (i.e., days) after implantation. Therefore, the question of whether chemistry or topography is more significant for enhancing the rate of new bone formation remains open.

6.2.1.2 *Sol−gel-formed titania and TiO_2/HAp composite coatings for bone attachment*

The formation of sol−gel-derived TiO_2 and TiO_2−HAp composite coatings over Ti or Ti alloy substrates on bone-interfacing implants is intended to (1) promote better adherence of an in vitro-formed calcium phosphate (nominally HAp) layer that can serve to enhance mineralization at the surface and implant osseointegration and (2) introduce additional topographic features at the nanomicron, submicron, and micron levels per se to promote faster mineralization and osseointegration.

The osseointegration benefits of TiO_2 for bone bonding were noted in the late 1960s and early 1970s by Branemark and colleagues with commercial purity Ti allowing virtually direct bone-to-implant apposition in vivo (as assessed by light microscopy) at the TiO_2 surface layer (so-called "osseointegration") (Brinker and Mukherjee, 1981). Results from in vitro studies in which Ti/TiO_2 samples were placed in simulated body fluid solutions for periods of days demonstrated calcium phosphate (nominally

HAp) formation on TiO_2 surface (Kim et al., 1996; Li and de Groot, 1993; Li et al., 1994a,b). The in vitro studies suggested the importance of negative surface charge and surface hydroxyl groups for promoting calcium phosphate formation and bone-to-implant attachment in vivo provided that the isoelectric point of the substrate surface oxide was below the pH at the implant site (Kokubo et al., 2000, Chapter. 16). TiO_2 satisfied these conditions as did other oxides (e.g., Ta_2O_5, Nb_2O_5, SiO_2, ZrO_2) (Li et al., 1994b; Miyazaki et al., 2001a,b; Uchida et al., 2001). Using appropriate precursors and processing conditions, formation of sol−gel-derived titania coatings of controlled thickness, microstructure, density, pore size, and surface topography has been reported (Advincula et al., 2005; Areva and Jokinen, 2008; Haddow et al., 1996; Jokinen et al., 1998; Peltola et al., 2000; Piveteau et al., 1999; Rossi et al., 2008; Wen et al., 2007) (and Table 6.2). The structural and topographic features of titania coatings formed this way were shown to significantly influence osteoconductivity and, consequently, the osseointegration potential of implants. Nano-sized pores observed with some of these coatings were suggested to be beneficial for osteogenesis resulting in more rapid osseointegration, a subject that continues to be studied.

TiO_2 formation by sol−gel processing uses various alkoxide precursors with final calcining/sintering anneals typically in the 500−600 °C range. Haddow et al. (1996) used titanium (IV) isopropoxide [$Ti(OCH(CH_3)_2)_4$] dissolved in isopropanol as a sol precursor. The study had as its goal optimization of TiO_2 films suitable for in vitro HAp formation as coatings on implant structures to promote osseointegration. Model substrates (glass slides) were used to investigate the effects of dip rate, sintering temperature, and time on coating characteristics (thickness, physical structure). Low dipping rates and higher sintering anneals (600 °C) resulted in thinner, crack-free films. A later study (Lim et al., 2001) used the same precursor to form functionally graded TiO_2/HAp coatings (calcium nitrate and phosphoric acid were used to form the HAp-forming precursor sol). In that study, the coating was applied to a Ti6Al4V substrate by spin coating, drying at 150 °C for 15 min in air, and calcining at 500 °C to sinter the structure and burn out organics. The graded coating structures were prepared using multiple coatings (10 or so layers with each layer ~0.12−0.13 μm thick) with a progressive decrease of TiO_2 and an increase of HAp from the substrate interface to the coating surface. In another study aimed at forming a dual-layered HAp/TiO_2 sol−gel coating over Ti−Zr alloy substrates (inner layer of TiO_2 and outer layer HAp), Wen et al. (2007) used tetrabutyl orthotitanate ($C_{16}H_{36}TiO_4$) diluted in ethanol as the precursor for the TiO_2 sol preparation and triethyl phosphate in anhydrous ethanol and calcium nitrate in ethanol as the sol for HAp preparation. Spin coating was used to deposit the appropriately aged sol−gel mixtures with final sintering (after drying at 80 °C) at 600 °C. The bilayer coating was thick (25 μm + 25 μm); therefore, not surprisingly, resulted in the TiO_2 (anatase) film cracking. It was suggested that the cracks were inconsequential because they were subsequently covered over by the HAp layer (the cracks may even have assisted in fixing the HAp to the TiO_2 layer). Part of the study rationale was for the deeper TiO_2 layer to promote HAp adherence as well as to act as a protective barrier layer. Peltoa et al. (2000) used tetraisopropyl orthotitanate [$Ti((CH_3)_2CHO)_4$], but dissolved it in absolute ethanol to form a solution that was

Table 6.2 Some titania and titania composite coatings for bone bonding—processing and characteristics

Coating-substrate	Precursor	Hydrolysis and aging conditions	Coating method	Drying conditions	Calcining/sintering conditions	Coating characteristics/notes	References
TiO_2−SiO_2 (glass slide)	Titanium (IV) isopropoxide dissolved in isopropanol	Stirred for 24 h	Dip coat; 1.5, 1.0, 0.5, 0.1 mm/s	Air dry for 1 h	100 and 600 °C for 1 or 3 h	No film cracking only with slowest withdrawal rate (i.e., 0.1 mm/s); films adhered for sintering $T > 300$ °C	Weng (1999)
HAp + TiO_2 −TiZr alloy	Tetrabutyl orthotitanate diluted with EtOH– > TiO_2 sol; TEP + $Ca(NO_3)_2 \cdot 4H_2O$– > HAp sol	TiO_2 sol hydrolyzed for 24 h; HAp as described previously	Spin coating; 3000 rpm for 15 s	80 °C for 2 h	600 °C for 20 min in argon	TiO_2 crystallized as anatase; cracked TiO_2 covered over by HAp	Wen et al. (2007)
Dense TiO_2−Ti	Tetra-n-butoxytitanate dissolved in *n*-butanol in Ar atmosphere	?	Dip coat; withdrawal rate = 1 mm/s	Air dry for 1 h	500 °C	Dense, crack-free coatings; biofunctionalized with amino groups	Lim et al. (2001)
Nanoporous TiO_2 −Ti	(A) Tetraethoxytitanate dissolved in EtOH and (B) nitric acid aqueous solution dissolved in dry ETOH; mix A and B	?	Dip coat over previously made dense TiO_2 coating; withdrawal rate = 1 mm/s	Store in saturated EtOH for 24 h, then supercritically dried in CO_2 for 3 days	500 °C	Biofunctionalized with amino groups	Faust et al. (2002)

mixed with a second solution made from ethyleneglycol monoethylether [$C_2H_5OCH_2$-CH_2OH], deionized water and fuming hydrochloric acid dissolved in ethanol to form a sol. The sol was kept cold (0 °C) to slow down the condensation reaction and then applied by dip coating. Final sintering was at 500 °C for 10 min. The objective of the study was to determine the effect of varying sol aging time on the structure and in vitro calcium phosphate deposition. It was shown that varying sol aging time had an effect on the structure of the outermost TiO_2 surface at the nanometer-scale level. It was suggested that this may significantly affect in vivo bone formation. Formation of dense or nano porous TiO_2 films was reported by others (Faust et al., 2002; Heidenau et al., 2001). Using tetra butoxytitanate dissolved in *n*-butanol under Ar atmosphere as the sol precursor for dip-coating titanium substrates, drying in air and calcining at 500 °C gave dense coatings. Using tetra ethoxytitanate dissolved in dry ethanol under Ar atmosphere and mixing with an aqueous nitric acid dissolved in dry ethanol precursor, dip coating, drying in air, and storage in saturated EtOH for 24 h before supercritical drying in CO_2 for 3 days and then calcining at 500 °C resulted in formation of a nano-porous titania coating. These studies illustrate how control precursors and processing conditions can be used to achieve desired coating microstructural features. To further promote osseointegration, biofunctionalization of sol–gel-formed, nano-porous TiO_2 coatings using adhesion peptides to promote better cell–coating interaction was investigated (Faust et al., 2002).

6.2.1.3 Other sol–gel-derived coatings for orthopedic/dental implants – Ta_2O_5, TiO_2/SiO_2, $CaTiSiO_3$ (ZrO_2)

Although the majority of reported studies on sol–gel-derived coatings for bone-interfacing implant applications and for achieving osseointegration have dealt with HAp, TiO_2, and TiO_2–HAp composite coatings placed over Ti-based substrates, other sol–gel-formed oxides have also been studied. The early studies by Hench et al. (1971) on bioactive glasses (glasses made with specific Na_2O-CaO–P_2O_5-SiO_2 formulations) suggested the importance of hydroxyl surface groups and negative surface charge in promoting calcium phosphate layers leading to bone attachment. Subsequent studies suggested a beneficial role of Si ion release in osteoinductivity leading to investigations of sol–gel-derived TiO_2–SiO_2 coatings (Aaritalo et al., 2007; Areva and Jokinen, 2008). In these studies, sols were prepared using tetraisopropylorthotitanate (TIPT, $Ti(CH_3)_2CHO)_4$) dissolved in ethanol and mixed with an ethyleneglycolmonoethylether ($C_2H_5OCH_2OH$), deionized water fuming hydrochloric acid, and ethanol solution to form the TiO_2 sol. This was mixed with the SiO_2-forming sol (tetraethyl orthosilicate (TEOS, $Si(OC_2H_5)_4$) ethanol and an HNO_3 catalyst, aged at 40 °C for 24 h and cooled to 0 °C for the dipping process. Coated samples were heat treated at 500 °C and the dipping process repeated to give the desired multilayered final coating thickness. The resulting TiO_2–SiO_2 coating was nanoporous (2–50-nm-sized pores) and compositionally heterogeneous with crystalline TiO_2 particles surrounded by amorphous SiO_2. The two oxides were bonded through Ti–O–Si bonds. Varying SiO_2:TiO_2 ratios through appropriate selection of sol ratios and processing parameters resulted in formation of coatings suitable for bone or soft-tissue attachment, thus highlighting a

novel feature of sol–gel coating preparation, namely the ability to "engineer" the coating by appropriate processing procedures for specific applications.

Arnould et al. (2009) formed a tantalum oxide coating by a modified two-step sol–gel process involving a first step of dipping the Ti substrate into a tantalum butoxide ($Ta(OCH_2CH_2CH_2CH_3)_5$)-ethanol/toluene solution followed by hydrolysis to form OH^- reaction groups followed by a second step involving immersion in a butane diphosphonic acid ($PO_3H_2–(CH_2)_4–PO_3H_2$) solution to functionalize the surface. The sample was then soaked for different periods (days) in SBF to form a calcium phosphate deposition layer.

6.2.2 Soft-tissue attachment

Achieving effective soft-tissue attachment to implants without the formation of a fibrous capsule interlayer between gingival or epithelial tissues is desirable for creating an effective "seal" at soft-tissue–implant junctions, thereby inhibiting bacterial ingress and implant-related infections along transcutaneous soft-tissue–implant tracts. Although it is generally recognized that surface roughness or microporous structures (i.e., features large enough to support bacterial ingress) are more susceptible to bacterial colonization than very smooth surfaces, nano-sized pores and topographical features appear to favor attachment of connective and epithelial tissues, thereby inhibiting biofilm formation. Studies have suggested that sol–gel-formed TiO_2 coatings may allow effective soft-tissue-to-implant attachment, an important consideration for dental implants and other transcutaneous implants. Effective attachment of soft tissues to nano-sized topographical features as can be formed with sol–gel-derived titania coatings has been reported [61] and suggests that it is a viable strategy for design of soft-tissue-interfacing transcutaneous/percutaneous implant components (Areva et al., 2004; Rossi et al., 2008). The topic is ripe for further investigation.

6.2.3 Sol–gel "barrier" coatings for biomaterials

Sol–gel coatings serving as protective layers over metallic biomaterials to achieve improved corrosion resistance represents another potential application in the biomedical field. Studies of coatings on 316L stainless steel (Galliano et al., 1998; Vijayalakshmi et al., 2008), Co-based alloys (Amato et al., 2005), Ti6Al4V (Duran et al., 2004), Mg (Shi et al., 2009), and noble dental casting alloys (Yoshida et al., 1999) have been reported (Table 6.3). Modification of 316L stainless steel for long-term implant use could provide a lower cost metal (compared with Ti or Ti alloys) for fabricating joint replacement implants. To this end SiO_2-containing sol–gel-derived coatings have been investigated (Duran et al., 2004; Galliano et al., 1998). To form SiO_2 coatings, Galliano et al. (1998) used tetraethylorthosilicate (TEOS, $Si(OC_2H_5)_4$) as a precursor alone or in combination with methyl-triethoxysilane (MTES, $CH_3Si(OCH_3)_3$) in a 1:1 M ratio resulting in protective layers of thickness ranging from 140 to 1400 nm over 316L stainless steel substrates. The dip-coated samples, after drying, were annealed at 500 °C for 1 h, resulting in dense crack-free coatings. Electrochemical impedance spectroscopy assessment of samples in an SBF solution at 37 °C and pH = 7.4 indicated

Table 6.3 Soft-tissue-interfacing, protective/barrier coatings − examples of processing and characteristics

Coating-substrate	Precursor	Hydrolysis and aging conditions	Coating method	Drying conditions	Calcining/sintering conditions	Coating characteristics/notes	References
TiO_2−SiO_2−titanium	TiO_2 and SiO_2 mixed sols; tetraisopropylorthotitanate and tetra ethylorthosilicate based, respectively	See the text and reference for details	Dip coat; 0.3 mm/s	−	500 °C for 10 min; repeated with 5 layers	Smooth coatings, 2−50 nm pores; silica release with SiO_2 enriched outer layer	Aaritalo et al. (2007)
SiO_2−316L stainless steel	A) Tetraethylorthosilicate (TEOS); B) TEOS + methyl-triethoxysilane (MTES)	(A) Stable for weeks; (B) stirred 2 h, sit 30 min	Dip coat; withdrawal rate between 10 and 40 cm/min	Air dry	500 °C for 1 h; multilayered	A) Crack-free coatings up to 350 nm; multilayer; B) coatings 1400 nm; excellent corrosion resistance	Galliano et al. (1998)
SiO_2 (with bioactive particles)−316L stainless steel	TEOS + MTES (+HAp, bioactive glass or glass-ceramic particles)	—	Dip coat; withdrawal rate = 4 cm/min	Air dry @ RT 30 min	450 °C for 30 min	Single- and double-layer coatings improve corrosion resistance; display bioactivity	Garcia et al. (2004)
Hybrid (SiO_2 + CH_3 groups) - CoCrMo alloy	TEOS + MTES	Sol made at 40 °C under reflux 3 h	Dip coat; withdrawal rate = 3.5 cm/s	Air dry for 21 h	450 °C or 550 °C for 30 min	Continuous defect-free coatings; enhanced corrosion resistance (more so for 450 °C sintered samples)	Amato et al. (2005)
Nanoporous TiO_2−Ti	A) Tetraethoxytitanate dissolved in EtOH, B) HNO_3 Aqueous solution dissolved in dry ETOH; mix A and B	—	Dip coat over previous dense TiO_2 coating; withdrawal rate = 1 mm/s	Store in saturated EtOH 24 h + supercritical dry in CO_2 for 3 days	500 °C	Biofunctionalized with amino groups	Faust et al. (2002)
TiO_2−Mg	Titanium butoxide + isobutanol	U/s agitated 30 min + aged 24 h	Dip coat; withdrawal rate = 240 mm/min @ 50 °C	Air dry 10 min	120 °C for 7−24 h	Increase in corrosion resistance	Shi et al. (2009)
HAp doped with $AgNO_3$−cpTi	Calcium nitrate tetrahydrate + triethyl phosphite (HAp sol) doped with $AgNO_3$ powder	Ca and P precursor sols mixed in Ar; aged @ 40 °C, 24 h, filtered, + 40 °C, 4 days	Spin coat; 5000 rpm for 50 s	Dried @ 70 °C 12 h	650 °C for 3 h	Reduced bacterial counts (*Staphylococcus epidermis* , *Staphylococcus aureus*); maintained osteoconductivity	Chung et al. (2006)

good corrosion protection for both the TEOS alone and TEOS-MTES−derived coatings, at least for the 200-h soaking periods studied. Duran et al. (2004) also used TEOS−MTES precursor solutions to form SiO_2 coatings on 316L stainless steel as well as on Co-based and Ti alloy substrates with the goal of inhibiting metal ion release. Coatings were applied by dipping with annealing after drying at 450 °C for 30 min. Single- and double-layer coatings were investigated using potentiodynamic polarization, electrochemical impedance spectroscopy, and plasma atomic emission spectroscopy to assess corrosion characteristics in vitro (samples in SBF at 37 °C and pH = 7.3 for 30 days). Reduced passive current densities resulted, but no improvement in breakdown potential was observed. Although the protective nature of such coatings was suggested by the lower corrosion currents observed in these relatively short-term studies, the longer term effectiveness remains to be demonstrated. These studies also investigated the inclusion of bioactive layers (either HAp or SiO_2−CaO−P_2O_5 coatings) over the SiO_2 layers deposited on 316L stainless steel as well as hybrid coatings containing HAp, bioactive glass or glass-ceramic particles. TEOS−MTES precursor solutions were used in these studies (Garcia et al., 2004). Contrary to these reported studies indicating the positive benefits for improved corrosion resistance of SiO_2 sol−gel-derived coatings, de Dambornenea et al. (1995) found no significant protection against electrochemical corrosion of 304 stainless steel samples coated using TEOS, ethanol, and distilled water sol-derived coatings. They proposed the lack of improvement to coating characteristics, namely micropores and microcracks produced during the sintering process. The use of a 304 stainless steel substrate, not as corrosion-resistant in the body environment as 316L stainless steel, may also have affected the outcome.

Sol−gel-derived HAp coatings on 316L stainless steel serving as protective barriers in addition to being bioactive were reported (Vijayalakshmi et al., 2008). The coatings were prepared using $Ca(NO_3)_2 \cdot 4H_2O$ and P_2O_5 precursors dissolved in ethanol and applied by spin coating to form triple-layered crack-free coatings ($\approx$16 μm total thickness). Good corrosion protection characteristics (in Ringer's solution) were reported with crystalline HAp coatings formed by sintering at 800 °C.

Cobalt-based alloys are used extensively for the bearing components of joint replacement implants primarily because of their superior wear resistance compared with other metallic biomaterials. The excellent wear resistance that properly processed CoCrMo alloys can display as well as their good corrosion resistance (related to formation of a Cr,Mo-containing passive oxide film) makes them a popular choice for these applications. Degradation and metal ion release to some extent, nevertheless, does occur in vivo. Cr and Co release are of particular concern due to reports of their ions promoting bone resorption (Lee et al., 1997; Mathiensen et al., 1991). To minimize metal ion release, Amato et al. (2005) used SiO_2 sol−gel-formed coatings, described as "hybrid" coatings in view of the inorganic−organic TEOS−MTES precursors used for their formation, over cast CoCrMo alloys. The dip-coating procedure used was similar to that described previously for coating stainless steel substrates with final sintering temperatures of 450 or 550 °C. Corrosion testing (potentiodynamic polarization and EIS assessment) with samples immersed in SBF solution at 37 °C, pH 7.3 for periods up to 720 h indicated improved corrosion resistance as a result of the

continuous defect-free coating that was reported, more so for coatings sintered at 450 °C. However, the protection was observed to decrease with increasing immersion time, a result of slow coating degradation.

Mg and Mg-based alloys are attracting considerable interest currently as possible biodegradable metals for use in fabricating fracture fixation devices. Mg is biocompatible but its' too-rapid rate of in vivo degradation limits its usefulness. Shi et al. (2009) reported on a TiO_2 sol−gel-formed coating placed over a micro-arc oxidized (MAO) Mg substrate as a possible approach for overcoming this limitation. The MAO of Mg results in a thick (∼12 μm) anodized oxide surface region with reported surface "pores" (more correctly described as "pits"). A sol−gel-derived TiO_2 coating applied by dipping over the MAO layer provides a more stable barrier over the MgO layer (also containing some MgF) while sealing the pores formed by the MAO process. The TiO_2 was prepared from a titanium butoxide ($Ti(OC_4H_9)_4$ and isobutanol (C_4H_9OH) precursor solution with dip coating at 50 °C, air drying, and then hydrothermal treatment at 120 °C for 7 h in water or steam to achieve coating densification. The TiO_2 so formed appeared amorphous and served to seal the pores of the MAO MgO/MgF coating. Corrosion testing demonstrated the effectiveness of the MAO−TiO_2 as a barrier to Mg corrosion early on. At later times (periods corresponding to completion or near-completion of fracture healing), degradation of the protective TiO_2 film occurred followed by rapid dissolution of Mg. Mg is known to be nontoxic and biocompatible and will eventually totally degrade in the body. The very small amount of TiO_2 remaining was considered by the investigators not to pose a significant toxicity issue.

A study on the use of sol−gel-formed protective SiO_2 coatings has been reported in the field of dental restorative materials. Yoshida et al. (1999) reported on formation of SiO_2 coatings over Ti-implanted Ag−Pd−Cu−Au dental casting alloys. A SiO_2 coating is applied by dip coating using a sol prepared from tetramethoxysilane oligomer [$Si(OCH_3)_4$] in a methyl alcohol solution containing toluene and sulfonic acid. After air drying, the coated samples are annealed at 120 °C for 20 min and then held at room temperature to form a SiO_2 coating approximately 0.5 μm thick. The SiO_2 coating proved effective in minimizing accumulation of plaque on the dental restoration. It was also claimed to reduce metal ion release from the Ag−Pd−Cu−Au device, thereby reducing the risk of an allergic response.

A novel application of sol−gel-formed HAp coatings as a barrier coating was recently reported in a study aimed at developing novel tissue-engineered implants for articular cartilage regeneration. Biphasic implants (i.e., porous calcium polyphosphate (CPP), a degradable inorganic polymer, with in vitro−formed cartilage) placed in defects formed in sheep knee sites appeared successful for defect repair but with low cartilage-to-CPP interfacial shear strength limiting usefulness (Kandel et al., 2006). Attempts to improve this interface strength by forming a zone of mineralized cartilage at the interface in vitro (simulating the calcified cartilage zone of natural cartilage−subchondral bone junctions) indicated that high rates of CPP degradation and accumulation of the degradation product at the junction appeared to inhibit cartilage mineralization at this location. To overcome this, a thin sol−gel-formed coating was deposited over the porous CPP using an Inorganic precursor by methods similar to

those reported by Gan and Pilliar (2004). The results indicated the effectiveness of the coating as a barrier limiting the rate of CPP degradation product build-up resulting in mineralized cartilage formation in direct contact with the CPP and a three- to four-fold increase in interfacial shear strength (Pierre et al., 2012). A more recent study using the organic route−formed HAp coating has resulted in a somewhat stronger interface presumably a result of the more continuous HAp coating formed via the organic route further inhibiting CPP degradation product release (Lee et al., under review).

6.2.4 Sol−gel-derived antibacterial coatings

Implant-associated infection is a major concern with modern-day implants. Estimates of this with orthopedic implants (fracture fixation devices and joint replacements) range from 0.5 to 1% at best and higher for complex cases (i.e., in patients with diabetes or undergoing revision arthroplasty) (Bedair and Della Valle, 2013, Chap. 100). For dental and other transcutaneous implants, the incidence is expected to be even higher although reliable published data are not available. As discussed previously, this is a strong motivator for development of implant designs to form reliable soft-tissue-to-implant "seals" with surfaces to combat bacterial adhesion and biofilm formation. Investigations to prevent bacterial adhesion can be divided into two camps: (1) use of antibiotics either tethered to implant surfaces or absorbed within pores or other surface depots that release bactericidal agents at an appropriate rate to combat infection (specific antibacterial drugs), and (2) controlled release of trace ions such as Ag^+ or Zn^{2+} known to be cytotoxic to bacteria (nonspecific agents). The growing awareness and concern over development of antibiotic drug-resistant bacteria favors the latter strategy. To this end, a limited number of studies incorporating Ag^+ or Zn^{2+} ions in sol−gel-derived coatings and films have been reported (Table 6.3). Chen et al. (2007) investigated Ag-containing HAp coatings applied over Ti6Al4V substrates. The precursors used for HAp coating formation were calcium nitrate tetrahydrate with methyl alcohol solutions to form the Ca precursor and triethyl phosphite in acetic acid as the P precursor. The two precursors were mixed, resulting in the formation of a calcium phosphate intermediate solution to which was added 1.0 or 1.5% silver nitrate. The mixed solution was aged for 4−5 days at 40 °C, applied to Ti alloy substrates by spin coating, dried at 70 °C, and then annealed at 650 °C for 3 h. Samples so formed were assessed in vitro for antimicrobial activity using *Staphylococcus epidermis* and *Staphylococcus aureus* bacterial strains. In addition, the response to an osteoblast precursor cell line (human embryonic palatal mesenchyme cells) was assessed. The coated samples appeared to be effective in inhibiting microbial adhesion while not affecting osteoblast precursor cell proliferation or differentiation, suggesting their usefulness with bone-interfacing implants and future in vivo studies to verify the response. In another in vitro study focusing on HAp sol−gel-formed coatings doped with Ag^+ or Zn^{2+} over Ti alloy dental implants for resisting attack by *Streptococcus mutans* on a human gingival fibroblast cell line, Chung et al. (2006) reported that both Ag^+ and Zn^{2+} were effective in inhibiting infection while retaining sample biocompatibility. The Ag^+-containing coatings were made using calcium nitrate tetrahydrate [$Ca(NO_3)_2{-}4H_2O$], triethyl phosphate [$(C_2H_5O)_3PO$]

and $AgNO_3$ in 2-methoxy ethanol to form the precursors, aging for 16 h at 80−90 °C, drying and then applying the gel by spin-coating, predrying at 150 °C, and annealing at 400 °C for 3 min. The procedure was repeated to achieve a desired final coating thickness ~20 μm, which was further annealed at 600 °C for 1 min. The intended application in this case was for coating the coronal implant region and abutment of endosseous dental implants to provide desirable soft-tissue−implant response at the transgingival interface region. Another model study demonstrating the effectiveness of Ag^+-doped sol−gel-derived antibacterial films with Ag-SiO_2 films formed on glass slides was reported by Jeon et al. (2003). Disc-shaped samples were dip coated with $AgNO_3$ being added to the sol prepared from TEOS, 2-ethoxyethanol, distilled water, and nitric acid. The SiO_2 sol was mixed and stirred at room temperature with the $AgNO_3$ being added after 4 h. Coated samples were dried at 100 °C for 30 min, and then annealed at temperatures between 300 °C and 600 °C, with the 600 °C anneal demonstrating the more effective antibacterial properties. In vitro assessment demonstrated the effectiveness of the Ag-doped coatings against *S. aureus* and *Escherichia coli* bacterial strains. Although limited in number and confined only to in vitro assessment, the results of the studies suggest potential effectiveness of such cation-doped HAp sol−gel-derived coatings to combat bacterial adhesion and early infection with implants.

6.3 Concluding remarks

Sol−gel-formed coatings represent one of a number of surface design strategies intended to improve implant performance. As noted in this review of reports on formation and characteristics of sol−gel coatings, the process offers the possibility of designing coating characteristics as required for specific applications through appropriate selection of precursors and conditions used through all stages of coating formation from the initial sol formation (hydrolysis and condensation reactions), transformation of the sol to a gel (particulate agglomeration, polymeric network formation), gel drying, and finally, calcining/sintering treatments. The process presents a relatively low-cost approach to implant surface modification. However, the complexities of processing in terms of selection of parameters through the different stages and the relative paucity of information on sensitivity to processing conditions present the challenge for further research and development of this promising technology for control of implant surface characteristics.

References

Aaritalo, V., Areva, S., Jokinen, M., Linden, M., & Peltola, T. (2007). Sol−gel-derived TiO_2−SiO_2 implant coatings for direct tissue attachment. Part I: design, preparation and characterization. *Journal of Materials Science: Materials in Medicine, 18*, 1863−1873.

Advincula, M., Fan, X., Lemons, J., & Advincula, R. (2005). Surface modification of surface sol-gel derived titanium oxide films by self-assembled monolayers (SAMs) and non-specific adsorption studies. *Colloids and Surfaces B: Biointerfaces, 42*, 29−43.

Amato, L. E., Lopez, D. A., Galliano, P. G., & Cere, S. M. (2005). Electrochemical characterization of sol-gel hybrid coatings in cobalt-based alloys for orthopaedic implants. *Materials Letters, 59*, 2026−2031.

Areva, S., Aaritalo, V., Tuusa, S., Jokinen, M., Linden, M., & Peltola, T. (2007). Sol-gel-derived TiO_2−SiO_2 implant coatings for direct tissue attachment. Part II: evaluation of cell response. *Journal of Materials Science: Materials in Medicine, 18*, 1633−1642.

Areva, S., & Jokinen, M. (2008). Ensuring implant fixation and sol-gel derived ceramic coatings. *Key Engineering Materials, 377*, 111−132.

Areva, S., Paldan, H., Peltola, T., Narhi, T., Jokinen, M., & Linden, M. (2004). Use of sol-gel-derived titania coating for direct soft tissue attachment. *Journal of Biomedical Materials Research, 70A*, 169−178.

Arnould, C., Volcke, C., Lamarque, C., Thiry, P. A., Delhalle, J., & Mekhalif, Z. (2009). Titanium modified with layer-by-layer sol-gel tantalum oxide and an organodiphosphonic acid: a coating for hydroxyapatite growth. *Journal of Colloid and Interface Science, 336*, 497−503.

Bedair, H., & Della Valle, C. J. (2013). Infection. In D. J. Berry, & J. R. Lieberman (Eds.), *Surgery of the hip* (pp. 1196−1206). Philadelphia, PA: Elsevier Saunders.

Bornside, D. E., Macosko, C. W., & Scriven, L. E. (1987). On modeling of spin coating. *Journal of Imaging Technology, 13*, 122−129.

Branemark, P. I., Hansson, B. O., Adell, R., Breine, U., Lindstrom, J., Hallen, O., et al. (1977). Osseointegrated implants in the treatment of the edentulous jaw, experience from a 10-year period. *Scandinavian Journal of Plastic and Reconstructive Surgery, 11* (Suppl. 16), 1−132.

Brendel, T., Engel, A., & Russel, C. (1992). Hydroxyapatite coatings by a polymeric route. *Journal of Materials Science: Materials in Medicine, 3*, 175−179.

Brinker, C. J., Frye, G. C., Hurd, A. J., & Ashley, C. S. (1991). Fundamentals of sol-gel dip coating. *Thin Solid Films, 201*, 97−108.

Brinker, C. J., & Mukherjee, S. P. (1981). Comparison of sol-gel-derived thin films with monoliths in a multicomponent silicate glass system. *Thin Solid Films, 77*, 141−148.

Brinker, C. J., & Scherer, G. (1990). *Sol-gel science. The physics and chemistry of sol-gel processing*. San Diego, CA: Academic Press, Inc.

Carrado, A. (2013). Development of bioactive hydroxyapatite coatings on titanium alloys. *Key Engineering Materials, 533*, 183−193.

Chai, C. S., & Ben-Nissan, B. (1999). Bioactive nanocrystalline sol−gel hydroxyapatite coatings. *Journal of Materials Science: Materials in Medicine, 10*, 465−469.

Chen, W., Oh, S., Ong, A. P., Oh, N., Liu, Y., Courtney, H. S., et al. (2007). Antibacterial and osteogenic properties of silver-containing hydroxyapatite coatings produced using a sol-gel process. *Journal of Biomedical Materials Research, 82A*, 899−906.

Choudhury, P., & Agrawal, D. C. (2011). Sol-gel derived hydroxyapatite coatings on titanium substrates. *Surface and Coatings Technology, 206*, 360−365.

Chung, R.-J., Hsieh, M.-A., Huang, C.-W., Peng, L.-H., Wen, H.-W., & Chin, T.-S. (2006). Antimicrobial effects and human gingival biocompatibility of hydroxyapatite sol-gel coatings. *Journal of Biomedical Materials Research, 76B*, 169−178.

de Dambornenea, J., Pellegrini, N., de Sanctis, O., & Duran, A. (1995). Electrochemical behaviour of Si sol-gel coatings on stainless steel. *Journal of Sol-Gel Science and Technology, 4*, 239−244.

Duran, A., Conde, A., Gomez Coedo, A., Dorado, T., Garcia, C., & Cere, S. (2004). Sol-gel for protection and bioactivation of metals used in orthopaedic devices. *Journal of Materials Chemistry, 14*, 2282−2290.

Emslie, A. G., Bonner, F. T., & Peck, L. G. (1958). Flow of a viscous fluid on a rotating disk. *Journal of Applied Physics, 29*, 858−862.

Esfahani, H., Dabir, F., Taheri, M., Sohrabi, N., & Toroghinejad, M. R. (2012). Sol-gel derived hydroxyapatite coating on TiB_2/TiB/Ti substrate. *Surface Engineering, 28*, 526−531.

Faust, V., Heidenau, F., Schmidgall, J., Stenzel, F., Lipps, G., & Ziegler, G. (2002). Biofunctionalized biocompatible titania coatings for implants. *Key Engineering Materials, 206−213*, 1547−1550.

Filiaggi, M. J., Pilliar, R. M., & Abdulla, D. (1996). Evaluating sol-gel ceramic thin films for metal implant applications. Part II: adhesion and fatigue properties of zirconia films on Ti-6Al-4V. *Journal of Applied Biomaterials, 33*, 239−256.

Galliano, P., de Damborena, J. J., Pascual, M., & Duran, A. (1998). Sol-gel coatings on 316L steel for clinical applications. *Journal of Sol-Gel Science and Technology, 13*, 723−727.

Gan, L., & Pilliar, R. M. (2004). Calcium phosphate sol-gel-derived thin films on porous-surfaced implants for enhanced osteoconductivity: I−synthesis and characterization. *Biomaterials, 25*, 5303−5312.

Gan, L., Wang, J., & Pilliar, R. M. (2004a). Evaluating interface strength of calcium phosphate sol-gel-derived thin films to Ti6Al4V substrate. *Biomaterials, 26*, 189−196.

Gan, L., Wang, J., Taché, A., Valiquette, N., Deporter, D. A., & Pilliar, R. (2004b). Calcium phosphate sol-gel-derived thin films on porous-surfaced implants for enhanced osteoconductivity: II−short-term in vivo studies. *Biomaterials, 25*, 5313−5321.

Garcia, C., Cere, S., & Duran, A. (2004). Bioactive coatings prepared by sol-gel on stainless steel 316L. *Journal of Non-Crystalline Solids, 348*, 218−224.

Gross, K. A., Chai, C. S., Kannangara, S. K., & Ben-Nissan, B. (1990). Thin hydroxyapatite coatings via sol-gel synthesis. *Journal of Materials Science: Materials in Medicine, 9*, 839−843.

Haddow, D. B., Kothari, S., James, P. F., Short, R.. D., Halton, P.. V., & van Noort, R. (1996). Synthetic implant surfaces 1. The formation and characterization of sol-gel titania films. *Biomaterials, 17*, 501−507.

Heidenau, F., Stenzel, F., & Ziegler, G. (2001). Structured porous titania as a coating for implant materials. *Key Engineering Materials, 192-195*, 87−90.

Hench, L. L., Splinter, R. J., Allen, W. C., & Greenlee, T. K. (1971). Bonding mechanisms at the interface of ceramic prosthetic materials. *Journal of Biomedical Materials Research Symposium, 2*, 117−141.

Hench, L. L., & West, J. (1990). The sol-gel process. *Chemical Reviews, 90*, 33−72.

Jeon, H.-J., Yi, S.-C., & Oh, S.-G. (2003). Preparation and antibacterial effects of Ag−SiO_2 thin films by sol-gel method. *Biomaterials, 24*, 4921−4928.

Jillavenkatesa, A., & Condrate, R. A., Sr. (1998). Sol-gel processing of hydroxyapatite. *Journal of Materials Science, 33*, 4111−4119.

Jokinen, M., Patsi, M., Rahaiala, H., Peltola, T., & Rosenholm, J. B. (1998). Influence of sol and surface properties on in vitro bioactivity of sol-gel-derived TiO_2 and TiO_2−SiO_2 films deposited by dip-coating method. *Journal of Biomedical Materials Research, 42*, 295−302.

Kandel, R. A., Grynpas, M., Pilliar, R., Lee, J., Waldman, S., Zalzal, P., et al. (2006). Repair of osteochondral defects with biphasic cartilage−calcium polyphosphate constructs in a sheep model. *Biomaterials, 27*, 4120−4131.

Kim, H.-M., Miyaji, F., Kokubo, T., & Nakamara, T. (1996). Preparation of bioactive Ti and its alloys via simple chemical surface treatment. *Journal of Biomedical Materials Research, 32*, 409−417.

Kokubo, T., Kim, H. M., Kawashita, M., & Nakamura, T. (2000). What kinds of materials exhibit bone-bonding? In J. E. Davies (Ed.), *Bone engineering* (pp. 190−194). Toronto, Canada: Em Squared Inc.

Landau, L. D., & Levich, B. G. (1942). Dragging of a liquid by a moving plate. *Acta Physiochimica U.R.S.S, 17*, 42−54.

Lee, S., Brennan, F., Jacobs, J., Urban, P., Ragusa, D., & Glant, T. (1997). Human monocyte/macrophage response to cobalt-chromium corrosion products and titanium particles in patients with total joint replacements. *Journal of Orthopaedic Research, 15*, 40−49.

Lee, W. D., Hurtig, M. B., Pilliar, R. M., Stanford, W. L., & Kandel, R. A. Scaffold-free engineering of hyaline cartilage with a calcified zone using bone marrow stromal cells, *Osteoarthritis and Cartilage* (under review).

Li, P., & de Groot, K. (1993). Calcium phosphate formation within sol-gel prepared titania in vitro and in vivo. *Journal of Biomedical Materials Research, 27*, 1495−1500.

Li, P., Kangasniemi, J., de Groot, K., & Kokubo, T. (1994a). Bonelike hydroxyapatite induction by a gel-derived titania on titanium substrate. *Journal of the American Ceramic Society, 77*, 1307−1312.

Li, P., Ohtsuki, C., Kokubo, T., Nakanishi, K., Soga, N., & de Groot, K. (1994b). The role of hydrated silica, titania, and alumina in inducing apatite on implants. *Journal of Biomedical Materials Research, 28*, 7−15.

Lim, Y.-M., Hwang, K.-S., & Park, Y.-J. (2001). Sol-gel functionally graded TiO_2/HAp films on Ti-6Al-4V implants. *Journal of Sol-Gel Science and Technology, 21*, 123−128.

Liu, D.-M., Yang, Q., Troczynski, T., & Hakimi, D. (2002a). Effect of hydrolysis on the phase evolution of water-based sol-gel hydroxyapatite and its application to bioactive coatings. *Journal of Materials Science: Materials in Medicine, 13*, 657−665.

Liu, D.-M., Yang, Q., Troczynski, T., & Tseng, W. (2001). Water-based sol-gel synthesis of hydroxyapatite process development. *Biomaterials, 22*, 1721−1730.

Liu, D.-M., Yang, Q., Troczynski, T., & Tseng, W. (2002b). Aging effect on the phase evolution of water-based sol-gel hydroxyapatite. *Biomaterials, 23*, 1227−1236.

Liu, D.-M., Yang, Q., Troczynski, T., & Tseng, W. J. (2002c). Structural evolution of sol-gel-derived hydroxyapatite. *Biomaterials, 23*, 1679−1687.

Liu, D.-M., Yang, Q., & Troczynski, T. (2002d). Sol-gel hydroxyapatite coatings on stainless steel substrates. *Biomaterials, 23*, 691−698.

Mathiensen, F., Lind Gren, J., Blomgren, G., & Reinbolt, F. (1991). Corrosion of modular hip prostheses. *Journal of Bone and Joint Surgery, 73B*, 569−575.

Mavis, B., & Cuneyt Tas, A. (2000). Dip coating of calcium hydroxyapatite on Ti-6Al-4V substrates. *Journal of the American Ceramic Society, 83*, 989−991.

Metikos-Hukovic, M., Tkalcec, E., Kwokal, A., & Piljac, J. (2003). An in vitro study of Ti and Ti-alloys coated with sol-gel derived hydroxyapatite coatings. *Surface and Coatings Technology, 165*, 40−50.

Meyerhofer, D. (1978). Characteristics of resist films produced by spinning. *Journal of Applied Physics, 49*, 3993−3997.

Miyazaki, T., Kim, H.-M., Kokubo, T., Kato, H., & Nakamura, T. (2001a). Induction and acceleration of bone-like apatite formation on tantalum oxide gel in simulated body fluid. *Journal of Sol-Gel Science and Technology, 21*, 83−88.

Miyazaki, T., Kim, H.-M., Kokubo, T., Ohtsuki, C., Kato, H., & Nakamura, T. (2001b). Apatite-forming ability of niobium oxide gels in a simulated body fluid. *Journal of the Ceramic Society of Japan, 109*, 929−933.

Nguyen, H. Q., Deporter, D. A., Pilliar, R. M., Valiquette, N., & Yakubovich, R. (2004). The effect of sol-gel-formed calcium phosphate coatings on bone ingrowth and osteo-conductivity of porous-surfaced Ti alloy implants. *Biomaterials, 25*, 865−876.

Paldan, H., Areva, S., Tirri, T., Peltola, T., Lindholm, T. C., Lassila, L., et al. (2008). Soft tissue attachment on sol-gel-treated titanium implants in vivo. *Journal of Materials Science: Materials in Medicine, 19*, 1283−1290.

Peltola, T., Jokinen, M., Rahiala, H., Patsi, M., Heikkila, J., Kangasniemi, I., et al. (2000). Effect of aging time on sol structure and in vitro calcium orthophosphate formation of sol-gel-derived titania films. *Journal of Biomedical Materials Research, 51*, 200−208.

Peltola, T., Patsi, M., Rahaiala, H., Kangasniemi, L., & Yli-Urpo, A. (1998). Calcium phosphate induction by sol-gel-derived titania coatings on titanium substrates in vitro. *Journal of Biomedical Materials Research, 41*, 504−510.

Piveteau, L.-D., Girona, M. I., Schlapbach, L., Parboux, P., Boilot, J.-P., & Gasser, B. (1999). Thin films of calcium orthophosphate and titanium dioxide by a sol-gel route: a new method for coating medical implants. *Journal of Materials Science: Materials in Medicine, 10*, 161−167.

Rossi, S., Tirri, T., Paldan, H., Kuntsi-Vaattovaara, H., Tulamo, R., & Narhi, T. (2008). Peri-implant tissue response to TiO_2 surface modified implants. *Clinical Oral Implants Research, 19*, 348−355.

Schmidt, H. (1988). Chemistry of material preparation by the sol-gel process. *Journal of Non-Crystalline Solids, 100*, 51−64.

Scriven, L. E. (1988). In C. J. Brinker, D. E. Clark, & D. R. Ulrich (Eds.), *Better ceramics through chemistry III* (pp. 717−729). Pittsburgh, PA: Mat Res Soc.

Shi, P., Ng, W. F., Wong, M. H., & Cheng, F. T. (2009). Improvement of corrosion resistance of pure magnesium in Hanks' solution by microarc oxidation with sol-gel TiO_2 sealing. *Journal of Alloys and Compounds, 469*, 286−292.

St. Pierre, J.-P., Gan, L., Wang, J., Pilliar, R. M., Grynpas, M. D., & Kandel, R. A. (2012). The incorporation of a zone of calcified cartilage improves the interfacial shear strength between in vitro-formed cartilage and the underlying substrate. *Acta Biomaterialia, 8*, 1603−1615.

Tache, A., Gan, L., Deporter, D., & Pilliar, R. M. (2004). Effect of surface chemistry on the rate of osseointegration of sintered porous-surfaced Ti-6Al-4V implants. *The International Journal of Oral & Maxillofacial Implants, 19*, 19−29.

Takahashi, H., Yashima, M., Kakihana, M., & Yoshimura, M. (1995). Synthesis of stoichiometric hydroxyapatite by a "gel" route from the aqueous solution of citric and phosphonoacetic acids. *European Journal of Solid State and Inorganic Chemistry, 32*, 829−835.

Uchida, M., Kim, H. M., Kokubo, T., & Nakamura, T. (2001). Bonelike apatite formation induced on zirconia gel in simulated body fluid and its modified solutions. *Journal of the American Ceramic Society, 84*, 2041−2044.

Vijayalakshmi, K., Prabakaran, K., & Rajeswari, S. (2008). Preparation and characterization of sol-gel hydroxyapatite and its electrochemical evaluation for biomedical applications. *Journal of Biomedical Materials Research, 87A*, 739−749.

Wen, C. E., Xu, W., Hu, W. Y., & Hodgson, P. D. (2007). Hydroxyapatite/titania sol-gel coatings on titanium−zirconium alloy for biomedical applications. *Acta Biomaterialia, 3*, 403−410.

Weng, W. (1999). Preparation and characterization of hydroxyapatite coatings on Ti6Al4V alloy by sol-gel method. *Journal of the American Ceramic Society, 82*, 27−32.

Weng, W., & Baptista, J. L. (1999). Preparation and characterization of hydroxyapatite coatings on Ti6Al4V alloy by a sol-gel method. *Journal of the American Ceramic Society, 82*, 27−32.

Yoshida, K., Tanagawa, M., Kamada, K., Hatada, R., Baba, K., Inoi, T., et al. (1999). Silica coatings formed on noble dental casting alloy by the sol-gel dipping process. *Journal of Biomedical Materials Research, 46*, 221−227.

Biomimetic surface modification of metallic biomaterials

7

T. Kokubo, S. Yamaguchi
Chubu University, Kasugai, Japan

7.1 Introduction

Various kinds of metallic materials such as stainless steel, Co−Cr−Mo alloys, Ti, and its alloys have been widely used as implants in orthopedics and dentistry. However, they do not bond to living bone, and hence their fixation is not stable over a long period. To confer a bone-bonding property to metallic materials, attempts have been made to coat their surfaces with a thin layer of bone-bonding ceramic, such as hydroxyapatite, using various techniques, such as plasma spray, flame spray, and sputtering. However, the coated layers are not stable over a long time in the living body because of cracking, transformation, and degradation. Attempts have also been made to deposit a bone-like apatite layer onto metallic materials in aqueous. However, this tends to crack and peel off because of shrinkage during the drying process subsequent to the deposition under wet conditions (Leeuwenburgh et al., 2008).

It has been shown that most of the bone-bonding ceramics form an apatite on their surfaces in the living body and bond to living bone through an apatite layer (Kokubo and Takadama, 2006). Therefore, even metallic material is expected to be able to bond to living bone if the surface is properly modified to form an apatite on its surface. In this chapter, such biomimetic surface modification of metallic materials and its clinical applications are reviewed.

7.2 Background of biomimetic surface modifications

Apatite formation on most bone-bonding ceramics can be reproduced in an acellular simulated body fluid (SBF) having ion concentrations essentially equal to those of human blood plasma (Kokubo and Takadama, 2006). Simple oxide gels with compositions such as TiO_2, ZrO_2, Nb_2O_5, and Ta_2O_5 also form an apatite on their surfaces in SBF (Kokubo and Takadama, 2006). This shows that metallic materials based on Ti, Zr, Nb, and/or Ta also form an apatite on their surfaces in the living body and bond to living bone through an apatite layer when their surfaces are slightly modified.

Surface Coating and Modification of Metallic Biomaterials. http://dx.doi.org/10.1016/B978-1-78242-303-4.00007-7
Copyright © 2015 Elsevier Ltd. All rights reserved.

7.3 Various approaches for biomimetic surface modification

Surface modifications of Ti metal and Ti-based alloys for the purpose of inducing apatite formation on their surfaces in SBF have been attempted by various methods including ion implantation (Armitage et al., 2007; Nayab et al., 2007; Rautray et al., 2010), hydrothermal treatment (Chen et al., 2009; Dong et al., 2007; Park et al., 2007, 2010; Ueda et al., 2009; Zhang et al., 2010), and electrochemical reactions (Bjursten et al., 2010; Diefenback et al., 2011; Minagar et al., 2013; Shibata et al., 2010; Suh, 2003; Whiteside et al., 2010; Xie et al., 2011; Zhang et al., 2013; Zhou et al., 2010, 2014). However, these techniques require special equipment and are not readily applicable to large-scale devices of complicated shapes or those composed of porous materials. In contrast to these techniques, simple chemical and heat treatments do not require any special equipment and are applicable to a broad range of shapes and materials.

Simple chemical and heat treatments for inducing apatite formation on Ti metal and Ti-based alloys in SBF have been attempted by various researchers (Cooper et al., 2006; Ferraris et al., 2011; Karthega and Rajendran, 2010; Lee et al., 2007; Li et al., 2010; Liu et al., 2007; Sugino et al., 2009; Takeuchi et al., 2005; Turkan and Guden, 2010; Wang et al., 2002; Wu et al., 2004; Zhao et al., 2005, 2007, 2008). However, the general principle governing apatite formation has not been revealed by these studies. The present authors have systematically studied the chemical and heat treatments effective for inducing apatite formation as a means of achieving the general principle of apatite formation.

7.4 Simple chemical and heat treatments for biomimetic surface modification

7.4.1 NaOH and heat treatments of Ti metal and its alloys

7.4.1.1 Surface structural change induced by the NaOH and heat treatments

A typical procedure of this method is soaking of Ti metal in a 5 M NaOH solution at 60 °C for 24 h and its subsequent heat treatment at 600 °C for 1 h in an ambient atmosphere. Sodium and oxygen enter into the surface of the Ti metal to 1 μm in thickness by the first NaOH treatment; only the oxygen among them penetrates into deeper regions upon subsequent heat treatment, as shown in Figure 7.1 (Kim et al., 1999). According to thin-film X-ray diffraction, sodium hydrogen titanate ($Na_xH_{2-x}Ti_yO_{2y+1}$; $0 < x < 2$ and $y = 2$, 3, or 4) appears in a fibrous form on the surface of the Ti metal within a level of 1 μm in thickness by the first NaOH treatment and is transformed into sodium titanate ($Na_2Ti_yO_{2y+1}$; $y = 5$, 6,

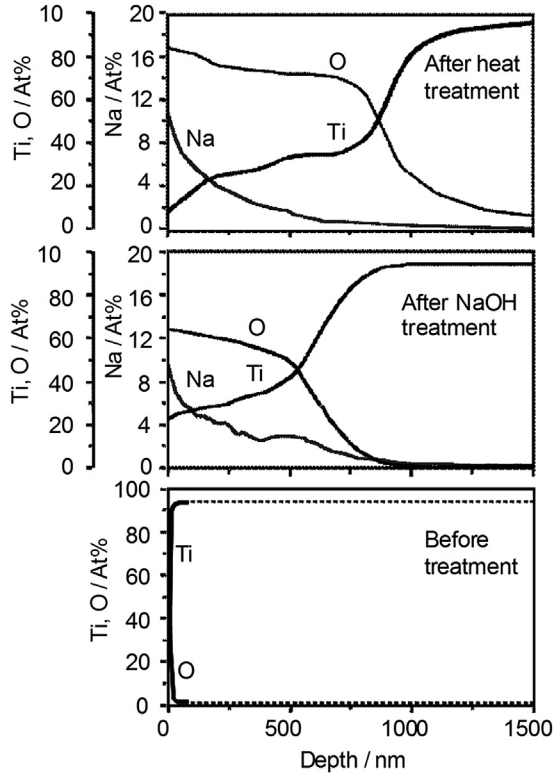


Figure 7.1 Depth profiles of Auger electron spectroscopy of Ti metal untreated and those subjected to NaOH and heat treatments.
Reproduced from Kim et al. (1999).

etc.) and rutile TiO_2 without appreciable morphological change by the subsequent heat treatment, as shown in Figure 7.2 (Yamaguchi et al., 2009).

Conventional Ti-based alloys such as Ti−6Al−4V (Kim et al., 1996; Ueno et al., 2011), Ti−6Al−2Nb−Ta (Kim et al., 1996), and Ti−15Mo−5Zr−3Al (Kim et al., 1996) also form sodium titanate and rutile, by the NaOH and heat treatments, since alloying elements such as Al, V, and Mo are selectively released from the surface of the alloys during the first NaOH treatment (Kim et al., 2000a,b).

7.4.1.2 *Apatite formation in SBF on the metal surfaces subjected to the NaOH and heat treatments*

The Ti metal subjected to the NaOH and heat treatments described previously fully forms an apatite on its surface within 1 day in SBF, as shown in Figure 7.3 (Yamaguchi et al., 2009).

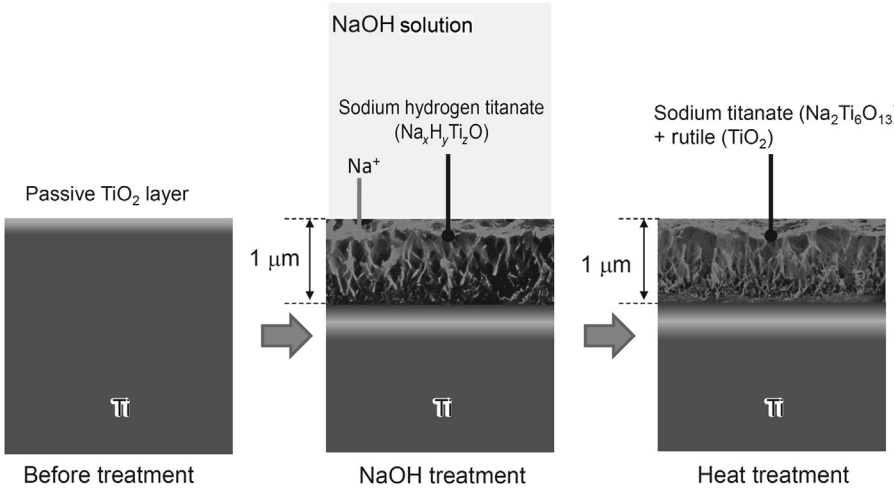


Figure 7.2 Structural change of the surface of the Ti metal by NaOH and heat treatments. Reproduced from Yamaguchi et al. (2009).

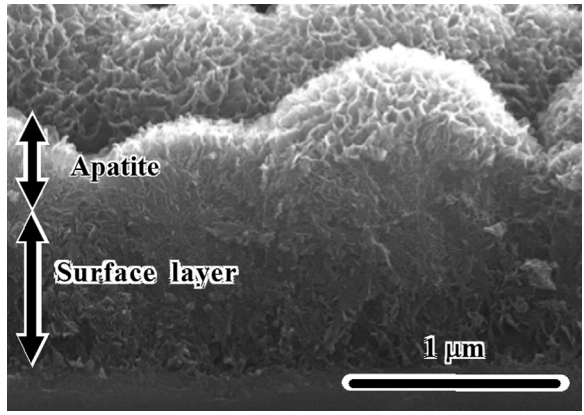


Figure 7.3 Scanning electron microscope photographs of a cross-section of the surface of a Ti metal soaked in SBF for 1 day, after NaOH and heat treatments.
Reproduced from Yamaguchi et al. (2009).

Based on X-ray photoelectron spectroscopy (Takadama et al., 2001a), transmission electron microscopy combined energy-dispersive X-ray analysis (Takadama et al., 2001b), and zeta potential measurement (Kim et al., 2003) on the Ti surface as a function of the soaking time in SBF, an apatite is formed during the process as shown in Figure 7.4 (Kim et al., 2003). Sodium ions are first released from the surface of the sodium titanate layer via exchange with H_3O^+ ions in SBF.

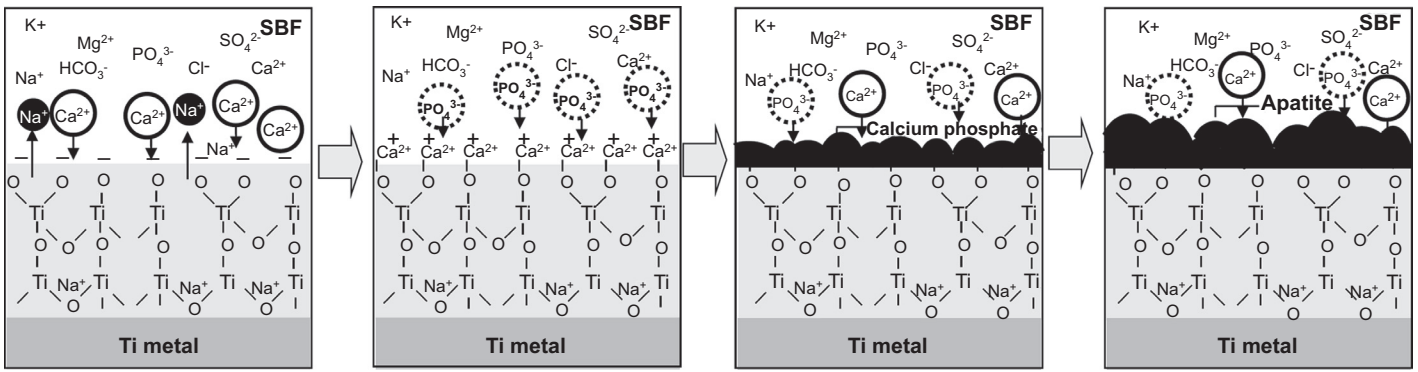


Figure 7.4 Process of apatite formation in SBF on Ti metal subjected to acid NaOH and heat treatments. Reproduced from Kim et al. (2003).

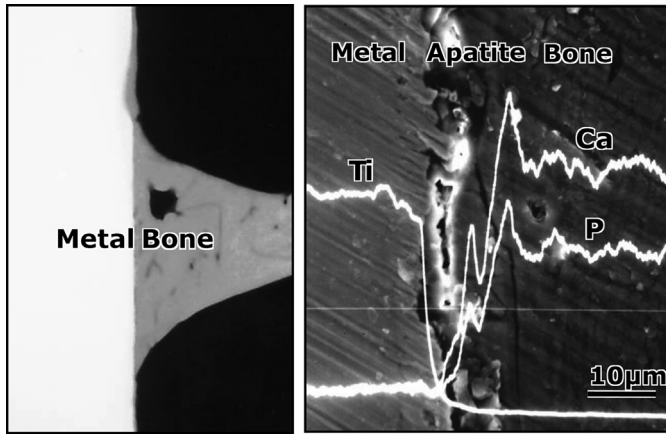


Figure 7.5 Contact microradiograph (left) and scanning electron microscope picture with energy-dispersive X-ray analysis (right) at the interface of Ti metal subjected to NaOH and heat treatments with neighboring bone 8 weeks after implantation into rabbit tibia. Reproduced from Yan et al. (1997).

As a result, the pH of the surrounding environment on the surface increases and the surface becomes negatively charged (Gold et al., 1989). The positively charged calcium ions are adsorbed on the negatively charged surface. As the calcium ions accumulate, the surface becomes positively charged and adsorbs the negatively charged phosphate ions, forming a calcium phosphate. This phase is metastable and eventually transforms into stable crystalline apatite.

The conventional Ti-based alloys such as Ti−6Al−4V (Kim et al., 1996; Ueno et al., 2011), Ti−6Al−2Nb−Ta (Kim et al., 1996), and Ti−15Mo−5Zr−3Al (Kim et al., 1996) − with similar treatment − also form an apatite layer on their surfaces in SBF.

7.4.1.3 *Bone-bonding of Ti metal and its alloys subjected to the NaOH and heat treatments*

The Ti metal subjected to the NaOH and heat treatments described previously forms an apatite layer on its surface in the living body of rabbit tibia, as in SBF, and so tightly bonds to the living bone, as shown in Figure 7.5 (Yan et al., 1997) so that fracture does not occur at the interface between the Ti metal and the bone under tensile stress. A Ti metal rod similarly treated cannot be pulled out from the medullary canal of a rabbit femur without being accompanied by bone fragment after implantation for 12 weeks, as shown in Figure 7.6 (Nishiguchi et al., 2003).

The conventional Ti-based alloys such as Ti−6Al−4V, Ti−6Al−2Nb−Ta, and Ti−15Mo−5Zr−3Al − after similar treatment − also tightly bond to the surrounding bone without the intervention of fibrous tissue at the interface between the alloys and the bone (Nishiguchi et al., 1999).

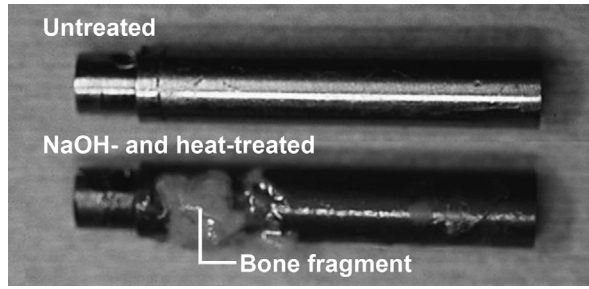


Figure 7.6 Untreated and NaOH- and heat-treated Ti metal rods pulled out from the medullary canal of a rabbit femur 12 weeks after implantation.
After Nishiguchi et al. (2003).

7.4.1.4 Some problems with NaOH and heat treatments

NaOH and heat treatments are simple, but they also have certain problems that need to be solved.

Ca contamination

When even a small amount of calcium ions are contained in an NaOH solution, it will preferentially enter into the sodium hydrogen titanate in place of the sodium ions during the first chemical treatment and remain in the sodium titanate formed by the subsequent heat treatment, inhibiting apatite formation by suppressing the release of sodium ions into SBF. Even a high-purity NaOH reagent often contains calcium contamination (Kizuki et al., 2013). Therefore, the reagent for the chemical treatment must be carefully chosen.

Humidity

The sodium ions of sodium titanate are easily released, even in a humid environment, via an exchange with the H_3O^+ ions in the humidity. As a result, the sodium concentration of the sodium titanate decreases before soaking in SBF or implantation and suppresses apatite formation in SBF and the living body. Therefore, the treated specimens must be carefully stored under dry conditions (Kawai et al., 2010).

Ti–Zr–Nb–Ta alloys

NaOH and heat treatments are effective not only for Ti metal, but also for conventional Ti-based alloys in inducing surface apatite formation in SBF as well as enhancing bone-bonding ability, as described previously. However, these treatments are not effective for new kinds of Ti-based alloys in the system Ti–Zr–Nb–Ta because alloying elements such as Zr, Nb, and Ta are barely released during the NaOH treatment and remain in the surface layer, inhibiting apatite formation by suppressing the release of the Na^+ ions (Yamaguchi et al., 2011).

These problems are overcome by the following methods.

7.4.2 NaOH, $CaCl_2$, heat, and water treatments of Ti and its alloys

7.4.2.1 Surface structural change by the NaOH, $CaCl_2$, heat, and water treatments

A typical procedure is to soak Ti metal in the NaOH solution under the same conditions as described previously, with successive soaking in 100 mM $CaCl_2$ solution at 40 °C for 24 h, subsequent heat treatment under the same conditions as described previously, and additional soaking in hot water at 80 °C for 24 h (Kizuki et al., 2010).

The sodium hydrogen titanate formed by the first NaOH treatment has a layered structure where the Na^+ ions are located at the interspace of the titanium oxide layers. These Na^+ ions are completely replaced with the Ca^{2+} ions during the subsequent $CaCl_2$ treatment and form a calcium hydrogen titanate. This transforms into calcium titanate and rutile by subsequent heat treatment, as shown in Figure 7.7. The calcium ions in the calcium titanate near the surface are partly replaced with H_3O^+ ions and form a calcium-deficient calcium titanate by the additional hot water treatment, as shown in Figure 7.8 (Kizuki et al., 2010).

The Ti-based alloys, including the new kind of alloys in the Ti−Zr−Nb−Ta system, also form essentially the same crystalline phases on their surfaces by the same treatments (Yamaguchi et al., 2010, 2012).

7.4.2.2 Apatite formation in SBF on the material surfaces subjected to NaOH, $CaCl_2$, heat, and water treatment

The Ti metal subjected to NaOH, $CaCl_2$, and heat treatment does not form an apatite on its surface in SBF within 3 days, but does forms it after subsequent hot water treatment, as shown in Figure 7.9 (Kizuki et al., 2010). This occurs because the calcium ions in the calcium titanate formed by the heat treatment are scarcely released in SBF, but

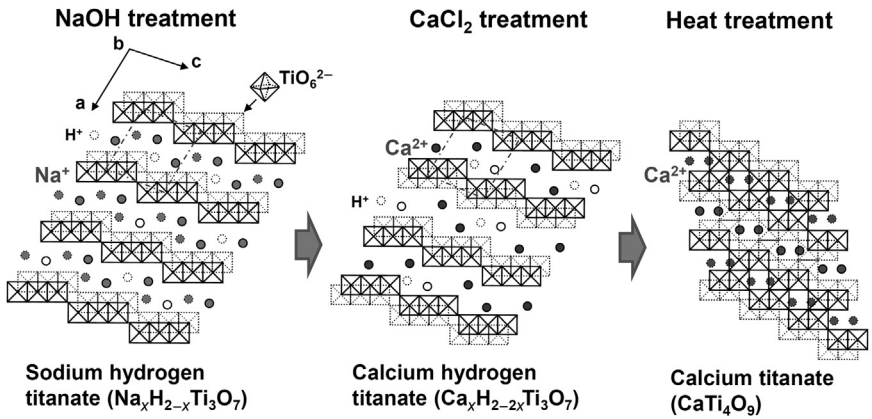


Figure 7.7 Structures of sodium hydrogen titanate, calcium hydrogen titanate, and calcium titanate.

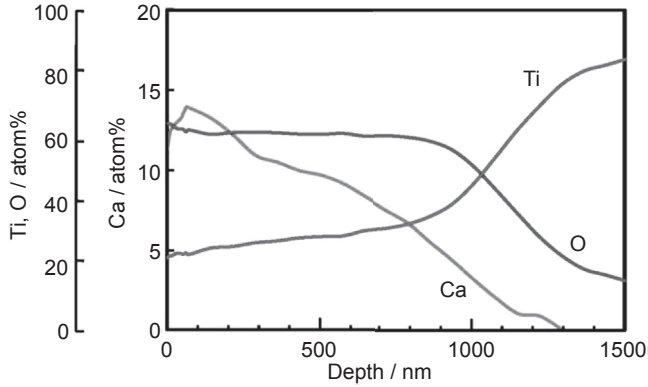


Figure 7.8 Depth profile of Auger electron spectroscopy of Ti metal subjected to NaOH, $CaCl_2$, heat, and water treatments.
Reproduced from Kizuki et al. (2010).

those in the calcium-deficient calcium titanate after the hot water treatment are easily released.

In contrast with the NaOH and heat treatments, the NaOH, $CaCl_2$, heat, and water treatments are effective not only for the Ti metal, but also for Ti-based alloys, including the new generation of Ti−Zr−Nb−Ta alloys in inducing apatite formation on their surfaces in SBF, as shown in Figure 7.9 (Yamaguchi et al., 2010, 2012). This occurs because the released calcium ions are more effective than the released sodium ions in forming apatites.

In contrast with the NaOH and heat treatments, the apatite-forming capacity conferred by the NaOH, $CaCl_2$, heat, and water treatments is maintained even after storage in a humid environment over a long period (Yamaguchi et al., 2010). This occurs because the calcium ions in the calcium-deficient calcium titanate are not as easily released in a humid environment as are the sodium ions of the sodium titanate.

7.4.2.3 *Bone bonding of the Ti metal and its alloys subjected to the NaOH, $CaCl_2$, heat, and water treatments*

Ti metal as well as Ti-based alloys, including the new generation of Ti−Zr−Nb−Ta alloys, bond to living bone without any intervention of fibrous tissue at the interface between the metals and the bone, as shown in Figure 7.10 (Fukuda et al., 2011a; Tanaka et al., 2014), when they are implanted into the tibia of a rabbit, after the NaOH, $CaCl_2$, heat, and water treatments. Under a tensile stress, fracture does not occur at their interfaces, but in the bone.

7.4.2.4 *The evolution of NaOH, $CaCl_2$, heat, and water treatments*

Various kinds of functional ions can be incorporated into calcium-deficient calcium titanate by adding them to the $CaCl_2$ solution because these ions are able to enter

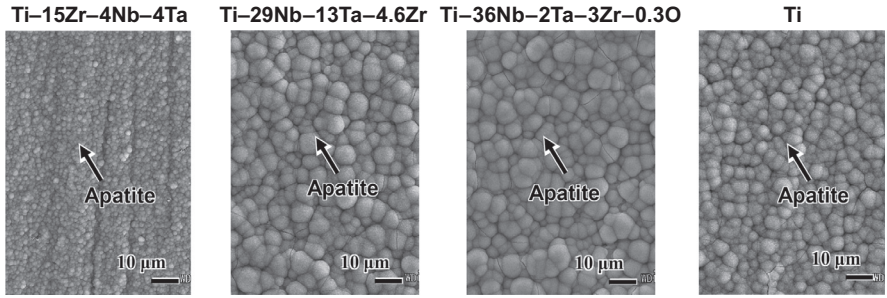


Figure 7.9 Scanning electron microscope photographs of Ti metal and its alloys subjected to NaOH, $CaCl_2$, heat, and water treatments, after soaking in SBF for 3 days.
Reproduced from Kizuki et al. (2010) and Yamaguchi et al. (2010, 2012).

the interspace of the titanium oxide layers of the calcium hydrogen titanate and transform it into calcium titanate that contains functional ions by the subsequent heat treatment. If these ions are also added to the water of the final treatment, the functional ions are only barely released during the water treatment. These incorporated functional ions are slowly released in the body environment and promote bone growth and antibacterial activity.

For example, Mg (Yamaguchi et al., 2013a), Sr (Yamaguchi et al., 2014), and Zn (Yamaguchi et al., 2013b) ions, which are known to promote bone growth, are incorporated into the calcium-deficient titanate layer surface by the modified NaOH, $CaCl_2$, heat, and water treatments, as shown in Figure 7.11 (Yamaguhci et al., 2014). The resultant products not only form an apatite on their surfaces in SBF, but also slowly release the functional ions into phosphate-buffered saline at 36.5 °C, as shown in Figure 7.12 (Yamaguchi et al., 2014). These ions would also be expected to be released from the Ti metal in the living body to promote growth of the surrounding bone. Consequently, an early bonding of the Ti metal with the surrounding bone takes place.

Silver ions, which are known to exhibit antibacterial activity, may also be incorporated into the surface calcium-deficient calcium titanate layer by adding $AgNO_3$ to the water of the final treatment, as shown in Figure 7.13 (Kizuki et al., 2014). The resultant product not only forms an apatite on its surface in SBF, but also slowly releases the

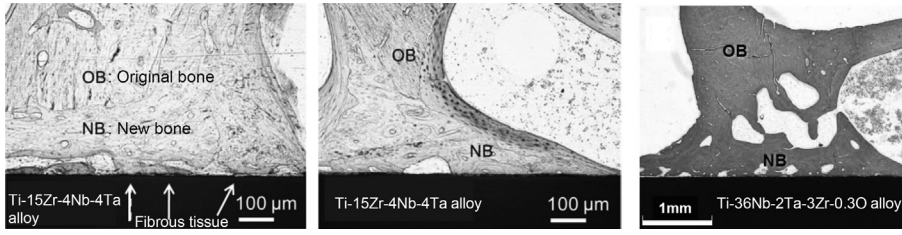


Figure 7.10 Optical micrograph of Ti−Zr−Nb−Ta alloys subjected to NaOH, $CaCl_2$, heat, and water treatments (center and right) at their interfaces with bone, in comparison with untreated (left), 16 weeks (left and center), and 26 weeks (right) after impanation into rabbit tibia.
Reproduced from Fukuda et al. (2011a) and Tanaka et al. (2014).

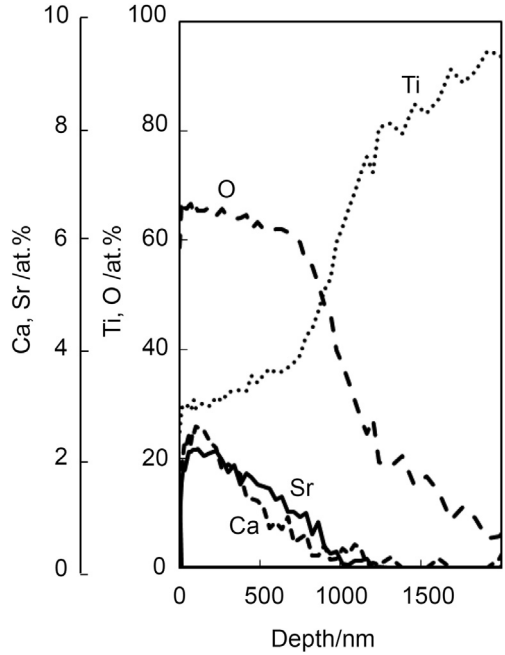


Figure 7.11 Depth profile of XPS of Ti metal subjected to NaOH, $CaCl_2/SrCl_2$, heat, and $SrCl_2$ treatments.
Reproduced from Yamaguchi et al. (2014).

Ag^+ ions into the fetal bovine serum and exhibits antibacterial activity. These Ag^+ ions are expected to be released from the Ti metal in the living body to prevent infection.

There still remain certain problems with both the NaOH and heat treatments as well as the NaOH, $CaCl_2$, heat, and water treatments. The surface layer formed by these treatments, which is approximately 1 μm thick with nanometer-scale roughness, is liable to be removed by shear stress—such as when the treated metals are screwed into bone. In addition, the Na^+ and Ca^{2+} ions released from the treated metals are liable to exert an adverse effect on living cell activity, especially in the narrow space of a porous metal. These problems are overcome by the following treatments.

7.4.3 Acid and heat treatments of the Ti metal

7.4.3.1 Surface structural change induced by the acid and heat treatments

A typical procedure for this method is to soak the Ti metal into 66.3% H_2SO_4/10.6% HCl = 1/1 mixed acid solution at 70 °C for 1 h, with a subsequent heat treatment at a temperature between 500 and 650 °C for 1 h in an ambient atmosphere (Kokubo et al., 2010).

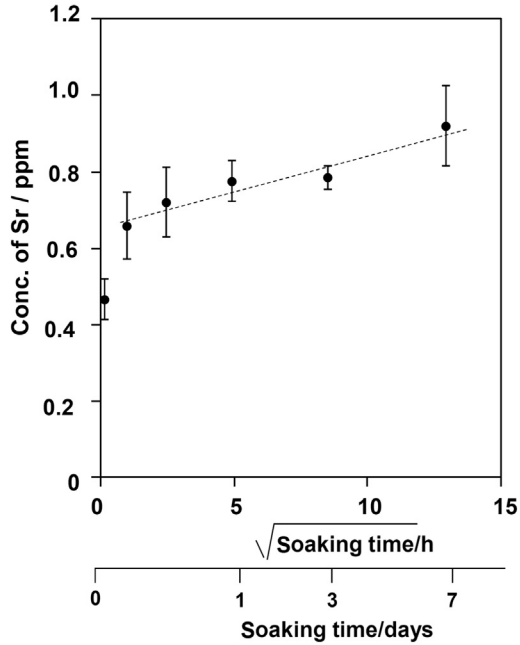


Figure 7.12 Sr ion release from Ti metal subjected to NaOH, $CaCl_2/SrCl_2$, heat, and $SrCl_2$ treatments into phosphate-buffered saline at 36.5 °C.
Reproduced from Yamaguchi et al. (2014).

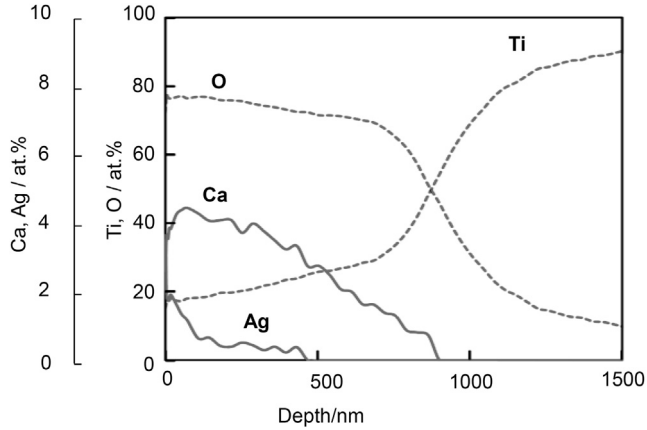


Figure 7.13 Depth profile of Auger electron spectroscopy of Ti metal subjected to NaOH, $CaCl_2$, heat, and $AgNO_3$ treatments.
Reproduced from Kizuki et al. (2014).

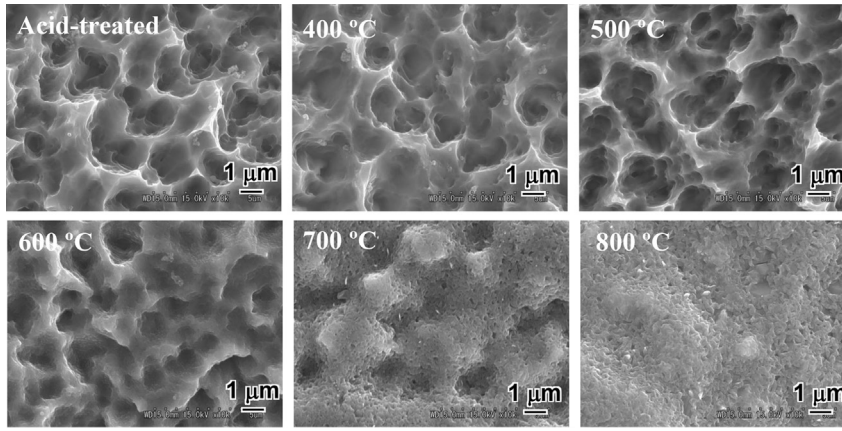


Figure 7.14 Scanning electron microscope photographs of surfaces of Ti metals subjected to acid and heat treatments.
Reproduced from Kokubo et al. (2010).

A layer of titanium hydride (TiH_x, where $0 < x < 2$) adsorbed with SO_4^{2-} and/or Cl^- ions, about 1 μm in thickness with a micrometer-scale roughness, is produced on the surface of the Ti metal by acid treatment. This is converted into a rutile TiO_2 adsorbed with SO_4^{2-} and/or Cl^- ions without appreciable morphological change by the subsequent heat treatment, as shown in Figure 7.14 (Kokubo et al., 2010).

7.4.3.2 *Apatite formation in SBF on the Ti surfaces subjected to acid and heat treatments*

The Ti metal subjected to the acid and heat treatments described previously forms apatite fully on its surface in SBF within 1 day, in contrast with that treated with acid, as shown in Figure 7.15 (Kokubo et al., 2010).

According to X-ray photoelectron spectroscopy and zeta potential measurement of the Ti surface as a function of the soaking time in SBF, an apatite is formed by the process shown in Figure 7.16 (Kokubo et al., 2010). The titanium oxide on the surface

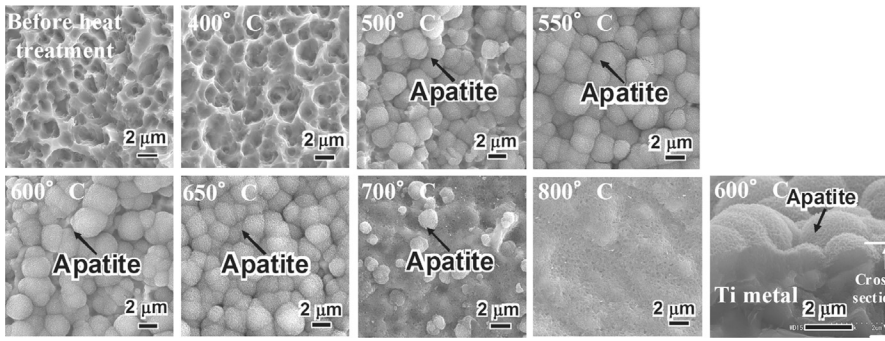


Figure 7.15 Scanning electron microscope photographs of surfaces of Ti metal soaked in SBF for 1 day after acid and heat treatments at various temperatures.
Reproduced from Kokubo et al. (2010).

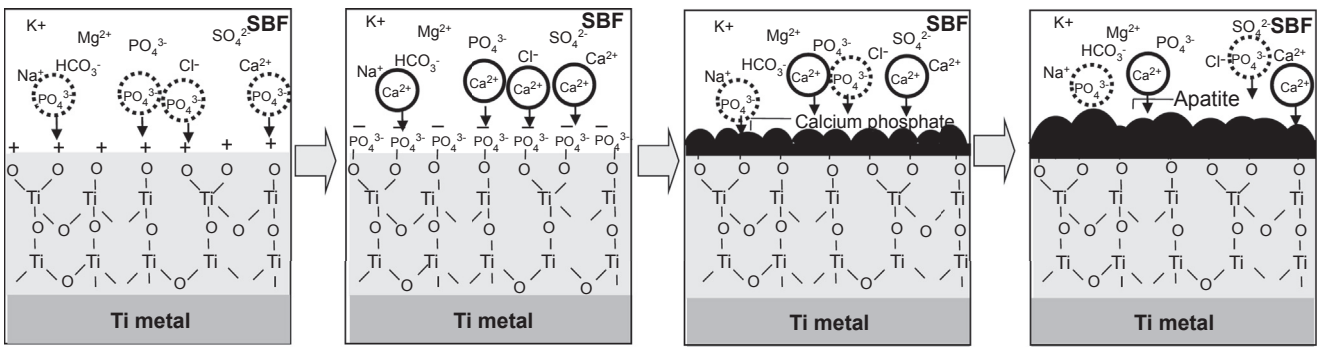


Figure 7.16 Process of apatite formation in SBF on Ti metal subjected to acid and heat treatments. Reproduced from Kokubo et al. (2010).

of the Ti metal dissociates the adsorbed SO_4^{2-} and/or Cl^- ions into SBF to produce an acidic environment. It is reported that titanium oxide is positively charged in an acidic environment (Gold et al., 1989); therefore, the surface of the titanium oxide is positively charged to preferentially adsorb the negatively charged phosphate ions in SBF. As the phosphate ions accumulate, the surface becomes negatively charged and adsorbs the positively charged calcium ions, forming calcium phosphate. This phase is metastable and eventually transforms into stable crystalline apatite.

The surface of the acid-treated Ti metal is not charged and hence does not induce apatite formation (Kokubo et al., 2010).

The apatite-forming capacity conferred by the acid and heat treatment is also maintained even after storage in a humid environment over a long period (Kokubo et al., 2010).

7.4.3.3 *Bone-bonding of the Ti metal subjected to the acid and heat treatments*

The Ti metal subjected to the acid and heat treatments described previously tightly bonds to the living bone without the intervention of fibrous tissue, in contrast to that of the acid- and heat-treated when it is implanted into the tibia of a rabbit, as shown in Figure 7.17 (Kawai et al., 2012). The Ti metal subjected to the acid and heat treatments does not produce a fracture at the interface between the metal and the bone under a tensile stress, but in the bone.

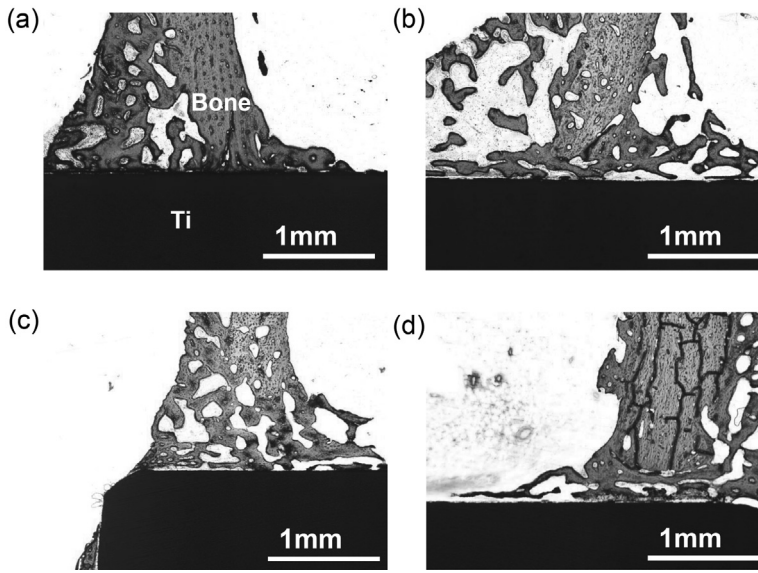


Figure 7.17 Optical micrographs of nondecalcified sections of Ti metals subjected to acid and heat treatments (a) in comparison with those subjected to no treatment (b), only heat treatment (c), and only acid treatment (d) 4 weeks after implantation into rabbit tibia. Reproduced from Kawai et al. (2012).

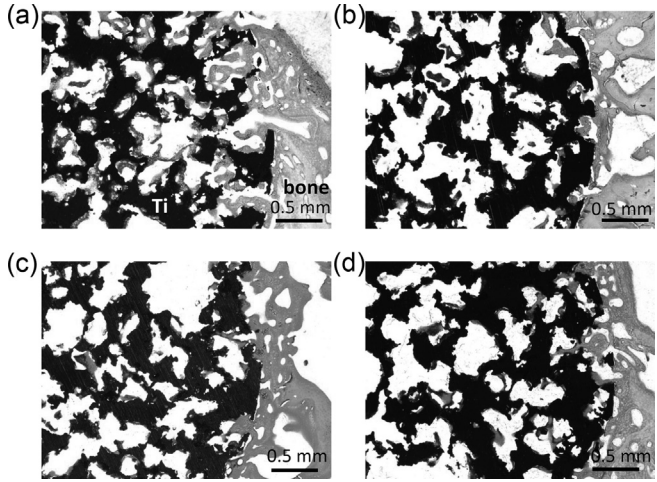


Figure 7.18 Optical micrographs of nondecalcified sections of porous Ti metals subjected to acid and heat treatments (a) in comparison with those subjected to no treatment (b), only heat treatment (c), and only acid treatment (d) 3 weeks after implantation into femoral condyle of rabbit.
Reproduced from Kawai et al. (2013).

7.4.3.4 Osteoconduction of the Ti metal subjected to the acid and heat treatments

When a porous Ti metal subjected to the acid and heat treatments described previously is implanted into a rabbit femur, the surrounding bone deeply penetrates into the porous structure within 3 weeks, in contrast to that of as-acid and as-heat-treatments, as shown in Figure 7.18 (Kawai et al., 2013).

7.4.3.5 Osteoinduction of the Ti metal subjected to the acid and heat treatments

When the same porous Ti metal subjected to the acid and heat treatments is implanted into the muscle of a dog, bone tissue is ectopically formed in the porous structure within 12 months, in contrast to that of the as-acid and as-heat-treatments, as shown in Figure 7.19 (Kawai et al., 2014).

7.4.4 The dependence of apatite formation on Ti metal on pH of the exposed solution

It has been shown by the experiments described previously that various chemical treatments followed by heat treatment are effective for inducing apatite formation on Ti metal in SBF. To investigate the dependence of apatite formation on Ti metal in SBF on the pH of the exposed solution, Ti metal was soaked in a solution with the pH systematically changed from approximately 0 to 14 by HCl and NaOH at 60 °C

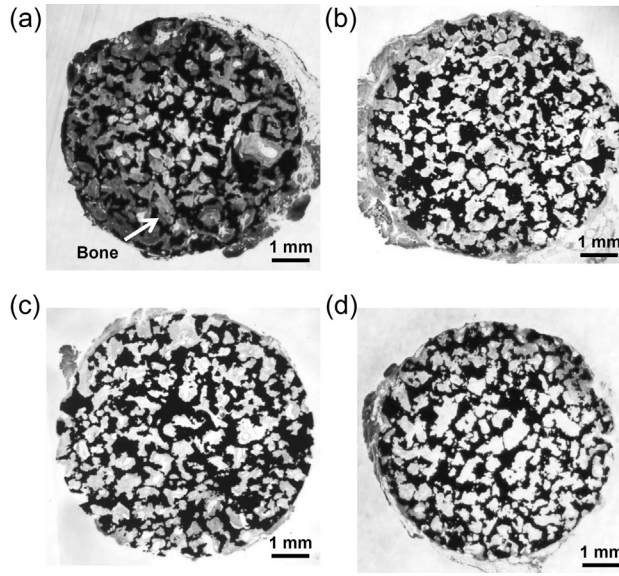


Figure 7.19 Optical micrographs of nondecalcified sections of porous Ti metal subjected to acid and heat treatment (a) in comparison with those subjected to no treatment (b), only heat treatment (c) and only acid treatment (d) 12 months after implantation into muscle of dog. Reproduced from Kawai et al. (2014).

for 24 h, and then heat-treated at 600 °C for 1 h. As a result, the Ti metal forms an apatite on its surface in SBF within 3 days when it was exposed to solutions of pH values lower than 1.1 or higher than 13.6, as shown in Figure 7.20 (Pattanayak et al., 2012).

Apatite formation depends on neither surface roughness nor specific crystalline phase, but rather on surface charge. The Ti metal is positively charged when heat-treated after exposure to strong acid solutions, whereas it is negatively charged when heat-treated after exposure to strong alkali solutions, as shown in Figure 7.21 (Pattanayak et al., 2012). The reason the Ti metal heat-treated after exposure to an

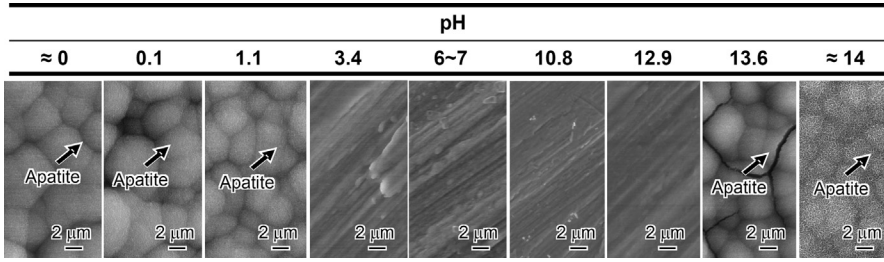


Figure 7.20 Scanning electron microscope photographs of surfaces of Ti metal soaked in SBF for 3 days after heat treatment after exposure to solutions with different pH levels. Reproduced form Pattanayak et al. (2012).

acid solution is positively charged in SBF was discussed in the section on acid and heat treatments. The reason the Ti metal heat-treated after exposure to the alkali solution is negatively charged was discussed in the section on NaOH and heat treatments. The reason the positively or negatively charged Ti metal forms an apatite on its surface in SBF was discussed through discussion of Figures 7.4 and 7.16.

It is clear from Figures 7.20 and 7.21 that the Ti metal forms an apatite on its surface in SBF when it is heat-treated after exposure to strong acid or alkali solutions, because it becomes positively or negatively charged on its surface, as shown in Figure 7.22 (Pattanayak et al., 2012). The natural Ti metal does not form an apatite on its surface in SBF even after heat treatment because it is neither positively nor negatively charged. This indicates that the Ti metal is able to bond to living bone if it is heat-treated after exposure to a strong acid or an alkali solution, even though the natural Ti metal is unable to do so on its own.

7.4.5 Biomimetic surface modification of metals other than the Ti metal and its alloys

A zirconia gel prepared by a sol−gel method also forms an apatite on its surface in SBF within 3 days, when it is heat-treated at 600 °C (Uchida et al., 2002a). This indicates the possibility for zirconium metal to form an apatite on its surface in SBF when its surface is slightly chemically modified. However, the zirconium metal only scarcely formed an apatite on its surface in SBF even after 28 days when it was treated with 5−15 M NaOH solution at 95 °C for 24 h (Uchida et al., 2002b). Chen et al. (2008) reported

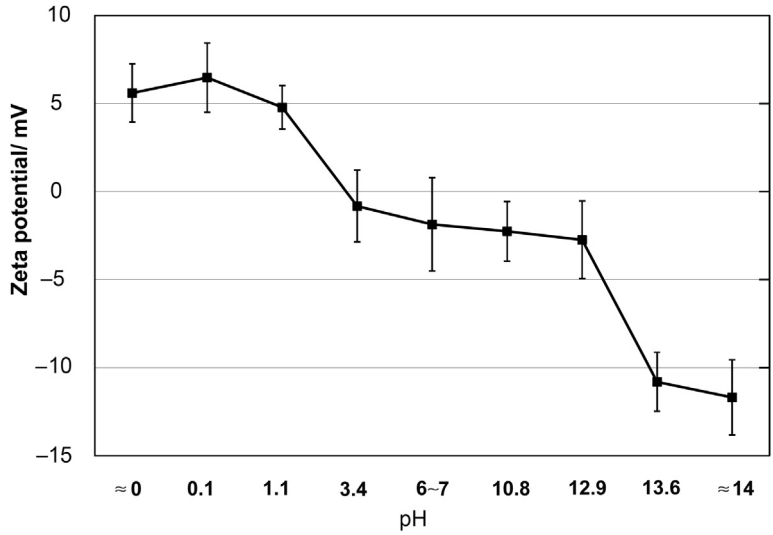


Figure 7.21 Zeta potentials of Ti metal heat-treated after exposure to solutions with different pH levels.
Reproduced from Pattanayak et al. (2012).

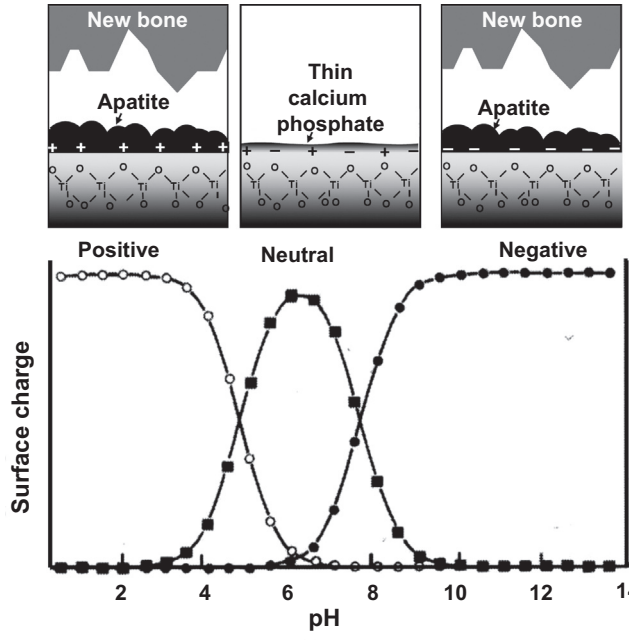


Figure 7.22 Surface charge of titanium oxide and apatite formation on its surface as a function of pH of exposed solution.
Reproduced from Pattanayak et al. (2012).

that the zirconium metal plate produced by sintering with Zr metal powders forms an apatite on its surface in SBF within 7 days when it was soaked in 10 M NaOH solution at 60 °C for 24 h and then heat-treated at 600 °C for 1 h in a vacuum.

A niobium oxide gel as prepared by a sol−gel method also forms an apatite on its surface in SBF within 7 days (Miyazaki et al., 2001c). This indicates that niobium metal might be able to form an apatite on its surface in SBF if the surface is chemically modified. However, niobium metal does not form an apatite on its surface within 14 days when treated with 0.5−2.0 M NaOH solution at 60 °C for 24 h (Miyazaki et al., 2001c). The treatment with an NaOH solution with concentrations greater than 2 M produced cracks on the surface of the metal. Wang et al. (2008) reported that the niobium metal formed an apatite on its surface in SBF within 7 days when soaked in 0.5 M NaOH solution at 80 °C for 24 h and then was heat-treated at 600 °C for 1 h in a vacuum.

A tantalum oxide gel as, prepared by a sol−gel method, also forms an apatite on its surface in SBF within 7 days (Miyazaki et al., 2001a). This indicates that tantalum metal forms an apatite on its surface in SBF when its surface is chemically modified. The tantalum metal forms an apatite on its surface in SBF without needing any surface chemical modification (Miyazaki et al., 2000a); however, it takes an induction period of as long as 4 weeks for an apatite to

form. It forms an apatite within 7 days, when treated with 0.2−0.5 M NaOH solution at 60 °C for 24 h and forms a sodium tantalate hydrogel layer on its surface. When it was subsequently heat-treated at 300 °C for 1 h after the NaOH treatment, the adhesive strength of the surface layer to the substrate increased without any decrease in its apatite-forming ability (Miyazaki et al., 2002; Miyazaki et al., 2001b). The tantalum metal subjected to 0.5 M NaOH treatment and heat treatment at 300 °C was confirmed to be strongly bonded to the living bone without any intervention of fibrous tissue at the bone interface within 16 weeks in an animal experiment using a rabbit tibia (Kato et al., 2000).

An alumina gel prepared by a sol−gel method does not form an apatite on its surface in SBF (Li et al., 1994). This indicates there is little possibility for aluminum metal to form an apatite on its surface in SBF, even if its surface is chemically modified.

7.5 Clinical applications of metallic biomaterials subjected to biomimetic surface modifications

7.5.1 Applications to total hip joints

A porous Ti metal layer formed on an acetabular shell and femoral stem of a total artificial hip joint made of Ti−6Al−2Nb−Ta alloy was subjected to NaOH and heat treatments to induce apatite formation on its surface in the living body. The resultant joint has been clinically used since 2007 in Japan, as shown in Figure 7.23 (Kawanabe et al., 2009). It was confirmed by two implants retrieved by treatment for bone fracture and infection that the Ti metal was tightly integrated with newly grown bone as early as 2 weeks after implantation (So et al., 2013).

7.5.2 Application to a spinal fusion device

The porous Ti metal subjected to NaOH and heat treatments to form the sodium titanate and rutile TiO_2 on its surface exhibits only low osteoinduction. However, if the same porous Ti metal is subjected to HCl treatment after the NaOH treatment to remove the sodium ions from the sodium hydrogen titanate (Pattanayak et al., 2009) and then subjected to heat treatment to form the rutile TiO_2 on its surface (Pattanayak et al. 2011a), the resultant product forms an apatite on its surface in SBF (Pattanayak et al. 2011b) and exhibits a high level of osteoinduction (Fujibayashi et al., 2004; Takemoto et al., 2006; Fukuda et al., 2011b) as well as osteoconduction (Takemoto et al., 2005), as shown in Figure 7.24 (Tanaka et al., 2009).

NaOH, HCl, and heat-treated porous Ti metal was applied to a spinal fusion device in a canine model (Takemoto et al., 2007). Based on this result, the metal was subjected to clinical trials for spinal fusion device for five patients between November

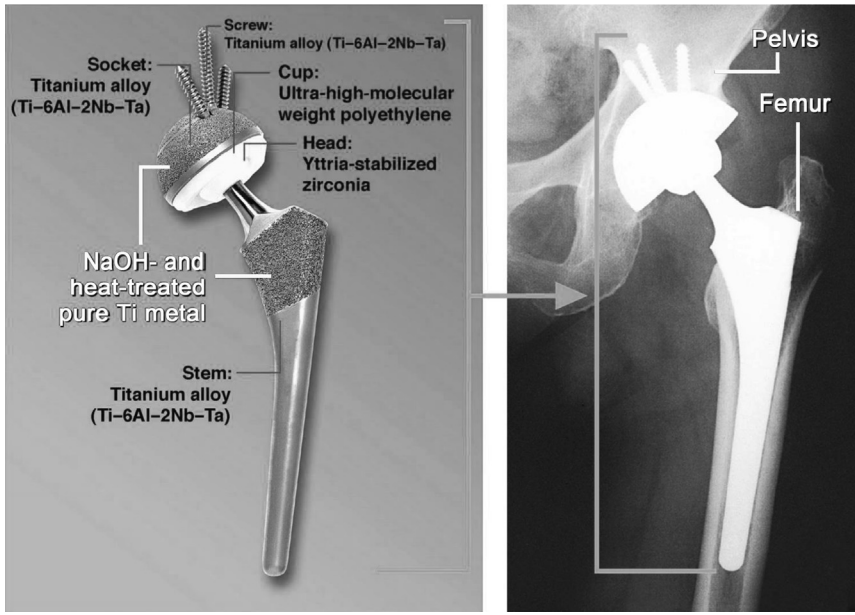


Figure 7.23 Application of NaOH and heat treatments to the porous Ti metal layer on an artificial hip joint.
After Kawanabe et al. (2009).

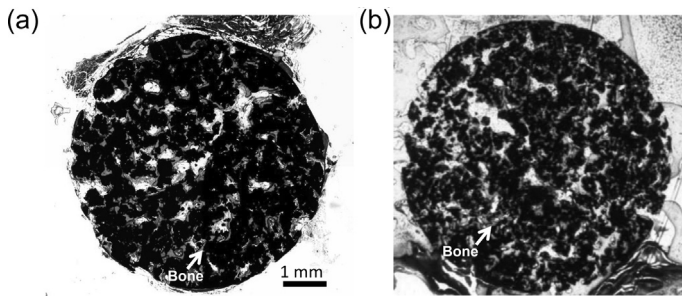


Figure 7.24 Optical micrographs of porous Ti metal subjected to NaOH, HCl, and heat treatments implanted into muscle of dog for 12 months (a) and into rabbit femur for 26 weeks (b).
Reproduced from Takemoto et al. (2006) and after Tanaka et al. (2009).

2008 and June 2009, as shown in Figure 7.25 (Fujibayashi et al., 2011). Conventional spinal fusion devices need an autograft for fixation to the surrounding bone because they cannot bond to living bone, whereas the present device can be fixed without an autograft because it does bond to living bone. All of the clinical cases to date have had a successful outcome.

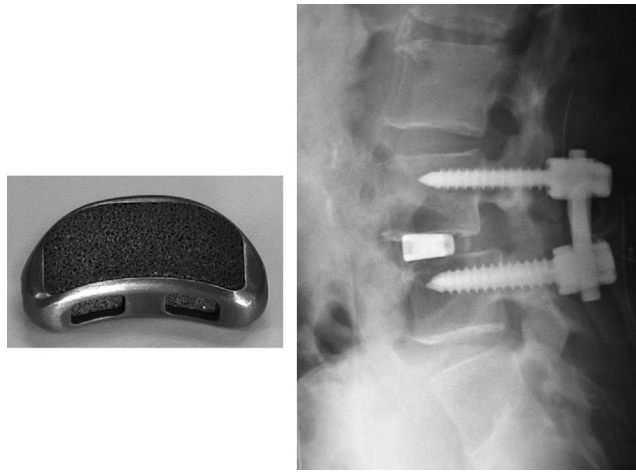


Figure 7.25 Spinal fusion device of porous Ti metal subjected to NaOH, HCl, and heat treatments (left) and its clinical application (right).
Reproduced from Fujibayashi et al. (2011).

7.6 Future aspect of the biomimetic surface modification

The general principle for obtaining a bone-bonding metal by biomimetic surface modification has been demonstrated for Ti metal and its alloys. The general principle for inducing the bone-bonding ability by biomimetic surface modification in general is expected to be seen even for different metals than just Ti metal and its alloys in the future. Various functions besides the bone-bonding ability are expected to be derived from metals by biomimetic surface modification.

Several bone-bonding ceramics have been developed and are being used clinically as important bone substitutes. However, they cannot be used under load-bearing conditions because their fracture toughness is insufficient. The present metals subjected to biomimetic surface modification can exhibit not only bone-bonding property but also high fracture toughness; therefore, these metals are likely to find broad applications in orthopedics and dentistry.

References

Armitage, D. A., Mihoc, R., Tate, T. J., McPhail, D. S., Chater, R., Hobkirk, J. A., et al. (2007). The oxidation of calcium implanted titanium in water: a depth profiling study. *Applied Surface Science, 253*, 4085−4093.

Bjursten, L. M., Rasmusson, L., Oh, S., Smith, G. C., Brammer, K. S., & Jin, S. (2010). Titanium dioxide nanotubes enhance bone bonding in vivo. *Journal of Biomedical Materials Research, 92A*, 1218−1224.

Chen, X.-B., Li, Y. C., Plessis, J. D., Hodgson, P. D., & Wen, C. (2009). Influence of calcium ion deposition on apatite-inducing ability of porous titanium for biomedical applications. *Acta Biomaterialia, 5*, 1808−1820.

Chen, X., Nouri, A., Li, Y., Lin, J., Hodgson, P. D., & Wen, C. (2008). Effect of surface roughness of Ti, Zr, and TiZr on apatite precipitation from simulated body fluid. *Biotechnology and Bioengineering, 101*, 378−387.

Cooper, L. F., Zhou, Y., Takebe, J., Guo, J., Abron, A., Holmen, A., et al. (2006). Fluoride modification effects on osteoblast behavior and bone formation at TiO_2 grit-blasted c.p. titanium endosseous implants. *Biomaterials, 27*, 926−936.

Diefenback, M., Muckley, T., Shrader, C., Schmidt, J., Zankovych, S., Bossert, J., et al. (2011). The effect of plasma chemical oxidation of titanium alloy on bone−implant contact in rats. *Biomaterials, 32*, 8041−8047.

Dong, W., Zhang, T., Epstein, J., Cooney, L., Wang, H., Li, Y., et al. (2007). Multifunctional nanowire bioscaffolds on titanium. *Chemistry of Materials, 19*, 4454−4459.

Ferraris, S., Spriano, S., Pan, G., Venturello, A., Bianchi, C. L., Chiesa, R., et al. (2011). Surface modification of T−6Al−4V alloy for biomineralization and specific biological response: part 1, inorganic modification. *Journal of Materials Science: Materials in Medicine, 22*, 533−545.

Fujibayashi, S., Neo, M., Kim, H.-M., Kokubo, T., & Nakamura, T. (2004). Osteoinduction of porous bioactive titanium metal. *Biomaterials, 25*, 443−450.

Fujibayashi, S., Takemoto, M., Neo, M., Matsushita, T., Kokubo, T., Doi, K., et al. (2011). A novel synthetic material for spinal fusion: a prospective clinical trial of porous bioactive titanium metal for lumber interbody fusion. *European Spine Journal, 20*, 1486−1495.

Fukuda, A., Takemoto, M., Saito, T., Fujibayashi, S., Neo, M., Yamaguchi, S., et al. (2011a). Bone bonding bioactivity of Ti metal and Ti−Zr−Nb−Ta alloys with Ca ions incorporated on their surfaces by simple chemical and heat treatments. *Acta Biomaterialia, 7*, 1379−1386.

Fukuda, A., Takemoto, M., Saito, T., Fujibayashi, S., Neo, M., Pattanayak, D. K., et al. (2011b). Osteoinduction of porous Ti implants with a channel structure fabricated by selective laser melting. *Acta Biomaterialia, 7*, 2327−2336.

Gold, J. M., Schmidt, M., & Steinmann, S. G. (1989). XPS study of amino acid adsorption to titanium surfaces. *Helvetica Physica Acta, 62*, 246−249.

Karthega, M., & Rajendran, N. (2010). Hydrogen peroxide treatment on Ti−6Al−4V alloy: a promising surface modification technique for orthopaedic application. *Applied Surface Science, 256*, 2176−2183.

Kato, H., Nakamura, T., Nishiguchi, S., Matsusue, Y., Kobayashi, M., Miyazaki, T., et al. (2000). Bonding of alkali- and heat-treated tantalum implants to bone. *Journal of Biomedical Materials Research, 53*, 28−35.

Kawai, T., Kizuki, T., Takadama, H., Matsushita, T., Unuma, T., Nakamura, T., et al. (2010). Apatite formation on surface titanate layer with different Na content on Ti metal. *Journal of the Ceramic Society of Japan, 118*, 19−24.

Kawai, T., Takemoto, M., Fujibayashi, S., Akiyama, H., Tanaka, S., Yamaguchi, S., et al. (2014). Osteoinduction on acid and heat treated porous Ti metal samples in canine muscle. *PLoS One, 9*, e88366.

Kawai, T., Takemoto, M., Fujibayashi, S., Akiyama, H., Yamaguchi, S., Pattanayak, D. K., et al. (2013). Osteoconduction of porous Ti metal enhanced by acid and heat treatments. *Journal of Materials Science: Materials in Medicine, 24*, 1701−1715.

Kawai, T., Takemoto, M., Fujibayashi, S., Neo, M., Akiyama, H., Yamaguchi, S., et al. (2012). Bone-bonding properties of Ti metal subjected to acid and heat treatments. *Journal of Materials Science: Materials in Medicine, 23*, 2981−2992.

Kawanae, K., Ise, K., Goto, K., Akiyama, H., Nakamura, T., Kaneuji, A., et al. (2009). A new cementless total hip arthroplasty with bioactive titanium porous-coating by alkaline and heat treatments: average 4.8-year results. *Journal of Biomedical Materials Research Part B: Applied Biomaterials, 90B*, 476−481.

Kim, H.-M., Himeno, T., Kawashita, M., Lee, J.-H., Kokubo, T., & Nakamura, T. (2003). Surface potential change in bioactive titanium metal during the process of apatite formation in simulated body fluid. *Journal of Biomedical Materials Research Part A, 67A*, 1305−1309.

Kim, H.-M., Miyaji, F., Kokubo, T., & Nakamura, T. (1996). Preparation of bioactive Ti and its alloys via simple chemical surface treatment. *Journal of Biomedical Materials Research, 32*, 409−417.

Kim, H.-M., Miyaji, F., Kokubo, T., Nishiguchi, S., & Nakamura, T. (1999). Graded surface structure of bioactive titanium prepared by chemical treatment. *Journal of Biomedical Materials Research, 45*, 100−107.

Kim, H.-M., Takadama, H., Kokubo, T., Nishiguchi, S., & Nakamura, T. (2000a). Formation of bioactive graded surface structure on Ti−15Mo−5Zr−3Al alloys by chemical treatment. *Biomaterials, 21*, 353−358.

Kim, H.-M., Takadama, H., Miyaji, F., Kokubo, T., Nishiguchi, S., & Nakamura, T. (2000b). Formation of bioactive functionally graded structure on Ti−6Al−4V alloy by chemical surface treatment. *Journal of Materials Science: Materials in Medicine, 11*, 555−559.

Kizuki, T., Matsushita, T., & Kokubo, T. (2014). Antibacterial and bioactive calcium titanate layers formed on Ti metal and its alloys. *Journal of Materials Science: Materials in Medicine, 25*, 1737−1746.

Kizuki, T., Takadama, H., Matsushita, T., Nakamura, T., & Kokubo, T. (2010). Preparation of bioactive Ti metal surface enriched with calcium ions by chemical treatment. *Acta Biomaterialia, 6*, 2836−2842.

Kizuki, T., Takadama, H., Matsushita, T., Nakamura, T., & Kokubo, T. (2013). Effect of Ca contamination on apatite formation in a Ti metal subjected to NaOH and heat treatments. *Journal of Materials Science: Materials in Medicine, 24*, 635−644.

Kokubo, T., Pattanayak, D. K., Yamaguchi, S., Takadama, H., Matsushita, T., Kawai, T., et al. (2010). Positively charged bioactive charged bioactive Ti metal prepared by simple chemical and heat treatments. *Journal of the Royal Society Interface, 7*, S503−S513.

Kokubo, T., & Takadama, H. (2006). How useful is SBF in predicting in vivo bone bioactivity? *Biomaterials, 15*, 2907−2915.

Lee, M.-H., Park, H.-S., Min, K.-S., Ahn, S.-G., Park, J.-M., Song, K.-Y., et al. (2007). Evaluation of in vitro tests for surface-modified titanium by H_2SO_4 and H_2O_2 treatment. *Metals and Materials International, 13*, 109−115.

Leeuwenburgh, S. C. G., Wolke, J. G. C., Jansen, J. A., & de Groot, K. (2008). Calcium phosphate coatings. In T. Kokubo (Ed.), *Bioceramics and their clinical applications* (pp. 464−484). Cambridge: Woodhead.

Li, P., Ohtsuki, C., Kokubo, T., Nakanishi, K., Soga, N., & de Groot, K. (1994). The role of hydrated silica, titania, and alumina in inducing apatite on implants. *Journal of Biomedical Materials Research, 28*, 7−15.

Li, Y., Zou, S., Wang, D., Feng, G., Bao, C., & Hu, J. (2010). The effect of hydrofluoric acid treatment on titanium implant osseointegration in ovariecomized rats. *Biomaterials, 31*, 3266−3273.

Liu, X., Zhao, Z., & Leng, Y. (2007). Biomimetic calcium phosphate coatings on nitric-acid-treated titanium surfaces. *Materials Science and Engineering: C, 27*, 700−708.

Minagar, S., Wang, J., Barndt, C. C., Ivanova, E. P., & Wen, C. (2013). Cell response of anodized nanotubes on titanium and titanium alloys. *Journal of Biomedical Materials Research Part A, 101A*, 2726−2739.

Miyazaki, T., Kim, H.-M., Kokubo, T., Kato, H., & Nakamura, T. (2000). Bioactive tantalum metal prepared by NaOH treatment. *Journal of Biomedical Materials Research, 50*, 35−42.

Miyazaki, T., Kim, H.-M., Kokubo, T., Kato, H., & Nakamura, T. (2001a). Induction and acceleration of bonelike apatite formation on tantalum oxide gel in simulated body fluid. *Journal of Sol−Gel Science and Technology, 21*, 83−88.

Miyazaki, T., Kim, H.-M., Kokubo, T., Miyaji, F., Kato, H., & Nakamura, T. (2001b). Effect of thermal treatment on apatite-forming ability on NaOH-treated tantalum metal. *Journal of Materials Science: Materials in Medicine, 12*, 683−687.

Miyazaki, T., Kim, H.-M., Kokubo, T., Ohtsuki, C., Kato, H., & Nakamura, T. (2002). Enhancement of bonding strength by graded structure at interface between apatite layer and bioactive tantalum metal. *Journal of Materials Science: Materials in Medicine, 13*, 651−655.

Miyazaki, T., Kim, H.-M., Kokubo, T., Ohtsuki, C., & Nakamura, T. (2001c). Apatite-forming ability of niobium oxide gels in a simulated body fluid. *Journal of the Ceramic Society of Japan, 109*, 929−933.

Nayab, S. N., Jones, F. H., & Olsen, I. (2007). Effects of calcium ion-implantation of titanium on bone cell function in vitro. *Journal of Biomedical Materials Research, 83A*, 296−302.

Nishiguchi, S., Fujibayashi, S., Kim, H.-M., Kokubo, T., & Nakamura, T. (2003). Biology of alkali- and heat-treated titanium implants. *Journal of Biomedical Materials Research, 67A*, 26−35.

Nishiguchi, S., Kato, H., Fujita, H., Kim, H.-M., Miyaji, F., Kokubo, T., et al. (1999). Enhancement of bone-bonding strengths of titanium alloy implants by alkali and heat treatments. *Journal of Biomedical Materials Research, 48*, 689−696.

Park, J.-W., Kim, Y.-J., Jang, J.-H., Kwon, T. G., Bae, Y.-C., & Suh, J.-Y. (2010). Effects of phosphoric acid treatment of titanium surface on surface properties, osteoblast response and removal of torque forces. *Acta Biomaterialia, 6*, 1661−1670.

Park, J.-W., Park, K. B., & Suh, J.-Y. (2007). Effects of calcium ion incorporation on bone healing of Ti−6Al−4V alloy implants in rabbit tibia. *Biomaterials, 28*, 3306−3313.

Pattanayak, D. K., Kawai, T., Matsushita, T., Takadama, H., Nakamura, T., & Kokubo, T. (2009). Effect of HCl concentrations on apatite-forming ability of NaOH−HCl- and heat-treated titanium metal. *Journal of Materials Science: Materials in Medicine, 20*, 2401−2411.

Pattanayak, D. K., Yamaguchi, S., Matsushita, T., & Kokubo, T. (2011a). Effect of heat treatments on apatite-forming ability of NaOH- and HCl-treated titanium metal. *Journal of Materials Science: Materials in Medicine, 22*, 273−278.

Pattanayak, D. K., Yamaguchi, S., Matsushita, T., & Kokubo, T. (2011b). Nanostructured positively charged bioactive TiO_2 layer formed on Ti metal by NaOH, acid and heat treatments. *Journal of Materials Science: Materials in Medicine, 22*, 1803−1812.

Pattanayak, D. K., Yamaguchi, S., Matsushita, T., Nakamura, T., & Kokubo, T. (2012). Apatite-forming ability of titanium in terms of pH of the exposed solution. *Journal of the Royal Society Interface, 9*, 2145−2155.

Rautray, T. R., Narayanan, R., Kwon, T.-Y., & Kim, K.-H. (2010). Surface modification of titanium and titanium alloys by ion implantation. *Journal of Biomedical Materials Research Part B: Applied Biomaterials, 93B*, 581−591.

Shibata, Y., Suzuki, D., Omori, S., Tanaka, R., Murakami, A., Ktaoka, Y., et al. (2010). The characteristics of in vitro biological activity of titanium surfaces anodically oxidized in chloride solution. *Biomaterials, 31*, 8546−8555.

So, K., Kaneuji, A., Matsumoto, T., Matsuda, S., & Akiyama, H. (2013). Is the bone-bonding ability of a cementless total hip prosthesis enhanced by alkaline and heat treatments? *Clinical Orthopaedics and Related Research, 471*, 3847−3855.

Sugino, A., Ohtsuki, C., Tsuru, K., Hayakawa, S., Nakano, T., Okazaki, Y., et al. (2009). Effect of spatial design and thermal oxidation on apatite formation on Ti−15Zr−4Ta−4Nb alloy. *Acta Biomaterialia, 5*, 298−304.

Suh, Y.-T. (2003). The significance of the surface properties of oxidized titanium to the bone response: special emphasis on potential biochemical bonding of oxidized titanium implant. *Biomaterials, 24*, 3893−3907.

Takadama, H., Kim, H.-M., Kokubo, T., & Nakamura, T. (2001a). An X-ray photoelectron spectroscopy study of the process of apatite formation on bioactive titanium metal. *Journal of Biomedical Materials Research, 55*, 185−193.

Takadama, H., Kim, H.-M., Kokubo, T., & Nakamura, T. (2001b). TEM-EDX study of mechanism of bonelike apatite formation on bioactive titanium metal in simulated body fluid. *Journal of Biomedical Materials Research, 57*, 441−448.

Takemoto, M., Fujibayashi, S., Neo, M., So, K., Akiyama, N., Matsushita, T., et al. (2007). A porous bioactive titanium implant for spinal interbody fusion: an experimental study using a canine model. *Journal of Neurosurgery: Spine, 7*, 435−443.

Takemoto, M., Fujibayashi, S., Neo, M., Suzuki, J., Kokubo, T., & Nakamura, T. (2005). Mechanical properties and osteoconductivity of porous bioactive titanium. *Biomaterials, 26*, 6014−6023.

Takemoto, M., Fujibayashi, S., Neo, M., Suzuki, J., Matsushita, T., Kokubo, T., et al. (2006). Osteoinductive porous titanium implants: effect of sodium removal by dilute HCl treatment. *Biomaterials, 27*, 2682−2691.

Takeuchi, K., Saruwatari, L., Nakamura, H., Yang, J.-M., & Ogawa, T. (2005). Enhanced intrinsic biomechanical properties of osteoblastic mineralized tissue on roughened titanium surface. *Journal of Biomedical Materials Research Part A, 72A*, 296−305.

Tanaka, M., Takemoto, M., Fujibayashi, S., Kawai, T., Yamaguchi, S., Kizuki, T., et al. (2014). Bone bonding ability of a chemically treated low elastic modulus Ti alloy; gum metal. *Journal of Materials Science: Materials in Medicine, 25*, 635−643.

Tanaka, K., Takemoto, M., Fujibayashi, S., Kawanabe, K., Matsushita, T., Kokubo, T., et al. (2009). Long term study of osteoconductivity of bioactive porous titanium metals: effects of sodium removal by dilute HCl treatment. *Key Engineering Materials, 396−398*, 353−356.

Turkan, U., & Guden, M. (2010). The effect of nitric acid surface treatment on CaP deposition on Ti−6Al−4V open-cell foams in SBF solution. *Surface and Coatings Technology, 205*, 1904−1916.

Uchida, M., Kim, H.-M., Kokubo, T., Tanaka, K., & Nakamura, T. (2002a). Structural dependence of apatite formation on zirconia gels in a simulated body fluid. *Journal of the Ceramic Society of Japan, 110*, 710−715.

Uchida, M., Kim, H.-M., Miyaji, F., Kokubo, T., & Nakamura, T. (2002b). Apatite formation on zirconium metal treated with aqueous NaOH. *Biomaterials, 23*, 313−317.

Ueda, M., Ikeda, M., & Ogawa, M. (2009). Chemical−hydrothermal combined surface modification of titanium for improvement of osteointegration. *Materials Science and Engineering: C, 29*, 994−1000.

Ueno, T., Tsukimura, N., Yamada, M., & Ogawa, T. (2011). Enhanced bone-integration capability of alkali-and heat-treated nanopolymorphic titanium in micro-to-nanoscale hierarchy. *Biomaterials, 32*, 7297−7308.

Wang, X.-X., Hayakawa, S., Tsuru, K., & Osaka, A. (2002). Bioactive titania gel layers formed by chemical treatment of Ti substrate with H_2O_2/HCl solution. *Biomaterials, 23*, 1353−1357.

Wang, X. J., Li, Y. C., Yamada, Y., Hodgson, P. D., & Wen, C. E. (2008). In vitro bioactivity evaluation of titanium and niobium metals with different surface morphologies. *Acta Biomaterialia, 4*, 1530−1535.

Whiteside, P., Matykina, E., Gough, J. E., Skeldon, P., & Thompson, G. E. (2010). In vitro evaluation of cell proliferation and collagen synthesis on titanium following plasma electrolytic oxidation. *Journal of Biomedical Materials Research Part A, 94A*, 38−46.

Wu, J.-M., Hayakawa, S., Tsuru, K., & Osaka, A. (2004). Low-temperature preparation of anatase and rutile layers on titanium substrates and their ability to induce in vitro apatite deposition. *Journal of the American Ceramic Society, 87*, 1635−1642.

Xie, L., Liao, X., Yin, G., Huang, Z., Yan, D., Yao, D., et al. (2011). Preparation, characterization, in vitro bioactivity, and osteoblast adhesion of multi-level porous titania layer on titanium by two-step anodization treatment. *Journal of Biomedical Materials Research Part A, 98A*, 312−320.

Yamaguchi, S., Kizuki, T., Takadama, H., Matsushita, T., Nakamura, T., & Kokubo, T. (2012). Formation of a bioactive calcium titanate layer on gum metal by chemical treatment. *Journal of Materials Science: Materials in Medicine, 23*, 873−883.

Yamaguchi, S., Matsushita, T., & Kokubo, T. (2013a). A bioactive Ti metal with a Ca-enriched surface layer releases Mg ions. *RSC Advances, 3*, 11274−11282.

Yamaguchi, S., Matsushita, T., Nakamura, T., & Kokubo, T. (2013b). Bioactive Ti metal with Ca-enriched surface layer able to release Zn ion. *Key Engineering Materials, 529−530*, 547−552.

Yamaguchi, S., Nath, S., Matsushita, T., & Kokubo, T. (2014). Controlled release of strontium ions from a bioactive Ti metal with a Ca-enriched surface layer. *Acta Biomaterialia, 10*, 2282−2289.

Yamaguchi, S., Takadama, H., Matsushita, T., Nakamura, T., & Kokubo, T. (2009). Cross-sectional analysis of the surface ceramic layer developed on Ti metal by NaOH−heat treatment and soaking in SBF. *Journal of the Ceramic Society of Japan, 117*, 1126−1130.

Yamaguchi, S., Takadama, H., Matsushita, T., Nakamura, T., & Kokubo, T. (2010). Apatite-forming ability of Ti−15Zr−4Nb−4Ta alloy induced by calcium solution treatment. *Journal of Materials Science: Materials in Medicine, 21*, 439−444.

Yamaguchi, S., Takadama, H., Matsushita, T., Nakamura, T., & Kokubo, T. (2011). Preparation of bioactive Ti−15Zr−4Nb−4Ta alloy from HCl and heat treatments after an NaOH treatment. *Journal of Biomedical Materials Research Part A, 97A*, 135−144.

Yan, W.-Q., Nakamura, T., Kobayashi, M., Kim, H.-M., Miyaji, F., & Kokubo, T. (1997). Bonding of chemically treated titanium implants to bone. *Journal of Biomedical Materials Research, 37*, 267−275.

Zhang, L., Ayukawa, Y., LeGeros, R. Z., Matsuya, S., Koyano, K., & Ishikawa, K. (2010). Tissue-response to calcium-bonded titanium surface. *Journal of Biomedical Materials Research Part A, 95A*, 33−39.

Zhang, P., Zhang, Z., Li, W., & Zhu, M. (2013). Effect of Ti−OH groups on microstructure and bioactivity of TiO_2 coating prepared by micro-arc oxidation. *Applied Surface Science, 268*, 381−386.

Zhao, X., Liu, X., & Ding, C. (2005). Acid-induced bioactive titania surface. *Journal of Biomedical Materials Research Part A, 75A*, 888−894.

Zhao, X., Liu, X., You, J., Chen, Z., & Ding, C. (2008). Bioactivity and cytocompatibility of plasma-sprayed titania coating treated by sulfuric acid treatment. *Surface and Coatings Technology, 202*, 3221−3226.

Zhao, L., Mei, S., Chu, P. K., Zhang, Y., & Wu, Z. (2010). The influence of hierarchical hybrid micro/nano-textured titanium surface with titania nanotubes on osteoblast functions. *Biomaterials, 31*, 5072−5082.

Zhou, R., Wei, D., Yang, H., Cheng, S., Feng, W., Li, B., et al. (2014). Osseointegration of bioactive microarc oxidized amorphous phase/TiO_2 nanocrystals composite coatings on titanium after implantation into rabbit tibia. *Journal of Materials Science: Materials in Medicine, 25*, 1307−1318.

Zhou, W., Zhou, X., Wu, X., Yuan, L., Shu, Q., Xia, Y., et al. (2007). Plasma-controlled nanocrystallinity and phase composition of TiO_2: a smart way to enhance biomimetic response. *Journal of Biomedical Materials Research Part A, 81A*, 453−464.

New nanoscale surface modifications of metallic biomaterials

8

N.C. Verissimo[1], *S. Chung*[2], *T.J. Webster*[2,3]
[1]State University of Campinas, Campinas, State of São Paulo, Brazil; [2]Northeastern University, Boston, MA, USA; [3]Center of Excellence for Advanced Materials Research, King Abdulaziz University, Jeddah, Saudi Arabia

8.1 Introduction

Biomaterials have been used extensively to improve the quality of human life, replacing dysfunctional or arthritic hips, atherosclerotic arteries, decaying teeth, and even repairing injured tissues such as cartilage and skin. The aging population will require even greater replacement and repair of soft and hard tissues such as bones, cartilage, blood vessels, or even entire organs (Holzapfel et al., 2013). Traditional materials such as metals, ceramics, polymers, semiconductors, and glasses are still used for material science and engineering; all of these materials have been used in a variety of biomedical applications such as cardiovascular stents and orthopedic implants. For biomaterials' applications, materials must be biocompatible and cannot induce toxicity (Callister and Rethwisch, 2007; Kumar et al., 2005). Thus, whereas the choice of materials has not changed significantly over the past decades, the variety of surface modification techniques has increased exponentially in the past few years to tailor such materials for specific biomedical applications. Recently, much progress has been made toward improving biomaterial properties by focusing at the nanoscale (material constituent dimensions on the order of 10^{-9} m) and at an atomic level. At these dimensions, it is possible to develop unique mechanical, electrical, magnetic, and other properties not otherwise possible with traditional micron-scale substrates (Callister and Rethwisch, 2007; Rosei, 2004). The use of nanotechnology has not been more apparent than through the modification of metals.

8.2 Metals for biological applications

8.2.1 Metallic biomaterials and their properties

Biomaterials are natural or synthetic substances that are tolerated transiently or permanently by various tissues in the human body and are typically used to construct artificial organs, rehabilitation devices, or implants to replace natural body tissues. More specifically, biomaterials are materials used in close or direct contact with the body

Surface Coating and Modification of Metallic Biomaterials. http://dx.doi.org/10.1016/B978-1-78242-303-4.00008-9
Copyright © 2015 Elsevier Ltd. All rights reserved.

to augment or replace materials that cause fracture after implantation in the human body (Bauer et al., 2013). Although the term "biocompatibility" is commonly used for a number of purposes, the most accepted definition for biocompatibility is "the ability of a material to develop a specific response to a suitable host in a specific application" (Brunette et al., 2001).

Ideally, biomedical materials should possess a number of unique properties. Naturally, the material must satisfy some requirements related to biocompatibility, corrosion resistance, and compatibility in physical and mechanical terms. These materials also should not have magnetic or ferromagnetic properties. Whenever a foreign substance is introduced into the human body (including biomaterials), rejection may occur, and the magnitude of the rejection may range from mild irritation or inflammation to death; therefore, it is important that the biomaterial possesses a high grade of biocompatibility (Bauer et al., 2013). A biocompatible material cannot generate by-products, caused by reactions with body fluids, which are toxic to the surrounding tissues, and they must remain intact under physiological conditions (Callister and Rethwisch, 2007). Suitable implant materials include metallic implants as well as polymers (Ganesh and Gross, 2012), ceramics (Rosengren et al., 2002), and composites thereof (Okereke et al., 2014). The strongest attributes of metals are their mechanical properties. The design of orthopedic biomaterials must also consider mechanical properties such as modulus of elasticity, yield strength, tensile strength, fatigue, fracture toughness, and ductility. Those properties are especially important for bone and hip replacements because of extreme body forces, such as weight, gravity, and external dynamic forces generated by the walking process. Orthopedic biomaterials must have similar properties with the human body but also withstand the sum of mechanical forces that actuate on it; if not, deterioration of the surrounding bone tissue and implant failure will ensure additional surgeries and prosthetic implants (Callister and Rethwisch, 2007; Martinu et al., 2010).

8.2.2 Metals used in biomedical applications

Metallic biomaterials, such as stainless steels, titanium alloys, and cobalt alloys, are widely used as implantable devices for different medical applications because of their excellent combinations of mechanical properties. For orthopedic applications, metallic materials are often used as plates, screws, and pins for fixation, artificial joints, artificial spines, and tooth implants (Navarro et al., 2008). Metallic biomaterials, specifically 316L stainless steel or L605 cobalt-based (Co) alloys, have been used as coronary stents.

An important class of new biologically active materials with biodegradable metals. Biodegradable alloys for biomedical applications have advantages over traditional materials such as inert metals, ceramics, and biodegradable polymers. These materials are especially important for orthopedic implants and load-bearing applications; they promote integration with the host tissue by stimulating new tissue growth and then dissolving in a time-dependent manner once the tissue regeneration process has been initiated. Thus, an important consideration is biocompatibility of the degradable

scaffold and the ability of the body to clear the scaffold materials (Holzapfel et al., 2013; Ren and Yang, 2013).

Magnesium (Mg)-based alloys are a new class of metallic biomaterials that have a unique blend of properties, biodegradability at physiological environments, and excellent mechanical properties that make them superior to other comparable materials such as polymers and ceramics (Holzapfel et al., 2013; Witte, 2010). Recent reports have also found that surface modifications that induce biological activity may improve tissue-specific endpoints. Mg has good compatibility, and Mg ions are present in large amounts in the human body, approximately 35 g per 70 kg body weight, with the daily nutritional demand for Mg around 375 mg. Thus, Mg-based alloys are promising candidates for orthopedic and cardiovascular implants and have attracted increasing attention because there is no requirement for a secondary removal surgery (Liu et al., 2004).

However, despite their many advantages, Mg-based materials suffer from disadvantages such as a high corrosion rate into the body, limiting applications of Mg-based devices. Because of their high corrosion rate, excessive generation of subcutaneous hydrogen gas is too much for the surrounding tissue to handle. Thus, for Mg devices to become effective bioabsorbable implants, Mg degradation rate must be slowed to match the natural human healing process, at least 12 weeks, to allow newly regenerated tissues to have sufficient structural integrity and support. The latest research has focused on retarding Mg degradability and stimulating tissue growth, with a strong emphasis on the use of surface modifications for achieving these goals (Poinern et al., 2012). Thus, investigation into the use of surface modifications for creating biologically active metallic biomaterials has become a new paradigm in the field (Mourino et al., 2012; Ren and Yang, 2013).

8.2.3 Common metal alloys

Permanent metallic implants based on stainless steel, cobalt−chromium (Co−Cr) alloys and titanium (Ti) or its alloys have been the metallic biomaterials of choice for decades. Replacement of hips, knees, and the spine as well as dental implants makes up the majority of all inserted metallic implants worldwide. However, classical metallic materials have some limitations, such as corrosion in the physiological environment. Such toxic elements such as nickel (Ni), chromium (Cr), and cobalt (Co) are released when they come into contact with body fluids and may cause serious conditions such as skin diseases or carcinogenesis (Bauer et al., 2013).

Among the metallic materials for biomedical applications, stainless steel, such as 316L (American Society for Testing and Materials F138), Cr−Co alloys, Co−Cr−Mo (ASTM F75, F799), Co−Ni−Cr−Mo (ASTM F562), commercially pure Ti, and Ti−6Al (Al)−4V (ASTMF67 and F136) are the most commonly used. These metals are most commonly used in orthopedic and implant devices and have been used as external materials to fix fractures. Some of their mechanical properties are shown in Table 8.1.

These devices are subject to failure from mechanical fracture, abrasion, corrosion, or some combination of these events. In this context, properties of resistance to

Table 8.1 Characteristic mechanical properties of various metallic biomedical materials (Bauer et al., 2013; Oréfice, 2006)

Material	Young's modulus (GPa)	Yield strength (MPa)	Tensile strength (MPa)
Ticp grade 1	102.7	240	170
Ticp grade 2	102.7	345	275
Ticp grade 3	103.4	450	380
Ticp grade 4	104.1	550	485
X_2CrNiMo 17122	190	331	586
AISI 316L	190	792	930
	190	1213	1351
Co−28Cr−6Mo	210	448−517	655−889
	210	896−1200	1399−1586
Co−20Cr−15W−10Ni	210	484−648	951−1220
	210	1606	1896
Ti−6Al−4V	100−110	830−1070	920−1140
Ti−6Al−17Nb	110	810−1010	870
Ti−5Al−2.5Fe	110−115	780	860
Ti−15Mo	78	1000−1060	874
Ti−12Mo−6Zr−2Fe	74−85	1000−1060	1060−1100
Ti−13Nb−13Zr	64−83	435−905	705−1035
Ti−29Nb−13Ta−4.6Zr	65	400	1000−1050
Ti−30Nb	63−80	500	700
Ti−30Ta	60−70	590	740

corrosion, abrasion, and fracture resistance are key requirements for a biomaterial. Many implants are exposed to heavy wear and high loads, with intense movement for a large number of cycles. These movements are highly aggressive and increase corrosion on the implants. On the other hand, metals with high Young's modulus values can induce a phenomenon known as stress shielding, leading to bone resorption. Among metallic materials, titanium and its alloys come closest to the elastic modulus of bone and can reduce bone resorption and enhance bone remodeling (Akahori and Niinomi, 1998; Bauer et al., 2013; Oréfice, 2006).

Titanium and its alloys have the best biocompatibility among various metallic materials such as stainless steel, alumina ceramics (Al_2O_3, 80−99%), Mg (pure, AZ31, AZ91D), and cobalt chrome alloys because of the formation of a stable

passive layer of titanium oxide, TiO_2, on its surface, and therefore they provide ideal corrosion resistance and superior biocompatibility. The Ti−6Al−4V alloy is the first titanium alloy registered as an implant material in terms of ASTM standards and is attractive because of its high specific strength. However, there are concerns about the possible release of toxic elements V and Al. Therefore, V-free titanium alloys such as Ti−6Al−7Nb have been developed and registered as a biomaterial (Akahori and Niinomi, 1998). New Ti alloys have been developed to include more biocompatible elements with more suitable mechanical properties; this has led to the development of low-modulus β-type titanium alloys in which niobium or iron is alloyed instead of vanadium. New developments in the field of Mg-based metal implants may change the paradigm of using insoluble metallic materials in the future (Holzapfel et al., 2013).

8.3 Nanoscience and nanotechnology

Between 2000 and 2010, research efforts in nanoscience and nanotechnology (that is, technology using building components in the size range of 1−100 nm) have become the most active research fields in the area of solid-state physics and engineering. The primary motivation behind this push is the need to fabricate new materials to decrease cost and to improve biocompatibility. Atoms, molecules, clusters, and nanoparticles can be used in advanced materials fabrication; these fundamentally smaller units allow for unprecedented tailoring of material properties through altering building block dimensions and control of surface geometry, chemistry, and assembly (Makarov, 2013; Rosei, 2004).

Nanotechnology has achieved tremendous progress over the past several decades. Recently, nanomaterials or nanostructured surfaces have received a great deal of attention toward improving disease prevention, diagnosis, and treatment (Zhang and Webster, 2009). The goal of nanotechnology today is to develop functional devices for tissue engineering purposes that can operate at submicron length scales resembling the human body (Rosei, 2004). The application of nanotechnology for biomedical purposes involves a two-dimensional association of surface features that can be arranged in an isotropic, organized, or an anisotropic, unorganized, fashion (Mendonça et al., 2008). For biomedical materials, implant surface modification is needed to optimize the properties of the implant and to maximize its bioactivity when interfacing with natural tissue. The biological characteristics of implants can be enhanced by adding materials with desired properties, changing the composition, or removing unwanted materials from the implant surface. These methods are known as *surface treatments* and can be classified into four categories: mechanical, physical, chemical, and biochemical surface modifications. Machining, grinding, polishing, and blasting are mechanical surface modifications. Physical surface treatments include thermal spraying, physical vapor deposition, ion implantation and deposition, and glow discharge plasma treatment. Chemical surface modifications include chemical treatment (acid, hydrogen peroxide, alkaline, etc.), anodic oxidation, sol−gel processes, and chemical vapor deposition (Minagar et al., 2012).

8.4 Surface modification techniques

At present, a great variety of methods for fabricating nanoparticles and nanomaterials are available. These techniques are based on two general approaches, "top-down" and "bottom-up." Top-down approaches are surface treatments that generate nanofeatures by etching away from a larger, macroscopic building block and make use of physical methods. Bottom-up approaches occur when atoms or molecules aggregate and react to form nanomaterials using chemical methods. In general, many of these techniques were first developed in the semiconductor industry before finding biomedical applications (e.g., anodization, ion beam etching, laser techniques) (Makarov, 2013). Table 8.2 summarizes all the techniques covered in this chapter and addresses the advantages and disadvantages as well as the areas of improvement for future research.

8.4.1 Physical techniques

Several special methods have been developed in recent decades that can be classified as physical methods for fabricating nanoparticles and nanomaterials. Many of these methods take advantage of the evaporation of a solid material and the subsequent vapor formation from which nanoparticles are generated as a result of homogeneous condensation. Evaporation is a process in which materials from a thermal vaporization source reach the substrate with little or no collision with gas molecules in the space between the source and the substrate and has a number of advantages: the coated material has good adhesion and controllable film structure; the deposition can occur at low temperatures and can even deposit alloys; and particle size can be controlled by switching the vapor source or reducing the atomic aggregation rate (Liu et al., 2010). Evaporation is an especially relevant surface modification technique and will be discussed at length with other physical modification techniques.

8.4.1.1 Laser-based techniques

In recent years, the use of laser surface modification techniques, especially for biological applications, has emerged as a promising method for creating micro- and nanoscale features because of its inherent fabrication advantages (Stratakis et al., 2009). Laser processing possesses a number of advantages over traditional processing:

1. It is versatile and can modify a variety of substrates (Pfleging et al., 2013). It is especially applied to materials with high melting points, hardness, or resistance to corrosion and brittleness.
2. Laser fabrication is a one-step, direct maskless fabrication technique. Furthermore, it is noncontact, allowing the manipulation of sensitive biological molecules without loss of cellular activity.
3. Laser fabrication does not require harsh production environments. Laser modifications have been conducted in gaseous environments, such as air (Chen et al., 2010) and sulfur hexafluoride (Baldacchini et al., 2006), and liquid environments, such as water (Shen et al., 2008) and ethyl alcohol. It also does not require clean-room operation.

Table 8.2 Summary of techniques discussed in the chapter and their varying advantages, disadvantages, and future directions to improve their suitability as metallic biomaterials

Technique	Type	Advantages	Disadvantages	Areas of improvement
Laser	Physical	Precise control of surface modification; one-step fabrication technique; does not require clean-room operation	High initial cost; produces homogenous surfaces that do not mimic the more graded architecture in nature	Reducing thermal damage such as melting and cracking; scale-up to include multiple length scales is still not possible
Plasma spray	Physical	Versatile process able to melt most ceramics, metals, or composites; good deposition rate; uniform coating; good control of coating process	High initial cost and scale-up issues; ion damage on surface; may cause residual stress	Reduce ion deposition; make process more homogenous
Physical vapor deposition (PVD)	Physical	Deposition for a large range of materials; rapid solidification process; low cost	Cannot control thin film and produces amorphous coatings; capacity limited for large-diameter wafers	Improve process control over thin film formation
Anodization	Chemical	Controlled way to create nano-roughness and nano-features; commonly used technique to increase thickness and oxide layer of atmosphere; promotes high corrosion resistance; good control of oxidation process	Choice of electrolytes must be carefully chosen and requires prior expertise	Improve the process to be used to incorporate drug delivery into titanium-based implants to enhance new bone formation; serving as reservoirs of chemical mediators

Continued

Table 8.2 Continued

Technique	Type	Advantages	Disadvantages	Areas of improvement
Chemical vapor deposition (CVD)	Chemical	Used to prepare inorganic nanostructures; good control of nanofeatures	Fast gas flow are required; reactors must be cleaned frequently; deposition occurs everywhere; fragile substrates can be damaged; film properties highly dependent on surface homogeneity	More biomaterial-specific research for CVD is needed; scale-up for biomaterial-specific CVD processes are needed for industrial applications
Chemical etching	Chemical	Inexpensive; high precision; low chemical deposition; applicable to small features	Poor anisotropy; poor process control because of high sensitivity to temperature; low control over particle size; high cost because of chemical disposal	Better control of patterning accuracy; provide mechanism for chemical etching process; explore extending metal-assisted chemical etching to non-silica surfaces

4. Lasers produce precise surface features that are tunable through physical parameters such as frequency of the light, the energy density, and exposure time. High-resolution features, micro- and nanoscale, may be produced on two- and three-dimensional scales. The advent of femtosecond (fs) lasers has significantly improved the precision offered by laser-based techniques at the nanoscale.

Laser-based techniques can be generally categorized as additive or subtractive. There are many well-known additive techniques, such as pulsed-laser deposition (PLD), matrix-assisted pulsed-laser evaporation (MAPLE), MAPLE direct write, and laser-induced forward transfer (LIFT). Laser is also one of the few physical methods capable of etching and modifying metallic surfaces. Pulsed lasers, especially fs lasers, have found increasing uses for physically modifying surface characteristics for various applications.

The most common laser printing method is PLD. This is mechanistically very similar to physical vapor deposition (PVD) and chemical vapor deposition (CVD), which will be further discussed at length later in this chapter. Inside a pressure chamber, a high-powered pulsed-laser beam is directed toward the target, causing the solid to transition into the plasma state. The plasma plume is then deposited onto the substrate. This process may occur in an ultra-high vacuum chamber or in the presence of background gas, such as oxygen to deposit oxide groups on the substrate surface. As with other deposition methods, PLD is attractive for orthopedics and implants because it is well suited for depositing bone-like chemistries, such as hydroxyapatite and calcium phosphates, onto metals (Hao and Lawrence, 2005). PLD allows for better control of deposited film characteristics than other deposition techniques such as PVD and CVD applied to the same biocompatible ceramics.

For PLD (Figure 8.1), laser wavelength, fluence, and pulse duration are critical parameters governing target ablation and subsequent formation for biomaterial films such as calcium phosphate films. They determine the morphology, phase, crystallinity, and stoichiometry of the deposited coatings; for those compounds, parameters should be 20−35 ns for generating pulses at 248 nm KrF and 193 nm ArF. For Ti devices, continuous-wave CO_2 lasers for homogenous heating are used for substrate deposition. A new generation of bioactive calcium phosphate, ($Ca_8(HPO_4)_2(PO_4)_4$-$5H_2O$), has

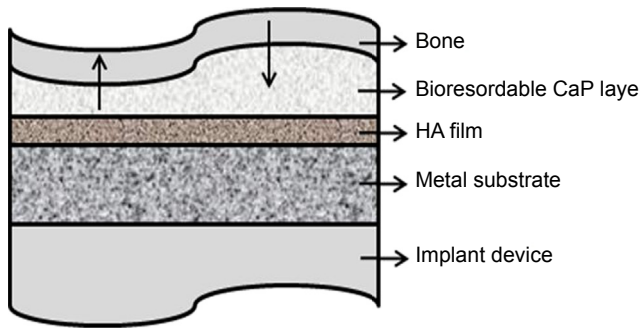


Figure 8.1 Scheme of a biofunctional bone implant using the PLD technique (Eason, 2007).

also been deposited by PLD (Iliescu et al., 2004; Socol et al., 2004). This material is formed in the precipitation of HA and natural BA. ($Ca_8(HPO_4)_2(PO_4)_4$-$5H_2O$) plays an essential role in the in vivo mineralization and ossification processes of mammalian bones and teeth as shown in Figure 8.1 (Eason, 2007).

In addition, PLD techniques, specifically MAPLE, may be used to transfer human cells. MAPLE is a gentler variation of the PLD technique and reduces the photochemical damage caused by ultraviolet (UV) laser light. MAPLE is a deposition technique designed for creating thin films that may be used to reconstruct different parts of bone tissue, teeth, or even whole organs, cell by cell, by accurately depositing specially prepared targets such as drugs, enzymes, cytokines, and pharmaceutical substances with specific regenerative activity on biomedical devices (Chen et al., 2013; Eason, 2007).

The biomaterial target is first dissolved in a solvent and then frozen to create a solid, ribbon target. A low-fluency flux integrated over time, pulsed laser evaporates the target for deposition on the substrate. MAPLE can be used across a variety of biomaterials, ranging from polymers, such as polyethylene glycol (Rodrigo et al., 2006), to cells, such as Chinese hamster ovary cells (Wu et al., 2001). Using masks, such as lines, dots, and arrays, pattern features as small as 20 μm can be deposited using different materials on a wide range of substrates.

MAPLE direct write is similar to MAPLE except the matrix containing the deposited material is placed directly on the substrate. The pulsed laser is then passed over the matrix and directly transfers the matrix material to the substrate in specific two- and three-dimensional features. Another commonly used laser direct-write method is the LIFT, in which a thin film of material is held over the substrate by a transparent support. When a laser pulse is focused on the film, a small fraction of the film is transferred to the receptor platform containing the substrate. The amount of material transferred depends on the laser fluence, laser wavelength, laser intensity, and the optical extinction coefficient of the target. At lower fluence levels, slightly above the melting threshold, small droplets of the transferred materials are formed. At higher fluence levels, the transferred materials are approximately the size of the laser spot. LIFT is versatile and can be used to transfer a wide range of materials in a solid or liquid state, such as conductors, dielectrics, and biomolecules in solution (Stratakis et al., 2009). Recent groups have also successfully transferred cells using a modified LIFT procedure (Ovsianikov et al., 2010).

In addition to additive methods, lasers can also directly alter the metallic surface. Pulsed lasers, traditional in the nanosecond (ns) range and increasingly transitioning into the fs range, have been used to directly modify physical surfaces of metals. These high-powered laser beams have pulse energies larger than 1 mJ, optical intensities greater than 10 TW/cm^2, and pulse repetition rates greater than 100 GHz. When directly applied to metal surfaces, lasers can etch through metallic surfaces, although increased pulse durations lead to thermal ablation of the surfaces (Keller, 2003). Thus, many researchers and investigators are interested in using ultrafast pulse lasers, such as fs lasers, to reduce thermal ablation while increasing spatial resolution. A common biological application of fs lasers is for modifying surface wettability. Laser-based techniques have successfully modified surface wettability using a wide range of

materials (silver, silicon, steel, polycarbonate, and poly-dimethylsiloxane), and recent groups have taken advantage of the improvements in laser technology to achieve precise topographical control using fs lasers (Fadeeva et al., 2009; Khorasani et al., 1999; Nuutinen and Vahimaa, 2013; Ranella et al., 2010). Despite the tremendous benefits of fs laser processing to modify surface wettability, there have been a few studies investigating cellular interactions with laser-ablated biomaterials. At the moment, fundamental knowledge about laser thermodynamics and phase transformations is still inadequate and require further research to resolve common laser associated problems such as microcracks and heat-affected zones.

8.4.1.2 Plasma-based techniques

Of all thermal spray processes, plasma spraying is the most versatile because it can melt virtually any material. Plasma spraying is a rapid heating−cooling solidification process. For the plasma technique, a range of materials can be deposited depending on the desired application and may be in the form of powders, rods, or wires, in fused or partially fused conditions, prepared over a substrate to form a film (Martinu et al., 2010). Controlled deposition of finer features is not possible with current technology. The technology of plasma spray imparts a metal substrate ceramic-coating system with the mechanical strength of a metal and the environmental stability of a ceramic material providing improving properties such as creep strength, fatigue strength, flexural strength, ductility, fracture toughness, coefficient of thermal expansion, heat conductivity, and porosity. The spray equipment generates the necessary heat to melt the material, and during plasma spraying, the temperature in the core region of the plasma beam is relatively constant at approximately 12,000 K, which melts most materials. As the material is heated, it turns into a molten or plastic state and is accelerated toward the substrate by a compressed gas. With the exception of large initial investment costs and problems with scale-up, plasma processing possesses a few major disadvantages. Figure 8.2 provides a scheme of plasma spray techniques.

The particle flux is directed to the substrate, and the particle strikes the surface at high speed, flattening out and forming layers that adhere and conform to surface irregularities and then cooling as the particles gradually form a lamellar structure (Liu et al., 2010). The plasma is generated by the plasma gun, which includes a cathode and an anode separated by a small chamber between the two. A direct current is applied to the cathode to generate an electric arc to the anode while the carrier gas is flowing through the chamber. The electric arc is powerful enough to turn electrostatic gas into the plasma state (Makarov, 2013). Plasma spray processes possess a number of advantages. It is possible to control surface layer length. Also, similar to noncontact laser techniques, plasma spray processes can avoid problems encountered in wet chemistry techniques, such as the presence of a residual solvent on the surface.

Among its many biomedical applications, plasma spray has been used to modify materials for various applications such as implants and devices for diagnosis and therapy, lenses, artificial veins, vascular grafts, catheters, dialysis membranes, and

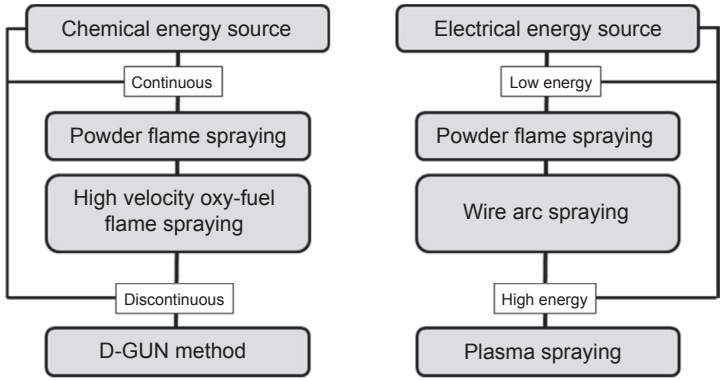


Figure 8.2 The thermal spray technique applied to metallic devices and divided by their energy sources (Martinu et al., 2010).

materials for repair bone and joint replacement. In addition, plasma spray has been used as an alternative to conventional biomaterial sterilization for heat-sensitive materials. Compared with the classical techniques of sterilization (heating and chemical), plasma provides three different linear segments instead of one. Plasma sterilization works by direct destruction (UV irradiation) of the genetic material of microorganisms, erosion of the microorganisms through intrinsic photo-desorption by UV irradiation, and erosion of the microorganisms through etching to form a volatile material emanating from the plasma.

In some cases, etching is further activated by UV photons, increasing the elimination rate of microorganisms. Compared with classical sterilization techniques, plasma spray sterilization is more efficient and does not produce toxic gases (Moisan et al., 2001; Zollfrank, 2014). For biomaterials, the plasma spray process has been used to generate nanoscale particles. One prominent example is a nanostructured zirconia coating, which is a conglomerate of two different types of particles: loose nanosized particles and a secondary structure consisting of microsized particles. The process gives the zirconia coating the same composition as the starting powder and creates uniform coating thickness. However, the thickness length is inconsistent, and research is being conducted to understand the effects of various preparations on plasma-sprayed nanostructured zirconia coatings. Commercially available TiO_2 have also been used in plasma spray for depositing onto alloys, such as Ti−6Al−4V substrates under modified spraying parameters (Liu et al., 2010). Plasma-sprayed titanium coatings with porous structures are used for the roots of teeth, hip, knee, and shoulder implant applications, because porous surfaces improve fixation via the growth of bone into the coating, forming a mechanical bond. Studies carried out by Vercaigne et al. (1998) show that plasma-spraying techniques can produce rough coatings that generate no particle release, overcoming a significant safety issue of very rough coatings (Liu et al., 2004; Vercaigne et al., 1998).

8.4.1.3 Physical vapor deposition

PVD is an atomistic deposition process in which materials are vaporized from a solid or liquid source, transported as vapor through vacuum or gas (or plasma) at low pressure to the substrate, and deposited onto the substrate via condensation. PVD is used to deposit films with a thickness of a few nanometers to thousands of nanometers (Liu et al., 2010). However, PVD can also form multiple layers, create thick compounds, and deposit film elements, alloys, and compounds using reactive deposition processes. In reactive deposition processes, the compounds are formed by reaction of the deposited materials with the gaseous atmosphere, such as nitrogen (for coating titanium nitride) or carbon (to form carbide titanium). The PVD process consists of evaporation, sputtering, vacuum arc deposition, ion plating, and ion implantation and deposition.

Fabricating thin films by the PVD technique involves a number of stages that are interdependent: such as (1) selecting the substrate; (2) defining the critical properties and determining those related to the substrate; (3) developing an appropriate surface preparation process; (4) selecting the film material and film structure to provide adhesion; (5) designing the fabrication process with the goal of providing reproducible coating properties and long-term stability; (6) developing production and fabrication equipment with proper processes and parameters; and (7) developing appropriate characterization techniques. One of the key applications of PVD is to modify existing injection molds. Two commonly used coatings for aluminum molds are titanium nitride and chromium nitride. Coating with these nitrides improves hardness on the mold surface, ensuring low porosity and high thermal and chemical stability. Physical vapor deposition can also be used to coat surgical instruments. The high hardness of the coating combined with a very low coefficient of friction provides a greater aptitude for cutting surgical instruments. The high-density layer provides an excellent barrier to any chemically aggressive environment as shown by Figure 8.3 (Liu et al., 2004; Mattox, 2010).

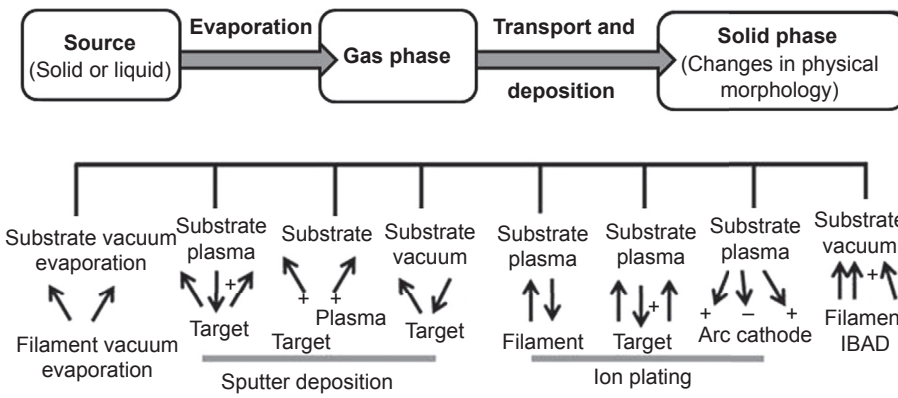


Figure 8.3 Schematic showing the configurations for various PVD deposition processes (Mattox, 2010).

PVD coatings also have a wide range of biomedical applications. Vacuum arc deposition is a process that uses vaporized materials emitted from an electrode under arcing conditions. Vacuum arc plasma deposited diamond-like carbon films with nanoscale thickness have been shown to have good biocompatibility properties and are promising coatings in biomedical devices including orthopedic implants (Xu and Pruitt, 1999). Recently, doped diamond films have attracted much attention, especially films doped with silver by pulsed deposition; these films are potentially useful biomaterials because of good blood compatibility and antimicrobial properties (Baba et al., 2012). Another approach is ion implantation, in which a negative high-voltage pulse is applied directly to a target. The ions from the plasma form gases such as nitrogen, oxygen, or hydrocarbons that are implanted onto the substrate surface. The technique has shown potential because of its versatility in modifying the surfaces of biomaterials and irregular shaped implants by changing surface structure, composition, functional groups, type of bimolecular or cellular bonding, and morphological features on the surface (Baba et al., 2012).

Ion plating is a PVD technique in which an energetic bombardment of particles alters the substrate surface and influences film formation. The materials for deposition are vaporized by evaporation, sputtering, arc erosion, or decomposition of chemical precursors. The energetic particles are usually ions of an inert or reactive gas or in some cases, ions of the condensing film materials. Ionic plasma deposition is an efficient method to deposit nanostructured films onto a variety of materials including metals and polymers; a cathode arc turns the deposited material, which includes metals and metals oxide, into plasma for deposition onto the substrate. Studies have shown that ionic plasma deposition treatment coating of titanium with silicone improved osteoblast function while decreasing fibroblast attachment and growth. This suggests that dry surface modification processes such as ion implantation, ion plating, ion beam mixing, and other ion-related modifications are useful in controlling the physiochemical nature of the surface, such as the surface energy and surface electrical charge, and developing tissue-compatible implants (Liu et al., 2010).

As with many other metallic modification techniques, electron beam (EB) evaporation or EB physical vapor deposition (EB-PVD) was originally developed in the semiconductor industry. In the EB-PVD process, the target material, in the shape of an ingot, is bombarded with high-powered electron beams, melting and evaporating atoms from the ingot. The gaseous atoms then precipitate into solids and coat everything in the vacuum chamber, including the substrate of interest. EB evaporation has a number of advantages. EB-PVD can be achieved through a wide range of deposition rates, as low as 1−100 nm/min. EB-PVD can generate either thin films or thick coatings and deposits uniformly. The main disadvantage to the EB-PVD process is the high equipment cost and the inability to generate more complicated or three-dimensional coating geometries. Also, filament degradation to the electron gun often results in "nonhomogeneous" power densities and evaporation rates.

Ion bean sputtering is a common method to deposit thin films, and its popularity stems from the simplicity of the physical processes involved, versatility, and flexibility. The mechanism of this technique is very similar to the mechanism of ion-bean PVD. Instead of an electron beam, an ion beam is used to bombard a target,

releasing atoms from the target. This technique can be used to either etch a target or sputter-coat a substrate. In sputtering, particles are vaporized from a target by some physical sputtering processes. In the ion sputtering method, ions are accelerated toward the target in the presence of a high-pressure inert gas and bombard the target, causing the surface particles to detach from the surface and aggregate into nanoparticles. This method was applied to obtain nanoparticles of metals and its alloys (Makarov, 2013). In addition, ion beam instruments can be used as components of diagnostic equipment; focused-ion-beam (FIB) instruments are commonly used to characterize thin films and have found increasing uses for more site-specific modification in biological applications (Liu et al., 2010).

8.4.2 Chemical methods

Nanostructured materials are usually synthesized under moderate reaction conditions. Nanoscale materials in the form of diluted salts, liquids, and foams are produced by chemical methods over rather long periods. The stages of seeding, particle growth, and growth arrest are frequently indivisible. Nanoparticle fabrication is usually initiated by mixing the reactants for synthesizing the nanoparticles, a coating for the nanoparticles, and a solvent. The most common chemical methods include: reduction; syntheses through solvothermal, photo, and electrochemical processes; arrested precipitation; thermolysis; and a number of other methods such as chemical reduction, e-beam lithography, metal reduction into solution reagents, photo-reduction in reverse micelles, and thermal decomposition of metal compounds.

8.4.2.1 Anodization

The anodization process is a classical metallurgical method that creates a protective and decorative oxide film over a metallic surface. Anodization is an improved process to classical electroprocessing. This process usually increases the thickness and density of the oxide layer formed on any metal surface exposed to the atmosphere. The metal or an alloy undergoing anodization serves as the anode and is connected to a positive terminal of a power supply and is placed in an electrolyte bath. The cathode, where hydrogen and oxygen is released, generally is an inert material such as platinum foil, graphite, or carbon. Once the anode and cathode are put inside the bath containing the proper electrolyte, reactions between the anode and cathode as well as in the electrolyte solution occur to form the oxide film at the substrate surface by processes such as anode oxidative degradation, migration of metal particles to the cathode, ion reduction to the zero-valence state, particle formation via nucleation and growth, growth arrest by capping agents, and particle precipitation (Mor et al., 2009). Anodization is used to synthesize metal nanoparticles of various sizes (starting from approximately 1 ± 5 nm), using metal palladium (Pd), nickel (Ni), Co, iron (Fe), Ti, silver (Ag), and gold (Au). The resulting oxide film properties such as nanometer roughness, morphology, and surface chemistry vary by a wide range depending on different process parameters such as applied potential, current density, electrolyte composition, pH, and temperature.

Anodization is the most popular technique for forming TiO_2 oxide layers, and much research and development has been done in the past 10 years. The first work related to this area was published in 1999 with anodization of Ti−6V4V alloys by Zwilling et al. (1999). Gong et al. (2001) developed CP-Ti anodization by using hydrofluoric acid (HF) solution, which allowed for the production of titanium nanotubes; this was later referred to as the first generation of anodization techniques of nanotubes (Gong et al., 2001). Commonly listed electrolytes used for anodization are acid electrolytes such as HF, phosphoric acid, sulfuric acid, and acetic acid; neutral salts; and organic and alkaline solutions (Makarov, 2013; Mor et al., 2009).

The first generation of nanotube synthesis was characterized by the use of acid electrolytes such as HF, sulfuric acid−HF, and HNO_3−HF. Experiments were initially performed using an electrochemical cell with constant voltage, a platinum foil as the cathode, and an electrolyte with mechanical stirring at room temperature. Studies on crystallization and structural transformation of these nanotubes showed that the application of specific heat treatments produces materials that are extremely sensitive to hydrogen gas materials as well as possessing excellent photocatalytic activity (Cai et al., 2005; Gong et al., 2001). Cai et al. (2005) were the first to produce TiO_2 nanotubes using KF and NaF with a pH change, ushering in second-generation production techniques of oriented nanotubes, which is characterized by the use of buffered solutions. These solutions gave longer nanotube lengths compared with the first-generation materials; however, pH control is necessary, because this directly changes the electrochemical behavior and consequently chemical dissolution.

Paulose et al. (2006) reported for the first time the anodization of CP-Ti based on NH_4F, $C_6H_6(CH_3)_3$, and formamide in combination with HF, NaF, and KF for generating fluoride ions, marking the third generation of anodization of nanotubes. This requires the reduction of water content to less than 5% of its volume to optimize the growth of the nanotubes. Because these solutions have low oxygen content, the formation of oriented oxide TiO_2 is weak. The dissolution of these compounds in water constitutes the source of oxygen required for anodizing; thus, this technique is only effective if water is no more than 5% of the total volume. The high conductivity of these electrolytes gives these nanotubes thin and elongated structures without internal deterioration (Hoyer, 1996; Jiang et al., 2012). Richter et al. (2007) reported the use of electrolytes without F in anodization, marking the beginning of the fourth generation. This generation is characterized by the substitution of fluoride ions by chloride (Cl) ions in the electrolyte because the Cl ions are able to perform similarly to F-based ions during anodization. The absence of F ions results in a new type of CP-Ti nanotube, with distinct morphological and chemical structures from the previous generation. The process of the formation of nanotubes is very fast, and the tubes are significantly thinner and longer than those previously reported in the literature (Gong et al., 2001; Richter et al., 2007).

Ti is a commonly used metal that has seen significant bioactive improvements because of the anodization process. Ti and its alloys are widely used as implants because of their high strength, biocompatibility, and high level of hemocompatibility. Hemocompatibility is conferred by the ability of Ti-based materials to form a dense and stable oxide layer on its surface in most environments, which makes the material

more suitable for biocompatible interaction. The amorphous oxide layer consists of TiO, Ti_2O_3 in the intermediate layer, and TiO_2 in the outer layer (Mor et al., 2009). The unanodized titania layer is bioinert and cannot form and maintain bonds easily with bone over long periods; thus, these implants tend to become loose and are not recommended for use over lengthy periods. Surface treatments are needed for Ti alloys to achieve better and faster osteo-induction or bonding to bone. The optimum surface treatment would create a stable passive layer on the surface of Ti implants with essential properties such as roughness, wettability, and electrostatic charges (Minagar et al., 2012). An ordered oxide layer can be tailored by controlling the type of electrolyte, applied current density, electrolyte concentration, electrolyte temperature, agitation speed, and cathode-to-anode surface area ratios (Sul et al., 2001).

Ti alloying elements include β-stabilizers, such as molybdenum, vanadium, niobium, and tantalum; eutectoids elements such as iron, tungsten, chromium, silicon, cobalt, and manganese; and finally neutral elements such as zirconium and tin. Organs and natural tissues have nanosized dimensions that cells can directly interact with to create nanostructured extracellular matrices. When biomaterials interact directly with biological tissues, nanostructured surface features provide a significant improvement in beneficial biological interactions by stimulating cell growth and, therefore, tissue regeneration (Zhang and Webster, 2009). The Ti−15Nb−4Ta−4Zr (TNZT) alloy is a beta alloy and is considered as a good choice for orthopedic and endo-prostheses. When compared with conventional Ti−6Al−4V, TNZT was found to have superior performance in terms of new bone formation and bone mineral density and mechanical properties (Minagar et al., 2012). Controllable metal oxide nanotubes can be fabricated by the anodization of titanium, titanium alloying metals (niobium, tantalum, and zirconium), and biocompatible titanium alloys such as Ti−Nb−Ta−Zr alloys and binary Ti−Nb, Ti−Ta, and Ti−Zr alloys. The nanotubes on titanium improve the mechanical properties of titanium and promote bonding to bone because of their high surface area and the ability for cells to form connections with the nanotubes (Minagar et al., 2012). The deposition of a TiO_2 nanotube layer seems to be a successful route toward the development of biomaterials based on Ti. The oxide layer exhibits a high surface-to-volume ratio, and researchers have seen a strong correlation between surface characteristics of an implant, morphology, and cytoskeletal organization (Oh et al., 2006).

In addition to Ti, other metals of interest in the anodization process include the valve metals such as Al, Nb, tantalum, and zirconium. It was demonstrated that a nanoporous oxide layer could be formed on these valve metals, forming a dense, stable, tightly adhering, and electrically insulating oxide layer on their surface (Minagar et al., 2012). Tantalum is more expensive and has a much higher density than titanium and, therefore, is not appropriate for implants. However, its chemical and physical properties, such as biocompatibility, radiopacity, dielectric properties, and high corrosion resistance to body fluids, are very attractive. Tantalum oxide has received a lot of attention as a protective coating material because of its corrosion resistance. Zirconium oxides have good properties such as chemical and thermal stability, mechanical strength, wear resistance, good ion exchange, and excellent biocompatibility (Liu et al., 2010).

8.4.2.2 Chemical vapor deposition

Similar to PVD, CVD produces gaseous atoms or molecules for deposition by high temperature reduction or decomposition. The deposited materials may react with other gaseous species in the system to yield compounds. Unlike PVD, CVD is a process involving chemical reactions between chemicals in the gas phase and the sample surface resulting in the deposition of a nonvolatile compound on the substrate (Liu et al., 2010). The sequential steps that occur in every CVD process include (1) convective and diffusive transport of reactants from the gas inlet to the reaction zone; (2) chemical reactions in the gas phase to produce new reactive species and by-products; (3) transport of the initial reactants to the substrate surface; (4) chemical and physical desorption and diffusion of these species onto the substrate surface; (5) heterogeneous reactions catalyzed by the surface leading to film formation; (6) desorption of the volatile by-products after surface reactions; and (7) convective and diffusive transport of the reaction by-products away from the reaction zone. The working temperature of these processes typically occurs around 1000 °C.

Thin films grown by CVD typically have better step coverage than films produced by PVD; therefore, CVD was initially used to coat microelectronic devices or objects with complex geometry. CVD is also now widely used to modify the mechanical and biological properties of Ti and Ti alloys. The CVD process begins with a predefined mixture of gas reagents and inert gases, introduced with a given flow inside of a chamber. The gas species move to the substrate, and the reactants are adsorbed on the surface of the substrate. The reactants undergo chemical reactions with the substrate to form the film, and the gaseous reaction products are evacuated from the camera reaction (Liu et al., 2010). There are many CVD processes, such as atmospheric-pressure chemical vapor deposition, low-pressure chemical vapor deposition, plasma-enhanced chemical vapor deposition, plasma-assisted chemical vapor deposition, laser-enhanced chemical vapor deposition (LE-CVD), and hybrid processes combining features of both physical and chemical vapor deposition (Liu et al., 2004).

CVD is most commonly used to prepare inorganic-oriented nanostructures such as ZnO, MoO_x, and nanostructured silver coatings. These nanostructured films are composed of isolated nanoparticles rather than a continuous film and have the potential to serve as enhanced biocide agents to kill gram-negative bacteria *Escherichia coli*. Nano-crystalline diamonds have tremendous potential in biomedical applications, especially for enhancing orthopedic implant durability, because of their superior hardness, low friction coefficient, high chemical resistance, and feasibility for coating on a variety of substrates such as metal matrix composites, alumina, silicon, and stainless steel (Liu et al., 2004, 2010).

Nano-crystalline diamond coating acts as a good biomaterial, producing a selective protective barrier between the implant and the human environment, preventing the release of metallic ions of the substrate device into the body. CVD production of diamonds has received a great deal of attention in the materials sciences because it allows many new applications of diamonds that had previously been considered too difficult to make economical. Those coatings present high resistance to bacterial colonization when compared with medical steel and titanium, preventing bacterial

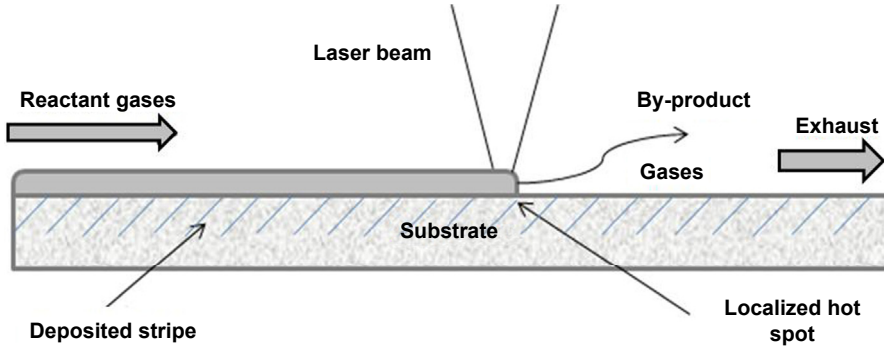


Figure 8.4 LE-CVD scheme of process of thin film deposition (Pierson, 1992).

infections and avoiding implant rejection and increasing the prosthesis life. Also, those nano-coatings can be produced by microwave plasma-enhanced CVD or traditional CVD to produce synthetic diamonds by creating the circumstances necessary for carbon atoms in a gas to settle onto a substrate in crystalline form, and can be treated in pure hydrogen plasma treatment at 300−800 W in the microwave plasma system at 5 mTorr (∼0.00666 mbar) for 2−15 min. Recently, other new nanotechniques such as polymer demixing, dip-pen lithography, photo or electron-beam nanolithography, and imprint lithography have been developed to construct a geometrically defined environment for patterning cells on the nanoscale. These fledgling techniques have led to more investigations of nanotopography-dependent mechanisms of integrin-mediated cell signaling (Liu et al., 2010).

For LE-CVD, the laser by itself produces a coherent, monochromatic high-energy beam of photons, which activates a CVD reaction, as shown in Figure 8.4. Laser CVD occurs as a result of the thermal energy from the laser coming in contact with and heating an absorbing substrate. The substrate is locally heated in a manner analogous to the local heating in a cold-wall reactor and deposition is restricted to the heated area (Pierson, 1992). Some examples of materials deposited by laser CVD are listed, with their respective parameters, such as aluminum (Al) with a pressure of 10 Torr (∼0.0133) and a laser range of 476−647 nm; Au with 1 Torr (∼0.00133) and atmospheric environment, elements such as platinum (Pt), tin (Sn), and indium (In) do not need any specific conditions to produce thin films by CVD (Pierson, 1992).

8.4.2.3 Chemical etching

Metal-assisted chemical etching is a simple and very promising technique to pattern mono-crystalline features into nanosized structures yielding high aspect ratios. In metal-assisted chemical etching, Ag, Au, Pt, and palladium are the most frequently used noble metals (Li et al., 2010). Metal-assisted etching requires three fundamental components: (1) an oxidant to dissolve silicon; (2) a suitable complexing agent to remove native silicon surface oxide and solubilize ionic silicon; and (3) a transition metal that locally enhances silicon dissolution in the vicinity of the metal.

An oxidant with higher reduction potential than silicon can only be used in the presence of an externally applied potential; once the reduction potential is lower, suitable oxidants are no longer required. Oxidant materials that have been previously investigated include Cr_2O_7, MnO^{4-}, HNO_3, $S_2O_8^{2-}$, Fe^{3+}, Pt^{3+}, Au^{3+}, Ag^{+}, and H_2O_2. It is believed that the dissolution of Si is facilitated by H_2O_2 reduction at the local metal cathode in the middle, whereas HF plays an important role in cleaning the silicon off surface oxides and producing fluorosilicates (SiF_6^{2-}) (Li et al., 2010; Smith et al., 2013). The addition of a metal is vital in metal-assisted etching processes and provides an attractive approach for triggering the formation of porous silicon in selected areas of a sample, forming a porous silicon pixel patterns. This method generates a Si layer with uniform pore size and within 100 nm provides longer durability of the porous microstructures in air or in aqueous media, which is a great advantage for biomedical applications (Li et al., 2010).

For biomedical applications, especially in orthopedics, metallic materials are usually chosen for their high load-bearing capacities, low cost, and low wear rates. However, repeated contact loading results in the formation of particulates from the simultaneous action of mechanical loading and electrochemical reactions in the corrosive physiological environment. Elastic interactions may lead to the development of surface residual stress, grooving, and surface roughness. An example is the Co—Cr alloy (ASTM F-76) under repeated contact loading, where amplitude of the dominant surface roughness mode may reach a steady value or decrease during the first few cycles. Using chemical etching treatment, alternating contact loading and nanoscale chemical etching destabilizes the evolution of the dominant roughness mode by decreasing during contact loading and increasing during exposure to an etchant. The increase in roughness during etching depends on the magnitude of the applied contact loads (Ryu et al., 2012).

Other techniques used to deposit metals onto substrates include thermal evaporation, sputtering, electron beam (e-beam) evaporation, electrolyte deposition, electrode deposition, FIB-assisted deposition, or spin-coating of particles via other methods. The metal deposited by FIB-assisted deposition is usually accompanied by a contamination with gallium and amorphous carbon, and the etching behavior is not predictable. Electrolyte deposition is a simple method for the deposition of noble metals and is normally used to deposit noble metals if there is no strict demand on the morphology of the resulting etched structures. Plating is typically a galvanic process where ions of the noble metal etch holes into the valence band of the substrate. In this process, the metal ions are reduced and form nuclei. The morphologies of the etched structures vary with the type of noble metal if isolated particles are used for metal-assisted chemical etching (Huang et al., 2010).

8.5 Conclusions

In recent years, new strategies in surface engineering and nanostructured materials have presented significant improvements in biomedical applications such as biomedical devices for orthopedics, orthodontics, and stents (Yang et al., 2010). Compared with ceramics or polymeric materials, metals are more suitable for load-bearing

applications because of their combination of high mechanical strength and fracture toughness. The general requirements for metallic biomaterials include biocompatibility, mechanical properties, and manufacturing besides nontoxicity, reproducibility, and stability.

Significant research is focused on designing, synthesizing, and fabricating biomaterials that have the appropriate mechanical properties, durability, and functionality. The biomaterials' field has developed revolutionary materials because of its increasingly multidisciplinary approach, with the convergence of molecular design and synthesis, materials science, molecular biology, surface science, and imaging techniques.

8.6 Future directions

Magnesium is an exciting base for future metallic biomaterial work because of its inherent advantages over conventional metals such as titanium. Mg and its alloys are essential for human metabolism and biocompatibility; in addition, Mg is biodegradable, allowing implants to support tissue regeneration and healing. Some mechanical properties like tensile strength, yield strength, modulus of elasticity, and density of Mg alloys are much more similar to natural bone compared with other types of metallic biomaterials. Early tests of bioabsorbable Mg stents in vitro and in vivo have confirmed that Mg-based materials are nontoxic and would be suitable for bone replacements except for rapid corrosion in physiological environments, which limits their potential for orthopedic applications (Yang et al., 2010).

In bone tissues, microtextured surfaces generate an advantageous three-dimensional environment leading to improved bone formation, at least during the initial stages of osteo-integration. However, to modulate proper cell signaling pathways for optimal tissue repair, nanoscale modifications are needed because cell/matrix/substrate interactions occur at this scale. These signals control cell attachment, cell spreading, migration, differentiation, and gene expression. Indeed, various cell types respond to nanotopography, and increased cellular responses have been reported in cultures grown on nano-phase ceramics, polymers with nanotopography, and nano-metric carbon fibers. In the future, materials will become more adaptive to physiological and cellular cues such as understanding of the interactions between nanotopography and cell signaling improves. Surface modification will become increasingly sophisticated and attuned to specific biomedical applications.

References

Akahori, T., & Niinomi, M. (1998). Fracture characteristics of fatigued Ti-6Al-4V ELI as an implant material. *Materials Science and Engineering: A, 243 (*(1−2), 237−243.

Baba, K., Hatada, R., Flege, S., & Ensinger, W. (2012). Preparation and properties of Ag-containing diamond-like carbon films by magnetron plasma source ion implantation. *Advances in Materials Science and Engineering*. http://dx.doi.org/10.1155/2012/536853. Article ID 536853, 5 pages.

Baldacchini, T., Carey, J. E., Zhou, M., & Mazur, E. (2006). Superhydrophobic surfaces prepared by microstructuring of silicon using a femtosecond laser. *Langmuir, 22*(11), 4917−4919.

Bauer, S., Schmuki, P., Von der Mark, K., & Park, J. (2013). Engineering biocompatible implant surfaces: part I: materials and surfaces. *Progress in Materials Science, 58*(3), 261−326.

Brunette, D. M., Tengvall, P., Textor, M., & Thomsen, P. (2001). *Titanium in medicine: Material science, surface science, engineering, biological responses, and medical applications*. New York: Springer-Verlag, Berlin Heidelberg.

Cai, Q., Paulose, M., & Grimes, C. A. (2005). The effect of electrolyte composition on the fabrication of self-organized titanium oxide nanotube arrays by anodic oxidation. *Journal Materials Research, 20*(1), 230−236.

Callister, W. D., & Rethwisch, D. G. (2007). *Materials science and engineering* (vol. 7). New York: Wiley.

Chen, F., Zhang, D., Yang, Q., Wang, X., Dai, B., Li, X., et al. (2010). Anisotropic wetting on microstrips surface fabricated by femtosecond laser. *Langmuir, 27*(1), 359−365.

Chen, F., Zhang, D., Yang, Q., Yong, J., Du, G., Si, J., et al. (2013). Bioinspired wetting surface via laser microfabrication. *ACS Applied Materials and Interfaces, 5*(15), 6777−6792.

Eason, R. (2007). *Pulsed laser deposition of thin films: Applications-led growth of functional materials*. Hoboken, NJ: Wiley.

Fadeeva, E., Schlie, S., Koch, J., Ngezahayo, A., & Chichkov, B. N. (2009). The hydrophobic properties of femtosecond laser fabricated spike structures and their effects on cell proliferation. *Physica Status Solidi (A), 206*(6), 1348−1351.

Ganesh, M., & Gross, R. A. (2012). Embedded enzymatic biomaterial degradation: flow conditions and relative humidity. *Polymer, 53*(16), 3454−3461.

Gong, D., Grimes, C. A., & Varghese, O. K. (2001). Titanium oxide nanotube arrays prepared by anodic oxidation. *Journal Materials Research, 16*, 3331−3334.

Hao, L., & Lawrence, J. (2005). *Laser surface treatment of bio-implant materials* (1st ed.). New York: Wiley.

Holzapfel, B. M., Reichert, J. C., Schantz, J. T., Gbureck, U., Rackwitz, L., Nöth, U., et al. (2013). How smart do biomaterials need to be? A translational science and clinical point of view. *Advanced Drug Delivery Reviews, 65*(4), 581−603.

Hoyer, P. (1996). Formation of a titanium dioxide nanotube array. *Langmuir, 12*, 1411−1413.

Huang, L., Ning, C. Q., Ding, D. Y., Bai, S., Qin, R., Li, M., et al. (2010). Wettability and in vitro bioactivity of doped TiO_2 nanotubes. *Journal of Inorganic Materials, 25*, 775−779.

Iliescu, M., Nelea, V., Werckmann, J., & Mihailescu, I. N. (2004). Transmission electron microscopy investigation of pulsed-laser deposited hydroxylapatite thin films prepared by tripod and focused ion beam techniques. *Surface and Coatings Technology, 187*(1), 131−140.

Jiang, A. F., Zheng, S., An, L., & Chen, H. (2012). Effect of calcination temperature on the adsorption and photocatalytic activity of hydrothermally synthesized TiO_2 nanotubes. *Applied Surface Science, 258*, 7188−7194.

Keller, U. (2003). Recent developments in compact ultrafast lasers. *Nature, 424*(6950), 831−838.

Khorasani, M. T., Mirzadeh, H., & Sammes, P. G. (1999). Laser surface modification of polymers to improve biocompatibility: HEMA grafted PDMS, in vitro assay—III. *Radiation Physics and Chemistry, 55*(5), 685−689.

Kumar, C. S. S. R., Hormes, J., & Leuschner, C. (2005). *Nanofabrication towards biomedical applications*. Weinheim: Wiley-VCH Verlag GmbH & Co.

Li, H. F., Han, H. M., Wu, Y. G., & Xiao, S. J. (2010). Biological functionalization and patterning of porous silicon prepared by Pt-assisted chemical etching. *Applied Surface Science, 256*(12), 4048−4051.

Liu, X., Chu, P. K., & Ding, C. (2004). Surface modification of titanium, titanium alloys, and related materials for biomedical applications. *Materials Science and Engineering: R: Reports, 47*, 49−121.

Liu, X., Chu, P. K., & Ding, C. (2010). Surface nano-functionalization of biomaterials. *Materials Science and Engineering: R: Reports, 70*(22), 275−302.

Makarov, G. N. (2013). Laser applications in nanotechnology: nanofabrication using laser ablation and laser nanolithography. *Physics, 56*(7), 643−682.

Martinu, L., Zabeida, O., & Klemberg-Sapieha, J. E. (2010). In P. Martin (Ed.), *Plasma-enhanced chemical vapor deposition of functional coatings* (3rd ed.). (pp. 392−465). Oxford: Elsevier.

Mattox, D. M. (2010). *Handbook of physical vapor deposition (PVD) processing* (2nd ed.). Burlington, MA: Elsevier.

Mendonça, G., Mendonça, D. B. S., Aragão, F. J. L., & Cooper, L. F. (2008). Advancing dental implant surface technology—from micron to nanotopography. *Biomaterials, 29*, 3822−3835.

Minagar, S., Berndt, C. C., Wang, J., Ivanova, E., & Wen, C. (2012). A review of the application of anodization for the fabrication of nanotubes on metal implant surfaces. *Acta Biomaterialia, 8*, 2875−2888.

Moisan, M., Barbeau, J., Moreau, S., Pelletier, J., Tabrizian, M., & Yahia, L. H. (2001). Low-temperature sterilization using gas plasmas: a review of the experiments and an analysis of the inactivation mechanisms. *International Journal of Pharmaceutics, 226*(1−2), 1−21.

Mor, G. K., Varghese, O. K., Paulose, M., Shankar, K., & Grimes, C. A. (2009). A review on highly ordered, vertically oriented TiO_2 nanotube arrays: fabrication, material properties, and solar energy applications. *Journal Solar Energy Materials and Solar Cells, 90*, 2011−2075.

Mourino, V., Cattalini, J. P., & Boccaccini, A. R. (2012). Metallic ions as therapeutic agents in tissue engineering scaffolds: an overview of their biological applications and strategies for new developments. *Journal of the Royal Society Interface, 9*(68), 401−419.

Navarro, M., Michiardi, A., Castano, O., & Planell, J. A. (2008). Biomaterials in orthopaedics. *Journal of the Royal Society Interface, 5*, 1137−1158.

Nuutinen, T., Silvennoinen, M., Päiväsaari, K., & Vahimaa, P. (2013). Control of cultured human cells with femtosecond laser ablated patterns on steel and plastic surfaces. *Biomedical Microdevices, 15*(2), 279−288.

Oh, S., Daraio, C., Chen, L. H., Pisanic, T. R., Fiñones, R. R., & Jin, S. (2006). Significantly accelerated osteoblast cell growth on aligned TiO_2 nanotubes. *Journal Biomedical Material Research Part A, 78*, 97−103.

Okereke, M. I., Akpoyomare, A. I., & Bingley, M. S. (2014). Virtual testing of advanced composites, cellular materials and biomaterials: a review. *Composites Part B: Engineering, 60*, 637−662.

Oréfice, R. L. (2006). *Biomateriais: Fundamentos e aplicações*. Rio de Janeiro: Cultura médica.

Ovsianikov, A., Gruene, M., Pflaum, M., Koch, L., Maiorana, F., Wilhelmi, M., et al. (2010). Laser printing of cells into 3D scaffolds. *Biofabrication, 2*(1), 014104.

Paulose, M., Shankar, K., Yoriya, S., Prakasam, H. E., Varghese, O. K., Mor, G. K., et al. (2006). Anodic growth of highly ordered TiO_2 nanotube arrays to 134 μm in length. *Journal Physical Chemistry B, 110*(33), 16179−16184.

Pfleging, W., Kohler, R., Südmeyer, I., & Rohde, M. (2013). *Laser-assisted fabrication of materials*. Berlin: Springer.

Pierson, H. O. (1992). *Handbook of chemical vapor deposition (CVD), principles, technology, and applications*. Park Ridge, NJ: Noyes.

Poinern, G. E. J., Brundavanam, S., & Fawcett, D. (2012). Biomedical magnesium alloys: a review of material properties, surface modifications and potential as a biodegradable orthopaedic implant. *American Journal of Biomedical Engineering, 2*(6), 218−240.

Ranella, A., Barberoglou, M., Bakogianni, S., Fotakis, C., & Stratakis, E. (2010). Tuning cell adhesion by controlling the roughness and wettability of 3D micro/nano silicon structures. *Acta Biomaterialia, 6*(7), 2711−2720.

Ren, L., & Yang, K. (2013). Bio-functional design for metal implants, a new concept for development of metallic biomaterials. *Journal of Materials Science and Technology, 29*(11), 1005−1010.

Richter, C., Wu, Z., Panaitescu, E., Willey, R. J., & Menon, L. (2007). Ultrahigh-aspect-ratio titania nanotubes. *Advanced Materials, 19*, 946−948.

Rodrigo, K., Czuba, P., Toftmann, B., Schou, J., & Pedrys, R. (2006). Surface morphology of polyethylene glycol films produced by matrix-assisted pulsed laser evaporation (MAPLE): dependence on substrate temperature. *Applied Surface Science, 252*(13), 4824−4828.

Rosei, F. (2004). Nanostructured surfaces: challenges and frontiers in nanotechnology. *Journal of Physics: Condensed Matter, 16*(17), 1373.

Rosengren, Å., Pavlovic, E., Oscarsson, S., Krajewski, A., Ravaglioli, A., & Piancastelli, A. (2002). Plasma protein adsorption pattern on characterized ceramic biomaterials. *Biomaterials, 23*(4), 1237−1247.

Ryu, J. J., Letchuman, S., & Shrotriya, P. (2012). Roughness evolution of metallic implant surfaces under contact loading and nanometer-scale chemical etching. *Journal of Mechanical Behavior of Biomedical Materials*, 55−66.

Shen, M., Carey, J. E., Crouch, C. H., Kandyla, M., Stone, H. A., & Mazur, E. (2008). High-density regular arrays of nanometer-scale rods formed on silicon surfaces via femtosecond laser irradiation in water. *Nano Letters, 8*(7), 2087−2091.

Smith, Z. R., Smith, R. L., & Collins, S. D. (2013). Mechanism of nanowire formation in metal assisted chemical etching. *Electrochimica Acta, 92*(1), 139−147.

Socol, G., Torricelli, P., Bracci, B., Iliescu, M., Miroiu, F., Bigi, A., et al. (2004). Biocompatible nanocrystalline octacalcium phosphate thin films obtained by pulsed laser deposition. *Biomaterials, 25*(13), 2539−2545.

Stratakis, E., Ranella, A., Farsari, M., & Fotakis, C. (2009). Laser-based micro/nanoengineering for biological applications. *Progress in Quantum Electronics, 33*(5), 127−163.

Sul, Y. T., Johansson, C. B., Jeong, Y., & Albrektsson, T. (2001). The electrochemical oxide growth behaviour on titanium in acid and alkaline electrolytes. *Medical Engineering Physics, 23*, 329−346.

Vercaigne, S., Wolke, J. G. C., Naert, I., & Jansen, J. A. (1998). Histomorphometrical and mechanical evaluation of titanium plasma-spray-coated implants placed in the cortical bone of goats. *Journal of Biomedical Materials Part A, 41*(1), 41−48.

Witte, F. (2010). The history of biodegradable magnesium implants: a review. *Acta Biomaterialia, 6*(5), 1680−1692.

Wu, P. K., Ringeisen, B. R., Callahan, J., Brooks, M., Bubb, D. M., Wu, H. D., et al. (2001). The deposition, structure, pattern deposition, and activity of biomaterial thin-films by matrix-assisted pulsed-laser evaporation (MAPLE) and MAPLE direct write. *Thin Solid Films, 398*, 607−614.

Xu, T., & Pruitt, L. (1999). Diamond-like carbon coatings for orthopaedic applications: an evaluation of tribological performance. *Journal of Materials Science: Materials in Medicine, 10*(2), 83−90.

Yang, J., Cui, Y. F., Lee, I. S., & Wang, X. (2010). Plasma surface modification of magnesium alloy for biomedical application. *Surface and Coatings Technology, 205*, 182−187.

Zhang, L., & Webster, T. J. (2009). Nanotechnology and nanomaterials: promises for improved tissue regeneration. *Nano Today, 4*(1), 66−80.

Zollfrank, C. (2014). Bioinspired material surfaces−Science or engineering? *Scripta Materialia, 74*, 3−8.

Zwilling, V., Aucouturier, M., & Darque-Ceretti, E. (1999). Anodic oxidation of titanium and TA6V alloy in chromic media: an electrochemical approach. *Electrochimica Acta, 45*, 921−929.

Functionalisation of metallic surfaces for biomedical applications

9

T. Hanawa
Tokyo Medical and Dental University, Chiyoda-ku, Tokyo, Japan

9.1 Introduction

Excellent biocompatibility and biofunction of some ceramics and polymers are expected to show excellent properties as biomaterials; in fact, many devices consisting of metals have been substituted by those consisting of ceramics and polymers. In spite of this event, more than 70% of implant devices in medical field including dentistry, especially more than 95% in orthopaedics, still consist of metals, and this share is currently maintained because of their high strength, toughness and durability. On the contrary, a disadvantage of using metals as biomaterials is that they are typically artificial materials and have no biofunction. Therefore, metal surface naturally forms a clear interface against living tissue that works as a barrier to conduct biofunctions. The concept of biosis−abiosis interface is shown in Figure 9.1. To add biocompatibility and biofunction to metals, in other words, to create a biosis−abiosis intelligent interface, surface modification is essential, because biofunction cannot be added during manufacturing processes of metals such as melting, casting, forging and heat treatment, as shown in Figure 9.2.

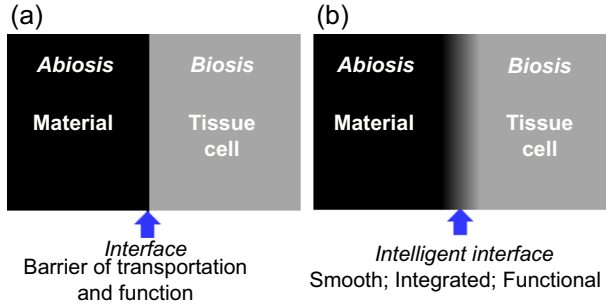


Figure 9.1 Clear interface against cell, bacteria and tissue: The interface works as a barrier for transportation of molecules and conduction of biofunction (a). Unclear and graded interface at which smooth transportation of molecules occurs, both material and tissue are integrated together, and biofunctions are conducted (b).

Surface Coating and Modification of Metallic Biomaterials. http://dx.doi.org/10.1016/B978-1-78242-303-4.00009-0
Copyright © 2015 Elsevier Ltd. All rights reserved.

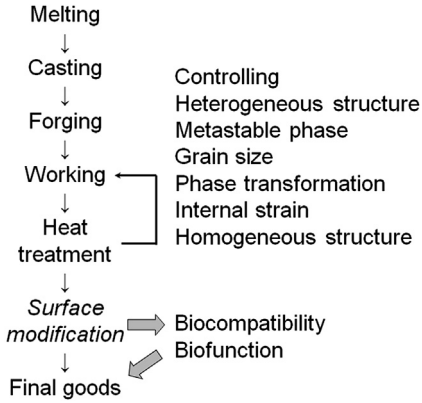


Figure 9.2 Manufacturing process of metallic materials and addition of biocompatibility and biofunction because of surface modification.

As mentioned previously, surface modification is an important and predominant technique for obtaining biofunction and biocompatibility in metals for biomedical use. One surface modification technique is a process that changes the surface composition, structure and morphology of a material, leaving the bulk mechanical properties intact. A second approach is the immobilisation of biofunctional molecules to the metal surface to control the adsorption of proteins and the adhesion of cells, platelets and bacteria.

In this chapter, (1) the motivation of surface modification of metallic materials to improve hard-tissue compatibility or bone formation, inhibit bacterial adhesion and inhibit platelet adhesion, (2) overview of the surface modification techniques, (3) challenge and application of the techniques and (4) expected future trends of the surface modification are reviewed to enhance the understanding of future surface modification techniques.

9.2 Motivations

The required properties for medical devices that are possibly obtained by surface modification are summarised in Table 9.1. The increase of wear resistance of artificial joints, increase of bone formation and bone bonding on the stem and cup of an artificial hip joint and fixture of a dental implant, prevention of bone formation on a bone screw and bone nail, increase of soft-tissue adhesion on a dental implant, trans-skin device, external fixation and pacemaker housing, inhibition of platelet adhesion on devices contacting blood, and inhibition of biofilm formation on all implant devices, are requested, and researchers are making the best effort to solve these problems with surface modification techniques.

9.2.1 Improvement of hard-tissue compatibility

'Osseointegration' is the first definition of the interface between a metallic material and living tissue. The definition of osseointegration is as follows: the formation of a

Table 9.1 Required properties for medical devices that are possibly obtained from surface modification

Required property	Target medical devices	Effect
Wear resistance	Artificial joint	Prevention of generation of wear debris; improvement of durability
Bone formation Bone bonding	Stem and cup of artificial hip joint; dental implant	Fixation of devices in bone
Prevention of bone formation	Bone screw; bone nail	Prevention of assimilation
Adhesion of soft tissue	Dental implant; trans-skin device; external fixation; pacemaker housing	Fixation in soft tissue; prevention of inflectional disease
Inhibition of platelet adhesion	Devices contacting blood	Prevention of thrombus
Inhibition of biofilm formation	All implant devices; treatment tools and apparatus	Prevention of infectious disease

direct interface between an implant and bone, without intervening soft tissue. No scar tissue, cartilage or ligament fibres are present between the bone and implant surface. The direct contact of bone and implant surface can be verified microscopically (Brånemark et al., 1977). This 'osseointegration' concept was immediately accepted by dentists and dental materials researchers in the world to show the biocompatible advantage of titanium among metals that makes it possible to occupy a major position in dental implant bodies. After percolating the concept of osseointegration, the elucidation of osseointegration mechanism including the investigation on the micro-interface structure between titanium and bone tissue has been actively studied.

Titanium and its alloys, which show good hard-tissue compatibility, are used for dental implants and artificial hip joints. However, the hard-tissue compatibility of these materials is lower than that of bioactive ceramics, such as hydroxyapatite and bioactive glasses. Therefore, numerous surface modification techniques to improve the hard-tissue compatibility of titanium have been developed, and some have been commercialised.

In the stems of artificial hip joints and dental implants, the chemical bonding of metal surfaces with bone is not expected. In other words, it is impossible for metals as typical artificial materials to chemically and naturally bond with bone as living tissue, especially in the human body with body fluid. Therefore, the surface morphology is sometimes controlled, and a rough and porous surface is formed in titanium. Living tissue, such as bone, is expected to grow into the rough porous

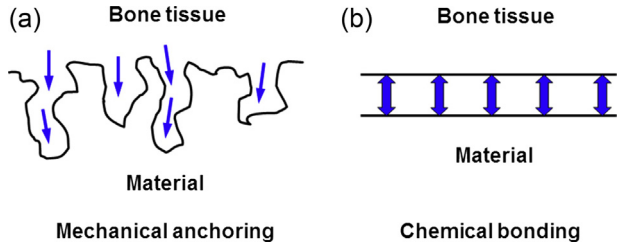


Figure 9.3 Mechanical anchoring (a) and chemical bonding (b) between bone and material.

surface, and the materials and bone are strongly connected as a result of the so-called anchoring effect. Figure 9.3 shows chemical bonding and a mechanical anchoring connection between bone and material.

9.2.2 Inhibition of bacterial adhesion

Some odontopathologies are caused by interactions between the implant or restorative materials and bacteria in the oral cavity. In the case of dental implants, the bacteria may enter into postoperative implanted sites, causing infections such as peri-implantal diseases (Dibart et al., 2005; Glauser et al., 2005; Tesmer et al., 2009). These infections are important issue not only in dental manipulations but also in orthopaedic applications such as spinal fixation devices (MacKintosh et al., 2006). The risk of infections caused by resistant pathogens such as methicillin-resistant *Staphylococcus aureus* is particularly high in patients with hip prosthesis, implanted spinal or vascular devices (Barberan et al., 2008; Sendi et al., 2006).

Biofilm formation is a multifactorial complicated process; occasionally referred to as a two-step process requiring initial bacterial adhesion to the surface followed by the bacteria−bacteria intercommunication leading to the formation of multiple layers of bacteria (Cramton et al., 1999). Once biofilms have formed, it becomes very difficult to eliminate the glucan-embedded pathogens because the bacteria in the interior of the biofilm remain protected from disinfectants and even from strong antibiotics. Therefore, a bacterial attachment-resistant surface or a surface which would allow the removal of biofilms with disinfectants or by applied physical forces is required for maximally efficient biomaterials.

Protein-resistant coatings are considered to be most useful for the inhibition of the biofilm formation because protein adsorption usually initiates this process on implant surfaces.

9.2.3 Control of platelet adhesion

As metals have high strength and toughness compared to ceramics and polymers, the demand for metals for blood-contacting devices as well as implants continues to be high. Stents and stent grafts must satisfy the mechanical requirements when they will contact blood. There are two types of stents: balloon-expandable and self-expandable. Balloon-expandable stents are usually made of stainless steel and Co−Cr

or Co−Ni−Cr alloys, whereas self-expandable stents are usually made of a Ti−Ni alloy. In addition, these metals and several other metals are commonly used for devices for long-term intravascular use, such as heart valves, blood pumps and pacemaker leads as well as for temporary intravascular use, such as catheters and guide-wires, because of their excellent mechanical properties. For metals to be used for intravascular devices, their blood compatibility is also important.

Protein adsorption and platelet adhesion to a material are important events for the formation of thrombus on the material and for the control of the blood compatibility of the material. The interaction of proteins with a metal surface occurs immediately after the metal contacts the blood, and then platelets attach to the surface. Because conventional metals are usually covered with surface oxide films, oxide films play an important role against protein adsorption and platelet adhesion to them. The compositions and chemical states of the surface oxide films on the above metals have been characterised. However, the relationship between those and the platelet adhesion behaviour on the metals remains unclear.

9.3 Overview of technologies

Surface modification is a process that changes a material's surface composition, structure and morphology, leaving the bulk mechanical properties intact. With surface modification, the tissue compatibility of the surface layer can be improved, as shown in Figure 9.4. Surface modification techniques by both dry and wet processes used in research and industry are summarised in Figure 9.5. Surface modification techniques

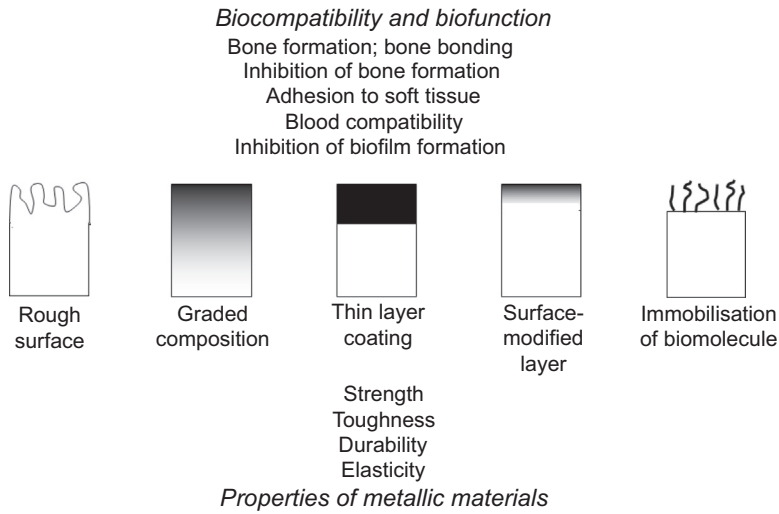


Figure 9.4 Category of surface modification of metallic materials to add biocompatibility and biofunctions remaining good mechanical property.

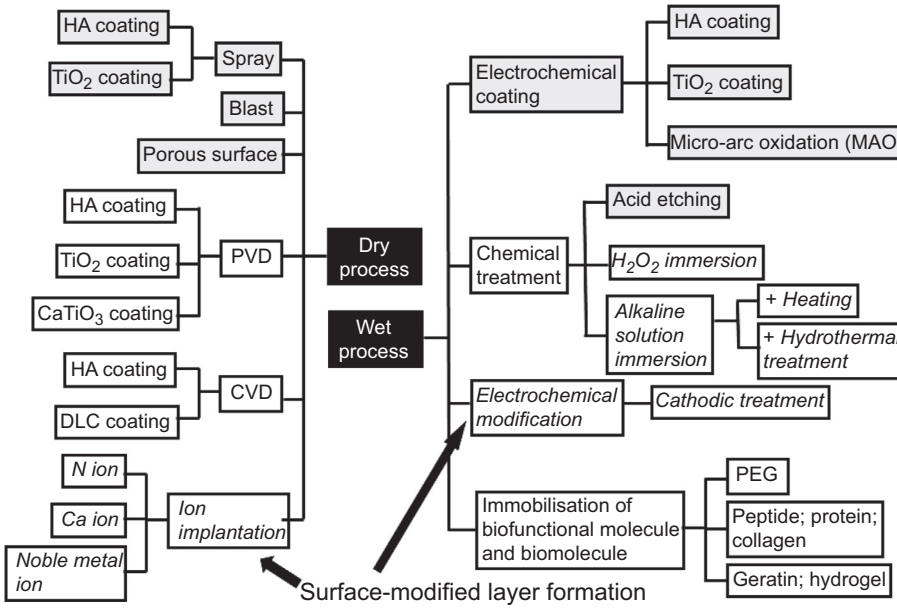


Figure 9.5 Surface modification techniques by dry and wet processes. Mechanical anchoring is expected by hatched processes.

are reviewed elsewhere (Hanawa, 2009, 2010). The current surface modification techniques for the improvement of hard-tissue compatibility focus on the effect of chemical bonding and/or mechanical anchoring as already explained. Even targeting chemical bonding, surface morphology always changes; there is sometimes mechanical anchoring factor.

9.4 Challenge and application

9.4.1 Inhibition of biofilm formation and platelet adhesion

Poly(ethylene glycol) (PEG) is an oligomer or a polymer of ethylene oxide, but historically PEG has tended to refer to oligomers and polymers with a molecular weight below 20,000. PEG is soluble in water, methanol, benzene and dichloromethane and is insoluble in diethyl ether and hexane. It is coupled to hydrophobic molecules to produce nonionic surfactants. This property, combined with the availability of PEGs with a wide range of end-functions, contributes to the wide use of PEGs in biomedical research: drug delivery, tissue engineering scaffolds, surface functionalisation and many other applications (Mahato, 2005), PEG is well known as a polymer inhibiting the adsorption of protein. Therefore, the immobilisation of the PEG molecule to the metal surface is possibly effective in inhibiting the adhesion of bacteria and platelet on it.

Both terminals of PEG (molecular weight: 1000) are terminated with $-NH_2$ ($NH_2-PEG-NH_2$). The cathodic potential was charged to Ti from the open circuit potential to -0.5 V versus a saturated calomel electrode and is maintained at this potential for 300 s. During charging, the terminated PEGs electrically migrate to and are immobilised on the Ti cathode, as shown in Figure 9.6(a). Not only electrodeposition but also immersion leads to the immobilisation of $NH_2-PEG-NH_2$ onto a Ti surface. However, more terminated amines combine with Ti oxide as an NH−O bond by electrodeposition, whereas more amines randomly exist as NH_3^+ in the $NH_2-PEG-NH_2$ molecule by immersion (Figure 9.6(b)) (Tanaka et al., 2007a,b). The amounts of the $NH_2-PEG-NH_2$ layer immobilised onto the metals are governed by the concentrations of the active hydroxyl groups on each surface oxide in the case of electrodeposition which is governed by the relative permittivity of the surface oxide in the case of immersion (Tanaka et al., 2008). The PEG-immobilised surface inhibits the adsorption of proteins and cells as well as the adhesion of platelets (Tanaka et al., 2010b) and bacteria (Tanaka et al., 2010a) (Figure 9.7), indicating that this electrodeposition technique is useful for the biofunctionalisation of metal surfaces. It is also useful for all electroconductive materials and materials even having complex surface topography.

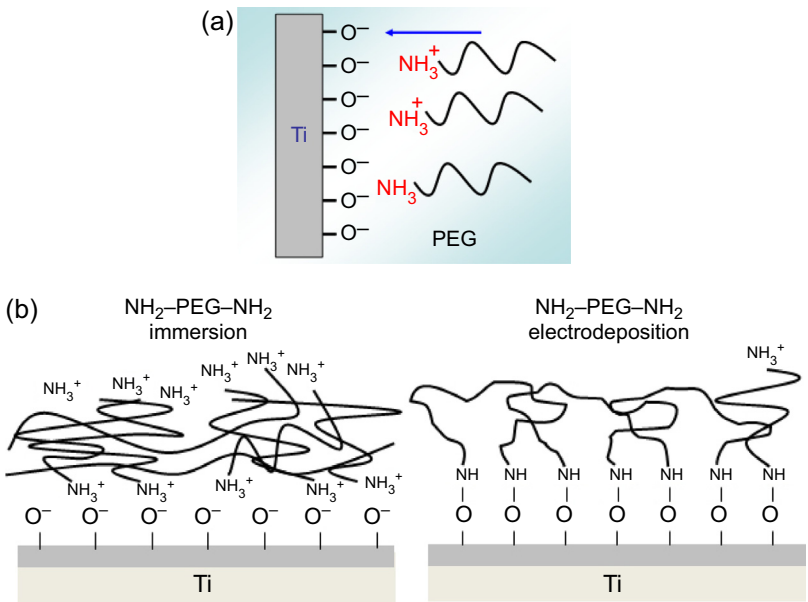


Figure 9.6 The immobilisation of $NH_2-PEG-NH_2$ by electrodeposition. The terminated PEGs electrically migrate to and are immobilised on the Ti cathode (a). More terminated amines combine with Ti oxide as an NH−O bond by electrodeposition, whereas more amines randomly exist as NH_3^+ in the PEG molecule by immersion (b).

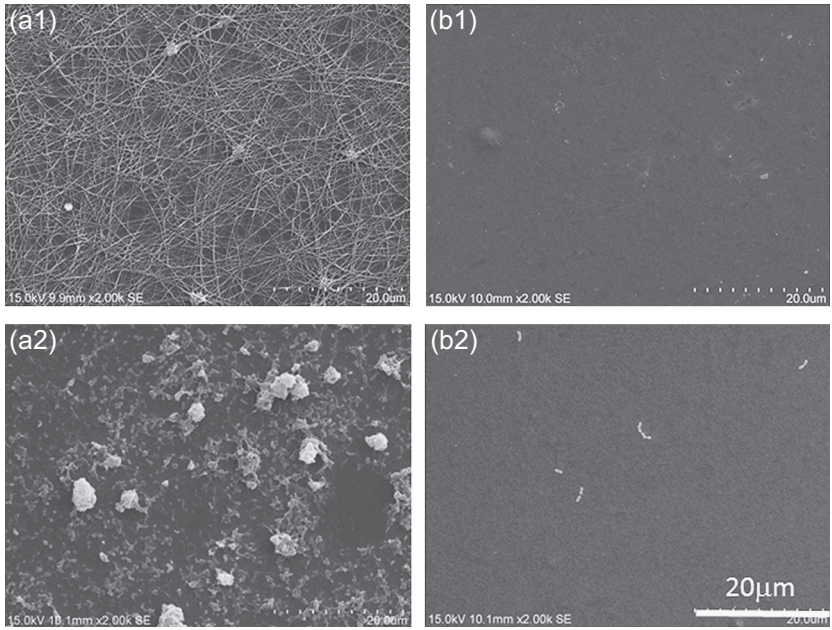


Figure 9.7 Inhibition of platelet adhesion and biofilm formation on Ti by immobilisation of NH_2−PEG−NH_2 by electrodeposition. (a1) Platelet adhesion and fibrin network on untreated Ti, (b1) inhibition of platelet adhesion on PEG-immobilised Ti by electrodeposition, (a2) biofilm formation on untreated Ti and (b2) inhibition of biofilm formation on PEG-immobilised Ti by electrodeposition.

9.4.2 Acceleration of bone formation

A peptide containing arginine-glycine-aspartic acid (Arg-Gly-Asp), which is known as RGD, accelerates cell attachment and the extension of bone cells on titanium (Rezania et al., 1997). RGD is a peptide that is known to be concerned with cell adhesion and involved in many extracellular matrix proteins (Pierschbacher and Ruoslahti, 1984). Bone formation is accelerated by immobilising RGD on a titanium surface (Schliephake et al., 2002).

Due to the main role of the RGD sequence in cell adhesion, several research groups have developed biofunctionalised surfaces by immobilisation of RGD peptides. Grafting RGD peptides has been performed on different biomaterials, such as Ti (Bagno et al., 2007; Elmengaard et al., 2005; Rammelt et al., 2006), and has been shown to improve osteoconduction in vitro.

To immobilise RGD to the electrodeposited PEG on Ti, PEG with an $-NH_2$ group and a −COOH group (NH_2−PEG−COOH) must be employed. One terminal group, $-NH_2$, is required to bind stably with a surface oxide on a metal. On the other hand, the other terminal group, −COOH, is useful to bond biofunctional molecules such as RGD as shown in Figure 9.8 (Tanaka et al., 2009). This RGD/PEG/Ti surface accelerates calcification by MC3T3-E1 cell (Oya et al., 2009). The calcification is the largest

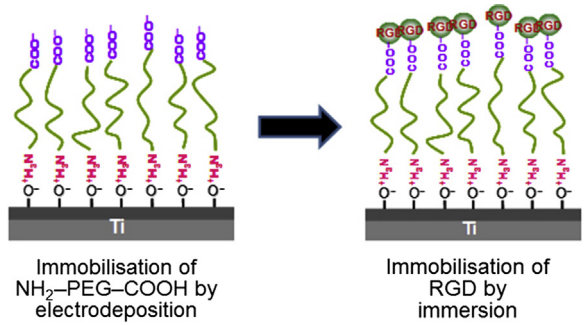


Figure 9.8 Immobilisation of RGD peptide through PEG with twitter ion electrodeposited Ti surface.

on the RGD/PEG/Ti surface and bone formation on the RGD/PEG/Ti surface is accelerated than the RGD/Ti surface in rabbit (Park et al., 2011).

9.5 Future trends

By referring to the stem of artificial hip joint and fixture of dental implant, history of surface modification techniques to improve hard-tissue compatibility at the research level is shown in Figure 9.9.

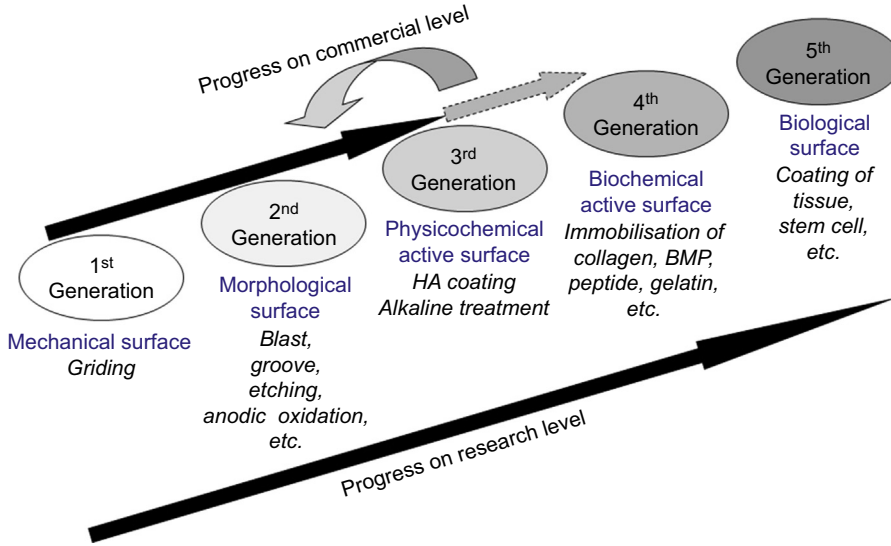


Figure 9.9 The evolution of surface modification techniques to improve hard-tissue compatibility at the research level.

First generation: grind machining of the surface.

Second generation: grooving, blast, acid etching, anodic oxidation and laser abrasion.

Third generation: chemical treatment and hydroxyapatite coating.

Fourth generation: immobilisation of biofunctional molecules (collagen, bone morphogenetic protein and peptide).

Fifth generation: coating of stem cells and tissues.

The bone formation of the material surface is accelerated when biomolecules concerning bone formation are immobilised on the material surface, such as in the fourth generation in Figure 9.9. Therefore, many studies have achieved good results in this direction. However, to increase the popularity of the immobilisation of biofunctional molecules, it is necessary to ensure the safety, quality maintenance during storage and dry-conditioned durability of the immobilised layer. Therefore, it is difficult for manufacturers to commercialise those research results. Most of commercialised goods are categorised into the second generation, a few belong to the third generation, and there is no prospect for the commercialisation of the fourth generation at present. The commercialisation went faster for the second than third generation possibly because materials employing mechanical anchoring are more practical than materials employing chemical bonding with bone.

On research developing new surface modification techniques, biocompatibility and biofunction are usually focused, whereas sometimes mechanical properties, durability and manufacturing process are left behind that may delay the utilisation of the technique. Most researchers make the best effort to evaluate biological effects with cell culture and animal tests; they hesitate to evaluate durability. They sometimes do not remember 'materials engineering', but remember only materials chemistry and biological evaluation.

Metallic materials are widely used in medicine not only for orthopaedic implants but also for cardiovascular devices and other purposes. Biomaterials are always used in contacting tissues. Therefore, inter-reactions among material surfaces and tissues must be well understood: this knowledge is essential to develop new novel materials. All evaluation techniques must be performed with this concept. In particular, reactions between metal surface and biomolecule and that between metal surface and cell reactions are important. The present regenerative medicine is categorised into three types as shown in Figure 9.10. Biofunctional and biocompatible metallic materials could be applied to regenerative medicine as a strong, flexible and tough scaffold.

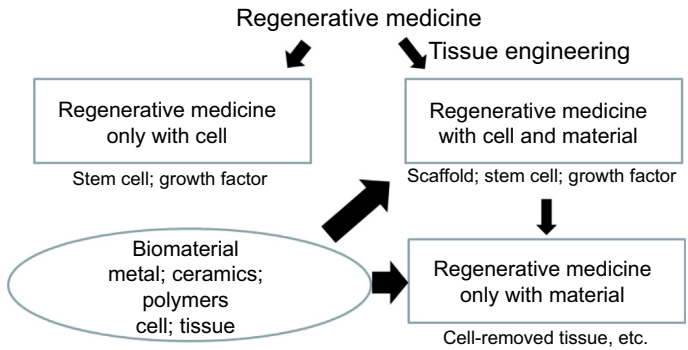


Figure 9.10 Category of regenerative medicine and the contribution of biomaterials.

References

Bagno, A., Piovan, A., Dettin, M., Chiarion, A., Brun, P., Gambaretto, R., et al. (2007). Human osteoblast-like cell adhesion on titanium substrates covalently functionalized with synthetic peptides. *Bone, 40*, 693−699.

Barberan, J., Aguilar, L., Gimenez, M. J., Carroquino, G., Granizo, J. J., & Prieto, J. (2008). Levofloxacin plus rifampicin conservative treatment of 25 early staphylococcal infections of osteosynthetic devices for rigid internal fixation. *International Journal of Antimicrobial Agents, 32*, 154−157.

Bränemark, P. I., Hansson, B. O., Adell, R., Breine, U., Lindström, J., Hallĕn, O., et al. (1977). Osseointegrated implants in the treatment of the edentulous jaw. Experience from a 10-year period. *Scandinavian Journal of Plastic and Reconstructive Surgery and Hand Surgery Supplementum, 16*, 1−132.

Cramton, S. E., Gerke, C., Schnell, N. F., Nichols, W. W., & Gotz, F. (1999). The intercellular adhesion (ica) locus is present in *Staphylococcus aureus* and is required for biofilm formation. *Infection and Immununity, 67*, 5427−5433.

Dibart, S., Warbington, M., Su, M. F., & Skobe, Z. (2005). In vitro evaluation of the implant-abutment bacterial seal: the locking taper system. *International Journal of Oral & Maxillofacial Implants, 20*, 732−737.

Elmengaard, B., Bechtold, J. E., & Soballe, K. (2005). In vivo study of the effect of RGD treatment on bone ongrowth on press-fit titanium alloy implants. *Biomaterials, 26*, 3521−3526.

Glauser, R., Schupbach, P., Gottlow, J., & Hammerle, C. H. F. (2005). Periimplant soft tissue barrier at experimental one-piece mini-implants with different surface topography in humans: a light-microscopic overview and histometric analysis. *Clinical Implant Dentistry and Related Research, 7*, S44−S51.

Hanawa, T. (2009). An overview of biofunctionalisation of metals in Japan. *Journal of the Royal Society Interface, 6*, S361−S369.

Hanawa, T. (2010). Biofunctionalization of titanium for dental implant. *Japanese Dental Science Review, 46*, 93−101.

MacKintosh, E. E., Patel, J. D., Marchant, R. E., & Anderson, J. M. (2006). Effects of biomaterial surface chemistry on the adhesion and biofilm formation of *Staphylococcus epidermidis* in vitro. *Journal of Biomedical Materials Research Part A, 78*, 836−842.

Mahato, R. I. (2005). *Biomaterials for delivery and targeting of proteins and nucleic acids*. Boca Raton, Florida: CRC Press (Ald. Cat. No. Z705102).

Oya, K., Tanaka, Y., Saito, H., Kurashima, K., Nogi, K., Tsutsumi, H., et al. (2009). Calcification by MC3T3-E1 cells on RGD peptide immobilised on titanium through electrodeposited PEG. *Biomaterials, 30*, 1281−1286.

Park, J. W., Kurashima, K., Tustusmi, Y., An, C. H., Suh, Y. J., Doi, H., et al. (2011). Bone healing of commercial oral implants with RGD immobilization through electrodeposited poly(ethylene glycol) in rabbit cancellous bone. *Acta Biomaterialia, 7*, 3222−3229.

Pierschbacher, M. D., & Ruoslahti, E. (1984). Cell attachment activity of fibronectin can be duplicated by small synthetic fragments of the molecule. *Nature, 309*, 30−33.

Rammelt, S., Illert, T., Bierbaum, S., Scharnweber, D., Zwipp, H., & Schneiders, W. (2006). Coating of titanium implants with collagen. RGD peptide and chondroitin sulfate. *Biomaterials, 27*, 5561−5571.

Rezania, A., Thomas, C. H., Branger, A. B., Waters, C. M., & Healy, K. E. (1997). The detachment strength and morphology of bone cells contacting materials modified with a peptide sequence found within bone sialoprotein. *Journal of Biomedical Materials Research, 37*, 9−19.

Schliephake, H., Scharnweber, D., Dard, M., Rössler, S., Sewing, A., Meyer, J., et al. (2002). Effect of RGD peptide coating of titanium implants on periimplant bone formation in the alveolar crest. An experimental pilot study in dogs. *Clinical Oral Implants Research, 13*, 312−319.

Sendi, P., Rohrbach, M., Graber, P., Frei, R., Ochsner, P. E., & Zimmerli, W. (2006). *Staphylococcus aureus* small colony variants in prosthetic joint infection. *Clinical Infectious Diseases, 43*, 961−967.

Tanaka, Y., Doi, H., Iwasaki, Y., Hiromoto, S., Yoneyama, T., Asami, K., et al. (2007a). Electrodeposition of amine-terminated-poly(ethylene glycol) to Ti surface. *Materials Science and Engineering Part C, 27*, 206−212.

Tanaka, Y., Doi, H., Kobayashi, E., Yoneyama, T., & Hanawa, T. (2007b). Determination of the immobilization manner of amine-terminated poly(ethylene glycol) electrodeposited on a Ti surface with XPS and GD-OES. *Materials Transactions, 48*, 287−292.

Tanaka, Y., Matin, K., Gyo, M., Okada, A., Tsutsumi, Y., Doi, H., et al. (2010a). Effects of electrodeposited poly(ethylene glycol) on biofilm adherence to titanium. *Journal of Biomedical Materials Research Part A, 95*, 1105−1113.

Tanaka, Y., Matsuo, Y., Komiya, T., Tsutsumi, Y., Doi, H., Yoneyama, T., et al. (2010b). Characterization of the spatial immobilization manner of poly(ethylene glycol) to a titanium surface with immersion and electrodeposition and its effects on platelet adhesion. *Journal of Biomedical Materials Research Part A, 92*, 350−358.

Tanaka, Y., Saito, H., Tsutsumi, Y., Doi, H., Imai, H., & Hanawa, T. (2008). Active hydroxyl groups on surface oxide film of Ti, 316l stainless steel, and cobalt−chromium−molybdenum alloy and its effect on the immobilization of poly(ethylene glycol). *Materials Transactions, 49*, 805−811.

Tanaka, Y., Saito, H., Tsutsumi, Y., Doi, H., Nomura, N., Imai, H., et al. (2009). Effect of pH on the interaction between zwitterion and titanium oxide. *Journal of Colloid and Interface Science, 330*, 138−143.

Tesmer, M., Wallet, S., Koutouzis, T., & Lundgren, T. (2009). Bacterial colonization of the dental implant fixture−abutment interface: an in vitro study. *Journal of Periodontology, 80*, 1991−1997.

Biocompatible coatings for metallic biomaterials

10

Y. Oshida[1,2], *Y. Guven*[3]
[1]Indiana University School of Dentistry, Indianapolis, IN, USA; [2]University of California San Francisco School of Dentistry, Orinda, CA, USA; [3]Istanbul University, Istanbul, Turkey

10.1 Introduction

About 20 pure elements can be used as base metals or as a major alloying element(s) in combination with an appropriate element(s) from a selection of 22 nonmetallic elements. Of the approximately 3500 binary (two-element) alloy system combinations possible, about 800 can be considered practical for use. From the 100,000 possible combinations for three-element (tertiary) alloy systems, only about 350 can serve as useful alloys. Hence, approximately 1200 metallic materials (in pure or alloy form) are available. Besides metallic materials, we still have polymeric, ceramic, and composite materials. Among polymeric materials, there are about 2000−5000 types of polymers, depending on molecular weight. In the realm of ceramic materials, about 10,000 different kinds exist. Additionally, there are composite materials of metal−matrix composite, plastic−matrix composite, or ceramic−matrix composite. All told, the materials available to us are of extraordinarily large number, and they can serve as structural and functional materials. The materials used in medical or dental applications may be referred to as biomaterials. The metals commonly used in dental/medical applications are stainless steels (e.g, 316L Mo-containing stainless steel), cobalt-based alloys (e.g., Cr−Co alloy), titanium alloys (e.g., Ti−6Al−4V, Ti−6Al−7Nb, etc.), NiTi shape memory alloy, zirconium-based alloys, and commercially pure titanium, zirconium, and tantalum. They are found mainly in orthopedic devices (e.g., joints, plates, screws, rods, and bars), dental devices (periodontal implants, orthodontic braces, and endodontic fillings), neurological implants (e.g., cochlear and pacemaker), and general surgery tools. The mechanical properties of metallic materials (modulus of elasticity, ultimate tensile and yield strengths, and ductility) have enabled the creation of devices with long-term in vivo stability. In addition, the passive surface oxide layers have provided chemical inertness and stability within biological environments, providing excellent biocompatibility. Porous metallic biomaterials have recently been developed. The hardness of some porous biomaterials has been reduced to magnitudes less than 50% of the nonporous alloys, which can be biomechanically compatible with adjacent hard tissue. An increase in effective surface area of such porous structure (3- to 10-fold) can be useful for bone ingrowth processes, although it has been reported that such biomaterials are prone to biocorrosion, resulting in elemental leaching into the tissues, which has biologic consequences (Corina and Felicia, 2008; Pike, 2009; Pilliar, 2009).

Surface Coating and Modification of Metallic Biomaterials. http://dx.doi.org/10.1016/B978-1-78242-303-4.00010-7
Copyright © 2015 Elsevier Ltd. All rights reserved.

In the field of biomaterials, many novel processing techniques and methods have been developed to improve the desirable characteristics of biomaterials. Today, the use of biomaterials is widespread. Estimates of the numbers of biomedical devices incorporating biomaterials used in the United States in 2002 include total hip joint replacements, 448,000; knee joint replacements, 452,000; shoulder joint replacements, 24,000; dental implants, 854,000; coronary stents, 1,204,000; and coronary catheters, 1,328,000 (Zivić et al., 2010). The clinical application of these devices is still a critical issue because of the tissue trauma that occurs during implantation and the presence of the device in the body. The in vivo functionality and durability of any implantable device can be compromised by the body's response to the foreign material. Numerous strategies to overcome negative body reactions have been reported. Some key issues of biomaterial/tissue interactions should include foreign body response and biocompatibility and biocompatibility assessment. General approaches used to overcome the in vivo instability of implantable devices can include the use of biocompatible biomaterial coatings (Morais et al., 2010; Sandberg et al., 2009).

Coatings, claddings, thin film deposition, and other surface additive modifications may be categorized in many ways. One of these is principally by the form of the material deposited at any given instant on a small area of the surface. Deposition may be categorized by (1) atomic size (including electrolytic deposition by electroplating, physical vapor deposition (PVD) by ion implantation, vacuum deposition, vacuum evaporation, ion beam, plasma deposition by sputter deposition, chemical vapor deposition (CVD) by spray pyrolysis, etc.); (2) particulate size (including thermal spray by flame spray, electric wire arc spray, plasma spray, spray and fuse/spray fuse thermal spray, etc.); (3) bulk coating or cladding (including wetting processes by dip coating, spin coating, cladding by explosive roll bonding, overlay by laser cladding, weld overlay, etc.); and (4) surface modification (including chemical conversion by electrolytic, anodization, chemical by thermal vapor or plasma vapor, mechanical by shot peening; thermal surface enhancement by diffusion from bulk, sputtering, or ion implantation) (Söderholm, 2012; Tucker, 2002). In many cases, a coating is applied to a substrate to improve its appearance or surface properties, such as surface roughness, adhesion, wettability, corrosion resistance, and wear resistance. Surface treatments serve several purposes: (1) to control tribological action (friction, lubrication, and wear); (2) to improve corrosion resistance (or passivation); (3) to change physical property, e.g., conductivity, resistivity, and reflection; (4) to alter surface mechanical properties (hardness, modulus of elasticity, etc.); (5) to change dimension (flatten, smooth, etc.); (6) to vary appearance, e.g., color and roughness; (7) to reduce cost (replace bulk material); (8) to provide an antiallergenic surface (Hallab et al., 2001; Rieu, 1993). It follows that coatings can also be considered a "key technology" (Fuchs et al., 2008) to promote biocompatibility and adhesion of foreign materials within a biological host.

In this chapter, the technology and methods for surface coating and additive modification, the materials for such surface engineering, and some advanced technologies that might be applicable in medical/dental fields will be discussed.

10.2 Biocompatibility

There are three basic requirements for placed implants to exhibit satisfactory biofunctionality: biological compatibility (or in short, biocompatibility), biomechanical compatibility, and morphological compatibility (Oshida, 2007a). Figure 10.1 shows the popularity of pure titanium (CpTi: commercially pure titanium) and its alloys (typically, Ti−6Al−4V and Ti−6Al−7Nb) in dental and medical fields by counting the manuscripts published in different peer-reviewed journals, and number of publications on the term "biocompatibility" (Oshida, 2007a; Williams, 2008). Referring to the figure, there are three straight lines in a semi-log plot that demonstrate the total accumulated number of published articles every five years. The uppermost line represents the accumulated number of all articles listed in chemical abstract. It represents a wide scattering of articles in many areas, including refining, metallurgy,

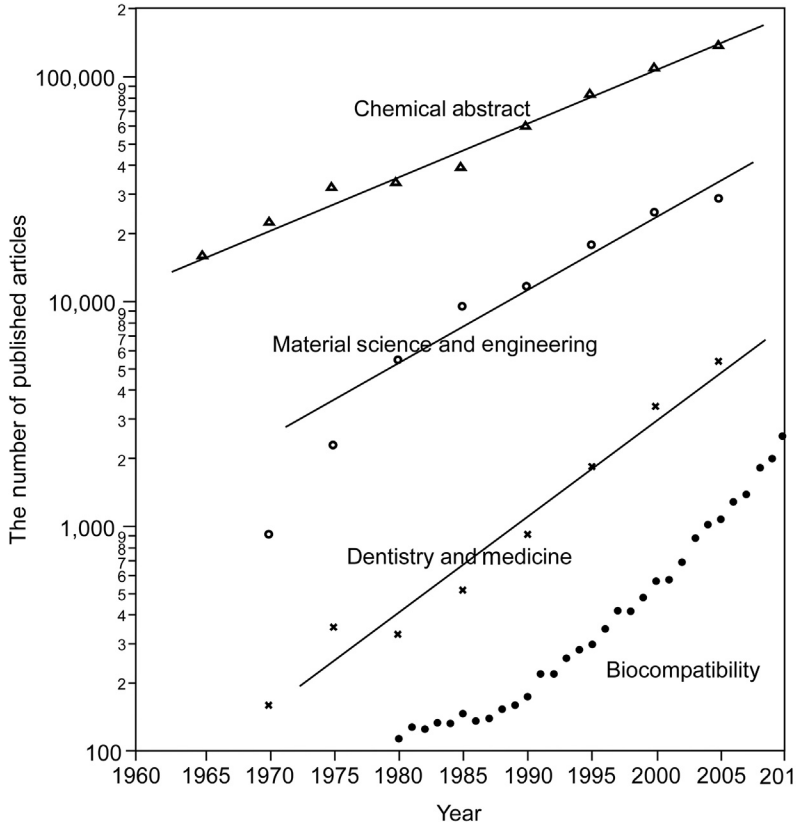


Figure 10.1 Accumulated numbers of published articles on titanium materials and biocompatibility.

dentistry, medicine, bioengineering, engineering, industries, pure chemistry, and chemical engineering. The second straight line from the top is obtained when the search area is limited to materials science in both the engineering and medical/dentistry fields. If our search is further defined within only the medicine/dentistry area, we still have an exponential increase in publications. If we search only for articles related to "biocompatibility," the number of published articles by year again appears to be increasing almost in parallel to those on titanium biomaterials in dentistry and medicine, indicating that the concept of biocompatibility is recognized as important when biomaterials are used for both dental (intraoral) and orthopedic (extraoral) implant systems.

Biomaterials are substances used to make medical devices for biological applications. A prerequisite for all biomaterials is that they are biocompatible. Biocompatibility is related to the behavior of biomaterials in various contexts (Mathieu, 2001). Modern medical devices and prostheses are often made of more than one material, so it might not always be sufficient to talk about the biocompatibility of a specific material. An implant may not always have to be positively bioactive, but it must not do any harm (either locally or systematically). At present, there are no known materials that completely satisfy these criteria. So, when a foreign material is placed into a biological environment, reactions inevitably occur that are detrimental to both host and material.

The biocompatibility of implantable devices remains a critical issue in extending device longevity and functionality. Also, the possible immune response to implantable devices may present a significant risk for some patients. Progress made in recent years in the areas of biotechnology, tissue engineering, biomaterials, cell and molecular biology, polymer science, and other related fields has resulted in numerous medical and pharmaceutical advances. Of particular significance are the advancements made in the areas of implantable devices and drug/device combination products, such as drug-eluting stents (Belverud et al., 2008; Frazier and Jacob, 2007; Kipshidze et al., 2005), artificial organs (Fine and Tobias, 2007; O'Connor et al., 2008), biosensors (Koschwanez and Reichert, 2007), catheters (Callahan and Natale, 2008), scaffolds for tissue engineering (Abukawa et al., 2006; Matsumoto et al., 2007), and heart valves (Nozyński et al., 2001). Various natural, synthetic, and semisynthetic materials are currently used in the fabrication of implantable devices. In addition, it has been shown that biological reactions that are adverse for a material in one application may not be adverse for the same material in a different application (Anderson and Langone, 1999; Onuki et al., 2008).

To implant a material, the hard tissue will be traumatized first. Injured or diseased tissues are removed to some extent in the process of implantation. The success of the entire operation depends on the kind and degree of tissue response (*biocompatibility*) toward the implants during the healing process. The tissue's response to the implantation trauma/injury may vary widely according to the site, contamination, etc. However, the inflammatory reaction and cellular response toward the wound for both intentional and accidental injuries are the same regardless of the site. There are many factors that influence implant biocompatibility, such as implant size, shape, material composition, and surface wettability, roughness and charge. For a material to

be deemed biocompatible, any adverse reactions that may ensue at the blood/material or tissue/material interface must be minimal. Having looked at different aspects related to the biocompatibility in the above, biocompatibility can be defined as the ability of a foreign material, device, or system to interact with a living host organism. It is clear that there must be various degrees of biocompatibility. Defining the term more closely, biocompatible materials are those for which the interaction between the material and vital soft/hard tissue is so minimal that the material is not detrimentally affected by the tissue nor the tissue by the material (Mikhalovsky et al., 2003; Williams, 2008).

To evaluate biocompatibility, it is generally necessary to evaluate the (1) implant itself; (2) ions dissolved from the implant surface (such ions should include corrosion products and/or biotribological reaction products); (3) tissue surrounding the placed implant; and (4) tissues nonproximal to the implant (Murabayashi and Nose, 2013).

10.3 Nature of surface and interface

Before discussing surface coating and additive modification in detail, it is worth reviewing briefly the nature of surface and interface. The surface of a material defines the boundary of an object and is not just a free end side of a substance, but it is a contact and boundary zone with other substances (either in gaseous, liquid, or solid). A physical system that comprises a homogeneous component such as solid, liquid, or gas and is clearly distinguishable from another is called a phase, and a boundary at which two or three of these individual phases are in contact is called an interface. Surface and interface reactions include reactions with organic or inorganic materials, vital or nonvital species, hostile or friendly environments, etc. Surface activities may vary from mechanical actions (fatigue crack initiation and propagation, stress intensification, dislocation movement, etc.), chemical action (discoloration, tarnishing, contamination, corrosion, oxidation, etc.), mechanochemical action (corrosion fatigue, stress-corrosion cracking, etc.), thermomechanical action (thermal fatigue and creep), and tribological and biotribological actions (wear and wear debris toxicity, friction, etc.) to physical and biophysical actions (surface contact and adhesion, adsorption, absorption, diffusion, cellular attachment, cell proliferation and differentiation, etc.). Consequently, the properties of the surface determine the interaction of the second material (Oshida, 2007b, 2013).

The surface has a certain characteristic thickness: (1) in cases in which interatomic reactions such as wetting or adhesion are dominant, it is important to target and analyze atoms up to a depth of 100 nm; (2) when mechanical interactions such as tribology and surface hardening come into play, a thickness of about $0.1 \sim 10$ μm will be important because the elasticity due to surface contact and the plastically deformed layer will be a governing area; and (3) for cases when mass transfer or corrosion is involved, the effective layer for preventing the diffusion will be within $1 \sim 100$ μm (Shabalovskaya et al., 2009). Because the thickness of the desired coating layer is accordingly selected, it becomes important to control the thickness

of coated or surface-modified film/layer. Coating is just a small portion of surface science and engineering. Structural elements beneath the surface function principally to support the surface and its characteristics determine not only esthetic appearance, but also interaction with the environment, including mechanical interactions, chemical interactions, optical and thermal interactions (Tucker, 2002), and of course biological interactions. Accordingly, the longevity, safety, reliability, and structural integrity of dental and medical materials and devices are greatly governed by these surface phenomena, which can be detected, observed, characterized, and analyzed by virtue of various means of equipment and technologies (Allen, 1996; Oshida, 1994, 2013).

10.4 Coating technologies

10.4.1 Introduction

There are various reasons for surface layers to receive alteration: for changing surface topology, for controlling surface energy, for managing hydrophilicity, for varying appearance, for enhancing surface chemistry and physics, for enriching surface elements or substances, etc. Methods for achieving such surface modification can be found in mechanical, chemical and electrochemical, physical, thermal, or combined techniques.

10.4.2 Mechanical modification

Although sand-blasting, shot-peening, and laser peening have been used for mainly (1) cleaning surface contaminants, (2) roughening surfaces to increase effective surface area, and (3) producing beneficial surface compressive residual stress, they are not directly used for coating purposes. However, there are two unique solid-state processes that can be used as a cladding method; the mechanical alloying process (a new method for producing composite metal powders with controlled microstructures) (Suryanarayana, 2001), and friction stir (or inertia) welding (Li et al., 2013; Mishra and Ma, 2005). These additive technologies can be used for modifying surface layers.

10.4.3 Chemical and electrochemical modifications

Generally, a chemical method has been adopted for (1) forming a stable oxide film and (2) the resulting surface having an appropriate level of surface roughness. On the other hand, the electrochemical method also possesses a two-fold purpose: (1) forming a stable oxide film, and (2) through an electrochemical reaction to deposit target substance(s) onto the substrate surface (Elias et al., 2008). Electrochemistry deals with charge transfer across interfaces. One of the first applications of electrochemistry was for coating conducting surfaces with either metals (e.g., electroplating) or by inorganic or organic substances (such as oxides and polymers). In either method,

enhanced biocompatibility of implants (in particular, titanium implants) highly depends on the possibility of achieving high degrees of surface functionalization for an enhanced mineralization of bioactive minerals (e.g., hydroxyapatite, HA) (Ajami and Aguey-Zinsou, 2011). Electrochemical coatings ranging from a monoatomic layers-to-microns thick have been carried out, which affected the physical and chemical properties of the coated surface (Guslitzer-Okner and Mandler, 2011).

Using an electrochemical reaction, deposition of biocompatible platinum foil (Pt) onto TiN substrate (Morcos et al., 2013) was reported. The conductive polymer, poly(3,4-ethylenedioxythiophene) film was coated onto biodegradable Mg substrate (Sebaa et al., 2013), and similarly it was reported that adhesive biodegradable polymer, poly(vinyl acetate) was coated by the dip processing onto biodegradable Mg alloy to control the degradation rate and enhance the biocompatibility of magnesium alloys (Abdal-hay et al., 2012). Moreover, (Ti,Al)N was coated electrochemically onto Ni−Cr dental base-alloy (Chung et al., 2004).

There are several techniques for the deposition of coatings on metals, including PVD, CVD, electrochemical deposition, plasma spraying, and sol−gel process. The sol−gel coating process possesses unique advantages: (1) it has excellent chemical stability, oxidation control, and enhanced corrosion resistance for metal substrates (Brinker et al., 1992; Wright and Sommerdijk, 2001); (2) it is an environmentally friendly technique of surface protection and has shown the potential for the replacement of toxic pretreatments and coatings that have traditionally been used for increasing corrosion resistance of metals (Durán et al., 2007; Wang and Bierwagen, 2009); (3) the processing temperature generally is low, frequently close to room temperature,and thus thermal volatilization and degradation of entrapped species, such as organic inhibitors, is minimized; (4) because liquid precursors are used, it is possible to cast coatings in complex shapes and to produce thin films without the need for machining or melting; and (5) the sol−gel films are formed by "green" coating technologies (Wang and Bierwagen, 2009).

Kado et al. (2012) developed a simple chemical modification method to immobilize cell-adhesive molecules on a titanium surface to improve its biocompatibility with human periodontal ligament cells (HPDLCs). It was concluded that cell-adhesive molecules successfully immobilized on the titanium surface and improved the compatibility of the surface with HPDLCs, suggesting that the collagen-immobilized titanium surface could be used for forming ligament-like tissues around titanium dental implants.

Lee et al. (2010a) examined the gelatin nano gold (GnG) composite for surface dipping modification of titanium in addition to insure biocompatibility on dental implants or biomaterials. The GnG composite was constructed by gelatin and hydrogen tetrachloroaurate in the presence of a reducing agent, sodium borohydrate ($NaBH_4$). It was reported that (1) the GnG composite showed well-dispersed character, the strong absorption at 530 nm, roughness, regular crystal, and clear C, Na, Cl, P, and Au signals onto titanium; and (2) further, this composite allowed MC-3T3 E1 cell growth and viability compared to gelatin and pure titanium, indicating that GnG composite-coated titanium surfaces have a good biocompatibility for osteoblast growth and attachment than is in intact by the simple and versatile dipping method.

10.4.4 Physical modification

In this section, we will discuss the micro-arc oxidation (MAO), ion implantation, including plasma immersion ion implantation (PIII or PI^3), other plasma treatments, and laser technologies.

Wu et al. (2010), using Ti−24Nb−4Zr−7.9Sn alloy (which is a newly developed β-titanium alloy having a low value of modulus of elasticity), evaluated the effects of MAO treatment on biological performance and reported that MAO treatment helps to form a porous surface with a biologically active bone-like apatite layer on Ti alloy. Because the TiO_2 surface possesses high apatite-forming ability, porous Ti was MAO processed to form a TiO_2 thin layer (Fan et al., 2012), and CpTi was subjected to MAO treatment to form porous TiO_2, indicating that the cortex-like coating was conducive to cell retention and implant stabilization (Liu et al., 2013). Most of the MAO application can be found in depositing bioactive or biocompatible substances onto biomaterials. The Ca- and P-containing electrolyte (α-$Ca(PO_3)_2$ or $CaTiO_3$) was coated on Ti−6Al−4V (Yu et al., 2007), and on Mg (Gan et al., 2013). HA was MAO-processed on titanium substrate, and a mixture of HA and TiO_2 was detected (Abbasi et al., 2012). Song et al. (2010) treated the MAO-processed CpTi surface (which has porous TiO_2) with an electrolyte containing Ca and P ions by hydrothermal treatment. It was reported that (1) a small number of micro-sized HA crystallites and a thin layer composed of nanosized HA were formed on the MAO-processed Ti, followed by treatment in an alkaline aqueous solution; whereas (2) a large number of micro-sized HA crystallites and dense anatase TiO_2 nanorods were formed on the MAO-processed Ti, followed by treatment in phosphorous-containing alkaline solution. A composite of potassium titanate ($K_2Ti_6O_{13}$) was also coated on a titanium surface, and it was indicated that the potassium/TiO_2 bioceramic coatings possess excellent capability of including bone-like apatite to deposit (Zhna et al., 2009).

A new technique combining MAO and electrophoresis was introduced to develop a biocompatible oxide layer on CpTi implant surface (Ma et al., 2010). Originally developed alkaline electrolyte containing nanoscale HA powder suspension was used. In the electric field, nanoscale HA powder was electrophoretically moved and sintered into the gradually formed oxide layer on titanium anode. An 8.5-μm-thick oxide layer with high surface energy and roughness, which was composed of titanium dioxide and calcium phosphates as well as HA, was formed on a titanium surface by the modified MAO technique. It was mentioned that the modified titanium surface, which is rough and porous, contains calcium phosphates and proved to be more biocompatible in vitro (Ma et al., 2010).

Plasma treatment (Coelho et al., 2012) is an interesting method to modify the implant surface. Not only can this treatment alter the surface charge, but this treatment can also alter the chemistry and the topography (Buser et al., 2004; Foest et al., 2006). To improve the properties of titanium and expand its clinical application, many methods have been applied to modify the surface of titanium, which should include the application of plasma surface modification technologies (such as plasma spraying and plasma immersion ion implantation and deposition), to

improve the bioactivity of titanium (Liu et al., 2004). Plasma technology can be applied not only to metallic materials, but also to polymeric materials. For biomedical polymers, the surface properties need to be altered to promote a good cell adhesion, growth, and proliferation and to make them suitable for implants and tissue-engineering scaffolds. For polymers, it is also important to know plasma polymerization and plasma-grafting techniques (Jacobs et al., 2012).

Because metallic biomaterials used for orthopedic and dental implants possess a paucity of reactive functional groups, bioactivity modification of these materials is challenging. Hu et al. (2011) treated the titanium discs and rods with carbon dioxide plasma and then incubated in a modified simulated body fluid (SBF) to obtain a HA layer. It was mentioned that the CpTi/SBF−Ti was more advantageous for new bone formation.

Plasma-based ion implantation and deposition techniques are widely used in many applications, including microelectronics, biomedical engineering, and nanotechnology (Chu, 2010). For improving biocompatibility, Chen et al. (2013a) conducted surface modification of different discharge gases (Ar, O_2, and Ar + O_2) plasma-treated polystyrene film by Ar plasma-induced graft polymerization, with biocompatible monomer *N*-vinyl-2-pyrrolidone. The modified film surface shows a better cell distribution and growth than that of the pristine polystyrene surface. From cell culture experiments, it was also observed that Ar + O_2 plasma is more capable of increasing cell adhesion and proliferation. Hence, it was concluded that the method can provide a potential and effective solution for grafting an useful component in future tissue-engineering applications.

Surface modification of biomaterials by ion-beam processing is becoming popular for improving medical device function and biocompatibility. Ion-beam-based processes, such as ion implantation and ion-beam-assisted deposition can provide beneficial surface layers with desirable properties without detrimentally affecting the bulk properties (Gupta, 2011). Ion implantation has been successful in biomaterials modification, such as in improving the wear resistance of artificial joint components, in improving wettability, anticoagulability, anticalcific behavior of biomedical polymers, in minimizing biofouling of medical devices, and depositing HA or Ca−P compounds (Lee et al., 2007b; Mändl et al., 2001). Application PIII technique to oxidation can be found in various references. Liu et al. (2012) reported a new method of titanium surface modification through ammonia (NH_3) PIII technique and its effect on the cellular behaviors of MC3T3-E1 osteoblastic cells. When MC3T3-E1 cells were cultured on NH_3−Ti substrates, it was found that cell proliferation was accelerated at four and seven days of culture. It was indicated that surface modification of titanium through NH_3 PIII favors osteoblastic proliferation and differentiation, and as a result, it may be used to improve the biocompatibility of Ti implants in vivo. Mändl (2007) treated NiTi and CpTi in oxygen-plasma immersion ion implantation method and found that a hard, dense, and thick rutile-type TiO_2 layer formed with excellent biocompatibility. Surface passivation can be achieved by PIII processing in an oxygen atmosphere on Ti (Yankov et al., 2004) and NiTi (Qi and Wu, 2013). PIII nitridization was conducted on Ti and/or NiTi (Firouzi-Arani et al., 2010). Byeli et al. (2012) conducted PIII treated pure Ti and Zr and reported that equal channel

angular pressing and nitrogen ion implantation can be efficiently used to improve bulk and surface properties of Ti- and-Zr based implants. Ti-based alloys,Ti−6Al−4V (Gordin et al., 2012) and Ti−5Al−2.5Fe (Leitão et al., 1997), were also subjected to PIII treatment, and it was reported that the treated surface was covered with Ti_2N. Furthermore, when such PIII nitride Ti-based alloys were immersed into Hank's balanced salt solution, it was reported that a Ca- and P-rich surface layer was detected by X-ray photoelectron spectroscopy. Pye (2004) had processed the steel to nitride to form FeN. Xie et al. (2005) investigated the effects of ($H_2O + H_2$)-implanted titanium by PIII technique on human osteoblast cell culture and concluded that ($H_2O + H_2$)-implanted titanium exhibited good adhesion and growth, suggesting that a practical means to improve the surface bioactivity and cytocompatibility of medical implants made of titanium.

The surface layers of titanium and titanium alloys were modified by ion-beam implantation (Rautray et al., 2010). A similar work was reported on NiTi (Liu et al., 2007). Both negative ion and positive ion are implanted for surface modification of materials. The calcium ion was implanted in titanium surface (Armitage et al., 2007; Byon et al., 2005), claiming that the Ca-implanted Ti specimen showed more active electrochemical behavior than the nonimplanted specimen and easier formation of apatite with good Ca/P ratio in the range of 1.38 and 1.60, revealing its potential as a bioactive material. Gallardo-Moreno et al. (2011) investigated the effects of surface modification by Si-ion implantation on 316L stainless steel on the biocompatibility and bacterial adhesion and reported that Si-ion implantation was an effective way of reducing bacterial adhesion on 316L stainless steel surfaces without compromising its good biocompatibility.

Among plasma technology, the most popular application is a plasma-spraying HA on titanium surface (Azarmi, 2005; Fomin et al., 2012; Xue et al., 2005). Recently, Latka et al. (2010) developed suspension plasma spraying that enables the production of finely grained nanometric or submicrometric coatings. The suspension (which is formulated with the use of fine powder particles in water or alcohol) is injected into plasma jet, and the liquid additives evaporate. The remaining fine solids are molten and subsequently agglomerate or remain solid. Suspension plasma coating of titanium oxide and HA was demonstrated successfully. Plasma oxidation was conducted in various ways (Huan et al., 2012; Montazeri et al., 2010; Silva et al., 2006). Montazeri et al. (2010), using plasma electrolytic oxidation, coated titania, and HA onto Ti-6Al-4V. It was reported that, by increasing the operation time, the amount of the formed HA increased, and the sample coated at 500 V and 15 min showed the best corrosion resistance in Ringer's solution. Ti was subjected to plasma oxidation and showed that improved wetting was obtained, which is potentially associated with shorter osseointegration periods. Huan et al. (2012) modified the surface of a NiTi shape memory alloy by plasma electrolytic oxidation in Na_3PO_4 with an aim to produce porous NiTi surfaces for biomedical applications. It was concluded that the wettability and surface free energy of NiTi increased significantly, indicating that the plasma oxidation process shows potential for expanding the biofunctionality of NiTi.

Similarly, plasma nitrization can be achieved. Ti−6Al−4V and Ti−4Al−2.5Fe (Rie et al., 1995) and Ti−24Al−10Nb intermetallic alloy (Abd El-Rahman et al., 2007) were plasma nitrided to form TiN film on these alloy surfaces. Fouquet et al. (2004) plasma treated Ti−6Al−4V using a N_2−H_2 gas mixture under 10 Pa. It was reported that (1) the plasma treatment enables the formation of a δ-TiN layer, which can act as a diffusion barrier for nitrogen, and (2) the underneath previously formed ε-Ti_2N grains undergo a nitrogen rearrangement with the remaining α-Ti grains, leading to the formation of a nitrogen-poor phase that was identified as the α-$TiN_{0.26}$ phase.

Chrzanowski et al. (2012) plasma treated NiTi because high nickel content such as in NiTi is believed to reduce the number of biomedical applications due to the reported toxicity of nickel. The reduction in nickel release and minimized exposure of the cell to nickel can optimize the biocompatibility of the alloy. Among many ideas proposed to prevent Ni element release from NiTi, it was hypothesized that the native surface of NiTi supports cell differentiation and insures good biocompatibility. Three types of surface modifications were investigated, thermal oxidation, alkali treatment, and plasma sputtering, and compared with smooth, ground surface. It was concluded that the most favorable cell responses were observed for ground and plasma-sputtered surfaces, suggesting that smooth, plasma-modified surfaces provide sufficient properties for cells to grow (Chrzanowski et al., 2012).

Diamond (or carbon) is highly biocompatible and has emerged as a potential biomaterial and was plasma CVD-treated onto pure titanium surface under various gas ratios of CH_4 and H_2 (Fu et al., 1999). It was reported that (1) growth of diamond crystals and coatings on TiC layer were observed; (2) pre-etching of Ti substrate with hydrogen plasma for a short time significantly increased nuclei density of diamond crystals; and (3) plasma power had a significant effect on the surface morphology and the mechanical properties of the deposited diamond coatings. Bazaka et al. (2011) treated biopolymer plasma modification to control bacterial cell attachment and biofilm formation. The application of atmospheric plasma is increasing in numerous situations especially in the biomedical field due to their practical capability to low-temperature-providing plasma that are not spatially bound or confined by electrodes (Dutt-Mazumder and Manna, 2011; Sawase et al., 2007).

Light amplification by stimulated emission of radiation (laser) is a coherent and monochromatic source of electromagnetic radiation that can propagate in a straight line with negligible divergence. As a result, laser finds diverse applications, ranging from mere mundane to most sophisticated uses either for totally commercial or purely scientific purposes, and from life-saving to life-threatening causes (Narayan et al., 2005). High-power lasers can produce intense heating and perform various manufacturing operations or material processing. The manufacturing processes have been broadly divided into four major categories, laser-assisted forming, joining, machining, and surface engineering. Surface engineering means the design and modification of a surface to enhance hardness, wear resistance, heat resistance, or some other properties. Although most laser surface engineering processes appear expensive to be compared to other technologies, in many cases they are actually

more cost-effective because of their precision and speed. Due to the intrinsic properties of high coherence and directionality, a laser beam can be focused onto a metallic surface to perform a broad range of treatments, such as remelting, alloying, and cladding, all of which are used to improve the wear and corrosion resistance of biomaterials (Narayan et al., 2005).

Bandyopadhyay et al. (2011) used a laser surface-modification method to improve mechanical and tribological properties of Ti biomaterials (CpTi and Ti−6Al−4V). To improve tribological properties of Ti−48Al−2Cr−2Nb intermetallic alloy, laser surface modification with NiCr−Cr_3C_2 precursor powders was conducted (Liu and Wang, 2006). An appropriate level of surface roughness of a titanium implant was created by laser modification to improve the biointegration (Trtica et al., 2006). Using localized melting and rapid solidification by laser energy, the surface of machined and Al_2O_3 blasted screw-shaped Ti dental implants was treated by Nd:glass laser and reported that surface treatment seems to be promising for the improvement of the osseointegration of dental implants (Pető et al., 2002). Laser surface treatment was used on electrophoretically deposited HA coatings on titanium to improve interfacial bonding. First, electrophoretic deposition was used to produce thick HA coatings on Ti substrate. Both heat treatment and laser surface treatment were used to create a strong metal−ceramic interface. X-ray diffraction results for laser-treated surface indicated the presence of HA and Ti phases along with $CaTiO_3$. A second layer of HA was electrophoretically deposited on laser-treated coatings to improve biological properties further. It was shown that laser surface treatment can eliminate delamination of weak interface of HA coatings by forming a strong Ti−HA composite layer at the interface. It was further reported that bone cell−material interactions for both laser-treated and untreated samples with human osteoprecursor cells showed no sign of toxicity due to laser processing and increased bioactivity due to HA coatings (Roy et al., 2008a).

Alloying can be achieved by not only conventional melting/casting method, but it can be also done by solid-state powder metallurgy, mechanical alloying, and laser alloying (Tian et al., 2005) and laser additive manufacturing (Gu et al., 2012). Another application of laser-assisted fabrication can be found in laser processing nylon 6,6 to enhance the wettability and bioactivity−osteoblast cell response (Waugh and Lawrence, 2013). Laser metal sintering has shown promising results, but no comparison with other commercially available surface has been performed. Witek et al. (2012) evaluated the biomechanical and histological early bone response to laser-sintered implants relative to alumina-blasted/acid-etched. Beagle dogs received four Ti−6Al−4V implants in each radius, remaining for one, three, and six weeks in vivo. Bone-to-implant contact (BIC) and bone area fraction occupancy (BAFO) were evaluated. Biomechanical evaluation was done by the torque-to-interface failure analysis. The laser-sintered surface presented higher S_a and S_q than alumina-blasted/acid-etched surfaces. Significantly higher torque was observed at one and six weeks for the laser-sintered surface, whereas at three weeks, no significant differences were observed. Significantly higher BIC and BAFO values were observed for the laser sintered only at one week, whereas no significant differences were observed at three and six weeks. It was also found that the laser-sintered implants presented

biocompatible and osseoconductive properties and improved biomechanical response compared with the alumina-blasted/acid-etched surface only at one and six weeks in vivo.

Laser deposition was performed to produce nanostructured TiO_2 films (Sanz et al., 2009; Walczak et al., 2009) and TiO_x nanoparticles (Kurland et al., 2010; Nikolov et al., 2009). Ca−P as well as HA can be deposited by laser treatment (Liang et al., 2008; Mihailescu et al., 2010). Thin films of calcium hydroxylapatite ($Ca_{10}(PO_4)_6(OH)_2$) were deposited on polished substrates of Ti−6Al−4V (Nikolov et al., 2009), and calcium phosphate compounds were deposited on acid- and alkali-treated Ti substrate (Kurland et al., 2010), indicating that such laser-treated surfaces enhance the biocompatibility of titanium and its alloys.

Laser oxidation and nitrization are other remarkable applications of laser technology. CpTi was treated using Q-switched Nd:YAG laser radiation to control early stage of oxidation, so that the oxygen content did not exceed 50 at% (TiO) (Lavisse et al., 2002). CpTi surfaces were subjected to laser nitrization (Carpene et al., 2005; Höche et al., 2007). It was reported that laser-treated CpTi was covered with δ-TiN phase or tetragonal δ'-Ti_2N phase, and it was mentioned that films containing tetragonal Ti_2N phases possess better mechanical properties, corrosion, and wear resistance in comparison with cubic TiN (Yue et al., 2002). Similarly, a Ti−6Al−4V alloy surface was laser-treated (Dahortre et al., 2013; Man et al., 2011). An excimer laser was used to improve the pitting corrosion resistance of the alloy, and it was found that pitting corrosion resistance was improved due to TiN precipitates acting as galvanic cathodes at high corrosion potentials (Yue et al., 2002). For improving tribological properties, laser diffusion nitriding was conducted (Dahortre et al., 2013; Man et al., 2011).

Laser chemical vapor deposition (LCVD) is a new manufacturing process that holds great potential for the production of small and complex metal and ceramic parts (Duty et al., 2001). A complex compound of silver nanoparticles (size 40 nm) combined with polymer blends (polyethylene glycol/polylactide−co-glycolide) was deposited through a laser-assisted pulsed evaporation method to cover the substrate surface with an antibacterial feature (Paun et al., 2013). Besides major surface coating and modification technology involved in the physical reaction as described above, there are still various methods available. Mishra et al. (2012) investigated synthesizing HA nanorods by microwave irradiation technique, taking ethylene diamine tetra-acetic acid as a complexing reagent. After examining calcinizing in the temperature range from 450 to 900 °C, it was found that the precursor was needed above 700 °C to produce nanorods with ~200 nm. Nanocomposite Ti−Si−N coating was performed by reactive dc magnetron sputtering in a mixture of Ar and N_2 gases onto bio-implantable 316L stainless steel substrates (Balasubramanian et al., 2012). It was found, by X-ray diffraction, that the thus processed Ti−Si−N nanocomposite coatings are mainly composed of amorphous Si_3N_4 and and TiN crystals as major constituents, with TiN, TiO_2, and Si_3N_4.

For modifying titanium dental implants, Yoshinari et al. (2002) used a dry process on a titanium surface, including the ion-beam dynamic mixing (thin calcium phosphates), ion implantation (Ca^+, N^+, F^+), titania spraying, ion plating (TiN, alumina),

and ion-beam mixing (Ag, Sn, Zn, Pt) with Ar^+ to enhance surface compatibility with the host bone tissue, subepithelial connective tissue, and epithelial tissue, so that the tissue-compatible surface can be obtained. It was concluded that dry-process surface modification was useful in controlling the physicochemical nature of surfaces, including the surface energy and the surface electrical charge, and in developing tissue-compatible implants. HA was cold-sprayed to biodegradable Mg alloy, and it was reported that biocompatible coatings of the order of 20−30 μm thickness was obtained by preheating at 400 °C prior to the cold spraying (Noorakma et al., 2013).

Cai et al. (2005), for improving the surface biocompatibility of titanium films, used the layer-by-layer self-assembly technique, based on the polyelectrolyte-mediated electrostatic adsorption of chitosan and gelatin. It was suggested that titanium films could be modified with chitosan and gelatin. The electrostatic layer-by-layer self-assembly technique was also used for producing polymers and enzymes (Ai et al., 2003). Because the presence of appropriate porosity is required for tissue ingrowth and for the concurrent degradation of implanted structure, formation of sufficiently large three-dimensional nanoporosity/macroporosity in bone scaffolds is important. Zhang et al. (2012b) introduced a new technique of combining the slip casting and polymer sponge methods using the slips with different powders to prepare HA scaffolds with bimodal pore sizes. It was reported that (1) the scaffolds were prepared with an open, uniform, and interconnected porous structure with a bimodal pore size of 100−300 μm; and (2) the bimodal porous HA scaffold sintered at 1200 °C had a large flexural strength of 73.3 MPa and a porosity of 52.5 vol%.

Sandblasting with large grit and acid-etching (SLA) treatment is considered to be a reliable modification to achieve an excellent titanium surface. However, contamination of hydrocarbons would make SLA surface hydrophobic and influence its bioactivity. Thus, appropriate methods of preservation or further treatments could be used for improvement. Li et al. (2012a) conducted preservation in deionized water and ultraviolet (UV) irradiation that were, respectively, applied to achieve SLA and UV-SLA surfaces. Surface characteristics were assessed by scanning electron microscopy, optical profilometer. and X-ray photoelectron spectroscopy as well as wettability by optical contact angle analyzer. Additionally, biocompatibility was evaluated by the response to osteoblast-like MG63 cells. It was mentioned that: (1) the SLA surface with fewer hydrocarbons (25.31%) remained hydrophilic and showed better affinity to mineralization of MG63 cells than hydrophobic polluted SLA surface; and (2) furthermore, with the lowest content of hydrocarbons (14.26%) and superhydrophilicity, the UV-SLA surface, which had the hydrocarbons effectively decomposed by photocatalysis and meanwhile acquired abundant hydroxyl groups, had most greatly promoted the attachment, proliferation, differentiation, and mineralization of MG63 cells. Therefore, hydrocarbons were found to be an important influencing factor to compatibility of biomaterials. It was also reported that UV irradiation was recognized as a trustworthy method for surface cleaning without change of topography and roughness and could even lead to greater biocompatibility of sandblasted and acid-etched titanium surface.

10.4.5 Thermal modification

Thermal spray is an established industrial method for the surfacing and resurfacing of metal parts and one of the most successful and versatile because of the wide range of coating materials and substrates that can be processed, e.g., from tape recording heads to print rollers and bridge structures. The benefits are typically lower cost, improved engineering performance, and/or increased component life. In addition to original equipment applications, thermal-spray coatings repair worn parts and those damaged ion service, and restore dimensions to mismachined parts (Dorfman, 2002; Puerta, 2013). Bioceramics such as HA mixed with TiO_2 on Ti−6Al−4V substrate (Lima et al., 2010) and rutile-type TiO_2 on surgical stainless steel substrate (Siva et al., 2005) were thermal sprayed.

Titanium surface was hydrothermally treated at a high pressure of 6.3 MPa (at 280 °C) in CaO solution or water to improve bioactivity and biocompatibility (Sultana et al., 2006) to form calcium titanate on the titanium surface. It was reported that, besides the calcium titanate, titanium oxide and titanium hydroxide layers were also formed as processing temperature and pressure increased. After immersing the thus surface-modified titanium in an SBF, needle-like apatite precipitation was observed, suggesting that surface modification of titanium with high-pressure hydrothermal treatment seemed to improve bioactivity and biocompatibility. A complex compound of a crystalline $CaTiO_3$ layer was formed on Ti−13Nb−13Zr alloy by the hydrothermal treatment (Park et al., 2011). An anatase-type TiO_2 along with $Ti(OH)_4$ was deposited on Ti (Drnovšek et al., 2009), and $Zn−PO_4$ was coated on Ti implants, forming zinc titanium phosphate (Valanezhad et al., 2012).

Dewidar and Lim (2008) fabricated porous-surfaced with solid core Ti−6Al−4V implant compacts by traditional powder metallurgy. The powder metallurgy technique was used to produce three different porous-surfaced implant compacts 30%, 50%, and 70% in a vacuum atmosphere. The solid core formed in the center of the compact shows a similar microstructure of near full density of Ti−6Al−4V. The compressive yield strength was up to 270 MPa and significantly depended on the surface porosity, core size, and temperature of sintering. Porous-surfaced Ti−6Al−4V implant compacts with a solid core have much higher compressive strengths compared to the human bone. The ingrowth of bone tissue into the outer porous surface layer results in part fixation, while the solid inner core region provides the necessary mechanical strength for a device used for the replacement of heavy load-bearing joint regions such as the hip and knee. Okazumi et al. (2011) investigated two-step thermal oxidation of CpTi with a focus on the formation of anatase-type TiO_2. A first-step treatment was conducted in an Ar-(0.1−20)%CO atmosphere at a temperature of 500−900 °C for a holding time of 0 or 1 h, and a subsequent second-step treatment was conducted in air at 200−600 °C for 1 h. It was reported that (1) titanium oxides and titanium oxycarbide were obtained in the first step, with relative amounts depending on heating temperature, holding time, and CO partial pressure; (2) an anatase-rich layer on Ti was obtained after second-step treatment in air at 300−350 °C in cases in which single-phase titanium

oxycarbide formed in the first step; and (3) the bonding strength of an anatase-rich layer with a thickness of 0.5 μm was calculated to be around 90 MPa.

Besides the above popular coating thermal methods, there are still several important methods for coating. Rodionov (2012) used the steam-thermal oxidation of medical titanium implants. Shenhar et al. (1999) developed the power immersed reaction-assisted coating nitriding method, which is suitable for surface modification of large complex-shape orthopedic implants. Ti−6Al−4V alloy samples were annealed at 850−1100 °C in sealed stainless steel containers that allow selective diffusion of nitrogen atoms from the atmosphere, and it was reported that (1) Ti_3Al intermetallic phase was detected at the Ti_2N/α-Ti interface acting as a barrier for nitrogen diffusion; and (2) importantly for biomedical applications, no toxic Al or V were detected in the surface layer nitrided Ti−6Al−4V alloy.

10.4.6 Combined technology

There is research that combined several methods mentioned above; some of it is conducted simultaneously, while the other studies are done consecutively. To improve the bioactivity of TiO_2 coatings, Zhang et al. (2013) conducted MAO in an electrolyte containing Ca and P ions and MAO in a 1-M NaOH electrolyte and reported that alkaline-treated TiO_2 surface was found to be a response for the rapid formation of HA during an SBF soaking, and the previous introduction of Ca and P can increase the opportunity to form HA. To increase osteoinduictivity and corrosive-wear resistance, a hybrid treatment of micro-arc discharge oxidation and electrophoretic deposition was conducted by forming a double-layer HA−TiO_2 coating on titanium alloys, with HA as the top layer and a dense TiO_2 film (which is believed to be effective as chemical barriers against the in vivo release of metal ions from the implants) as the inner layer, so that a good combination of bioactivity, chemical stability, and mechanical integrity can be expected (Nie et al., 2000). It was reported that a hybrid combination of MAO and electrophoretic deposition provided a phase-pure HA top layer and anticorrosive TiO_2 interlayer, which should show good mechanical and biochemical stability in the corrosive environment of the human body. MAO was combined with hydrothermal treatment in electrolytes containing calcium glycerophosphate and calcium acetate on Ti−6Al−4V, and it was found that (1) the film with a Ca/P ratio equivalent to HA was obtained when the final voltage and current density were 350 V and 200 A/m^2 in the electrolyte containing 0.06 M calcium glycerophosphate and 0.25 M calcium acetate; and (2) after hydrothermal treatment, the HA was precipitated on the surface of the film obtained by MAO with a thickness of about 4 μm (Liu et al., 2005).

Wei et al. (2008) heat-treated NiTi alloy in air at 600 °C to form TiO_2 film and alkali-treated in NaOH solutions (1 M, 2 M, 3 M, 5 M) to improve their bioactivity, followed by soaking SBF to evaluate their in vitro performance, and reported that (1) the 3-M NaOH treatment is the most appropriate method; (2) a large amount of apatite formed within 1 day's soaking in SBF; and (3) after 7 days' soaking, a TiO_2/HA composite layer formed on the NiTi surface.

Plasma-coated HA possesses a few crucial problems, including easy dissolution or resorption in living tissue and a potentially weak interfacial bond between the coating and a metal substrate, so that the low stability of the HA coating may lead to the failure of the implant. Besides, HA cannot be deposited uniformly due to geometrical limitations such as on inner or undercut surfaces of a porous structure. Ishizawa and Ogino (1996) used combined methods of electrochemical and hydrothermal reactions to precipitate HA crystals on porous Ti. HA ceramic has been applied on Ti implants (which was previously modified by laser beam irradiation) to increase the corrosion resistance and gain better biocompatibility and implant−bone tissue biological adhesion, by coating polyvinyl dense fluoride/HA composite that was obtained by casting method, and it was reported that uniform coating with a small thickness variation along the coated surface was successfully obtained (Ribeiro et al., 2009). Moreover, to control surface topography (roughness and blind porosity), surface chemistry, and wettability affecting the osseointegration, Shtansky et al. (2012) used a combination of various techniques, such as cold spray, selective laser sintering, pulsed electro-erosion treatment, and magnetron sputtering, on Ti materials. In particular, for modifying surface chemistry, multifunctional bioactive nanostructured TiCaPCON films were deposited on cold-sprayed, laser-sintered, and electro-erosion treated surfaces using a composite $TiC_{0.5} + Ca_3(PO_4)_2$ target. Following are reported (1) the wettability measurements showed that the cold-sprayed and electro-erosion treated surfaces exhibit high values of water contact angle; and (2) ion etching in vacuum and TiCaPCON film deposition made the samples highly hydrophilic; concluding that the combination of high surface roughness and blind porosity with hydrophilicity and biocompatibility makes the fabricated metal−ceramic materials promising candidates for applications involving tissue regeneration.

10.5 Coating materials

10.5.1 Introduction

Coating surface layers is a valuable way to achieve the surface transformation, including carburizing, oxidizing, or nitrizing. In this section, we will discuss coating materials (metallic, polymeric, ceramics, composites, and biomimetrics) and their preparations.

10.5.2 Metallic materials

As we will see in this section, metal elements and alloys are chosen and used extensively as coating materials. A nanotopographic noble metal (Ag, Au, Pd) coating has been applied on commercial urinary catheters and used in more than 80,000 patients, and it was indicated that it is possible to modulate inflammation and fibrosis in soft tissue (Suska et al., 2010). Use of the silver element was due to the excellent

antibacterial property (Chen et al., 2009). Bioactive coatings are in high demand to increase the functions of cells for numerous medical devices. The metal element (Au,Ti) was coated on several potential orthopedic polymeric materials (specifically, ultrahigh-molecular-weight polyethylene, polyetheretherketone [PEEK] and polytetrafluoroethylene [PTFE]) by an ionic plasma deposition process that creates a surface-engineered nanostructure (with features below 100 nm), and their osteoblast (bone-forming cell) adhesion was improved (Yao et al., 2007).

A solid Ti metal was widely selected as a coating element. Ti was coated on surgical 316L stainless steel substrate, and it was reported that cell proliferation, alkaline phosphatase activity, migration, and adhesion were increased, and osteoblast-like cells on the grit-blasted, titanium-coated, micro-arc-oxidated surface were strongly adhered and proliferated well (Young et al., 2011). Nanoscale titanium was coated on silicon surfaces and increased cell spreading, and proliferation rates were reported on surfaces with 50-nm-thick Ti coatings (Mwenifumbo et al., 2007). Nanostructures entail a high potential for improving implant surfaces, for instance, in stent applications. Ti nanoparticles were coated on an electropolished NiTi stent surface (Neumeister et al., 2012). The solid solution phases of β-(Ti, Nb) (Fallah et al., 2010) and Ti−6Al−4V film (Sonoda et al., 2006) were also selected as coating materials. Although carbon fiber-reinforced polyetheretherketone (CF/PEEK) exhibits properties suitable for load-bearing orthopedic implants, its hydrophobicity induces the deposition of a peri-implant fibrous tissue capsule, preventing bone apposition. Devine et al. (2013) coated CF/PEEK screws with titanium by vacuum plasma spraying and PVD and found that Ti coating of CF/PEEK screws significantly improve bone apposition and removal torque compared with uncoated CF/PEEK screws.

Tantalum (Ta) metal has been successfully used for implants due to excellent biocompatibility (Dolatshahi-Pirouz et al., 2010; Kovacs and Davidson, 1996; Matsuno et al., 2001). It has been found that tantalum coatings show great potential within both industrial and medical applications (Lee et al., 1999). Coating tantalum, having a very ductile nature, is suitable when a product can be improved by combining material characteristics of the substrate with an exceptional corrosion-resistant surface (Macionczyk et al., 2001). As a result, tantalum is an excellent candidate for usage as a coating for NiTi alloys to improve its anticorrosion property and radiopacity (Cheng et al., 2006). Ta was also coated on Co−Cr alloy with excellent outcomes of good mechanical properties (high elastic modulus, high hardness value, low friction coefficient, high wear resistance) and chemical properties (high wettability, good corrosion resistance), so that it is of interest for joints presenting good biocompatibility and great longevity (Pham et al., 2012; Spriano et al., 2009). Porous tantalum (which possesses a low modulus metal with a characteristic appearance similar to cancellous bone) is currently available for use in several orthopedic applications (hip and knee arthroplasty, spine surgery, and bone graft substitute). It was reported that this transition metal maintains several interesting biomaterial properties, including a high volumetric porosity (70−80%), low modulus of elasticity (3 MPa), and high frictional characteristics with an excellent biocompatibility, and tantalum−chondrocyte composites have yielded successful early results in vitro and may afford an option for joint resurfacing in the future, suggesting a promising applications in orthopedic surgery (Balla et al.,

2010; Levine et al., 2006; Macheras et al., 2006). In other work, it was reported that Ta and TaO were coated on surgical 316L stainless steel, and it was mentioned that (1) the mechanical stability and repassivation properties of the material are guaranteed up to the onset of substrate plastic deformation; (2) biocompatibility is obtained by tantalum oxide; and (3) the ductility is achieved by the tantalum interface, which, at the same time, ensures continued film adhesion, even after plastic deformation of the steel substrate (Macionczyk et al., 2001).

Olivares-Navarrete et al. (2011) deposited niobium (Nb) by magnetron sputtering as a possible surface modification for stainless steel substrates in biomedical implants, and the biocompatibility of the coatings was evaluated using human alveolar bone-derived cells, in terms of cellular adhesion, proliferation, and viability. It was observed that (1) no toxic response was observed for any of the surfaces, indicating that the Nb coatings act as a biocompatible and bioinert material; (2) a cell morphology test confirmed the healthy state of the cells on the Nb surface; and (3) water contact angle measurements showed that the Nb surface is more hydrophobic than the stainless steel substrate. Nb thin film and NbN were deposited on stainless steel to evaluate the biocompatibility of the surfaces by testing the cellular adhesion and viability/proliferation of human cementoblasts during different culture times, up to 7 days (Ramírez et al., 2011). It was reported that (1) the niobium oxide films were amorphous and of stoichiometric Nb_2O_5, while the niobium nitride films were crystalline in the FCC phase (*c*-NbN) and were also stoichiometric with a Nb-to-N ratio of one; (2) the biocompatibility of the stainless steel could be improved by any of the two films, but neither was better than the Ti-6Al-4V alloy; and (3) on the other hand, comparing the two films, the *c*-NbN seemed to be a better surface than the oxide in terms of the adhesion and proliferation of human cemetoblasts.

High-purity biodegradable magnesium (Mg) is believed to exhibit excellent biocompatibility, and coating of Mg element is expected to be shown as appropriate for implant applications and to improve the interaction between the implant and the biological environment (Bansiddhi et al., 2008). In recent years, research on magnesium alloys has increased significantly for hard tissue replacement and stent application due to their outstanding advantages, because (1) Mg alloys have mechanical properties similar to bone, which can avoid stress shielding; (2) they are biocompatible essential to the human metabolism as a factor for many enzymes; (3) the main degradation product Mg is an essential trace element for human enzymes; and (4) the most important reason is they are perfectly biodegradable in the body fluid (Salunke et al., 2011). Mg−Y−Nd was evaluated for its feasibility in bone implant applications, mainly focused on biocompatibility and corrosion resistance (Yuen and Ip, 2010). It was concluded that the biodegradable Mg−Y−Nd implant is superior to the control Ti−6Al−4V with respect to both bone/implant interface strength and osseointegration. Mg−Zr−Sr alloys have recently been developed as biodegradable implant materials (Li et al., 2012b). It was reported that (1) both Zr and Sr are evaluated as excellent alloying elements in manufacturing biodegradable Mg alloy implants; (2) the Zr addition refined the grain size, improved the ductility, smoothed the grain boundaries, and enhanced the corrosion resistance of Mg alloys; (3) the Sr addition led to an increase in compressive strength, better in vitro biocompatibility, and significantly higher bone

formation in vivo; and (4) Mg−xZr−ySr alloys with x and $y \leq 5$ wt% would make excellent biodegradable implant materials for load-bearing applications. Biodegradable Mg−Zn−Zr was also developed as an orthopedic implant material due to its biodegradable feature and suitable mechanical properties (Yang et al., 2013). Amorphous Si film (which was prepared by plasma-enhanced CVD of SiH_4) was coated on Mg−Y−Nd alloy for biomedical applications (Li et al., 2012b). The hemolysis test and blood platelets adhesion test were conducted, and it was reported that the hemolysis of Mg−Y−Nd alloy decreased after being coated by Si and the platelets attached on the Si film were at the inactivated stage with a round shape.

Functionally graded, hard and wear-resistant Co−Cr−Mo alloy was coated on Ti−6Al−4V alloy, and it was shown that the addition of the Co−Cr−Mo alloy significantly increased the surface hardness without any intermetallic phases in the transition region (Krishna et al., 2008).

Selenium (in the form of sodium selenite) coating onto Ti material was evaluated, and it was found that there was no inhibitory effect of the selenium coating on the osteoblastic cell growth, and Se coating is a promising method to reduce bacterial attachment on prosthetic material (Holinka et al., 2013).

10.5.3 Polymeric materials

Biodegradable polymers (which perform a structural application and are designed to be completely resorbed and to become weaker over time) form a unique class of materials that created an entirely new concept when originally proposed as biomaterials. Recently, in tissue engineering, a biodegradable scaffold seeded with an appropriate cell type provided a substitute for damaged human tissue while the natural process of regeneration was completed (Gomes and Reis, 2004a,b). An adhesive biodegradable polymer, poly(vinyl acetate) (PVA), was coated on Mg-based alloys by the dip-coating technique to control the degradation rate and enhance the biocompatibility of magnesium alloys. Because the cytocompatibility of osteoblast cells (MC3T3) revealed high adherence, proliferation, and survival on the porous structure of PVA-coated Mg alloy, which was not observed for the uncoated samples, it was concluded that the PVA coating is a promising candidate for biodegradable implant materials, which might widen the use of Mg-based implants (Abdal-hay et al., 2012). A biodegradable polymeric membrane fabricated by polycaprolactone and dichloromethane was coated on an Mg-based alloy to control high corrosion rate, and accumulation of hydrogen gas on degradation hinders its clinical application (Wong et al., 2010).

Polyurethane (Tepe et al., 2006) and polyhedral oligomeric silsesquioxanes and poly(carbonate-urea)urethane (Bakhshi et al., 2011) were coated onto NiTi stent to control thrombogenicity. When Ti−6Al−4V alloy is used in several ventricular assist devices, the thrombogenecity resistance is highly required. A plasma-induced graft polymerization of 2-methacryloyloxyethyl phosphorylcholine (MPC) was carried out and poly(MPC) (PMPC) chains were covalently attached onto the Ti−6Al−4V surface (Ye et al., 2009). It was reported that platelet deposition was markedly reduced on the PMPC-grafted surfaces, and platelet activation in blood that contacted the PMPC-grafted samples was significantly reduced relative to the

unmodified Ti−6Al−4V and polystyrene control surfaces. For bone and teeth repairs, biomaterials are demanded of both good biocompatibility and reliable mechanical properties for long periods. Due to the nature of the HA of low fracture toughness and fracture energy, there are several ways to overcome these disadvantages of HA materials, including incorporating with ZrO_2 or Al_2O_3. Nakahira et al. (2002) infiltrated porous HA with nylon to improve fracture toughness of HA with 1.65 MPa$\sqrt{m}$.

10.5.4 Ceramics − metallic oxides, nitrides, and carbides

Bioactive TiO_2 was deposited on surface-modified polyethylene terephthalate plates by using a sol−gel method, and it was indicated that this modification possesses a mechanically stable surface-modified layer, excellent bone-bonding ability, osteoconductive ability, and biocompatibility in bone (Saito et al., 2011). Ti-O film was deposited on surgical 316L stainless steel by PIII and deposit method (Xie et al., 2013).

Titania (TiO_2) thin films were deposited on NiTi surgical alloy by the sol−gel method. It was found that, according to the in vitro evaluation on blood compatibility of the film and NiTi alloy by dynamic clotting time and blood platelets adhesion tests, an NiTi alloy coated with TiO_2 film possessed an improved blood biocompatibility (Liu et al., 2003). Titanium oxide coatings were conducted by MAO in galvanostatic regime on biomedical NiTi alloy in H_3PO_4 electrolyte using DC power supply (Wang et al., 2011b). Sugita et al. (2011) using a slow-rate sputter deposition of molten TiO_2 nanoparticles, coated acid-etched microroughened titanium surfaces with a TiO_2 layer of 300 pm to 6.3 nm thickness that increased the surface oxygen levels without altering the existing microtopography. It was reported that (1) a superthin TiO_2 coating of pico-to-nanometer thickness enhances the biological properties of the proven microroughened titanium surfaces; and (2) the improvements in proliferation and differentiation of osteoblasts attained by this chemical modification is of great significance, providing a new insight into how to develop new implant surfaces for better osseointegration, based on the established microtopographic surfaces. Titanium oxide (TiO_2) films were deposited onto the polymer substrates of polytetrafluoroethylene, polyethylene, and polyethylene terephthalate, which were premodified with polydopamine coating, by a simple liquid-phase deposition process. It was indicated that the fabricated TiO_2 films could markedly improve the in vitro cytocompatibility (Ou et al., 2010). TiO_2 was coated on Ti−6Al−4V substrate by air plasma-spraying method. It was reported that, according to the osteoblast adhesion morphology and proliferation tests, osteoblast-like cell morphology was not influenced by process parameters, but cell proliferation was affected to some extent by surface roughness and porosity among TiO_2.

Silicon substrate was also coated with titania films by different methods—by spray pyrolysis method (Ou et al., 2008), ion irradiation (Acik et al., 2009), and sol−gel method (Rawat et al., 2008). Ultrathin film of titanium oxide (TiO_x) was coated on silicon wafers. It was found that (1) the surface sol−gel process predominantly formed homogeneous, but rough and porous titanium oxide layers; and (2) the protein

adsorption was dependent primarily on the silane chemistry, packing of the alkyl chains, morphology (porosity and roughness), and wettability of the sol−gel oxide.

Thin porous titania film was also coated differently. Porous titania film is prepared by alkali (in NaOH) treatment of NiTi alloy, followed by soaking treatment in HCl solution. The benefit of this porous titania film as an interlayer to improve adhesion and integrity of the sol−gel titania coating on NiTi alloy substrate is evidenced by surface morphological observations (Advincula et al., 2005). Effective immobilization of bioactive substances such as adhesive proteins, synthetic peptides, and growth factors on metallic substrates is required for a number of medical applications. It was reported that (1) an alkoxy-derived nanoporous titanium oxide coating (which was synthesized electrochemically on titanium in methanolic electrolytes) may act as an effective interface for functionalizing a titanium surface; and (2) nanoporous oxide coatings could facilitate fast diffusion of small organic molecules within the oxide network and form strong chemical bonds with the functional groups of these molecules at room temperature.

Porous TiO_2 coating was achieved on Ti surface by MAO process, and it was mentioned that the cortex-like coating was conducive to cell retention and implant stabilization (Fu et al., 2011).

Nanotubes of titania were coated. Oriented aligned TiO_2 nanotube arrays were fabricated by anodizing titanium foil in 0.5% HF electrolyte solution (Lai et al., 2005). A net-like structured TiO_2 film was produced with a low-temperature hydrothermal process, followed by acid washing and calcination in air, and was deposited on surgical 316L stainless steel substrate (Yun et al., 2008). For improving cell adhesion and differentiation and as a result of these improvements, nanofibrous modification of dental and bone implants might enhance osseointegration (Lim et al., 2008). TiO_2 nanofibers were fabricated by the electrospinning method using a mixture of Ti isopropoxide and poly(vinyl pyrrolidone) (PVP) in acidic alcohol solution. It was reported that the diameter of the TiO_2 nanofibers was controlled within the range of 20−350 nm.

Titania composites were also chosen as coating materials. To improve the bioactivity of titanium, CpTi was hydrothermally treated in 0.1 mol/L $MgCl_2$ solutions with different pH values (5.5, 7.5, and 9.5) at 200 °C for 24 h. It was reported that (1) nanosized anatase precipitations (including $MgTiO_3$ at low pH and $Mg(OH)_2$ at high pH) were obtained; and (2) hydrothermal treatment in $MgCl_2$ solution can improve the bioactivity of titanium by immobilizing Mg into oxide layer; however, the chemical state and amount of Mg should be well controlled (Shi et al., 2013). Mg-incorporated titania was produced by hydrothermally treating Ti in an alkaline Mg-containing solution. It was concluded that the Mg-incorporated submicroporous Ti oxide surface produced by hydrothermal treatment may improve implant osseointegration by enhancing the attachment, spreading, and differentiation of osteoblastic cells (Park et al., 2010). A mixture of TiO_2 and TiN was deposited on titanium alloy by plasma nitriding and oxidizing under glow discharge conditions. It was reported that nitriding and oxidizing under glow discharge conditions have provided new possibilities of producing nontoxic, human fibroblast-compatible surface layers on parts made of titanium alloys (Czarnowska et al., 1999). Ni_2O_3-doped TiO_2 nanotubes

were deposited on NiTi alloy using an electrochemical anodization method. It was reported that: (1) forming of Ni_2O_3-doped TiO_2 film on the surface of NiTi alloy increased its wettability, especially for 600 °C annealed sample, so the biological response is expected to be improved; and (2) annealing the Ni_2O_3-doped TiO_2 film coated NiTi alloy at 450 °C is desirable for cardiovascular applications (Huang et al., 2009).

There are still several different types of oxides that are ready for coating processing. A mixture of TiO_2 and ZnO was sputter-coated on glass substrates (Hang et al., 2012). To improve corrosion resistance and biocompatibility, Fe-O film was coated on iron stents (Zhu et al., 2009). It was reported that the results of human umbilical vein endothelial cells culture showed the cells had good adhesion and proliferation behavior on the Fe−O film, and, after depositing Fe−O thin film by PIII and deposition technique under the low oxygen flux, the corrosion resistance and biocompatibility of pure iron were effectively improved.

Due to excellent mechanical stability and repassivation, properties of the tantalum (Ta) are guaranteed up to the onset of substrate plastic deformation. Macionczyk et al. (2001) coated TaO onto stainless steel implants and obtained results indicating that, while biocompatibility is obtained by tantalum oxide, the ductility is achieved by the tantalum interface, which, at the same time, ensures continued film adhesion, even after the steel substrate was plastically deformed. Thin TaO film was also coated on Ti material by layer-by-layer sol−gel deposition technique (Arnould et al., 2009). A composite of TaO and carbon was coated on Ti surface to improve its propensity to a long-term degradation in physiological conditions and its weak osseointegrative capacities (Maho et al., 2012).

Zirconia (ZrO_2) coating was evaluated by the histologic analysis, indicating that (1) bone growth is more evident around coating fixtures than in controls; and (2) a more mature bone is present in the peri-implant coated surface than in controls; hence zirconium oxide coating can enhance implant osseointegration (Sollazzo et al., 2008). Yan et al. (2008) prepared macroporous and nanocrystalline zirconia coating film by MAO, followed by chemical treatment in H_2SO_4 or NaOH aqueous solution to evaluate the apatite-forming ability. Monolithic zirconia and zirconia−HA composites were prepared by joining by cold isostatic pressing (at 300 MPa) and subsequently by glass-encapsulated hot isostatic pressing (at 1225 °C, for 1 h and under 200 MPa) (Balla et al., 2009). A zirconia (ZrO_2) was coated on Ti and Zr to exhibit lower friction and superior wear properties, suggesting that they could be used in hip and knee implants.

Now moving to metal nitrides, TiN film was coated on mild steel by a new combined laser/sol−gel processing technique, indicating that nanohardness measurements revealed a hardness value of the order of 22−27 GPa (Ezz et al., 2007). Titanium and Ti−6Al−4V alloy samples were coated using a powder immersion reaction-assisted coating nitriding method to modify their surface properties, and it was reported that strongly adherent single (TiN)- or double (Ti_2N/TiN)-layer coatings were obtained on both substrates, suggesting that titanium nitride coatings can provide surgical titanium alloys with the enhanced fretting wear and corrosion-resistant surface, thereby minimizing the ion- and particulate-generating potential of modular orthopedic

implants (Shenhar et al., 2000). TiN was coated on surgical Ti−6Al−4V ELI alloy to improve tribological and corrosion properties by means of plasma etching in an argon/nitrogen atmosphere protection of surfaces (Hübler, 1999). Nanostructured TiN film was prepared by reactive plasma spraying in the air. The coated film was identified as mainly composed of TiN (max. 86.3%) and a small quantity of Ti_3O (Xiao et al., 2007). Sinter-coating combines sintering and TiN coating in one step by sintering the green specimens in N_2 atmosphere conducted on titanium foam to produce a TiN film layer (Mutlu, 2013). It was reported that, after the alkali treatment by soaking the foams in NaOH solution and then heating at 600 °C, treated foams were immersed into SBF to induce a bone-like apatite layer on foam surface. TiN-based composite coatings with and without the addition of Cr were prepared and deposited by reactive plasma spraying in air. Both sintered and mixed powder of Ti and B_4C were used for this process. It was found that the coating deposited using sintered Ti and B_4C powder is composed of two main phases (TiN and $TiN_{0.3}$), two minor phases (Ti_2O_3 and TiB_2), and a small fraction of TiC phase, and the composition of the coating deposited using the mixed powder with Cr added is predominantly in the TiN and TiB_2 phases, a smaller phase fraction of Ti_2O_3 and TiO_2, and some unreacted Cr (Mao et al., 2007). TiN/Ti multilayer was deposited on 18Cr−8Ni (type 304) stainless steel by magnetron sputtering to improve pitting corrosion resistance (Flores et al., 2007). TiN was also coated on cellulosic fiber substrates by atomic layer deposition to produce biocompatible cellulose and other implant materials (Hyde et al., 2009).

In the TiN group, there are several composites prepared for coating purposes. To improve cytotoxicity, cell adherency, and tribological performance, TiN particle reinforced Ti−6Al−4V composite coatings were prepared. It was found that (1) the composite coatings contain distinct TiN particles embedded in $\alpha + \beta$ phase matrix; (2) the average top surface hardness of Ti−6Al−4V alloy increased from 394 ± 8 HV to 1138 ± 61 HV with 40 wt% TiN reinforcement; and (3) among the composite coatings, the coatings reinforced with 40 wt% TiN exhibited the highest wear resistance of 3.74×10^{-6} mm^3/Nm, which is lower than the wear rate, 1.04×10^{-5} mm^3/Nm, of laser processed Co-Cr-Mo alloy tested under identical experimental conditions (Balla et al., 2012). Titanium nitride oxide ($TiNO_x$) coating were preformed on roughened Ti and stainless steel by plasma/PVD deposition technique and on cellulose fiber substrates by atomic layer deposition (Rieder et al., 2012). It was reported that $TiNO_x$ coatings yield similar proliferation and differentiation rates when applied onto roughened Ti and stainless steel, suggesting that a more effective osseointegration of endosseous implants can be produced.

Titanium aluminum nitride (Ti,Al)N was coated on 304 stainless steel substrate. After the coated implants were placed into the mid-shaft of the femur of Wistar rats, it was found that: (1) all implants exhibited a favorable response in bone with no evidence of fibrous encapsulation; (2) there was no significant difference in the amount of new bone formed around the different rods (osseoconduction); and (3) there was a greater degree of shrinkage separation of bone from the coated rods than from the plain rods, suggesting that titanium aluminum nitride coating may result in reduced osseointegration between bone and implant (Freeman and Brook, 2006). Mukherjee et al. (2005) coated the hard Ti-based coating TiAlN on stainless steel by plasma immersion

ion implantation-assisted deposition to improve wear resistance in orthopedic conditions. Furthermore, titanium aluminum nitride oxide (TiAlNO) coatings were deposited on the corning glass by means of the co-sputtering technique. It was indicated that TiAlNO is versatile material that could be used for both mechanical and electronic applications; however, it is important to control fabrication conditions (Garcib et al., 2013). Shtansky et al. (2011) studied intricate composite of TiCaPCON films that were prepared by DC magnetron sputtering of composite comprising $TiC_{0.5}$ and $Ca_3(PO_4)_2$ target produced by self-propagating high-temperature synthesis. It was reported that: (1) the in vitro studies showed that human fibroblasts well adhered and spread on the surface of the PTFE (polytetrafluoroethylene) sample coated with TiCaPCON films; and (2) the in vivo studies using rat hip and rabbit calvarial defect models demonstrated a high osseointegration potential of the TiCaPCON/PTFE implants.

Titanium carbide (TiC) was coated on titanium substrate by pulsed laser deposition method to improve implant hardness, biocompatibility through surface stability, and osseointegration through improved bone growth (Brama et al., 2007), and TiC and TiB(titanium boride) were coated by laser surface alloying of Ti−6Al−4V with graphite and boron mixed powders to enhance wear resistance (Tian et al., 2006). Levashov et al. (2012) coated a composite of TiCCaPCON on NiTi by rapid plastic deformation technology, thermomechanical treatment, and magnetron sputtering.

10.5.5 Ceramics − nonmetallic compounds

In recent years, implants coated with bioactive layers to promote fixation through an osseointegration mechanism have become increasingly common. Fabrication routes that provide control over features such as biocompatibility and bioreactivity through management of coating chemistry and structure are still being developed. Current coating fabrication technology includes plasma spraying, rf sputtering, CVD, laser ablation, and sol−gel processing, although plasma spraying is used to produce most commonly available bioceramic coatings for orthopedic and dental implants (Rogers et al., 2004).

HA was coated on titanium plates (Guo et al., 2012; Hahn et al., 2009; Hirai et al., 2004; Stiegler et al., 2012). HA coating on titanium was performed by a sol−gel process combined with conventional heat treatment and with UV irradiation at ambient temperature. It was reported that the sol−gel coated titanium had slightly higher bone apposition than uncoated titanium as a control material (Hirai et al., 2004). To improve biocompatibility of Ti substrates, Hahn et al. (2009) coated 1-μm thick nanostructured HA, deposited on the substrates through aerosol deposition, which sprays HA powder with an average particle size of 3.2 μm at room temperature in vacuum. Ti−6Al−4V is also a popular biomedical metallic substrate for HA coating (Hung et al., 2012; Luo et al., 2013; Mansur et al., 2013; Parast et al., 2011). Hung et al. (2012) coated HA on Ti−6Al−4V extra low interstitial surfaces by plasma spraying method. HA-coated surfaces were immersed in an SBF. It was found that: (1) after 28 days, the crystallinity level of the HA coatings in the SBF increased from 54.88 % to 74.39 %; (2) the released calcium-ion concentration increased from 44.9 ppm up to

79.27 ppm; and (3) the coatings contained no significant phase components such as tricalcium phosphate (α-TCP or β-TCP) or tetracalcium phosphate. NiTi shape memory alloy was coated with HA for improving biocompatibility and bioactivity, and TiO_2 for preventing Ni ion release (Maleki-Ghaleh et al., 2012). Gopi et al. (2013) passivated surgical grade stainless steel (316L) in borate through poly-*ortho*-phenylenediamine, followed by subsequent HA coating by a dip-coating method to minimize the release of metallic ions. Nonmetallic substrates are also subjected to HA coatings. To improve bioactivity and to enhance osseointegration of titanium implant materials, nanotubular TiO_2 structure was subject to HA coating, and the bond strength was further improved by annealing the HA-coated nanoporous titania in an argon atmosphere (Kar et al., 2006). Cao et al. (2010) coated the fusion cage-like carbon fiber reinforced carbon composite implants with HA by the plasma-spraying technique for bone tissue reconstruction. After autogenously bone filled fusion cage-like implants were grafted in hybrid goats' tibia for 328 days, it was reported that the coating can significantly speed up the bone-defect healing process and improve the surface bioactivity of carbon fiber reinforced carbon composites. Nanocomposite $ZrO_2-Al_2O_3$ was HA-coated for improving biocompatibility, and from the mechanical and biological evaluations, it was concluded that a mixture of coated HA with 30 vol% and 70 vol% of $ZrO_2-Al_2O_3$ composite was found to be the optimal composition for load-bearing biological applications (Kong et al., 2005).

HA material as a coating species is not limited in the form of a relatively thick solid layer, but it can be formed in various shapes. HA thin films for applications in the biomedical field were grown by pulsed laser deposition and radio-frequency magnetron sputtering techniques (Grigorescu et al., 2007; Jeong et al., 2013; Lee et al., 2010b; Nelea et al., 2004; Yang et al., 2009b). Nelea et al. (2004) coated HA thin film on Ti−5Al−2.5Fe alloys substrates with controlled thickness from 1 μm to 350 nm. To achieve excellent biocompatibility of metal-based implants, HA thin film was coated on nanotube-formed Ti−35Nb−10Zr alloys after femtosecond laser texturing (Jeong et al., 2013). The thus-treated surface was found to be a composite with TiO_2, Nb_2O_5, and ZrO_2. It was furthermore reported that (1) the HA-coated surface on the nanotubes showed the lowest contact angle compared with the other surfaces; and (2) scanning electron microscopy observation revealed that cell attachment and spreading of MG 63 cells showed significantly higher tendency for surfaces covered by HA coating and nanotubes. Not only thickness, but the size is also controlled for coating HA material (Khalid et al., 2012; Lee et al., 2007; Roy et al., 2011a). Lee et al. (2007a) coated a nanosized HA layer on a Ti substrate with a titanium oxide (TiO_2) buffer layer by the electron-beam deposition method and concluded that the nanosized HA coating with the TiO_2 buffer layer holds great promise as a bioactive coating system. A highly crystalline nano HA was coated on CpTi using inductively coupled radio-frequency plasma spray (Roy et al., 2011). It was characterized that (1) depending on the plasma processing conditions, a coating thickness between 300 and 400 μm was achieved in which the adhesive bond strengths were found to be between 4.8 and 24 MPa; and (2) the coating was made of multigrain HA particles of $\sim$200 nm in size, which consisted of recrystallized HA grains in the size range of 15−20 nm.

In most cases, HA has been prepared as synthetic material, but Duta et al. (2013) prepared HA as the synthesis of novel ovine and bovine-derived HA thin films and coated it on titanium substrates by pulsed laser deposition. It was reported that (1) the micrographs of the films showed a uniform distribution of spheroidal particulates with a mean diameter of ~ 2 μm; (2) pull-off measurements demonstrated excellent bonding strength values between the HA films and the titanium substrates; and (3) because of their physiochemical properties and low-cost fabrication from renewable resources, these new coating materials could be considered as a prospective competitor to synthetic HA used for implant applications (Balani et al., 2007). Based on this variation possibility, there are several ion substitutions inside the HA structure (which is a hexagonal closed-packed crystalline structure). Among proposed variations, fluoridated HA seems to be the major one (Balani et al., 2007; Li et al., 2012c; Tredwin et al., 2013; Zhou et al., 2011). Carbon can be incorporated in HA structure to show the excellent mechanical property of carbon in form of nanotube (Balani et al., 2007) or carbonate (Zhou et al., 2011) with biocompatible HA. Li et al. (2012c) coated Na-doped HA (which was, in turn, Ca-deficient) directly prepared onto carbon/carbon composites using electrochemical deposition. It was reported that (1) the Na/P molar ratio of the coating formed on carbon/carbon substrate was 0.097; (2) the mean thickness of the coating was approximately 10 ± 2 μm; (3) the average shear bonding strength of Na−HA coating on carbon/carbon was 5.55 ± 0.77 MPa; and (4), after soaking the samples in an SBF for 14 days, the Na−HA-coated carbon/carbon composites can rapidly induce bone-like apatite nucleation and growth on its surface in SBF, suggesting that the Na−HA coating might be an effective method to improve the surface bioactivity and biocompatibility of carbon/carbon composites.

Silicon-substituted HA was prepared and was coated on Ti substrate via a magnetron co-sputtering technique, and coated surfaces were subjected to an in vitro study using primary human osteoblast cells to evaluate their biological property (Thian et al., 2011). It was reported that (1) although human osteoblast cells showed initial poor adhesion and spreading on hydrophobic Ti surface, Si-incorporated HA coatings on Ti substrates render the surface more hydrophilic, with water contact angles between 30 and 40°; (2) human osteoblast cells attached, spread, and proliferated well on these coatings; (3) enhanced calcification (formation of calcium phosphate nodules across the collagenous matrices) was observed on Si−HA coatings with increasing Si content, suggesting that Si-incorporation into HA structure enhances the surface wettability and promotes cell proliferation and calcification. Guo et al. (2009) investigated the physicochemical properties and biocompatibilities of La-containing apatites with the formula $La_2Ca_8(PO_4)_6O_2$ as the typical one. It was reported that the sintered La-incorporated apatite block achieves a maximal flexure strength of 66.69 ± 0.98 MPa at 5% La content with 320% increase when compared with the La-free apatite, suggesting that the La-incorporated apatite possesses application potential in developing a new type of bioactive coating material for metal implants and also as a promising La carrier for further exploring the beneficial functions of La in the human body. Strontium (Sr)-substituted HA was prepared with 10 mol% Ca^{2+} replaced by Sr^{2+}, and the implant fixation in ovariectomized rats was investigated after

Sr−HA was coated on Ti implant by the sol−gel dip methods (Li et al., 2010). It was reported that (1) Sr−HA-coated implants revealed improved osseointegration compared to HA, with the bone area ratio and bone-to-implant contact increased by 70.9% and 49.9%, respectively, in histomorphometry; (2) the bone volume ratio and percent osseointegration increased by 73.7% and 45.2%, respectively, in micro-computed tomography evaluation; and (3) the maximal push-out force and ultimate shear strength increased by 107.2% and 132.9%, respectively in a push-out test, suggesting that the feasibility of using Sr−HA coatings to improve implant fixation in osteoporotic bone. Similarly, Sr−HA was also coated on Mg−Sr (with Sr in the range of 0.3−2.5%) (Bornapour et al., 2013).

HA-based composites are also prepared. Ji et al. (2012) prepared HA-carbon nanotube/titania double layer and coated it on titanium substrates intended for biomedical applications, reporting that the composite HA coating promoted the adhesion of preosteoblasts and the unique surfaces combined with the osteoconductive properties of HA exhibited the excellent mechanical properties. A double coating layer of the first thin precoating made with polyalkoxysilanes was prepared to promote the adhesion of HA/polyalkoxysilanes composite second layer (Damia et al., 2006). Furthermore, HA was admixed with tri-calcium phosphate with a Ca/P molar ratio from 1.56 to 1.77 (Tkalcec et al., 2001), with TiO_2 with bonding strength between HA coating and substrate of 27.2 ± 1.6 MPa (Wang et al., 2011a) and ZrO_2 (Chou and Chang, 2003).

Biocompatible calcium phosphate (Ca−P) has been widely used as a coating material for improving the substrate's biocompatibility. Ca−P was coated on CpTi substrates (Junker et al., 2010; Leem and Lim, 2010; Ribeiro et al., 2013; Zhang et al., 2010) and various Ti-based alloys, including Ti−6Al−4V (Durdu et al., 2013; Paital et al., 2011; Symietz et al., 2011), Ti−7.5Mo alloy (Hsu et al., 2010) and Ti−3Zr−2Sn−3Mo−25Nb (Yu et al., 2011). Uniquely, Wang et al. (1999) prepared functionally graded bioceramic coating composed of essentially calcium phosphate compounds. It was expected that the coating was graded in accordance with adhesive strength, bioactivity, and bioresorbability; i.e., the bond coat on the Ti-6Al-4V substrate is deposited with a particle range of the HA that provides a high adhesive strength and bioactivity, but has poor bioresorption properties; while the top coat is composed of predominantly α-TCP that is highly bioresorbable. Chen et al. (2011) used electrochemically deposited dicalcium phosphate dihydrate coating of a porous substrate on CpTi implant surface and reported that Ca_2P coatings improve the extent of cancellous bone ingrowth in the early postoperative phase following uncemented arthroplasty.

Titanium substrate has been also coated with another type of Ca-containing species. Load-bearing Ti implants were coated with TCP (Lin et al., 2011a; Roy et al., 2008b). Ti was also coated with Ag−HA composite (Mo et al., 2008) or TCP doped by Mg element in the form of $Ca_{2.8}Mn_{0.2}(PO_4)_2$ (Sima et al., 2007). Ti−6Al−4V alloy was coated with bioactive calcium alkali phosphate (Symietz et al., 2011), Ca_2SiO_4 (Mirhosseini et al., 2007), $CaTiSiO_5$ (sphene) (Wu et al., 2008), $TiO_2 + CaP$ compound (Ng et al., 2005), corrosion-resistant zeolite (aluminosilicate) for eliminating the release of cytotoxic Al and V ions (Bedi et al., 2009), or ceramics treated in $K_4ZrF_6-H_3PO_4$ and $NaAlO_2-Na_3PO_4$ solutions (Yao et al., 2008).

Bioglass should be included in this group as biocompatible coating material. CpTi and Ti-based alloys were coated with bioglass; two-phase ($\alpha + \beta$) Ti−6Al−7Nb titanium alloy was coated with a composite polyetheretherketone (PEEK) + bioglass (Moskalewicz et al., 2013), and Ti−6Al−4V was coated with bioactive borate glass comprising a $Na_2O-CaO-B_2O_3$ system, modified by additions of SiO_2, Al_2O_3, and P_2O_5 with adhesive strengths of 36 ± 2 MPa (Peddi et al., 2008), or alkali-free bioglass thin films with the highest mean value of pull-out adherence (60.3 ± 4.6 MPa) (Stan et al., 2013).

10.5.6 Composites, hybrids, functional gradient materials, and biomimetic materials

There are a huge number of papers published on HA-based biocompatible composites. HA−TiO_2 composites (Lee, 2012; Lima et al., 2010; Montazeri et al., 2010; Sarao et al., 2012) and HA−ZrO_2 composites (Evis et al., 2005; Evis and Doremus, 2007) were prepared. Moreover, HA−glass composites (Lee et al., 2006; Tanaskovic et al., 2007), HA−carbon composites (Facca et al., 2011; Pei et al., 2011), and HA−Wollastonite ($CaSiO_3$) composites (Lin et al., 2011b; Pattanayak et al., 2006) were also produced. To enhance the hard tissue biocompatibility and excellent osteoconductivity, HA was admixed with chitosan (Pang and Zhitomirsky, 2009; Rath et al., 2012). To improve bioactivity, the initial cell proliferation, and finally the osseointegration, HA has been also incorporated with collagen (Sugata et al., 2011; Xia et al., 2012; Yang et al., 2011). For promoting implant osseointegration or bone tissue engineering, biomimetic coating materials were introduced, e.g., HA−amelogenin composite (Du et al., 2005) and HA−fibronectin (Wang et al., 2010).

Titania (TiO_2) has been admixed/incorporated with Zn element (Zhang et al., 2012a), Ag element (Dastjerdi et al., 2010), carbon (Cho et al., 2008; Yang and Lu, 2013), $CaTiSiO_5$ (sphene) (Cheng et al., 2011), SiO_2 (Wang et al., 2013), and $CaSiO_3$ (Hu et al., 2013). Similarly, zirconia (ZrO_2) is admixed with Ca−P (Pardun et al., 2013) or with poly-pyrrole (Kumar and Rajendran, 2012) for improving corrosion resistance and biocompatibility. As nitride composites, there are reports on AlN−SiO_2 (Gazia et al., 2011) and TiN−carbon composites (Sokołowska et al., 2005).

Other metallic oxide composites are also prepared. Gurappa (2002) deposited a mixture of alumina, magnesia-stabilized zirconia, and yttria-stabilized zirconia with different thicknesses on 316L stainless steel substrate by the air plasma-spray technique to improve corrosion resistance. Dense and ultrafine alumina−zirconia composites (Al_2O_3−16 wt%ZrO_2 and ZrO_2−20 wt%Al_2O_3) were prepared to enhance the bioactivity (Martorana et al., 2009). Nelson et al. (2011) deposited a mixture of powders of titanium alloy (Ti−6Al−4V) and bioactive glass by flame spraying to fabricate composite porous coatings for potential use in bone fixation implants. After immersing samples in SBF, it was reported that HA was found on the bioactive glass−alloy composite coatings after 7 days of immersion, while no HA was observed after 14 days on the pure titanium alloy control coating. Balasubramanian et al. (2012) prepared nanocomposite Ti−Si−N coatings by reactive dc magnetron sputtering in a mixture of Ar and N_2 gases and deposited the composite on implantable 316L stainless

steel substrates. It was reported that theta−Si−N nanocomposite coatings exhibited superior corrosion resistance compared with the Si_3N_4, TiN single layer, and the bare substrate in SBF solution.

With an attempt of achieving faster osseointegration to hasten the overall treatment process, the use of biomimetic agents represents a growing area of research in implant dentistry. Major biomimetic agents should include (1) biocompatible ceramics, (2) bioactive agents, (3) ions, and (4) polymers, and their respective importance in the early stages of osseointegration. The potential bioactive agents include bone morphogenetic proteins, growth factors, type-I collagen, RGD peptide, fluoride, or chitosan, among others. The ideal characteristics that biomimetic agents should uphold and factors that may influence their effectiveness are reviewed by Avila et al. (2009). It was pointed out that (1) some of these agents, such as bioceramics (calcium phosphate salts) or ions (fluoride) are already commercially available and have shown clinical success; (2) others such as bone morphogenetic proteins are promising, with an excellent therapeutic potential; and (3) a specific implant surface coating may enhance the percentage of bone-to-implant contact and speed of osseointegration that allows clinicians to overcome many challenging clinical scenarios. In implantology, in particular dental implants, the increased demand on implant performance and the broadened treatment indications have led to the development of new moderately rough surfaces and alterations in both the surface chemistry and topography for chemical influences on bone tissue (or bioactivity) (Åstrand et al., 2008; Bougas et al., 2012; Jemt, 2008). Furthermore, surface alterations should include manipulations for surface energy, surface wettability, cellular maturation state, nutrition status, and micro-stresses that alter the degree of bioactivity (Jemt, 2008). It was reported that implant roughness promotes bacterial colonization (Fröjd et al., 2011). To enhance bone formation, implants have been coated with bone-specific biomolecules (Abtahi et al., 2012; Thorey et al., 2011).

He et al. (2008) reported on the pretreatment of the metal surface and comparison of the efficacy of three treatments for the binding ability of collagen and chitosan. The compound of collagen and chitosan was immobilized on the titanium oxide, and the morphology and chemical composition were used to characterize the titanium surfaces by scanning electron microscope and X-ray photoelectron spectrometry. The results showed that the surface displayed irregularities after roughness treatments, and the rough surface was beneficial to the adsorption and attachment of collagen and chitosan. Collagen is a highly versatile material, extensively used in the medical, dental, and pharmacological fields. Resorbable forms of collagen have been used to dress oral wounds, for closure of graft and extraction sites, and to promote healing. Collagen-based membranes also have been used in periodontal and implant therapy as barriers to prevent epithelial migration and allow cells with regenerative capacity to repopulate the defect area (Patino et al., 2002). In particular, collagen type-I is a major component of the extracellular matrix of most tissues, and it is increasingly used for surface engineering of biomaterials to accelerate receptor-mediated cell adhesion (Müller et al., 2006). Collagen was coated on Ti-based (Morra et al., 2003; Rammelt et al., 2006) and Co-based biomaterials or stainless steel (Müller et al., 2005), suggesting that collagen coating can enhance the rate of bone healing and increase new bone

formation at the implant surface. Collagen was even coated on poly(DL-lactide-co-glycolide) fibers (Glattauer et al., 2012) and TiO_x surface oxide layer (Yang et al., 2009a). Recently, Schulz et al. (2014) coated dental implants with components of the extracellular matrix and found that it was a promising approach to enhance osseointegration in compromised peri-implant bone.

Fibronectin functions in cell adhesion, migration, survival, proliferation, and differentiation as well as tissue organization and interacts with other biomolecules, such as collagen, proteoglycan, heparin, hyaluronic acid, fibrin/fibrinogen, plasmin, gangliosides, complement components, and also integral proteins of cell plasma membrane-integrins, as well as with itself (Elias et al., 2012; Miyamoto et al., 1998). Fibronectin was coated on Ti surface (Elias et al., 2012; Petrie et al., 2008) and the porous TiO_2/perlite composite (Erli et al., 2006; von Walter et al., 2005), and fibronectin coating improved cellular spreading and enhanced the tissue ingrowth.

Immobilization of bone morphogenetic proteins as growth factor onto material surfaces is promising, because these proteins can accelerate and enhance the quality of osseointegration (Haruyama et al., 2005; Simon et al., 2006). Protein was coated on Ti substrate (Cai et al., 2005; Guillot et al., 2013; Nayak et al., 2013) and on Ti−6Al−4V (Guillot et al., 2013). Fe−Pd-based ferromagnetic shape memory actuators for medical applications were also coated with protein (Allenstein et al., 2013). Covalently bound recombinant human tropoelastin as a major regulator of vascular cells in vivo was prepared to enhance endothelial cell interactions, suggesting that such coating for metal alloys with multifaceted biocompatibility can resist delamination and is nonthrombogenic, with implications for improving coronary stent efficacy (Waterhouse et al., 2010).

Prevention of bacterial colonization and formation of a bacterial biofilm on implant surfaces has been a challenge in orthopedic surgery (Kazemzadeh-Narbat et al., 2013). The antimicrobial peptide was coated on Ti biomaterials (Meyers et al., 2009; Werner et al., 2009; Yazici et al., 2013), suggesting that the integration of soft tissue on titanium dental implants was improved by significantly protecting implants from peri-implant inflammation and enhancing long-term implant stabilization. Similarly, for the prevention of the peri-implant infection in orthopedics, Ca−P-coated titanium surface was coated with the peptide (Kazemzadeh-Narbat et al., 2010). To prevent the unwanted infection on and around titanium implants, antibacterial coatings were performed on titanium implants (Busscher et al., 2010; Zhao et al., 2009). Reyes et al. (2007) coated a titanium implant surface with glycine-phenylalanine-hydroxyproline-glycine-glutamate-arginine collagen-mimetic peptide to improve osseointegration and reported that a biologically active and clinically relevant implant-coating that enhances bone repair and orthopedic implant integration was developed. Chitosan is the deacetylated derivative of the natural polysaccharide, chitin. Chitosan has been shown to be biocompatible, biodegradable, and osteoconductive and to accelerate wound healing (Darder et al., 2012; Leedy et al., 2011). Ti was coated with chitosan to promote osteointegration (Bumgardner et al., 2007).

Frosch et al. (2006) coated titanium implant surfaces with stem cell to evaluate the partial surface replacement of the knee and to provide a basis for a successful treatment

of large osteochondral defects, indicating that a partial joint resurfacing of the knee with stem cell-coated titanium implants occur. Similarly, the stem cell was coated to functionalized titanium films, reporting that stemcell-coated titanium films are beneficial for sustained in situ inducing osteoprogenitor cells to differentiate into mature osteoblasts over a long time (Hu et al., 2009). Achneck et al. (2011) evaluated the viability and adherence of peripheral blood-derived porcine endothelial progenitor cells on thin Ti layers and reported that (1) peripheral blood-derived cells adhere and function normally on Ti surfaces; and (2) the cells may be used to seed cardiovascular devices prior to implantation to ameliorate platelet activation and thrombus formation. Moreover, electrochemically functionalized Ti-alloy surfaces were coated with a cell specific aptamer to enhance the cell adhesion and by aptamer-based capture molecules on cell adhesion (Guo et al., 2007).

10.6 Future trends

Development of materials for manufacturing of the biomedical implants in medicine biomaterials (metals and alloys, polymers, ceramics, and hybrids and composites) is directly determined by the characteristics and nature of the tissue, organs, and systems that are being replaced or supplemented (Zivić et al., 2010). The application of biomaterials requires knowledge of their complex nature and different variables in regard to biocompatibility, corrosion behavior, mechanical characteristics, stability, and durability in an aggressive environment, wear mechanisms and wear rates during exploitation, and many others (Goodman et al., 2013). Additive manufacturing technologies, rapid manufacturing, rapid prototyping, three-dimensional printing, and nanotechnology are general terms that describe a variety of methods used to directly fabricate physical objects (three-dimensional models and end-use products) from electronic CAD data. Biologic coatings have been incorporated into orthopedic implants to modulate the surrounding biological environment. While many of these coatings are still in the preclinical testing stage, bioengineers, material scientists, and surgeons continue to explore surface coatings as a means of improving the clinical outcome of patients undergoing orthopedic surgery. In this section, we will introduce newly developed biomaterials new structures, texturing methods, and technologies that are currently in use in the medical and dental fields or possess potential application.

In application of biomedical materials, particularly orthopedics and dental implantology areas, biomechanical compatibility is a sine-qua-non requirement between implant surface zone and receiving bone structure, so that stress-shielding and weak interfacial bond between the tissue and the implant can be eliminated. Recently, bone-like material (which should possess similar label of modulus of elasticity) has been developed in forms of porous materials (Bencharit et al., 2013; Chae et al., 2013), hybridization with more slight weight compounds, HA + ZrO_2 (Matsumoto et al., 2011) or TiO_2+PMMA (Khaled et al., 2007). These bone-like materials' rigidity allows for stress forces to be transmitted; with the new formation of bone cells, it also fosters healing of the implant. Consequently, stress can and should be applied to the

implant immediately after implant insertion. In addition to these porosity-controlled materials, there are several studies on different types of material nanotubes, including carbon nanotubes (Dong et al., 2013; Yang and Lu, 2013), titania nanotubes (Kowalski et al., 2013; Lei et al., 2010; Ma et al., 2012; Wang and Luo, 2011), zirconia nanotubes (Ma et al., 2012), Ti metal nanotubes (Choe, 2011; Grigorescu et al., 2013), and composite nanotubes (Chen et al., 2013b).

Material composed of multilayers, with each layer having unique characteristics, yet adjacent layers having some similarity, is called functionally gradient (or gradient function) material (FGM) (Oshida, 2007c). FGM had been developed as a potential implant material to replace titanium for its improved capability of initial osseointegration. The idea behind FGM dental implants is that their properties can be tailored in accordance with the biomechanical needs at different regions, adapting to its hosting bony tissues and therefore creating an improved overall integration and stability in the entire restoration. When putting FGM concept into an applicable structure (for example, orthopedic or dental implants), the core zone of the implant materials should be strong and rigid, while from core to case zone the mechanical properties (strength and rigidity) should be gradually reduced to reach the similar levels of bone structure. To achieve this realization, there are several newly developed coating and manufacturing technologies, such as three-dimensional bioprinting (Lembo, 2003; Sparrow, 2013), electrospinning (Aznar-Cervantes et al., 2012; Martins et al., 2008; Supaphol et al., 2012), advanced laser technology (Mangano et al., 2013; Ng et al., 2011; Schade et al., 2013; Xiao et al., 2013), atmospheric plasma treatment (Gotoh et al., 2012; Thomas and Mittal, 2013), friction stir welding (Çam, 2011; Li et al., 2013), or direct-write technique (Ringeisen et al., 2001). At the extreme outlayer of the FGM, several biomimetic functionalizations (Jung et al., 2013; Khatayevich et al., 2010; Laydi et al., 2013; Ravichandran et al., 2012; Ren et al., 2011; Sala et al., 2010; Tan et al., 2013) can be done to establish a perfect osseointegration at an early stage of treatment.

Although not directly relevant to the scope of this chapter, it is valuable to introduce the recently addressed issue of the time-depending aging process of biomedical materials. Suzuki et al. (2009) investigated the effect of UV light irradiation on rejuvenating the aged titanium, so that the original bioactivity can be regained. Fresh Ti, aged Ti, and UV-treated Ti were subjected to the test. It was reported that proliferation, alkaline phosphatase activity, and calcium deposition of the cells were substantially lower on the aged surfaces than on the fresh surfaces, while those on the UV-treated aged surfaces were higher than on the fresh surfaces, suggesting that the bioactivity of titanium surfaces degrades with time and that UV treatment of the aged surface increases the bioactivity over the level of the freshly prepared surface. It is, therefore, concluded that UV treatment overcomes time-related degrading bioactivity of titanium. Similar results are reported elsewhere (Att et al., 2009; Hori et al., 2010).

Despite the substantial contribution of titanium implants in the field of dental and orthopedic constructive therapy, there is a crucial unaddressed question of why bone−implant contact does not reach the ideal 100%. Lee and Ogawa (2012) introduced the recently reported time-dependent reduction in osteoconductivity and other biological capabilities of titanium since processing. This phenomenon is

defined as the biological aging of titanium and provides insight to significantly advance the understanding of osseointegration and to further improve implant surfaces in the future.

References

Abbasi, S., Golestani-Fard, F., Rezaie, H. R., & Mirhosseini, S. M. M. (2012). MAO-derived hydroxyapatite/TiO_2 nanostructured multi-layer coatings on titanium substrate. *Applied Surface Science, 261*, 37−42.

Abd El-Rahman, A. M., Maitz, M. F., Kassem, M. A., El-Hossary, F. M., Prokert, F., Reuther, H., et al. (2007). Surface improvement and biocompatibility of $TiAl_{24}Nb_{10}$ intermetallic alloy using rf plasma nitriding. *Applied Surface Science, 253*, 9067−9072.

Abdal-hay, A., Dewidar, M., & Lim, J. K. (2012). Biocorrosion behavior and cell viability of adhesive polymer coated magnesium based alloys for medical implants. *Applied Surface Science, 261*, 536−546.

Abtahi, J., Tengvall, P., & Aspenberg, P. (2012). A bisphosphonate-coating improves the fixation of metal implants in human bone: a randomized trial of dental implants. *Bone, 50*, 1148−1151.

Abukawa, H., Papadaki, M., Abulikemu, M., Leaf, J., Vacanti, J. P., Kaban, L. B., et al. (2006). The engineering of craniofacial tissues in the laboratory: a review of biomaterials for scaffolds and implant coatings. *Dental Clinics of North America, 50*, 205−216.

Achneck, H. E., Jamiolkowski, R. M., Jantzen, A. E., Haseltine, J. M., Lane, W. O., Huang, J. K., et al. (2011). The biocompatibility of titanium cardiovascular devices seeded with autologous blood-derived endothelial progenitor cells: EPC-seeded antithrombotic Ti Implants. *Biomaterials, 32*, 10−18.

Acik, I. O., Junolainen, A., Mikli, V., Danilson, M., & Krunks, M. (2009). Growth of ultra-thin TiO_2 films by spray pyrolysis on different substrates. *Applied Surface Science, 256*, 1391−1394.

Advincula, M., Fan, X., Lemons, J., & Advincula, R. (2005). Surface modification of surface sol-gel derived titanium oxide films by self-assembled monolayers (SAMs) and non-specific protein adsorption studies. *Colloids and Surfaces B: Biointerfaces, 42*, 29−43.

Ai, H., Jones, S. A., & Lvov, Y. M. (2003). Biomedical applications of electrostatic layer-by-layer nano-assembly of polymers, enzymes, and nanoparticles. *Cell Biochemistry and Biophysics, 39*, 23−43.

Ajami, E., & Aguey-Zinsou, K.-F. (2011). Formation of OTS self-assembled monolayers at chemically treated titanium surfaces. *Journal of Materials Science: Materials in Medicine, 22*, 1813−1824.

Allen, P. (1996). Titanium alloy development. *Advanced Materials and Processes, 154*, 35−37.

Allenstein, U., Ma, Y., Arabi-Hashemi, A., Zink, M., & Mayr, S. G. (2013). Fe−Pd based ferromagnetic shape memory actuators for medical applications: biocompatibility, effect of surface roughness and protein coatings. *Acta Biomaterialia, 9*, 5845−5853.

Anderson, J. M., & Langone, J. J. (1999). Issues and perspectives on the biocompatibility and immunotoxicity evaluation of implanted controlled release systems. *Journal of Controlled Release, 57*, 107−113.

Armitage, D. A., Mihoc, R., Tate, T. J., McPhail, D. S., Chater, R., Hobkirk, J. A., et al. (2007). The oxidation of calcium implanted titanium in water: a depth profiling study. *Applied Surface Science, 253*, 4085−4093.

Arnould, C., Volcke, C., Lamarque, C., Thiry, P. A., Delhalle, J., & Mekhalif, Z. (2009). Titanium modified with layer-by-layer sol-gel tantalum oxide and an organodiphosphonic acid: a coating for hydroxyapatite growth. *Journal of Colloid and Interface Science, 336*, 497−503.

Åstrand, P., Ahlqvist, J., Gunne, J., & Nilson, H. (2008). Implant treatment of patients with edentulous jaws: a 20-year follow-up. *Clinical Implant Dentistry and Related Research, 10*, 207−217.

Att, W., Hori, N., Takeuchi, M., Ouyang, J., Yang, Y., Anpo, M., et al. (2009). Time-dependent degradation of titanium osteoconductivity: an implication of biological aging of implant materials. *Biomaterials, 30*, 5352−5363.

Avila, G., Misch, K., Galindo-Moreno, P., & Wang, H.-L. (2009). Implant surface treatment using biomimetic agents. *Implant Dentistry, 18*, 17−26.

Azarmi, F. (2005). Vacuum plasma spraying. *Advanced Materials and Processes, 163*, 37−39.

Aznar-Cervantes, S., Roca, M. I., Martinez, J. G., Meseguer-Olmo, L., Cenis, J. L., Moraleda, J. M., et al. (2012). Fabrication of conductive electrospun silk fibroin scaffolds by coating with polypyrrole for biomedical applications. *Bioelectrochemistry, 85*, 36−43.

Bakhshi, R., Darbyshire, A., Evans, J. E., You, Z., Lu, J., & Seifalian, A. M. (2011). Polymeric coating of surface modified nitinol stent with POSS-nanocomposite polymer. *Colloids and Surfaces B: Biointerfaces, 86*, 93−105.

Balani, K., Anderson, R., Laha, T., Andara, M., Tercero, J., Crumpler, E., et al. (2007). Plasma-sprayed carbon nanotube reinforced hydroxyapatite coatings and their interaction with human osteoblasts in vitro. *Biomaterials, 28*, 618−624.

Balasubramanian, S., Ramadoss, A., Kobayashi, A., & Muthirulandi, J. (2012). Nanocomposite Ti−Si−N coatings deposited by reactive dc magnetron sputtering for biomedical applications. *Journal of the American Ceramic Society, 95*, 2746−2752.

Balla, V. K., Bhat, A., Bose, S., & Bandyopadhyay, A. (2012). Laser processed TiN reinforced Ti6Al4V composite coatings. *Journal of the Mechanical Behavior of Biomedical Materials, 6*, 9−20.

Balla, V. K., Bodhak, S., Bose, S., & Bandyopadhyay, A. (2010). Porous tantalum structures for bone implants: fabrication, mechanical and in vitro biological properties. *Acta Biomaterialia, 6*, 3349−3359.

Balla, V. K., Xue, W., Bose, S., & Bandyopadhyay, A. (2009). Laser-assisted Zr/ZrO_2 coating on Ti for load-bearing implants. *Acta Biomaterialia, 5*, 2800−2809.

Bandyopadhyay, A., Balla, V. K., Roy, M., & Bose, S. (2011). Laser surface modification of metallic biomaterials. *Journal of Metals, 63*, 94−99.

Bansiddhi, A., Sargeant, T. D., Stupp, S. I., & Dunand, D. C. (2008). Porous NiTi for bone implants: a review. *Acta Biomaterialia, 4*, 773−782.

Bazaka, K., Jacob, M. V., Crawford, R. J., & Ivanova, E. P. (2011). Plasma-assisted surface modification of organic biopolymers to prevent bacterial attachment. *Acta Biomaterialia, 7*, 2015−2028.

Bedi, R. S., Beving, D. E., Zanello, L. P., & Yan, Y. (2009). Biocompatibility of corrosion-resistant zeolite coatings for titanium alloy biomedical implants. *Acta Biomaterialia, 5*, 3265−3271.

Belverud, S., Mogilner, A., & Schulder, M. (2008). Intrathecal pumps. *Neurotherapeutics, 5*, 114−122.

Bencharit, S., Byrd, W. C., Altarawneh, S., Hosseini, B., Leong, A., Reside, G., Morelli, T., & Offenbacher, S. (2014). Development and applications of porous tantalum trabecular metal-enhanced titanium dental implants. *Clinical Implant Dentistry and Related Research, 16*, 817−826. http://dx.doi.org/10.1111/cid.12059.

Bornapour, M., Muja, N., Shum-Tim, D., Cerruti, M., & Pekguleryuz, M. (2013). Biocompatibility and biodegradability of Mg−Sr alloys: the formation of Sr-substituted hydroxyapatite. *Acta Biomaterialia, 9*, 5319−5330.

Bougas, K., Jimbo, R., Xue, Y., Mustafa, K., & Wennerberg, A. (2012). Novel implant coating agent promotes gene expression of osteogenic markers in rats during early osseointegration. *International Journal of Biomaterials, 2012*. http://dx.doi.org/10.1155/2012/579274.

Brama, M., Rhodes, N., Hunt, J., Ricci, A., Teghil, R., Migliaccio, S., et al. (2007). Effect of titanium carbide coating on the osseointegration response in vitro and in vivo. *Biomaterials, 28*, 595−608.

Brinker, C. J., Hurd, A. J., Shunrk, P. R., Frye, G. C., & Asley, C. S. (1992). Review of sol-gel thin film formation. *Journal of Non-Crystalline Solids, 147*, 424−436.

Bumgardner, J. D., Chesnutt, B. M., Yuan, Y., Yang, Y., Appleford, M., Oh, S., et al. (2007). The integration of chitosan-coated titanium in bone: an in vivo study in rabbits. *Implant Dentistry, 16*, 66−79.

Buser, D., Broggini, N., & Wieland, M. (2004). Enhanced bone apposition to a chemically modified SLA titanium surface. *Journal of Dental Research, 83*, 529−533.

Busscher, H. J., Rinastiti, M., Siswomihardjo, W., & van der Mei, H. C. (2010). Biofilm formation on dental restorative and implant materials. *Journal of Dental Research, 89*, 657−665.

Byeli, A. V., Kukareko, V. A., & Kononov, A. G. (2012). Titanium and zirconium based alloys modified by intensive plastic deformation and nitrogen ion implantation for biocompatible implants. *Journal of the Mechanical Behavior of Biomedical Materials, 6*, 89−94.

Byon, E., Moon, S., Cho, S.-B., Jeong, C.-Y., Jeong, Y., & Sul, Y.-T. (2005). Electrochemical property and apatite formation of metal ion implanted titanium for medical implants. *Surface and Coatings Technology, 200*, 1018−1021.

Cai, K., Rechtenbach, A., Hao, J., Bossert, J., & Jandt, K. D. (2005). Polysaccharide-protein surface modification of titanium via a layer-by-layer technique: characterization and cell behaviour aspects. *Biomaterials, 26*, 5960−5971.

Callahan, T. D., & Natale, A. (2008). Catheter ablation of atrial fibrillation. *Medical Clinics of North America, 92*, 179−201.

Çam, G. (2011). Friction stir welded structural materials: beyond Al-alloys. *International Materials Reviews, 56*, 1−48.

Cao, N., Dong, J., Wang, Q., Ma, Q., Xue, C., & Li, M. (2010). An experimental bone defect healing with hydroxyapatite coating plasma sprayed on carbon/carbon composite implants. *Surface and Coatings Technology, 205*, 1150−1156.

Carpene, E., Shinn, M., & Schaaf, P. (2005). Free-electron laser surface processing of titanium in nitrogen atmosphere. *Applied Surface Science, 247*, 307−312.

Chae, T., Yang, H., Leung, V., Ko, F., & Troczynski, T. (2013). Novel biomimetic hydroxyapatite/alginate nanocomposite fibrous scaffolds for bone tissue regeneration. *Journal of Materials Science: Materials in Medicine, 24*, 1885−1894.

Chen, D., Bertollo, N., Lau, A., Taki, N., Nishino, T., Mishima, H., et al. (2011). Osseointegration of porous titanium implants with and without electrochemically deposited DCPD coating in an ovine model. *Journal of Orthopaedic Surgery and Reserch, 6*. http://dx.doi.org/10.1186/1749−799X-6-56.

Chen, Y., Gao, Q., Wan, H., Yi, J., Wei, Y., & Liu, P. (2013a). Surface modification and biocompatible improvement of polystyrene film by Ar, O_2 and Ar + O_2 plasma. *Applied Surface Science, 265*, 452−457.

Chen, L., Hu, J., Shen, X., & Hua Tong, H. (2013b). Synthesis and characterization of chitosan−multiwalled carbon nanotubes/hydroxyapatite nanocomposites for bone tissue engineering. *Journal of Materials Science: Materials in Medicine, 24*, 1843−1851.

Chen, Y., Zheng, X., Xie, Y., Ji, H., & Ding, C. (2009). Antibacterial properties of vacuum plasma sprayed titanium coatings after chemical treatment. *Surface and Coatings Technology, 204*, 685−690.

Cheng, Y., Cai, W., Li, H. T., & Zheng, Y. F. (2006). Surface modification of NiTi alloy with tantalum to improve its biocompatibility and radiopacity. *Journal of Materials Science, 41*, 4961−4964.

Cheng, S., Wei, D., & Zhou, Y. (2011). Formation and structure of sphene/titania composite coatings on titanium formed by a hybrid technique of microarc oxidation and heat-treatment. *Applied Surface Science, 257*, 340−3411.

Cho, J., Schaab, S., Roether, J. A., & Boccaccini, A. R. (2008). Nanostructured carbon nanotube/TiO_2 composite coatings using electrophoretic deposition (EPD). *Journal of Nanoparticle Research, 10*, 99−105.

Choe, H.-C. (2011). Nanotubular surface and morphology of Ti-binary and Ti-ternary alloys for biocompatibility. *Thin Solid Films, 519*, 4652−4657.

Chou, B.-Y., & Chang, E. (2003). Influence of deposition temperature on mechanical properties of plasma-sprayed hydroxyapatite coating on titanium alloy with ZrO_2 intermediate layer. *Journal of Thermal Spray Technology, 12*, 199−207.

Chrzanowski, W., Szade, J., Hart, A. D., Knowles, J. C., & Dalby, M. J. (2012). Biocompatible, smooth, plasma-treated nickel−titanium surface—an adequate platform for cell growth. *Journal of Biomaterials Applications, 26*, 707−731.

Chu, P. K. (2010). Recent applications of plasma-based ion implantation and deposition to microelectronic, nano-structured, and biomedical materials. *Surface and Coatings Technology, 204*, 2853−2863.

Chung, K. H., Liu, G. T., Duh, J. G., & Wang, J. H. (2004). Biocompatibility of a titanium-aluminum nitride film coating on a dental alloy. *Surface and Coatings Technology, 188/189*, 745−749.

Coelho, P. G., Giro, G., Teixeira, H. S., Marin, C., Witek, L., Thompson, V. P., et al. (2012). Argon-based atmospheric pressure plasma enhances early bone response to rough titanium surfaces. *Journal of Biomedical Materials Research Part A, 100*, 1901−1906.

Corina, B., & Felicia, S. (2008). About the tribological behavior of ceramic materials. *Tribology in Industry, 30*, 10−14.

Czarnowska, E., Wierzchoń, T., & Maranda-Niedbała, A. (1999). Properties of the surface layers on titanium alloy and their biocompatibility in vitro tests. *Journal of Materials Processing Technology, 92/93*, 190−194.

Dahortre, S. N., Vora, H. D., Pavani, K., & Banerjee, R. (2013). An integrated experimental and computational approach to laser surface nitriding of Ti-6Al-4V. *Applied Surface Science, 271*, 141−148.

Damia, C., Sarda, S., Deydier, E., & Sharrock, P. (2006). Study of two hydroxyapatite/poly (alkoxysilane) implant coatings. *Surface and Coatings Technology, 201*, 3008−3015.

Darder, M., Aranda, P., & Eduardo Ruiz-Hitzky, E. (2012). Chitosan-clay bio-nanocomposites. In L. Avérous, & E. Pollet (Eds.), *Environmental silicate nano-biocomposites* (pp. 365−391). London: Springer-Verlag.

Dastjerdi, R., Montazer, M., & Shahsavan, S. (2010). A novel technique for producing durable multifunctional textiles using nanocomposite coating. *Colloids and Surfaces B: Biointerfaces, 81*, 32−41.

Devine, D. M., Hahn, J., Richards, R. G., Gruner, H., Wieling, R., & Pearce, S. G. (2013). Coating of carbon fiber-reinforced polyetheretherketone implants with titanium to improve bone apposition. *Journal of Biomedical Materials Research Part B, 101B*, 591−598.

Dewidar, M. M., & Lim, J. K. (2008). Properties of solid core and porous surface Ti-6Al-4V implants manufactured by powder metallurgy. *Journal of Alloys and Compounds, 454*, 442−446.

Dolatshahi-Pirouz, A., Jensen, T., Kraft, D. C., Foss, M., Kingshott, P., Hansen, J. L., et al. (2010). Fibronectin adsorption, cell adhesion, and proliferation on nanostructured tantalum surfaces. *ACS Nano, 4*, 2874−2882.

Dong, C., Campell, A. S., Eldawud, R., Perhinschi, G., Rojanasakul, Y., & Dinu, C. Z. (2013). Effects of acid treatment on structure, properties and biocompatibility of carbon nanotubes. *Applied Surface Science, 264*, 261−268.

Dorfman, M. R. (2002). Thermal spray—basics. *Advanced Materials and Processes, 160*, 47−50.

Drnovšek, N., Daneu, N., Rečnik, A., Mazaj, M., Kovač, J., & Novak, S. (2009). Hydrothermal synthesis of a nanocrystalline anatase layer on Ti6A4V implants. *Surface and Coatings Technology, 203*, 1462−1468.

Du, C., Schneider, G. B., Zaharias, R., Abbott, C., Seabold, D., Stanford, C., et al. (2005). Apatite/amelogenin coating on titanium promotes osteogenic gene expression. *Journal of Dental Research, 84*, 1070−1074.

Durán, A., Castro, Y., Aparicio, M., Conde, A., & de Damborenea, J. J. (2007). Protection and surface modification of metals with sol-gel coatings. *International Materials Reviews, 52*, 175−192.

Durdu, S., Deniz, Ö. F., Kutbay, I., & Usta, M. (2013). Characterization and formation of hydroxyapatite on Ti6Al4V coated by plasma electrolytic oxidation. *Journal of Alloys and Compounds, 551*, 422−429.

Duta, L., Oktar, F. N., Stan, G. E., Popescu-Pelin, G., Serban, N., Luculescu, C., et al. (2013). Novel doped hydroxyapatite thin films obtained by pulsed laser deposition. *Applied Surface Science, 265*, 41−49.

Dutta-Mazumdar, J., & Manna, I. (2011). Laser material processing. *International Materials Reviews, 56*, 341−388.

Duty, C., Jean, D., & Lackey, W. J. (2001). Laser chemical vapour deposition: materials, modelling, and process control. *International Materials Reviews, 46*, 271−287.

Elias, C. N., Gravina, P. A., de Filho, C. S., & Pedro Augusto de Paula Nascente, P. A. (2012). Preparation of bioactive titanium surfaces via fluoride and fibronectin retention. *International Journal of Biomaterials, 2012*. http://dx.doi.org/10.1155/2012/290179.

Elias, C. N., Oshida, Y., Lima, J. H. C., & Muller, C. A. (2008). Relationship between surface properties (roughness, wettability and morphology) of titanium and dental implant removal torque. *Journal of the Mechanical Behavior of Biomedical Materials, 1*, 234−242.

Erli, H.-J., Rüger, M., Ragoß, C., Jahnen-Dechent, W., Hollander, D. A., Paar, O., et al. (2006). The effect of surface modification of a porous TiO_2/perlite composite on the ingrowth of bone tissue in vivo. *Biomaterials, 27*, 1270−1276.

Evis, Z., & Doremus, R. H. (2007). Hot-pressed hydroxyapatite/monoclinic zirconia composites with improved mechanical properties. *Journal of Materials Science, 42*, 2426−2431.

Evis, Z., Ergun, C., & Doremus, R. H. (2005). Hydroxyapatite-zirconia composites: thermal stability of phases and sinterability as related to the Cao-ZrO_2 phase diagram. *Journal of Materials Science, 40*, 127−1134.

Ezz, T., Crouse, P., Li, L., & Liu, Z. (2007). Synthesis of TiN thin films by a new combined laser/sol−gel processing technique. *Applied Surface Science, 253*, 7903−7907.

Facca, S., Lahiri, D., Fioretti, F., Messadeq, N., Mainard, D., Benkirane-Jessel, N., et al. (2011). Invivo osseointegration of nano-designed composite coatings on titanium implants. *ACS Nano, 5*, 4790−4799.

Fallah, V., Corbin, S. F., & Khajepour, A. (2010). Process optimization of Ti-Nb alloy coatings on a Ti-6Al-4V plate using a fiber laser and blended elemental powders. *Journal of Materials Processing Technology, 210*, 2081−2087.

Fan, X., Feng, B., Di, Y., Lu, X., Duan, K., Wang, J., et al. (2012). Preparation of bioactive TiO film on porous titanium by micro-arc oxidation. *Applied Surface Science, 258*, 7584−7588.

Fine, D. M., & Tobias, A. H. (2007). Cardiovascular device infections in dogs: report of 8 cases and review of the literature. *Journal of Veterinary Internal Medicine, 21*, 1265−1271.

Firouzi-Arani, M., Savaloni, H., & Ghoranneviss, M. (2010). Dependence of surface nanostructural modifications of Ti implanted by N^+ ions on temperature. *Applied Surface Science, 256*, 4502−4511.

Flores, M., Huerta, L., Escamilla, R., Andrade, E., & Muhl, S. (2007). Effect of substrate bias voltage on corrosion of TiN/Ti multilayers deposited by magnetron sputtering. *Applied Surface Science, 253*, 7192−7196.

Foest, R., Schmidt, M., & Becker, K. (2006). Microplasmas, an emerging field of low-temperature plasma science and technology. *International Journal of Mass Spectrometry, 248*, 87−102.

Fomin, A. A., Steinhauer, A. B., Lyasnikov, V. N., Wenig, S. B., & Zakharevich, A. M. (2012). Nanocrystalline structure of the surface layer of plasma-sprayed hydroxyapatite coatings obtained upon preliminary induction heat treatment of metal base. *Technical Physics Letters, 38*, 481−483.

Fouquet, V., Pichon, L., Drouet, M., & Sraboni, A. (2004). Plasma assisted nitridation of Ti-6Al-4V. *Applied Surface Science, 221*, 248−258.

Frazier, O. H., & Jacob, L. P. (2007). Small pumps for ventricular assistance: progress in mechanical circulatory support. *Cardiology Clinics, 25*, 553−564.

Freeman, C. O., & Brook, I. M. (2006). Bone response to a titanium aluminium nitride coating on metallic implants. *Journal of Materials Science: Materials in Medicine, 17*, 465−470.

Fröjd, V., de Paz, L. C., Andersson, M., Wennerberg, A., Davies, J. R., & Svensäter, G. (2011). In situ analysis of multispecies biofilm formation on customized titanium surfaces. *Molecular Oral Microbiology, 26*, 241−252.

Frosch, K.-H., Drengk, A., Krause, P., Viereck, V., Miosge, N., Werner, C., et al. (2006). Stem cell-coated titanium implants for the partial joint resurfacing of the knee. *Biomaterials, 27*, 2542−2549.

Fu, T., Liu, B. G., Zhou, Y. M., & Wu, X. M. (2011). Sol-gel titania coating on NiTi alloy with a porous titania film as interlayer. *Journal of Sol-Gel Science and Technology, 58*, 307−311.

Fu, Y., Yan, B., Loh, N. L., Sun, C. O., & Hing, P. (1999). Deposition of diamond coating on pure titanium using micro-wave plasma assisted chemical vapor deposition. *Journal of Materials Science, 34*, 2269−2283.

Fuchs, T., Schmidmaier, G., Raschke, M. J., & Stange, R. (2008). Bioactive-coated implants in trauma surgery. *European Journal of Trauma and Emergency Surgery, 34*, 60−68.

Gallardo-Moreno, A. M., Multigner, M., Calzado-Martín, A., Méndez-Vilas, A., Saldaña, L., Galván, J. C., et al. (2011). Bacterial adhesion reduction on a biocompatible Si^+ ion implanted austenitic stainless steel. *Materials Science and Engineering: C, 31*, 1567−1576.

Gan, J., Tan, L., Yang, K., Hu, Z., Zhang, Q., Fan, X., et al. (2013). Bioactive Ca-P coating with self-sealing structure on pure magnesium. *Journal of Materials Science: Materials in Medicine, 24*, 889−901.

García, G. L., Hernández, T. J., Flores, R. N., Argumedo, M. P., López, V. A., Araujo, L. D. J., et al. (2013). Influence of nitrogen in TiAlNO coatings fabricated by co-sputtering. *IOP Conference Series: Materials Science and Engineering, 45*. http://dx.doi.org/10.1088/1757−899X/45/1/012024.

Gazia, R., Mandracci, P., Mussano, F., & Stefano Carossa, S. (2011). AlN_x and a-SiO_x coatings with corrosion resistance properties for dental implants. *Surface and Coatings Technology, 206*, 1109−1115.

Glattauer, V., Briggs, K. L., Zappe, S., Ramshaw, J. A. M., & Truong, Y. B. (2012). Collagen-based layer-by-layer coating on electrospun polymer scaffolds. *Biomaterials, 33*, 9198−9204.

Gomes, M. E., & Reis, R. L. (2004a). Biodegradable polymers and composites in biomedical applications: from catgut to tissue engineering. Part 1: available systems and their properties. *International Materials Reviews, 49*, 261−273.

Gomes, M. E., & Reis, R. L. (2004b). Biodegradable polymers and composites in biomedical applications: from catgut to tissue engineering. Part 2: systems for temporary replacement and advanced tissue regeneration. *International Materials Reviews, 49*, 274−285.

Goodman, S. B., Yao, Z., Keeney, M., & Yang, F. (2013). The future of biologic coatings for orthopaedic implants. *Biomaterials, 34*, 3174−3183.

Gopi, D., Indira, J., Kavitha, L., & Ferreira, J. M. F. (2013). Hydroxyapatite coating on selectively passivated and sensitively polymer-protected surgical grade stainless steel. *Journal of Applied Electrochemistry, 43*, 331−345.

Gordin, D. M., Gloriant, T., Chane-Pane, V., Busardo, D., Mitran, V., Höche, D., et al. (2012). Surface characterization and biocompatibility of titanium alloys implanted with nitrogen by Hardion+ technology. *Journal of Materials Science: Materilas in Medicine, 23*, 2953−2966.

Gotoh, K., Yasukawa, A., & Tanuguchi, K. (2012). Water contact angles on poly(ethylene terephthalate) films exposed to atmospheric pressure plasma. *Journal of Adhesion Science and Technology, 25*, 307−322.

Grigorescu, S., Carradò, A., Ulhaq, C., Faerber, J., Ristoscu, C., Dorcioman, G., et al. (2007). Study of the gradual interface between hydroxyapatite thin films PLD grown onto Ti-controlled sublayers. *Applied Surface Science, 254*, 1150−1154.

Grigorescu, S., Ungureanu, C., Kirchgeorg, R., Schmuki, P., & Demetrescu, I. (2013). Various sized nanotubes on TiZr for antibacterial surfaces. *Applied Surface Science, 270*, 190−196.

Gu, D. D., Meiners, W., Wissenbach, K., & Poprawe, R. (2012). Laser additive manufacturing of metallic components: materials, processes and mechanisms. *International Materials Reviews, 57*, 133−164.

Guillot, R., Gilde, F., Becquart, P., Sailhan, F., Lapeyrere, A., Logeart-Avramoglou, D., et al. (2013). The stability of BMP loaded polyelectrolyte multilayer coatings on titanium. *Biomaterials, 34*, 5737−5746.

Guo, K.-T., Scharnweber, D., Schwenzer, B., Ziemer, G., & Wendel, H. P. (2007). The effect of electrochemical functionalization of Ti-alloy surfaces by aptamer-based capture molecules on cell adhesion. *Biomaterials, 28*, 468−474.

Guo, C. Y., Tang, A. T. H., & Jukka Pekka Matinlinna, J. P. (2012). Insights into surface treatment methods of titanium dental implants. *Journal of Adhesion Science and Technology, 26*, 189−205.

Guo, D. G., Wang, A. H., Han, Y., & Xu, K. W. (2009). Characterization, physicochemical properties and biocompatibility of La-incorporated apatites. *Acta Biomaterialia, 5*, 3512−3523.

Gupta, D. (2011). Plasma immersion ion implantation (PIII) process—physics and technology. *International Journal of Advanced Manufacturing Technology, 2*, 471−490.

Gurappa, I. (2002). Development of appropriate thickness ceramic coatings on 316 L stainless steel for biomedical applications. *Surface and Coatings Technology, 161*, 70−78.

Guslitzer-Okner, R., & Mandler, D. (2011). Applications of electrochemistry and nanotechnology in biology and medicine, I: electrochemical coating of medical implants. *Modern Aspects of Electrochemistry, 52*, 291−342.

Hahn, B.-D., Park, D.-S., Choi, J.-J., Ryu, J., Yoon, W.-H., Kim, K.-H., et al. (2009). Dense nanostructured hydroxyapatite coating on titanium by aerosol deposition. *Journal of the American Ceramic Society, 92*, 68−687.

Hallab, N., Merritt, K., & Jacobs, J. J. (2001). Metal sensitivity in patients with orthopaedic implants. *Journal of Bone and Joint Surgery American Volume, 83*, 428−438.

Hang, R., Huang, X., Tian, L., He, Z., & Tang, B. (2012). Preparation, characterization, corrosion behavior and bioactivity of Ni_2O_3-doped TiO_2 nanotubes on NiTi alloy. *Electrochimica Acta, 70*, 382−393.

Haruyama, T., Sakai, T., & Matsuno, K. (2005). Protein layer coating method on metal surface by electrochemical process through genetical introduced tag. *Biomaterials, 26*, 4944−4947.

He, H. W., Liu, M. L., Zhu, Z. L., Yang, M. Z., Li, Q. L., & Chen, Z. Q. (2008). Influence of surface morphology of cpTi on the adsorption and attachment of collagen/chitosan. *Applied Surface Science, 255*, 509−511.

Hirai, S., Nishinaka, K., Shimakage, K., Uo, M., & Watari, F. (2004). Hydroxyapatite coating on titanium substrate by the sol-gel; process. *Journal of the American Ceramic Society, 87*, 29−34.

Höche, D., Rapin, G., & Schaaf, P. (2007). FEM simulation of the laser plasma interaction during laser nitriding of titanium. *Applied Surface Science, 254*, 888−892.

Holinka, J., Pilz, M., Kubista, B., Presterl, E., & Windhager, R. (2013). Effects of selenium coating of orthopaedic implant surfaces on bacterial adherence and osteoblastic cell growth. *Bone & Joint Journal, 95*, 678−682.

Hori, N., Ueno, T., Suzuki, T., Yamada, M., Att, W., Okada, S., et al. (2010). Ultraviolet light treatment for the restoration of age-related degradation of titanium bioactivity. *International Journal of Oral & Maxillofacial Implants, 25*, 49−62.

Hsu, H.-C., Wu, S.-C., Fu, C.-É., & Ho, W.-F. (2010). Formation of calcium phosphates on low-moldulus Ti-7.5 Mo alloy by acid and alkali treatments. *Journal of Materials Science, 45*, 3661−3670.

Hu, Y., Cai, K., Luo, Z., Zhang, R., Yang, L., Deng, L., et al. (2009). Surface mediated *in situ* differentiation of mesenchymal stem cells on gene-functionalized titanium films fabricated by layer-by-layer technique. *Biomaterials, 30*, 3626−3635.

Hu, H., Qiao, Y., Meng, F., Liu, X., & Ding, C. (2013). Enhanced apatite-forming ability and cytocompatibility of porous and nanostructured TiO_2/$CaSiO_3$ coating on titanium. *Colloids and Surfaces B: Biointerfaces, 101*, 83−90.

Hu, X., Shen, H., Shuai, K., Zhang, E., Bai, Y., Cheng, Y., et al. (2011). Surface bioactivity modification of titanium by CO_2 plasma treatment and induction of hydroxyapatite: in vitro and in vivo studies. *Applied Surface Science, 257*, 1813−1823.

Huan, Z., Fratila-Apachitei, L. E., Apachitei, I., & Duszczyk, J. (2012). Porous NiTi surfaces for biomedical applications. *Applied Surface Science, 258*, 5244−5249.

Huang, F., Xie, B., Wu, B., Shao, L., Li, M., Wang, H., et al. (2009). Enhancing the crystallinity and surface roughness of sputtered TiO_2 thin film by ZnO underlayer. *Applied Surface Science, 255*, 6781−6785.

Hübler, R. (1999). Hardness and corrosion protection enhancement behaviour of surgical implant surfaces treated with ceramic thin films. *Surface and Coatings Technology, 116/119*, 1111−1115.

Hung, K.-Y., Lo, S.-C., Shih, C.-S., Yang, Y.-C., Feng, H.-P., & Lin, Y.-C. (2012). Titanium surface modified by hydroxyapatite coating for dental implants. *Surface and Coatings Technology, 231*, 337−345.

Hyde, G. K., McCullen, S. D., Jeon, S., Stewart, S. M., Jeon, H., Loboa, E. G., et al. (2009). Atomic layer deposition and biocompatibility of titanium nitride nano-coatings on cellulose fiber substrates. *Biomedical Materials, 4*. http://dx.doi.org/10.1088/1748−6041/4/2/025001.

Ishizawa, H., & Ogino, M. (1996). Thin hydroxyapatite layers formed on porous titanium using electrochemical and hydrothermal reaction. *Journal of Materials Science, 31*, 6279−6284.

Jacobs, T., Morent, R., De Geyter, N., Dubruel, P., & Leys, C. (2012). Plasma surface modification of biomedical polymers: influence on cell-material interaction. *Plasma Chemistry and Plasma Processing, 32*, 1039−1073.

Jemt, T. (2008). Single implants in the anterior maxilla after 15 years of follow-up: comparison with central implants in the edentulous maxilla. *International Journal of Prosthodontics, 21*, 400−408.

Jeong, Y.-H., Choe, H.-C., Brantley, W. A., & Sohn, I.-B. (2013). Hydroxyapatite thin film coatings on nanotube-formed Ti−35Nb−10Zr alloys after femtosecond laser texturing. *Surface and Coatings Technology, 217*, 13−22.

Ji, X., Lou, W., Wang, Q., Ma, J., Xu, H., Bai, Q., et al. (2012). Sol-gel- derived hydroxyapatite-carbon nanotube/titania coatings on titanium substrates. *International Journal of Molecular Sciences, 13*, 5242−5253.

Jung, G.-B., Kim, J.-H., Jin Sik Burm, J. S., & Park, H.-K. (2013). Fabrication of chitosan-silver nanoparticle hybrid 3D porous structure as a SERS substrate for biomedical applications. *Applied Surface Science, 273*, 179−183.

Junker, R., Manders, P. J. D., Wolke, J., Borisov, Y., Braceras, I., & Jansen, J. A. (2010). Loaded microplasma-sprayed CaP-coated implants in vivo. *Journal of Dental Research, 89*, 1489−1493.

Kado, T., Hidaka, T., Aita, H., Endo, K., & Furuichi, Y. (2012). Enhanced compatibility of chemically modified titanium surface with periodontal ligament cells. *Appled Surface Science, 262*, 240−247.

Kar, A., Raja, K. S., & Misra, M. (2006). Electrodeposition of hydroxyapatite onto nanotubular TiO_2 for implant applications. *Surface and Coatings Technology, 201*, 3723−3731.

Kazemzadeh-Narbat, M., Kindrachuk, J., Duan, K., Jenssen, H., Hancock, R. E. W., & Wang, R. (2010). Antimicrobial peptides on calcium phosphate-coated titanium for the prevention of implant-associated infections. *Biomaterials, 31*, 9519−9526.

Kazemzadeh-Narbat, M., Lai, B. F. L., Ding, C., Kizhakkedathu, J. N., Hancock, R. E. W., & Wang, R. (2013). Multilayered coating on titanium for controlled release of antimicrobial peptides for the prevention of implant-associated infections. *Biomaterials, 34*, 5969−5977.

Khaled, S. M., Sui, R., Charpentier, P. A., & Rizkalla, A. S. (2007). Synthesis of TiO_2−PMMA nanocomposite: using methacrylic acid as a coupling agent. *Langmuir, 23*, 3988−3995.

Khalid, H. M., Jauhari, I., & Dom, A. H. M. (2012). Development of nanolayer hydroxyapatite (HA) on titanium alloy *via* superplastic deformation method. *Metallurgical and Materials Transactions A, 43*, 3776−3785.

Khatayevich, D., Gungormus, M., Yazici, H., So, C., Cetinel, S., Ma, H., et al. (2010). Biofunctionalization of materials for implants using engineered peptides. *Acta Biomaterialia, 6*, 4634−4641.

Kipshidze, N. N., Tsapenko, M. V., Leon, M. B., Stone, G. W., & Moses, J. W. (2005). Update on drug-eluting coronary stents. *Expert Review of Cardiovascular Therapy, 3*, 953−968.

Kong, Y.-M., Bae, C.-J., Lee, S.-H., Kim, H.-W., & Kim, H.-E. (2005). Improvement in biocompatibility of by addition of HA. *Biomaterials, 26*, 509−517.

Koschwanez, H. E., & Reichert, W. M. (2007). In vitro, in vivo and post explantation testing of glucose-detecting biosensors: current methods and recommendations. *Biomaterials, 28*, 3687−3703.

Kovacs, P., & Davidson, J. A. (1996). Medical applications of titanium and its alloys: the material and biological issues. In S. A. Brown, & J. E. Lemons (Eds.), *Chemical, electrochemical aspects of the biocompatibility of titanium and its alloys* (pp. 163−165). Philadelphia, PA.

Kowalski, D., Kim, D., & Schmuki, P. (2013). TiO_2 nanotubes, nanochannels and mesosponge: self-organized formation and applications. *Nano Today, 8*, 235−264.

Krishna, B. V., Xue, W., Bose, S., & Bandyopadhyay, A. (2008). Functionally graded Co-Cr-Mo coating on Ti-6Al-4V alloy structures. *Acta Biomaterialia, 4*, 697−706.

Kumar, A. M., & Rajendran, N. (2012). Influence of zirconia nanoparticles on the surface and electrochemical behaviour of polypyrrole nanocomposite coated 316L SS in simulated body fluid. *Surface and Coatings Technology, 213*, 155−166.

Kurland, H.-D., Stötzel, C., Grabow, J., Zink, I., Müller, E., Staupendahl, G., et al. (2010). Preparation of spherical titania nanoparticles by CO_2 laser evaporation and process-integrated particle coating. *Journal of the American Ceramic Society, 93*, 1282−1289.

Lai, Y. K., Sun, L., Chen, C., Nie, C. G., Zuo, J., & Lin, C. J. (2005). Optical and electrical characterization of TiO_2 nanotube arrays on titanium substrate. *Applied Surface Science, 252*, 1101−1106.

Latka, L., Goryachev, S. B., Kozerski, S., & Pawlowski, L. (2010). Sintering of fine particles in suspension plasma sprayed coatings. *Materials, 3*, 3845−3866.

Lavisse, L., Grevey, D., Langlade, C., & Vannes, B. (2002). The early stage of the laser-induced oxidation of titanium substrates. *Applied Surface Science, 186*, 150−155.

Laydi, F., Rahouadj, R., Vuchois, G., Stoltz, J.-F., & de Isla, N. (2013). Hydroxyapatite incorporated into collagen gels for mesenchymal stem cell culture. *Bio-Medical Materials and Engineering, 23*, 311−315.

Lee, C.-K. (2012). Fabrication, characterization and wear corrosion testing of bioactive hydroxyapatite/nano-TiO_2 composite coatings on anodic Ti-6Al-4V substrate for biomedical applications. *Materials Science and Engineeing: B, 177*, 810−818.

Lee, Y.-H., Bhattarai, G., Aryal, S., Lee, N.-H., Lee, M.-H., Kim, T.-G., et al. (2010a). Modified titanium surface with gelatin nano gold composite increases osteoblast cell biocompatibility. *Applied Surface Science, 256*, 5882−5887.

Lee, E.-J., Chae, S.-Y., Kim, H.-E., & Kim, H.-W. (2006). Improvement in biocompatibility of fluoridated apatite with addition of resorbable glass. *Journal of the American Ceramic Society, 89*, 1748−1751.

Lee, K., Choe, H.-C., Kim, B.-H., & Ko, Y.-M. (2010b). The biocompatibility of HA thin films deposition on anodized titanium alloys. *Surface and Coatings Technology, 205*, S267−S270.

Lee, S. L., Cipollo, M., Windover, D., & Rickard, C. (1999). Analysis of magnetron-sputtered tantalum coatings versus electrochemically deposited tantalum from molten salt. *Surface and Coatings Technology, 120/121*, 44−52.

Lee, S.-H., Kim, H.-E., & Kim, H.-W. (2007a). Nano-sized hydroxyapatite coatings on Ti substrate with TiO_2 buffer layer by e-beam deposition. *Journal of the American Ceramic Society, 90*, 50−56.

Lee, J. H., & Ogawa, T. (2012). The biological aging of titanium implants. *Implant Dentistry, 21*, 415−421.

Lee, I.-S., Zhao, B., Lee, G.-H., Choi, S.-H., & Chung, S.-M. (2007b). Industrial application of ion beam assisted deposition on medical implants. *Surface and Coatings Technology, 201*, 5132−5137.

Leedy, M. R., Martin, H. J., Norowski, P. A., Jennings, J. A., Haggard, W. O., & Bumgardner, J. D. (2011). Use of chitosan as a bioactive implant coating for bone-implant applications; chitosan for biomaterials. *Advances in Polymer Science, 244*, 129−165.

Leem, J. M., & Lim, Y. J. (2010). In vitro investigation of anodization and CaP deposited titanium surface using MG63 osteoblast-like cells. *Applied Surface Science, 256*, 3086−3092.

Lei, L., Yuming, C., Bo, L., Xingfu, Z., & Weiping, D. (2010). Study on the surface erosion route to the fabrication of TiO_2 hollow spheres. *Applied Surface Science, 256*, 2596−2601.

Leitão, E., Silva, R. A., & Barbosa, M. A. (1997). Electrochemical and surface modifications on N^+-ION implanted Ti-5Al-2.5Fe immersed in HBSS. *Corrosion Science, 39*, 377−383.

Lembo, J. (2003). Three-dimensional printing. *Advanced Materials and Processes, 161*, 52−53.

Levashov, E. A., Petrzhik, M. I., Kiryukhantsev-Korneev, F. V., Shtansky, D. V., Prokoshkin, S. D., Gunderov, D. V., et al. (2012). Structure and mechanical behavior during indentation of biocompatible nanostructured titanium alloys and coatings. *Metallurgist, 56*, 395−407.

Levine, B. R., Sporer, S., Poggie, R. A., Della Valle, C. J., & Jacobs, J. J. (2006). Experimental and clinical performance of porous tantalum in orthopedic surgery. *Biomaterials, 27*, 4671−4681.

Li, Y., Li, Q., Zhu, S., Luo, E., Li, J., Feng, G., et al. (2010). The effect of strontium-substituted hydroxyapatite coating on implant fixation in ovariectomized rats. *Biomaterials, 31*, 9006−9014.

Li, S., Ni, J., Liu, X., Zhang, X., Yin, S., Rong, M., et al. (2012a). Surface characteristics and biocompatibility of sandblasted and acid-etched titanium surface modified by ultraviolet irradiation: an *in vitro* study. *Journal of Biomedical Materials Research Part B, 100B*, 1587−1598.

Li, B., Shen, Y., & Hu, W. (2013). Surface nitriding on Ti-6Al-4V alloy via friction stir processing method under nitrogen atmosphere. *Applied Surface Science, 274*, 356−364.

Li, Y., Wen, C., Mushahary, D., Sravanthi, R., Harishankar, N., Pande, G., et al. (2012b). Mg−Zr−Sr alloys as biodegradable implant materials. *Acta Biomaterialia, 8*, 3177−3188.

Li, H., Zhao, X., Cao, S., Li, K., Chen, M., Xu, Z., et al. (2012c). Na-doped hydroxyapatite coating on carbon/carbon composites: preparation, in vitro bioactivity and biocompatibility. *Applied Surface Science, 263*, 163−173.

Liang, C. Y., Yang, X. J., Wei, Q., & Cui, Z. D. (2008). Comparison of calcium phosphate coatings formed on femtosecond laser-induced and sand-blasted titanium. *Applied Surface Science, 255*, 515−518.

Lim, J. I., Yu, B., Woo, K. M., & Lee, Y.-K. (2008). Immobilization of TiO_2 nanofibers on titanium plates for implant applications. *Applied Surface Science, 255*, 2456−2460.

Lima, R. S., Dimitrievska, S., Bureau, M. N., Marple, B. R., Petit, A., Mwale, F., et al. (2010). HVOF-sprayed nano TiO_2-HA coatings exhibiting enhanced biocompatibility. *Journal of Thermal Spray Technology, 19*, 336−343.

Lin, K., Yuan, W., Wang, L., Lu, J., Chen, L., & Jiang, Z. W. (2011a). Evaluation of host inflammatory responses of β-tricalcium phosphate bioceramics caused by calcium pyrophosphate impurity using a subcutaneous model. *Journal of Biomedical Materials Research Part B, 99B*, 350−358.

Lin, K., Zhang, M., Zhai, W., Qu, H., & Chang, J. (2011b). Fabrication and characterization of hydroxyapatite/wollastonite composite bioceramics with controllable properties for hard tissue repair. *Journal of the American Ceramic Society, 94*, 99−105.

Liu, F., Li, B., Sun, J., Li, H., Wang, B., & Zhang, S. (2012). Proliferation and differentiation of osteoblastic cells on titanium modified by ammonia plasma immersion ion implantation. *Applied Surface Science, 258*, 4322−4327.

Liu, X., Poon, R. W. Y., Kwoka, S. C. H., Chu, P. K., & Ding, C. (2004). Plasma surface modification of titanium for hard tissue replacements. *Surface and Coatings Technology, 186*, 227−233.

Liu, X.-B., & Wang, H.-M. (2006). Modification of tribology and high-temperature behavior of Ti−48Al−2Cr−2Nb intermetallic alloy by laser cladding. *Applied Surface Science, 252*, 5735−5744.

Liu, Z., Wang, W., Liu, H., Wang, T., & Min Qi, M. (2013). Formation and characterization of titania coatings with cortex-like slots formed on Ti by micro-arc oxidation treatment. *Applied Surface Science, 266*, 250−255.

Liu, F., Wang, F., Shimizu, T., Igarashi, K., & Zhao, L. (2005). Formation of hydroxyapatite on Ti−6Al−4V alloy by microarc oxidation and hydrothermal treatment. *Surface and Coatings Technology, 199*, 220−224.

Liu, X. M., Wu, S. L., Chu, P. K., Chung, C. Y., Chu, C. L., Yeung, K. W. K., et al. (2007). Effects of water plasma immersion ion implantation on surface electrochemical behavior of NiTi shape memory alloys in simulated body fluids. *Applied Surface Science, 253*, 3154−3159.

Liu, J.-X., Yang, D.-Z., Shi, F., & Cai, Y.-J. (2003). Sol-gel deposited TiO_2 film on NiTi surgical alloy for biocompatibility improvement. *Thin Solid Films, 429*, 225−230.

Luo, R., Liu, Z., Yan, F., Kong, Y., & Zhang, Y. (2013). The biocompatibility of hydroxyapatite film deposition on micro-arc oxidation Ti6Al4V alloy. *Applied Surface Science, 266*, 57−61.

Ma, P. W., Wang, S.-H., Wu, G.-F., Liu, B.-L., Wei, J.-H., Xie, C., et al. (2010). Preparation and *in vitro* biocompatibility of hybrid oxide layer on titanium surface. *Surface and Coatings Technology, 205*, 1736−1742.

Ma, Y., Zhan, G., Ma, M., Wang, X., & Li, C. (2012). Direct electron transfer of hemoglobin in a biocompatible electrochemical system based on zirconium dioxide nanotubes and ionic liquid. *Bioelectrochemistry, 84*, 6−10.

Macheras, G. A., Papagelopoulos, P. J., Kateros, K., Kostakos, A. T., Baltas, D., & Karachalios, T. S. (2006). Radiological evaluation of the metal-bone interface of a porous tantalum monoblock acetabular component. *Journal of Bone and Joint Surgery (British volume), 88*, 304−309.

Macionczyk, R., Gerold, B., & Thull, R. (2001). Repassivating tantalum/tantalum oxide surface modification on stainless steel implants. *Surface and Coatings Technology, 142/144*, 1084−1087.

Maho, A., Linden, S., Arnould, C., Detriche, S., Delhalle, J., & Mekhalif, Z. (2012). Tantalum oxide/carbon nanotubes composite coatings on titanium, and their functionalization with organophosphonic molecular films: a high quality scaffold for hydroxyapatite growth. *Journal of Colloid and Interface Science, 371*, 150−158.

Maleki-Ghaleh, H., Khalili, V., Khalil-Allafi, J., & Javidi, M. (2012). Hydroxyapatite coating on NiTi shape memory alloy by electrophoretic deposition process. *Surface and Coatings Technology, 208*, 57−63.

Man, H. C., Bai, M., & Cheng, F. T. (2011). Laser diffusion nitriding of Ti-6Al-4V for improving hardness and wear resistance. *Applied Surface Science, 258*, 436−441.

Mändl, S. (2007). PIII treatment of Ti alloys and NiTi for medical applications. *Surface and Coatings Technology, 201*, 6833−6838.

Mändl, S., Krause, D., Thorwarth, G., Sader, R., Zeilhofer, F., Horch, H. H., et al. (2001). Plasma immersion ion implantation treatment of medical implants. *Surface and Coatings Technology, 142/144*, 1046−1050.

Mangano, C., Piattelli, A., Mangano, F., Rustichelli, F., Shibli, J. A., Iezzi, G., et al. (2013). Histological and synchrotron radiation-based computed microtomography study of 2 human-retrieved direct laser metal formed titanium implants. *Implant Dentistry, 22*, 175−181.

Mansur, M. R., Wang, J., & Berndt, C. C. (2013). Microstructure, composition and hardness of laser assisted hydroxyapatite and Ti-6Al-4V composite coatings. *Surface and Coatings Technology, 232*, 482−488.

Mao, Z., Ma, J., Wang, J., & Sun, B. (2007). The effect of powder preparation method on the corrosion and mechanical properties of TiN-based coatings by reactive plasma spraying. *Applied Surface Science, 255*, 3784−3788.

Martins, A., Reis, R. L., & Neves, N. M. (2008). Electrospinning: processing technique for tissue engineering scaffolding. *International Materials Reviews, 53*, 257−274.

Martorana, S., Fedele, A., Mazzocchi, M., & Bellosi, A. (2009). Surface coatings of bioactive glasses on high strength ceramic composites. *Applied Surface Science, 255*, 6679−6685.

Mathieu, H. J. (2001). Bioengineered material surfaces for medical applications. *Surface and Interface Analysis, 32*, 3−9.

Matsumoto, T. J., An, S.-H., Ishimoto, T., Nakano, T., Matsumoto, T., & Imazato, S. (2011). Zirconia−hydroxyapatite composite material with microporous structure. *Dental Materials, 27*, e205−e212.

Matsumoto, T. J., Okazaki, M., Nakahira, A., Sasaki, J., Egusa, H., & Sohmura, T. (2007). Modification of apatite materials for bone tissue engineering and drug delivery carriers. *Current Medical Chemistry, 14*, 2726−2733.

Matsuno, H., Yokoyama, A., Watari, F., Uno, M., & Kawasaki, T. (2001). Biocompatibility and osteogenesis of refractory metal implants, titanium, hafnium, niobium, tantalum and rhenium. *Biomaterials, 22*, 1253−1262.

Meyers, S. R., Khoo, X., Huang, X., Walsh, E. B., Grinstaff, M. W., & Kenan, D. J. (2009). The development of peptide-based interfacial biomaterials for generating biological functionality on the surface of bioinert materials. *Biomaterials, 30*, 277−286.

Mihailescu, I. N., Ristoscu, C., Bigi, A., & Mayer, I. (2010). Laser-surface interactions for newmaterials production. In *Advanced biomimetic implants based on nanostructured coatings synthesized by pulsed laser technologies* (Vol. 130). Springer Series in Materials Science. pp. 235−260.

Mikhalovsky, S. V., Santin, M., Mikhalovska, L. I., Lloyd, A. W., & Denyer, S. P. (2003). Nanostructured materials and coatings for biomedical and sensor applications. *NATO Science Series, 102*, 15−26.

Mirhosseini, N., Crouse, P. L., Li, L., & Garrod, D. (2007). Combined laser/sol−gel synthesis of calcium silicate coating on Ti−6Al−4V substrates for improved cell integration. *Applied Surface Science, 253*, 7998−8002.

Mishra, R. S., & Ma, Z. Y. (2005). Friction stir welding and processing. *Materials Science and Engineering, R50*, 1−78.

Mishra, V. K., Srivastava, S. K., Asthana, B. P., & Kumar, D. (2012). Structural and Spectroscopic studies of hydroxyapatite nanorods formed via microwave-assisted synthesis route. *Journal of the American Ceramic Society, 95*, 2709−2715.

Miyamoto, S., Katz, B. Z., Lafrenie, R. M., & Yamada, K. M. (1998). Fibronectin and integrins in cell adhesion, signaling, and morphogenesis. *Ann NY Acad Sci, 857*, 119−129.

Mo, A., Liao, J., Xu, W., Xian, S., Li, Y., & Bai, S. (2008). Preparation and antibacterial effect of silver−hydroxyapatite/titania nanocomposite thin film on titanium. *Applied Surface Science, 255*, 435−438.

Montazeri, M., Dehghanian, C., Shokouhfar, M., & Baradaran, A. (2010). Investigation of the voltage and time effects on the formation of hydroxyapatite-containing titania prepared by plasma electrolytic oxidation on Ti−6Al−4V alloy and its corrosion behavior. *Applied Surface Science, 257*, 7268−7275.

Morais, J. M., Papadimitrakopoulos, F., & Burgess, D. J. (2010). Biomaterials/tissue interactions: possible solutions to overcome foreign body response. *Amer Ass Pharm Sci J, 12*, 188−196.

Morcos, B. M., O'Callaghan, J. M., Amira, M. F., Van Hoof, C., & de Beeck, M. O. (2013). Electrodeposition of platinum thin films as interconnects material for implantable medical applications electrochemical/electroless deposition. *Journal of the Electrochemical Society, 160*, D300−D306.

Morra, M., Cassinelli, C., Cascardo, G., Cahalan, P., Cahalan, L., Fini, M., et al. (2003). Surface engineering of titanium by collagen immobilization; surface characterization and in vitro and in vivo studies. *Biomaterials, 24*, 4639−4654.

Moskalewicz, T., Seuss, S., & Boccaccini, A. R. (2013). Microstructure and properties of composite polyetheretherketone/Bioglass® coatings deposited on Ti-6Al-7Nb alloy for medical applications. *Applied Surface Science, 273*, 62−67.

Mukherjee, S., Maitz, M. F., Pham, M. T., Richter, E., Prokert, F., & Moeller, W. (2005). Development and biocompatibility of hard Ti-based coatings using plasma immersion ion implantation-assisted deposition. *Surface and Coatings Technology, 196*, 312−316.

Müller, R., Abke, J., Schnell, E., Macionczyk, F., Gbureck, U., Mehrl, R., et al. (2005). Surface engineering of stainless steel materials by covalent collagen immobilization to improve implant biocompatibility. *Biomaterials, 26*, 6962−6972.

Müller, R., Abke, J., Schnell, E., Scharnweber, D., Kujat, R., Englert, C., et al. (2006). Influence of surface pretreatment of titanium- and cobalt-based biomaterials on covalent immobilization of fibrillar collagen. *Biomaterials, 27*, 4059−4068.

Murabayashi, S., & Nose, Y. (2013). Biocompatibility: bioengineering aspects. *Bio-Medical Materials and Engineering, 23*, 129−142.

Mutlu, I. (2013). Sinter-coating method for production of TiN coated titanium foam for biomedical implant applications. *Surface and Coatings Technology, 232*, 396−402.

Mwenifumbo, S., Li, M., Chen, J., Beye, A., & Soboyejo, W. (2007). Cell/surface interactions on laser micro-textured titanium-coated silicon surfaces. *Journal of Materials Science: Materials in Medicine, 18*, 9−23.

Nakahira, A., Tamai, M., Miki, S., & Pezzotti, G. (2002). Fracture behavior and biocompatibility evaluation of nylon-infiltrated porous hydroxyapatite. *Journal of Materials Science, 37*, 4425−4430.

Narayan, R. J., Jin, C., Patz, T., Doraiswamy, A., Modi, R., Chrisey, D. B., et al. (2005). Laser processing of advanced biomaterials. *Advanced Materials and Processes, 163*, 39−42.

Nayak, S., Dey, T., Naskar, D., & Kundu, S. C. (2013). The promotion of osseointegration of titanium surfaces by coating with silk protein sericin. *Biomaterials, 34*, 2855−2864.

Nelea, V., Morosanu, C., Iliescu, M., & Mihailescu, I. N. (2004). Hydroxyapatite thin films grown by pulsed laser deposition and radio-frequency magnetron sputtering: comparative study. *Applied Surface Science, 228*, 346−356.

Nelson, G. M., Nychka, J. A., & McDonald, A. G. (2011). Flame spray deposition of titanium alloy-bioactive glass composite coatings. *Journal of Thermal Spray Technology, 20*, 1339−1351.

Neumeister, A., Bartke, D., Bärsch, N., Weingärtner, T., Guetaz, L., Montani, A., et al. (2012). Interface of nanoparticle-coated electropolished stents. *Langmuir, 28*, 12060−12066.

Ng, B. S., Annergren, I., Soutar, A. M., Khor, K. A., & Jarfors, A. E. W. (2005). Characterisation of a duplex TiO_2/CaP coating on Ti6Al4V for hard tissue replacement. *Biomaterials, 26*, 1087−1095.

Ng, K. W., Man, H. C., & Yue, T. M. (2011). Characterization and corrosion study of NiTi laser surface alloyed with Nb or Co. *Applied Surface Science, 257*, 3269−3274.

Nie, X., Leyland, A., & Matthews, A. (2000). Deposition of layered bioceramic hydroxyapatite/TiO_2 coatings on titanium alloys using a hybrid technique of micro-arc oxidation and electrophoresis. *Surface and Coatings Technology, 125*, 407−414.

Nikolov, A. S., Atanasov, P. A., Milev, D. R., Stoyanchov, T. R., Deleva, A. D., & Peshev, Z. Y. (2009). Synthesis and characterization of TiO*x* nanoparticles prepared by pulsed-laser ablation of Ti target in water. *Applied Surface Science, 255*, 5351−5354.

Noorakma, A. C. W., Zuhailawati, H., Aishvarya, V., & Dhindaw, B. K. (2013). Hydroxyapatite-coated magnesium-based biodegradable alloy: cold Spray deposition and simulated body fluid studies. *Journal of Materials Engineering and Performance, 22*, 2997−3004. http://dx.doi.org/10.1007/s11665-013-0589-9.

Nozyński, J. K., Religa, Z., Wszołek, J., Zembala-Nozyńska, E., & Rozentryt, P. (2001). Biological heart valve—an alternative to mechanical valve. *Medical Science Monitor, 7*, 550−562.

Okazumi, T., Ueda, K., Tajima, K., Umetsu, U., & Narushima, T. (2011). Anatase formation on titanium by two-step thermal treatment. *Journal of Material Science, 46*, 2998−3005.

Olivares-Navarrete, R., Olaya, J. J., Ramírez, C., & Rodil, S. E. (2011). Biocompatibility of niobium coatings. *Coatings, 1*, 72−87.

Onuki, Y., Bhardwaj, U., Pharm, M., Papadimitrakopoulos, F., & Burgess, D. J. (2008). A review of the biocompatibility of implantable devices: current challenges to overcome foreign body response. *Journal of Diabetes Science and Technology, 2*, 1003−1015.

Oshida, Y. (2007a). *Bioscience and bioengineering of titanium materials*. London, UK: Elsevier. pp. 4−5.

Oshida, Y. (2007b). *Bioscience and bioengineering of titanium materials* (1st ed.). London, UK: Elsevier.

Oshida, Y. (2007c). *Bioscience and bioengineering of titanium materials*. London, UK: Elsevier. pp. 389−390.

Oshida, Y. (2013). *Bioscience and bioengineering of titanium materials* (2nd ed.). London, UK: Elsevier.

Oshida, Y., Hashem, A., Nishihara, T., & Yapchulay, M. V. (1994). Fractal dimension analysis of mandibular bones—toward a morphological compatibility of implants. *Journal of Bio-Medical Materials and Engineering, 4*, 397−407.

Ou, K.-L., Shih, Y.-H., Huang, C.-F., Chen, C.-C., & Liu, C.-M. (2008). Preparation of bioactive amorphous-like titanium oxide layer on titanium by plasma oxidation treatment. *Applied Surface Science, 255*, 2046−2051.

Ou, J., Wang, J., Zhang, D., Zhang, P., Liu, S., Yan, P., et al. (2010). Fabrication and biocompatibility investigation of TiO_2 films on the polymer substrates obtained via a novel and versatile route. *Colloids and Surfaces B: Biointerfaces, 76*, 123−127.

O'Connor, R. C., Lyon, M. B., Guralnick, M. L., & Bales, G. T. (2008). Long-term follow-up of single versus double cuff artificial urinary sphincter insertion for the treatment of severe postprostatectomy stress urinary incontinence. *Urology, 71*, 90−93.

Paital, S. R., Bunce, N., Nandwana, P., Honrao, C., Nag, S., He, W., et al. (2011). Laser surface modification for synthesis of textured bioactive and biocompatible Ca−P coatings on Ti−6Al−4V. *Journal of Material Science: Materials in Medcine, 22*, 1393−1406.

Pang, S. X., & Zhitomirsky, I. (2009). Electrophoretic deposition of composite hydroxyapatite−chitosan−heparin coatings. *Journal of Material Processing Technology, 209*, 1597−1606.

Parast, S. Y., Jauhari, I., & Zaeem, M. A. (2011). Implantation of HA into superplastic Ti-6Al-4V: kinetics and mechanical behaviors of implanted layer. *Metallurgical and Materials Transaction A, 42*, 219−226.

Pardun, K., Treccani, L., Volkmann, E., Li Destri, G., Marletta, G., Streckbein, P., et al. (2013). Characterization of wet powder-sprayed zirconia/calcium phosphate coating for dental implants. *Clinical Implant Dentistry and Related Research, 2013*. http://dx.doi.org/10.1111/cid, 12071.

Park, J.-W., Kim, Y.-J., Jang, J.-H., & An, C.-H. (2010). *In vitro* biocompatibility of magnesium-incorporated submicro-porous titanium oxide surface produced by hydrothermal treatment. *Applied Surface Science, 257*, 925−931.

Park, J.-W., Tsutsumi, Y., Lee, C. S., Park, C. H., Kim, Y.-J., Jang, J.-H., et al. (2011). Surface structures and osteoblast response of hydrothermally produced $CaTiO_3$ thin film on Ti-13Nb-13Zr alloy. *Applied Surface Science, 257*, 7856−7863.

Patino, M. G., Neiders, M. E., Andreana, S., Noble, B., & Cohen, R. E. (2002). Collagen as an implantable material in medicine and dentistry. *Journal of Oral Implantology, 28*, 220−225.

Pattanayak, D. K., Prasad, R. C., Rao, B. T., & Mohan, T. R. R. (2006). Apatite Wollastonite−titanium biocomposites: synthesis and in vitro evaluation. *Journal of the American Ceramic Society, 89*, 2172−2176.

Paun, I. A., Moldovan, A., Luculescu, C. R., & Dinescu, M. (2013). Antibacterial polymeric coatings grown by matrix assisted pulsed laser evaporation. *Applied Physics, A, 110*, 895−902.

Peddi, L., Brow, R. K., & Brown, R. F. (2008). Bioactive borate glass coatings for titanium alloys. *Journal of Materials Science: Materials in Medicine, 19*, 3145−3152.

Pei, X., Wang, J., Wan, Q., Kang, L., Xiao, M., & Bao, H. (2011). Functionally graded carbon nanotubes/hydroxyapatite composite coating by laser cladding. *Surface and Coatings Technology, 205*, 4380−4387.

Petrie, T. A., Raynor, J. E., Reyes, C. D., Burns, K. L., Collard, D. M., & García, A. J. (2008). The effect of integrin-specific bioactive coatings on tissue healing and implant osseointegration. *Biomaterials, 29*, 2849−2857.

Pető, G., Karacs, A., Pászti, Z., Guczi, L., Divinyi, T., & Joób, A. (2002). Surface treatment of screw shaped titanium dental implants by high intensity laser pulses. *Applied Surface Science, 186*, 7−13.

Pham, V.-H., Lee, S.-H., Li, Y., Kim, H.-E., Shin, K.-H., & Koh, Y.-H. (2012). Utility of tantalum (Ta) coating to improve surface hardness *in vitro* bioactivity and biocompatibility of Co-Cr. *Thin Solid Films, 536*, 269−274.

Pike, M. (2009). Medical device materials. *Advanced Materials and Processes, 167*, 50−56.

Pilliar, R. M. (2009). Metallic biomaterials. In R. Narayan (Ed.), *Biomedical materials* (pp. 41−42). Springer Science and Business Media.

Puerta, D. G. (2013). Thermal spray coating—characterization and evaluation. *Advanced Materials and Processes, 171*, 16−19.

Pye, D. (2004). Ion nitriding—basics. *Advanced Materials and Processes, 162*, 41−43.

Qi, H., & Wu, H. Y. (2013). Effect of surface modification of pure Ti on tribological and biological properties of bone tissue. *Surface Engineering, 29*, 300−305.

Ramírez, G., Rodil, S. E., Arzate, H., Muhl, S., & Olaya, J. J. (2011). Niobium based coatings for dental implants. *Applied Surface Science, 257*, 2555−2559.

Rammelt, S., Illert, T., Bierbaum, S., Scharnweber, D., Zwipp, H., & Schneiders, W. (2006). Coating of titanium implants with collagen, RGD peptide and chondroitin sulfate. *Biomaterials, 27*, 5561−5571.

Rath, P. C., Singh, B. P., Besra, L., & Bhattacharjee, S. (2012). Multiwalled carbon nanotubes reinforced hydroxyapatite-chitosan composite coating on Ti metal: corrosion and mechanical properties. *Journal of the American Ceramic Society, 95*, 2725−2731.

Rautray, T. R., Narayanan, R., Kwon, T.-Y., & Kim, K.-H. (2010). Surface modification of titanium and titanium alloys by ion implantation. *Journal of Biomedical Materials Research Part B, 93B*, 581−591.

Ravichandran, R., Ng, C. C. H., Liao, S., Pliszka, D., Raghunath, M., Ramakrishna, S., et al. (2012). Biomimetic surface modification of titanium surfaces for early cell capture by advanced electrospinning. *Biomedical Materials, 7*. http://dx.doi.org/10.1088/1748−6041/7/1/015001.

Rawat, R. S., Aggarwal, V., Hassan, M., Lee, P., Springham, S. V., Tan, T. L., et al. (2008). Nano-phase titanium dioxide thin film deposited by repetitive plasma focus: ion irradiation and annealing based phase transformation and agglomeration. *Applied Surface Science, 255*, 2932−2941.

Ren, X., Wu, Y., Cheng, Y., Ma, H., & Wei, S. (2011). Fibronectin and bone morphogenetic protein-2-decorated poly(OEGMA-*r*-HEMA) brushes promote osseointegration of titanium surfaces. *Langmuir, 27*, 12069−12073.

Reyes, C. D., Petrie, T. A., Burns, K. L., Schwartz, Z., & García, A. J. (2007). Biomolecular surface coating to enhance orthopaedic tissue healing and integration. *Biomaterials, 28*, 3228−3235.

Ribeiro, A. A., Balestra, R. M., Rocha, M. N., Peripolli, S. B., Andrade, M. C., Pereira, L. C., et al. (2013). Dense and porous titanium substrates with a biomimetic calcium phosphate coating. *Applied Surface Science, 265*, 250−256.

Ribeiro, A. A., Marques, R. F. C., Guastaldi, A. C., & Sinézio, J. C. C. (2009). Hydroxyapatite deposition study through polymeric process on commercially pure Ti surfaces modified by laser beam irradiation. *Journal of Materials Science, 44*, 4056−4062.

Rie, K.-T., Stucky, T., Silva, R. A., Leitao, E., Bordji, K., Jouzeau, J.-Y., et al. (1995). Plasma surface treatment and PACVD on Ti alloys for surgical implants. *Surface and Coatings Technology, 74/75*, 973−980.

Rieder, P., Scherrer, S., Filieri, A., Wiskott, H. W. A., & Durual, S. (2012). TiNO*x* coatings increase human primary osteoblasts proliferation independently of the substrate—a short report. *Bio-Medical Materials and Engineering, 22*, 277−281.

Rieu, J. (1993). Ceramic formation on metallic surfaces (ceramization) for medical applications. *Clinical Materials, 12*, 227−235.

Ringeisen, B. R., Chrisey, D. B., Piqué, A., Krizman, D., Bronks, M., & Spargo, B. (2001). Direct write technology and a tool to rapidly prototype patterns of biological and electronic systems. *Nanotechnology, 1*, 414−417.

Rodionov, I. V. (2012). Steam-thermal oxide coatings for titanium medical implants. *Biomedical Engineering, 46*, 58−61.

Rogers, K. D., Etok, S. E., & Scott, R. (2004). Structural characterization of apatite coatings. *Journal of Materials Science, 39*, 5747−5754.

Roy, M., Bandyopadhyay, A., & Bose, S. (2008a). Laser surface modification of electrophoretically deposited hydroxyapatite coating on titanium. *Journal of the American Ceramic Society, 91*, 3517−3521.

Roy, M., Bandyopadhyay, A., & Bose, S. (2011). Induction plasma sprayed nano hydroxyapatite coatings on titanium for orthopaedic and dental implants. *Surface and Coatings Technology, 205*, 2785−2792.

Roy, M., Krishna, B. V., Bandyopadhyay, A., & Bose, S. (2008b). Laser processing of bioactive tricalcium phosphate coating on titanium for load-bearing implants. *Acta Biomaterialia, 4*, 324−333.

Saito, T., Takemoto, M., Fukuda, A., Kuroda, Y., Fujibayashi, S., Neo, M., et al. (2011). Effect of titania-based surface modification of polyethylene terephthalate on bone−implant bonding and peri-implant tissue reaction. *Acta Biomaterialia, 7*, 1558−1569.

Sala, A., Ehrbar, M., Trentin, D., Schoenmakers, R. G., Vörös, J., & Weber, F. E. (2010). Enzyme mediated site-specific surface modification. *Langmuir, 26*, 11127−11134.

Salunke, P., Shanov, V., & Witte, F. (2011). High purity biodegradable magnesium coating for implant application. *Materials Science and Engineering B, 176*, 1711−1717.

Sandberg, T., Carlsson, J., & Ott, M. K. (2009). Interactions between human neutrophils and mucin-coated surfaces. *Journal of Materials Science: Materials in Medicine, 20*, 621−631.

Sanz, M., Walczak, M., de Nalda, R., Oujja, M., Marco, J. F., Rodriguez, J., et al. (2009). Femtosecond pulsed laser deposition of nanostructured TiO_2 films. *Applied Surface Science, 255*, 5206−5210.

Sarao, T. P. S., Sidhu, H. S., & Singh, H. (2012). Characterization and *in vitro* corrosion investigations of thermal sprayed hydroxyapatite and hydroxyapatite-titania coatings on Ti alloy. *Metallurgical and Materials Transactions A, 43*, 4365−4376.

Sawase, T., Jimbo, R., Wennerberg, A., Suketa, N., Tanaka, Y., & Atsuta, M. (2007). A novel characteristic of porous titanium oxide implants. *Clinical Oral Implants Research, 18*, 680−685.

Schade, L., Franzka, S., Hardt, S., Wiggers, H., & Hartmann, N. (2013). Sintering of thin titanium dioxide nanoparticle films via photothermal processing with ultraviolet continuous-wave lasers. *Applied Surface Science, 278*, 336−340.

Schulz, M. C., Korn, P., Stadlinger, B., Range, U., Möller, S., Becher, J., et al. (2014). Coating with artificial matrices from collagen and sulfated hyaluronan influences the osseointegration of dental implants. *Journal of Materials Science: Materials in Medicine, 25*, 247−258.

Sebaa, M. A., Dhillon, S., & Liu, H. (2013). Electrochemical deposition and evaluation of electrically conductive polymer coating on biodegradable magnesium implants for neural applications. *Journal of Materials Science: Materials in Medicine, 24*, 307−316.

Shabalovskaya, S. A., Tian, H., Anderegg, J. W., Schryvers, D. U., Carroll, W. U., & Van Humbeeck, J. (2009). The influence of surface oxides on the distribution and release of nickel from Nitinol wires. *Biomaterials, 30*, 468−477.

Shenhar, A., Gotman, I., Gutmanas, E. Y., & Ducheyne, P. (1999). Surface modification of titanium alloy orthopaedic implants via novel powder immersion reaction assisted coating nitriding method. *Materials Science and Engineering: A, 268*, 40−46.

Shenhar, A., Gotman, I., Radin, S., Ducheyne, P., & Gutmanas, E. Y. (2000). Titanium nitride coatings on surgical titanium alloys produced by a powder immersion reaction assisted coating method: residual stresses and fretting behavior. *Surface and Coatings Technology, 126*, 210−218.

Shi, X., Tsuru, K., Xu, L., Kawachi, G., & Ishikawa, K. (2013). Effects of solution pH on the structure and biocompatibility of Mg-containing TiO_2 layer fabricated on titanium by hydrothermal treatment. *Applied Surface Science, 270*, 445−451.

Shtansky, D. V., Batenina, I. V., Yadroitsev, I. A., Ryashin, N. S., Kiryukhantsev-Korneev, P. V., Kudryashov, A. E., et al. (2012). A new combined approach to metal-ceramic implants with controllable surface topography, chemistry, blind porosity, and wettability. *Surface and Coatings Technology, 208*, 14−23.

Shtansky, D. V., Grigoryan, A. S., Toporkova, A. K., Arkhipov, A. V., Sheveyko, A. N., & Kiryukhantsev-Korneev, P. V. (2011). Modification of polytetrafluoroethylene implants by depositing TiCaPCON films with and without stem cells. *Surface and Coatings Technology, 206*, 1188−1195.

Silva, M. A. M., Martinelli, A. E., Alves, C., Nascimento, R. M., Távora, M. P., & Vilar, C. D. (2006). Surface modification of Ti implants by plasma oxidation in hollow cathode discharge. *Surface and Coatings Technology, 200*, 2618−2626.

Sima, F., Socol, G., Axente, E., Mihailescu, I. N., Zdrentu, L., Petrescu, S. M., et al. (2007). Biocompatible and bioactive coatings of Mn^{2+}-doped β-tricalcium phosphate synthesized by pulsed laser deposition. *Applied Surface Science, 254*, 1155−1159.

Simon, Z., Deporter, D. A., Pilliar, R. M., & Clokie, C. M. (2006). Heterotopic bone formation around sintered porous-surfaced Ti-6Al-4V implants coated with native bone morphogenetic proteins. *Implant Dentistry, 15*, 265−274.

Siva, D., Krishna, R., & Sun, Y. (2005). Thermally oxidised rutile-TiO_2 coating on stainless steel for tribological properties and corrosion resistance enhancement. *Applied Surface Science, 252*, 1107−1116.

Söderholm, K.-J. M. (2012). Review: coatings in dentistry—a review of some basic principles. *Coatings, 2*, 138−159.

Sokołowska, A., Rudnicki, J., Niedzielski, P., Boczkowska, A., Bogusławski, G., Wierzchoń, T., et al. (2005). TiN−NCD composite coating produced on the Ti6Al4V alloy for medical applications. *Surface and Coatings Technology, 200*, 87−89.

Sollazzo, V., Pezzetti, F., Scarano, A., Piattelli, A., Bignozzi, C. A., Massari, L., et al. (2008). Zirconium oxide coating improves implant osseointegration in vivo. *Dental Materials, 24*, 357−361.

Song, H.-J., Kim, J.-W., Kook, M.-S., Moon, W.-J., & Park, Y.-J. (2010). Fabrication of hydroxyapatite and TiO_2 nanorods on microarc-oxidized titanium surface using hydrothermal treatment. *Applied Surface Science, 256*, 7056−7061.

Sonoda, T., Saito, T., Watazu, A., Katou, K., & Asahina, T. (2006). Coating of Ti−6Al−4V alloy with pure titanium film by sputter-deposition for improving biocompatibility. *Surface and Interface Analysis, 38*, 797−800.

Sparrow, N. (2013). How 3-D printing is transforming medical technology. *European Medical Device Technology, 23*, 1−3.

Spriano, S., Vernè, E., Guala, C., Faga, M. G., & Eitel, F. (2009). Surface modification of cobalt alloys for articular prostheses. *Journal of Bone & Joint Surgery (British Volume), 91-B*, 265−266.

Stan, G. E., Popa, A. C., Galca, A. C., Aldica, G., & Ferreira, J. M. F. (2013). Strong bonding between sputtered bioglass−ceramic films and Ti-substrate implants induced by atomic inter-diffusion post-deposition heat-treatments. *Applied Surface Science, 280*, 530−538.

Stiegler, N., Bellucci, D., Bolelli, G., Cannillo, V., Gadow, R., Killinger, A., et al. (2012). High-velocity suspension flame sprayed (HVSFS) hydroxyapatite coatings for biomedical applications. *Journal of Thermal Spray Technology, 21*, 275−287.

Sugata, Y., Sotome, S., Yuasa, M., Hirano, M., Shinomiya, K., & Okawa, A. (2011). Effects of the systemic administration of alendronate on bone formation in a porous hydroxyapatite/collagen composite and resorption by osteoclasts in a bone defect model in rabbits. *Journal of Bone & Joint Surgery, 93-B*, 510−516.

Sugita, Y., Ishizaki, K., Iwasa, F., Ueno, T., Minamikawa, H., Yamada, M., et al. (2011). Effects of pico-to-nanometer-thin TiO_2 coating on the biological properties of microroughened titanium. *Biomaterials, 32*, 8374−8384.

Sultana, R., Kon, M., Hirakata, L. M., Fujihara, E., Asaoka, K., & Ichikawa, T. (2006). Surface modification of titanium with hydrothermal treatment at high pressure. *Dental Materials Journal, 25*, 470−479.

Supaphol, P., Suwantong, O., Sangsanoh, P., Srinivasan, S., Jayakumar, R., & Nair, S. V. (2012). Electrospinning of biocompatible polymers and their potentials in biomedical applications. *Advances in Polymer Science, 246*, 213−239.

Suryanarayana, C. (2001). Mechanical alloying and milling. *Progress in Materials Science, 46*, 1−184.

Suska, F., Svensson, S., Johansson, A., Emanuelsson, L., Karlholm, H., Ohrlander, M., et al. (2010). In vivo evaluation of noble metal coatings. *Journal of Biomedical Materials Research Part B, 92B*, 86−94.

Suzuki, T., Hori, N., Att, W., Kubo, K., Iwasa, F., Ueno, T., et al. (2009). Ultraviolet treatment overcomes time-related degrading bioactivity of titanium. *Tissue Engineering Part A, 15*, 3679−3688.

Symietz, C., Lehmann, E., Gildenhaar, R., Koter, R., Berger, G., & Krüger, J. (2011). Fixation of bioactive calcium alkali phosphate on Ti6Al4V implant material with femtosecond laser pulses. *Applied Surface Science, 257*, 5208−5212.

Tan, G., Zhou, L., Ning, C., Tan, Y., Ni, G., Liao, J., et al. (2013). Biomimetically-mineralized composite coatings on titanium functionalized with gelatin methacrylate hydrogels. *Appl Surf Sci, 279*, 293−299.

Tanaskovic, D., Jokic, B., Socol, G., Popescu, A., Mihailescu, I. N., Petrovic, R., et al. (2007). Synthesis of functionally graded bioactive glass-apatite multistructures on Ti substrates by pulsed laser deposition. *Applied Surface Science, 254*, 1279−1282.

Tepe, G., Schmehl, J., Wendel, H. P., Schaffner, S., Heller, S., Gianotti, M., et al. (2006). Reduced thrombogenicity of nitinol stents—in vitro evaluation of different surface modifications and coatings. *Biomaterials, 27*, 643−650.

Thian, E. S., Huang, J., Barber, Z. H., Best, S. M., & Bonfield, W. (2011). Surface modification of magnetron-sputtered hydroxyapatite thin films via silicon substitution for orthopaedic and dental applications. *Surface and Coatings Technology, 205*, 3472−3477.

Thomas, M., & Mittal, K. L. (2013). *Atmospheric pressure plasma treatments of polymers: relevance to adhesion*. Wiley, Schilevener Publishing.

Thorey, F., Menzel, H., Lorenz, C., Gross, G., Hoffmann, A., & Windhagen, H. (2011). Osseointegration by bone morphogenetic protein-2 and transforming growth factor beta2 coated titanium implants in femora of New Zealand white rabbits. *Indian Journal of Orthopaedics, 45*, 57−62.

Tian, Y. S., Chen, C. Z., Chen, L. B., & Chen, L. X. (2006). Study on the microstructure and wear resistance of the composite coatings fabricated on Ti-6Al-4V under different processing conditions. *Applied Surface Science, 253*, 1494−1499.

Tian, Y. S., Chen, C. Z., Wang, D. Y., Huo, Q. H., & Lei, T. Q. (2005). Laser surface alloying of pure titanium with TiN-B-S-Ni mixed powders. *Applied Surface Science, 250*, 223−227.

Tkalcec, E., Sauer, M., Nonninger, R., & Schmidt, H. (2001). Sol-gel-derived hydroxyapatite powders and coatings. *Journal of Materials Science, 36*, 5253−5263.

Tredwin, C. J., Georgiou, G., Kim, H.-W., & Knowles, J. C. (2013). Hydroxyapatite, fluorhydroxyapatite and fluorapatite produced via the sol−gel method: bonding to titanium and scanning electron microscopy. *Dental Materials, 29*, 521−529.

Trtica, M., Gakovic, B., Batani, D., Desai, T., Panjan, P., & Radak, B. (2006). Surface modifications of a titanium implant by a picosecond Nd:YAG laser operating at 1064 and 532 nm. *Applied Surface Science, 253*, 255−2556.

Tucker, R. C. (2002). Surface engineering. *Journal of Metals, 160*, 1−3.

Valanezhad, A., Tsuru, K., Maruta, M., Kawachi, G., Matsuya, S., & Ishikawa, K. (2012). A new biocompatible coating layer applied on titanium substrates using a modified zinc phosphatizing method. *Surface and Coatings Technology, 206*, 2207−2212.

Walczak, M., Papadopoulou, E. L., Sanz, M., Manousaki, A., Marco, J. F., & Castillejo, M. (2009). Structural and morphological characterization of TiO_2 nanostructured films grown by nanosecond pulsed laser deposition. *Applied Surface Science, 255*, 5267−5270.

von Walter, M., Rüger, M., Ragoß, C., Steffens, G. C. M., Hollander, D. A., Paar, O., et al. (2005). In vitro behavior of a porous TiO_2/perlite composite and its surface modification with fibronectin. *Biomaterials, 26*, 2813−2826.

Wang, D., & Bierwagen, G. P. (2009). Sol-gel coatings on metals for corrosion protection. *Progress in Organic Coatings, 64*, 327−338.

Wang, Y., Khor, K. A., & Cheang, P. (1999). Thermal spraying of functionally graded calcium phosphate coatings for biomedical implants. *Journal of Thermal Spray Technology, 7*, 50−57.

Wang, N., Li, H., Lü, W., Li, J., Wang, J., Zhang, Z., et al. (2011a). Effects of TiO_2 nanotubes with different diameters on gene expression and osseointegration of implants in minipigs. *Biomaterials, 32*, 6900−6911.

Wang, H. R., Liu, F., Zhang, Y. P., Yu, D. Z., & Wang, F. P. (2011b). Preparation and properties of titanium oxide film on NiTi alloy by micro-arc oxidation. *Applied Surface Science, 257*, 5576−5580.

Wang, L., & Luo, J. (2011). Formation of hydroxyapatite coating on anodic titanium dioxide nanotubes *via* an efficient dipping treatment. *Metallurgical and Materials Transactions A, 42*, 3255−3264.

Wang, X., Wu, G., Zhou, B., & Jun Shen, J. (2013). Thermal annealing effect on optical properties of binary TiO_2-SiO_2 sol-gel coatings. *Materials, 6*, 76−84.

Wang, G., Yang, H., Li, M., Lu, S., Chen, X., & Cai, X. (2010). The use of silk fibroin/hydroxyapatite composite co-cultured with rabbit bone-marrow stromal cells in the healing of a segmental bone defect. *Journal of Bone and Joint Surgery, 92-B*, 320−325.

Waterhouse, A., Yin, Y., Wise, S. G., Bax, D. V., McKenzie, D. R., Bilek, M. M. M., et al. (2010). The immobilization of recombinant human tropoelastin on metals using a plasma-activated coating to improve the biocompatibility of coronary stents. *Biomaterials, 31*, 8332−8340.

Waugh, D., & Lawrence, J. (2013). Laser surface processing of polymers for biomedical applications in laser-assisted fabrication of materials. *Springer Series in Materials Science, 161*, 275−318.

Wei, Q., Cui, Z.-D., Yang, X.-J., & Shi, J. (2008). Improving the bioactivity of NiTi shape memory alloy by heat and alkali treatment. *Applied Surface Science, 255*, 462−465.

Werner, S., Huck, O., Frisch, B., Vautier, D., Elkaim, R., Voegel, J.-C., et al. (2009). The effect of microstructured surfaces and laminin-derived peptide coatings on soft tissue interactions with titanium dental implants. *Biomaterials, 30*, 2291−2301.

Williams, D. F. (2008). On the mechanisms of biocompatibility. *Biomaterials, 29*, 2941−2953.

Witek, L., Marin, C., Granato, R., Bonfante, E. A., Campos, F., Bisinotto, J., et al. (2012). Characterization and *in vivo* evaluation of laser sintered dental endosseous implants in dogs. *Journal of Biomedical Materials Research Part B, 100B*, 1566−1573.

Wong, H. M., Yeung, K. W. K., Lam, K. O., Tam, V., Chu, P. K., Luk, K. D. K., et al. (2010). A biodegradable polymer-based coating to control the performance of magnesium alloy orthopaedic implants. *Biomaterials, 31*, 2084−2096.

Wright, J. D., & Sommerdijk, N. A. J. (2001). *Sol-gel materials chemistry and applications*. CRC Press, OPA Overseas Publishers Association.

Wu, J., Liu, Z.-M., Zhao, X.-H., Gao, Y., Hu, J., & Bo Gao, B. (2010). Improved biological performance of microarc-oxidized low-modulus Ti-24Nb-4Zr-7.9Sn alloy. *Journal of Biomedical Materials Research Part B, 92B*, 298−306.

Wu, C., Ramaswamy, Y., Gale, D., Yang, W., Xiao, K., Zhang, L., et al. (2008). Novel sphene coatings on Ti−6Al−4V for orthopedic implants using sol-gel method. *Acta Biomaterialia, 4*, 569−576.

Xia, Z., Yu, X., & Wei, M. (2012). Biomimetic collagen/apatite coating formation on Ti6Al4V substrates. *Journal of Biomedical Materials Research Part B, 100B*, 871−881.

Xiao, L., Yan, D., He, J., Zhu, L., Dong, Y., Zhang, J., et al. (2007). Nanostructured TiN coating prepared by reactive plasma spraying in atmosphere. *Applied Surface Science, 253*, 7535−7539.

Xiao, D., Yang, Y., Su, X., Wang, D., & Su, J. (2013). An integrated approach of topology optimized design and selective laser melting process for titanium implants materials. *Bio-Medical Materials and Engineering, 23*, 433−445.

Xie, Y., Liu, X., Huang, A., Ding, C., & Chu, P. K. (2005). Improvement of surface bioactivity on titanium by water and hydrogen plasma immersion ion implantation. *Biomaterials, 26*, 6129−6135.

Xie, D., Wan, G., Maitz, M. F., Sun, H., & Huang, N. (2013). Deformation and corrosion behaviors of Ti−O film deposited 316L stainless steel by plasma immersion ion implantation and deposition. *Surface and Coatings Technology, 214*, 117−123.

Xue, W., Liu, X., Zheng, X.-B., & Ding, C. (2005). In vivo evaluation of plasma-sprayed titanium coating after alkali modification. *Biomaterials, 26*, 3029−3037.

Yan, Y., Han, Y., & Lu, C. (2008). The effect of chemical treatment on apatite-forming ability of the macroporous zirconia films formed by micro-arc oxidation. *Applied Surface Science, 254*, 4833−4839.

Yang, C.-C., Huang, C.-Y., Lin, C.-C., & Yen, S.-K. (2011). Electrolytic deposition of collagen/HA composite on Post HA/TiO_2 coated Ti6Al4V implant alloy electrochemical synthesis and engineering. *Journal of the Electrochemical Society, 158*, E13−E20.

Yang, X., Jiang, B., Huang, Y., Tian, Y., Chen, H., Chen, J., et al. (2009a). Collagen nanofilm immobilized on at surfaces by electrodeposition method. *Journal of Biomedical Materials Research Part B, 90B*, 608−613.

Yang, X., Li, M., Lin, X., Tan, L., Lan, G., Li, L., et al. (2013). Enhanced in vitro biocompatibility/bioactivity of biodegradable Mg−Zn−Zr alloy by micro-arc oxidation coating contained Mg_2SiO_4. *Surface and Coatings Technology, 233*, 65−73.

Yang, X. F., & Lu, J. (2013). A new way to synthesize carbon nanofiber film on bulk titanium via hybrid surface mechanical attrition treatment. *Applied Surface Science, 264*, 91−196.

Yang, S., Xing, W., & Man, H. C. (2009b). Pulsed laser deposition of hydroxyapatite film on laser gas nitriding NiTi substrate. *Applied Surface Science, 255*, 9889−9892.

Yankov, R. A., Shevchenko, N., Rogozin, A., Maitz, M. F., Richter, E., Möller, W., et al. (2004). Reactive plasma immersion ion implantation for surface passivation. *Surface and Coatings Technology, 201*, 6752−6758.

Yao, Z., Jiang, Y., Jia, F., Jiang, Z., & Wang, F. (2008). Growth characteristics of plasma electrolytic oxidation ceramic coatings on Ti-6Al-4V alloy. *Applied Surface Science, 254*, 4084−4091.

Yao, C., Storey, D., & Webster, T. (2007). Nanostructured metal coatings on polymers increase osteoblast attachment. *International Journal of Nanomedicine, 2*, 487−492.

Yazici, H., Fong, H., Wilson, B., Oren, E. E., Amos, F. A., Zhang, H., et al. (2013). Biological response on a titanium implant-grade surface functionalized with modular peptides. *Acta Biomaterialia, 9*, 5341−5352.

Ye, S. H., Johnson, C. A., Jr., Woolley, R., Oh, H.-I., Gamble, L. J., Ishihara, K., et al. (2009). Surface modification of a titanium alloy with a phospholipid polymer prepared by a plasma-induced grafting technique to improve surface thromboresistance. *Colloids and Surfaces B: Biointerfaces, 74*, 96−102.

Yoshinari, M., Oda, Y., Inoue, T., & Shimono, M. (2002). Dry-process surface modification for titanium dental implants. *Metallurgical and Materials Transactions A, 33*, 511−519.

Young, L., Soon, K., Doo, S., & Yong, K. (2011). Enhanced biocompatibility of stainless steel implants by titanium coating and microarc oxidation. *Clinical Orthopaedics and Related Research, 469*, 330−338.

Yu, S., Yang, X., Yang, L., Liu, Y., & Yu, Y. (2007). Novel technique for preparing Ca- and P-containing ceramic coating on Ti-6Al-4V by micro-arc oxidation. *Journal of Biomedical Materials Research Part B, 83B*, 623−627.

Yu, S., Yu, Z., Wang, G., Han, J., Ma, X., & Dargusch, M. S. (2011). Biocompatibility and osteoconduction of active porous calcium−phosphate films on a novel Ti-3Zr-2Sn-3Mo-25Nb biomedical alloy. *Colloids and Surfaces B: Biointerfaces, 85*, 103−115.

Yue, T. M., Yu, J. K., Mei, Z., & Man, H. C. (2002). Excimer laser surface treatment of Ti-6Al-4V alloy for corrosion resistance enhancement. *Materials Letters, 52*, 206−212.

Yuen, C. K., & Ip, W. Y. (2010). Theoretical risk assessment of magnesium alloys as degradable biomedical implants. *Acta Biomaterialia, 6*, 1808−1812.

Yun, H., Lin, C., Li, J., Wang, J., & Chen, H. (2008). Low-temperature hydrothermal formation of a net-like structured TiO_2 film and its performance of photogenerated cathode protection. *Applied Surface Science, 255*, 2113−2117.

Zhang, Z., Gu, B., Zhang, W., Kan, G., & Sun, J. (2012a). The enhanced characteristics of osteoblast adhesion to porous Zinc-TiO_2 coating prepared by plasma electrolytic oxidation. *Applied Surface Science, 258*, 6504−6511.

Zhang, Y., Kong, D., Yokogawa, Y., Feng, X., Tao, Y., & Tai Qiu, T. (2012b). Fabrication of porous hydroxyapatite ceramic scaffolds with high flexural strength through the double slip-casting method using fine powders. *Journal of the American Ceramic Society, 95*, 147−152.

Zhang, B., Lu, J., Chen, J., Zhang, X., Gu, Z., & Yang, X. (2010). Biomimetic Ca-P coating on pre-calcified Ti plates by electrodeposition method. *Applied Surface Science, 256*, 2700−2704.

Zhang, P., Zhang, Z., Li, W., & Zhu, M. (2013). Effect of Ti-OH groups on microstructure and bioactivity of TiO_2 coating prepared by micro-arc oxidation. *Applied Surface Science, 268*, 381−386.

Zhao, L., Chu, P. K., Zhang, Y., & Wu, Z. (2009). Antibacterial coatings on titanium implants. *Journal of Biomedical Materials Research Part B, 91B*, 470−480.

Zhna, Z., Chen, X., Chen, A., Huo, G., & Li, H. (2009). Preparation of K2Ti6O13/TiO_2 bioceramic on titanium substrate by micro-arc oxidation. *Journal of Materials Science, 44*, 6310−6316.

Zhou, H., Lawrence, J. G., Touny, A. H., & Bhaduri, S. B. (2011). Biomimetic coating of bisphosphonate incorporated CDHA on Ti6Al4V. *Journal of Materials Science: Materials in Medicine, 23*, 365−374.

Zhu, S., Huang, N., Xu, L., Zhang, Y., Liu, H., Lei, Y., et al. (2009). Biocompatibility of Fe−O films synthesized by plasma immersion ion implantation and deposition. *Surface and Coatings Technology, 203*, 1523−1529.

Zivić, F., Babić, M., Grujović, N., & Mitrović, S. (2010). Tribometry of materials for bioengineering applications. *Tribology in Industry, 32*, 25−32.

Coatings for osseointegration of metallic biomaterials

11

D. Wang[1], G. Wu[1], X. Lin[1,2], Y. Liu[1]
[1]VU University and University of Amsterdam, Amsterdam, The Netherlands;
[2]University of Nanjing, Nanjing, China

11.1 Clinical background

Medical metallic implants, such as dental implants and hip implants, have been widely used in the past few decades. Diseases or complications that are caused by disordered bone tissue (such as trauma and inflammation) affect millions of patients every year (Govender et al., 2002). The affected bone tissues often appear as a bone defect and its biological function is impaired. They need to be repaired by the implantation of metallic biomaterials (dental implants or hip implants) (Geurs et al., 2002; Landor et al., 2007). Therefore, the function of surrounding tissues is regained and the life quality of patients is improved.

The currently used metallic implants can achieve satisfactory efficacy for most cases. However, it is still great challenge to gain proper osseointegration in some circumstances, such as a low bone density. Patients with medical conditions, such as diabetes, radiation treatment for cancer, xerostomia, and osteoporosis, often exhibit compromised bone conditions for placing metallic implants (Diz et al., 2013). These conditions may significantly decrease the survival rates of metallic implants. This situation has led to continuous efforts for improving the surface of implants to achieve proper osseointegration. In addition, immediate and early loading of implants is needed to decrease the waiting time for the functioning of implants. This needs an acceleration of the osseointegration process. Therefore, various methods have been developed to prepare the coatings on the surface of implants to enhance and accelerate osseointegration (Hunziker et al., 2012).

11.2 Osseointegration

11.2.1 Definition of osseointegration

In 1952, Per-Ingvar Brånemark accidently found that the titanium chamber could completely integrate into surrounding bone in rabbits. He named the phenomenon "osseointegration" and saw the possibilities for human use. Brånemark (1985) defined osseointegration as "the direct structural and functional connection between the ordered, living bone and the surface of a load-carrying implant." With the development of modern medicine, the definition of osseointegration has been developed. The most

Surface Coating and Modification of Metallic Biomaterials. http://dx.doi.org/10.1016/B978-1-78242-303-4.00011-9
Copyright © 2015 Elsevier Ltd. All rights reserved.

widely accepted definition of osseointegration is that it is the formation of a direct structural and functional connection between the implant and surrounding bone tissues without any intervening connective tissue (Guo et al., 2012). This is a definition based on a histological view. In addition, a more clinically oriented definition for osseointegration is advised as a process in which clinically asymptomatic rigid fixation of alloplastic materials is achieved and maintained in bone during functional loading (Zarb and Schmitt, 1991).

11.2.2 Biological process of osseointegration

Biomaterials can trigger a biological reaction from the host after being implanted. A different biological response happens according to the surface properties of metallic biomaterials. An inappropriate metallic biomaterial surface can lead to an encapsulation of the material with dense connective tissues and a consequent isolation from the body fluid (Allan, 1999). On the other hand, the well-designed implant surface could form an interlock with the surrounding bone and achieve osseointegration, which indicates the biocompatibility of the metallic biomaterial (Brunski, 1988).

The first step of the body's reaction to a biomaterial is the adsorption of the molecules onto the surface of biomaterials from the surrounding fluid (Hu et al., 2001). This is essential for the subsequent cell adhesion because the protein film bridges the biomaterial and the cells to assure cell adhesion. The cells are mainly considered to be mesenchymal stem cells (Vagaska et al., 2010). The second step is the proliferation of mesenchymal stem cells, which are in need of various growth factors. In the third stage, the multipotent mesenchymal stem cells would differentiate into osteoblasts (Eslaminejad et al., 2009) and produce cross-linked collagen and several additional specialized proteins in much smaller quantities (such as osteocalcin and osteopontin) to form the organic matrix of bone. The organic matrix is subsequently calcified to form a mineralized bone matrix (El-Amin et al., 2003), which follows the remodeling process of the newly formed woven bone (Raisz, 1999). In the remodeling phase, the woven bone is transformed into lamellar bone. Gradually, the trabccular bone is formed along the pressure trajectories. This remodeling phase represents the most active period of osteogenesis with high levels of osteoblast and osteoclast activity. Osteoblasts synthesize very dense and cross-linked collagen to form an organic matrix of bone. Osteoclasts are responsible for remodeling newly formed bone along press trajectories by demineralizing the matrix and degrading the organic components with proteinases (Katagiri and Takahashi, 2002). The outcome of the bone remodeling stage is the establishment of the osseointegration of metallic implants. The construction of osseointegration is the biological foundation of the secondary stability of dental implants.

11.2.3 Methods of evaluating osseointegration

The in vitro parameters that are used to evaluate the osseointegration are the adhesion, proliferation, differentiation, and mineralization of osteogenic cells on the surface of an implant.

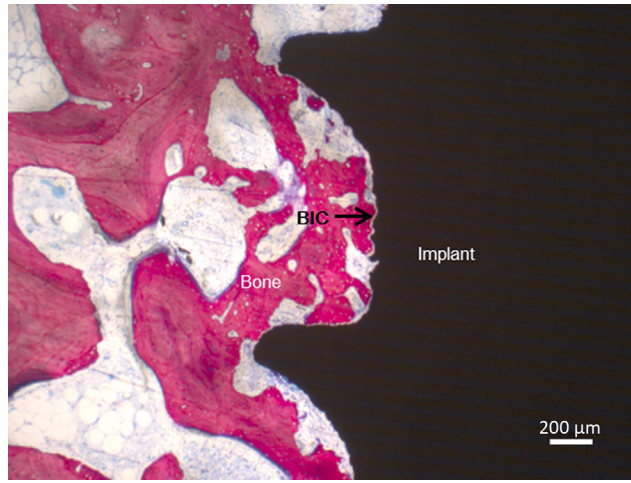
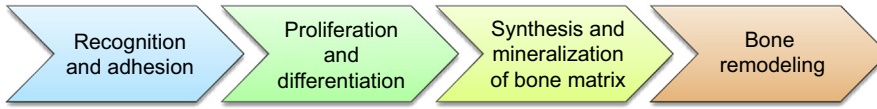


Figure 11.1 Histological micrograph showing BIC. Dental implant implanted in a sheep femur (after 12 weeks postoperatively), retrieved with the surrounding tissue and stained with McNeil's tetrachrome, basic fuchsin, and Toluidine Blue O.

Histomorphometric parameters and biomechanical testing are recommended as direct measurable indicators for assessing osseointegration in vivo. Bone-to-implant contact (BIC) is the most widely used parameter in in vivo studies to assess osseointegration quantitatively (Figure 11.1). The biomechanical testing is used to measure the force required to break the bone−implant interface.

11.3 Overview of coatings for osseointegration of metallic biomaterials

As above mentioned, the biological process of osseointegration of biocompatible implants can be divided roughly into four phases: first, recognition and adhesion; second, proliferation and differentiation; third, synthesis and mineralization of bone matrix; and fourth, bone remodeling.



Various kinds of coatings on implant surfaces have been designed to regulate these four phases to promote osseointegration, either by improving the function of osteoblast lineage or by adjusting the function of osteoclasts. The coatings mentioned in this chapter refer to an biological functionalized additional layer on the surface of an implant.

11.3.1 Improve recognition and adhesion of cells

Once implants are placed, the molecules from the surrounding environment adsorb onto the surface of biomaterials. These molecules are critical for cell adhesion.

These molecules are mainly considered as an extracellular matrix (ECM). The process of recognition and adhesion is initiated by cell-to-ECM contact. It is achieved by cells binding to ECM through adhesion receptors on cell membranes, for example, integrins (De Jonge et al., 2008). ECM consists of a variety of proteins, such as collagen type I, fibronectin, vitronectin, osteopontin, and bone sialoprotein. These proteins all have the specific amino acid sequences, arginine-glycine-aspartic acid (Arg-Gly-Asp), which is known as RGD (Avila et al., 2009). RGD has a high affinity for some proteins from the integrin family, and it is of great importance for the cell-to-ECM contacts. This has led to development of the coatings carrying RGD peptides or proteins with an RGD amino acid sequence, which are used to improve the osseointegration of metallic implants (Junker et al., 2009). But the effect of RGD to improve osseointegration is still controversial. On the one hand, RGD peptides were found to significantly increase the adhesion of MC3T3-E1 mouse osteoblasts onto titanium surfaces (Roessler et al., 2001). In the same line of research, RGD peptides were also found to improve the properties of their coatings on biomaterials such as hydroxyapatite (HA) (Avila et al., 2009). On the other hand, another in vitro study showed that the presence of the RGD sequence did not improve the adhesion onto titanium (Senyah et al., 2005). These findings were in line with other in vivo animal studies that was unable to confirm any increased bone regeneration or BIC around titanium transplants treated with RGD peptides (Avila et al., 2009; Yang et al., 2009). Another study suggested that the effects of RGD peptides could be related to checking time points. In general, significantly different results were observed mainly in the early stage between implants coated with RGD or ECM and implants carrying no peptides, whereas in the later stage almost no difference can be detected. Coating of titanium pins with collagen I showed that the cellular reaction on the implants appeared to be more intense in the early stages of bone healing in a rat tibia model compared with uncoated pins. Four days after implantation, cathepsin D, osteopontin, and osteonectin-positive cells were detected in higher numbers around the collagen I−coated Ti pins compared with the uncoated Ti pins. The early appearance of these proteins around collagen I−coated Ti pins indicated an earlier onset of the bone remodeling process compared with uncoated Ti pins. After 28 days, both the direct BIC and the amount of newly formed bone showed no statistically significant influence in collagen I−coated pins compared with Ti pins. A similar phenomenon was observed in a different animal model. In a sheep tibia model, the coating of Ti implants with collagen I under loaded conditions (external fixator pins) was investigated (Rammelt et al., 2007). The extraction torque of the pins fixed externally was not altered by collagen I coating 6 weeks after implantation. However, a significantly increased activity of osteoblasts around pins suggested an increased remodeling of the bone around the collagen I−coated implants. All the data indicated that the faster remodeling by collagen I coating affected primarily the earlier stages of bone healing without altering mechanical stability.

Not only do the positive results of the early stage lacked credibility but also the results of the later stage needed further discussion. In some instances, RGD peptides either had no effect on the synthesis of new bone (Barber et al., 2007) or they were actually detrimental (Ho et al., 2007). Hennessy et al. (2008) proposed that this can be explained by a competitive inhibition between the endogenous adhesive agents and the coated RGD. They found that the coated RGD could disturb the adsorption of fibronectin, vitronectin, and fibrinogen from blood onto the implant surface. Like RGD, which binds to integrins on cells, there are other multiple domains within fibronectin, vitronectin, and fibrinogen that also bind to integrins and subsequently stimulate either synergistically or additively the integrin signaling (Ruoslahti, 1996). Hence, the RGD sequence by itself elicited weaker integrin activation than the full-length adhesion proteins. This resulted in poor cell adhesion and thus osseointegration (Hennessy et al., 2008).

11.3.2 Enhance cell proliferation and differentiation

Adhesion of osteogenic cells on a biomaterial surface is necessary but not sufficient to on cells ensure osseointegration. More signals are needed for the proliferation and differentiation of osteogenic cells.

Bone morphogenetic protein-2 (BMP-2) is the most intensively studied growth factor for this purpose. BMP-2 has shown considerable potency for stimulating bone formation both in ectopic sites (Yoshida et al., 1998) and in orthotopic sites in different species (Teixeira and Urist, 1998). Because BMP-2 possesses a high osteoinductive potential, it is considered to be an interesting candidate for a growth factor to coat titanium implants (Junker et al., 2009). Over the past decade, recombinant human bone morphogenetic protein-2 (rhBMP-2) has been studied as a bone-modulating agent for applications in dentistry, oral and maxillofacial surgery, and other biomedical settings (Boyne, 2001). Animal model studies have corroborated its capacity for inducing bone formation (Wikesjo et al., 2001). The induced bone has demonstrated a long-term stability after the placement of loaded implants. It is found that the success of BMP-2−functionalized coatings was strongly dependent on the concentration (Wikesjo et al., 2008a) and delivery mode of BMP-2 (Liu et al., 2007).

In the critical-size, supraalveolar, peri-implant defect dog model, Wikesjo et al. (2008a) examined the ability of rhBMP-2 coated onto a titanium porous oxide implant surface to stimulate the formation of local bone including osseointegration and vertical augmentation of the alveolar ridge. Animals received either implants coated with 0.75, 1.5, or 3 mg/mL rhBMP-2, or uncoated control implants. After 8 weeks of healing, cortex formation was observed in sites receiving implants coated with rhBMP-2 at 0.75 or 1.5 mg/mL. Sites receiving implants coated with rhBMP-2 at 3.0 mg/mL exhibited more immature trabecular bone formation, seroma formation, peri-implant bone remodeling, and an undesirable displacement of the implant. The authors concluded that higher concentrations of rhBMP-2 were associated with problematic effects. Similar dose-dependent bone remodeling and seroma formation have been observed in the previous studies evaluating implants coated with rhBMP-2

at 0.2 and 4.0 mg/mL in the alveolar bone in dogs (Wikesjo et al., 2008b). The mechanisms accounting for the side effects of overdosed BMP-2 could be that BMPs stimulate the recruitment, proliferation, and differentiation of osteoclasts (Chen et al., 2004). Hence, they may promote the resorption of newly formed bone almost as soon as it has been laid down onto a titanium implant surface (Huh et al., 2012). Another possible mechanism was that the overdosed BMPs could trigger the production of intrinsic BMP inhibitors, such as noggin (Rosen, 2006). Therefore, the applied dose of BMP-2 was critical in gaining optimal bone regeneration. In contrast to the enhancement desired of bone regeneration at the bone−implant interface, an excessive dose of BMP-2 may possibly impair the osteoconductivity of the implant surface (Liu et al., 2007).

The delivery mode of BMP-2 can also have a dramatic influence on osseointegration. Liu et al. (2007) assessed the effects of BMP-2 and its mode of delivery on the osteoconductivity of dental implants in the maxillae of miniature pigs. Six different types of surfaces were evaluated: uncoated titanium surfaces (Ti), BMP-2 adsorbed to Ti (Ti/BMP-2 ads), biomimetic calcium phosphate (CaP) coated surfaces, BMP-2 adsorbed to CaP (CaP/BMP-2 ads), and BMP-2 incorporated into CaP (CaP/BMP-2 inc) as well as BMP-2 adsorbed onto and incorporated into CaP (CaP/BMP-2 ads and inc). After 3 weeks, implants bearing only adsorbed BMP-2 displayed the lowest volume of bone deposited within the osteoconductive space and the lowest bone-interface coverage among all the groups. The authors concluded that the osteoconductivity of functionalized implant surfaces was drastically impaired when BMP-2 was present as a superficially adsorbed depot upon CaP-coated or uncoated surfaces. The phenomenon might be due to the burst release of adsorbed BMP-2 to the sites of bone defect, which caused an excessive application of BMP-2 and subsequently resulted in side effects of stimulating the degradation of the bone.

Therefore, the sustained delivery of a moderate amount of BMP-2 is essential for maximizing its osteoinductivity. A biomimetic CaP coating can be a suitable carrier for the sustained release of BMP-2. The composition of CaP is quite similar to the inorganic phase of bone tissue. CaP coating is also widely considered as an osteogenic drug carrier. The preparation of a CaP coating with a biomimetic method enables the co-precipitation of osteogenic drugs into the latticework of CaP coatings. Biomimetic deposition is a method whereby a biologically active bone-like apatite layer is formed on a substrate surface by immersing the substrate in simulated body fluid under physiological conditions of temperature (37 °C) and pH (7.4) (Kokubo and Takadama, 2006) instead of the exceedingly high temperatures that can make osteogenic drugs inactive.

Liu et al. (2001) developed a biomimetic two-layer CaP coating on a titanium-alloy plate (Figure 11.2). The first layer was the initial "rainbow" coating made of a layer of CaP. The second layer was then biomimetically prepared by coprecipitating protein and CaP upon the first layer. Scanning electron microscope images suggested that protein has been incorporated into the mineral latticework instead of being deposited upon its surface. To assess the delivery mode of CaP coating as a carrier system, the coated titanium-alloy plates were dissolved in a simulated

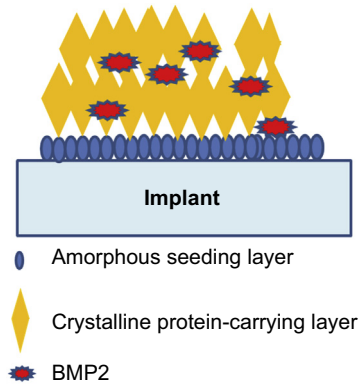


Figure 11.2 Illustration of the biomimetic CaP-coating technique. The coating was coprecipitated with the bone growth factor of BMP-2 on the surface of a titanium implant. The growth factor was incorporated into the crystal layer of CaP without losing their bioactivities.

physiological solution to observe the release kinetics of the incorporated protein. Preformed CaP coatings, which had been immersed later in solutions containing protein, lost about 3% of their associated protein during the first 2 h of incubation at pH 7.3. The dissociation process was completed within 6 h. This burst release was highly characteristic of superficially adsorbed material, but coatings prepared by the co-precipitation of CaP and protein released only 0.3% of their associated protein during the first 2 h of incubation and no more than 0.85% after 6 days. The small burst release component almost certainly represented superficially adsorbed protein. Mere 0.85% of the protein was released after 6 days demonstrated that this protein formed an integral part of the mineral matrix.

The biological property of the implants that were coated with BMP-2 was studied in vitro (Liu et al., 2004). Titanium-alloy implants were coated biomimetically with a layer of CaP in the presence of different concentrations of rhBMP-2 (0.1−10 μg/mL). Protein blot staining showed that rhBMP-2 was successfully incorporated into the crystal latticework. The absorption of rhBMP-2 by the CaP coatings was dependent on the dose, as determined by enzyme-linked immunosorbent assay. Rat bone marrow stromal cells were grown directly on these coatings for 8 days. Their osteogenicity was then assessed quantitatively by monitoring the alkaline phosphatase activity, which increased as a function of rhBMP-2 concentrations within the coating medium. The rhBMP-2 incorporated into CaP coatings was more potent in stimulating the alkaline phosphatase activity of the adhering cell layer compared with the stimulation of the cell layers grown on a plastic substratum using the freely suspended drug. The osteoinductivity of BMP-2−incorporated implant coating was also evaluated in an ectopic rat model (Liu et al., 2005). Bone formation along implants, which was used to describe osteoinductivity of implant materials, was first observed 2 weeks after implantation and thereafter continued unabated until 5 weeks. By the end of the fifth week, implants with BMP-2−incorporated CaP coating were almost completely encapsulated by woven bone (Figure 11.3).

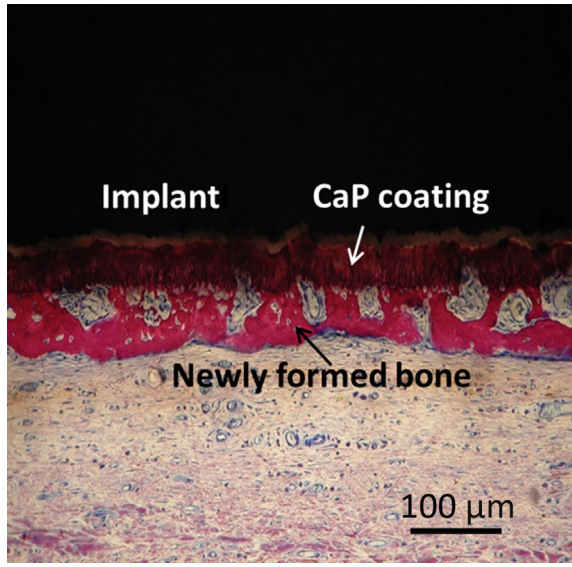


Figure 11.3 Light micrograph of titanium-alloy disc bearing a coprecipitated layer of calcium phosphate and BMP-2 (subcutaneous place in rat), retrieved with the surrounding tissue 5 weeks after implantation and stained with McNeil's tetrachrome, basic fuchsin, and Toluidine Blue O.

11.3.3 Promoting mineralization of bone matrix

The organic matrix produced by osteoblasts needs to calcify to form mineralized bone matrix (El-Amin et al., 2003). This can be modulated by drugs such as fluorine. The implants that are treated with fluorine are currently available for the clinician to use. The mechanism relies upon the property of fluoride, which interacts with HA that is present in bone tissue or teeth and generates fluorapatite. Fluorapatite has better crystallinity and a lower dissolution rate compared with HA (Caverzasio et al., 1998). Hence, a tight junction between bone and the fluoapatite-coated implant was noted. The incorporation of fluoride into CaP coating on implants was supposed to improve the bone formation along the implant surface.

Farley et al. (1983) studied the effect of fluoride on osteoblasts in an in vitro model of avian cells. They reported that fluoride increased the proliferation and alkaline phosphatase activity of osteoblasts. Based on the biomechanical and histomorphometric data, the titanium implants modified with fluoride demonstrated a firmer bone anchorage than the unmodified titanium implants. These implants achieved a greater osseointegration after a shorter healing time than unmodified titanium implants (Ellingsen et al., 2004). These findings were later confirmed by others (Hall, 1987; Modrowski et al., 1992). Results from these studies suggested that the application of fluoride can facilitate a very specific stimulus on osteoblasts so as to lead to an increase in the bone apposition rate in the early phases of osteogenesis.

11.3.4 Regulation of bone remodeling by inhibiting the osteoclast function

A current clinical challenge in the field of orthopedics is to obtain a stably fixed implant in weak osteoporotic bones. The fixation of orthopedic implants in bone relies strongly upon the initial stability of the implant (Stadelmann et al., 2008). For osteoporotic patients this early phase is particularly delicate as the bone is already weak before the surgery. The resorption of a small amount of bone near the implant may induce a dramatic decrease in early fixation, accelerating failure (Stadelmann et al., 2008). Bisphosphonates are a class of drugs that prevent the loss of bone mass by inhibiting the osteoclast activity. They are used to treat osteoporosis and similar diseases. Therefore, bisphosphonates can be used to reduce peri-prosthetic osteolysis, which allows orthopedic implants to achieve a stronger primary fixation (Hilding et al., 2000).

There are two classes of bisphosphonates: the N-containing and non−N-containing bisphosphonates. The two types of bisphosphonates work differently in inhibiting osteoclast cells. Zoledronate, one the N-containing bisphosphonates, was studied as a coating agent for osteoporotic bone (Stadelmann et al., 2008). Four implants coated with zoledronate and two control implants were inserted in the femoral condyle of ovariectomized sheep for 4 weeks. The amount of bone on the implant surface was 50% higher in the zoledronate group than in the control group. This was significant up to a distance of 400 μm from the implant surface. These results were similar to those observed in the osteoporotic rat model. This finding suggested that the concept of releasing zoledronate locally from the implant to increase the implant fixation was not species-specific. The results of this trial support the claimed that local zoledronate could increase the fixation of an implant in weak bone (Stadelmann et al., 2008).

The mechanism of bisphosphonates for improving osseointegration can be explained by the following study (Aspenberg, 2009) where bisphosphonate-coated screws were used for fracture fixation. Histological results showed that a shell of new bone had formed around the screw, inside the marrow cavity. This was not seen in the control group (Wermelin et al., 2008a,b). It can be explained that very scant, patchy loose bone or osteoid also formed around the control screws after 1 week, but disappeared later when resorption was not suppressed. When protected by the bisphosphonate, this early, scant new bone can serve as a scaffold for continued bone growth so as to lead to the formation of a bony shell. It proved that bisphosphonate coatings took effects by the inhibiting of bone resorption rather than promoting bone formation.

11.4 Clinical application and future trends

11.4.1 Current clinical application

Although a variety of coatings have been developed for improving osseointegration in preclinical studies, only a few have been evaluated in clinical applications, such as HA and bisphosphonate coatings (Abtahi et al., 2012).

HA coating has been most extensively studied in clinical applications that are applied mainly on hip implants and dental implants and in rare cases on knee prostheses (Hansson et al., 2008). HA coating could dramatically enhance the osseointegration and the survival rate of implants when placed under a compromised bone condition. Interestingly, HA-coated implants showed hardly any statistically significant difference compared with noncoated implants as long as the surrounding bone tissue exhibited sufficient quantity and quality of the bone to achieve initial stability. This phenomenon was observed in dental (Geurs et al., 2002; Morris et al., 2000), hip (Johnston et al., 2001; Landor et al., 2007; Tanzer et al., 2004), and knee implants (Hansson et al., 2008).

According to the classification of Lekholm and Zarb, bone is divided into four types (I, II, III, and IV). The bone quality is more and more challenging for achieving the initial stability going from type I to type IV. Saadoun and Legall (1992) studied 673 Steri-Oss (Denar) implants (titanium screws, HA-titanium screws, and HA−titanium cylinders) during a 5-year period. They recommended that the choice of the design should be based on implant lengths, bone quality, and anatomic region. They recommended that the closer the bone was to type IV, the greater the indication was for HA−titanium cylinders. The effect of the coating on the survival rate as a function of bone quality has been studied (Truhlar et al., 2000). HA-coated implants had an overall failure rate of 3.9% over 36 months for all bone qualities combined, whereas noncoated implants had a 13.4% failure rate for the same parameters. The highest failure rates for noncoated implants were in bone qualities III and IV (19.1 and 25.5%, respectively). Therefore, HA-coated implants were more appropriate for patients with a compromised bone quality, whereas HA-coated implants should not be recommended for cases with an acceptable bone quality.

Caution should also be taken on applying HA-coated to patients since an HA coating was found to have negative effects on bone formation. Reports in the literature (Albrektsson and Sennerby, 1991; Johnson, 1992) have suggested that HA coatings are unstable, more susceptible to bacterial infection, may be predisposed to rapid osseous breakdown, and do not demonstrate any significant advantages over titanium implants (Truhlar et al., 2000). Furthermore, it was discovered the HA was not able to improve the long-term outcome of bipolar hemiarthroplasty, because in the initially well-fixed HA-coated prostheses, the sealing effect of an HA coating created high concentrations of polyethylene in the limited joint space, which resulted in massive proximal femoral osteolysis. Consequently, an HA coating introduced a new failure mechanism, and HA-coated implants should only be recommended for patients with a compromised bone quality.

Bisphosphonate-coated dental implants were also studied in clinical trials. Apart from the conventional therapy using systemic treatment with bisphosphonates for patients suffering from osteoporosis, bisphosphonate-coated dental implants were developed to release bisphosphonate locally (Abtahi et al., 2012). The promising results may lead to new possibilities for orthopedic surgery in osteoporotic bone and for dental implants.

11.4.2 Potential modification of coatings for clinical use

Several implants that have been surface-treated with bioceramics or drugs are available commercially. They have been shown to accelerate and enhance osseointegration formation. Nevertheless, taking BMP-2 for example, there are other promising bioactive agents the true potential of which for application as biomimetic agents on implant coatings has yet to be established (Avila et al., 2009). RhBMP-2 has been approved by US Food and Drug Administration to be used for spinal fusion and has been shown to induce bone formation in animal studies and clinical trials (Govender et al., 2002; Liu et al., 2005). Moreover, CaP coatings have proved to be an efficient carrier of BMP-2 so as to stimulate differentiation of rat bone marrow stromal cells in vitro. It would therefore be worthwhile to perform clinical trials to evaluate the osseointegration of implants bearing CaP coatings incorporated with BMP-2.

References

Abtahi, J., Tengvall, P., & Aspenberg, P. (2012). A bisphosphonate-coating improves the fixation of metal implants in human bone. A randomized trial of dental implants. *Bone, 50*, 1148−1151.

Albrektsson, T., & Sennerby, L. (1991). State of the art in oral implants. *Journal of Clinical Periodontology, 18*, 474−481.

Allan, B. (1999). Closer to nature: new biomaterials and tissue engineering in ophthalmology. *British Journal of Ophthalmology, 83*, 1235−1240.

Aspenberg, P. (2009). Bisphosphonates and implants: an overview. *Acta Orthopaedica, 80*, 119−123.

Avila, G., Misch, K., Galindo-Moreno, P., & Wang, H. L. (2009). Implant surface treatment using biomimetic agents. *Implant Dentistry, 18*, 17−26.

Barber, T. A., Ho, J. E., De Ranieri, A., Virdi, A. S., Sumner, D. R., & Healy, K. E. (2007). Peri-implant bone formation and implant integration strength of peptide-modified p(AAM-co-EG/AAC) interpenetrating polymer network-coated titanium implants. *Journal of Biomedical Materials Research A, 80*, 306−320.

Boyne, P. J. (2001). Application of bone morphogenetic proteins in the treatment of clinical oral and maxillofacial osseous defects. *Journal of Bone and Joint Surgery America, 83-A*(Suppl. 1), S146−S150.

Brånemark, P. I. (1985). Introduction to osseointegration. In P. I. Branemark, G. A Zarb, & T. Albrektsson (Eds.), *Tissue-Integrated Prosthese: Osseointegration in Clinical Dentistry* (pp. 11−76). Chicago: Quintessence.

Brunski, J. B. (1988). Biomaterials and biomechanics in dental implant design. *The International Journal of Oral & Maxillofacial Implants, 3*, 85−97.

Caverzasio, J., Palmer, G., & Bonjour, J. P. (1998). Fluoride: mode of action. *Bone, 22*, 585−589.

Chen, D., Zhao, M., & Mundy, G. R. (2004). Bone morphogenetic proteins. *Growth Factor, 22*, 233−241.

De Jonge, L. T., Leeuwenburgh, S. C., Wolke, J. G., & Jansen, J. A. (2008). Organic−inorganic surface modifications for titanium implant surfaces. *Pharmaceutical Research, 25*, 2357−2369.

Diz, P., Scully, C., & Sanz, M. (2013). Dental implants in the medically compromised patient. *Journal of Dentistry, 41*, 195−206.

El-Amin, S. F., Lu, H. H., Khan, Y., Burems, J., Mitchell, J., Tuan, R. S., et al. (2003). Extracellular matrix production by human osteoblasts cultured on biodegradable polymers applicable for tissue engineering. *Biomaterials, 24*, 1213−1221.

Ellingsen, J. E., Johansson, C. B., Wennerberg, A., & Holmen, A. (2004). Improved retention and bone-to-implant contact with fluoride-modified titanium implants. *The International Journal of Oral & Maxillofacial Implants, 19*, 659−666.

Eslaminejad, M. B., Mirzadeh, H., Nickmahzar, A., Mohamadi, Y., & Mivehchi, H. (2009). Type I collagen gel in seeding medium improves murine mesenchymal stem cell loading onto the scaffold, increases their subsequent proliferation, and enhances culture mineralization. *Journal of Biomedical Materials Research B: Applied Biomaterials, 90*, 659−667.

Farley, J. R., Wergedal, J. E., & Baylink, D. J. (1983). Fluoride directly stimulates proliferation and alkaline phosphatase activity of bone-forming cells. *Science, 222*, 330−332.

Geurs, N. C., Jeffcoat, R. L., Mcglumphy, E. A., Reddy, M. S., & Jeffcoat, M. K. (2002). Influence of implant geometry and surface characteristics on progressive osseointegration. *The International Journal of Oral & Maxillofacial Implants, 17*, 811−815.

Govender, S., Csimma, C., Genant, H. K., Valentin-Opran, A., Amit, Y., Arbel, R., et al. (2002). Recombinant human bone morphogenetic protein-2 for treatment of open tibial fractures: a prospective, controlled, randomized study of four hundred and fifty patients. *Journal of Bone and Joint Surgery America, 84-A*, 2123−2134.

Guo, C. Y., Matinlinna, J. P., & Tang, A. T. (2012). Effects of surface charges on dental implants: past, present, and future. *International Journal of Biomaterials, 2012*, 381535.

Hall, B. K. (1987). Sodium fluoride as an initiator of osteogenesis from embryonic mesenchyme in vitro. *Bone, 8*, 111−116.

Hansson, U., Ryd, L., & Toksvig-Larsen, S. (2008). A randomised RSA study of peri-apatite HA coating of a total knee prosthesis. *Knee, 15*, 211−216.

Hennessy, K. M., Clem, W. C., Phipps, M. C., Sawyer, A. A., Shaikh, F. M., & Bellis, S. L. (2008). The effect of RGD peptides on osseointegration of hydroxyapatite biomaterials. *Biomaterials, 29*, 3075−3083.

Hilding, M., Ryd, L., Toksvig-Larsen, S., & Aspenberg, P. (2000). Clodronate prevents prosthetic migration: a randomized radiostereometric study of 50 total knee patients. *Acta Orthopaedica Scandinavica, 71*, 553−557.

Ho, J. E., Barber, T. A., Virdi, A. S., Sumner, D. R., & Healy, K. E. (2007). The effect of enzymatically degradable IPN coatings on peri-implant bone formation and implant fixation. *Journal of Biomedical Materials Research A, 81*, 720−727.

Hu, W. J., Eaton, J. W., Ugarova, T. P., & Tang, L. (2001). Molecular basis of biomaterial-mediated foreign body reactions. *Blood, 98*, 1231−1238.

Huh, J. B., Kim, S. E., Kim, H. E., Kang, S. S., Choi, K. H., Jeong, C. M., et al. (2012). Effects of anodized implants coated with *Escherichia coli*-derived rhBMP-2 in beagle dogs. *International Journal of Oral & Maxillofacial Surgery, 41*, 1577−1584.

Hunziker, E. B., Enggist, L., Kuffer, A., Buser, D., & Liu, Y. (2012). Osseointegration: the slow delivery of BMP-2 enhances osteoinductivity. *Bone, 51*, 98−106.

Johnson, B. W. (1992). HA-coated dental implants: long-term consequences. *Journal of the California Dental Association, 20*, 33−41.

Johnston, D. W., Davies, D. M., Beaupre, L. A., & Lavoie, G. (2001). Standard anatomical medullary locking (AML) versus tricalcium phosphate-coated AML femoral prostheses. *Canadian Journal of Surgery, 44*, 421−427.

Junker, R., Dimakis, A., Thoneick, M., & Jansen, J. A. (2009). Effects of implant surface coatings and composition on bone integration: a systematic review. *Clinical Oral Implants Research, 20*(Suppl. 4), 185−206.

Katagiri, T., & Takahashi, N. (2002). Regulatory mechanisms of osteoblast and osteoclast differentiation. *Oral Diseases, 8*, 147−159.

Kokubo, T., & Takadama, H. (2006). How useful is SBF in predicting in vivo bone bioactivity? *Biomaterials, 27*, 2907−2915.

Landor, I., Vavrik, P., Sosna, A., Jahoda, D., Hahn, H., & Daniel, M. (2007). Hydroxyapatite porous coating and the osteointegration of the total hip replacement. *Archives of Orthopaedic and Trauma Surgery, 127*, 81−89.

Liu, Y., De Groot, K., & Hunziker, E. B. (2005). BMP-2 liberated from biomimetic implant coatings induces and sustains direct ossification in an ectopic rat model. *Bone, 36*, 745−757.

Liu, Y., Enggist, L., Kuffer, A. F., Buser, D., & Hunziker, E. B. (2007). The influence of BMP-2 and its mode of delivery on the osteoconductivity of implant surfaces during the early phase of osseointegration. *Biomaterials, 28*, 2677−2686.

Liu, Y., Hunziker, E. B., Layrolle, P., De Bruijn, J. D., & De Groot, K. (2004). Bone morphogenetic protein 2 incorporated into biomimetic coatings retains its biological activity. *Tissue Engineering, 10*, 101−108.

Liu, Y., Layrolle, P., De Bruijn, J., Van Blitterswijk, C., & De Groot, K. (2001). Biomimetic coprecipitation of calcium phosphate and bovine serum albumin on titanium alloy. *Journal of Biomedical Materials Research, 57*, 327−335.

Modrowski, D., Miravet, L., Feuga, M., Bannie, F., & Marie, P. J. (1992). Effect of fluoride on bone and bone cells in ovariectomized rats. *Journal of Bone and Mineral Research, 7*, 961−969.

Morris, H. F., Ochi, S., Spray, J. R., & Olson, J. W. (2000). Periodontal-type measurements associated with hydroxyapatite-coated and non-HA-coated implants: uncovering to 36 months. *Annals of Periodontology, 5*, 56−67.

Raisz, L. G. (1999). Physiology and pathophysiology of bone remodeling. *Clinical Chemistry, 45*, 1353−1358.

Rammelt, S., Heck, C., Bernhardt, R., Bierbaum, S., Scharnweber, D., Goebbels, J., et al. (2007). In vivo effects of coating loaded and unloaded Ti implants with collagen, chondroitin sulfate, and hydroxyapatite in the sheep tibia. *Journal of Orthopaedic Research, 25*, 1052−1061.

Roessler, S., Born, R., Scharnweber, D., Worch, H., Sewing, A., & Dard, M. (2001). Biomimetic coatings functionalized with adhesion peptides for dental implants. *Journal of Materials Science: Materials in Medicine, 12*, 871−877.

Rosen, V. (2006). BMP and BMP inhibitors in bone. *Annals of the New York Academy of Sciences, 1068*, 19−25.

Ruoslahti, E. (1996). RGD and other recognition sequences for integrins. *Annual Review of Cell and Developmental Biology, 12*, 697−715.

Saadoun, A. P., & Legall, M. L. (1992). Clinical results and guidelines on Steri-Oss endosseous implants. *The International Journal of Periodontics and Restorative Dentistry, 12*, 486−495.

Senyah, N., Hildebrand, G., & Liefeith, K. (2005). Comparison between RGD-peptide-modified titanium and borosilicate surfaces. *Analytical and Bioanalytical Chemistry, 383*, 758−762.

Stadelmann, V. A., Gauthier, O., Terrier, A., Bouler, J. M., & Pioletti, D. P. (2008). Implants delivering bisphosphonate locally increase periprosthetic bone density in an osteoporotic sheep model. A pilot study. *European Cells and Materials, 16*, 10−16.

Tanzer, M., Gollish, J., Leighton, R., Orrell, K., Giacchino, A., Welsh, P., et al. (2004). The effect of adjuvant calcium phosphate coating on a porous-coated femoral stem. *Clinical Orthopaedics and Related Research*, 153−160.

Teixeira, J. O., & Urist, M. R. (1998). Bone morphogenetic protein induced repair of compartmentalized segmental diaphyseal defects. *Archives of Orthopaedic and Trauma Surgery, 117*, 27−34.

Truhlar, R. S., Morris, H. F., & Ochi, S. (2000). Implant surface coating and bone quality-related survival outcomes through 36 months post-placement of root-form endosseous dental implants. *Annals of Periodontology, 5*, 109−118.

Vagaska, B., Bacakova, L., Filova, E., & Balik, K. (2010). Osteogenic cells on bio-inspired materials for bone tissue engineering. *Physiological Research, 59*, 309−322.

Wermelin, K., Aspenberg, P., Linderback, P., & Tengvall, P. (2008a). Bisphosphonate coating on titanium screws increases mechanical fixation in rat tibia after two weeks. *Journal of Biomedical Materials Research A, 86*, 220−227.

Wermelin, K., Suska, F., Tengvall, P., Thomsen, P., & Aspenberg, P. (2008b). Stainless steel screws coated with bisphosphonates gave stronger fixation and more surrounding bone. Histomorphometry in rats. *Bone, 42*, 365−371.

Wikesjo, U. M., Qahash, M., Polimeni, G., Susin, C., Shanaman, R. H., Rohrer, M. D., et al. (2008a). Alveolar ridge augmentation using implants coated with recombinant human bone morphogenetic protein-2: histologic observations. *Journal of Clinical Periodontology, 35*, 1001−1010.

Wikesjo, U. M., Sorensen, R. G., & Wozney, J. M. (2001). Augmentation of alveolar bone and dental implant osseointegration: clinical implications of studies with rhBMP-2. *Journal of Bone and Joint Surgery America, 83-A*(Suppl. 1), S136−S145.

Wikesjo, U. M., Xiropaidis, A. V., Qahash, M., Lim, W. H., Sorensen, R. G., Rohrer, M. D., et al. (2008b). Bone formation at recombinant human bone morphogenetic protein-2-coated titanium implants in the posterior mandible (type II bone) in dogs. *Journal of Clinical Periodontology, 35*, 985−991.

Yang, G. L., He, F. M., Yang, X. F., Wang, X. X., & Zhao, S. F. (2009). In vivo evaluation of bone-bonding ability of RGD-coated porous implant using layer-by-layer electrostatic self-assembly. *Journal of Biomedical Materials Research A, 90*, 175−185.

Yoshida, K., Bessho, K., Fujimura, K., Kusumoto, K., Ogawa, Y., Tani, Y., et al. (1998). Osteoinduction capability of recombinant human bone morphogenetic protein-2 in intramuscular and subcutaneous sites: an experimental study. *Journal of Cranio-Maxillo-Facial Surgery, 26*, 112−115.

Zarb, G. A., & Schmitt, A. (1991). Osseointegration and the edentulous predicament. The 10-year-old Toronto study. *British Dental Journal, 170*, 439−444.

Bioactive polymer–calcium phosphate composite coatings by electrophoretic deposition

12

F. Pishbin[1], L. Cordero-Arias[2], S. Cabanas-Polo[2], A.R. Boccaccini[1,2]
[1]Imperial College London, London, UK; [2]University of Erlangen-Nuremberg, Erlangen, Germany

12.1 Introduction

12.1.1 Bioactive coatings

Indisputably one of the research fields that has been reaching attention and increasing activity through the last two decades is the field of biomaterials. The evolution and development of new biomaterials, both in the academic and industrial sectors, have been encouraged due to the population ageing in the western societies, mainly induced by a higher life expectancy, lower birth rate and dramatic improvement in medicine and medical technology. However a higher life expectancy implies new spectra of challenges related with the dealing of age-related chronic diseases, e.g. circulatory system problems and osteoporosis. Trying to find a solution to these problems, new techniques must be developed to repair soft and hard tissues, e.g. bone and blood vessels, or even complete organs. According to Holzapfel et al. (2013), the biomaterials market for 2014 was estimated to be in the order of US$58.1 billion, with annual growth rates that can reach 15%. Today, approximately 1.5 million surgical procedures/year are done in the world in which an orthopaedic implant is involved, with a cost of around US$10 billion (Holzapfel et al., 2013). These numbers highlight the importance of this market in near future.

The main problem of orthopaedic implants today, and where new efforts and investigations are being carried out, is the general lack of a positive interaction between the metallic implant and the body to enhance the osseointegration with the existing bone tissue (Goodman et al., 2013). Normally, the implant is perceived as a strange body which can be isolated from the rest of the organism by fibrous tissue, which leads to micromovements of the implant, migration and possible loosening (Aro et al., 2012; Goodman et al., 2013). This encapsulation reduces the lifetime of the implant and can result in a second surgery after few years of implantation, with its subsequent problems and costs. To tackle this problem, a solution currently under investigation is the development of novel implant surface coatings with the ability to induce the osseointegration of the implant with the host tissue.

To achieve osseointegration, different materials based on calcium phosphates, mainly hydroxylapatite (HA), have been used to coat metallic implants. HA has

Surface Coating and Modification of Metallic Biomaterials. http://dx.doi.org/10.1016/B978-1-78242-303-4.00012-0
Copyright © 2015 Elsevier Ltd. All rights reserved.

been proven to increase the osseointegration of metallic prosthesis with bone tissue (Furth et al., 2007). Preventing the formation of fibrous tissue around the implant. To produce HA coatings, a variety of techniques have been explored: sputtering, pulse layer deposition, electrostatic multilayer deposits and, the most extended, spray coating.

A second general problem with implants is the risk of bacterial growth leading to possible infections, causing posterior procedures well as the risk of an elevated use of antibiotics or other drugs. It has been reported that infections of orthopaedic implants occur in 5% of cases, for a total amount of 100,000 cases per year just in the United States (Holzapfel et al., 2013). This problem is originated by the bacterial colonization on the implant surface, where the bacteria form a biofilm causing the infection of the existing bone and surrounding tissues (Gristina et al., 1990). This phenomenon not only induces retarded bone healing but it can also lead to total implant loosening. To avoid this problem, antibiotics are prescribed, with some disadvantages of systemic administration such as relatively low drug concentration at the target site. Another disadvantage is that the antibiotic acts on the whole body, exposing all the tissues and organs to potential systemic adverse effects (Holzapfel et al., 2013). To avoid adverse effects and have a better treatment against infections, the implant could also be coated with antibiotics or other biomolecules (Goodman et al., 2013; Lovsky et al., 2010; Poortinga et al., 2000), localizing the treatment where is required. With this approach, different antibiotics and other biomolecules have been used including: growth factors, proteins (e.g. collagen) and even DNA molecules (Auernheimer et al., 2005; Elmengaard et al., 2005; Wojtowicz et al., 2010).

Currently, the most extended technique to produce coatings on metallic orthopaedic implants is the spray coating method; however, due to the high processing temperatures involved, biological entities, e.g. antibiotics, proteins, etc., cannot be incorporated into the coatings. Different coating technologies, like dip coating, electrospraying, sol−gel, layer by layer (LbL) and electrophoretic deposition (EPD), are being put forward to solve this problem. With these techniques, a huge variety of ceramic, metallic and polymer materials can be deposited, with the advantage that they can be used at room temperature, avoiding thermal damage and enabling the direct deposition of biological entities. In this chapter, we will discuss EPD and its role on the development of coatings for bone replacement applications, with a focus in polymer−calcium phosphate composite coating systems.

12.1.2 Electrophoretic deposition

EPD is a colloidal processing technique that consists of two different steps. In the first step, named electrophoresis, charged particles in suspension move towards an oppositely charged substrate under the influence of an applied electric field. In the second one, the deposition itself, the particles coagulate to create a coherent and homogeneous coating on the surface of the conductive substrate (Sarkar and Nicholson, 1996). This technique has been widely used over the last couple of decades to produce a wide range of coatings in composition and thickness intended for biomedical applications (Boccaccini et al., 2010). In fact, any particulate system (metals, polymers, ceramics,

glasses, biological entities and the combination of these materials) can be deposited using EPD (Van der Biest and Vadeperre, 1999). Although the EPD technique was first reported back in the nineteenth century, its practical applications were not described until 1933 (Besra and Liu, 2007), and even today the mechanisms of the deposition are still under investigation (Besra and Liu, 2007; Grillon et al., 1992; Zhitomirsky, 2006).

For polymer systems in polar solvents, in which the functional groups of the polymeric chains are dissociated, it is believed that the deposition mechanism consists of the recombination of the polymer with the protons (H^+) or hydroxyl groups (OH^-) that are generated at the interface between the suspension and the electrode, i.e. the particle charge neutralization mechanism (Grillon et al., 1992). In this way, cationic polymers, which develop a positive charge in the suspension, would move towards the negative electrode (cathode) and would recombine with the OH^- groups developed at the cathode interface (Figure 12.1). This recombination would neutralize the polymer and would make it to coagulate on the electrode surface (Zhitomirsky, 2006). On the other hand, for anionic polymers, the recombination with H^+ groups would occur at the anode surface.

In the case of metals, ceramics, and glasses, the particle charge neutralization mechanism can also be applied, and the loss of stability in the suspension plays a major role in the deposition kinetics. Colloidal stability is one of the key parameters required to achieve homogeneous and reproducible coatings by EPD. There are many factors affecting the particle stability in suspensions, but for polar solvents the most accepted

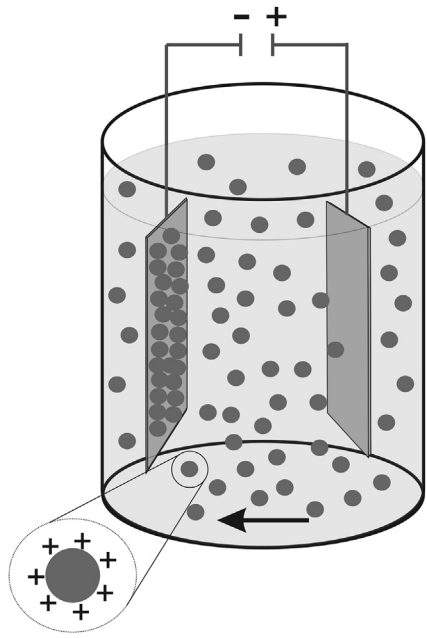


Figure 12.1 Scheme of a cathodic electrophoretic deposition where positively charged particles (or polymer molecules) move towards a negatively charged electrode under the influence of an electric field (the arrow indicates the direction of the particles movement).

stabilization mechanisms are electrostatic (due to repulsive forces of equally charged particles in the suspension) and electrosteric (in which the charge is provided by polyelectrolytes that create both electrostatic and steric repulsion) interactions (Dickerson and Boccaccini, 2012). Regarding the EPD mechanism, flocculation by particle accumulation suggests that the applied electric field makes the incoming particles create enough pressure on the particles next to the deposit to overcome the repulsive forces that keep them stable in suspension and accumulate on the surface of the electrode (Hamaker, 1940; Heavens, 1990), while the coagulation mechanism implies that a decrease of the zeta potential of the particles, due to an increase of electrolytes near the interface between the suspension and the electrode, makes the particles flocculate and become part of the deposit (Koelmans, 1995). Another accepted mechanism is the one proposed by Sarkar and Nicholson (1996), which is based on the distortion of the electrical double layer (EDL) under the effect of the electric field: when a particle is moving toward the oppositely charge electrode, the head of the EDL (the closest to the electrode) becomes thinner, while the tail becomes thicker. This phenomenon also results in the decrease of the repulsive forces between the incoming particles and the ones already deposited and, therefore, in an increase of the attractive London and Van der Waals forces, this including coagulation and deposition of the particles. This mechanism was later modified by De and Nicholson for cathodic EPD (De and Nicholson, 1999). In this case, particle discharge and other chemical reactions generate a drop in the H^+ concentration at the cathode surface, increasing the pH toward the isoelectric point (IEP) of the particles (pH value at which the zeta potential becomes zero and the particles reach their maximum instability), thus, therefore decreasing the zeta potential makes the particles coagulate.

EPD presents a series of advantages: it is a cost-effective technique that requires simple equipment and inexpensive precursors; high reproducibility and homogeneity of the coatings can be obtained; and thickness of the coating can be tuned by controlling the voltage and deposition time during the process because the kinetics of the process is governed by the Hamaker equation (Eqn (12.1)), which correlates the mass (m) deposited per area (A) with the applied electric field (E), the deposition time (t), the electrophoretic mobility of the particles (μ_e) and the concentration of the particles in the suspension (C).

$$m/A = EC\,\mu_e t \tag{12.1}$$

Moreover, one-dimensional wires, two-dimensional sheets or three-dimensional porous structures can be coated, and by controlling the deposition system, not only metals, ceramics, glasses or polymers can be deposited, but also biological entities as mentioned above (Besra and Liu, 2007; Boccaccini et al., 2010; Seuss and Boccaccini, 2013). All these advantages have made EPD a versatile technique to be used in a wide range of applications, such as functionally graded ceramics (Put et al., 2003), dye-sensitized solar cells (Kim et al., 2006), thermal barrier (Li et al., 2011) and oxidation protection coatings (Liu et al., 2012), electrodes for lithium batteries (Caballero et al., 2013), layered ceramics (Ferrari et al., 1998), superconductors (Maiti et al., 1989), carbon nanotube film (Du et al., 2002), thick silica films

(Hasegawa et al., 1999) nano ceramics (Corni et al., 2008) and hydroxyapatite coatings on metal substrates for biomedical applications (Wei et al., 2001) to name a selection of EPD applications.

The application of EPD to the field of biomaterials started with the development of an HA coating on Ti substrates for bone replacement applications (Boccaccini et al., 2010), and since then a large variety of coatings have been investigated. Between 2000 and 2010, EPD has received increasing attention due to the possibility of combining bioactive ceramics or glasses, which induce bone formation, with biocompatible polymers (Boccaccini et al., 2010). The obtained organic/inorganic composite coatings ('soft coatings') does not require a sintering process to consolidate the inorganic structure, because the polymer acts as a binder and provides sufficient mechanical consistency to the inorganic phase. By avoiding the sintering process, not only transformation or crystallization of the bioactive ceramic or glass material is avoided, but also the possible morphological changes that arise from contraction or dilatation during the heating process or the cracking and detachment of the coating due to mismatches between the thermal expansion coefficients and between the metallic substrate and the inorganic phase can be eliminated.

12.2 Organic–inorganic composite coatings

Human bone can be considered a natural organic–inorganic composite. The inorganic phase is mainly formed by nanocrystals of a hydrated calcium phosphate component, hydroxycarbonate apatite (HCA), while the organic matrix of bone mainly consists of type I collagen (Posner, 1969). This combination confers proper toughness as well as stiffness to the bone. Polymers are flexible, but lack mechanical strength, while inorganic materials such as ceramics are stiff and brittle. On the other hand, although processing of polymers into complex shapes is easier, they are not bioactive and cannot provide osseointegration. Therefore, inspired by the structure of the bone, one promising approach is the fabrication of biodegradable polymer/bioactive ceramic (or bioactive glass) composite materials (Rezwan et al., 2006). The first advantage of this type of composite systems is an improved mechanical property of the biomedical device in terms of combination of strength, stiffness and fracture toughness provided by the polymer–inorganic material composite. Second, increased bioactivity and bone-bonding capability of the structure due to the incorporation of bioactive ceramic or glass is expected. Moreover, the bioactive phase introduces a specific topography on the polymer surface (nanoscale or microscale roughness), which, if tuned, can be favourable for cell adhesion and deposition of extracellular matrix components (Misra and Boccaccini, 2007). Additionally, many degradable synthetic polymers are resorbed by hydrolysis of the polymer chains, which in several systems leads to an acidic environment with autocatalytic effect on polymer degradation. Addition of a material such as bioactive glass leads to a buffering effect of the surrounding medium and controls the fast degradation rate of polymers (Boccaccini and Maquet, 2003; Li and Chang, 2005). Finally, not only the polymer degradation kinetics is controlled by a

higher amount of water absorption at the interfaces between the polymer and the more hydrophilic bioactive phase (Kim et al., 2005), but also the ionic release rate of the bioactive ceramic included in the degrading polymer phase can be controlled, which should lead to superior bone growth (Stamboulis and Hench, 2000).

Because there is an increasing interest in adding surface functionality to bioinert metallic implants, recent efforts are concentrated on developing polymer/inorganic composite coatings. These coatings can enhance bioactivity, chemical stability and antimicrobial function of the implants (Boccaccini et al., 2010; Pang and Zhitomirsky, 2007). Furthermore, the need for sintering and densification of ceramic coatings is resolved, because the polymer provides a suitable template in which the ceramic particles are embedded and guarantee their adhesion to the substrate.

There are different techniques available to produce polymer−matrix composite coatings. Composite chitosan (CS)/apatite coatings have been fabricated on titanium (Ti) alloy substrates by mixing different ratios of CS and apatite powders, followed by dip coating of metal and a subsequent alkaline transformation at room temperature (Peña et al., 2006). In a novel approach, silica xerogel/CS film was spin-coated on Ti discs at room temperature. These hybrid films displayed more hydrophilicity and improved osteoblastic proliferation compared to pure CS (Jun et al., 2010).

Bioactive ceramic-coated implants can also be infiltrated by the polymer to attain a composite structure (Muzzarelli et al., 2001). CS-infiltrated plasma-sprayed HA coatings on Ti alloy substrates have displayed improved antibacterial activity proportional to the CS concentration (Song et al., 2011). Degradable and nondegradable sutures have been dip-coated with Bioglass®/poly-DL-lactide films for bioactive wound healing applications. A two-step coating process has been shown to improve the adherence of glass particles to the substrate (Chen et al., 2006, p. 354). Tamjid et al. (2011) have demonstrated a significant increase in the elastic modulus of polycaprolactone (PCL) polymer by reinforcing it with bioactive glass particles. In a similar study, a 20% increase in the Young's modulus of CS films has been obtained by the addition of montmorillonite nanoparticles. This effect has been attributed to the formation of hydrogen bonds and van der Waals interactions between the two phases (Paluszkiewicz et al., 2011).

Another approach is LBL deposition, by which polyelectrolyte multilayers of nanostructured organic/inorganic composites can be obtained. The idea to construct these structures has been inspired by nacre, a natural material that has a regular brick-and-mortar arrangement of aragonite ($CaCO_3$) crystals infiltrated by tight layers of a protein. Although 95% of nacre is made of ceramic, it exhibits excellent toughness and inelasticity (Wang, 2004). Based on LBL methodology, composite coatings have been generated by sequential deposition of CS (as polycation) and bioactive glass nanoparticles (as anionic component) (Couto et al., 2008). This approach has been used to form polysaccharide coatings of alginate (Alg)−CS on Si wafers on which calcium phosphate carbonate was nucleated and grown to mimic the composite structure of bone (Peng et al., 2009). Composite coatings with antibacterial properties can also be produced by LBL deposition. It has been

achieved by coating poly (ethylene terephthalate) substrate with multifunctional CS/heparin films. These films have been loaded with TiO_2 nanoparticles as a contact-active antibacterial agent and nanosilver as a release-active antibacterial agent (Yuan et al., 2008).

As a promising technique, there is an increasing interest in EPD of composites based on polysaccharides. This is due to an investigation showing the role of these natural polymers in forming interfaces between organic and inorganic components in bone and governing crystallization of HA nanoparticles (Wise et al., 2007). HA/Alg (Cheong and Zhitomirsky, 2008), multiwalled carbon nanotubes (MWCNT)/Alg and MWCNT/hyaluronic acid (HYH) coatings (Grandfield et al., 2009) are examples of this type of coatings.

Moreover, EPD of composite coatings containing bioactive glasses is drawing increasing attention (Boccaccini et al., 2006; Ma et al., 2010a,b; Sun et al., 2008; Zhitomirsky et al., 2009). The aqueous suspension stability of Bioglass® particles can be improved by electrosteric and electrostatic effects of positively charged CS molecules in the solution, and hence better deposition rate is achieved on the cathode. (Sun et al., 2008; Zhitomirsky et al., 2009). Similarly, polyanions of Alg (Zhitomirsky et al., 2009) and hyaluronate (Ma et al., 2010a,b) provide anodic deposition of bioactive particles. Water electrolysis and consequent hydrogen and oxygen gas releases at the electrodes result in a pH increase at the cathode and a pH decrease at the anode, respectively. At the vicinity of the electrode, CS deposits due to alkaline pH and alginic acid and HYH deposits due to acidic pH. In another study, the influence of EPD parameters on co-deposition of Bioglass® 45S5 and CS from aqueous medium has been reported (Pishbin et al., 2011). Recently in a similar way, sol–gel bioactive glass particles and CS have been deposited from ethanol–water suspensions (Mehdipour and Afshar, 2012). EPD has also been applied to prepare composite antibacterial coatings of CS/Bioglass®/silver nanoparticles. In this study, in situ single-step formation and deposition of silver nanoparticles in the composite coatings was shown for the first time using EPD (Pishbin et al., 2013).

Because certain compounds of calcium phosphates have chemical similarity with the mineral phase of bone, they are of great interest for use in composite orthopaedic coatings. A comprehensive discussion of the polymer–calcium phosphate composite coatings, focusing on EPD of such coatings, is presented in the following section.

12.3 Composite coatings based on calcium phosphates

The most popular synthetic calcium phosphate ceramic for bone repair application is HA, which has the following chemical formula: $Ca_{10}(PO_4)_6(OH)_2$. HA bonds to bone and is osteoconductive. Its bone-bonding mechanism has been attributed to cellular activity at the implant surface, leading to partial dissolution of Ca and P ions. These ions combined with other ions from body fluids form HCA microcrystals that bond to the host bone (Oonishi et al., 2000). Sintered HA is clinically used to coat metal

alloys to improve osseointegration between the bone and the implant and to remove the need for applying bone cements (Groot et al., 1998). If HA is to be subjected to thermal processing, the Ca/P ratio gains significant importance; a slight deviation from stoichiometry of the material may lead to the formation of phases such as β-tricalcium phosphate (TCP), tetracalcium phosphate or calcium oxide, which can adversely affect the biological response to the material (Fanovich and Porto Lopez, 1998).

Another well-known calcium phosphate is TCP with the formula $Ca_3(PO_4)_2$. It is biodegradable and is present in four polymorphs, the most common being TCP-α and TCP-β. To adjust the rate of resorption of calcium phosphate with that of tissue regrowth, the use of mixtures of HA and TCP has been suggested (Daculsi et al., 2003).

Electrodeposition techniques have been extensively used to produce polymer/inorganic composite coatings containing calcium phosphate ceramics (Boccaccini et al., 2010). This is due to the low cost, tuneable deposition properties and low-temperature processing this method provides. Electrodeposition can be divided into two methods: (1) electrochemical deposition (ED); and (2) EPD.

The Co-ED of calcium phosphates with CS on Ti alloy has been reported (Ballesteros et al., 2010; Wang et al., 2004, 2008). Compared to electrodeposited calcium phosphate coatings, these composites display higher proliferation rate, increased alkaline phosphatase activity and higher collagen expression of osteoblast-like cells (Wang et al., 2008). Likewise, collagen/octacalcium phosphate coatings have been electrodeposited (Wang et al., 2009). The coatings possessed hierarchically porous structures in nano/micrometer scale, similar to bone structure. Additionally, when immersed in simulated body fluid, the coatings stimulated formation of an apatite layer that, in terms of crystalline orientation and structural composition, was very similar to natural bone apatite.

Considering EPD-based techniques, different polymer-based composite coatings have been achieved. For example, Silicon-substituted HA/PCL composite coatings were prepared by EPD to bioactivate Ti substrates. PCL enhanced the bonding strength of HA to Ti (Xiao et al., 2009a,b). Ti implants have been coated via constant voltage EPD with CS reinforced apatite−wollastonite films. These homogeneous coatings were found to have interconnected pores, and the adhesive strength of the coating was evaluated by nanoindentation (Young's modulus = 9.23 GPa). It was found that the presence of CS triggers sheet-like apatite formation due to provision of a dense negatively charged surface. Suspension pH and current density were recognized as the most important factors in EPD (Sharma et al., 2009b,c). Implantation of these coated Ti implants in rabbit tibia demonstrated good haemocompatibility and fast bone healing (Sharma et al., 2009a).

Among polysaccharides, various studies have used CS as the organic matrix for HA-containing composite coating. A significant finding is that HA/CS films deposited by EPD have preferred HA *c*-axis crystallographic orientation, similar to natural bone (Pang and Zhitomirsky, 2007). By varying EPD parameters, monolayer and functionally graded coatings of HA−silica−CS have been deposited on different substrates such as Ti foil and 316L stainless steel (Grandfield and Zhitomirsky, 2008). In another

study, the biocompatibility and physiological corrosion resistance of Ni–Ti shape memory alloys have been enhanced by three-phase component EPD of CS/MWCNT/HA (Grandfield et al., 2009). EPD of CS has also enabled co-deposition of HA and $CaSiO_3$ at room temperature. CS molecules adsorbed on HA nanoparticles provided electrosteric stabilization of the HA suspension. These coatings also improved the physiological corrosion resistance of AISI 316L SS substrate (Pang et al., 2009). In a recent attempt, Ti_6Al_4V substrate has been electrophoretically coated by calcium carbonate film. This film was changed to HCA by immersing in phosphate-buffered saline and finally dip-coated with CS to obtain a composite film. By this novel approach, the morphology, adhesion, spreading and proliferation of human bone mesenchymal stem cells were improved compared to the noncomposite film (Tang et al., 2014).

A novel application of EPD is that coatings can be deposited in the form of laminates comprising layers of different functionality (Pang et al., 2009; Sun et al., 2008, 2009). HA/silver/CS monolayers and multilayers of individual HA/CS and silver/CS layers, as shown in Figure 12.2, have been fabricated (Pang and Zhitomirsky, 2008). In addition, Sun et al. (2009) have successfully applied EPD to prepare multilayers of HA/CS and heparin/CS. Incorporation of heparin in these functionally graded coatings can improve the blood compatibility of the implants.

Implantation of a biomedical device in the body is always associated with a risk of bacterial adhesion to the implant surface and consequent microbial infection, which is more severe in open-fractured bones and joint-revision surgeries (Duan and Wang, 2006). More importantly, formation of bacterial biofilms on the implant presents additional complications, because they are extremely resistant to both the immune system and antibiotics (Davies, 2003). While systemic drug administration is used to address implant-related infections, it might not be sufficiently effective against bacterial biofilms formation due to impaired blood circulation at the injury site and low local concentration of the drug. Therefore, local delivery of drugs and

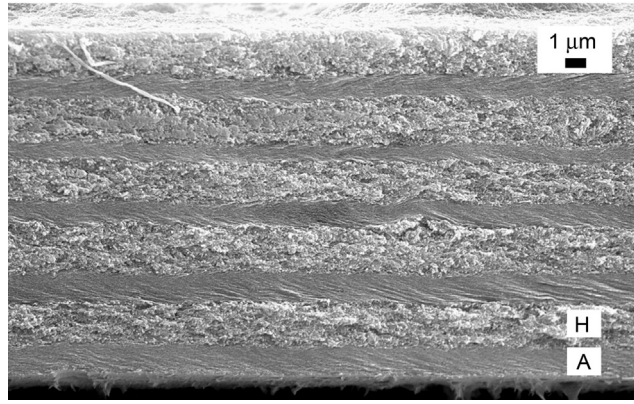


Figure 12.2 Multilayer composite coating with chitosan/HA (H) and chitosan/AgNO3 (A) layers deposited by EPD, adapted from reference [78] and reproduced with permission of Elsevier.

biomolecules can be a promising approach to effectively treat such conditions. With this approach, specific local levels of drug concentration with long-term controlled release can be administered without the risk of systemic toxicity or formation of biofilms (Popat et al., 2007). There is a wealth of literature on organic and inorganic drug-delivery systems for orthopaedic applications (Kanellakopoulou and Giamarellos-Bourboulis, 2000; Mourino and Boccaccini, 2010). Moreover, the EPD technique has been used in few studies for drug loading. Model protein bovine serum albumin (Ma et al., 2010a,b), heparin (anticoagulant) (Sun et al., 2009) and salicylic acid (anti-inflammatory) (Ma et al., 2010a,b) are examples of components electrophoretically loaded in CS and HYH polymers.

Composite release systems have also been studied. Zhou and co-workers (Zhou et al., 2011) demonstrated that the release of gentamicin from electrochemically deposited CS/CaP coating is controlled by the chemical composition and surface topography. In another study, a Ti alloy was dip-coated with gelatin/HA composite coatings and loaded with an ibuprofen anti-inflammatory drug (Xiao et al., 2009a). The coatings had a thin dense outer layer and thick porous inner layer. The in vitro release rate from this system was always zero order and lasted for 30 days. In another study, CS/nano HA film capped with poly(β-amino ester)-based film incorporating physiological amounts of rhBMP-2 exhibited an increased rate of mesenchymal stem cells differentiation (Shah et al., 2012).

Because increased antibiotic resistance is a major medical concern, silver, an agent that has not developed bacterial resistance, is emerging as a high potential antibacterial component. It works against a broad range of gram-positive (e.g. *Staphylococcus aureus*, *Staphylococcus epidermidis*) and gram-negative (*e.g. Escherichia coli*, *Pseudomonas aeruginosa*) bacteria (Lansdown, 2002). Silver exhibits bactericidal effect at low concentrations (as low as 35 ppb) without toxicity to human cells (Ewald et al., 2011). One mechanism suggested is that Ag^{+} reacts with the bacteria cell membrane and metabolic proteins and enzymes and disrupts their function by binding to DNA and thiol groups of proteins (Feng et al., 2000).

Silver has been incorporated in a variety of organic matrices. Silver/polyamide composite films were shown to actively release silver ion due to interaction between diffused water and silver particles in the matrix (Kumar and Münstedt, 2005). In a recent approach, intrinsically antibacterial polyurethane anionomers were prepared by neutralising its backbone carboxyl groups by metal ions of Ag(I), Cu(II), Zn(II), Al(III) and Fe(III) (Francolini et al., 2010). The best result was obtained by silver ion containing-polymer, which inhibited *S. epidermidis* growth up to 16 days. It was shown that silver nanoparticles have larger surface area to come in contact with bacterial cells and hence have a higher level of interaction and faster release rate (Rai et al., 2009). Pang and Zhitomirsky (2008) have applied EPD to co-deposit multilayers of composite CS/silver/HA nanoparticles. The formation of amorphous Ag−CS complexes in the coatings was reported and it was shown that control of the release kinetics of ionic silver from these coatings could be achieved by application of an additional CS film.

All of the above mentioned examples demonstrate the vast extent of current research activities to obtain an implant composite coating with desirable properties.

Table 12.1 summarizes the literature on EPD of orthopaedic polymer–calcium phosphate composite coatings.

Table 12.1 Summary of the literature on EPD of orthopaedic polymer/calcium phosphate coatings

Coating	EPD parameters	Substrate	Reference
CS/HA	CS: 0–0.7 g/l in 17 vol% ethanol–water (1 vol% AA) HA: 0.5–8 g/l IED: 15 mm Current: 0.1 mA/cm^2 Time: 3–10 min	Pt foil 316L SS foil and wire	Pang and Zhitomirsky (2007)
	CS: 0.5 g/l in 60–87 vol% ethanol–water (1 vol% AA) HA: 0–4 g/l IED: 15 mm Voltage: 10–50 V Time: 5 min	Nitinol Graphite	Grandfield et al. (2009)
	CS: 0.5 g/l in 87 vol% ethanol–water (1 vol% AA) HA: 1 g/l IED: 15 mm Voltage: 10–30 V	Nitinol foil and wire	Sun et al. (2008)
	CS: 0.5 g/l (1 vol% AA) HA: 1, 4 g/l IED: 15 mm Voltage:10–30 V	Pt foil 304 SS Graphite	Sun et al. (2009)
CS/CaP	CS: 0.05, 0.1, 0.15, 0.2 g/l (1 vol% AA) Supersaturated CaP solution Current: 2 mA/cm^2 Time: 15 h pH = 6.8–6.9 Temperature: 52 °C	Ti_6Al_4V	Wang et al. (2004, 2008), Ballesteros et al. (2010)
CS/CaP/ gentamicin	CS: 5 g/l CaP: 30–10 mM $Ca(NO_3)_2$ and 10–0 mM NaH_2PO_4 Voltage: 28 V Time: 30 min IED: 15 mm pH = 5.8 Then 40 g/l gentamicin was pipetted over the coatings	Ti	Zhou et al. (2011)

Continued

Table 12.1 Continued

Coating	EPD parameters	Substrate	Reference
CS/HA/MWCNT	CS: 0.5 g/l in 60–87 vol% ethanol–water (1 vol% AA) HA: 0–4 g/l MWCNT: 0–0.5 g/l IED: 15 mm Voltage: 10–50 V 5 min	Nitinol Graphite	Grandfield et al. (2009)
CS/HA/silica	CS: 0.5 g/l in 17 vol% ethanol–water (1 vol% AA) HA: 0.25, 2.5, 5 g/l Silica: 0.9, 1.8, 3.6 g/l IED: 15 mm Voltage: 10–30 V	Ti foil 316L SS foil and wire Graphite	Grandfield and Zhitomirsky (2008)
CS/HA/$CaSiO_3$	CS: 0–0.7 g/l in 17 vol% ethanol–water (1 vol% AA) HA: 0–4 g/l $CaSiO_3$: 0.1–0.5 g/l IED: 15 mm Voltage: 20 V	Pt foil 316L SS foil Graphite	Pang et al. (2009)
CS/HA/silver	CS: 0–0.7 g/l in 17 vol% ethanol–water (1 vol% AA) HA: 0.5–2 g/l $AgNO_3$: 0.5–1 mM IED: 15 mm Current: 0.1 mA/cm^2 Time: 10–20 min	Pt foil 316L SS foil and gauze Graphite	Pang and Zhitomirsky (2008)
CS/HA/BG	CS: 0.5 g/l in 87 vol% ethanol-water (1 vol% AA) HA: 1 g/l BG: 0.5 g/l IED: 15 mm Voltage: 10–30 V	Nitinol wire and foil	Sun et al. (2008)
CS/AW	CS: 0.2 g/l (2 vol% AA) AW: 2 g/l in ethanol (pH = 1.6) Current for CS: 1 mA/cm^2 Time for CS: 1 min Current for AW: 5, 7, 9 mA/cm^2 Time for AW: 1, 3, 5 min	Ti	Sharma et al. (2009a,b)

Table 12.1 Continued

Coating	EPD parameters	Substrate	Reference
CS/HCA	Calcium carbonate coating: 1.25 g $CaCo_3$ in 250 ml ethanol (pH = 6.5, IED: 10 mm, voltage: 90 V, time: 1 min) Then transformed to HCA in phosphate buffered saline Then soaked in CS 10 g/l (20 vol% AA)	Ti_6Al_4V	Tang et al. (2014)
PCL/Si-HA	PCL: 0–16 g/l Si-HA: 20 g/l 34% *n*-butanol and 16% chloroform IED: 7.5 mm Voltage: 30 V Time: 90 s	Ti	Xiao et al. (2009a)
Alg/HA	Alg: 1–2 g/l HA: 0–8 g/l Current: 2 mA/cm^2 Time: 5 min	NiTi shape memory alloy Platinized silicon wafer	Cheong and Zhitomirsky (2008)
Alg/HA/BG	Alg: 0.5 g/l HA: 0–1 g/l BG: 0–2 g/l IED: 15 mm Voltage: 10–30 V	Ti Pt 316L SS Platinized silicon wafer	Zhitomirsky et al. (2009)
HYH/HA/BG	HYNa: 0.5 g/l HA: 0.6 g/l BG: 0.15 g/l Voltage: 3–12 V/cm Time: 0–10 min	Pt foil 316L SS foil Graphite	Ma et al. (2010b)
Collagen/ octacalcium phosphate	Collagen: 0.333 g/l 0.028 M $Ca(NO_3)_2$–0.017 M $NH_4H_2PO_4$ pH = 4.2 Temperature: 65 °C Current: 0.5 mA/cm^2 Time: 20 min	Ti	Wang et al. (2009)

CS: chitosan; HA: hydroxyapatite; CaP: calcium phosphate; MWCNT: multiwalled carbon nanotubes; AW: apatite–wollastonite; HCA: hydroxycarbonate apatite; Si-HA: silicon-substituted hydroxyapatite; Alg: alginate; BG: bioactive glass; HYH: hyaluronic acid; PCL: polycaprolactone; PT: platinum; SS: stainless steel; AA: acetic acid; IED: inter-electrode distance.

12.4 Conclusions

EPD is a coatings technique exhibiting versatility in producing organic/inorganic coatings with a large variety of materials for a wide spectrum of applications. Coatings of orthopaedic implants have concentrated large research efforts, leading to significant advancement on the last years. Specific coating systems based on biopolymer−CaP composites have been discussed in this chapter. Important challenges remain for the further optimization of such coating systems which can be summarized as follows:.

- Processing techniques: Most previous investigations have focused on flat substrates; EPD-based coating techniques must be developed to coat real implants (three-dimensional structures). To fulfil this goal, studies of the counter-electrode design, form and control of the electrical field, etc. have to be done.
- Mechanical properties: The adhesion of the coatings to the substrate, scratch resistance and wear behaviour are key parameters that until now have been marginally studied. This is a key factor during the surgery procedure (to ensure the permanence of the coating) and service life of the coating once inside the body.
- Degradation of the coating and results of in-vivo tests: These two aspects have also been marginally studied. More in-vivo tests should be performed to approximate these coatings to real applications and to be able to suggest these coatings as real alternatives compared to coatings obtained via conventional methods, e.g. thermal spraying.
- Addition of biomolecules: Beyond the incorporation of antibacterial or anti-inflammatory drugs, other molecules, such as growth factors, bioactive molecules and DNA, should be studied.

Summarizing, it can be stated that EPD of organic/inorganic biomedical coatings is a relatively new field of investigation that has been attracting increasing interest between 2000 and 2010. It is expected that more work will be done in the near future to tackle the issues mentioned above, which should lead to producing superior coatings for orthopaedic applications using EPD as core coating method.

Acknowledgements

L. Cordero-Arias wishes to thank the German Academic Exchange Service (DAAD) (Bonn, Germany) for a scholarship. The authors acknowledge EU FP-7 project “ITN-GlaCERCo” for financial support.

References

Aro, H. T., Alm, J. J., Moritz, N., Makinen, T. J., & Lankinen, P. (2012). Low BMD affects initial stability and delays stem osseointegration in cementless total hip arthroplasty in women. A 2-year RSA study of 39 patients. *Acta Orthopaedica, 83*, 107−114.

Auernheimer, J., Zukowski, D., Dahmen, C., Kantlehner, M., Enderle, A., Goodman, S. L., et al. (2005). Titanium implant materials with improved biocompatibility through coating with phosphonate-anchored cyclic RGD peptides. *ChemBioChem: A European Journal of Chemical Biology, 6*, 2034−2040.

Ballesteros, D. Y. P., Duran, H. A. E., Tutta, E. M. C., Martinez, R., & Quintero, C. V. (2010). Chitosan/calcium phosphate coating obtained by electrodeposition on titanium alloy. *Revista Facultad de Ingenieria Universidad de Antioquia*, 15–23.

Besra, L., & Liu, M. (2007). A review on fundamentals and applications of electrophoretic deposition (EPD). *Progress in Materials Science, 52*, 1–61.

Boccaccini, A. R., Keim, S., Ma, R., Li, Y., & Zhitomorsky, I. (2010). Electrophoretic deposition of biomaterials. *Journal of the Royal Society Interface, 7*, S581–S613.

Boccaccini, A. R., & Maquet, V. (2003). Bioresorbable and bioactive polymer/Bioglass® composites with tailored pore structure for tissue engineering applications. *Porous Materials, 63*, 2417–2429.

Boccaccini, A., Peters, C., Roether, J., Eifler, D., Misra, S., & Minay, E. (2006). Electrophoretic deposition of polyetheretherketone (PEEK) and PEEK/Bioglass® coatings on NiTi shape memory alloy wires. *Journal of Materials Science, 41*, 8152–8159.

Caballero, A., Hernán, L., Morales, J., Cabanas-Polo, S., Ferrari, B., Sanchez-Herencia, A. J., et al. (2013). Electrochemical properties of ultrasonically prepared $Ni(OH)_2$ nanosheets in lithium cells. *Journal of Power Sources, 238*, 366–371.

Chen, Q. Z., Blaker, J. J., & Boccaccini, A. R. (2006). Bioactive and mechanically strong Bioglass®-poly(d,l-lactic acid) composite coatings on surgical sutures. *Journal of Biomedical Materials Research Part B: Applied Biomaterials, 76B*(2), 354–363. http://dx.doi.org/10.1002/jbm.b.30379.

Cheong, M., & Zhitomirsky, I. (2008). Electrodeposition of alginic acid and composite films. *Colloids and Surfaces A: Physicochemical and Engineering Aspects, 328*, 73–78.

Couto, D. S., Alves, N. M., & Mano, F. J. (2008). Nanostructured multilayer coatings combining chitosan with bioactive glass nanoparticles. *Journal of Nanoscience and Nanotechnology, 8*, 1–8.

Corni, I., Ryan, M. P., & Boccaccini, A. R. (2008). Electrophoretic deposition: From traditional ceramics to nanotechnology. *Journal of the European Ceramic Society, 28*(7), 1353–1367. http://dx.doi.org/10.1016/j.jeurceramsoc.2007.12.011.

Daculsi, G., Laboux, O., Malard, O., & Weiss, P. (2003). Current state of the art of biphasic calcium phosphate bioceramics. *Journal of Materials Science Materials in Medicine, 14*, 195–200.

Davies, D. (2003). Understanding biofilm resistance to antibacterial agents. *Nature Reviews Drug Discovery, 2*, 114–122.

De, D., & Nicholson, P. S. (1999). Role of ionic depletion in deposition during electrophoretic deposition. *Journal of the American Ceramic Society, 82*, 3031–3036.

Dickerson, J. H., & Boccaccini, A. R. (2012). *Electrophoretic deposition of nanomaterials*. Springer.

Duan, K., & Wang, R. (2006). Surface modifications of bone implants through wet chemistry. *Journal of Materials Chemistry, 16*, 2309–2321.

Du, C., Heldbrant, D., & Pan, N. (2002). Preparation and preliminary property study of carbon nanotubes films by electrophoretic deposition. *Materials Letters, 57*, 434–438.

Elmengaard, B., Bechtold, J. E., & Søballe, K. (2005). In vivo study of the effect of RGD treatment on bone ongrowth on press-fit titanium alloy implants. *Biomaterials, 26*, 3521–3526.

Ewald, A., Hösel, D., Patel, S., Grover, L. M., Barralet, J. E., & Gbureck, U. (2011). Silver-doped calcium phosphate cements with antimicrobial activity. *Acta Biomaterialia, 7*, 4064–4070.

Fanovich, M. A., & Porto Lopez, J. M. (1998). Influence of temperature and additives on the microstructure and sintering behaviour of hydroxyapatites with different Ca/P ratios. *Journal of Materials Science: Materials in Medicine, 9*, 53–60.

Feng, Q. L., Wu, J., Chen, G. Q., Cui, F. Z., Kim, T. N., & Kim, J. O. (2000). A mechanistic study of the antibacterial effect of silver ions on *Escherichia coli* and *Staphylococcus aureus*. *Journal of Biomedical Materials Research, 52*, 662−668.

Ferrari, B., Sánchez-Herencia, A. J., & Moreno, R. (1998). Electrophoretic forming of Al_2O_3/Y-TZP layered ceramics from aqueous suspensions. *Materials Research Bulletin, 33*, 487−499.

Francolini, I., D'Ilario, L., Guaglianone, E., Donelli, G., Martinelli, A., & Piozzi, A. (2010). Polyurethane anionomers containing metal ions with antimicrobial properties: thermal, mechanical and biological characterization. *Acta Biomaterialia, 6*, 3482−3490.

Furth, M. E., Atala, A., & Van Dyke, M. E. (2007). Smart biomaterials design for tissue engineering and regenerative medicine. *Biomaterials, 28*, 5068−5073.

Goodman, S. B., Yao, Z., Keeney, M., & Yang, F. (2013). The future of biologic coatings for orthopaedic implants. *Biomaterials, 34*, 3174−3183.

Grandfield, K., Sun, F., FitzPatrick, M., Cheong, M., & Zhitomirsky, I. (2009). Electrophoretic deposition of polymer-carbon nanotube−hydroxyapatite composites. *Surface & Coatings Technology, 203*, 1481−1487.

Grandfield, K., & Zhitomirsky, I. (2008). Electrophoretic deposition of composite hydroxyapatite−silica−chitosan coatings. *Materials Characterization, 59*, 61−67.

Grillon, F., Fayeulle, D., & Jeandin, M. (1992). Quantitative image-analysis of electrophoretic coatings. *Journal of Materials Science Letters, 11*, 272−275.

Gristina, A., Naylor, P., & Myrvik, Q. (1990). Biomaterial-centered infections: microbial adhesion versus tissue integration. In T. Wadström, I. Eliasson, I. Holder, & Å. Ljungh (Eds.), *Pathogenesis of wound and biomaterial-associated infections*. London: Springer.

Groot, K., Wolke, J. G. C., & Jansen, J. A. (1998). Calcium phosphate coatings for medical implants. *Proceedings of the Institution of Mechanical Engineers, Part B: Journal of Engineering Manufacture, 212*, 137−147.

Hamaker, H. C. (1940). Formation of a deposit by electrophoresis. *Transactions of the Faraday Society, 35*, 279−287.

Hasegawa, K., Kunugi, S., Tatsumisago, M., & Minami, T. (1999). Preparation of thick films by electrophoretic deposition using surface modified silica particles derived from sol−gel method. *Journal of Sol-Gel Science and Technology, 15*, 243−249.

Heavens, N. (1990). Electrophoretic deposition as a processing route for ceramics. In G. P. Binner (Ed.), *Advanced ceramics processing & technology*. Park Ridge: Noyes Publications.

Holzapfel, B. M., Reichert, J. C., Schantz, J.-T., Gbureck, U., Rackwitz, L., Nöth, U., et al. (2013). How smart do biomaterials need to be? A translational science and clinical point of view. *Advanced Drug Delivery Reviews, 65*, 581−603.

Jun, S. H., Lee, E. J., Yook, S. W., Kim, H. E., Kim, H. W., & Koh, Y. H. (2010). A bioactive coating of a silica xerogel/chitosan hybrid on titanium by a room temperature sol−gel process. *Acta Biomaterialia, 6*, 302−307.

Kanellakopoulou, K., & Giamarellos-Bourboulis, E. J. (2000). Carrier systems for the local delivery of antibiotics in bone infections. *Drugs, 59*, 1223−1232.

Kim, H., Lee, E. J., Jun, I. K., Kim, H. E., & Knowles, J. C. (2005). Degradation and drug release of phosphate glass/polycaprolactone biological composites for hard-tissue regeneration. *Journal of Biomedical Materials Research, 75*, 34−41.

Kim, G.-S., Seo, H.-K., Godble, V. P., Kim, Y.-S., Yang, O. B., & Shin, H.-S. (2006). Electrophoretic deposition of titanate nanotubes from commercial titania nanoparticles: application to dye-sensitized solar cells. *Electrochemistry Communications, 8*, 961−966.

Koelmans, H. (1995). Suspensions in nonaqueous media. *Philips Research Reports, 10*, 161.

Kumar, R., & Münstedt, H. (2005). Silver ion release from antimicrobial polyamide/silver composites. *Biomaterials, 26*, 2081−2088.

Lansdown, A. B. (2002). Silver. I: its antibacterial properties and mechanism of action. *Journal of Wound Care, 11*, 125−130.

Li, H., & Chang, J. (2005). pH-compensation effect of bioactive inorganic fillers on the degradation of PLGA. *Composites Science and Technology, 65*, 2226−2232.

Li, Z., Qian, S., & Wang, W. (2011). Characterization and oxidation behaviour of NiCoCrAlY coating fabricated by electrophoretic deposition and vacuum heat treatment. *Applied Surface Science, 257*, 4616−4620.

Liu, J., Cao, L.-Y., Huang, J.-F., Xin, Y., Yang, W.-D., Fei, J., et al. (2012). A $ZrSiO_4$/SiC oxidation protective coating for carbon/carbon composites. *Surface and Coatings Technology, 206*, 3270−3274.

Lovsky, Y., Lewis, A., Sukenik, C., & Grushka, E. (2010). Atomic-force-controlled capillary electrophoretic nanoprinting of proteins. *Analytical and Bioanalytical Chemistry, 396*, 133−138.

Ma, R., Epand, R. F., & Zhitomirsky, I. (2010a). Electrodeposition of hyaluronic acid and hyaluronic acid−bovine serum albumin films from aqueous solutions. *Colloids and Surfaces B: Biointerfaces, 77*, 279−285.

Maiti, H. S., Datta, S., & Basu, R. N. (1989). High-Tc superconductor coating on metal substrates by an electrophoretic technique. *Journal of the American Ceramic Society, 72*, 1733−1735.

Ma, R., Li, Y., & Zhitomirsky, I. (2010b). Electrophoretic deposition of hyaluronic acid and composite films for biomedical applications. *JOM, 62*, 72−75.

Mehdipour, M., & Afshar, A. (2012). A study of the electrophoretic deposition of bioactive glass−chitosan composite coating. *Ceramics International, 38*, 471−476.

Misra, S. K., & Boccaccini, A. R. (2007). Biodegradable and bioactive polymer/ceramic composite scaffolds. In A. R. Boccaccini, & J. E. Gough (Eds.), *Tissue engineering using ceramics and polymers* (pp. 72−92). England: Woodhead Publishing Limited.

Mourino, V., & Boccaccini, A. R. (2010). Bone tissue engineering therapeutics: controlled drug delivery in three-dimensional scaffolds. *Journal of the Royal Society Interface, 7*, 209−227.

Muzzarelli, R. A. A., Biagini, G., DeBenedittis, A., Mengucci, P., Majni, G., & Tosi, G. (2001). Chitosan−oxychitin coatings for prosthetic materials. *Carbohydrate Polymers, 45*, 35−41.

Oonishi, H., Hench, L. L., Wilson, J., Sugihara, F., Tsuji, E., Matsuura, M., et al. (2000). Quantitative comparison of bone growth behavior in granules of Bioglass, A-W glass-ceramic, and hydroxyapatite. *Journal of Biomedical Materials Research, 51*, 37−46.

Paluszkiewicz, C., Stodolak, E., Hasik, M., & Blazewicz, M. (2011). FT-IR study of montmorillonite−chitosan nanocomposite materials. *Spectrochimica Acta Part A: Molecular and Biomolecular Spectroscopy, 79*, 784−788.

Pang, X., Casagrande, T., & Zhitomirsky, I. (2009). Electrophoretic deposition of hydroxyapatite−$CaSiO_3$−chitosan composite coatings. *Journal of Colloid and Interface Science, 330*, 323−329.

Pang, X., & Zhitomirsky, I. (2007). Electrophoretic deposition of composite hydroxyapatite−chitosan coatings. *Materials Characterization, 58*, 339−348.

Pang, X., & Zhitomirsky, I. (2008). Electrodeposition of hydroxyapatite−silver−chitosan nanocomposite coatings. *Surface and Coatings Technology, 202*, 3815−3821.

Peña, J., Izquierdo-Barba, I., García, M. A., & Vallet-Regí, M. (2006). Room temperature synthesis of chitosan/apatite powders and coatings. *Journal of the European Ceramic Society, 26*, 3631−3638.

Peng, P., Dietzel, L., Miller, T., & Meagher, L. (2009). Rapid fabrication of bio-inspired, mineralized polysaccharide coatings. *Materials Science and Engineering: C, 29*, 2208−2212.

Pishbin, F., Mourino, V., Gilchrist, J. B., McComb, D. W., Kreppel, S., Salih, V., et al. (2013). Single-step electrochemical deposition of antimicrobial orthopaedic coatings based on a bioactive glass/chitosan/nano-silver composite system. *Acta Biomaterialia, 9*, 7469−7479.

Pishbin, F., Simchi, A., Ryan, M. P., & Boccaccini, A. R. (2011). Electrophoretic deposition of chitosan/45S5 Bioglass® composite coatings for orthopaedic applications. *Surface & Coatings Technology, 205*, 5260−5268.

Poortinga, A. T., Bos, R., & Busscher, H. J. (2000). Controlled electrophoretic deposition of bacteria to surfaces for the design of biofilms. *Biotechnology and Bioengineering, 67*, 117−120.

Popat, K. C., Eltgroth, M., LaTempa, T. J., Grimes, C. A., & Desai, T. A. (2007). Titania nanotubes: a novel platform for drug-eluting coatings for medical implants? *Small, 3*, 1878−1881.

Posner, A. S. (1969). Crystal chemistry of bone mineral. *Physiological Reviews, 49*, 760−792.

Put, S., Vleugels, J., Anné, G., & Van der Biest, O. (2003). Functionally graded ceramic and ceramic−metal composites shaped by electrophoretic deposition. *Colloids and Surfaces A: Physicochemical and Engineering Aspects, 222*, 223−232.

Rai, M., Yadav, A., & Gade, A. (2009). Silver nanoparticles as a new generation of antimicrobials. *Biotechnology Advances, 27*, 76−83.

Rezwan, K., Chen, Q. Z., Blaker, J. J., & Boccaccini, A. R. (2006). Biodegradable and bioactive porous polymer/inorganic composite scaffolds for bone tissue engineering. *Biomaterials, 27*, 3413−3431.

Sarkar, P., & Nicholson, P. S. (1996). Electrophoretic deposition (EPD): mechanisms, kinetics, and application to ceramics. *Journal of the American Ceramic Society, 79*, 1987−2002.

Seuss, S., & Boccaccini, A. R. (2013). Electrophoretic deposition of biological macromolecules, drugs, and cells. *Biomacromolecules, 14*, 3355−3369.

Shah, N. J., Hong, J., Hyder, M. N., & Hammond, P. T. (2012). Osteophilic multilayer coatings for accelerated bone tissue growth. *Advanced Materials, 24*, 1445−1450.

Sharma, S., Patil, D. J., Soni, V. P., Sarkate, L. B., Khandekar, G. S., & Bellare, J. R. (2009a). Bone healing performance of electrophoretically deposited apatite−wollastonite/chitosan coating on titanium implants in rabbit tibiae. *Journal of Tissue Engineering and Regenerative Medicine, 3*, 501−511.

Sharma, S., Soni, V., & Bellare, J. (2009b). Chitosan reinforced apatite−wollastonite coating by electrophoretic deposition on titanium implants. *Journal of Materials Science: Materials in Medicine, 20*, 1427−1436.

Sharma, S., Soni, V., & Bellare, J. (2009c). Electrophoretic deposition of nanobiocomposites for orthopaedic applications: influence of current density and coating duration. *Journal of Materials Sciense: Materials in Medicine, 20*, S93−S100.

Song, L., Gan, L., Xiao, Y. F., Wu, Y., Wu, F., & Cu, Z. W. (2011). Antibacterial hydroxyapatite/chitosan complex coatings with superior osteoblastic cell response. *Materials Letters, 65*, 974−977.

Stamboulis, A., & Hench, L. L. (2001). Bioresorbable polymers: their potential as scaffolds for bioglass composites. *Key Engineering Materials, 192-195*, 729−732. Retrieved from http://www.scopus.com/inward/record.url?eid=2-s2.0-0035147951&partnerID=tZOtx3y1.

Sun, F., Pang, X., & Zhitomirsky, I. (2009). Electrophoretic deposition of composite hydroxyapatite−chitosan−heparin coatings. *Journal of Materials Processing Technology, 209*, 1597−1606.

Sun, F., Sask, K. N., Brash, J. L., & Zhitomirsky, I. (2008). Surface modifications of Nitinol for biomedical applications. *Colloids and Surfaces B: Biointerfaces, 67*, 132−139.

Tamjid, E., Bagheri, R., Vossoughi, M., & Simchi, A. (2011). Effect of particle size on the in vitro bioactivity, hydrophilicity and mechanical properties of bioactive glass-reinforced polycaprolactone composites. *Materials Science and Engineering: C, 31*, 1526−1533.

Tang, S., Tian, B., Guo, Y.-J., Zhu, Z.-A., & Guo, Y.-P. (2014). Chitosan/carbonated hydroxyapatite composite coatings: fabrication, structure and biocompatibility. *Surface and Coatings Technology, 251*, 210−216.

Van der Biest, O. O., & Vadeperre, L. J. (1999). Electrophoretic deposition of materials. *Annual Review of Materials Science, 29*, 327−352.

Wang, R. (2004). *Pearl powder bio-coating and patterning by electrophoretic deposition*. Andover, Hants, United Kingdom: Chapman Hall. pp. 4961−4964.

Wang, J., de Boer, J., & de Groot, K. (2004). Preparation and characterization of electrodeposited calcium phosphate/chitosan coating on Ti_6Al_4V plates. *Journal of Dental Research, 83*, 296−301.

Wang, J., de Boer, J., & de Groot, K. (2008). Proliferation and differentiation of MC3T3-E1 cells on calcium phosphate/chitosan coatings. *Journal of Dental Research, 87*, 650−654.

Wang, H., Lin, C., & Hu, R. (2009). Effects of structure and composition of the CaP composite coatings on apatite formation and bioactivity in simulated body fluid. *Applied Surface Science, 255*, 4074−4081.

Wei, M., Ruys, A. J., Milthorpe, B. K., Sorrell, C. C., & Evans, J. H. (2001). Electrophoretic deposition of hydroxyapatite coatings on metal substrates: a nanoparticulate dual-coating approach. *Journal of Sol−Gel Science and Technology, 21*, 39−48.

Wise, E. R., Maltsev, S., Davies, M. E., Duer, M. J., Jaeger, C., Loveridge, N., et al. (2007). The organic−mineral interface in bone is predominantly polysaccharide. *Chemistry of Materials, 19*, 5055−5057.

Wojtowicz, A. M., Shekaran, A., Oest, M. E., Dupont, K. M., Templeman, K. L., Hutmacher, D. W., et al. (2010). Coating of biomaterial scaffolds with the collagen-mimetic peptide GFOGER for bone defect repair. *Biomaterials, 31*, 2574−2582.

Xiao, X., Liu, R., & Tang, X. (2009a). Electrophoretic deposition of silicon-substituted hydroxyapatite/poly(epsilon-caprolactone) composite coatings. *Journal of Materials Science: Materials in Medicine, 20*, 691−697.

Xiao, J. W., Zhu, Y. C., Liu, Y. Y., Zeng, Y., & Xu, F. F. (2009b). An asymmetric coating composed of gelatin and hydroxyapatite for the delivery of water insoluble drug. *Journal of Materials Science: Materials in Medicine, 20*, 889−896.

Yuan, W., Ji, J., Fu, J., & Shen, J. (2008). A facile method to construct hybrid multilayered films as a strong and multifunctional antibacterial coating. *Journal of Biomedical Materials Research Part B: Applied Biomaterials, 85B*, 556−563.

Zhitomirsky, I. (2006). Electrophoretic deposition of organic−inorganic nanocomposites. *Journal of Materials Science, 41*, 8186−8195.

Zhitomirsky, D., Roether, J. A., Boccaccini, A. R., & Zhitomirsky, I. (2009). Electrophoretic deposition of bioactive glass/polymer composite coatings with and without HA nanoparticle inclusions for biomedical applications. *Journal of Materials Processing Technology, 209*, 1853−1860.

Zhou, J., Cai, X., Cheng, K., Weng, W., Song, C., Du, P., et al. (2011). Release behaviors of drug loaded chitosan/calcium phosphate coatings on titanium. *Thin Solid Films, 519*, 4658−4662.

Antimicrobial coatings for metallic biomaterials

13

B.D. Hatton
University of Toronto, Toronto, ON, Canada

13.1 Introduction

Metallic implants represent a significant component of biomedical treatments involving bone fracture, reconstruction, and replacement and have significantly improved the quality of life for patients in recent years. In fact, of biomaterial implants, metallic implants represent a major class of components (particularly for orthopedic fracture treatment and joint replacement) and have been largely successful since the development of advanced titanium (Ti), cobalt (Co), and stainless-steel alloys. Further, a whole new generation of three-dimensional printed Ti orthopedic implant components, directly modeled on a patient's own bone structure, is on the horizon. A recent estimate for the 2010 global annual market for orthopedic implant devices was about $30 billion, with an annual growth rate of 8.2%, which represents an overall market value upward of $50 billion by 2018 (Kargupta et al., 2014).

However, despite these successes, there are some persistent biomaterial-associated complications, such as implant loosening and infection, that affect a not insignificant percentage of clinical applications. In a 2004 study, of the 2.6 million orthopedic implants (annually, in the United States), approximately 4.3% developed infections (Darouiche, 2004). In fact, the infection rate of cardiovascular implants was even higher (7.4%). In fact, to consider all indwelling devices, the number of implant-associated infections was approximately 1 million per year in the United States alone (Darouiche, 2004). Of course, the increased rise of antibiotic-resistant bacterial strains (such as methicillin-resistant *Staphylococcus aureus*) has serious implications for the treatment of these implant-associated infections (Davies and Davies, 2010; Kåhrström, 2013). An unfortunate consequence is that implant removal (revision surgery) and/or amputation are increasingly necessary. Such incidents cause human pain and suffering, and implant-associated infections also represent a significant economic burden. In 2004 (in the United States), the direct medical cost of such infections was estimated to exceed $3 billion annually (Darouiche, 2004). Of course, in an aging society, the problem is only projected to get worse, as more patients receive biomedical implants such as hip and knee joint replacements.

This review looks specifically at coating and surface treatment approaches for reducing and preventing the bacterial infection of metallic implants. There are already some excellent reviews on antimicrobial treatments for medical implants, which cover different aspects of this subject, on general aspects of antifouling surfaces (Banerjee et al., 2011) and bacterial−surface interactions (Anselme et al., 2010;

Surface Coating and Modification of Metallic Biomaterials. http://dx.doi.org/10.1016/B978-1-78242-303-4.00013-2
Copyright © 2015 Elsevier Ltd. All rights reserved.

Harris and Richards, 2006; Hasan et al., 2013a), antibacterial coatings in general (Montali, 2006), active-release approaches (Hetrick and Schoenfisch, 2006), immobilized antibiotics on implants (Hickok and Shapiro, 2012), on the design of medical devices (Desrousseaux et al., 2013; Zilberman and Elsner, 2008), and specific approaches for orthopedic implants (Goodman et al., 2013; Kargupta et al., 2014; Zhao et al., 2009). Herein, this review does not claim to present an exhaustive list of all antimicrobial designs for metal implants, but hopes to give a broad overview of approaches to the problem, from drug release to surface nanostructure design, and present some of the latest interesting developments.

Implant-associated infections are the result of bacterial adhesion to a biomaterial surface, as the first stage in the development of a biofilm colony (Costerton et al., 1987; De Beer and Stoodley, 2006; Gilbert et al., 2003). Planktonic bacteria spontaneously seek out and adhere to surfaces, generally to derive nutrients and as a self-preservation strategy to evade an immune response. Immediately after implantation, a competition begins between the adhesion of bacteria and human cells (such as fibroblasts) to the implant surface. This competition can be considered part of the early foreign body response (Gristina, 1987). If bacteria populate and colonize that surface substantially and win that competition, they can initiate the formation of a biofilm, which has a protective extracellular matrix and is much more resistant to an immune system attack. The formation of a bacterial biofilm on an implant surface is often the origin of persistent infections within the body and can be difficult to diagnose and treat (Costerton et al., 1987; De Beer and Stoodley, 2006; Gilbert et al., 2003).

Many studies have investigated the interaction between bacteria and biomaterial implant surfaces and the material (and cellular) design factors that control bacterial cell adhesion (Anselme et al., 2010; Dunne, 2002; Gristina, 1987; Harris and Richards, 2006). Bacterial colonization of implants is enhanced by the body wound response to implantation. In particular, the body rapidly coats implanted materials with serum proteins that promote cell recruitment and tissue repair. However, these same proteins are used by pathogenic bacteria for surface adhesion. Strains such as *S. aureus* are commonly found in contaminated fracture surgery sites and compete with the host human cells to colonize the implant surface. The bacteria have a certain advantage in this 'race,' in that they divide rapidly and can be very adaptable to changing environments. The immune system of the body is typically locally weakened by the presence of a foreign body and a fractured bone (and other potential tissue injury due to surgery), and as a result, bacteria can gain an advantage in the competition (Darouiche, 2004; Gilbert et al., 2003; Gristina, 1987; Zimmerli and Ochsner, 2003).

Many approaches have been taken to prevent implant colonization by microorganisms, which can be generally classed as antiadhesion (prevents cell attachment altogether) or antibiotic (killing cells on the surface or in the local environment) (Desrousseaux et al., 2013; Gilbert et al., 2003; Zhao et al., 2009). A third approach can include the design of surface structure to encourage the proliferation of tissue on the implant, to help exclude bacterial contamination. In either respect, it is ideal to design this antibacterial property of the biomaterial implant without loss of

biocompatibility. In other words, such surface coatings or treatments should not be cytotoxic, induce an increase immune response, or delay rates of wound repair and implant integration (Goodman et al., 2013; Harris and Richards, 2006). Therefore, in the development of any antimicrobial surface treatment or coating, it is highly important to optimize the biocompatibility of the implant itself. Minimizing the foreign body response and the extent of the inflammatory zone and fibrous tissue formation around the implant will improve the long-term integration of the implant, which also directly and indirectly reduces the likelihood of infection.

13.2 Chemical/drug release

Antibiotics are typically administered following the implantation surgery of metallic implants, but despite their efficacy, systemic delivery (whole body) of antibiotics does have certain limitations in preventing infection at the implant site (Zilberman and Elsner, 2008). Toxicity can sometimes be an issue, and the amount of drug penetration into ischemic or necrotic tissue can be inadequate. If the regions surrounding the implant are not sufficiently reached by antibiotics, then bacteria may colonize (or continue to colonize) that surface, and there is a real possibility of more serious infection (Gristina, 1987). This challenge defines the need for surface coatings or treatments to prevent local bacterial attachment, colonization, infection or viability.

Most antimicrobial coatings for metallic implants involve some active chemical or drug release. As a result, an antibacterial coating that is present at the first stages of implantation will generally start releasing the active substance immediately. This type of coating has been found to work prophylactically to avoid bacterial colonization of the implant surface (Harris and Richards, 2006; Hetrick and Schoenfisch, 2006; Montali, 2006). However, the chemical release rate can be difficult to control or maintain consistently over time. At first, there is often a high local antimicrobial concentration, which can be far above the minimal inhibitory concentration (MIC) of any resident bacteria, but it drops in time (Harris and Richards, 2006; Hetrick and Schoenfisch, 2006; Montali, 2006).

There are a number of mechanisms for drug containment and release that have been investigated, which range from those at a research stage to those that are clinically applied. The drug can be incorporated into a deposited coating (polymer or inorganic), loaded into the implant by ion implantation (in the case of metal ion release), or loaded into a nanoporous surface structure, which may be coated or etched into the implant material (such as anodized nanotube surfaces (Minagar et al., 2012)).

13.2.1 Metal ion release

The release of metal ions (i.e., inorganic antimicrobial elements, such as Ag) from surface treatments or coatings is an attractive approach because such species have good antibacterial activity, excellent biocompatibility, and suitable stability under physiological conditions. Among these species, silver is the best known, based on

its usage as an antimicrobial treatment for wounds since Roman times and particularly in the twentieth century (Alexander, 2009). There are several advantages of silver as a dopant for metal implant coatings: (1) it is effective against both gram-positive and gram-negative bacteria (and some drug-resistance bacteria (Necula et al., 2009)) at low parts per billion concentrations (Chernousova and Epple, 2013; Melaiye and Youngs, 2005), (2) silver is less prone to resistance development, although there is some evidence of growing resistance, and (3) it has good biocompatibility without cytotoxicity and few signs of adverse effects (in vivo) (Bosetti et al., 2002; Chernousova and Epple, 2013; Hardes et al., 2007). In terms of biomaterial performance, silver doping seems to inhibit bacterial adhesion and growth without compromising the activity of osteoblasts and epithelial cells (Chen et al., 2006; Gosheger et al., 2004).

Silver has been added as a dopant (typically as nanoparticles) to a wide range of biomaterial types, including polymers, bioactive glass and ceramics, and metals (Chernousova and Epple, 2013). Cui and Luo (1999) have reviewed methods of ion-beam-based processes, such as ion implantation and ion-beam-assisted deposition.

Based on this extensive background, there are several examples of silver being added to metallic implants. For example, for Ti, silver has been ion implanted into Ti and Ti−Al−Nb alloys (Wan et al., 2007). In another example, a particulate silver coating was deposited on stainless steel (Devasconcellos et al., 2012). Moseke et al. (2011) used physical vapor deposition to deposit silver-doped TiN coatings on Ti substrates, in which the TiN coating maintains good mechanical strength against wear. Svensson et al. (2013) tested the deposition and antimicrobial activity of a nanostructured coating consisting of palladium, gold, and silver to Ti screws for bone repair.

There are also several examples of hydroxyapatite (HAp) coatings containing silver particles. A silver-containing HAp coating has been produced on Ti by magnetron sputtering (Chen et al., 2006), and plasma-sprayed HAp coatings (Fielding et al., 2012).

Copper has also been tested as an antimicrobial additive (Heidenau et al., 2005; Wan et al., 2007). Heidenau et al. (2005) showed that the best antibacterial effectiveness was reached for a Cu−TiO_2 surface coating, which caused a decrease of surface bacteria counts by more than six orders of magnitude. They proposed that even high copper ion concentrations are tolerable for tissue cells. Also, nitric oxide can act as a potent antimicrobial agent (Fang, 1997). Nablo et al. (2005) deposited nitric oxide-releasing xerogel coatings onto stainless-steel substrates to assess their antibacterial activity for orthopedic implant applications. The coated stainless steel was shown to significantly reduce *Pseudomonas aeruginosa* adhesion, compared to controls (xerogel-coated and bare stainless steel). The authors also found significant reduction for *S. aureus* and *S. epidermidis*, using zeolite-based coatings (Fox et al., 2010).

13.2.2 Antibiotic drug release

Antibiotics are generally administered to patients who receive implants as a systemic prophylaxis to prevent infection postsurgery (Ketonis et al., 2012; Zilberman and

Elsner, 2008). However, as mentioned above, a systemic dose of antibiotics can result in a relatively low-drug concentration at the target site. Sublethal antibiotic concentrations provide an ideal environment for selecting resistant bacterial strains, which can contribute to the growing problem of antibiotic resistance. As a result, the local, topical delivery of antibiotics has certain important advantages over systemic delivery and has been developed and used for the past 40 years (Lucke et al., 2003; Radin and Ducheyne, 2007; Zilberman and Elsner, 2008).

Gentamicin is perhaps the most widely used antibiotic for coatings on metal implants and is one of the few types of antibiotics that is thermally stable. Gentamicin is an aminoglycoside antibiotic and is relatively broadly effective, although there are many others with broad antibacterial activity, such as vancomycin and amoxicillin, that have also been used in bone implant coatings.

Antibiotics have usually been loaded onto (or into) metallic implants by means of a porous ceramic coating or loaded into the nanopores of an anodized oxide surface (Hatton, 2013; Minagar et al., 2012). Calcium phosphate coatings are biocompatible and osteoconductive (Bose and Tarafder, 2012; Verron et al., 2010), and various studies have involved porous HAp coatings loaded with antibiotics (Alt et al., 2006; Radin et al., 1997; Stigter et al., 2004; Yamamura et al., 1992). The drug-loaded HAp coatings typically show significant improvement in infection prophylaxis (compared with standard HAp coatings in vivo). But one problem is that antibiotics cannot be incorporated directly into the calcium phosphate coatings formed by plasma spraying due to the high processing temperatures. Also, physical absorption onto the surface of calcium phosphates after deposition can be limited, which reduces the total drug amount and control over the release rates. As a result, several studies have developed co-precipitation methods for calcium phosphate deposition with drug incorporation (Stigter et al., 2004).

The concentrations of antibiotics near the implant surface can become significant shortly after the release from an antibiotic-loaded implant coating.

It is important that any antibacterial coating be designed with two important factors in mind: the choice of an antibiotic and the delivery release kinetics. The latter must be designed to minimize any antibiotic exposure time at concentrations below the minimum inhibitory concentration (MIC) of the bacteria present. Therefore, there is always a potential risk of developing a resistance, compared to the potential benefit to prevent an implant-related infection.

Another approach for antibiotic drug release is the use of biodegradable polymer coatings, such as poly (D,L-lactide) (PDLLA). Gollwitzer et al. (2003) showed that PDLLA coatings containing gentamicin showed a continuous drug release for 96 h, with an initial burst in the first 6 h. As expected, this drug release was shown to kill bacteria (*S. epidermidis*) locally; however, this particular example does not allow for longer-term control of release.

Hickok and Shapiro (2012) have reviewed the application and success of immobilized antibiotics for orthopedic implants. In some cases, the activity of the antibiotic is retained even when the biomolecule is covalently bound to the surface. Vancomycin has been successfully covalently bonded to titanium, and its antibacterial activity is

retained when tested in vitro. This approach has some advantages in that the antibiotics are not released and lost in the body (with potential adverse effects), but because proteins are quickly deposited onto the implant surface following implantation, it is not clear if surface-bound antibiotics are still active through this protein layer.

13.2.3 Organic antimicrobial drug release

Non-antibiotic (organic) antimicrobial agents, such as chlorhexidine, chloroxylenol, and poly(hexamethylenebiguanide), are good alternatives to antibiotics because of the potential for drug resistance with antibiotics (Nigam et al., 2014; Zilberman and Elsner, 2008). Non-antibiotic antimicrobials have a broad spectrum of antimicrobial activity and a much lower chance of drug resistance. Certain of these drugs, such as chlorhexidine, are commonly used in dentistry to treat periodontal infection and in various brands of mouthwash.

Various approaches have been made to test the release of antimicrobial agents (chlorhexidine) from metal implant surfaces. The simplest approach has been desorption from the (unmodified) metal surface, such as Ti. The physical adsorption of chlorhexidine onto the TiO_2 surface is spontaneous and desorption occurs over several days, but there is little room for control or ways of extending that release time (Kozlovsky et al., 2006).

Other studies have incorporated chlorhexidine into coatings such as polymer (Harris et al., 2006), mineral (Campbell et al., 2000), and collagen-based layers. Harris et al. (2006) have compared the release rates of chlorhexidine from several kinds of polymer coatings, such as PDLLA and polyurethane, on titanium surfaces. They found that PDLLA allowed the slowest release (over 200 h), but is not cytotoxic and has suitable mechanical properties.

13.3 Surface treatments to affect physical adhesion

13.3.1 PEG and surface exclusion

In the past 20 years, there has been a significant study into the exclusion of protein adsorption and bacterial adhesion by hydrophilic polymer coatings such as poly(methacrylic acid) and poly(ethylene glycol) (PEG) (Michel et al., 2005; Ostuni et al., 2001). These polymers are covalently grafted onto substrates and often form a 'brush' structure, oriented perpendicular to the surface. These polymer coatings appear to prevent or delay bacterial adhesion by attracting a local, 'structured' water layer at the material surface. Such coatings can be deposited onto metal implant surfaces by relatively simple methods (Gao et al., 2011; Harris et al., 2004).

While bacterial adhesion is impaired, one problem is that human cell adhesion (osteoblast and fibroblast) is also impaired and reduced by the same mechanism. However, the human cell activity and function can be improved by the addition of bioactive molecules having the arginine-glycine-aspartic acid (RGD) sequence.

Khoo et al. (2009) showed that a PEG coating could be developed with noncovalent binding by using a short peptide possessing affinity for Ti (identified using a phage display screening process), to simplify the coating process. This PEG-modified analog of the peptide was coated onto Ti and found to prevent the adsorption of fibronectin and significantly reduce *S. aureus* attachment and biofilm formation in vitro.

Gao et al. (2011) tested the bacterial activity of polymer brush coatings on metal implants consisting of hydrophilic polymer chains conjugated with an optimized series of antimicrobial peptides. They found a broad spectrum antimicrobial activity in vitro and in vivo to resist biofilm formation.

13.3.2 Surface topology and wetting modification

There is a strong incentive to find nanostuctured and microstructured topologies that can affect and prevent bacterial attachment to metallic implants, because this kind of approach should have broad spectrum activity and would avoid regulatory approvals involving chemically modified surfaces and coatings. The effects of surface nanostructured roughness (topology) on bacterial attachment and biofilm formation are complex and not fully understood (Anselme et al., 2010; Crawford et al., 2012). Graham and Cady (2014) have presented a recent review on the effects of nanoscale and microscale topologies on bacterial adhesion and growth. These are new areas of research — there are few examples, so far, of implementations of surface roughness or wettability properties to control bacterial adhesion in metal implants, but research is underway.

Surfaces with roughness or surface topologies at the microscale have been shown to influence cell orientation, and in some cases, cell attachment rates. Hochbaum and Aizenberg (2010) showed that the spacing of submicron Si posts can affect the general order of cell orientation, but there were no overall effects on the rates of biofilm growth.

Diaz et al. (2009) showed that ordered groove microstructures can have a small (but measurable) effect to reduce biofilm growth rates. There is likely some role of local, microfluidic flow effects at the surface due to these surface microstructures, which remains an area of research to fully understand (Halder et al., 2013). An often-cited study, based on the reproduction of shark skin surface morphology, suggests that these structures can reduce bacterial biofilm growth, although the mechanism for this is not well developed and may be related to microfluidic effects (Chung et al., 2007).

Ivanova et al. (2012) suggested that high aspect ratio, sharp nanoscale features, such as those found on cicada wings, dragonfly wings, and black silicon can physically damage and kill bacterial cells (Figure 13.2) (Hasan et al., 2013b). These results are promising for the development of coatings for metal implants, but the details of this mechanism remain unclear.

Patterned surface wettability has been shown to affect bacterial retention. Bos et al. (2000) tested bacterial adhesion on a surface patterned with hydrophobic and hydrophilic patches of 10-μm size. They found that the adhesion rates were similar for all surfaces, but that the strength of cell adhesion (using a parallel plate flow chamber) was much less for hydrophobic surfaces.

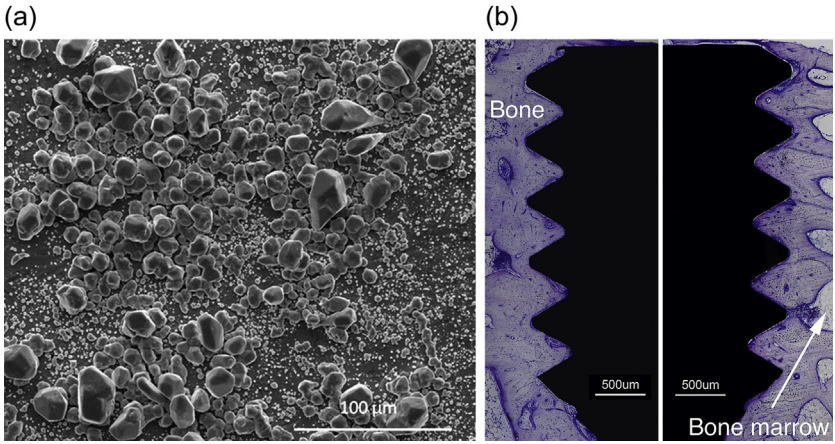


Figure 13.1 (a) Scanning electron microscopy images of electro-deposited silver particles on 316L stainless steel. (From Devasconcellos et al. (2012).) (b) Histological sections showing the extent of bone formation in a rabbit femur, after 12 weeks of implantation for Ti screws coated with a mixed noble metal plating of Pd, Ag, and Au. (From Svensson et al. (2013).) There was no histological difference between the noble metal coated (right) and control (left) implants, indicating insignificant signs of cytotoxicity.

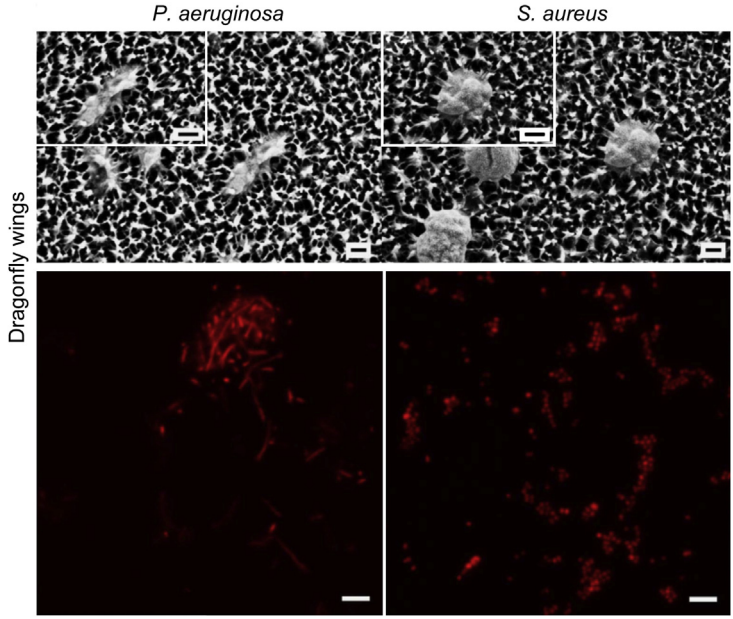


Figure 13.2 Scanning electron microscopy images of *Pseudomonas aeruginosa* and *Staphylococcus aureus* (top) and confocal fluorescence images (bottom), showing physical damage of cells on a nanostructured dragonfly wing. (From Ivanova et al. (2013).) The red color indicates the presence of dead cells, through live/dead staining.

Genzer and Efimenko (2006) have reviewed the applications of superhydrophobic surfaces, which are non-wetting surfaces with high contact angles (>150°), to prevent biofouling in general. The Cassie-Baxter superhydrophobic condition keeps the liquid interface at the tips of rough, hydrophobic topological features. While this should prevent bacterial attachment and biofilm formation, it has been found that this wetting state is metastable and does not persist for long, especially in long-term, implant conditions.

A new approach altogether to prevent bacterial attachment is to design a microstructured surface to contain a thin, inert lubricant liquid layer that is energetically bound to the surface, known as slippery liquid-infused porous surfaces, or SLIPS (Wong et al., 2011). A few studies on different SLIPS have demonstrated a real resistance to protein and bacterial cell adhesion (Epstein et al., 2012; Maccallum et al., 2015; Vogel et al., 2013). However, as for hydrophilic polymer brush surfaces (such as PEG), complete nonadhesion to proteins and other biomolecules also will impair the adhesion of cells such as fibroblasts and osteoblasts. Therefore, SLIPS still need some development for biomaterial implant applications.

13.4 Summary and conclusions

Metal implants and biomaterial implants in general improve the quality of life through the treatment of disease and by offsetting the effects of aging. The general trend of increasing life expectancy will consistently lead to a greater demand for medical implants, such as orthopedic joint replacements. As a result, we should also expect to see consistent problems of implant-associated infections as this trend continues.

This review has attempted to summarize some of the approaches taken to treat the surfaces of metal implants to reduce the rates of bacterial adhesion, colonization, biofilm formation and the general problem of implant-related infection within the body. All of these approaches must deal with the same challenge of providing a surface treatment that does not compromise the function of the implant itself, prevents bacterial colonization (by antimicrobial drug activity or by preventing adhesion itself), and is not toxic to the host tissue itself. There are a number of challenges in this research, to assess the performance of such coatings in vivo and ultimately develop them for clinical use. Nevertheless, the high financial and medical costs of implant infections ensure that such research will continue, and new approaches to control bacterial infection on metal biomaterial implants will emerge.

References

Alexander, J. W. (2009). History of the medical use of silver. *Surgical Infections, 10*, 289–292.

Alt, V., Bitschnau, A., Österling, J., Sewing, A., Meyer, C., Kraus, R., et al. (2006). The effects of combined gentamicin–hydroxyapatite coating for cementless joint prostheses on the reduction of infection rates in a rabbit infection prophylaxis model. *Biomaterials, 27*, 4627–4634.

Anselme, K., Davidson, P., Popa, A., Giazzon, M., Liley, M., & Ploux, L. (2010). The interaction of cells and bacteria with surfaces structured at the nanometre scale. *Acta Biomaterialia, 6*, 3824−3846.

Banerjee, I., Pangule, R. C., & Kane, R. S. (2011). Antifouling coatings: recent developments in the design of surfaces that prevent fouling by proteins, bacteria, and marine organisms. *Advanced Materials, 23*, 690−718.

Bose, S., & Tarafder, S. (2012). Calcium phosphate ceramic systems in growth factor and drug delivery for bone tissue engineering: a review. *Acta Biomaterialia, 8*, 1401−1421.

Bosetti, M., Masse, A., Tobin, E., & Cannas, M. (2002). Silver coated materials for external fixation devices: in vitro biocompatibility and genotoxicity. *Biomaterials, 23*, 887−892.

Bos, R., Van Der Mei, H. C., Gold, J., & Busscher, H. J. (2000). Retention of bacteria on a substratum surface with micro-patterned hydrophobicity. *FEMS Microbiology Letters, 189*, 311−315.

Campbell, A. A., Song, L., Li, X. S., Nelson, B. J., Bottoni, C., Brooks, D. E., et al. (2000). Development, characterization, and anti-microbial efficacy of hydroxyapatite−chlorhexidine coatings produced by surface-induced mineralization. *Journal of Biomedical Materials Research, 53*, 400−407.

Chen, W., Liu, Y., Courtney, H., Bettenga, M., Agrawal, C., Bumgardner, J., et al. (2006). In vitro anti-bacterial and biological properties of magnetron co-sputtered silver-containing hydroxyapatite coating. *Biomaterials, 27*, 5512−5517.

Chernousova, S., & Epple, M. (2013). Silver as antibacterial agent: ion, nanoparticle, and metal. *Angewandte Chemie International Edition, 52*, 1636−1653.

Chung, K. K., Schumacher, J. F., Sampson, E. M., Burne, R. A., Antonelli, P. J., & Brennan, A. B. (2007). Impact of engineered surface microtopography on biofilm formation of *Staphylococcus aureus*. *Biointerphases, 2*, 89−94.

Costerton, J. W., Cheng, K. J., Geesey, G. G., Ladd, T. I., Nickel, J. C., Dasgupta, M., et al. (1987). Bacterial biofilms in nature and disease. *Annual Review of Microbiology, 41*, 435−464.

Crawford, R. J., Webb, H. K., Truong, V. K., Hasan, J., & Ivanova, E. P. (2012). Surface topographical factors influencing bacterial attachment. *Advances in Colloid and Interface Science, 179*, 142−149.

Cui, F., & Luo, Z. (1999). Biomaterials modification by ion-beam processing. *Surface and Coatings Technology, 112*, 278−285.

Darouiche, R. O. (2004). Treatment of infections associated with surgical implants. *New England Journal of Medicine, 350*, 1422−1429.

Davies, J., & Davies, D. (2010). Origins and evolution of antibiotic resistance. *Microbiology and Molecular Biology Reviews, 74*, 417−433.

De Beer, D., & Stoodley, P. (2006). Microbial biofilms. *Prokaryotes, 1*, 904−937.

Desrousseaux, C., Sautou, V., Descamps, S., & Traoré, O. (2013). Modification of the surfaces of medical devices to prevent microbial adhesion and biofilm formation. *Journal of Hospital Infection, 85*, 87−93.

Devasconcellos, P., Bose, S., Beyenal, H., Bandyopadhyay, A., & Zirkle, L. G. (2012). Antimicrobial particulate silver coatings on stainless steel implants for fracture management. *Materials Science and Engineering: C, 32*, 1112−1120.

Diaz, C., Schilardi, P. L., Dos Santos Claro, P. C., Salvarezza, R. C., & Fernandez Lorenzo De Mele, M. A. (2009). Submicron trenches reduce the *Pseudomonas fluorescens* colonization rate on solid surfaces. *ACS Applied Materials and Interfaces, 1*(1), 136−143.

Dunne, W. M. (2002). Bacterial adhesion: seen any good biofilms lately? *Clinical Microbiology Reviews, 15*, 155−166.

Epstein, A. K., Wong, T. S., Belisle, R. A., Boggs, E. M., & Aizenberg, J. (2012). Liquid-infused structured surfaces with exceptional anti-biofouling performance. *Proceedings of the National Academy of Sciences, 109*, 13182−13187.

Fang, F. C. (1997). Perspectives series: host/pathogen interactions. Mechanisms of nitric oxide-related antimicrobial activity. *Journal of Clinical Investigation, 99*, 2818.

Fielding, G. A., Roy, M., Bandyopadhyay, A., & Bose, S. (2012). Antibacterial and biological characteristics of silver containing and strontium doped plasma sprayed hydroxyapatite coatings. *Acta Biomaterialia, 8*, 3144−3152.

Fox, S., Wilkinson, T. S., Wheatley, P. S., Xiao, B., Morris, R. E., Sutherland, A., et al. (2010). NO-loaded Zn^{2+}-exchanged zeolite materials: a potential bifunctional anti-bacterial strategy. *Acta Biomaterialia, 6*, 1515−1521.

Gao, G., Lange, D., Hilpert, K., Kindrachuk, J., Zou, Y., Cheng, J. T., et al. (2011). The biocompatibility and biofilm resistance of implant coatings based on hydrophilic polymer brushes conjugated with antimicrobial peptides. *Biomaterials, 32*, 3899−3909.

Genzer, J., & Efimenko, K. (2006). Recent developments in superhydrophobic surfaces and their relevance to marine fouling: a review. *Biofouling, 22*, 339−360.

Gilbert, P., Mcbain, A. J., Rickard, A. H., & Schooling, S. R. (2003). Control of biofilms associated with implanted medical devices. *Medical Biofilms: Detection, Prevention and Control*, 73−96.

Gollwitzer, H., Ibrahim, K., Meyer, H., Mittelmeier, W., Busch, R., & Stemberger, A. (2003). Antibacterial poly (D, l-lactic acid) coating of medical implants using a biodegradable drug delivery technology. *Journal of Antimicrobial Chemotherapy, 51*, 585−591.

Goodman, S. B., Yao, Z., Keeney, M., & Yang, F. (2013). The future of biologic coatings for orthopaedic implants. *Biomaterials, 34*, 3174−3183.

Gosheger, G., Hardes, J., Ahrens, H., Streitburger, A., Buerger, H., Erren, M., et al. (2004). Silver-coated megaendoprostheses in a rabbit model—an analysis of the infection rate and toxicological side effects. *Biomaterials, 25*, 5547−5556.

Graham, M. V., & Cady, N. C. (2014). Nano and microscale topographies for the prevention of bacterial surface fouling. *Coatings, 4*, 37−59.

Gristina, A. G. (1987). Biomaterial-centered infection: microbial adhesion versus tissue integration. *Science, 237*, 1588−1595.

Halder, P., Nasabi, M., Lopez, F. J. T., Jayasuriya, N., Bhattacharya, S., Deighton, M., et al. (2013). A novel approach to determine the efficacy of patterned surfaces for biofouling control in relation to its microfluidic environment. *Biofouling, 29*, 697−713.

Hardes, J., Ahrens, H., Gebert, C., Streitbuerger, A., Buerger, H., Erren, M., et al. (2007). Lack of toxicological side-effects in silver-coated megaprostheses in humans. *Biomaterials, 28*, 2869−2875.

Harris, L., Mead, L., Müller-Oberländer, E., & Richards, R. (2006). Bacteria and cell cytocompatibility studies on coated medical grade titanium surfaces. *Journal of Biomedical Materials Research Part A, 78*, 50−58.

Harris, L. G., & Richards, R. G. (2006). Staphylococci and implant surfaces: a review. *Injury, 37*, S3−S14.

Harris, L., Tosatti, S., Wieland, M., Textor, M., & Richards, R. (2004). *Staphylococcus aureus* adhesion to titanium oxide surfaces coated with non-functionalized and peptide-functionalized poly (L-lysine)-grafted-poly (ethylene glycol) copolymers. *Biomaterials, 25*, 4135−4148.

Hasan, J., Crawford, R. J., & Ivanova, E. P. (2013a). Antibacterial surfaces: the quest for a new generation of biomaterials. *Trends in Biotechnology, 31*, 295−304.

Hasan, J., Webb, H. K., Truong, V. K., Pogodin, S., Baulin, V. A., Watson, G. S., et al. (2013b). Selective bactericidal activity of nanopatterned superhydrophobic cicada Psaltoda claripennis wing surfaces. *Applied Microbiology and Biotechnology, 97*, 9257−9262.

Hatton, B. D. (2013). Engineering nanoporous biomaterials. In A. K. Gaharwar, S. Sant, M. J. Hancock, & S. A. Hacking (Eds.), *Nanomaterials in tissue engineering*. Woodhead Publishing.

Heidenau, F., Mittelmeier, W., Detsch, R., Haenle, M., Stenzel, F., Ziegler, G., et al. (2005). A novel antibacterial titania coating: metal ion toxicity and in vitro surface colonization. *Journal of Materials Science: Materials in Medicine, 16*, 883−888.

Hetrick, E. M., & Schoenfisch, M. H. (2006). Reducing implant-related infections: active release strategies. *Chemical Society Reviews, 35*, 780−789.

Hickok, N. J., & Shapiro, I. M. (2012). Immobilized antibiotics to prevent orthopaedic implant infections. *Advanced Drug Delivery Reviews, 64*, 1165−1176.

Hochbaum, A. I., & Aizenberg, J. (2010). Bacteria pattern spontaneously on periodic nanostructure arrays. *Nano Letters, 10*, 3717−3721.

Ivanova, E. P., Hasan, J., Webb, H. K., Gervinskas, G., Juodkazis, S., Truong, V. K., et al. (2013). Bactericidal activity of black silicon. *Nature Communications, 4*, 1−7.

Ivanova, E. P., Hasan, J., Webb, H. K., Truong, V. K., Watson, G. S., Watson, J. A., et al. (2012). Natural bactericidal surfaces: mechanical rupture of *Pseudomonas aeruginosa* cells by cicada wings. *Small, 8*, 2489−2494.

Kåhrström, C. T. (2013). Entering a post-antibiotic era? *Nature Reviews Microbiology, 11*, 146, 146.

Kargupta, R., Bok, S., Darr, C. M., Crist, B. D., Gangopadhyay, K., Gangopadhyay, S., et al. (2014). Coatings and surface modifications imparting antimicrobial activity to orthopedic implants. *Wiley Interdisciplinary Reviews: Nanomedicine and Nanobiotechnology, 6*, 475−495.

Ketonis, C., Parvizi, J., & Jones, L. C. (2012). Evolving strategies to prevent implant-associated infections. *Journal of the American Academy of Orthopaedic Surgeons, 20*, 478−480.

Khoo, X., Hamilton, P., O'toole, G. A., Snyder, B. D., Kenan, D. J., & Grinstaff, M. W. (2009). Directed assembly of PEGylated-peptide coatings for infection-resistant titanium metal. *Journal of the American Chemical Society, 131*, 10992−10997.

Kozlovsky, A., Artzi, Z., Moses, O., Kamin-Belsky, N., & Greenstein, R. B.-N. (2006). Interaction of chlorhexidine with smooth and rough types of titanium surfaces. *Journal of Periodontology, 77*, 1194−1200.

Lucke, M., Schmidmaier, G., Sadoni, S., Wildemann, B., Schiller, R., Haas, N., et al. (2003). Gentamicin coating of metallic implants reduces implant-related osteomyelitis in rats. *Bone, 32*, 521−531.

Maccallum, N., Friedlander, R., Howell, C., Lin, J., Sun, D., Wong, T. S., et al. (2015). Oil-infused silicone tubing as a biomedical material that prevents bacterial accumulation. *ACS Biomaterials Science and Engineering, 1*, 43−51.

Melaiye, A., & Youngs, W. J. (2005). Silver and its application as an antimicrobial agent. *Expert Opinion on Therapeutic Patents, 15*, 125−130.

Michel, R., Pasche, S., Textor, M., & Castner, D. G. (2005). Influence of PEG architecture on protein adsorption and conformation. *Langmuir, 21*, 12327−12332.

Minagar, S., Berndt, C. C., Wang, J., Ivanova, E., & Wen, C. (2012). A review of the application of anodization for the fabrication of nanotubes on metal implant surfaces. *Acta Biomaterialia, 8*, 2875−2888.

Montali, A. (2006). Antibacterial coating systems. *Injury, 37*, S81−S86.

Moseke, C., Gbureck, U., Elter, P., Drechsler, P., Zoll, A., Thull, R., et al. (2011). Hard implant coatings with antimicrobial properties. *Journal of Materials Science: Materials in Medicine, 22*, 2711−2720.

Nablo, B. J., Rothrock, A. R., & Schoenfisch, M. H. (2005). Nitric oxide-releasing sol−gels as antibacterial coatings for orthopedic implants. *Biomaterials, 26*, 917−924.

Necula, B. S., Fratila-Apachitei, L. E., Zaat, S. A., Apachitei, I., & Duszczyk, J. (2009). In vitro antibacterial activity of porous TiO_2−Ag composite layers against methicillin-resistant *Staphylococcus aureus*. *Acta Biomaterialia, 5*, 3573−3580.

Nigam, A., Gupta, D., & Sharma, A. (2014). Treatment of infectious disease: beyond antibiotics. *Microbiological Research, 169*(9-10), 643−651.

Ostuni, E., Chapman, R. G., Liang, M. N., Meluleni, G., Pier, G., Ingber, D. E., et al. (2001). Self-assembled monolayers that resist the adsorption of proteins and the adhesion of bacterial and mammalian cells. *Langmuir, 17*, 6336−6343.

Radin, S., Campbell, J. T., Ducheyne, P., & Cuckler, J. M. (1997). Calcium phosphate ceramic coatings as carriers of vancomycin. *Biomaterials, 18*, 777−782.

Radin, S., & Ducheyne, P. (2007). Controlled release of vancomycin from thin sol−gel films on titanium alloy fracture plate material. *Biomaterials, 28*, 1721−1729.

Stigter, M., Bezemer, J., De Groot, K., & Layrolle, P. (2004). Incorporation of different antibiotics into carbonated hydroxyapatite coatings on titanium implants, release and antibiotic efficacy. *Journal of Controlled Release, 99*, 127−137.

Svensson, S., Suska, F., Emanuelsson, L., Palmquist, A., Norlindh, B., Trobos, M., et al. (2013). Osseointegration of titanium with an antimicrobial nanostructured noble metal coating. *Nanomedicine: Nanotechnology, Biology and Medicine, 9*, 1048−1056.

Verron, E., Khairoun, I., Guicheux, J., & Bouler, J.-M. (2010). Calcium phosphate biomaterials as bone drug delivery systems: a review. *Drug Discovery Today, 15*, 547−552.

Vogel, N., Belisle, R., Hatton, B. D., Wong, T. S., & Aizenberg, J. (2013). Fully transparent, omniphobic surfaces and based on inverse colloidal monolayers. *Nature Communications, 4*.

Wan, Y., Raman, S., He, F., & Huang, Y. (2007). Surface modification of medical metals by ion implantation of silver and copper. *Vacuum, 81*, 1114−1118.

Wong, T. S., Kang, S. H., Tang, S. K. Y., Smythe, E. J., Hatton, B. D., Grinthal, A., et al. (2011). Bioinspired self-repairing slippery surfaces with pressure-stable omniphobicity. *Nature, 477*, 443−447.

Yamamura, K., Iwata, H., & Yotsuyanagi, T. (1992). Synthesis of antibiotic-loaded hydroxyapatite beads and in vitro drug release testing. *Journal of Biomedical Materials Research, 26*, 1053−1064.

Zhao, L., Chu, P. K., Zhang, Y., & Wu, Z. (2009). Antibacterial coatings on titanium implants. *Journal of Biomedical Materials Research Part B: Applied Biomaterials, 91*, 470−480.

Zilberman, M., & Elsner, J. J. (2008). Antibiotic-eluting medical devices for various applications. *Journal of Controlled Release, 130*, 202−215.

Zimmerli, W., & Ochsner, P. (2003). Management of infection associated with prosthetic joints. *Infection, 31*, 99−108.

Polymer-based degradable coatings for metallic biomaterials

14

N. Scharnagl, C. Blawert
Helmholtz-Zentrum Geesthacht, Centre for Materials and Coastal Research, Institute of Materials Research, Geesthacht, Germany

14.1 Introduction

As material science and biomedical technology advance together, the need for biomaterials that can temporarily or permanently replace damaged tissue and induce tissue regeneration is also increasing (Langer and Vacanti, 1993; Williams, 2009). Tissue engineering, encompassing the efforts from biomedical and material science, aims to develop biomaterials and technologies so that the damaged tissues can be either replaced by biomaterial substitutes (e.g. biomaterial implants) (Arcos et al., 2014) or regenerated with the help of biomaterials as temporary substitute for the extracellular matrix. Thus, biomaterials play a crucial role in tissue engineering (Zdrahala and Zdrahala, 1999b), which covers the area of controlling individual cellular behavior and providing the microenvironment to support regeneration such as being a matrix to direct tissue formation and promote vascularization (Barbieri et al., 2013; Langer, 2013; Scharnagl et al., 2010).

Surface modification is a very useful tool for manipulating surface characteristics. This technology is even more important when it comes to implantable metallic or nonmetallic biomedical materials (Sankara Narayanan et al., 2014), because specific interactions with in vivo environments mostly occur on the surface or subsurface and these phenomena are often unpredictable and uncontrollable. Therefore, many biomedical devices are coated or grafted with target molecules, proteins, particles, or polymers. The current trend in biomaterial development is moving toward the use of degradable materials that have extended functionalities and advantages in the fields of tissue engineering and drug delivery. Therefore the material has to fulfil the specific therapeutic tasks and has to degrade subsequently while being harmlessly excreted from the body over time. Furthermore, in cases in which they are used as coatings for erodible metallic implants, their functionality has to be extended for taking over the control of the degradation process (e.g. if magnesium or magnesium alloys are used).

This requires that the materials which are used as biodegradable medical implants or devices have to provide the following important properties:

- Degradation time for coating, implant material, and complete component should be matched to the regeneration or required therapy time
- Mechanical properties of the complete component must be suited to the required task

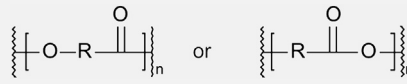
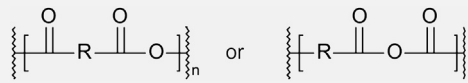
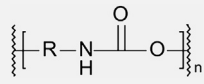
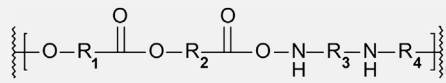
Surface Coating and Modification of Metallic Biomaterials. http://dx.doi.org/10.1016/B978-1-78242-303-4.00014-4
Copyright © 2015 Elsevier Ltd. All rights reserved.

- The materials have to be nontoxic and endotoxin-free, aiming to minimize unwanted foreign body responses upon implantation
- Degradation products should be nontoxic and readily cleared from the body
- Materials must be easily processed to allow tailoring for the required task.

For a long time, natural polymers have been used in medical applications. However, synthetic polymers are also valuable and have the advantage to allow tailoring of properties such as mechanical strength and degradation behavior (Phua et al., 2011). The disadvantage of natural polymers is their degradation by enzymatic mechanisms at a rate that might be more or less undefined and makes them not usable for clinical applications. Furthermore, critical effects are caused by their inherent biological activity. Therefore synthetic polymers that are biodegradable have been adopted more and more for medical applications. The following chapters deal with the mostly used synthetic polymer classes that are presented in Table 14.1.

Today, many of the polymers applied for clinical applications are linear homopolymers like polystyrene. For these polymers the chemical structure is determined by the repeating unit resulting from the chemical structure of the monomer. Up to a certain limit the physical properties depend on the molecular weight (M_n) of a polymer. For example, up to a certain M_n, melting and boiling temperatures increase as well as the glass transition temperature, strength, and toughness, whereas the chain mobility decreases. Influences of polymer end groups are only relevant for low molecular weights where the ratio of the end group to the repeating unit is low. With increasing M_n, the ratio is shifted toward the number of repeating units and the number of end groups, which can offer interface for fixing the coating on a substrate as well as interaction with cells from the environment, become more and more negligible.

Table 14.1 Examples of synthetic polymer classes used as biodegradable material

Polyesters (PEs)	
Polyanhydrides (PAs)	
Polyurethanes (PUs)	
Poly(ester amide)s (PEAs)	

Synthetic copolymers typically contain only two or three different repeating units in comparison to natural copolymers. They can be classified according to their sequence structure including:

- Random copolymers representing copolymers in which the sequence of repeating units follows a statistical random distribution
- Alternating copolymers with regular alternating A and B units
- Block copolymers comprising two or more homopolymer chain segments linked by covalent bonds.

The sequence structure can be characterized by nuclear magnetic resonance methods.

These include: Besides linear chains, macromolecules can have different molecular architectures. The deviation from linearity in such architectures essentially arises from the incorporation of branching points along the polymeric chains. In this way, polymers with three-dimensional geometries can be prepared. This extra dimensionality is based on the molecular, subnanometer scale, but it can have far-reaching consequences for the bulk properties of polymeric materials as a whole. The most relevant architectures to be considered for current biomaterials (Albertsson and Varma, 2003) are schematically shown in Figure 14.1. These common two-dimensional structures

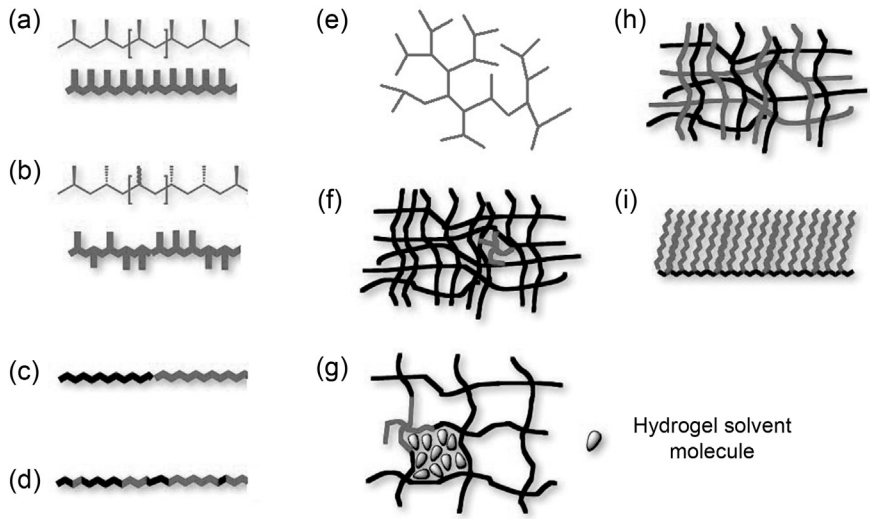


Figure 14.1 Schematic view of common polymer structures and architectures employed in the preparation of cell-specific materials including: (a) isotactic linear homopolymer; (b) atactic linear homopolymer; (c) block copolymer; (d) random copolymer; and (e) hyperbranched polymer showing the abundance of end groups; (f) collapsed polymer network constructed from a tetrameric macromonomer (gray); (g) swollen hydrogel network constructed of a tetrameric macromonomer (bottom left void space drawn with solvent molecules included); (h) interpenetrating networks (IPN) formulated from two polymer networks (gray and black); (i) grafted polymer brush.
Reprinted from Scharnagl et al. (2010) – reproduced with permission from The Royal Society of Chemistry.

may be described as grafted polymers (polymer brushes), hyperbranched polymers, or polymer networks.

14.2 Degradable polymer systems

14.2.1 Polyesters and copolyesters

In principle, polyesters can be synthesized from alcohols, diols, and carboxylic or dicarboxylic acids by a direct polycondensation reaction. Other synthesis processes are self-polycondensation of hydroxycarboxylic acids or ring-opening polymerization of lactides and lactones (Figure 14.2), which is the most used method for commercially available biodegradable polyesters (Okada, 2002). The major disadvantages for synthesis by condensation reaction are high reaction temperatures and long reaction times to obtain high-molecular-weight polymers, whereas, in addition, these polymers do not have well-controllable chain lengths. Although there is a restriction in monomers, ring-opening polymerization can be carried out under milder conditions and produces high-molecular-weight polymers within less time. Development and progress in initiators and catalytic compounds also for living polymerization enabled the production of polyesters with controlled chain length and copolyesters with specific composition. The development of enzyme-catalyzed polymerization processes offered a way toward high regiospecificity and stereospecificity of the synthesis.

The huge number of catalysts represent the popularity of the ring-opening polymerization mechanism, whereas the nature of the initiator might be anionic, cationic, and nucleophilic or it starts a coordinative chain growth. The variability of catalysts also represents the still-ongoing discussion of reaction mechanisms for the ring-opening

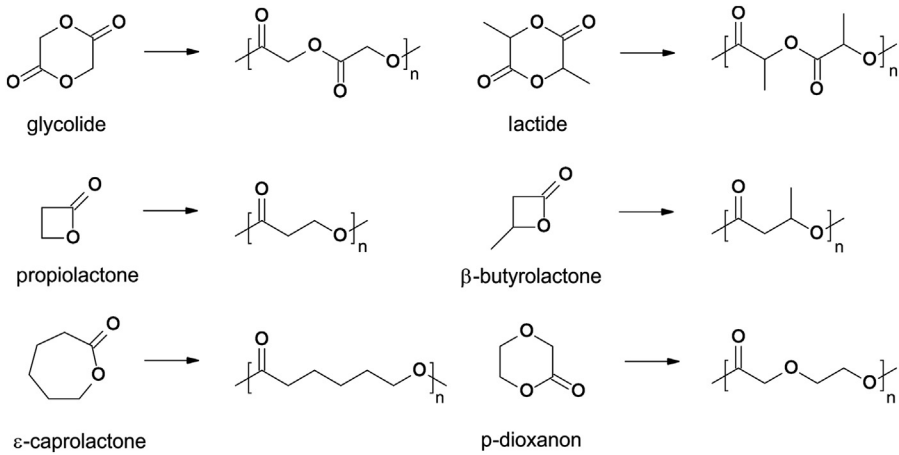


Figure 14.2 Monomers for ring-opening polymerization.

polymerization (Dechy-Cabaret et al., 2004; Gupta and Kumar, 2007). One of the most efficient initiators is tin(II)octanoate. With a concentration of less than 0.05 wt% of the initiator polyesters, high molecular weights and narrow weight distributions can be obtained. By adding alcohols, the efficiency can be increased (Kowalski et al., 2000). However, the reactivity for different lactones is different. Glycolide polymerization is faster than the polymerization of lactide, which is otherwise faster than that of β-butyrolactone (3-hydroxybutyric acid). In case of using monomers or lactones with asymmetric carbon atoms, optical active polyesters will be obtained (e.g. poly-L-lactide from L,L-dilactide). Using racemic monomers, blocks of different tacticities will be achieved. High regular isotactic, alternating syndiotactic, or randomly organized atactic blocks will exist, which have consequences for the properties of the resulting polymer (Kricheldorf et al., 1988, 1994).

Because homopolymers or copolymers from glycolide and L-lactide (Table 14.2) have mechanical properties that are similar to human bones, ligaments, or tendons (E-modulus 2−7 GPa; tensile strength 41−58 MPa), they are useful for biomaterial applications like temporary scaffolds and make them sufficient for the production of fibers (Sabir et al., 2009).

To improve the variability of the properties of aliphatic biodegradable polyesters, various copolyesters have been prepared. An example is the copolymerization of β-butyrolactone with δ-valerolactone (3-hydroxyvaleric acid) (Poirier et al., 1993). The incorporation of δ-valerolactone increases the elasticity and the softness of the resulting material (Table 14.3). Another way to prepare tailored mechanical properties is the syntheses of block copolymers. Lendlein et al. presented a system with a crystallizable unit and an elastic unit. The crystallizable segment gives the material the necessary strength and acts as a crosslinking unit while the elastic segment is amorphous and has a low T_g (Lendlein et al., 1998). Unfortunately, scrambling often becomes a problem during the synthesis of block copolymers. This can be avoided by the presence of a diol during the ring-opening polymerization of lactones resulting in a prepolymer terminated by secondary hydroxyl groups. This syntheses is followed by a copolymerization with L-lactide to obtain a triblock-copolymer of type A-B-A where the poly-L-lactide represents block A and the prepolymer becomes block B. For this block copolymer, the molecular weight and the unit composition of the produced copolymer can be successfully controlled by changing the L-lactide/poly-lactone ratio in the feedstock. Its characterization revealed that this block copolymer has high potential for use as a biodegradable thermoplastic elastomer (Hiki et al., 2000). Manifold properties of polyesters arise from their molecular architecture. For example, dendrimers (symmetrically branched around the core) and hyperbranched macromolecules are attracting, both scientifically and industrially. Approaches have been made to dendritic aliphatic block-copolymers using a series of substituted ε-caprolatones containing methyl, ethyl, phenyl, and dimethyl groups. These comonomers prevent crystallization and impart desirable mechanical properties to the dendritic polyesters ranging from thermoplastic elastomer to rubber-toughened systems. The hyperbranched systems can be realized by cocondensation of different intrinsically branched AB_x macromolecules

Table 14.2 Material properties of various polyesters

Polyester	Crystallinity (%)	T_g (°C)	T_m (°C)	E (GPa)	σ_B (MPa)	ε_B (%)	Elongation (%)
Polyglycolide	40–50	36	228	7.0	–	–	15–20
Poly-L-lactide	37	57	174	3.6	58	2.1	–
Poly(3-hydroxybutyrate)*	60–80	10	179	3.5	–	6	–
Poly(ε-caprolactone)	–	−60	59–64	0.4	–	–	300–500
Polydioxanone	55	−10 to 0	115	1.5	–	–	–

–, data not available.
* Bacterially produced.

Table 14.3 Physical properties of copolyesters from β-butyrolactone and δ-valerolactone

Amount of δ-valerolactone (mol-%)	T_g (°C)	T_m (°C)	E (GPa)
0	10	179	3.5
9	6	162	1.9
20	−1	145	1.2
25	−6	137	0.7

Lendlein (1999), Poirier et al. (1993) with permission of WILEY-VCH Verlag GmbH & Co. KGaA, Weinheim Copyright © 1999.

(Trollsas et al., 1999). Another route to block copolymers with controlled branching uses a type of molecular architecture, denoted as dendrimer-like star polymers. These block copolymers are described by a radial geometry where the different layers or generations consist of high-molecular-weight polymer emanating from a central core. With this architecture, more control in the placement of the different blocks is achieved over the hyperbranched analog. Irrespective of the molecular architecture, microphase morphologies were observed when poly(L-lactide) was employed as one of the blocks.

14.2.2 Polyanhydrides

Polyanhydrides are an important class of biodegradable polymers that are closely related to the polyesters. Today, polyanhydrides can be regarded as "tailor-made" polymers because they can be synthesized in such a way to produce polymers with various degrees of crystallinity, degradation behavior, branching, and crosslinking. Polyanhydrides are of great interest because they are biocompatible (they show no evidence of inflammatory reaction) and degrade in vitro as well as in vivo into their acid counterparts (Figure 14.3) as nonmutagenic and noncytotoxic products that are either eliminated from the body as metabolites or excreted in feces/urine (Kumar et al., 2002). Polyanhydrides have been considered to be useful biomaterials as carriers of drugs to various organs of the human body such as brain, bone, blood vessels, and

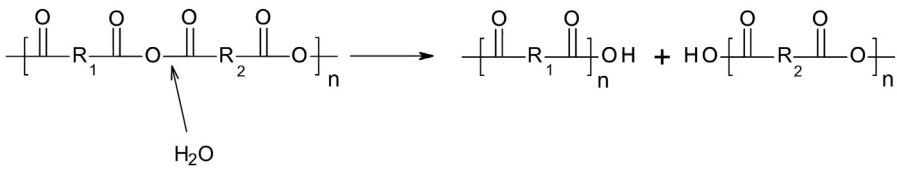


Figure 14.3 Hydrolytic degradation of polyanhydrides.

eyes. For clarification, the class of polyanhydrides discussed here belongs to those polyanhydrides that have the anhydride group in the polymer backbone. Other polyanhydrides exist wherein the anhydride group is a side group and is not a part of the backbone. For example, poly(maleic anhydride) is a polyethylene chain having the anhydride groups as side groups to the polymeric backbone. This causes a significant change in the degradation behavior. Although the breakdown of anhydride groups in the backbone causes a decrease in the initial molecular weight, the breakdown of these groups in side chains do not initiate a change of the initial molecular weight. The main limitation of polyanhydrides is their storage stability requiring storage under refrigeration.

For a drug delivery system with constant release rate, a surface-eroding device might be desirable. Therefore the polymer must be hydrophobic but contain water labile linkages (Tamada and Langer, 1992). Mechanical properties of, e.g. polyanhydrides, can be enhanced by the introduction of imide groups, while the presence of polyethylene glycol in polyanhydrides increases their hydrophilicity and induces fast drug release because of the bulk degradation properties of the polyethylene glycol. In general, high hydrolytic reactivity of the anhydride linkage of the polyanhydrides provides an intrinsic advantage in flexibility and control of the degradation rates. Variation in monomer ratio and type of monomer (Figures 14.4 and 14.5) allows preparation and design of certain degradation times of surface-eroding polymers within rates of 1 week to several years. Pure aliphatic polyanhydrides may have degradation times of some days, whereas more complex architectures of aromatic polyanhydrides degrade over a few years. Polyanhydrides of only aromatic diacids offer several advantages compared with aliphatic polymers. This includes longer release and degradation times as well as higher mechanical strength and stability. However, aromatic polyanhydrides are insoluble in common organic solvents and melt at high temperatures. These properties limit the use of purely aromatic polyanhydrides because they cannot be fabricated as films or coatings using solvent or melt techniques. Because of these limitations, aromatic copolyanhydrides based on the common diacids isophthalic acid, terephthalic acid, 1,3-bis(carboxyphenoxy)propane, fumaric acid, and sebacic acid have been synthesized. The copolymers are highly soluble in chloroform or dichloromethane (>20% w/w) and melt at temperatures between 80 and 130 °C (Domb, 1992; Domb et al., 1989).

14.2.3 Polyurethanes

The development of biodegradable polyurethanes (PURs) started in the early 1960s. Nowadays, PURs belong to the most popular materials used as biomaterials in medical applications and devices because of their extended properties in biocompatibility, biostability, durability, and toughness. However, in the field of regenerative medicine, biodegradability is more and more required, thus new PURs with more or less tailored biodegradation properties are produced. In principle, PURs are synthesized from a diol and a diisocyanate. Most often, chain-extending agents are used to improve the biodegradation behavior (Figures 14.6 and 14.7). Unfortunately, some of the aromatic diamines and diisocyanates are suspected to cause cancer (Cardy, 1979; Schoental, 1968).

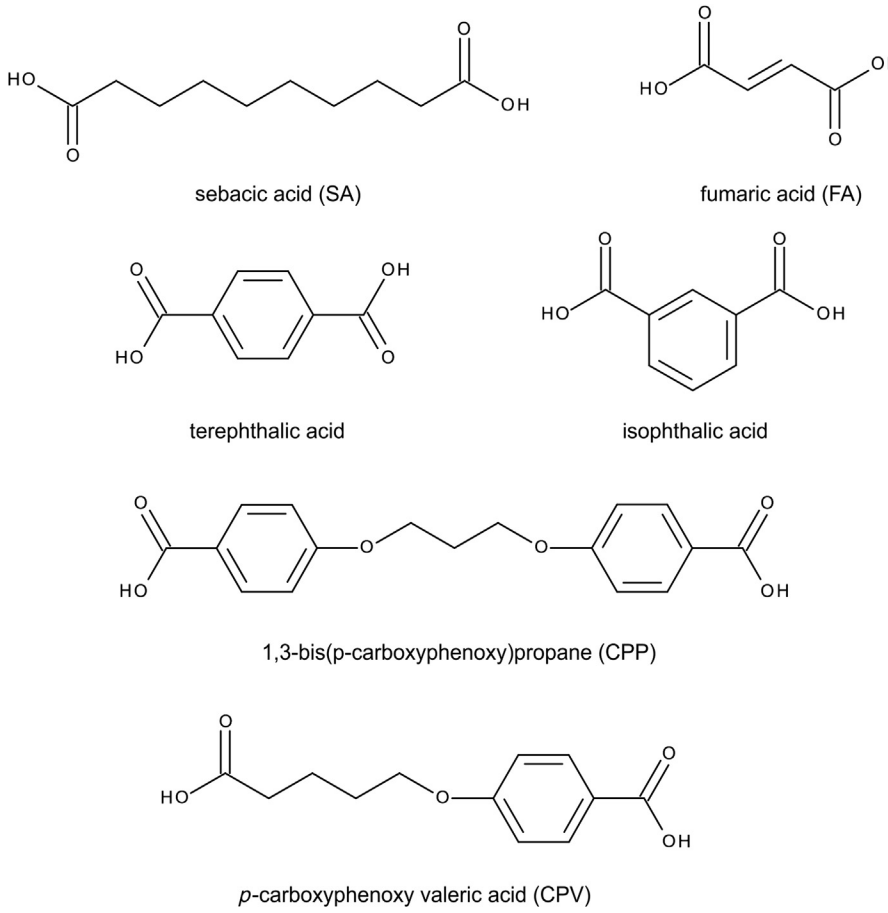
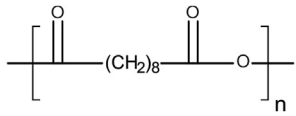
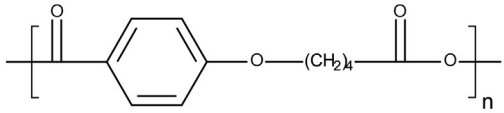


Figure 14.4 Examples of monomers for polyanhydride synthesis.

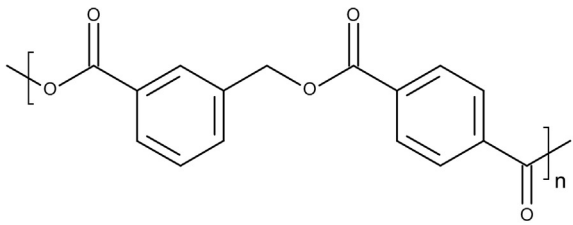
Therefore as diisocyanate compounds mostly 1,6-hexamethylene diisocyanate, 1,4-butane diisocyanate, or lysinemethylester diisocyanate, whose degradation products are all nontoxic, as well as some corresponding aliphatic diamines are used. For synthesis of biodegradable PUR, polymers of low-molecular-weight diols with hydroxyl end groups are often used. The backbone of these polymeric diols mostly corresponds to a polyester or a polyether that has beneficial degradation abilities. As described previously, polyester-based diols can be prepared by ring-opening polymerization of lactones (Sawhney and Hubbell, 1990) and furthermore, heteroatoms like S, Si, N, or P can be incorporated during the ring-opening polymerization reaction (Penczek et al., 2007). Depending on the type of diol, the polymers result either in polyether-urethane or polyester-urethane. In case of hydrophobic polyester diols, the hydrophilicity of the resulting polyester-urethane can be increased if polyethylene glycol is mixed with the diol. Additionally, this approach increases the rate of biodegradation and in some cases an improved cell attachment can be observed (Gorna and Gogolewski, 2002b). Using this



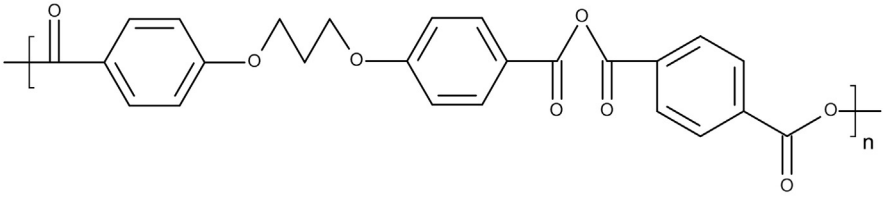
poly(sebacic acid) (PSA)



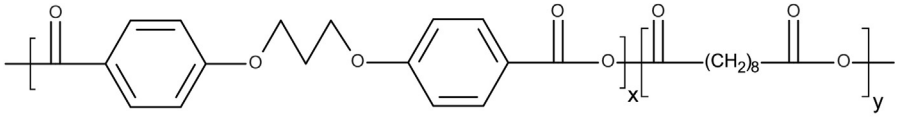
poly-1,3-bis(p-carboxyphenoxy)valerate (P(CPV))



poly-(terephthalic acid)-*co*-(isophthalic acid) (P(TA-IPA))



poly-((1,3-bis(p-carboxyphenoxy)propane)-*co*-(isophthalic acid) (P(CPP-*co*-IPA))



poly-(1,3-bis(p-carboxyphenoxy)propane)-poly(sebacic acid) (PCPP-PSA)

Figure 14.5 Structures of several polyanhydrides.

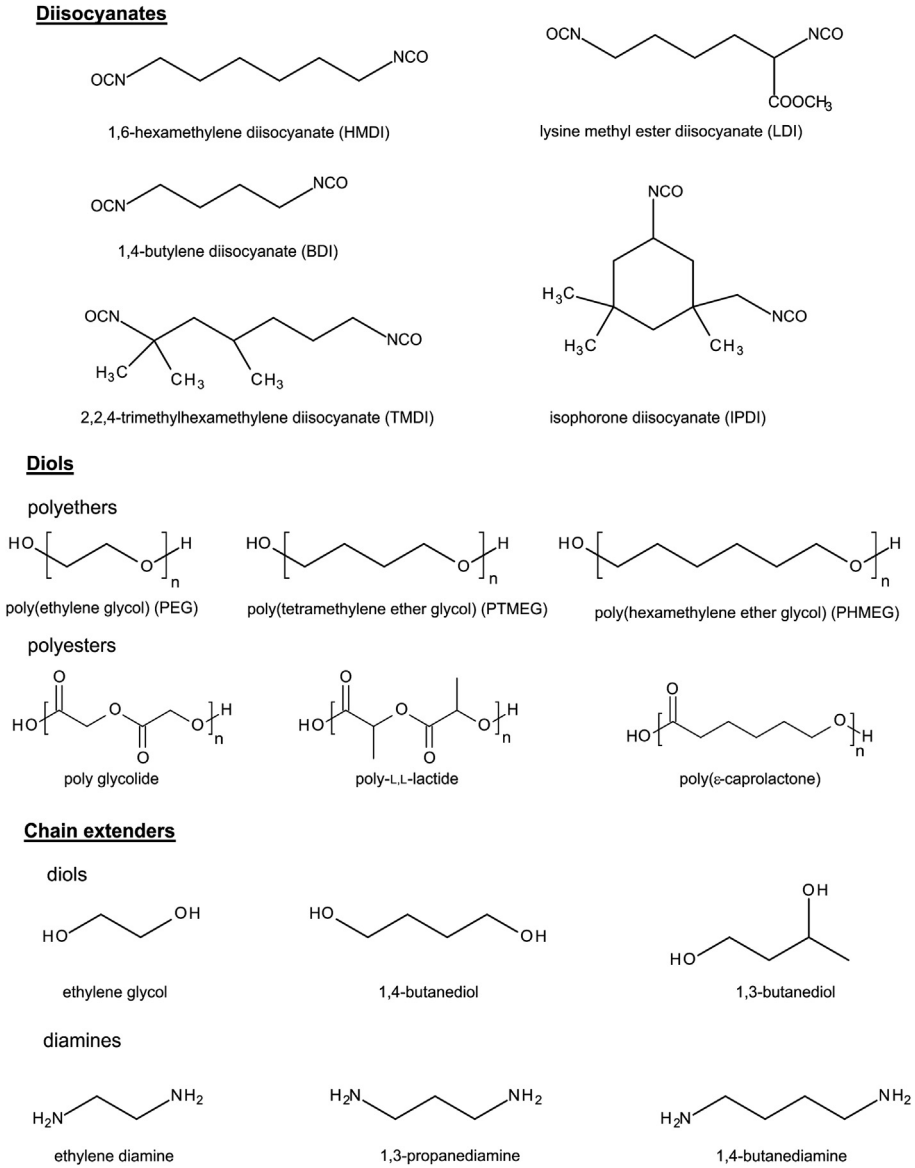


Figure 14.6 Raw materials for synthesis of biodegradable polyurethanes (PURs).

principle opens the way to adjusted hydrophilicity of polyurethanes (decreasing water contact angle, sessile drop method, from 77° to 40°).

In general, polyurethanes contain different segments. They include nonpolar hard segments (HS) as well as polar soft segments derived from the chain extender and the diisocyanate. Therefore, microphase separation is possible, which has consequences for the mechanical properties of the PURs (Spaans et al., 1998).

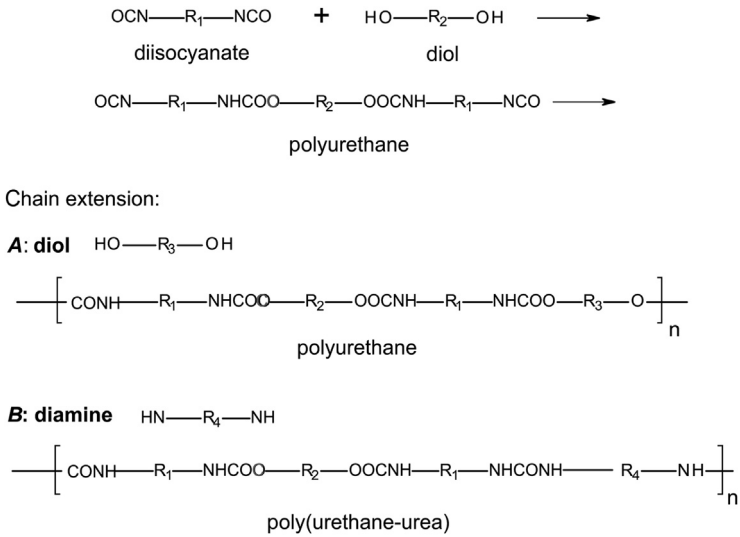


Figure 14.7 Synthesis and chain extension of polyurethanes (PURs).

Reconsidering this, various parameters influence the mechanical behavior of PURs (Gisselfalt et al., 2002). Decreasing the molecular weight of the macrodiol and/or increasing the chain extender to diol ratio lead to harder and stiffer polyurethanes with higher tensile strength and lower elongation at break. HS with higher melting temperature and hardness can be obtained by use of diamine-based chain extenders. Aromatic diisocyanates increase chain stiffness and facilitate aggregation of the hard phases by π-electron association, but one should keep in mind that they might behave carcinogenically. Still the flexibility of the molecular chains can be influenced by variation in the number of substitutions and spacing between and within branch chains. Finally, the HS content determines the resulting mechanical properties (Table 14.4). HS below 15 wt% is considered soft material, HS between 15 and 40 wt% is rubbery elastomer, whereas tough elastomer might be available for an HS between 40 and 65 wt% and at HS >65 wt% a strong engineering polymer is obtained (Zdrahala and Zdrahala, 1999a).

14.2.4 Natural polymeric materials

Not only synthetic polymeric materials are used for biomedical applications, but natural polymeric materials also play a significant role. Because of their excellent biocompatibility, they are used for bone and cartilage tissue engineering. To this group of degradable polymers belong collagen, fibrin, hyaluronic acid, alginic acid, and chitosan. All of these materials serve as intrinsic templates for cell attachment and growth and can stimulate an immune response at the same time. Natural polymeric materials are well-organized and interact directly with cells by cellular substances that can be bound to cell receptors. Unfortunately, the disadvantages of these polymers are difficulties in processability for clinical applications, less bulk quantity because they are

Table 14.4 Mechanical properties of polyester-urethane with different chain length of the soft segment from PCL

MW PCL	HS (%)	Young's modulus (MPa)	Strain at break (%)	Tensile strength (MPa)	Yield stress (MPa)	Yield strain (%)
750	33	263.9	870	38.7	16.2	10.1
100	27	149.0	994	37.8	10.3	11.2
600	19	64.6	1081	43.6	6.4	19.2
1900	16	54.6	1173	55.0	5.5	27.1
2200	14	30.1	1150	38.4	4.8	29.6
2800	12	33.8	1196	47.8	4.7	58.1

1,4-butandiol, chain extension; BDI, diisocyanate; HS, hard segment content; MW, molecular weight; PCL, poly(ε-caprolactone).
Heijkants et al. (2005).

not a mass product, and their price. Additionally, their degradation rate is different from patient to patient as it is based on an enzymatic process where the enzyme varies with every patient.

Collagen matrices in the form of fibers, coatings, and films are used extensively in biomaterial and biomedical applications. The specific properties of these matrices, both in terms of physical and chemical characteristics, have a direct impact on cellular adhesion, spreading, and proliferation rates, and ultimately on the rate and extent of new extracellular matrix formation in vitro or in vivo (Abraham et al., 2008). Collagen is widely used for repair and regeneration of tissues. Furthermore, the structure and remodeling of collagen in vivo is critical to the pathology and healing of many human diseases. In recent studies, it has also been shown that collagen matrix structure can have a major impact on cell and tissue outcomes related to cellular aging and differentiation potential (Blair et al., 2002). The collagen structure is complex because of diversity of source materials, chemistry, and structural hierarchy. New spongy collagen matrices containing oxidized cellulose (Kang et al., 1999) were recently introduced in the US and European markets for treating diabetic and ulcer wounds. Variations in physical, chemical, and degradation properties as well as the risk of infections, and difficult-to-handle properties are the drawbacks of collagen.

Similar to collagen is *fibrin*, which is involved in the blood clotting process. It is formed from fibrinogen by the protease thrombin. Fibrin is always used in conjunction with other scaffold materials where it acts as cell carrier. It is completely degradable but has poor mechanical strength for articular cartilage engineering applications.

Chitosan is a polysaccharide consisting of β-(1→4)-linked D-glucosamine with randomly located N-acetyl-D-glucosamine units. It is produced commercially by deacetylation of chitin, which is the structural element in the exoskeleton of crustaceans and cell walls of fungi. Because of its extended biocompatibility, it is useful

in bandages to reduce bleeding and as an antibacterial agent; it can also be used to help deliver drugs through the skin. Additionally, chitosan has a potential as scaffold material for tissue engineering including cartilage and bone.

Another linear polysaccharide is *hyaluronic acid* (HyA, hyalorunan) which consists of alternating units of β-(1→4) and β-(1→3)-linked N-acetyl-D-glucosamine and D-glucuronic acid. Hyaluronic acid has a polyanionic structure with a range of corresponding cations (e.g. Na^+, K^+, and H^+). Because of HyA's immunoneutrality and its capability of tissue repair by promoting mesenchymal and epithelial cell migration, differentiation and enhancing collagen deposition and angiogenesis HyA can be used in irregular shaped defects. On the other hand, it has only weak mechanical properties that limit the number of applications.

A nonhuman natural polymer is *alginic acid*, which is a nonbranched, binary copolymer of β-(1→4)-glycosidically linked β-D-mannuronic acid and α-L-guluronic acid monomers. It can be regarded as a true block copolymer composed of homopolymeric β-D-mannuronic acid and α-L-guluronic acid regions, interspersed with regions of alternating structure. The physicochemical properties of alginate have been found to be highly affected by the β-D-mannuronic acid/α-L-guluronic acid ratio as well as by the structure of the alternating zones. The high functionality of alginic acid makes it biocompatible. For specific medical applications, materials with an increased guluronic acid ratio exhibit a much better compatibility (De Vos et al., 1997). It is widely used as cell transplantation vehicles to grow new tissues as well as wound dressing. The drawbacks of these polymer materials are their slow degradation and their insufficient mechanical integrity which makes them unsuitable for long-term implants.

All of these natural polymer materials have their own advantages such as available in abundance, synergic with bioactive components, biodegradable and/or bioabsorbable, nontoxic, and biocompatible. Generally naturally occurring biomaterials may create a native cellular milieu. However, large batch-to-batch variations upon separation from biological tissues are the main restriction for their wide applications.

14.3 Degradation mechanisms

For biodegradable polymeric materials, the obvious question is why some polymers degrade, whereas others do not. To understand this, knowledge is necessary about the mechanisms through which polymeric materials biodegrade. Biodegradation is usually defined as degradation caused by biological activity. However, it will occur simultaneously with abiotic degradation such as photodegradation and simple hydrolysis. A great number of polymers, such as polyesters, polyanhydrides, polyamides, polycarbonates, polyurethanes, polyureas, polyacetals, and polyorthoesters, are subject to hydrolysis. In medical applications, biodegradable polymeric materials are only needed for a certain amount of time and if a second surgery for removal of the implant should be avoided, such as controlled drug release implants, internal sutures, and applications in tissue engineering and induced autoregeneration. To fulfill these application-driven requirements the degradation mechanisms of the individual

synthetic biodegradable materials are based on the cleavage of specific bonds of the material under physiological conditions. The cleavage itself proceeds through hydrolysis or miscellaneous mechanisms such as reduction of the disulfide bonds, and can be in the backbone, side chains, or pendant groups, depending on the monomers and architecture of the polymer (Guo and Chu, 2007; Kumar et al., 2002; Lenaerts et al., 1984). Additionally, other parameters affect the chemical bond degradation such as the pH, the temperature, and the water uptake (hydrophilicity) (Göpferich, 1996). In biodegradable materials, cleavage of the bonds results in polymer fragments, which can be excreted from the body. The metabolites should be water-soluble, nontoxic, and ideally eliminated by the kidney or metabolized analog to the natural cell metabolism. Additionally, the kinetics of degradation have to be considered, because a too high concentration of degradation products may also be toxic. The degradation process of the polymer materials can be observed on different levels, including mass loss, change of molecular weight, change of thermomechanical properties, and the occurrence of degradation products. The degradation rate can generally be adjusted by the types of monomers, the sequence structure, and the architecture of the polymer, as well as by the morphology (Gorna and Gogolewski, 2002a) (Figure 14.8).

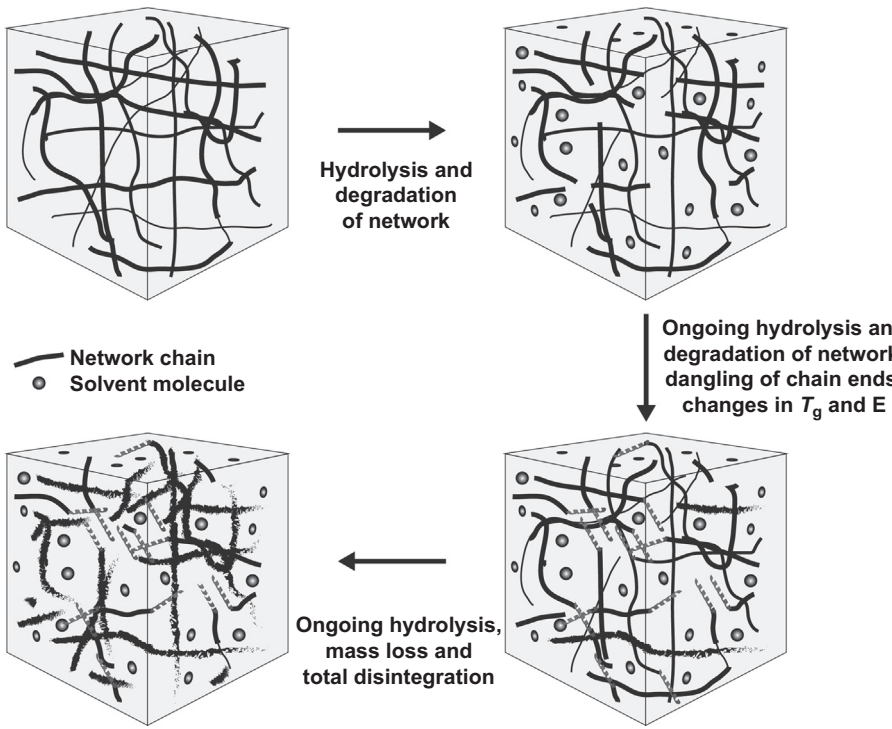


Figure 14.8 Degradation of polyester urethane network with changes in thermomechanical properties.
Adapted from Neffe et al. (2010) with permission of WILEY-VCH Verlag GmbH & Co. KGaA, Weinheim Copyright © 2010.

14.3.1 Bulk degradation

A typical hydrolytic bulk degradation takes place in the whole sample. It is the dominant mechanism if the ingress and diffusion of water is faster than the rate of degradation of the polymer (Figure 14.9). For polyesters and copolyesters, the hydrolytic degradation rate may be adjusted by the sequence structure or the ratio of the comonomers (Table 14.5). For poly-((ε-caprolactone)-*co*-glycolide), the glycolide units speed up the hydrolysis for ester bonds regardless of whether they form the hydroxy or carboxy component. Therefore, ester bonds of diads which consist of two glycolide units are the most easily hydrolysable bonds. This explains the faster degradation of a block-copolyester in comparison to a randomized copolyester with identical comonomer ratio (Lendlein et al., 2001).

Polyester urethane networks are versatile polymer systems because it is possible to tailor their mechanical properties and their hydrolytic degradation profile. For biomedical applications, the biodegradability as well as the thermomechanical properties of the polymer networks during the course of degradation is of importance (Neffe et al., 2010). Although hydrolytic degradation is always connected to mass loss and water uptake, changes in the thermomechanical properties of the polymer networks during the degradation can be observed. For polyester urethane networks, first the uptake of small amounts of water leads to some bond cleavages. The ongoing hydrolysis by time causes further cleavages that result in a decrease of T_g of the network, whereas entanglement of fragments with remaining part of the network increases the elongation at break, ε_b. As bond cleavage goes on soluble fragments are built which result in mass loss and a change in composition of the network. Finally, the network is destroyed.

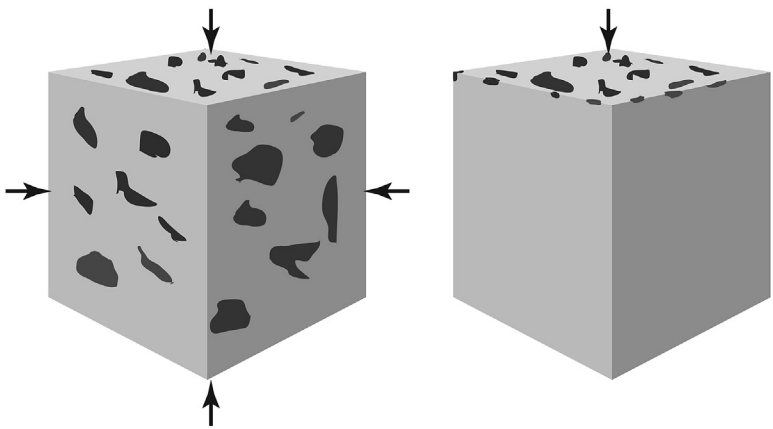


Figure 14.9 Scheme of bulk degradation (left) and surface erosion (right); arrows show the erosion path.

Table 14.5 Degradation times and products of polyesters and copolyesters

Polymer	Degradation time (months)	Degradation product
Polyglycolide	2–4	Glycolic acid
Poly(L-lactide)	18–24	L-Lactic acid
Poly(*rac*-lactide)	12–16	*rac*-Lactic acid
Poly(3-hydroxybutyrate)	>36	3-Hydroxybutyric acid
Polydioxanone	6–12	–
Poly(ε-caprolactone)	>24	Caproic acid
Poly[(L-lactide)-*co*-(glycolide)] 10:90	3–4	L-Lactic acid and glycolic acid
Poly[(L-lactide)-*co*-(glycolide)] 50:50	2	L-Lactic acid and glycolic acid
Poly[(L-lactide)-*co*-(glycolide)] 75:25	1–2	L-Lactic acid and glycolic acid
Poly[(*rac*-lactide)-*co*-(glycolide)] 50:50	0.5	*rac*-Lactic acid and glycolic acid
Poly[(*rac*-lactide)-*co*-(glycolide)] 75:25	1–2	*rac*-Lactic acid and glycolic acid
Poly[(*rac*-lactide)-*co*-(glycolide)] 85:15	5	*rac*-Lactic acid and glycolic acid
Poly[(*rac*-lactide)-*co*-(ε-caprolactone)] 90:10	2	*rac*-Lactic acid and caproic acid

Lendlein (1999), Sabir et al. (2009).

14.3.2 Surface degradation

For a surface degrading device – as these are favorably used for drug delivery systems – the polymer or the polymer coating must be hydrophobic but contain water-labile linkages. For these surface-eroding materials, the drug delivery rate is nearly directly proportional to the degradation rate, which yields a constant drug release rate. Under normal conditions, polyanhydrides are typically undergoing surface degradation. This is a consequence of the high water lability of the anhydride bonds on the surface of the material, whereas the hydrophobicity of the backbone restricts water penetration into the bulk. A decrease in the material thickness during the degradation process, maintenance of the structural integrity, and the nearly zero-order degradation kinetics suggest the dominancy of the heterogeneous surface erosion

(Kumar et al., 2002). A similar decrease as a function of time was also observed among the aliphatic−aromatic copolyanhydrides (Domb et al., 1989; Domb and Langer, 1989) and imide-containing polyanhydrides (Staubli et al., 1991). As an example poly(*o*-CPH) polymer hydrolytically degrades in vitro by nearly linear degradation rate into 2-(6-(2-carboxyphenoxy)hexoxy)benzoic acid and acetic acid as byproduct (Bedell et al., 2001).

14.4 Applications

Biomedical engineering is defined as an extension of materials and chemical engineering toward biomaterials (Peppas and Langer, 2004). Tissue engineering is one of its main branches. It makes use of the fact that if cells are located close enough to each other, they build shapes and structures identical to those the same species of cells would create in a living body because living cells are able to exchange signals with their neighboring ones. Based on a balanced combination of cell culture growth with biomaterials to support it and on bioactive molecules to enhance and direct it, tissue engineering opens a way of replacement or repair of damaged or failed tissues with viable ones. Therefore it offers an environment that supports the native capacity of cells to integrate, differentiate, and proliferate. An ambitious aim would be the generation of new tissues and organs. For creating the required environment normally three-dimensional scaffolds seeded with appropriate living cells are implanted. The proliferation of these cells is usually supported by the addition of growth factors.

Nowadays, regenerative medicine is one of the major scientific challenges. It aims to support the regeneration of damaged cells, tissues, and organs through developing and applying innovative medical therapies. It requires integration of emerging knowledge in the physical and life sciences with bioengineering and with clinical medicine to learn how to trigger the failed human tissues and organs. One of the strategies being pursued in regenerative medicine is induced autoregeneration, and it necessitates the development of biomaterials that can control individual cellular behavior and provide a proper microenvironment to support regeneration, such as being a matrix to direct tissue formation and promote vascularization, rather than simply provide mechanical support.

For both fields, tissue engineering and regenerative medicine, coatings are an essential tool as they can be custom-designed and multifunctional. Polymeric coatings may influence toxicity, cell adhesion (including proliferation and differentiation), biofilm formation, inflammation, oxidation of the supporting material, and drug carrying as well as drug delivery (Bryaskova et al., 2013; Busch et al., 2014; Daghighi et al., 2013; Scholz et al., 2011; Thorfve et al., 2014). In the following chapters, a selection of possible applications is presented, albeit it cannot be complete because the huge number of published applications would go far beyond the scope of the topic.

14.4.1 Cardiovascular applications

Stenosis and/or formation of thrombus on arteries bringing blood to the heart may be a precursor of a cardiac infarct. Medical treatment may involve insertion of a stent

into the obstructed blood vessel, expected to restore the normal blood flow. The use of bare metallic stents for such treatments may, however, cause severe problems such as ingrowth of the stent followed by inflammation or restenosis. Therefore biodegradable polymer coatings are commonly applied in micro- or nanoscale thickness, especially for drug-eluting stents (DESs). It is recognized that rapid reendothelialization is a promising method for preventing the previously mentioned complications. The endothelial progenitor cell compatibility and hemocompatibility of titanium used for stents are improved by coating an extracellular matrix−like film with heparin and collagen using a layer-by-layer self-assembly technique (Chen et al., 2010).

For DES design, biodegradable polymer coating on the metal stent is a key technology along with the drug release control, because the polymer degradation rate can be closely associated with the release pattern of therapeutic drugs. Most commercially available DESs consist of stainless steel or cobalt−chrome alloys coated with polymer and drug. Because there are disadvantages of the chemical vapor deposition method (e.g. expensive equipment or hypersensitivity associated with thrombosis), a method of securing polymer coating on the metal surface by applying direct surface-initiated ring-opening polymerization of L,L-lactide is used (Choi et al., 2011).

Another progress in cardiovascular applications is the use of complete biodegradable stents. They offer the possibility that blood vessels are only supported as long as they require to regenerate for stabilizing themselves. The benefit is obvious because it will no longer be necessary to administer substances to the patient for extended periods of time and the risk of vascular occlusion and infarction is decreasing. Furthermore, in case of an emergency heart or artery surgery it can be performed easier and at lower risk because no metallic implant has to be removed that could damage the blood vessel sustainably. Besides fully polymeric DESs, mostly from polyesters or polyanhydrides, the development of degradable stents from magnesium is a field of research during the past few years (Peng et al., 2013; Sternberg et al., 2012). Unfortunately, tailoring of the degradation properties, especially of the degradation rate, is still a challenge (Zeng et al., 2008). Therefore various combinations of coatings by biodegradable polymeric materials such as poly(ε-caprolactone) or poly(L-lactide) and different magnesium alloys are in the focus of research work (Chen et al., 2011) to adjust the biodegradability. Nevertheless, first patent applications are also being submitted now (Mangiardi, 2013).

14.4.2 Musculoskeletal applications

Biodegradable polymer systems are often used as scaffold material for bone growth and tissue engineering (Jagur-Grodzinski, 2006). The development of bone scaffolds depends on the porosity providing interconnected pores, suitable mechanical strength, and sufficient microchemistry of the surface. Additionally, it should support cell activities such as proliferation, migration, adhesion, and differentiation. There are many factors for bone tissue engineering, but all include the following key ingredients: (1) harvested cells, (2) recombinant signaling molecules, and (3) three-dimensional

matrices (Cheung et al., 2007). During tissue regeneration, all of these factors play very important roles for the healing process.

Applications of polymers for bone tissue repair and reinforcement, for regeneration of cartilage associated with bones, for helping in partial replacement of bones by metallic parts, and as carriers of antibiotics to the infected bone tissues, have been extensively investigated (Jagur-Grodzinski, 2006). For example, degradable biomaterials containing high-molecular-weight hyaluronan (HyA)-based polymers with excellent histocompatibility and biodegradability were prepared for the synthetic bioskin and biosynthetic osteocartilage used for the reconstruction of tissues. The addition of growth factors and cytokines promoted cell migration and proliferation and formation of a new tissue (Mori et al., 2004). The natural repair of osteochondral defects can be enhanced by using biocompatible materials that support repair process. HyA-based scaffolds seem to allow faster cell infiltration, leading to faster tissue formation than the synthetic polylactides and their copolymers. This may be due to the polysaccharides provided by the natural polymers (Solchaga et al., 2005; Yoo et al., 2005).

Because metallic biomaterials are in principle bioinert, but not bioactive, coating is a tool for biofunctionalizing of these implants. Especially for orthopedics, this method allows the combination of mechanical optimized metallic implant with ceramics, or polymers and incorporated bioactive factors (Strobel et al., 2011a,b). Polyesters and copolyesters based on polylactide, polyglycolide, and polyanhydrides fulfill the necessary mechanical requirements and are able to act as reservoirs for drug delivery systems supporting the healing process.

In case of degradable metallic implants, especially by use of magnesium-based materials (Rosemann et al., 2013), biodegradable polymer systems can have a key function in controlling the disintegration of the device. Because magnesium implants degrade less uniformly (Witte et al., 2005), they seem not to be very suitable for applications such as temporary or permanent implants. Coatings with poly((*rac*-lactide)-*co*-(glycolide)), which has been used in medical applications because of its good blood compatibility, can offer an effective protection against corrosion. A prerequisite is that it has a relative molecular mass of about 200,000 Da. It shows an obvious reduction in mass loss of the coating over pure Mg in Hank's solutions (Huang et al., 2007). This polymer coating may be a good choice for degradable implants. But because of its bulk degradation mechanism, it will not provide sufficient protection for a bone replacement. Thus, it is still crucial to seek a potential polymer coating, which is suitable for Mg-based permanent implants. Besides the necessary alloy development, the final challenge for polymers in combination with Mg-based devices may be the degradability, the proliferation of huge number of cells, and to resist wear (Li and Zheng, 2013).

14.5 Challenges

One of the most important challenges is that the materials used for all kinds of implants have to be nontoxic and endotoxin-free, aiming to minimize unwanted foreign body

responses upon implantation. Cellular functions are the result of highly diverse interactions between cells and biomaterials (Scharnagl et al., 2010). Unfortunately, most biomaterials, polymer based as well as metal based, do not completely meet the complex demands therefore. The materials are not specifically adapted for applications in contact with blood, cells, or other biomedical environments. For commercially available polymers, mostly neither biological relevant data nor information about their medical grade purity (chemical purity, cytotoxicity, or endotoxin content) are available. The standard production methods for the polymers often include extrusion or solution processes. Especially in the case of coatings, organic solvents are often used. This makes the resulting biomaterial potentially toxic for cells because these solvents cannot be completely removed by any drying method or reprecipitation procedure because of the strong intermolecular interaction of the solvent (Fiore and Degrassi, 1999; Sjogren and Anderson, 2000). Furthermore, pretreatment processes of the metal that is to be coated as well as catalysts used for polymerization reactions have to be taken into account as they may induce cytotoxicity to the final biomaterial (Tanzi et al., 1994).

The sterilization of implant materials is a precondition for their biomedical use to minimize the risk of introducing unwanted foreign particles or pathogens by biomaterials, which can affect the cell behavior. Sterilization is defined as the act or process, physical or chemical, which destroys or eliminates all forms of life, especially microorganisms (Block, 2000; FDA, 2002). Because the sterilization process itself affects the biomaterial's physical and chemical properties (Carrascosa et al., 2003; Filipczak et al., 2006; Loo et al., 2005; Montanari et al., 1998; Rickert et al., 2003; Williams et al., 2006), it is important to choose a knowledge-based proper sterilization plan. For polymeric materials, and especially for hydrolytically degradable biomaterials in general, mainly the low temperature sterilization methods based on gamma- or e-beam-irradiation, hydrogen peroxide vapor, low temperature gas plasma, or ethylene oxide treatment are used. In addition the biocompatibility of sterilized substrates can be limited by endotoxins (Gorbet and Sefton, 2005), also called lipopolysaccharides, which are pyrogenic hydrophobic residues of the outer cell membrane of gram-negative bacteria that contaminated the material before sterilization. Endotoxins are highly heat stable and are not destroyed under regular sterilizing conditions. According to the Food and Drug Administration guidelines for medical devices the endotoxin load in substrate eluates may not exceed 0.5 endotoxic units (EU)/mL (20 EU/device), and if the device comes into contact with cerebrospinal fluid this limit is as low as 0.06 EU/mL (2.4 EU/device) (FDA, 1987).

Immediately after biomaterials come into contact with cell culture medium in vitro (even common serum-free medium, which still contains proteins) or surrounding tissue in vivo, protein adsorption to its surface occurs (Chen et al., 2009). This process occurs within seconds. Consequently, cells almost never come into direct contact with the material surface; they instead interact with the layer of adsorbed proteins. This layer mediates the cell adhesion and also provides signals to the cell by the cell adhesion receptors, mainly integrins. In this way, it determines the cellular response to the biomaterial. The type, amount, and conformation of adsorbed proteins strongly depend

on the physicochemical properties of the material surface and significantly affect the cell behavior (Tzoneva et al., 2008).

In addition to the pure biological aspects, the treatment of the metallic substrate before carrying out any coating plays a major role for the polymer−metal interaction as well as for the degradation behavior. For degradable metallic implants, especially for Mg alloys, the major challenge is their high susceptibility to galvanic corrosion attack. Even microgalvanic corrosion of the alloys without contact to other metals is possible because of heavy metal impurities such as iron, copper, or nickel and their own different phases of the alloy. Therefore, the degradation can be minimized by the use of single-phase high-purity alloys that maintain heavy metal impurities below the tolerance limits and alloying elements below the solubility limits. The removal of bad design, flux inclusions, surface contaminations, and galvanic couples and the avoidance of inadequate or incorrectly applied surface protection schemes can also significantly decrease the degradation. In most cases, the substrate needs a cleaning step followed by performing a conversion or primer treatment, taking into account the biocompatibility of the device (da Conceição et al., 2012; Nwaogu et al., 2009).

A perfect adhesion of the polymer on the metallic substrate is necessary to implement an effective and risk-minimized use of coated material in medical applications (Abdal-hay et al., 2014, Kannan and Liyanaarachchi, 2013). The prevention of early delamination or peeling of polymer coating from metal substrates requires much attention. In fact, polymer and metal have totally different physicochemical and mechanical properties so that weak bonding at the interface can cause significant deformation of the coated polymer once an implant is deployed. Pieces of polymer can be delaminated from the metal surface (e.g. because of very high blood pressure in the in situ implantation milieu of stents). Furthermore, the internal residual stresses from mechanical load may have a negative impact on the stability of the polymer coating. Therefore, the interfacial adhesion between polymer and metal should be firmly secured and fully evaluated.

14.6 Future trends

Because of the shift in morbidity spectrum during past few decades and the recent demographic developments, clinical medicine has to deal more and more with diseases that are gradually leading to a loss of function of important cell and organ systems. In many cases, these diseases cannot be cured by the currently available therapies and the patients have to remain in permanent therapy resulting in high costs. Regenerative medicine is highly interdisciplinary and deals with the restitution, substitution, regeneration of nonfunctional or more or less functionally impaired cells, tissues, organs through biological replacements, for example, through tissues produced in vitro or through the stimulation of the body's own regeneration and/or repair process (Mason and Dunnill, 2007, 2008). Important success in stem cell research (Bajada et al., 2008; Slater et al., 2008) and the extracorporeal tissue growth in bioreactors show the potential of regenerative medicine

(Breymann et al., 2006; Schulz and Bader, 2007). The euphoric visions to grow complete and functional organs in vitro were recognized however to be premature. This is also from a lack in basic research and the development of multifunctional implant materials (Shastri and Lendlein, 2009). The experience with polymer-based implants used in medicine led to a profile of requirements for future implant materials and the functionality of implant materials has to be broadened. The next generation of biomaterials for regenerative therapies requires the development of substances, which are able to influence and activate specific phenotype characteristics of cells and tissues. They should be stimuli-sensitive (Lendlein and Kelch, 2005) and, for example, change their physicochemical behavior due to external stimuli or to biological processes induced at the site of implantation. Bioactive peptides, proteins, or carbohydrates might be immobilized by polymers or released from implants in a well-defined process. The most up-to-date trend in polymer sciences is the development of degradable biomaterials showing multifunctionality. This implies that specific functionalities like hydrolytic degradation, physiological, and biomechanical tissue compatibilities (Razavi et al., 2014; Scharnagl et al., 2012; Trescher et al., 2012), and shape-memory can be adjusted to regiospecific requirements at the site of implantation (Gall et al., 2005; Langer and Tirrell, 2004). Research toward this aim has resulted in an increasing number of reports about material-induced cellular functions and cell−cell interactions.

Stem cells, which have the capacity for self-renewal and capability of differentiation to various cell lineages, represent an important building block for regenerative medicine and tissue engineering. These cells can broadly be classified into embryonic stem cells and nonembryonic stem cells comprising adult stem cells. Embryonic stem cells are called pluripotent and can differentiate in all cell types of the three embryonic germ layers. Adult stem cells are multipotent and the differentiation of these cells is committed to only one of the germ layers. Embryonic stem cells have a great potential, but their use is limited by several ethical and scientific considerations. Limiting factors for the use of adult and embryonic stem cells next to ethical considerations (Shapiro, 2008) are problems associated with extensive cell expansion in vitro (Unger et al., 2008), problems with in vitro cultivation on implant materials (Burdick and Vunjak-Novakovic, 2009; Little et al., 2008), and cell apoptosis following implantation (Vacanti, 2006) as well as vascularization (Griffith et al., 2005).

Based on the progress in polymer chemistry, multifunctional coated metallic implant materials are available nowadays, which can selectively initiate biological processes in a physiological environment and/or change their physiochemical characteristics in reaction to external stimuli. The availability of such multifunctional implant materials and the progress in tissue engineering resulted in the establishment of novel therapeutical options in different medical fields. Applying stem cell technology, further progress is expected for the reconstruction of different tissues based on the principles of tissue engineering. To benefit from this potential, clinicians have to get involved in these interdisciplinary research fields of regenerative medicine. For reaching the high-level goal, new, fast, and efficient predictive tools for engineering, evaluating, and validating of biomaterials such as virtual

laboratories or virtual frameworks (Okereke et al., 2014) will have to be improved and established.

References

Abdal-hay, A., Dewidar, M., Lim, J., & Lim, J. K. (2014). Enhanced biocorrosion resistance of surface modified magnesium alloys using inorganic/organic composite layer for biomedical applications. *Ceramics International, 40*(1), 2237−2247.

Abraham, L. C., Zuena, E., Perez-Ramirez, B., & Kaplan, D. L. (2008). Guide to collagen characterization for biomaterial studies. *Journal of Biomedical Materials Research Part B, 87B*(1), 264−285.

Albertsson, A.-C., & Varma, I. K. (2003). Recent developments in ring opening polymerization of lactones for biomedical applications. *Biomacromolecules, 4*(6), 1466−1486.

Arcos, D., Boccaccini, A. R., Bohner, M., Díez-Pérez, A., Epple, M., Gómez-Barrena, E., et al. (2014). The relevance of biomaterials to the prevention and treatment of osteoporosis. Opinion paper. *Acta Biomaterialia, 10*(5), 1793−1805.

Bajada, S., Mazakova, I., Richardson, J. B., & Ashammakhi, N. (2008). Updates on stem cells and their applications in regenerative medicine. *Journal of Tissue Engineering and Regenerative Medicine, 2*(4), 169−183.

Barbieri, D., Yuan, H., Luo, X., Farè, S., Grijpma, D. W., & de Bruijn, J. D. (2013). Influence of polymer molecular weight in osteoinductive composites for bone tissue regeneration. *Acta Biomaterialia, 9*(12), 9401−9413.

Bedell, C., Deng, M., Anastasiou, T. J., & Uhrich, K. E. (2001). Processing and hydrolytic degradation of aromatic, ortho-substituted polyanhydrides. *The Journal of Applied Polymer Science, 80*(1), 32−38.

Blair, H. C., Zaidi, M., & Schlesinger, P. H. (2002). Mechanisms balancing skeletal matrix synthesis and degradation. *Biochemical Journal, 364*, 329−341.

Block, S. A. (2000). *Disinfection, sterilization, and preservation* (5 ed). Lippincott: Williams & Williams.

Breymann, C., Schmidt, D., & Hoerstrup, S. P. (2006). Umbilical cord cells as a source of cardiovascular tissue engineering. *Stem Cell Reviews, 2*(2), 87−92.

Bryaskova, R., Georgieva, N., Andreeva, T., & Tzoneva, R. (2013). Cell adhesive behavior of PVA-based hybrid materials with silver nanoparticles. *Surface and Coatings Technology, 235*, 186−191.

Burdick, J. A., & Vunjak-Novakovic, G. (2009). Engineered microenvironments for controlled stem cell differentiation. *Tissue Engineering Part A, 15*(2), 205−219.

Busch, R., Strohbach, A., Rethfeldt, S., Walz, S., Busch, M., Petersen, S., et al. (2014). New stent surface materials: the impact of polymer-dependent interactions of human endothelial cells, smooth muscle cells, and platelets. *Acta Biomaterialia, 10*(2), 688−700.

Cardy, R. H. (1979). Carcinogenicity and chronic toxicity of 2,4-toluenediamine in F344 rats. *Journal of the National Cancer Institute, 62*(4), 1107−1116.

Carrascosa, C., Espejo, L., Torrado, S., & Torrado, J. J. (2003). Effect of gamma-sterilization process on PLGA microspheres loaded with insulin-like growth factor-I (IGF-I). *Journal of Biomaterials Applications, 18*(2), 95−108.

Chen, J., Chen, C., Chen, Z., Chen, J., Li, Q., & Huang, N. (2010). Collagen/heparin coating on titanium surface improves the biocompatibility of titanium applied as a blood-contacting biomaterial. *Journal of Biomedical Materials Research Part A, 95A*(2), 341−349.

Chen, Y., Song, Y., Zhang, S., Li, J., Zhao, C., & Zhang, X. (2011). Interaction between a high purity magnesium surface and PCL and PLA coatings during dynamic degradation. *Biomedical Materials (Bristol, England), 6*(2), 025005/1−025005/8.

Chen, Z. P., Xu, R. Z., Zhang, Y., & Gu, N. (2009). Effects of proteins from culture medium on surface property of silanes-functionalized magnetic nanoparticles. *Nanoscale Research Letters, 4*(3), 204−209.

Cheung, H. Y., Lau, K. T., Lu, T. P., & Hui, D. (2007). A critical review on polymer-based bio-engineered materials for scaffold development. *Composites Part B—Engineering, 38*(3), 291−300.

Choi, J., Cho, S. B., Lee, B. S., Joung, Y. K., Park, K., & Han, D. K. (2011). Improvement of interfacial adhesion of biodegradable polymers coated on metal surface by nanocoupling. *Langmuir, 27*(23), 14232−14239.

da Conceição, T. F., Scharnagl, N., Dietzel, W., & Kainer, K. U. (2012). Controlled degradation of a magnesium alloy in simulated body fluid using hydrofluoric acid treatment followed by polyacrylonitrile coating. *Corrosion Science, 62*, 83−89.

Daghighi, S., Sjollema, J., van der Mei, H. C., Busscher, H. J., & Rochford, E. T. J. (2013). Infection resistance of degradable versus non-degradable biomaterials: an assessment of the potential mechanisms. *Biomaterials, 34*(33), 8013−8017.

De Vos, P., De Haan, B., & Van Schilfgaarde, R. (1997). Effect of the alginate composition on the biocompatibility of alginate−polylysine microcapsules. *Biomaterials, 18*(3), 273−278.

Dechy-Cabaret, O., Martin-Vaca, B., & Bourissou, D. (2004). Controlled ring-opening polymerization of lactide and glycolide. *Chemical Reviews, 104*(12), 6147−6176.

Domb, A. J. (1992). Synthesis and characterization of biodegradable aromatic anhydride copolymers. *Macromolecules, 25*(1), 12−17.

Domb, A. J., Gallardo, C. F., & Langer, R. (1989). Poly(anhydrides) .3. poly(anhydrides) based on aliphatic aromatic diacids. *Macromolecules, 22*(8), 3200−3204.

Domb, A. J., & Langer, R. (1989). Solid-state and solution stability of poly(anhydrides) and poly(esters). *Macromolecules, 22*(5), 2117−2122.

FDA. (1987). *Guideline on validation of the limulus amebocyte lysate test as an end-product endotoxin test for human and animal parenteral drugs, biological products, and medical devices*.

FDA. (2002). *Sterility review guidance K90-1; updated 510(k), final guidance for Industry and FDA*. FDA.

Filipczak, K., Wozniak, M., Ulanski, P., Olah, L., Przybytniak, G., Olkowski, R. M., et al. (2006). Poly(epsilon-caprolactone) biomaterial sterilized by E-beam irradiation. *Macromolecular Bioscience, 6*(4), 261−273.

Fiore, M., & Degrassi, F. (1999). Dimethyl sulfoxide restores contact inhibition-induced growth arrest and inhibits cell density-dependent apoptosis in hamster cells. *Experimental Cell Research, 251*, 102−110 (Copyright (C) 2011 American Chemical Society (ACS). All Rights Reserved.).

Gall, K., Yakacki, C. M., Liu, Y. P., Shandas, R., Willett, N., & Anseth, K. S. (2005). Thermomechanics of the shape memory effect in polymers for biomedical applications. *Journal of Biomedical Materials Research Part A, 73A*(3), 339−348.

Gisselfalt, K., Edberg, B., & Flodin, P. (2002). Synthesis and properties of degradable poly(urethane urea)s to be used for ligament reconstructions. *Biomacromolecules, 3*(5), 951−958.

Göpferich, A. (1996). Mechanisms of polymer degradation and erosion. *Biomaterials, 17*(2), 103−114.

Gorbet, M. B., & Sefton, M. V. (2005). Endotoxin: the uninvited guest. *Biomaterials, 26*(34), 6811−6817.

Gorna, K., & Gogolewski, S. (2002a). Biodegradable polyurethanes for implants. II. In vitro degradation and calcification of materials from poly(epsilon-caprolactone)−poly(ethylene oxide) diols and various chain extenders. *Journal of Biomedical Materials Research, 60*(4), 592−606.

Gorna, K., & Gogolewski, S. (2002b). In vitro degradation of novel medical biodegradable aliphatic polyurethanes based on epsilon-caprolactone and pluronics (R) with various hydrophilicities. *Polymer Degradation and Stability, 75*(1), 113−122.

Griffith, C. K., Miller, C., Sainson, R. C. A., Calvert, J. W., Jeon, N. L., Hughes, C. C. W., et al. (2005). Diffusion limits of an in vitro thick prevascularized tissue. *Tissue Engineering, 11*(1−2), 257−266.

Guo, K., & Chu, C. C. (2007). Biodegradation of unsaturated poly(ester-amide)s and their hydrogels. *Biomaterials, 28*(22), 3284−3294.

Gupta, A. P., & Kumar, V. (2007). New emerging trends in synthetic biodegradable polymers—polylactide: a critique. *European Polymer Journal, 43*(10), 4053−4074.

Heijkants, R. G. J. C., van, C. R. V., van, T. T. G., de, G. J. H., Buma, P., Pennings, A. J., et al. (2005). Uncatalyzed synthesis, thermal and mechanical properties of polyurethanes based on poly(ε-caprolactone) and 1,4-butane diisocyanate with uniform hard segment. *Biomaterials, 26*(20), 4219−4228.

Hiki, S., Miyamoto, M., & Kimura, Y. (2000). Synthesis and characterization of hydroxy-terminated [RS]-poly(3-hydroxybutyrate) and its utilization to block copolymerization with L-lactide to obtain a biodegradable thermoplastic elastomer. *Polymer, 41*(20), 7369−7379.

Huang, J. J., Ren, Y. B., Zhang, B. C., & Yang, K. (2007). Study on biocompatility of magnesium and its alloys. *Rare Metal Materials and Engineering, 36*(6), 1102−1105.

Jagur-Grodzinski, J. (2006). Polymers for tissue engineering, medical devices, and regenerative medicine. Concise general review of recent studies. *Polymers for Advanced Technologies, 17*(6), 395−418.

Kang, H. W., Tabata, Y., & Ikada, Y. (1999). Fabrication of porous gelatin scaffolds for tissue engineering. *Biomaterials, 20*(14), 1339−1344.

Kannan, M. B., & Liyanaarachchi, S. (2013). Hybrid coating on a magnesium alloy for minimizing the localized degradation for load-bearing biodegradable mini-implant applications. *Materials Chemistry and Physics, 142*(1), 350−354.

Kowalski, A., Duda, A., & Penczek, S. (2000). Kinetics and mechanism of cyclic esters polymerization initiated with tin(II) octoate. 3. polymerization of L,L-dilactide. *Macromolecules, 33*(20), 7359−7370.

Kricheldorf, H. R., Berl, M., & Scharnagl, N. (1988). Poly(lactones). 9. polymerization mechanism of metal alkoxide initiated polymerizations of lactide and various lactones. *Macromolecules, 21*(2), 286−293.

Kricheldorf, H. R., Lee, S.-R., & Scharnagl, N. (1994). Polylactones. 28. syndiotactic poly(β-D,L-hydroxybutyrate) by ring-opening polymerization of β-D,L-butyrolactone with butyltin methoxides. *Macromolecules, 27*(12), 3139−3146.

Kumar, N., Langer, R. S., & Domb, A. J. (2002). Polyanhydrides: an overview. *Advanced Drug Delivery Reviews, 54*(7), 889−910.

Langer, R. (2013). Biomaterials and biotechnology: from the discovery of the first angiogenesis inhibitors to the development of controlled drug delivery systems and the foundation of tissue engineering. *Journal of Biomedical Materials Research Part A, 101A*(9), 2449−2455.

Langer, R., & Tirrell, D. A. (2004). Designing materials for biology and medicine. *Nature, 428*(6982), 487−492.

Langer, R., & Vacanti, J. (1993). Tissue engineering. *Science, 260*(5110), 920−926.

Lenaerts, V., Couvreur, P., Christiaensleyh, D., Joiris, E., Roland, M., Rollman, B., et al. (1984). Degradation of poly (isobutyl cyanoacrylate) nanoparticles. *Biomaterials, 5*(2), 65−68.

Lendlein, A. (1999). Polymere als Implantatwerkstoffe. *Chemie in unserer Zeit, 33*(5), 279−295.

Lendlein, A., Colussi, M., Neuenschwander, P., & Suter, U. W. (2001). Hydrolytic degradation of phase-segregated multiblock copoly(ester urethane)s containing weak links. *Macromolecular Chemistry and Physics, 202*(13), 2702−2711.

Lendlein, A., & Kelch, S. (2005). Shape-memory polymers as stimuli-sensitive implant materials. *Clinical Hemorheology and Microcirculation, 32*(2), 105−116.

Lendlein, A., Neuenschwander, P., & Suter, U. W. (1998). Tissue-compatible multiblock copolymers for medical applications, controllable in degradation rate and mechanical properties. *Macromolecular Chemistry and Physics, 199*(12), 2785−2796.

Little, L., Healy, K. E., & Schaffer, D. (2008). Engineering biomaterials for synthetic neural stem cell microenvironments. *Chemical Reviews, 108*(5), 1787−1796.

Li, N., & Zheng, Y. F. (2013). Novel magnesium alloys developed for biomedical application: a review. *Journal of Materials Science & Technology, 29*(6), 489−502.

Loo, S. C., Ooi, C. P., & Boey, Y. C. (2005). Influence of electron-beam radiation on the hydrolytic degradation behaviour of poly(lactide-co-glycolide) (PLGA). *Biomaterials, 26*(18), 3809−3817.

Mangiardi, E. K. (2013). *Biodegradable supporting device*. USA: Eventions, LLC, 15pp; Chemical Indexing Equivalent to 159:475836 (WO).

Mason, C., & Dunnill, P. (2007). Lessons for the nascent regenerative medicine industry from the biotech sector. *Regenerative Medicine, 2*(5), 753−756.

Mason, C., & Dunnill, P. (2008). A brief definition of regenerative medicine. *Regenerative Medicine, 3*(1), 1−5.

Montanari, L., Costantini, M., Signoretti, E. C., Valvo, L., Santucci, M., Bartolomei, M., et al. (1998). Gamma irradiation effects on poly(DL-lactictide-co-glycolide) microspheres. *Journal of Controlled Release, 56*(1−3), 219−229.

Mori, M., Yamaguchi, M., Sumitomo, S., & Takai, Y. (2004). Hyaluronan-based biomaterials in tissue engineering. *Acta Histochemica Et Cytochemica, 37*(1), 1−5.

Neffe, A. T., Tronci, G., Alteheld, A., & Lendlein, A. (2010). Controlled change of mechanical properties during hydrolytic degradation of polyester urethane networks. *Macromolecular Chemistry and Physics, 211*(2), 182−194.

Nwaogu, U. C., Blawert, C., Scharnagl, N., Dietzel, W., & Kainer, K. U. (2009). Influence of inorganic acid pickling on the corrosion resistance of magnesium alloy AZ31 sheet. *Corrosion Science, 51*(11), 2544−2556.

Okada, M. (2002). Chemical syntheses of biodegradable polymers. *Progress in Polymer Science, 27*(1), 87−133.

Okereke, M. I., Akpoyomare, A. I., & Bingley, M. S. (2014). Virtual testing of advanced composites, cellular materials and biomaterials: a review. *Composites Part B: Engineering, 60*, 637−662.

Penczek, S., Cypryk, M., Duda, A., Kubisa, P., & Słomkowski, S. (2007). Living ring-opening polymerizations of heterocyclic monomers. *Progress in Polymer Science, 32*(2), 247−282.

Peng, Q., Li, K., Han, Z., Wang, E., Xu, Z., Liu, R., et al. (2013). Degradable magnesium-based implant materials with anti-inflammatory activity. *Journal of Biomedical Materials Research Part A, 101A*(7), 1898−1906.

Peppas, N. A., & Langer, R. (2004). Origins and development of biomedical engineering within chemical engineering. *Aiche Journal, 50*(3), 536−546.

Phua, K. K. L., Roberts, E. R. H., & Leong, K. W. (2011). Degradable polymers. In D. Paul (Ed.), *Comprehensive biomaterials* (pp. 381−415). Oxford: Elsevier.

Poirier, Y., Dennis, D. E., Nawrath, C., & Somerville, C. (1993). Progress toward biologically produced biodegradable thermoplastics. *Advanced Materials, 5*(1), 30−37.

Razavi, M., Fathi, M., Savabi, O., Beni, B. H., Razavi, S. M., Vashaee, D., et al. (2014). Surface modification of biodegradable magnesium alloy bone implants using nanostructured diopside (CaMgSi2O6) coating. *Applied Surface Science, 288*, 130−137.

Rickert, D., Lendlein, A., Schmidt, A. M., Kelch, S., Roehlke, W., Fuhrmann, R., et al. (2003). In vitro cytotoxicity testing of AB-polymer networks based on oligo(ε-caprolactone) segments after different sterilization techniques. *Journal of Biomedical Materials Research Part B, 67B*, 722−731 (Copyright © 2010 American Chemical Society (ACS). All Rights Reserved.).

Rosemann, P., Schmidt, J., & Heyn, A. (2013). Short and long term degradation behavior of Mg-1Ca magnesium alloys and protective coatings based on plasma-chemical oxidation and biodegradable polymer coating in synthetic body fluid. *Materials and Corrosion, 64*(8), 714−722.

Sabir, M. I., Xu, X. X., & Li, L. (2009). A review on biodegradable polymeric materials for bone tissue engineering applications. *Journal of Materials Science, 44*(21), 5713−5724.

Sankara Narayanan, T. S. N., Park, I. S., & Lee, M. H. (2014). Strategies to improve the corrosion resistance of microarc oxidation (MAO) coated magnesium alloys for degradable implants: prospects and challenges. *Progress in Materials Science, 60*(0), 1−71.

Sawhney, A. S., & Hubbell, J. A. (1990). Rapidly degraded terpolymers of Dl-lactide, glycolide, and epsilon-caprolactone with increased hydrophilicity by copolymerization with polyethers. *Journal of Biomedical Materials Research, 24*(10), 1397−1411.

Scharnagl, N., Hiebl, B., Trescher, K., Zierke, M., Behl, M., Kratz, K., et al. (2012). Behaviour of fibroblasts on water born acrylonitrile-based copolymers containing different cationic and anionic moieties. *Clinical Hemorheology and Microcirculation, 52*(2−4), 295−311.

Scharnagl, N., Lee, S., Hiebl, B., Sisson, A., & Lendlein, A. (2010). Design principles for polymers as substratum for adherent cells. *Journal of Materials Chemistry, 20*(40), 8789−8802.

Schoental, R. (1968). Carcinogenic and chronic effects of 4,4'-diaminodiphenylmethane, an epoxyresin hardener. *Nature, 219*(5159), 1162.

Scholz, M. S., Blanchfield, J. P., Bloom, L. D., Coburn, B. H., Elkington, M., Fuller, J. D., et al. (2011). The use of composite materials in modern orthopaedic medicine and prosthetic devices: a review. *Composites Science and Technology, 71*(16), 1791−1803.

Schulz, R. M., & Bader, A. (2007). Cartilage tissue engineering and bioreactor systems for the cultivation and stimulation of chondrocytes. *European Biophysics Journal with Biophysics Letters, 36*(4−5), 539−568.

Shapiro, R. S. (2008). Future issues in transplantation ethics: ethical and legal controversies in xenotransplantation, stem cell, and cloning research. *Transplant Reviews (Orlando), 22*(3), 210−214.

Shastri, V. P., & Lendlein, A. (2009). Materials in regenerative medicine. *Advanced Materials, 21*(32−33), 3231−3234.

Sjogren, F., & Anderson, C. (2000). The spectrum of inflammatory cell response to dimethyl sulfoxide. *Contact Dermatitis, 42*, 216−221 (Copyright © 2011 American Chemical Society (ACS). All Rights Reserved.).

Slater, B. J., Kwan, M. D., Gupta, D. M., Panetta, N. J., & Longaker, M. (2008). Mesenchymal cells for skeletal tissue engineering. *Expert Opinion on Biological Therapy, 8*(7), 885−893.

Solchaga, L. A., Temenoff, J. S., Gao, J., Mikos, A. G., Caplan, A. I., & Goldberg, V. M. (2005). Repair of osteochondral defects with hyaluronan- and polyester-based scaffolds. *Osteoarthritis Cartilage, 13*(4), 297−309.

Spaans, C. J., de Groot, J. H., Dekens, F. G., & Pennings, A. J. (1998). High molecular weight polyurethanes and a polyurethane urea based on 1,4-butanediisocyanate. *Polymer Bulletin, 41*(2), 131−138.

Staubli, A., Mathiowitz, E., Lucarelli, M., & Langer, R. (1991). Characterization of hydrolytically degradable amino acid containing poly(anhydride-co-imides). *Macromolecules, 24*(9), 2283−2290.

Sternberg, K., Gratz, M., Koeck, K., Mostertz, J., Begunk, R., Loebler, M., et al. (2012). Magnesium used in bioabsorbable stents controls smooth muscle cell proliferation and stimulates endothelial cells in vitro. *Journal of Biomedical Materials Research Part B, 100B*(1), 41−50.

Strobel, C., Kadow-Romacker, A., Witascheck, T., Schmidmaier, G., & Wildemann, B. (2011a). Evaluation of process parameter of an automated dip-coating. *Materials Letters, 65*(23−24), 3621−3624.

Strobel, C., Schmidmaier, G., & Wildemann, B. (2011b). Changing the release kinetics of gentamicin from poly(D,L-lactide) implant coating using only one polymer. *The Journal of Artificial Organs, 34*(3), 304−316.

Tamada, J., & Langer, R. (1992). The development of polyanhydrides for drug delivery applications. *Journal of Biomaterials Science, Polymer Edition, 3*(4), 315−353.

Tanzi, M. C., Verderio, P., Lampugnani, M. G., Resnati, M., Dejana, E., & Sturani, E. (1994). Cytotoxicity of some catalysts commonly used in the synthesis of copolymers for biomedical use. *Journal of Materials Science Materials in Medicine, 5*, 393−396 (Copyright © 2011 American Chemical Society (ACS). All Rights Reserved.).

Thorfve, A., Lindahl, C., Xia, W., Igawa, K., Lindahl, A., Thomsen, P., et al. (2014). Hydroxyapatite coating affects the Wnt signaling pathway during peri-implant healing in vivo. *Acta Biomaterialia, 10*(3), 1451−1462.

Trescher, K., Scharnagl, N., Kratz, K., Roch, T., Lendlein, A., & Jung, F. (2012). Adherence and viability of primary human keratinocytes and primary human dermal fibroblasts on acrylonitrile-based copolymers with different concentrations of positively charged functional groups. *Clinical Hemorheology and Microcirculation, 52*(2−4), 391−401.

Trollsas, M., Kelly, M. A., Claesson, H., Siemens, R., & Hedrick, J. L. (1999). Highly branched block copolymers: design, synthesis, and morphology. *Macromolecules, 32*(15), 4917−4924.

Tzoneva, R., Seifert, B., Albrecht, W., Richau, K., Lendlein, A., & Groth, T. (2008). Poly(ether imide) membranes: studies on the effect of surface modification and protein pre-adsorption on endothelial cell adhesion, growth and function. *Journal of Biomaterials Science, Polymer Edition, 19*, 837−852 (Copyright © 2010 American Chemical Society (ACS). All Rights Reserved.).

Unger, C., Skottman, H., Blomberg, P., Dilber, M. S., & Hovatta, O. (2008). Good manufacturing practice and clinical-grade human embryonic stem cell lines. *Human Molecular Genetics, 17*, R48−R53.

Vacanti, C. A. (2006). History of tissue engineering and a glimpse into its future. *Tissue Engineering, 12*(5), 1137−1142.

Williams, D. F. (2009). On the nature of biomaterials. *Biomaterials, 30*(30), 5897−5909.

Williams, H., Huxley, J., Claybourn, M., Booth, J., Hobbs, M., Mehan, E., et al. (2006). The effect of gamma-irradiation and polymer composition on the stability of PLG polymer and microspheres. *Polymer Degradation and Stability, 91*, 2171.

Witte, F., Kaese, V., Haferkamp, H., Switzer, E., Meyer-Lindenberg, A., Wirth, C. J., et al. (2005). In vivo corrosion of four magnesium alloys and the associated bone response. *Biomaterials, 26*(17), 3557−3563.

Yoo, H. S., Lee, E. A., Yoon, J. J., & Park, T. G. (2005). Hyaluronic acid modified biodegradable scaffolds for cartilage tissue engineering. *Biomaterials, 26*(14), 1925−1933.

Zdrahala, R. J., & Zdrahala, I. J. (1999a). Biomedical applications of polyurethanes: a review of past promises, present realities, and a vibrant future. *Journal of Biomaterials Applications, 14*(1), 67−90.

Zdrahala, R. J., & Zdrahala, I. J. (1999b). In vivo tissue engineering: Part I. Concept genesis and guidelines for its realization. *Journal of Biomaterials Applications, 14*(2), 192−209.

Zeng, R., Dietzel, W., Witte, F., Hort, N., & Blawert, C. (2008). Progress and challenge for magnesium alloys as biomaterials. *Advanced Engineering Materials, 10*(8), B3−B14.

Index

Note: Page numbers followed by "f" and "t" indicate figures and tables respectively.

A
Acid treatment, 162–166, 164f–165f, 167f–168f
Adsorption, 34–35
  protein, 13–14, 26–28
Albumin, 26–27
Aldehydes, chemical structure of, 15t–16t
Alginic acid, 406
Alkali treatment, 166–176, 169f–174f
Alkenes, chemical structure of, 15t–16t
Alumina gel, biomimetic surface modification of, 238
Amides, chemical structure of, 15t–16t
Amines, chemical structure of, 15t–16t
Anchoring effect, 277–278, 278f
Anodization, 32–33, 263–265
Antibacterial coatings, 211–212
Antibacterial property, 4, 380–381
  silver element, 303–304
Antibiotic drug release, 382–384
Antimicrobial coatings, 379–392
  antibiotic drug release, 382–384
  chemical/drug release, 381–384
  metal ion release, 381–382
  organic antimicrobial drug release, 384
  surface treatments to affect physical adhesion, 384–387
    PEG and surface exclusion, 384–385
    surface topology and wetting modification, 385–387, 386f
Apatite formation, 159–161, 170–172, 220
  on bone-bonding ceramics, 219
  in SBF on metal surfaces
    subjected to NaOH and heat treatments, 221–224, 223f
    subjected to NaOH, $CaCl_2$, heat, and water treatment, 226–227
  in SBF on Ti
    subjected to acid and heat treatments, 231–233, 232f
    on pH of exposed solution, 234–236
Arginine-glycine-aspartic acid (Arg-Gly-Asp), 348. *See also* RGD (Arg-Gly-Asp) sequence
Aryl, chemical structure of, 15t–16t
Atomic force microscopy (ATM), 73–74, 73f
Attenuated total reflection (ATR), 63–64, 64f

B
Bacterial adhesion, inhibition of, 278
Barrier coatings, 207–211, 208t
Bioactive coatings, 359–360
Bioactive polymer-calcium phosphate composite coatings, by electrophoretic deposition, 359–378
Bioactivity of metallic biomaterials, 126–129
  plasma immersion ion implanted surfaces, 126–127
  plasma-polymerized and plasma-grafted surfaces, 127–128
  plasma-sprayed surfaces, 128–129
Biochemical surface modification, 34–36
Biocompatibility, 126–129, 249–250, 289–291, 289f. *See also* Bioactivity of metallic biomaterials; Biocompatible coatings
Biocompatible coatings, 287–344
  future trends of, 318–320
  materials, 303–318
    biomimetic materials, 315–318
    ceramics, 307–315
    composites, 315–318
    functional gradient materials, 315–318

Biocompatible coatings (*Continued*)
hybrids, 315–318
metallic materials, 303–306
polymeric materials, 306–307
surface and interface, nature of, 291–292
technologies of, 292–303
chemical and electrochemical modifications, 292–293
combined technology, 302–303
mechanical modification, 292
physical modification, 294–300
thermal modification, 301–302
Biocorrosion of magnesium, 88–90
key issues of, 88–89
in vitro–in vivo comparison, 89–90, 89t
Biodegradation, 406–407
Biofilm formation, inhibition of, 280–281, 282f
Biological applications, of metallic biomaterials, 249–250
Biological interactions, on metallic biomaterials surface, 24–30, 25f
cell adhesion and cell–surface interaction, 28–30
protein adsorption, 26–28
Biomaterials. *See* Metallic biomaterials
Biomedical applications, of metallic biomaterials, 17–24, 250–251
cobalt–chromium alloys, 18–19
dental metals, 22
essential requirements, 7t
magnesium, 22–23
platinum group metals, 23
shape memory alloys, 21
silver, 23
stainless steels, 17–18
superelastic alloys, 21
tantalum, 24
titanium, 19–21
zirconium alloys, 24
Biomimetic surface modification, 38, 219
alumina gel, 238
approaches for, 220
background of, 219
future of, 240
metallic biomaterials, clinical applications of, 238–239
spinal fusion devices, 238–239, 239f–240f
total hip joints, 238, 239f
niobium oxide gel, 237
tantalum oxide gel, 237–238
Ti metals, acid and heat treatments of, 229–234
bone-bonding, 233, 233f
osteoconduction, 234, 234f
osteoinduction, 234, 235f
simulated body fluid, apatite formation in, 231–233, 231f–232f
surface structural change, 229–231, 231f
Ti metals/alloys in NaOH/$CaCl_2$ solution, heat and water treatments of, 226–229
bone-bonding, 227, 228f
evolution of, 227–229, 229f–230f
simulated body fluid, apatite formation in, 226–227, 228f
surface structural change, 226, 226f–227f
Ti metals/alloys in NaOH solution, heat treatments of, 220–225
bone-bonding, 224, 224f–225f
problems associated with, 225
simulated body fluid, apatite formation in, 221–224, 222f–223f
surface structural change, 220–221, 221f–222f
Ti metals on pH of exposed solution, apatite formation dependence on, 234–236, 235f–237f
zirconia gel, 236–237
Bioprinting, three-dimensional, 319
Biosis–abiosis interface, 275, 275f
Blue light interferometer, 162f
Bone area fraction occupancy (BAFO), 298–299
Bone bonding
Ti metals, acid and heat treatments of, 233, 233f
Ti metals/alloys in NaOH/$CaCl_2$ solution, 227, 228f
Ti metals/alloys in NaOH solution, 224, 224f–225f
Bone formation, acceleration of, 282–283
Bone interfacing implants, 195–207
Bone-like apatite, 38
Bone matrix mineralization, promoting, 352

Bone morphogenetic protein-2 (BMP-2), 349–351, 352f
Bone remodeling, regulation of, 353
Bone-to-implant contact (BIC), 298–299, 347, 347f
Bulk degradation, 408, 408f, 409t

C
Calcium contamination, in Ti metals/alloys, 225
Calcium hydroxyapatite sol–gel-derived coating, 196–203
Calcium phosphate (Ca-P), 37–41
  biocompatible coatings, 314
  coatings, for osseointegration, 350–351, 351f
  composite coatings based on, 365–369, 367f
  glass-ceramic coatings, 41
  sol–gel-derived coatings, 196–203, 198t–200t, 202f
Carbides, 307–311
Carbon layer coatings, 44
Carboxylic acids, chemical structure of, 15t–16t
Cardiovascular applications, of degradable polymer materials, 410–411
$CaTiSiO_3$ sol–gel-derived coating, 206–207
  TiO_2–HAp composite coatings, 203–206, 205t
  titania coating, 203–206, 205t
Cell adhesion, 28–30, 348–349
Cell differentiation, 349–351
Cell proliferation, 349–351
Cell–surface interaction, 28–30
Ceramics, 307–315
Chemical/drug release, 381–384
Chemical etching, 32, 267–268
Chemical surface modification, 159, 292–293
  acid treatment, 162–166, 164f–165f, 167f–168f
  alkali treatment, 166–176, 169f–174f
  challenges to, 177
  future trends of, 177
  hydrogen peroxide treatment, 159–162, 160f–161f
  thermal oxidation, 176–177
  treatment methods for, 177t
Chemical vapor deposition (CVD), 257, 266–267
  laser-enhanced, 267, 267f, 299
Chitosan, 405–406
Coatings, 31f, 36–45
  adhesion to substrate, 41
  antimicrobial, 379–392
  bioactive, 359–360
  bioactive polymer-calcium phosphate composite. *See* Bioactive polymer-calcium phosphate composite coatings, by electrophoretic deposition
  biocompatible. *See* Biocompatible coatings
  calcium phosphate. *See* Calcium phosphate (Ca-P)
  carbon layer, 44
  composite, 42
  hydrogel, 45
  layer-by-layer method, 44–45
  organic–inorganic composite, 363–365
  for osseointegration, 345–358
  oxide, 42–44
  plasma-sprayed, 117t–120t
  polymer-based degradable. *See* Polymer-based degradable coatings
  sol–gel-derived. *See* Sol–gel-derived coatings
  stability of, 40
  thickness of, 40
Cobalt–chromium (Co–Cr) alloys, biomedical applications of, 18–19
Collagen, 405
Composite coatings, 42
Contact angle goniometry, 70–71
Contact guidance, 11
Copolyesters, 396–399
  physical properties of, 399t
Corrosion
  crevice, 91, 94f–95f
  magnesium. *See* Magnesium corrosion
  resistance, 132–136, 133t–135t
  self-corrosion, 98
Covalent attachment, 34–35
Crevice corrosion, 91, 94f–95f

D
Degradable polymer systems, 396–406
  copolyesters, 396–399, 399t
  natural polymeric materials, 404–406

Degradable polymer systems (*Continued*)
polyanhydrides, 399–400, 399f, 401f–402f
polyesters, 396–399, 398t
polyurethanes, 400–404, 403f–404f, 405t
Dental metals, biomedical applications of, 22
Diffuse reflectance infrared Fourier transform infrared spectroscopy (DRIFTS), 64f, 65
Dip sol–gel-derived coating, 189–191, 189f–190f
Drug-eluting stents (DES), 410–411

E
Electrochemical modification, 32–33, 292–293
Electro-erosion, 33
Electron beam physical vapor deposition (EB-PVD), 262
Electrophoretic deposition (EPD), 360–363, 361f, 369t–371t
bioactive polymer-calcium phosphate composite coatings by, 359–378
Electropolishing, 33
Entrapment, 34–35
Esters, chemical structure of, 15t–16t
Etching
chemical, 32, 267–268
physical, 260
plasma, 108, 122
reactive ion, 108
sandblasting with large grit and acid-etching, 300
Ethers, chemical structure of, 15t–16t
Extracellular matrix (ECM), 29–30, 348

F
Fibrin, 405
Fibrinogen, 27–28
Fibrous capsule, 25–26
Foreign body giant cells (FBGC), 25–26
Fourier transform infrared spectroscopy (FTIR), 63
Functionally gradient material (FGM), 315–319

G
Gentamicin, 383
Grit-blasting, 32

H
Hard-tissue compatibility, improvement of, 276–278
Hip joints, clinical applications of metallic biomaterials, 238
Hooke's law, 73
Hyaluronic acid, 406
Hydrochloric acid (HCl), 163–166
Hydrogel coating, 45
Hydrogen peroxide (H_2O_2), 106
treatment, 159–162, 160f–161f
Hydroxyapatite (HA)
-based composites, 314
bioactive polymer-calcium phosphate composite coatings, 359–360, 364
biocompatible coatings, 311–313
mechanical properties of, 129–131
osseointegration, coatings for, 348
plasma-sprayed, 128, 296
silicon substituted, 313–314
tribological behaviour, 131–132
Hydroxycarbonate apatite (HCA), 363–364
Hydroxyl, chemical structure of, 15t–16t
Hyluronate, 365

I
Ion beam-assisted deposition (IBAD), 33, 37
Ion beam-based processes, 33–34
Ion beam sputtering, 262–263

J
Joint replacement, 6, 126, 211–212
implants, 207–210
cementless implants, 195–196
total hip joints, 238

K
Ketones, chemical structure of, 15t–16t

L
Laser-based techniques, 254–259, 257f
Laser-enhanced chemical vapor deposition (LE-CVD), 267, 267f, 299
Laser-induced forward transfer (LIFT), 258
Laser nitrization, 299
Laser oxidation, 299
Laser surface modification, 34

Layer-by-layer (LbL) deposition, 44–45, 364–365
Low-temperature isotropic pyrolytic carbon (LTIC), 127

M
Magnesium (Mg)
  -based metals, biomedical applications of, 251
  biodegradation, 92–95
  biomedical applications of, 22–23
  corrosion. *See* Magnesium corrosion
Magnesium corrosion, 81
  biocorrosion, 88–90
    key issues of, 88–89
    in vitro–in vivo comparison, 89–90, 89t
  mechanism of, 98
  pure Mg corrosion, tolerance limits of, 81–86, 82f–85f
  rate measurement, 90–98
    apparent valence of, 96–98, 97f–98f
    crevice corrosion, 91, 94f–95f
    issues of, 92
    plug-in specimen, 90–92, 92f
    solutions, 92–96
    techniques of, 90, 91f
    time of, 91–92
  stainless magnesium, 81–88
    melt purification, 88, 88f–89f
    pure Mg corrosion, tolerance limits of, 81–86, 82f–85f
    ultra-high-purity Mg alloys corrosion, requirements for, 86–88, 86f–87f
Matrix-assisted pulsed-laser evaporation (MAPLE), 258
  MAPLE direct write, 258
Mechanical modification, 292
Mechanical properties of metallic biomaterials, 129–131
Medical devices, properties of, 277t
Melt purification, 88, 88f–89f
Metal alloys, mechanical properties of, 251–253, 252t
Metal ion release, 381–382
Metallic biomaterials, 3–60
  biological applications of, 249–250
  biomedical applications of, 250–251
  coatings, 31f, 36–45
    calcium phosphate, 37–41
    calcium phosphate glass-ceramic, 41
    carbon layer, 44
    composite, 42
    hydrogel, 45
    layer-by-layer method, 44–45
    oxide, 42–44
  future trends of, 45–46
  manufacturing process of, 276f
  pros and cons of, 5–6
  surface, biological interactions on, 24–30, 25f
    cell adhesion and cell–surface interaction, 28–30
    protein adsorption, 26–28
  surface characteristics of, 6–17, 8f
    surface charge, 12
    surface chemistry, 8–9
    surface energy and wettability, 12–17
    topography and surface roughness, 9–12
  surface modification of, 4, 12, 31f
    biochemical, 34–36
    physicochemical, 32–34
    reasons for, 4–5
Metallic materials, 303–306
Metallic oxides, 307–311
Metallic surfaces, functionalisation of, 275
  challenges and applications, 280–283
    biofilm formation and platelet adhesion, inhibition of, 280–281, 282f
    bone formation, acceleration of, 282–283
  future trends of, 283–284
  motivations for, 276–279
    bacterial adhesion, inhibition of, 278
    hard-tissue compatibility, improvement of, 276–278
    platelet adhesion, control of, 278–279
  technologies overview, 279–280
Methyl, chemical structure of, 15t–16t
Micro-arc oxidation (MAO), 294
Microelectromechanical systems (MEMS), 108
Multinucleated giant cells, 25–26
Musculoskeletal applications, of degradable polymer materials, 411–412

N
Nanoparticles, 254, 262–263
Nanoscale surface modification, 249, 255t–256t
  chemical methods, 263–268
    anodization, 263–265
    chemical etching, 269
    chemical vapor deposition, 266–267, 267f
  future directions of, 255t–256t, 269
  physical techniques, 254–263
    laser-based techniques, 254–259, 257f
    physical vapor deposition, 261–263, 261f
    plasma-based techniques, 259–260, 260f
Nanoscience, 253
Nanotechnology, 253
Natural polymeric materials, 404–406
NH_2–PEG–NH_2, immobilization of, 281f
Niobium oxide gel, biomimetic surface modification of, 237
Nitrides, 307–311
Nonthermal plasma, 103–104

O
Organic-inorganic composite coatings, 363–365
Osseointegration, 195–207, 276–277
  biological process of, 346
  clinical background of, 345
  coatings for, 345–358
    bone matrix mineralization, promoting, 352
    bone remodeling, regulation of, 353
    clinical applications of, 353–355
    future trends of, 353–355
    proliferation and differentiation, 349–351
    recognition and adhesion, 348–349
  definition of, 345–346
  evaluation methods of, 346–347
Osteoconduction, 125, 138, 238
  in vitro, 282
  Ti metals, acid and heat treatments of, 234, 234f
Osteoinduction, 238
  Ti metals, acid and heat treatments of, 234, 235f
Oxide coatings, 42–44

P
Phenols, chemical structure of, 15t–16t
Physical etching, 260
Physical surface modification, 254–263, 294–300
  laser-based techniques, 254–259, 257f
  physical vapor deposition. *See* Physical vapor deposition (PVD)
  plasma-based techniques, 259–260, 260f
Physical vapor deposition (PVD), 257, 261–263, 261f
  electron beam, 262
Physicochemical surface modification, 32–34
Plasma-based techniques, 259–260, 260f
Plasma etching, 108, 122
Plasma grafting, 112–114, 113f, 122–126, 128
  grafted surfaces, 127–128
Plasma immersion ion implantation (PIII), 108–110, 109f, 111t, 122–127, 295–296
Plasma immersion ion implantation and deposition (PIII&D), 108–110
Plasma immersion ion implanted surfaces, 126–127, 127f
Plasma nitrization, 297
Plasma polymerization, 110–112, 112t, 113f, 122–126
Plasma-polymerized surfaces, 127–128
Plasma spraying, 38, 40–41, 114–121, 124–125, 259–260, 296
  coatings, 117t–120t
  plasma-sprayed surfaces, 128–129
  torch, 115f
Plasma sputtering, 106–108
Plasma sterilization, 105–106, 107f
Plasma surface modification, 103
  arithmetic roughness average values, 124t
  applications of, 136–138
  challenges to, 138–140, 139f
  classification of, 106f
  future trends of, 138–140, 139f
  overview of, 103–105
  plasma etching. *See* Plasma etching
  plasma grafting. *See* Plasma grafting
  plasma immersion ion implantation. *See* Plasma immersion ion implantation (PIII)

plasma polymerization. *See* Plasma polymerization
plasma spraying. *See* Plasma spraying
plasma sputtering. *See* Plasma sputtering
plasma sterilization. *See* Plasma sterilization
primary requirements of, 122f
surface properties from, 121–136
biocompatibility and bioactivity, 126–129
corrosion resistance, 132–136, 133t–135t
mechanical properties, 129–131
surface chemistry, 125–126
surface morphology, 121–125, 123f
tribological behaviour, 131–132
Plasma treatment, 294–295
Platelet adhesion
control of, 278–279
inhibition of, 280–281, 282f
Platinum group metals (PGM), biomedical applications of, 23
Polyanhydrides (PAs), 394t, 399–400, 399f, 401f–402f
Polycaprolactone (PCL), 364
Poly(ester amide)s (PEAs), 394t
Polyesters (PEs), 394t, 396–399
material properties of, 398t
Polyethylene, 303–304
Poly(ethylene glycol) (PEG), 280–283, 384–385, 387
Poly(ethylene glycol)methacrylate (PEGMA) grafting, 128
Poly(D,L-lactide) (PDLLA), 383–384
Poly(2-methacryloxyloxyethyl phosphorylcholine) (PMPC), 128
Poly(vinyl acetate) (PVA), 306
Polymer, structures and architectures, 395f
Polymer-based biomaterials. *See* Polymer-based degradable coatings
Polymer-based degradable coatings, 393–422
applications of, 410–412
cardiovascular applications, 410–411
musculoskeletal applications, 411–412
challenges to, 412–414
degradable polymer systems, 396–406
copolyesters, 396–399, 399t
natural polymeric materials, 404–406
polyanhydrides, 399–400, 399f, 401f–402f
polyesters, 396–399, 398t
polyurethanes, 400–404, 403f–404f, 405t
degradation mechanisms, 406–410, 407f
bulk degradation, 408, 408f, 409t
surface degradation, 409–410
future trends of, 414–415
Polymeric materials, 306–307
Polytetrafluoroethylene (PTFE), 303–304
Polyurethanes (PURs), 394t, 400–404
mechanical properties of, 405t
synthesis of
and chain extension of, 404f
raw materials for, 403f
Profilometry techniques, 74–75
Protein adsorption, 13–14, 26–28
Protein–surface interactions, 28
Pulsed laser deposition (PLD), 257–258, 257f

Q

Quantitative osseointegration, 347, 347f

R

Reactive ion etching (RIE), 108
Recombinant human bone morphogenetic protein-2 (rhBMP-2), 349–351
Regenerative medicine, category of, 284f
RGD (Arg-Gly-Asp) sequence, 282–283, 283f, 348–349
Ring-opening polymerization, monomers for, 396f

S

Sandblasting with large grit and acid-etching (SLA), 300
Scanning electron microscopy (SEM), 71–73, 72f
Secondary ion mass spectrometer (SIMS), 67–68, 67f
Self-corrosion, 98
Shape memory alloys, biomedical applications of, 21
Silver, biomedical applications of, 23

Simulated body fluid (SBF), 38–39, 41, 219–220, 295
apatite formation in
Ti metal on pH of exposed solution, dependence of, 234–236, 235f–237f
Ti metals, acid and heat treatments of, 231–233, 231f–232f
Ti metals/alloys in NaOH solution, 221–224, 222f–223f
Ti metals/alloys in NaOH/$CaCl_2$ solution, 226–227, 228f
Slippery liquid-infused porous surfaces (SLIPS), 387
Smooth muscle cells (SMCs), 6
Soft tissue attachment, 207, 208t
Sol–gel-derived coatings, 188
application of, 195–212
antibacterial coatings, 211–212
barrier coatings, 207–211, 208t
Ca-P sol–gel-derived coatings, 196–203, 198t–200t, 202f
soft tissue attachment, 207, 208t
Ta_2O_5 sol–gel-derived coating, 206–207
TiO_2/SiO_2 sol–gel-derived coating, 206–207
characterization of, 194–195
coating sintering, 193
dip coating, 189–191, 189f–190f
microstructure, factors affecting, 193–194
spin coating, 191–192, 191f
Sol–gel surface modification, 39–41, 185
coatings. *See* Sol–gel-derived coatings
general, 185–186
process, 186–188
Specular reflectance, 64–65, 64f
Spinal fusion devices, metallic biomaterials applications in, 238–239, 239f–240f
Spin sol–gel-derived coating, 191–192, 191f
Stainless magnesium, corrosion of, 81–88
melt purification, 88, 88f–89f
pure Mg corrosion, tolerance limits of, 81–86, 82f–85f
ultra-high-purity Mg alloys corrosion, requirements for, 86–88, 86f–87f
Stainless steels, biomedical applications of, 17–18
Superelastic alloys, biomedical applications of, 21
Surface characterization, 61–62
Surface charges, 12, 75
Surface chemistry, 62–68
attenuated total reflection, 63–64, 64f
diffuse reflectance infrared FTIR, 64f, 65
Fourier transform infrared spectroscopy (FTIR), 63
of metallic biomaterials, 8–9
plasma-modified, 125–126
secondary ion mass spectrometer, 67–68, 67f
specular reflectance, 64–65, 64f
X-ray photoelectron spectroscopy, 65–66, 66f
Surface degradation, 409–410
Surface energy, of metallic biomaterials, 12–17
Surface exclusion, 384–385
Surface modification, 4, 12, 31f, 219
biochemical, 34–36
biomimetic. *See* Biomimetic surface modification
category of, 279f
chemical. *See* Chemical surface modification
evolution of, 283f
nanoscale. *See* Nanoscale surface modification
physicochemical, 32–34
plasma. *See* Plasma surface modification
reasons for, 4–5
techniques by dry and wet processes, 280f
Surface-modified layer formation, 33–34
Surface morphology, plasma-modified, 121–125, 123f
Surface properties, 61–78
surface charges, 75
surface chemistry, 62–68, 64f, 66f–67f. *See also* Surface chemistry
surface texture, 71–75, 72f–73f. *See also* Surface texture
surface wettability. *See* Surface wettability
Surface roughness, of metallic biomaterials, 9–12
Surface texture, 71–75
atomic force microscopy, 73–74, 73f
profilometry techniques, 74–75
scanning electron microscopy, 71–73, 72f
Surface topology, 385–387, 386f

Surface treatments, 4, 253
Surface wettability, 12–17, 68–71, 69f

T
Tantalum, biomedical applications of, 24
Tantalum oxide gel, biomimetic surface modification of, 237–238
Ta_2O_5 sol–gel-derived coating, 206–207
Thermal modification, 301–302
Thermal oxidation, 176–177
Thermal plasma, 103–104
  high-temperature, 104t
  low-temperature, 104t
Thin film formation, 33–34
Thiols, chemical structure of, 15t–16t
Titania sol–gel-derived coating, 203–206, 205t
Titanium alloys
  biomedical applications of, 19–21
  surface morphology of, 123f
  Ti–Zr–Nb–Ta alloys, 225
Titanium aluminum nitride, 310–311
Titanium carbide (TiC), 311
Ti metals/alloys in NaOH/$CaCl_2$ solution, heat and water treatments of, 226–229
  bone-bonding, 227, 228f
  evolution of, 227–229, 229f–230f
  simulated body fluid, apatite formation in, 226–227, 228f
  surface structural change, 226, 226f–227f
Ti metals/alloys in NaOH solution, heat treatments of, 220–225
  bone-bonding, 224, 224f–225f
  problems associated with, 225
    Ca contamination, 225
    humidity, 225
    Ti–Zr–Nb–Ta alloys, 225
  simulated body fluid, apatite formation in, 221–224, 222f–223f
  surface structural change, 220–221, 221f–222f
Ti metals on pH of exposed solution, apatite formation dependence on, 234–236, 235f–237f
TiO_2–HAp sol–gel-derived coating, 203–206, 205t
TiO_2/SiO_2 sol–gel-derived coating, 206–207
Tissue-biomaterial interactions, 24–25, 25f
Topography, of metallic biomaterials, 9–12
Total hip joints, metallic biomaterials applications in, 238, 239f
Tribological behaviour, 131–132
Trichlorosilanes, chemical structure of, 15t–16t
Trifluoromethyl, chemical structure of, 15t–16t

U
Ultra-high-purity Mg alloys corrosion, requirements for, 86–88, 86f–87f
Uni-positive Mg^+, 98

V
Vapor deposition. *See individual vapor disposition*
Vroman effect, 26, 27f

W
Wetting modification, 385–387, 386f

X
X-ray photoelectron spectroscopy (XPS), 65–66, 66f

Y
Yield strain, 405t
Yield strength, 14, 23, 252t, 405t
Young's modulus, 7t, 405t

Z
Zeta potential analysis, 75
Zirconia coating, 24, 236–237, 309
Zisman method, 69